Integrating climate and satellite remote sensing to assess the reaction of *Vitis vinifera* L. cv. Cabernet Sauvignon to a changing environment

by

TO Southey

Dissertation presented for the degree of
Doctor of Philosophy
(Agricultural Sciences)
at
Stellenbosch University
Department of Viticulture and Oenology, Faculty of AgriSciences

Supervisor: Dr AE Strever

March 2017

DECLARATION

By submitting this thesis electronically, I declare that the entirety of the work contained therein is my own, original work, that I am the sole author thereof (save to the extent explicitly otherwise stated), that reproduction and publication thereof by Stellenbosch University will not infringe any third party rights and that I have not previously in its entirety or in part submitted it for obtaining any qualification.

Date: March 2017

SUMMARY

Context - In the context of climate change, factors such as seasonal variability and limitations of available water resources, have increased pressures on the production of table wines, and could continue to do so without effective adaptive strategies.

Problem formulation and aims (objective) - The classification of the climate in the Western Cape as well as long term and in-season monitoring are complicated due to the difficulties in accessing climate data, quality of the data is not assured, and limitations due to the sparse spatial distribution of currently logging weather stations. Reliable climate data can be costly, and currently requires intensive data validation; hence the study aimed to find an alternative resource to quantify the climate over the spatial extent of the Western Cape, for possible semi-real time applications. Temperature is one of the main climatic variables driving grapevine response; hence this study validated the use of freely available remote sensing land surface temperature images - a collection of daily maximum and minimum temperature layers. The aims of the study were to quantify climate change and seasonal variability in the Western Cape with the best station network possible within the limits of the spatial and temporal resolution availability.

Study design - The study included extreme climatic conditions by selecting sites over a climatic band, and multiple factor analysis was used to evaluate the interaction of climate with grapevine phenology, growth, ripening and wine attributes. This was done to highlight the possible driving factors that can be used in future climatic modelling.

Findings and impact - For the estimation of mean weather station temperature, the results from this study can be considered promising, given the simplicity of the statistical models employed, the robustness of the resampling techniques and the high accuracy achieved under these limitations. The weather station mean temperature can therefore be supplemented/predicted using the mean land surface temperatures, based on the regression equations attained from the final analysis with a calibration error of 2.4°C and a prediction error of 2.6°C. The daily mean land surface temperature and weather station temperature data exhibited a strong linear relationship ($r = 0.86$, $p < 0.001$, and $N = 29$), and good prediction accuracy. These land surface temperature maps are intrinsically spatialised, providing daily temperature values that in the past would have only been possible by spatial interpolation of sparse weather station networks, which could only be as accurate as the input data.

Seasonal variability was prominent in driving grapevine response. The variability was seemingly intensified by extreme climate events such as extreme wind, rainfall or higher temperatures earlier in growing season as well as during the ripening period. This confirmed the difficulty to predict seasonal conditions in the context of climate change. Seasonal variability and grapevine responses could better be described with finer scale analysis of the climate profile, considering and accounting for the amount of hours in specific temperature, wind and relative humidity ranges. This was a novel approach, as it allowed analysis of the climate data without preconceived ideas around specified thresholds. This could possibly explain grapevine responses outside of a conventional scientific frame of reference. Grapevine phenological stages seemed to be more affected by temperatures outside of the growing season, which highlighted a need for reviewing the current climatic indices used to describe the growing season. Temperatures throughout the year, with the exception of August and September, seemed to affect flowering. The summer months (December, January and February) with more observed hours between 30-35°C and 35-40°C, had a negative correlation with flowering date as days after 1 September (the flowering and vintage precocity indices were earlier). In this study, the date of flowering was most affected by

temperature and tended to “set the pace” for phenology in the season. Flowering date as days after budburst could also potentially be used to predict harvest date for Cabernet Sauvignon over sites with an accuracy of only a few days.

The study proved that within a general warming trend, the climate in the Western Cape could be both warming and cooling, depending on the area or months in the context of the long term mean. This emphasises the need for continuous semi-real time climate data, such as the daily land surface temperature layers that can be used as an alternative to supplement weather station networks using a regression model to account for the remote sensing imaging. The acquisition and processing of the land surface temperature layers can be automated and extended to other crops cultivated in South Africa.

This study has provided some insights into the understanding of cultivating Cabernet Sauvignon in the context of warmer and cooler climatic conditions. Almost every response of the grapevine was affected by climate. It was shown that grapevine growth tempo and final shoot length were sensitive to seasonal variability and water constraints and indirectly affected leaf area per vine that in turn could alter ripening tempo and final wine quality. The seasonal climatic conditions could be masked with more detailed viticultural management practices to ensure a balanced grapevine through the selection of trellis system, pruning and canopy management. In the context of climate change, the aim is to match the cultivar growth and ripening response to the climatic conditions of a site. Finer scale analysis of the climate using hourly frequency data approaches may aid in improving adaptive strategies for the future. This is especially relevant in the context of climate change and the complex terrain of the Western Cape affecting the diurnal shifts of climate over seasons and short distances. The study showed that warm to moderate climatic conditions where grapevines experience moderate water constraints tended to be more balanced in terms of growth and ripening, yielding complex wines with favourable attributes for Cabernet Sauvignon.

Prospectives for future work would include the integration of climate maps in the context of grapevine modelling along with a spatial view of the seasonal shifts. This could help with improved management and adaptation. This further emphasises the need for within season monitoring of temperature, plant water status as well as other environmental parameters. It can also be further unlocked by remote sensing products, also in the context of water management in the future.

The study provided some foundations for a larger database of climate, land surface temperature and phenology for the identification of cultivar distributions compared to more ideal cultivar distribution in the context of a warmer future with possibly more limited water resources.

OPSOMMING

Konteks - In die konteks van klimaatsverandering het faktore soos die seisoenale wisselvalligheid en beperkings in beskikbare waterhulpbronne die druk op die produksie van tafelwyn verhoog en kan dit so voortduur as daar nie doeltreffende aanpassingstrategieë is nie.

Probleemformulering en doelwitte - Die klassifikasie van die klimaat in die Wes-Kaap, sowel as langtermyn en binne-seisoen monitering, word belemmer deur moeilik bekombare klimaatsdata, die kwaliteit van die data wat nie verseker is nie, sowel as beperkings met betrekking tot die yl verspreide weerstasies wat tans funksioneer. Die doelwitte van hierdie studie was om klimaatsverandering en seisoenale wisselvalligheid in die Wes-Kaap te kwantifiseer met die beste netwerk van stasies moontlik binne die perke van die beskikbare ruimtelike en tydsresolusie. Betroubare klimaatsdata kan duur wees en vereis tans intensiewe data validasie; die studie het dus gemik om ’n alternatiewe hulpbron te vind om die klimaat oor die ruimtelike omvang van die Wes-Kaap te kwantifiseer vir moontlike semi-intydse toepassings. Temperatuur is een van die vernaamste klimaatsveranderlikes wat die wingerdrespons dryf; hierdie studie het dus die gebruik van vrylik beskikbare afstandswaarnemingsbeelde van grondoppervlaktemperatuur gestaaf in die vorm van ’n versameling van daaglikse maksimum- en minimum temperatuurlae.

Studie ontwerp – Die studie het ekstreme klimaatstoestande ingesluit deur liggings oor ’n klimaatsband te kies, en veelvuldige faktoranalise is gebruik om die interaksie van klimaat met wingerdfenologie, groei, rypwording en wyneienskappe te evalueer. Dit is gedoen om die moontlike dryfvere uit te lig wat in toekomstige klimaatsmodellering gebruik kan word.

Bevindings en impak - Vir die skatting van die gemiddelde weerstasietemperatuur kan die uitslae van hierdie studie as belowend beskou word, gegewe die eenvoudigheid van die statistiese modelle wat gebruik is, die robuustheid van die tegnieke vir beeldverwerking en die hoë akkuraatheid wat onder hierdie beperkings verkry is. Die gemiddelde temperatuur van die weerstasie kan dus aangevul/voorspel word deur die gemiddelde temperature van die grondoppervlak te gebruik, gebaseer op die regressievergelykings wat vanaf die finale analise met ’n kalibrasiefout van 2.4°C en ’n voorspellingsfout van 2.6°C verkry is. Die daaglikse gemiddelde grondoppervlaktemperatuur en die temperatuurdata van die weerstasie het ’n sterk liniêre verhouding gewys (r = 0.86, p < 0.001, en N = 29), en goeie voorspellingsakkuraatheid. Hierdie kaarte van grondoppervlaktemperatuur is opsigself ruimtelik, en verskaf dus daaglikse temperatuurwaardes wat in die verlede slegs moontlik sou gewees het deur die ruimtelike interpolasie van yl weerstasienetwerke, wat net so akkuraat soos die insetdata sou wees.

Seisoenale wisselvalligheid is ’n prominente aspek wat die wingerdstokrespons dryf. Die wisselvalligheid word skynbaar vergroot deur uiterste klimaatsgebeure, soos uiterste wind, reënval of hoër temperature vroeër in die groeiseisoen, asook tydens rypwording. Hierdie het die moeilikheid om seisoenale toestande in die konteks van klimaatsverandering te voorspel, bevestig. Seisoenale wisselvalligheid en wingerdstokresponse kon beter beskryf word binne die fyner skaalanalise van die klimaatsprofiel, wat die aantal ure binne spesifieke temperatuur-, wind- en relatiewe humiditeitsreekse beter weerspieël. Hierdie was ’n nuwe benadering, aangesien dit voorsiening gemaak het vir die analise van klimaatsdata sonder enige vooroordele as gevolg van spesifieke drempelwaardes. Dit kan moontlik wingerdstokresponse buite ’n konvensionele wetenskaplike verwysingsraamwerk verklaar. Die fenologiese stadiums van die wingerdstok het geblyk om meer deur temperature buite die groeiseisoen geaffekteer te word, wat die behoefte na vore gebring het om die huidige klimaatsindekse wat gebruik word om die groeiseisoen te beskryf, te hersien. Temperature dwarsdeur die jaar, buiten in Augustus en September, blyk om blom te

beïnvloed. Die somermaande (Desember, Januarie en Februarie), met meer waargenome ure tussen 30-35°C en 35-40°C, het ’n negatiewe korrelasie gehad met blomdatum as dae ná 1 September (die blom- en oes-vroegheidsindekse het vroeër waardes getoon). In hierdie studie was blomdatum die meeste geaffekteer deur temperatuur en het dit geneig om die toon aan te gee vir fenologie in die seisoen. Blomdatum as dae ná bot kan ook potensieel gebruik word om die oesdatum van Cabernet Sauvignon oor liggings te voorspel met ’n akkuraatheid van slegs ’n paar dae.

Hierdie studie het bewys dat, binne ’n algemene neiging tot warmer toestande, die klimaat in die Wes-Kaap beide kan opwarm of afkoel, afhangend van die gebied of maande in die konteks van die langtermyn gemiddelde. Dít benadruk die behoefte aan volgehoue semi-intydse klimaatsdata, soos die daaglikse grondoppervlak- temperatuurlae wat gebruik kan word as ’n alternatief om weerstasienetwerke aan te vul deur middel van ’n regressiemodel om rekenskap te gee van die afstandswaarnemingsbeelde. Die verkryging en prosessering van die grondoppervlak-temperatuurlae kan geoutomatiseer word en aan ander gewasse wat in Suid-Afrika gekweek word, uitgebrei word.

Hierdie studie verskaf sekere insigte wat ons begrip van Cabernet Sauvignon in die konteks van warmer en koeler klimaatstoestande verbeter. Feitlik elke reaksie van die wingerdstok word deur klimaat beïnvloed. Daar is getoon dat die groeitempo en finale lootlengte van die wingerdstok gevoelig was vir seisoenale wisselvalligheid en waterstremming en indirek beïnvloed is deur blaaroppervlak per stok, wat op sy beurt weer die rypwordingstempo en finale wynkwaliteit kon verander. Die seisoenale klimaatstoestande kon gemaskeer word deur aangepaste wingerdkundige bestuurspraktyke om ’n gebalanseerde wingerdstok te verseker deur die keuse van opleistelsel, snoei en lowerbestuur. In die konteks van klimaatsverandering, is die doel om die kultivar se groei- en rypwordingsreaksie by die klimaatstoestande van ’n ligging te pas. Fyner skaalanalises van die klimaat deur gebruik te maak van uurlikse frekwensie- databenaderings kan moontlik help om aanpassingstrategieë vir die toekoms te verbeter. Hierdie is veral relevant in die konteks van klimaatsverandering en die kompleksie Wes-Kaapse terrein wat daaglikse verskuiwings in weer/klimaat oor seisoene en kort afstande beïnvloed. Die studie het getoon dat warm tot matige klimaatstoestande waarbinne wingerdstokke matige waterspanning ervaar het, meer gebalanseerd was in terme van groei en rypheid en komplekse wyne met gunstige eienskappe vir Cabernet Sauvignon is gelewer.

Moontlikhede vir toekomstige werk kan insluit die integrasie van klimaatskaarte in die konteks van wingerdstokmodellering, tesame met ’n ruimtelike ontleding van die seisoenale verskuiwings. Dit sal help om bestuur en aanpassing te verbeter. Dit benadruk ook verder die behoefte aan binne-seisoen monitering van temperatuur, plantwaterstatus asook ander omgewingsparameters. Hierdie kan ook verder ontsluit word deur afstandswaarnemingsprodukte te gebruik, asook in die toekoms in die konteks van waterbestuur.

Hierdie studie verskaf etlike grondslae vir ’n groter databasis van klimaat, grondoppervlaktemperatuur en fenologie, vir die identifisering van huidige kultivarverspreiding in vergelyking met meer ideale verspreiding in die konteks van ’n warmer toekoms met moontlik meer beperkte waterhulpbronne.

This thesis is dedicated to my Mother Kim Olivia Mehmel who has thought me courage, perseverance and tenacity to keep on keeping on.

"Count it all joy when you meet trials of various kinds, for you know the testing of your faith produces steadfastness. And let steadfastness have its full effect, that you may be perfect and complete lacking nothing…blessed is the man who remains steadfast under trail, for when he has stood the test he will receive the crown of life, which God has promised to those who love him"

James 1:2-4,12

"Rejoice always, pray without ceasing, give thanks in all circumstances" 1 Thess 5:16-18

BIOGRAPHICAL SKETCH

Tara Olivia Southey was born on 27 May 1985 in Cape Town, her younger years spent on a farm in the Karoo. She started her school career at Somerset House in Somerset West, and matriculated from Somerset College in 2003. She obtained her BscAgric- degree in 2007 from Stellenbosch University, majoring in Viticulture and Oenology. In 2008 she obtained her HonsBScAgric-degree in Viticulture at the same University. She completed her MScAgric-degree entitled “Effect of climate and soil water status on Cabernet Sauvignon (*Vitis vinifera* L.) grapevines” in March 2010 at Stellenbosch University. She was employed as a Research Technician in November 2009 at the Department of Viticulture and Oenology, Stellenbosch University, transitioning into a Junior Lecturer position in Viticulture in 2011. Since January 2013, she has been a Junior Researcher in the Department of Viticulture at Oenology, Stellenbosch University. Her research has focused on Climate, Geographic Information Systems (GIS), Satellite remote sensing and grapevine responses in the field. She completed two GIS and remote sensing modules through the Department of Geography, Stellenbosch University in 2012. She enrolled for a part time PhD (Agric)-degree in Viticulture at Stellenbosch University in 2013, focusing on climate, satellite remote sensing, GIS, and grapevine responses to climate, while continuing as a Junior Researcher in Viticulture. In 2013 she spent three months collaborating with the PGIS group in San Michelle, Italy and Rennes2University, France to enrich her knowledge in climate and remote sensing.

ACKNOWLEDGEMENTS

I wish to express my sincere gratitude and appreciation to the following persons and institutions:

- **My Heavenly Father**, Jesus, the way the truth and the life, this would not have been possible without His enabling grace, strength, peace and joy to overcome every mountain.
- My supervisor, **Dr Albert Strever**, for his vision and support in the establishment of the project, for his guidance, kindness and incredible patience for the duration of the study. His passion for viticulture and broad knowledge base has been challenging and inspiring and motivated me into a better researcher. This Dissertation would not have been possible without his valuable inputs and guidance.
- My husband, best friend, **Justin Southey**, for his incredible support, from field work to writing up, being awake every hour I have been awake, his endurance and support has been more than words could ever encompass.
- The Wine Industry Network for Expertise and Technology (Winetech) for funding and interest during the project, in particularly **Anel Andrag**, **Gerard Martin** and **Jan Booysen** for the opportunity to continue working and studying in viticulture.
- **Dr Philip Myburgh,** for his guidance and patience during my MSc, teaching me skills that made this PhD possible, his gentle guidance, positivity and belief in me.
- **Dr Carolyn Howell,** for her friendship, support, encouragement, guidance and many long hours editing the dissertation.
- **Emma Moffat,** for her friendship, encouragement, wisdom and laughter to make the longest days more bearable and for assistance in field and data processing.
- **Dr Caren Jarmain**, for her encouragement, wisdom, kindness and support scientifically, emotionally and spiritually for the duration of the study. For her willingness to help me in field work, especially with predawn measurements.
- **Mr Vink Lategan**, for his friendship, continual support, encouragement and valuable scientific support. For guidance and help with soil profiles and soil classifications at some of the experimental study sites.
- **Commercial wine farms** over the climatic band of the study, for their generous cooperation, both with respect to proving vineyards for the field studies, but for allowing me to come onto their farms any time for measurements, in particular:
    - Thelema/Sutherland – I would like to thank the owner **Gyles Webb** for his support and kindness is giving us vineyards to study on two of his commercial wine farms. I would like to thank the viticulturist/manage **Werner Shultz**, **Simon Thompson** and **Chris Watermeyer** for their support and for being do considerate of the field trials.
    - Vergelegen – I would like to thank the viticulturist **Dwayne Lottering** for the collaboration with Stellenbosch University, to study the grapevine reactions using more invasive measurements for normal commercial farming, such as the installation of loggers, the eddy covariance and opening up areas of the soil for root studies to be done. Thank you for accommodating us, for making this possible and for farming around our installations for the duration of the study.
    - Vredendal – I would like thank **Tehan Engelbrecht** for providing the study with two commercial vineyards to study, for his enthusiasm and willingness to go the extra mile in the project. **Gert Engelbrecht**, for his kindness and willingness to help when I was unable to get to Vredendal.
    - Rustenberg – I would like to thank the Owner **Simon Barlow** for his willingness for collaboration, and the viticulturist **Tessa Moffat** for managing the collaboration.

- **Dr Valerie Bonnardot**, for her mentorship, value inputs and encouragement throughout the study and hosting me at Rennes2University, France for scientific collaboration aspects of the study.

- **Dr Roberto Zorer**, for mentorship, valuable inputs and his encouragement for the study, and the **PGIS unit** at San Michelle Univeristy, Italy for hosting me for a scientific collaboration and growing my scientific knowledge in the field of satellite remote sensing.

- **Prof Martin Kidd** of the Centre for Statistical consultation, Stellenbosch University for his kindness, patience, guidance and processing of these statistical analyses.

- Technical support for field measurements from **Hendrik September**, **Dirk Swart**, **Emma Moffat**, **Katharina Muller**, **Larisa van der Vyver**, **Talitha Venter**, **Leonard Adams**, **Christo Kotze**, **Annette Laker**, **Jacobus Els** and **Tessa Moffat**.

- **Prof JJ Hunter**, for his heart for viticulture, his enthusiasm in the establishment of the study. For the opportunity to visit abroad and broaden my horizon of science.

- **Prof A Deloire**, for his initial support in helping this PhD take off, for opening up opportunities for me to make this venture viable financially.

- **Karin Vergeer,** for her kindness, encouragement and positively throughout my studies at Stellenbosch University, for the willingness to go the extra mile.

- My family, my mother **Kim Mehmel**, my sisters **Lorrae** and **Carla**, my father in law **Geoff Southey** for their love, encouragement and prayers that have carried me.

- **Winetech**, **Thrip** and **Stellenbosch University** for financial support of the study that has made this dissertation possible.

PREFACE

This dissertation is presented as a compilation of nine chapters. Each chapter is introduced separately and is written according to the style of the South African Journal of Enology and Viticulture.

Chapter 1 **General introduction and project aims**

Chapter 2 **Literature review**
A review of the environment for viticulture in South Africa

Chapter 3 **Literature review**
Satellite remote sensing and its application in agriculture to monitor land surface temperature

Chapter 4 **Research results**
High resolution monitoring of seasonal weather variation over four growing seasons, over a climatic band

Chapter 5 **Research results**
Overview of long term climate trends in the Western Cape and the possible impacts for the future of viticulture

Chapter 6 **Research results**
Evaluating the suitability of Satellite Land surface temperature data to supplement weather station temperature data for *Vitis vinifera* L.

Chapter 7 **Research results**
Phenology expression of *Vitis vinifera* L. in the context of climate shifts over sites and seasons

Chapter 8 **Research results**
Interactive effects of site and season on the preformance of (*Vitis vinifera* L.) *cv*. Cabernet Sauvignon and Shiraz

Chapter 9 **General discussion and conclusions**

TABLE OF CONTENTS

Chapter 1

Introduction and project aims

CHAPTER 1: INTRODUCTION AND PROJECT AIMS

1.1 Introduction

In view of climate change, economic pressures and future limitation of water availability to the agricultural sector, informative decisions regarding the suitability of environments for viticulture are paramount. Understanding the interaction between the atmosphere and biosphere is important for the improvement of models relating to the physical system of the earth, and to monitor the impact of global climate change (Cleland *et al.*, 2007). The plant's reaction to seasonality of environments can be seen in phenology, a sensitive indicator of climate change (Zhao *et al.*, 2013). Availability of climate and weather data at spatial and temporal level is crucial to support grapevine phenology, growth, and ripening models, and this can be achieved by integrating existing weather station networks and remote sensing resources (Bonnardot & Carey, 2007; Carey *et al.*, 2007; Zorer *et al.*, 2011; Zorer *et al.*, 2013). In this work, our understanding of climate is meteorological variables in a given region over a long period, usually over a 30 year interval, as opposed to weather which is a particular condition at a particular place over a short period of time within years or over years.

Every local environment has unique diurnal temperature variations due to the inland penetration of the sea breeze, and other local effects such as wind, topography, coastline orientation, slope angle and aspect. Continuous monitoring of extreme environments is hampered by the sparse and/or irregular distribution of meteorological stations, the difficulties in performing ground surveys and the complexity of interpolating existing station data. Climate data accuracy strongly relate to surface resolution, as climate variability information can be lost at lower spatial resolutions. The local environment can be inferred using higher resolution models, either atmospheric (Soltanzadeh *et al.*, 2016) or geostatistical models (Van Niekerk & Joubert, 2011), to describe the environment over regions and vineyards. The application of traditional geospatial interpolation methods in complex terrain remains challenging and difficult to optimise (Benali *et al.*, 2012). Regardless of the method, interpolation accuracy is highly dependent on station network density and the scale of spatial and temporal variability of the parameter (Vogt *et al.*, 1997).

Techniques to increase resolution and integrity of climate data by integrating existing networks and remote sensing resources, using mostly freely available open source software will add significant value to local research in viticulture. An important potential application of the land surface temperature (LST) retrieved from satellite data is to validate and improve the global meteorological model prediction (Neteler, 2010; Zorer, 2013). Intrinsically spatialised thermal remote sensing data can be used as an alternative source (Neteler, 2010). This data can greatly improve the estimation of temperature in spatiotemporal patterns, thus improving the knowledge of both climate and biological processes in the wine industry on regional and global spatial scales (Prihodko & Goward, 1997).

Global classification of climate has been performed (Le Roux, 1974; Jones & Davis, 2000) and suitable areas for viticulture demarcated (Carey, 2001). This laid the foundation for further regional studies with focus on cultivar adaptation to climate change. Factors such as aspect, altitude, site exposure, and distance from the sea or large water bodies generate various mesoclimates and environments for viticulture. High resolution climate data, in time and space, from which spatial temperature maps can be compiled for regions are important, therefore it is relevant to assess vineyard response to climate on regional (macro) to site (meso) to grapevine variability (micro) scale.

Climatic features that affect key grapevine physiological processes need to be assessed on a finer scale in order to optimise distribution of a grapevine cultivar in a specific environment, based on grapevine physiology thresholds in the context of climate change (Hunter & Bonnardot, 2011). Matching cultivar and terroir requires cultivar-specific studies, such as those described in (Van Schalkwyk & Schmidt, 2009), and knowledge of grapevine reaction in terms of growth and ripening when confronted with different climatic/extreme weather conditions. Limitations in understanding phenological mechanisms of the plant exist in relation to: a) interactions between grapevines and their direct environmental conditions, b) integration of field observations and remote sensing data, c) threshold ranges for cultivar suitability and sensitivity to climate shifts (in-season extreme weather conditions), and d) fine scale modelling uncertainties to forecast impact of climate shifts and change.

1.2 Problem statement and project aims

1.2.1 Study area, problem statement/research question

This study's general aim is to improve our international viticultural knowledge of cultivar-environment interactions through creating an understanding of the driving factors influencing grapevine phenology, growth and ripening on a meso- and micro scale, with a possibility of integrating these factors into site selection models in the near future for the Western Cape study are. This would allow maximum utilisation for informed decision making regarding site suitability within a climate profile.

1.2.2 Study aims

The study tests the hypothesis that the grapevine is responding to climate change through altered phenology, growth and ripening responses, considering that the grapevine's performance is affected by global environmental parameters despite differences on vineyard and site level.

The study has four main aims with its respective objectives:

1. To perform climate analysis on a site and regional scale within the study area of the Western Cape (Chapter 4 and 5)
    a. To analyse hourly data for different sites selected over a climatic band, focusing on temperature and other selected variables (relative humidity, rainfall and wind).
    b. Climate analysis to identify trends and shifts for the study area of the Western Cape.

2. To evaluate the use of land surface temperature for supplementing weather station temperature networks within the study area of the Western Cape (Chapter 6)
    a. Establish an automated workflow to acquire freely available land surface temperature data for any site within South Africa.
    b. Testing the reliability of land surface temperature (LST) data to supplement daily weather station temperatures in the complex terrain of the Western Cape.

3. To study grapevine phenological variability in relation to climate (Chapter 7)
    a. Monitoring main phenological stages for a network of *Vitis vinifera* L. cvs Cabernet Sauvignon and Shiraz vineyards selected over a climatic band within the study area of the Western Cape for four growing seasons.
    b. Including some other commercial sites and cultivars to assess possible climatic impacts on phenology.

4. To study grapevine growth, ripening and wine attributes in relation to climate (Chapter 8)
   a. Monitoring grapevine vegetative responses for the mentioned sites, as well as areas within the vineyards with differing vigour, for four growing seasons.
   b. Correlating final wine chemical and sensory attributes to climate for the Cabernet Sauvignon sites.
   c. Isolating possible factors affecting grapevine growth, ripening and wine attributes in relation to climate.

The dissertation has 9 chapters, chapter 2 and 3 are literature reviews of climate and remote sensing and the possible applications to viticulture, chapter 4 to 8 represents the core of he dissertation. Chapter 4 is a presentation of the spatial and seasonal variability of climate in the Western Cape with application to viticulture and chapter 5 focusing on climate trends for various wine regions of the Western Cape. Chapter 6 presents the use of remote sensing images as a solution to supplement climate data. The last two chapters, 7 and 8 will focus on the interaction between climate and grapevine physiology (chapter 7) and berry compostion and wine aromas (chapter 8). Chapter 9 is the final chapter of the dissertation, summarising the findings of the study.

1.3 References

Benali, A., Carvalho, A.C., Nunes, J.P., Carvalhais, N. & Santos, A., 2012. Estimating air surface temperature in Portugal using MODIS LST data. Remote Sens. Environ. 124, 108-121.

Bonnardot, V. & Carey, V., 2007. Climate change: observed trends, simulations, impacts and response strategy for the South African vineyards. In: Proc. Global warming, which potential impacts on the vineyards? pp. 1-13.

Carey, V., Archer, E., Barbeau, G. & Saayman, D., 2007. The use of local knowledge relating to vineyard performance to identify viticultural terroirs in Stellenbosch and surrounds. Acta Horticulturae 754, 385-392.

Carey, V.A., 2001. Spatial characteristic of natural terroir units for viticulture in the Bottelaryberg-Simonsberg-Helderberg winegrowing area. Thesis, Stellenbosch University, Private Bag X1, 7602 Matieland (Stellenbosch), South Africa.

Cleland, E.E., Chuine, I., Menzel, A., Mooney, H.A. & Schwartz, M.D., 2007. Shifting plant phenology in response to global change. Ecol. Evol 22, 357-365.

Hunter, J.J. & Bonnardot, V., 2011. Suitability of some climatic parameters for grapevine cultivation in South Africa, with focus on key physiological processes. S. Afr. J. Enol. Vitic 32, 137-154.

Jones, G.V. & Davis, R.E., 2000. Climate influences on grapevine phenology, grape composition, and wine production and quality for Bordeaux, France. Am. J. Enol. Vitic. 51, 249-261.

Le Roux, E.G., 1974. A climate classification for the South Western Cape viticultural areas (in Afrikaanse). Thesis, Stellenbosch University, Private Bag X1, 7602 Matieland (Stellenbosch), South Africa.

Neteler, M., 2010. Estimating daily land surface temperatures in mountainous environments by reconstructed MODIS LST data. Remote Sens. 2, 333-351.

Prihodko, L. & Goward, S.N., 1997. Estimation of ait temperature from remotely sensed surface observations. Remote Sens. Environ. 60, 335-346.

Soltanzadeh, I., Bonnardot, V., Sturman, A., Quénol, H. & Zawar-Reza, P., 2016. Assessment of the ARW-WRF model over complex terrain: the case of the Stellenbosch Wine of Origin district of South Africa. Theor. Appl. Climatol., 1-21.

Van Niekerk, A. & Joubert, S.J., 2011. Input variable selection for interpolating high-resolution climate surfaces for the Western Cape. Water SA 37, 271-280.

Van Schalkwyk, D. & Schmidt, A., 2009. Cultivation of Pinotage in various climatic regions (Part 1): Climatic differences. Wynboer, February, 7-11.

Vogt, J.V., Viau, A.A. & Paquet, F., 1997. Mapping regional air temperature fields using satellite-derived surface skin temperatures. Int. J. Climatol. 17, 1559-1579.

Zhao, M., Peng, C., Xiang, W., Deng, X., Tian, D., Zhou, Z., Yu, G., He, H. & Zhao, Z., 2013. Plant phenological modeling and its application in global climate change research: Overview and future challenges. Environ. Rev. 21, 1-14.

Zorer, R., Rocchini, R., Delucchi, L., Zottele, F., Meggio, F. & Neteler, M., 2011. Use of multi-annual MODIS land surface temperature data for the characterization of the heat requirements for grapevine varieties. In: Proc. Analysis of Multi-temporal Remote Sensing Images (Multi-Temp), 2011 6th International Workshop pp. 225-228.

Zorer, R., Rocchini, D., Metz, M., Delucchi, L., Zottele, F., Meggio, F. & Neteler, M., 2013. Daily MODIS land surface temperature data for the analysis of the heat requirements of grapevine varieties. IEEE T. Geosci. Remote 51, 2128-2135.

Chapter 2

Literature review

A review of the environment for viticulture in South Africa

CHAPTER 2: A REVIEW OF THE ENVIRONMENT FOR VITICULTURE IN SOUTH AFRICA

2.1 Viticultural environment in South Africa

South Africa is a relatively young wine producing country, and the wine industry presents an important diversity of unique grapevine growing conditions (Vink *et al.*, 2010). The first South African wine was made by Jan van Riebeeck in 1659 from grapevines which were planted in 1655 (Robinson, 1994). In 1685, another Cape Governor, Simon van der Stel, purchased a large estate, now known as Constantia. In Van der Stel's travel journal, he described a fertile valley with a stream (the Eerste River) and a wooded island, which he named Stellenbosch (Smuts, 1979). Further development was initially slow, as the Dutch colonists were not traditional wine farmers. The advent of the French Huguenots is reputed to have been a great stimulus and viticulture expanded during the 1670's to 1680's when Wine Berg, Rondebosch, Stellenbosch and Drakenstein districts were opened up for colonisation (Van Zyl, 1975; Saayman, 2010). By 1685, most of the well-known farms that we know today had already been established in Stellenbosch, forming a circle around the island (Smuts, 1979), with maximum river frontage to ensure water rights (Van Huyssteen, 1983). The wine industry gained international recognition in the early 19th century with the production of Constantia wines, highlighting the geographic potential for high quality wine grape cultivation (Saayman, 1977). Wine production increased dramatically in the early 19th century as a result of some of the British fleet being stationed at the Cape during the first and second periods of occupation. During this period, extensive plantings were undertaken and Stellenbosch farmers became true wine producers (Van Zyl, 1979). Over production in the early 1900's lead to great quantities of wine being poured down the local rivers and streams with the low prices caused by the imbalance between the supply and demand. This prompted the South African government to fund the formation of the Koöperatieve Wijnbouwers Vereniging van Zuid-Afrika Bpkt (KWV) in 1918. Initially started as a co-operative, the KWV soon grew in power and prominence, setting policies and prices for the entire South African wine industry, restricting yields and setting minimum prices as well as encouraging the production of brandy and fortified wines. A shift was made towards production focussed on quality rather than quantity, resulting in the introduction of the Wine of Origin (WOO) legislation in 1973. This appellation scheme, created a hierarchy of regions, districts and wards in order to better manage production (Figure 1 and Figure 2). According to this legislation, when the term "Wine of Origin" appears together with the name of a production area, it confirms that 100% of the grapes used for the production of the wine came from that area (Theron, 1995). "Region" and "District" are more administrative in nature but a "Ward" is defined according to soil, climate and ecological factors, and named according to a real geographical place name (Carey, 2001).

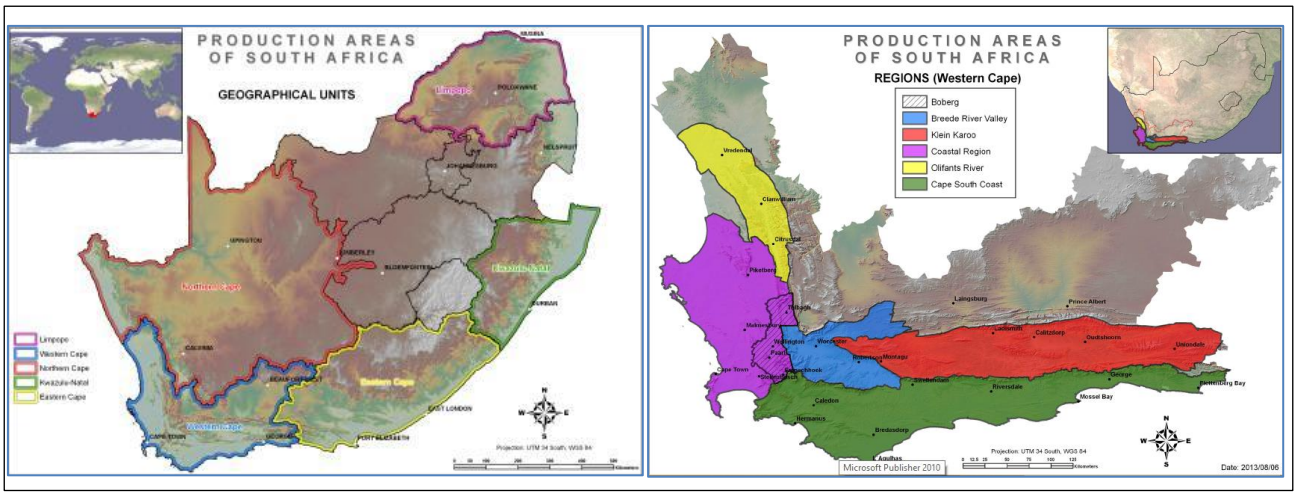

Figure 1 Production areas of South Africa divided in five geographical units (SAWIS) (left), and Wine of Origin Regional demarcation (right).

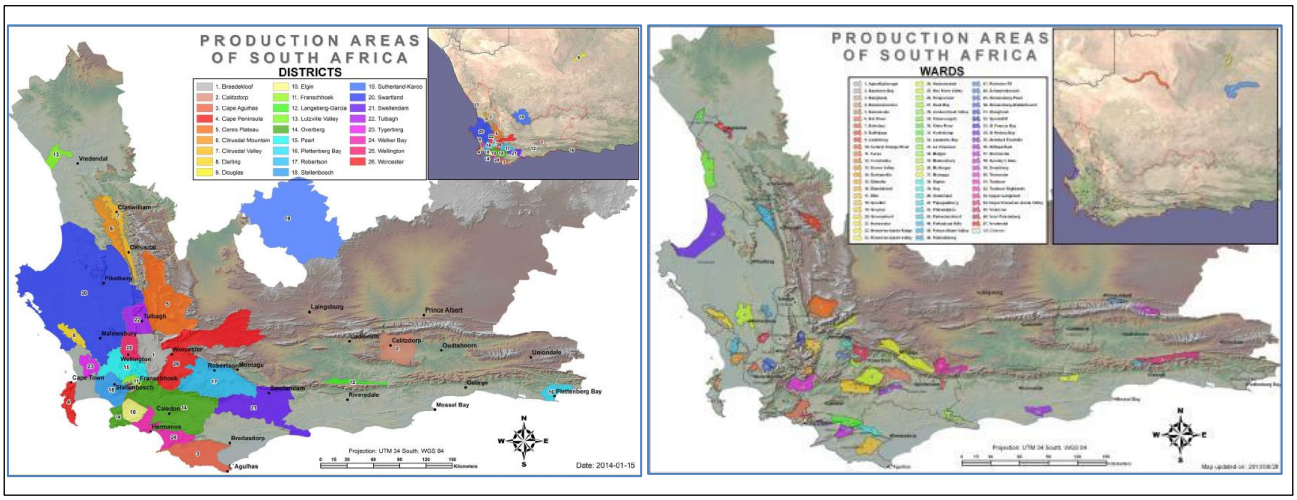

Figure 2 Wine of Origin demarcation, Districts (Left) and Wards (right) (SAWIS, 2015).

The Western Cape Province (centered at 33°S latitude) of South Africa (centered at 30°S latitude, 34-35°S) which occupies the most southwestern part of the country is classified as a temperate coastal area, with temperate to cold interiors (Figure **3**), in contrast to much of southern Africa which experiences summer rains and dry winters. Along the southern and western coasts (the winter rainfall zone), with the mean annual precipitation falling between April and September, rainfall results from temperate frontal systems embedded in the westerlies, hence the Western Cape receives the bulk of its rainfall in winter months, and experiences relatively dry summers (Tyson *et al.*, 2002; Peel *et al.*, 2007; Conradie, 2012). South Africa falls within the high-pressure belt and is edged by the circumpolar westerly circulation to the south, which has a stronger influence in winter when the South Atlantic high pressure moves northwards. In summer the mid latitude influences are weaker and easterly troughs extend from Namibia over western South Africa, including the Western Cape, resulting in high temperatures and relative humidity as well as possible convection rainfall (Soltanzadeh *et al.*, 2016).

This climatic pattern is driven mainly by the position of the southern African subcontinent in relation to the band of westerlies and associated low pressure systems that move from west to east at 40º and 50º S. These systems bring rainfall to south-western South Africa seasonally in the form of cold fronts, affecting seasonal and annual rainfall in the region of the Western Cape, predominantly between march and May and from September to November (Chase & Meadows, 2007;

Soltanzadeh *et al.*, 2016). The associated rainfall is amplified by a significant contribution of orographic rain due to the extensive mountain ranges in the area, creating a drier interior compared to a wetter coastal region (Figure 4). Cut-off low pressure systems are unstable atmospheric systems that spin off from frontal systems, generally occurring in autumn and spring months and these may cause extreme rainfall events and flooding over South Africa (Midgley *et al.*, 2016). The annual mean maximum temperatures are higher in the inland and cooler near the coasts, with annual mean minimum temperatures higher closer to the coast.

Another significant weather phenomenon in the Western Cape climate is the weak low pressure systems along the southern African coast, having a vertical extent limited by the height of the inversion along the coastal mountains and a diameter less than 100km, propagating an internal Kelvin wave in the marine boundary layer down the west and south coast of South Africa (Reason & Jury, 1990). These systems cause an offshore hot and dry “berg” wind to blow over the landmass southwards from the interior, causing extreme warm conditions generally during late winter and early spring (Soltanzadeh *et al.*, 2016).

The Western Cape region has the cold Benguela current on the West and the warm Agulhas on the east. The Benguela current is on the eastern side of the South Atlantic subtropical gyre consisting of two elements, namely the Ekman drift that makes up the main Benguela Current and the wind-driven upwelling along the coast (Peterson & Stramma, 1991; Reason *et al.*, 2006b). The warm Agulhas current flows south westward along the east coast to the point where it leaves the coast as the continental shelf widens off the south coast of South Africa and becomes a more westward flow, before bending back on itself and returning to the South Indian Ocean (Reason *et al.*, 2006a; Soltanzadeh *et al.*, 2016). The Benguela oceanic current flowing northward in the South Atlantic Ocean along the west coast and the prevailing southerly and south easterly winds produce upwelling of cold water (Soltanzadeh *et al.*, 2016). The strong temperature gradients contribute to the development of local sea breeze circulations, contributing to the unique diversity of viticulture in the Western Cape (Bonnardot *et al.*, 2002; Bonnardot *et al.*, 2005).

Due to this geographic and climatic complexity, the Western Cape must be amongst the most agriculturally diversified regions in the world, with crops ranging from rain-fed extensive commercial cereals to high value endemic crops such as Rooibos tea, irrigated horticultural and viticultural production, as well as several intensive and extensive animal production systems in operation (Midgley *et al.*, 2016).

One of the outstanding natural components of the Western Cape vineyard and wine landscapes is the distinctive diversity in topography and geology as highlighted in the satellite image (Figure 4). The diverse landscapes of the Western Cape are characterised by Sandstone Mountains, granite foothill bases, low mountains and prominent ranges of hills, merging into undulating shale hills. Various weather cycles and several periods of inundation by the sea, together with the pronounced and varied geography of the Western Cape, gave rise to great soil diversity over short distances (Saayman, 2014). Although viticulture in the Western Cape is young, the geology is old and directly or indirectly linked to terroir, through the soil assemblages and mesoclimates. Geological processes have led to the creation of unique mesoclimates through the variation in altitiude, sunlight interception and exposure to prevailing winds and their effects on temperature and water availability, along with soil (Saayman, 2014).

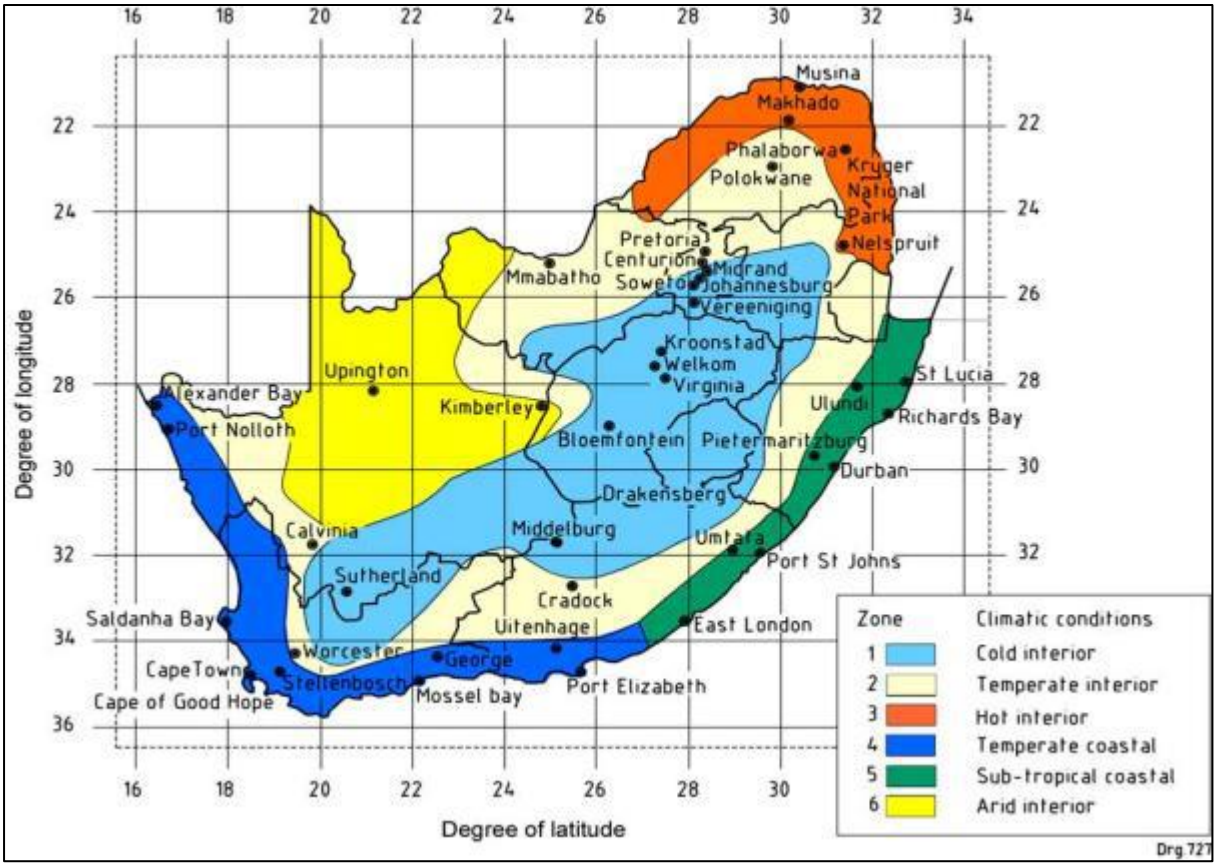

Figure 3 A new SANS 204-2 standard climatic zone map recognises six main climatic regions in South Africa (Peel *et al*., 2007; Conradie, 2012).

Figure 4 Satellite image showing the diverse topography and oceanic influence bordering the Western Cape Province, creating a unique and complex agricultural environment (Midgley *et al.*, 2015)**.**

A good overview of the different climatic regions of South Africa is described by the South African Köppen-Geiger climate classification map given in Figure 5. The Köppen-Geiger indicating that 0.2% of the country's area is equatorial, 70.89% arid and 28.91% has a warm temperate climate. When adopting this finding for the prediction of climatic regions, the impact of regional humidity variations should be factored in separately as the simulations do not consider humidity directly (Conradie, 2012). The classification system incorporates precipitation and temperature in the index, highlighting the complexity of the terrain, driving vegetation diversity in the Western Cape. The five vegetation groups of the Köppen classification distinguish between plants of the equatorial zone (A), the arid zone (B), the warm temperate zone (C), the snow zone (D) and the polar zone (E). A second letter in the classification considers the precipitation and a third letter the air temperature. The Köppen classification therefore essentially uses combinations of temperature and precipitation to classify and describe the environment in terms of agricultural use (Peel *et al.*, 2007; Conradie, 2012). The inclusion of precipitation and climate in the calculation index is important and of value for future adaptations strategies in the context of climate change due to shifts in rainfall and increasing temperature extremes. Recently, spatial units or agroclimatic zones have been identified for the Western Cape though through the aggregation of the more than 80 Relatively Homogeneous Farming Areas (RHFAs) based on climatic, vegetative and productive attributes (Midgley *et al.*, 2005; Midgley *et al.*, 2016). The Homogeneous Farming Areas demarcate areas where the main agricultural activities practiced are common, and within which the pertinent climatic factors do not vary sufficiently to influence production practices and potential. These agro ecological zones provide an excellent spatial unit for representing the specific agricultural character, current enterprises and climatic potential of a locality.

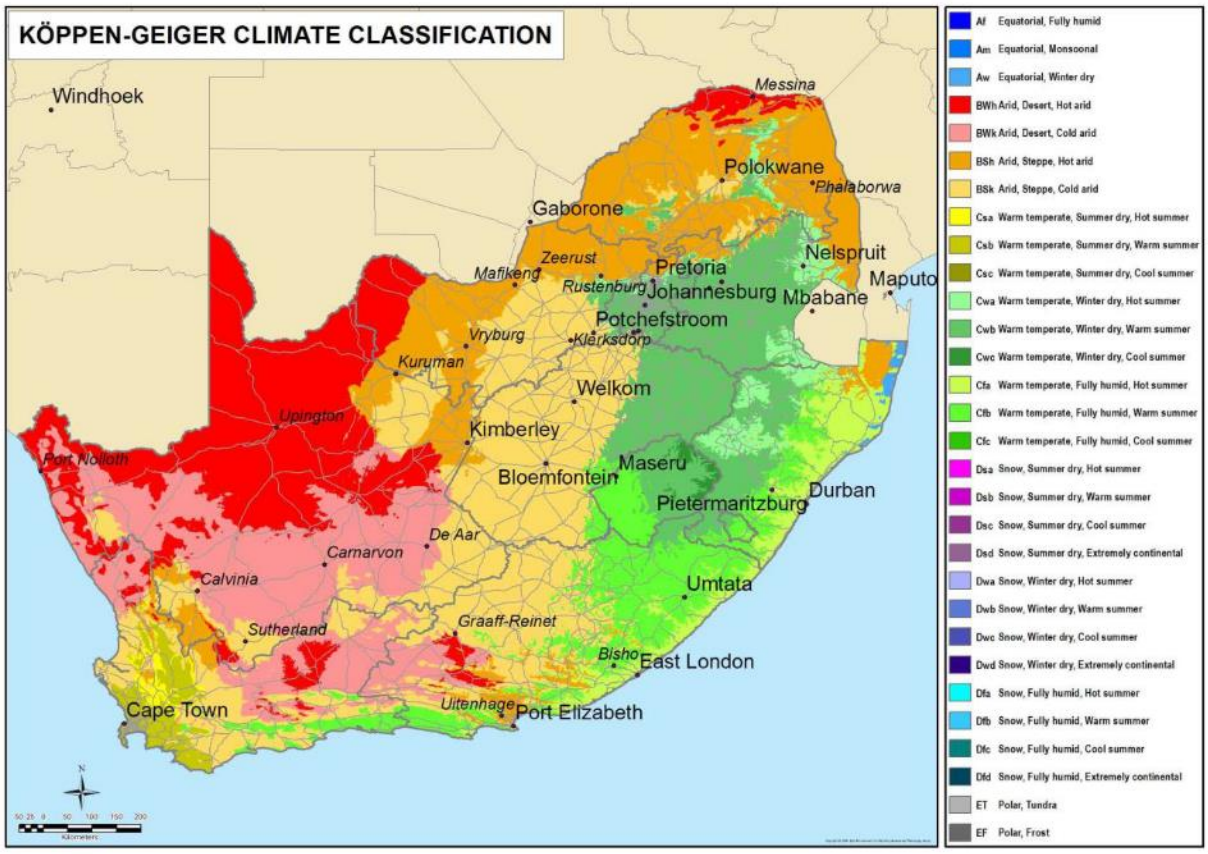

Figure 5 Köppen-Geiger map based on 1985 to 2005 South African Weather Services data on a very fine 1 km x 1 km grid (Conradie, 2012).

2.2 Wine of Origin System

The demarcation of region districts and wards is based on land types, a concept unique to South Africa proposed in 1974. A land type is defined as a class of land over which the macro climate, the terrain form and the soil pattern each displays a marked degree of uniformity. One land type differs from another in terms of one or more of macro climate, terrain form or soil pattern (Saayman, 1999). These demarcations are currently being used in the South African wine industry as demarcation areas for cultivation and marketing under the region, districts, and wards representing a specific wine style. However, the regions and districts are too large for the identification of unique mesoclimates, and not all cultivated areas fall into wards and districts. The wine of origin system needs to be reviewed for the future especially in the context of climate change.

The wine production regions in South Africa are located in the Western Cape, represented as five regions (Cape South Coast, Klein Karoo, Breede River Valley, Coastal, Olifants River). According to the South African Wine Industry Information and Statistics, an additional region (Boberg) was demarcated within the Coastal Region (SAWIS, 2015) (Figure 1). The South African wine producing area is divided into 26 Districts, mostly in the Western Cape, with the exception of Sutherland-Karroo and Douglas in the Northern Cape (Figure 2). Stellenbosch, Paarl and Franschhoek regions are the original South African wine producing regions where viticulture was practiced at the end of the 17th century. "Wards" may contain different viticultural environments or terroirs and produce wines of differing character despite their demarcation. There are 67 Wards demarcated in the South African wine producing area, with 64 of them in the Western Cape and the other 3 (Central Orange River; Hartswater and Rietrivier FS) in the Northern Cape (Figure 2).

The pronounced diversity in Western Cape vineyard and wine landscapes where most of the wine of high quality is produced is unique and a great advantage for the creation of unique world class wines. The WOO system imposes no specific limitations on cultivar, grape quality, viticulture and winemaking techniques on the producer (Vink *et al.*, 2010). The importance of these natural factors in determining wine character and style had been realised since the establishment of viti-viniculture at the Cape, and have since been scientifically verified and today forms the basis on which South Africa's wines of origin areas are identified, demarcated and protected (Saayman, 2014). Today there are several 'layers' of geographical indications available to utilise and better explain the diversity, from broad regions to individual vineyards. The importance of zoning and demarcation of areas of origin is accepted by the industry, and was supported by relatively recent research (Carey, 2001; Bonnardot *et al.*, 2002; Carey *et al.*, 2002). The scheme was instituted in 1973 and protects wines of origin and wines made of specific cultivars and/or vintages (Theron, 1995).

Regions are demarcated around common geographic traits, such as a river or a plateau (*eg* Coastal Region). Districts are also built around macro characteristics such as mountain ranges and rivers, but with a more specific character than regions, even though they still encompass a wide variety of soil types, topographies, *etc.* (*eg* Stellenbosch, most recognised district internationally). Wards are where soil, climate and ecological factors start to have a distinctive and more easily recognisable impact on the character of wine. Wards isolate unique pockets in the complexity of the Western Cape, such as warm climate and cool climate wards, Franschhoek and Elgin respectively (Vink *et al.*, 2010). These then are the natural heritage factors that dominated the shaping of the present vineyard and wine landscapes along the coastal regions of the Western Cape. Viticultural terroirs are there to be discovered and developed to their full potential with the diversity of the Western Cape.

The planting of cultivars directed towards quality wine production in the late 1980s has led to an increased focus on the implications of terroir for viticultural management, wine style and quality. Demarcation to identify relatively homogenous viticultural terroirs is of national and international importance, and allows areas to express their specific wine style and character instead of proving their originality (Saayman, 1999). Identifying preliminary viticultural terroirs in the complexity of the South Western Cape wine-growing areas is of high importance (Carey, 2001). The wine consumer is interested in the origin and uniqueness of the product. The identification of natural terroir units with specific application to viticulture is an important step in meeting the consumer challenge and reaching an important market. The WOO demarcation was taken further with a focused study within a popular District, namely Stellenbosch, to apply suitable methods of research and interpretation to take into account all the factors of the viticultural ecosystem including the characteristics of the soil, climate, interactions between variety and site and the effects of the human factors on the maturation and the quality of the grape (Carey, 2001), highlighting a large number of natural terroir units for the cultivars Cabernet Sauvignon and Sauvignon blanc (Carey, 2005).

In the late 1980's, the varieties planted shifted from being predominantly white cultivars to red cultivars selected for red wine production of higher quality to satisfy the market demand expanded in line with increased exports after 1994. The South African wine industry is mostly concentrated in the Western Cape (Figure 1 and Figure 2) and the total hectares of wine producing vineyards remained approximately 100 000 hectares over several years. Until 2006, the total surface showed an annual increase of grapevine cultivation, however since then has decreased steadily, due to limited re-establishment in many areas. The percentage of total vineyard area increased in some regions such as Robertson, Breedekloof and Worcester regions, while decreasing in the Paarl, Swartland and Stellenbosch regions for the period 2005 to 2015 (SAWIS, 2015, 2016).

There was no significant change in the hectare percentage white and red wine grapes in the various regions over the last decade. Varieties remained relatively constant, with Chenin blanc and Colombar remaining the most planted white varieties, followed by Cabernet Sauvignon and Shiraz as the most planted red varieties overall. The main individual wine grape varieties represented in total wine surface is Chenin blanc (18.2%), Colombar (11.2%), Cabernet Sauvignon (13.4%), Pinotage (6.4%), Chardonnay (7.8%), Shiraz (9.6%), Sauvignon blanc (7.5%). Sauvignon blanc and Shiraz has increased significantly since 2005, as well as less planted varieties such as Pinot Noir, Nouvelle, Mouvedre, Pinot Gris, Grenache (Red) and Villard blanc(SAWIS, 2015).

2.3 Terroir and grapevine interaction

The interaction of the grapevine with its immediate environment has long been a research focus in South Africa (Buys, 1971; Le Roux, 1974; Saayman, 1977; Saayman & Kleynhans, 1978). Terroir is defined as a spatial and temporal entity, which is characterised by homogeneous or dominant features that are of significance for grapes and/or wine; *i.e.* soil, landscape and climate, at a given scale-duration, within a territory that has been founded on social and historical experience and genotype related technical choices (Vaudour, 2002; Van Leeuwen *et al.*, 2004). A natural component of the terroir or Natural Terroir Unit (Carey *et al.*, 2008) is defined by the interactions at a specific scale of climatic and topographical factors. The effects of different terroirs on wine character have been scientifically verified (Conradie *et al.*, 2002).

The effects of climate, soil and cultivar have been found to be highly significant with regard to grapevine behaviour and berry composition, with the greatest effect seen to be climate and soil

and its effects mediated through grapevine water status (Van Leeuwen *et al.*, 2004). Soil and climate are the primary environmental factors to which the grapevine is subjected. For this reason, terroir-related studies are mainly focused on the effects of soil and climate on typicity and quality expression of wine (Hunter & Bonnardot, 2011). The climatic conditions of the vintage can influence grape quality through the amount of insolation, temperature or water balance (Smart *et al.*, 1985; Van Leeuwen *et al.*, 2004). Climate is important for the choice of grapevine varieties, as each variety requires a minimum temperature summation to reach maturity (Tonietto & Carbonneau, 2004; Deloire *et al.*, 2005). The best terroir expression is obtained when grapevine varieties suit the climate, therefore reaching complete ripeness at the end of the season. The complexity of soil influences the cultivation of grapevines in the Western Cape, with extremes in soil water holding capacity and other soil properties affecting grapevine water status. Hence the Western Cape is a highly coveted vineyard landscape and known for high quality due to the complexity in soil and climate over very short distances complemented by the elevated hills, exposure to sea breezes which allow for great variety in terroirs.

Geographical variables, distance from the ocean and the altitude contribute significantly to the variability of average temperature of the ripening months in the Western Cape wine growing regions (Myburgh, 2005). Distance to the ocean influences the continentality of the climate, playing a role in the thermal range and rainfall regime of each terroir. On average, air temperature in South Africa decreases at a rate of 0.3°C per 100 m increase in altitude compared to 0.6°C for Europe (Conradie *et al.*, 2002). The presence of large water bodies will also influence air temperature over the adjacent land via land-sea breeze circulation. During daytime, the sea breeze circulation will induce prominent cooling near the coastline, especially during January/February when temperature difference over sea and land is the greatest. The cooling effect declines rapidly with an increase in distance from False Bay. The sea breeze effect has been recorded as far as 100 km inland from False Bay. Depending on the synoptic wind, the effect on temperature and relative humidity is reduced and stopped at a certain distance inland (Bonnardot *et al.*, 2002; Bonnardot *et al.*, 2005; Myburgh, 2005). The traditional wine regions along the coastal zone are seldom further than 50 km from the sea, with the more reputable areas being 12-15 km from the sea, benefiting from the prevailing local breezes and synoptic summer winds blowing from the sea (Bonnardot *et al.*, 2005). The altitude combined with the distance from the ocean may affect grapevine physiology as it decreases air temperature during the warmest hours of the day (Bonnardot *et al.*, 2005; Myburgh, 2005).

Environmental parameters such as climate (rainfall, relative humidity, air temperature, soil temperature, direction and intensity of dominant winds), topography (slope, exposition, sunlight exposure and landscape form) and soil (mineralogy, compaction, soil water reserve, depth, and colour) have an overriding effect on the performance of grapevines with regards to phenology, growth, yield, berry composition and wine (Deloire *et al.*, 2005; Bonnardot *et al.*, 2011; Hunter & Bonnardot, 2011; Conradie, 2012; Van Schalkwyk, 2013).

The grapevine has always been a good indicator of climate change, as it is a perennial plant with different growth stages correlated with known bioclimatic indexes, and because there are many historical documents on past climate in ancient vineyards (Jones & Davis, 2000; Parker *et al.*, 2011; Webb *et al.*, 2012; Fraga *et al.*, 2015). The relationship between the vine growth cycle and climate has been studied to assess the impact of climate change on viticulture. In the late 90s, early work on the impact of climate change consisted in analysing bioclimatic indices such as the dates of phenological stages and harvest, and sugar content. Results showed that during the twentieth century, the average annual temperature has increased in most of the world's wine

regions with a high variability between countries (Carey, 2001; Webb *et al.*, 2007a). Spatial variability of climate in a region will influence the grapevine's reactions with the warmest locations in the region to have earlier harvest dates compared to the cooler locations. Climate impacts vary according to the wine regions and other environmental factors such as water availability, topography *etc,* but overall a significant advance of the phenological stages of grapevines and changes in the composition of grapes result with increased temperature (Jones & Davis, 2000; Spayd *et al.*, 2002; Webb *et al.*, 2007b; Le Roux *et al.*, 2015). Further climate change over the coming decades is studied in the context of adaptation strategies, and it has been shown that certain wine growing regions have met or exceeded their optimum conditions for growing grapevines, making wine grape growing more complicated for adaption and shifting to new regions (Carey, 2005). This is more a possibility in new world wine producing countries compared to old world countries due to appellation systems.

2.3.1 General grapevine response to climate

Air temperature is one of the most important atmospheric variables for viticulture (Myburgh, 2005) as it plays an important role in grapevine development and ultimately influencing juice and final wine quality and aroma (Le Roux, 1974; De Villiers *et al.*, 1996). Temperature is one of the most important parameters affecting grapevine growth, and has an effect on almost every aspect of the grapevine's physiological functioning (Carey, 2001). Phenological development and growth of the grapevine is temperature driven, every facet of plant growth and development, each physical process, enzymatic reaction, membrane field, transport processes and phase transition is separately subjected to the influence of temperature (Coombe, 1987; Carey, 2001).

The observed phenology of the grapevine in different localities in Europe has steadily advanced over the past 50 years with harvest now almost three to four weeks earlier and suggested warming trends are likely to be cause (Jones & Davis, 2000; Jones *et al.*, 2005; Webb *et al.*, 2007a; Le Roux *et al.*, 2015). Some local studies have showed that the phenology of Cabernet Sauvignon was predominantly affected by seasonal climate with little to no contribution of site (Carey, 2005; Van Schalkwyk, 2013).

Increases in temperature, and increases in CO_2 (increased since 1955 to 2005 from 315 to 380 ppm), elevated CO_2 increases the capacity of the leaf to produce sugar at high temperatures, as the photosynthetic activity of the leaves increase with the increase of CO_2 in the atmosphere. Although leaves are more tolerant of high temperatures at elevated CO_2 levels, photosynthetic rates and carbon accumulation can be higher at these high temperatures, compressing the vintage and potentially increasing sugar accumulation (Long, 1991; Ainsworth *et al.*, 2004). This was confirmed in a CO_2 enrichment field trail, which showed that CO_2 increased crop growth by *c.a.* 20%, decreased water loss and increased the canopy temperature (Ainsworth *et al.*, 2004; Mountinho-Pereira *et al.*, 2009). Factors such as wind exposure, water stress and excessive shading in the canopy could reduce the photosynthetic activity of leaves, resulting in increased potassium accumulation in berries, with implication for wine pH (Freeman *et al.*, 1982; Carey, 2005).

Grapevine water status is influenced by the varying amounts of summer rainfall in different vintages, while the soil influences grapevine water status through its water holding capacity. Van Leeuwen *et al.* (2004) found the best vintages for wine quality to be those in which the plant water potential from flowering to harvest was most negative, and the best soils to be those which induce deficits earlier in the season. Water deficits earlier in the season limited excessive vegetative

growth, reducing the berry size and increasing the sugar loading as the berries are greater sinks for photosynthates. Moderate water stress retards shoot growth without notably affecting photosynthetic activity, facilitating the distribution of sugars in the berries during ripening (Wang *et al.*, 2003a; Wang *et al.*, 2003b). Primary shoot length is used to provide information on the dynamic of plant growth and directly linked to the plants nitrogen and plant water status (Deloire *et al.*, 2005). Rootstocks are the link between soil and the reproductive portion of the vine, they modify shoot growth rate, but do not influence leaf photosynthetic capacity (at ambient CO_2 concentration) in the absence of water deficits (Ollat *et al.*, 2003). Moderate water constraints also have a positive effect on the phenolic compound synthesis and grape quality, with optimum quality being obtained in seasons with low summer rain, leading to water deficit stress (Van Leeuwen *et al.*, 2004).

The kinetic monitoring of the amount of sugar per berry is a viable method of measuring the plants physiological functioning, mainly photosynthesis which is a reliable indicator of the temperature that the grapevine is subjected to and grape grapevine water status (Wang *et al.*, 2003a; Hunter & Deloire, 2005). Sugar per berry also gives an indication of colour and quality as sugars and anthocyanins have been shown to be co-regulated in the grapes (Kennedy, 2002). Anthocyanin biosynthesis is stimulated by sunlight quality in the bunch zone (Smart *et al.*, 1985; Spayd *et al.*, 2002; Downey *et al.*, 2004) and high temperatures reduce anthocyanin accumulation. The optimum temperature range for anthocyanin synthesis is between 30°C and 35°C (Spayd *et al.*, 2002).

Titratable acidity of Cabernet Sauvignon wine is predominately related to climate, especially temperature during the green berry stage. Hence, temperature has also been acknowledged to have a major influence on grape composition and quality (Coombe, 1987). Higher temperatures cause respiration of malic acid, therefore decreasing the total acidity in the grape juice. Grape derived secondary metabolites are the principle sources of wine colour, aroma and flavour. There is a significant effect of vintage and soil type on berry anthocyanin content and it is not determined by cultivar (Van Leeuwen *et al.*, 2004).

Climate of the season appeared to have a very strong influence on aroma characteristics of Cabernet Sauvignon wine. Warmer sites with normal seasonal rainfall can be expected to have more intense berry aroma characteristics (Carey *et al.*, 2008) and the cooler climates a more vegetative character. The biochemical evolution of berries, together with the monitoring of the water status of the grapevine, provides a more rapid determination of the vintage effect for specific cultivars on a specific terroir. Cabernet Sauvignon wines from seasons or sites with a higher rainfall during the month before harvest were described as having more intense berry aroma characteristics. Various studies (literature cited in Noble *et al.* (1995)) have suggested that berry aromas are associated with soils having a lower water holding capacity (Carey, 2005; Mehmel, 2010).

2.4 Spatial and temporal climate variability

There are three main scales at which climate is referred to in viticultural research and these are related to differences in the scales used to describe surface and time (Figure 6), namely macroclimate on a regional scale, microclimate on a site scale and microclimate inside the canopy (Smart, 1985; Deloire *et al.*, 2005).

The macroclimate describes the climate of a wide area or region, which extends over hundreds of kilometres and is studied over a long time-period (usually 30 years or more) using annual, seasonal and/or monthly data (Deloire *et al.*, 2005). Temperature on a macro scale can aid in denominating areas for specific crops, *i.e.* during the determination of land suitability. Temperature

on such a scale directly impacts temperature on a meso- and micro- scale, which can be affected by other climatic factors such as wind speed, cloud cover, humidity and precipitation.

The mesoclimate describes the climate within smaller areas, which extend from less than a kilometre (*e.g.* vineyards) to several kilometres (*e.g.* an estate) and over shorter periods of time using hourly or daily data. It is also known as topoclimate, as it is influenced by the surrounding topographic factors of elevation, slope inclination, aspect and proximity to bodies of water (Bonnardot *et al.*, 2002). Mesoclimate therefore refers to a smaller denomination, with the goal of describing the climate of a specific vineyard. Recent studies have emphasised the important effects of mesoclimate, especially for marginal growing conditions (Smart, 1985).

The microclimate is the climate immediately within or surrounding the plant canopy and differences occur within a few centimetres/meters and seconds/minutes. It is affected by grapevine vigour and cultural practices (inter alia canopy management, row orientation and spacing), but also by the soil surface characteristics (Deloire *et al.*, 2005). Canopy temperature is directly influenced by the amount and distribution of leaf area and its interaction with the above ground climate and soil surface characteristics (Smart, 1985) which may also impact on grape bunch temperature regime and related implications for ripening and flavour development (Moffat, 2013).

Moving down the climatic levels from a macro to micro scale, there is an increase in the variability due to spatial resolution increasing and furthermore there is a need for an increase in the temporal resolution as a result of faster changing conditions, especially on a microclimatic level.

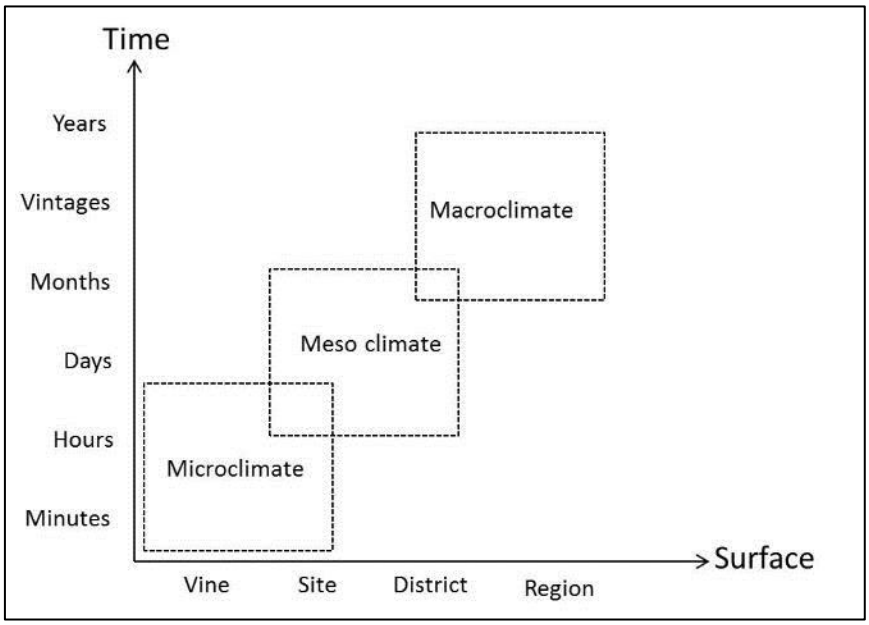

Figure 6 Temporal (y-axis) and Spatial (x-axis) display of temperature scale measurements used in the calculations to quantify climate and seasons for agriculture. Source: Carey (2001).

2.5 Surface modelling in South Africa

In order to estimate a region's climate, it is possible to simulate the many processes that are responsible for the climatic conditions experienced by using a climate model. Such models attempt to describe the climate system in terms of basic physical, chemical and biological principles by means of a series of numerical equations expressing these laws (McGuffie & Henderson-Sellers, 2005 (3rd ed)).

The choice of sites for viticulture depends on many natural factors, with soil and climate being of particular importance. Climate monitoring networks are frequently of insufficient temporal and spatial resolution to provide a clear picture of the temperature patterns in regions of complex terrains such ase the Western Cape. Improved temperature surface layers of higher temporal and spatial resolution would aid in better decision making for future cultivation into new or existing areas, for in vineyard management of heterogeneous vineyard blocks (precision viticulture) and highlighting areas more susceptible to temperature increases as a result of global warming (Bonnardot *et al.*, 2011). Numerical simulations over the wine-producing areas of South Africa, using high grid resolutions is necessary to assess the local air circulations in greater detail in the context of the bigger climate picture. The modelling outputs help in identifying locations based on their potential to meet climatic requirements for optimum physiological performance of the grapevine and to facilitate recommendations for terroir selection and zoning (Bonnardot & Cautenet, 2009; Hunter & Bonnardot, 2011).

High resolution historic climate layers, in time climate layers as well as project climate layers from atmospheric and geostatistical modelling will compliment agriculture in the future and in the context of climate change. The modelling methods should be selected based on the application needs, country wide versus high resolution vineyard level studies.

2.5.1 Atmospheric modelling over South Africa

Global Climate Models (GCMs) is said to be an appropriate tool for addressing future climate change in many scientific studies (Hudson & Jones 2002). Reliable climate change information is usually required at finer spatial scales than that of a typical GCM grid-cell (which is usually >300 × 300 km). Thus, although GCMs provide adequate simulations of atmospheric circulation at the continental scale, they do not capture the detail required for regional and national assessments. Over estimating the impact of projected climate change, as shown in a study where the future South African wine industry is predicted to be non-viable by 2050 (Hannah *et al.*, 2013), in this study the interpretation of the bioclimatic indices was the problem, more than the GCM. This extreme over and under estimation of temperatures is particularly true for heterogeneous regions (like the Western Cape), where sub GCM grid scale variations in topography, vegetation, soils and coastlines have a significant effect on the climate over short distances (Hudson & Jones 2002).

A controversial study using GCMs for regional scale analysis, on the level of the grapevine's physiological functions and therefore the economic viability of grapevine farming activity for the future, showed 50% decrease of viticulture surfaces could be observed by 2050 in the world wine-producing regions, according to the greenhouse gas emission projections (Hannah *et al.*, 2013). Van Leeuwen *et al.* (2013) showed their conclusion that most of the present wine growing regions will become unsuitable for viticulture is mistaken. Van Leeuwen *et al.* (2013) pointed out major methodological flaws in the Hannah *et al.* (2013) study, mostly linked to the misuse of bibliographical data to compute suitability index, resulting in the under estimation of adaptations of viticulture to warmer conditions, and the inadequacy of the monthly time step in the suitability approach. The suitability index used in the study for the grapevine maturity groupings (Jones, 2006), was constructed from empirical observations collected in wine growing areas and not based on grapevine physiological modelling as suggested by Hannah *et al.* (2013). Hence, the difficulty to establish precise upper limits for the variety for growing high-quality wines, and hence the statement is overestimated and totally unrealistic. This dispute from the study highlights the need for localised scale studies and groupings of cultivars based on the grapevines physiological

function in different extreme climatic environments (Hunter & Bonnardot, 2011) and the correct or comparable bioclimatic indices should be used in the context of climate change.

Some key climatic processes relevant for South Africa appear not to be adequately represented by the GCMs or the downscaling methods currently in use, the strengths and weaknesses of model simulations of the recent historical climate (1960–2010), based on comparisons of observed and modelled trends. Observed temperature trends since 2000 have not increased as steeply as projected by model simulations. Rainfall trends are unpredictable, observed reductions in autumn rainfall are not reproduced by the models, and the models tend to show opposite trends (DEA, 2013).

High horizontal resolution (< 1 km) is important in characterising the climate potential of viticultural environments (Bonnardot & Cautenet, 2009), and therefore considered necessary to properly identify and characterise the climate of wine producing regions and to determine its vulnerability. The Regional Atmospheric Modelling System (RAMS) has been used to investigate sea breeze circulations over the vineyards of the South Western Cape in South Africa (Bonnardot *et al.*, 2005). The simulations of 1 km and 200 m resolution were superior to the 5 km resolution simulation, especially in reproducing the local air circulations (sea and slope breezes) because of a better representation of the local terrain (topography and vegetation cover) at 5 km. The use of a high resolution grid (200 m) may be of greater value in the identification of potential terrains for viticulture for the future (Bonnardot *et al.*, 2005; Bonnardot & Cautenet, 2009).

Another RCM described and used by Roux (2009), the conformed-cubic atmospheric model (CCAM) was employed in stretched-grid mode to simulate climate for the period 1976-2005 at four different spatial resolutions (60 km, 8 km, 1 km and 200 m) (Roux, 2009). The 60 km CCAM simulation gives a good representation of the synoptic scale weather over southern Africa, with realistic seasonal circulation patterns and rainfall percentages as well as intra-annual rainfall totals over various regions. The meso-scale climate over the Western Cape is captured by the 8 km simulation, especially with respect to seasonal variations in temperature and rainfall percentages although underestimating the actual rainfall over the south-western tip of the Western Cape. The ultra-high-resolution (200 m to 1 km) simulated diurnal cycle of temperature, relative humidity and screen level wind speed compared well against observations for the month of February (Roux, 2009). The CCAM climate simulations may not be accurate enough for some of the very sensitive studies at finer scale resolutions, but it can have great value for the demarcation of areas which are climatically suited for viticulture as the simulations verify well against observed datasets, and generally capture the important climatic features over the area of interest, such as a region or a district.

Farm and vineyard level environments require higher definition modelling to quantify for the atmospheric variability over shorted distances. A recent study by Soltanzadeh *et al.* (2016) applied the Advanced Research Weather Research and Forecasting (ARW-WRF) model of high-resolution (500 m), known to have positive results in areas of high complexity (Zhang *et al.*, 2013). This is a three-dimensional atmospheric numerical model which is used to map spatial and temporal variability of temperature in the wine-producing region of Stellenbosch in the Western Cape Province in South Africa. This model identifies the potential areas with high daytime temperature stress most likely to affect grapevine photosynthesis and grape composition. The differences are that diurnal temperatures are highlighted due to synoptic and local environmental factors, often associated with the influence of terrain (Soltanzadeh *et al.*, 2016). Although the results showed that the WRF was unable to represent weather associated with low level temperature inversions, it

seems this is a common problem when preforming numerical simulation in complex terrain (Zhang *et al.*, 2013).

Soltanzadeh *et al.* (2016) shows that even though there are many environmental factors such as mesoscale and synoptic scale wind systems, topography, coastline orientation and slope angle and aspect each have significant effects on the thermal regime of the vineyard region (Carey *et al.*, 2008), and it can be inferred from the statistical analysis provided in the study using the WRF model, with the exception of a few difficult sites. The WRF model can therefore effectively simulate the local scale meteorology in complex wine growing area of Stellenbosch.

On a daily basis, grapevines experience a range of thermal conditions that have an impact on vine growth and the development of primary (*e.g.* sugar and organic acids) and secondary (*e.g.* colour and aroma) grape quality compounds (Carey, 2005; Deloire *et al.*, 2005). These conditions were largely controlled by the prevailing large-scale weather conditions and complexity of the local terrain (Bonnardot *et al.*, 2011). Finer scale models as mentioned above can therefore be used to identify areas in which the vines are likely to be under significant climatic stress in relation to the large-scale weather conditions. In particular, areas in which low/high night temperature stress was likely to affect grape composition, and where low/high day temperature stress is likely to affect grapevine photosynthesis, can be identified in future climate change scenarios.

2.5.2 Geostatistical Modelling over South Africa

Geostatistical modelling can be used alongside or as an alternative for higher spatial interpolated outputs, but accuracy is highly dependent on input resolutions. Air temperature modelling is challenging in complex terrains and meteorological stations are often spread sparsely, especially at high elevation or in uninhabited areas (Zorer *et al.*, 2013). Thus, it is difficult to obtain precise climatic maps because reconstruction of temperature fields involves interpolating sparse data over large distances (Benavides *et al.*, 2007). This may lead to unreliable traditional geospatial interpolation results. Different interpolation methods have been used to model the spatial distribution of air temperature; the most widely used being the inverse distance interpolation weighting, Voronoi tessellation, regression analysis or, more recently, geostatistical methods (Benavides *et al.*, 2007). Relationships have been derived between temperature and other topographic variables, together with elevation data, such as exposure, continentality, latitude and solar radiation. Maps of bioclimatic indices are commonly generated by spatial interpolation of data collected from weather stations.

The resolution and accuracy of existing spatially interpolated climate data (Schulze, 1997; Hijmans *et al.*, 2005) is often not sufficient for applications at regional and local scales. This is true for the Western Cape Province of South Africa (Van Niekerk & Joubert, 2011). Climate surface accuracy strongly relates to surface resolution, as climate variability is often lost at lower spatial resolutions, therefore interpolations with higher resolutions are more likely to accurately represent the variability in climate when mapping (Hijmans *et al.*, 2005). Interpolated climate surface accuracy is determined by the interpolation algorithm employed, the resolution of the generated surfaces, and the quality and density of the input data used. Although the primary input data of climate interpolations are usually meteorological data, other related (independent) variables such as elevation (known to have a strong influence on climate) are frequently incorporated in the interpolation process (Van Niekerk & Joubert, 2011).

Interpolated climate layers need to be updated continually to keep up with the new technologies of advances of interpolation methods and in the context of the climate changing. Currently the

existing climate layers available are the South African Atlas of Agrohydrology and Climatology (SAAAC) (Schulze, 1997) and the WorldClim climate surface layer (Hijmans *et al.*, 2005) for the whole of South Africa at 1.6 km and 1 km resolution respectively. The Western Cape Climate Surfaces (WCCS) (Joubert, 2007) layer was created using the monthly temperature means of meteorological stations to generate a new set of surfaces. The SAAAC surfaces differentiate for specific areas, as sub-region specific multiple regression equations were used for the temperature surfaces (Schulze & Maharaj, 2006). A pair-wise comparison of the new interpolated surfaces (WCCS) with existing climate surfaces revealed that the surfaces created using new methodology on a finer scale are more accurate than any existing interpolations at 1.6 km and 1 km (Figure 7), with the accuracy in Figure 8 highlighting that the new layer WCCS is more comparable to the actual weather station values.

The limitations of this layer is the limited input of 125 meteorological stations logging for 30 years (spatial and temporal inputs), which hindered the accuracy assessment and the use of the layer as a climate source for decision making. The criticism of this method is that it was presumed that the input stations acquired for the WCCS layer would be comparable to that used for the creation of the SAAAC and WorldClim surface. However, the methodology is advanced and since this analysis has advanced significantly, with better climate data as an input this could be great climate layer to use in decision making for adaptation to climate change.

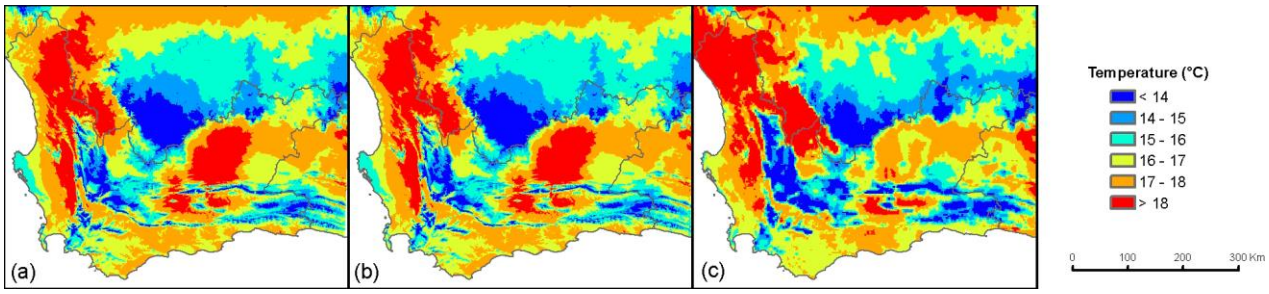

Figure 7 Comparison of the (a) WCCS annual mean temperature surface with those produced by (b) WorldClim and (c) SAAAC (Van Niekerk & Joubert 2011).

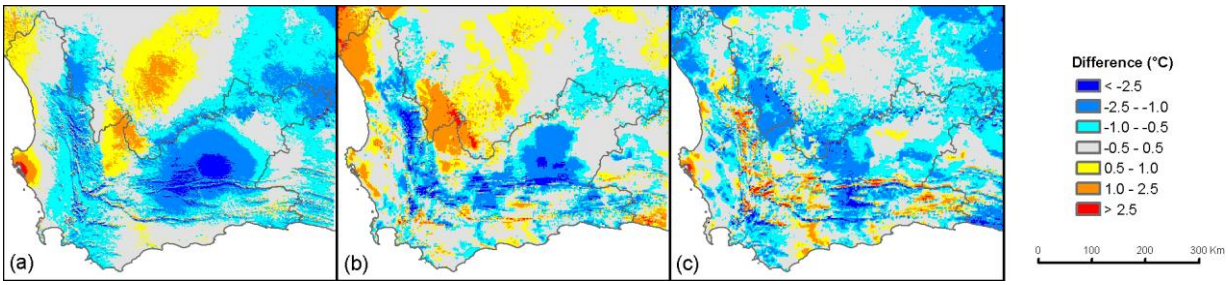

Figure 8 Pair-wise difference comparison of mean temperature:(a) WorldClim – WCCS, (b) SAAAC – WCCS and (c) WorldClim – SAAAC (Van Niekerk & Joubert 2011).

Spatial maps created for the Western Cape are of value for future adaptions to climate change, and for finer scale decision making using geographical information systems (GIS). A study was conducted in the Stellenbosch district to isolate the natural terroir units (NTU), defined as a unit of land that is characterised by relatively homogenous topography, climate, geological substrate and soil within the complexity of Stellenbosch. The aim of the study was to use geostatistical modelling to characterise the Stellenbosch Wine of Origin District using existing digital information (such as topographic features and soil association data) into NTUs using GIS. Terrain morphological units, altitude, aspect and soil type were used as primary keys for the identification of NTUs. Each of the

identified units was further described with respect to the extent of the expected sea breeze effect and, for certain of the soil types, the associated parent material. Figure 9 is the output of the geostatistical modelling as a map of terroirs identified for Cabernet Sauvignon and Sauvignon Blanc in the Stellenbosch Wine of Origin associated to the viticultural potential oenological performance is given in Figure 9 (Carey, 2005).

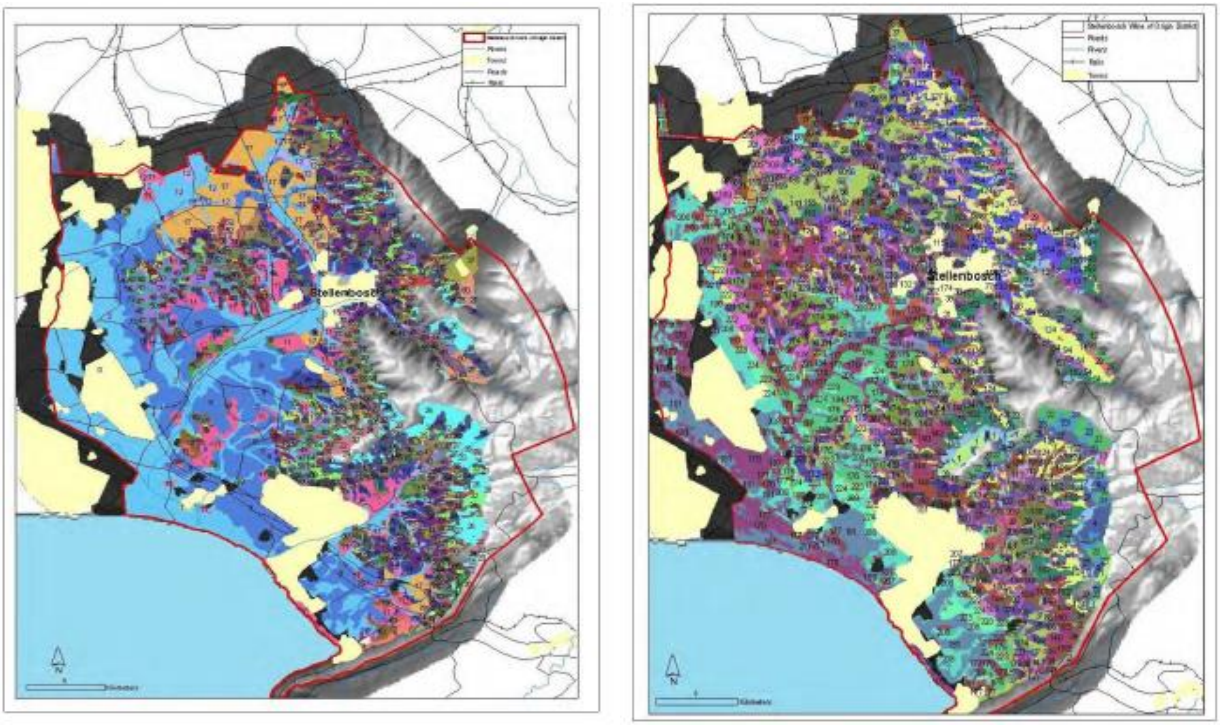

Figure 9 Map of terroirs identified for Cabernet Sauvignon and Sauvignon blanc in the Stellenbosch Wine of Origin District (Carey, 2005).

The number of NTU's could be grouped for practical applications in the future, and the analysis could also be done over more regions and cultivars. With more geospatial layers, adaptions to climate change could be more effectively planned, applying modelling in semi-real time resolution for example modelling grapevine responses, like phenology maps for analysis and forecasting (Mariani *et al.*, 2013).

Remote sensing can be used as an alternative resource to atmospheric and geostatistical modelling to monitor the climate and environment in time and space. The great advantage is that the layers are intrinsically spatialised and consider a lot of the variables discussed previously (Neteler, 2010; Zorer *et al.*, 2013). The layers are, however, available at lower resolutions than that of the WRF model and geostatistical modelling; downscaling of the remote sensing layers improves the resolution. The integration of the modelling discussed above and remote sensing allows for detailed studies of the natural environment surrounding the vineyard, also allowing for in time monitoring of climate change, advancing the adaptive strategies to be more in time with seasonal management.

2.6 Climate classification systems

2.6.1 Climatic indices

Climate, namely temperature, rainfall, relative humidity, sunshine duration and water balance, are combined components that are used to describe the viticultural potential of a region at different

climate scales (macro-micro) (Deloire *et al.*, 2005). The climate of a location is affected by its latitude, terrain and altitude, as well as nearby water bodies and their currents. Climates can be classified according to the average and the typical ranges of different variables, most commonly temperature and precipitation (Conradie, 2012).

Regions and local sites are classified based on bioclimatic indices and climatic parameters (temperature, rainfall *etc*), to describe the climatic potential and characteristics favourable for specific wine grape cultivars and the general wine style that can be produced within a given climate (Jones *et al.*, 2010; Anderson *et al.*, 2012). The indices are a summation over a period of time (growth season or a whole year), but may also use mean data of a single month. They are normally established for a specific country or region, but may be adapted to other regions or used for a systematic global classification of the climate (Tonietto & Carbonneau, 2004). Subsequent adaptations have made them more applicable to specific countries and regions (Amerine & Winkler, 1944; Le Roux, 1974; De Villiers *et al.*, 1996).

The average daily maximum and minimum temperatures are used to derive climatic indices for areas of interest, namely the growing season average temperature index (GST), standard growing degree-days (GDD) as represented in the Winkler Index (WI) (Amerine & Winkler, 1944), the Huglin Index (HI) (Tonietto & Carbonneau, 2004), and a biologically effective degree-day index (BEDD). A summary of the indices is given in Table 1.

The GST index is the average temperature over the seven growing months, i.e. from September to March. The calculated values were then categorised into five classes using designations of cool, intermediate, warm, hot, and very hot, with values ranging from 13 °C to 24 °C (Table 1). The GST index can be used broadly to categorise wine grape growing regions based on maturity potential or climate suitability in addition to delineating maximum and minimum latitudes for viticulture (Jones *et al.*, 2010; Anderson *et al.*, 2012) (Figure 10).

One of the most well-known temperature indices for viticulture is that of the GDD, as first suggested by Amerine and Winkler (1944) for California (hereafter referred to as the Winkler index). Le Roux (1974) applied the heat summation technique to the Western Cape wine producing regions and adapted the growing season and classification to make it relevant for South African conditions. The growing season was changed to start at 1 September, differing from the 1 October start if the Northern Hemisphere equivalent is used, lasting until 30th March and it is calculated as a summation of the daily mean temperature above 10˚C. The GDD is calculated using the standard formula (Table 1) with a base temperature of 10°C representing a theoretical lower limit for growth of the grapevine, summating the daily values over the September to March months, classified into eight classes of region categories (too cool <850, to too hot >2700) based on the climatic suitability for cultivation of grapes (Anderson *et al.*, 2012).

The heliothermal index, a.k.a. the Huglin index (HI) is used worldwide to describe the potential of a region for viticulture (Huglin, 1978). This index is based on the mean and maximum monthly temperatures from October to March (Tonietto & Carbonneau, 2004; Blanco-Ward *et al.*, 2007). The calculation incorporates a coefficient to allow for the greater photosynthetic active radiation that occurs with longer days at higher altitudes. A coefficient of 1 is used for the South Western Cape (latitude 34˚ South), and the index provides information regarding the level of heliothermal potential at a site. It provides a better indication of the sugar loading potential according to the varieties, rather than the classic temperature summations, thereby providing qualitative information (Tonietto & Carbonneau, 2004). As can be seen in Table 1, The HI was calculated similarly to GDD but includes in its calculation a stronger weighting for maximum temperature (subtracting the

base temperature from both the maximum and the mean before averaging; (Table 1) and an adjustment based on the length of the day at its latitude (Huglin, 1978). Summating the daily values from October to March, the calculated values were placed in eight class categories (Anderson *et al.*, 2012). Both indices are therefore based on a summation method and calculated according to a base temperature of 10°C, which has been widely accepted for grapevine as below which little vegetative growth occurs (Zorer *et al.*, 2011), although this is likely cultivar specific (Jones *et al.*, 2010; Anderson *et al.*, 2012).

Using the HI in conjunction with the cool night index (CI), provides a better insight into a region's climatic influence on growth and ripening respectively (Tonietto & Carbonneau, 2004). The CI is the night coolness variable and is quantified using the mean minimum (night) temperature during the month preceding harvest (Tonietto & Carbonneau, 2004). It is used to determine the qualitative potential of wine growing regions with respect to wine colour and aroma, notably in relation to secondary metabolites (polyphenols and aromas) in grapes.

The BEDD index assumes a minimum base value for plant growth (10°C) but also places an upper threshold on temperature (19°C), beyond which significant additional growth potential is unlikely, and the index uses an adjustment to account for day length at varying latitudes (Anderson *et al.*, 2012). It also assumes potential plant growth is not linear at all temperatures (Gladstones, 1992), and includes an adjustment based on the daily temperature range (upward if the temperature is greater than 13°C and downward if it is less than 10°C). The BEDD values are assigned to five classification classes (Hall & Jones, 2010; Jones *et al.*, 2010; Anderson *et al.*, 2012).

Table 1 Equations of climatic indices used to calculate and classify the climate.

Equation	Climatic Indices	Calculations	References
Eq 1	Growing season average Temperature (GST)	$GST = \frac{\sum_{31.03}^{01.09}(Tmax + Tmin)/2}{n}$	(Anderson *et al.* 2012)
Eq 2	Growing Degree Days (GDD)/ Winkler Index (WI)	$GDD = \sum_{31.03}^{01.09}(Tmax - Tmin)/2 - 10°C; \geq 0$	Winkler index (Amerine & Winkler, 1944) as adapted by Le Roux (1974)
Eq 3	Huglin index	$HI = \sum_{31.03}^{01.10}\frac{(Tmean - 10°C) + (Tmax - 10\ °C)}{2}\ \mathrm{d}; \geq 0$	(Huglin, 1978)
Eq 7	Biologically Effective Degree Days (BEDD)	$BEDD = \sum_{31.03}^{01.09}\frac{\min[\max([Tmax + Tmin]}{2} - 10{,}0)K + DTRadj, 9$	(Anderson *et al.* 2012)
Eq 4	Fresh Night Index (FNI) / CI (Cool night Index)	Mean Minimum March temperature	(Tonietto & Carbonneau 2004)
Eq 5	MJT	Mean January temperature	(Smart & Dry, 1980)
Eq 6	MFT	Mean February temperature	Smart & Dry (1980) and adapted by De (Villiers *et al.,* 1996)

Long term weather data, *e.g.* mean February temperature (MFT), is used as a criterion to determine wine quality potential of a specific region (De Villiers *et al.*, 1996; Myburgh, 2005). Mean February temperature is based on the concept of Smart and Dry (1980) ("temperature of the warmest month within the growing season") and was adapted by De Villiers *et al.* (1996), where the South Western Cape was also divided into different climatic regions according to the MFT values. It is accepted that February is the warmest month in many parts of the Western Cape and it is the month during which the majority of the grapes ripen, in many cases this is not true. In many wine growing areas of the Western Cape, January is the warmest month from past records, *i.e.* the Robertson area. Cultivar ripening ranges from January (early ripening cultivars) to March (late ripening cultivars), therefore ripening does not only occur in February, especially in the context of climate shifts. In the future, the mean January temperature (MJT) and possibly the mean March

temperature (MMT) should also be considered as an index of value to describe the ripening months for early and late cultivars.

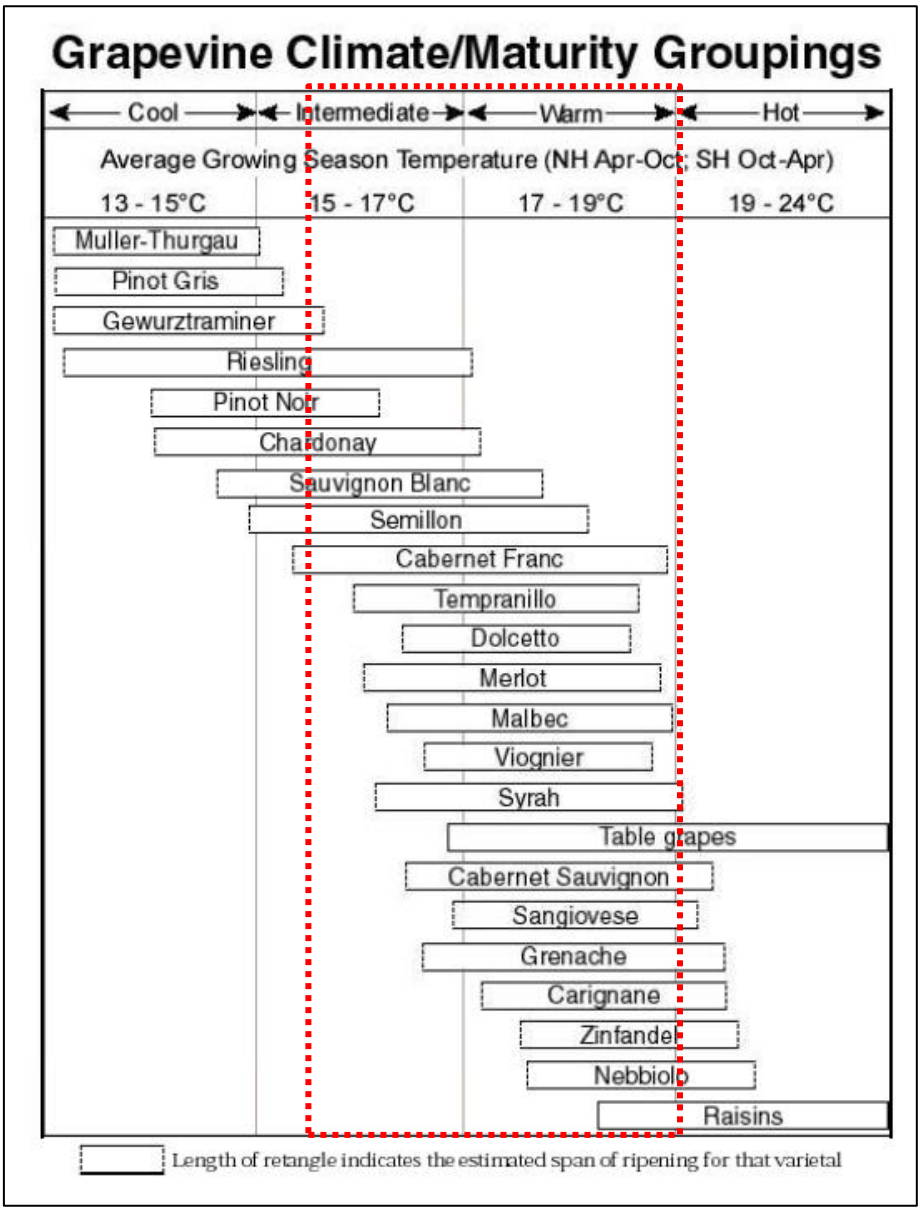

Figure 10 Climate-maturity groupings based on relationships between phenological requirements and growing season average temperatures for high to premium quality wine production in the world's benchmark regions for many of the world's most common cultivars (Jones, 2006). The red dashed line indicates the average growing season demarcation for Syrah and Cabernet Sauvignon.

2.6.2 Cultivar selection based on climate

There are a great variety of white and red cultivars planted in the Western Cape, and the harvest season can range from early January (early cultivars) to early April (late cultivars). The diversity of cultivars is an advantage in the context of the climate change. A further advantage is that in South Africa there is no limitation on which cultivar should be planted where. However, in the context of climate change, future strategies of adaption should include past knowledge of how cultivars fared in certain regions.

Grapevines, which are considered drought-tolerant plants, are characterised by diverse hydraulic and photosynthetic behaviours, depending on the cultivar. The hydraulic and photosynthetic

variance of grapevine cultivars may have important practical implications on daily management by applying different irrigation regimes to different cultivars in order to maximise crop performance in the context of increased temperatures (Hochberg *et al.*, 2013). The management of water resources and availability of water to the grapevine will be a significant factor for warmer to hot regions to continue cultivating grapevines. The grapevine is the only known species to possess both isohydric and anisohydric behaviour, which are different strategies to cope with water constraints, and indicate substantial quantitative differences between the different cultivars (Schultz, 2003b; Hochberg *et al.*, 2013). Isohydric (pessimist) represents a plant behaviour in which leaf water potential is kept steady (regardless of soil water status), whereas anisohydric (optimistic) represents a plant behaviour in which, under decreased water availability, leaf water potential decreases accordingly (Hochberg *et al.*, 2013). Near isohydric cultivars such as Cabernet Sauvignon can modify their growth and physiology to conserve current resources and to control their demand for future resources whereas an near anisohydric cultivar such as Shiraz will use all the resources available to them in expectation of more arriving (Schultz, 2003a).

Water scarcity is a critical limitation for agricultural systems, exacerbated with increases in temperature, hence selecting the correct cultivar in the context of growth nature as isohydric or anisohydric, selecting late and early ripening cultivars based on conditions at the localised area of interest. Early ripening and late cultivars, matching to the cultivar to the ripening period of an area (early cultivars to be harvest before hottest part of the season arrives). Selecting grapevine cultivars to match specific regions for optimal functioning is an adaptive strategy to apply in the context of climate and seasons shifting.

2.6.3 Viticultural climatic index limitations

These indices (heat summations over the growing season) result in classification of climatic regions broad enough to take short-term variation in climate into account. Grapevine growth and ripening is linked to the geographical situation through the induced meso-scale climatic regimes. Many indices are thus based on climate variables and can be used to classify the winemaking regions at a world-wide scale (Tonietto & Carbonneau, 2004) and at a regional scale. Research on climatic suitability for grapevine cultivation usually focuses on these temperature analyses at monthly or seasonal scales (Jones *et al.*, 2010). Jones (2006) created optimum climatic thresholds for wine production, regarding the cultivars based on the growing season temperatures (Figure 10). This cultivar suitability classification showing ‘Grapevine Climate/Maturity groupings’ (Jones, 2006), is not likely to be applicable on a regional scale due to the variability between regions and the complexity within a region that is generalised in these groupings. The methods and field observations used for the cultivar groupings have significant limitations as it was constructed from empirical observations collected in premium wine growing areas and not based on grapevine physiological modelling. The upper limits set on the groupings per cultivar for growing high quality wines are underestimated (Van Leeuwen *et al.*, 2013), and this was illustrated in a study in Germany and France (Burgundy and Rhone valley) based on Pinot noir. Comparing the growing seasons temperature from 1970 to 1999 and 2000 to 2012, Pinot noir is past the upper limit demarcated in Figure 10 but still produces high quality wines (Van Leeuwen *et al.*, 2013) . Climate-maturity groupings were based on relationships between phenological requirements and growing season average temperatures for high to premium quality wine production in the world’s benchmark regions for many of the world’s most common cultivars. The dashed line at the end of the bars in Figure 10 indicates that some adjustments may occur as more data become available, but changes of more than ± 0.2 – 0.5°C are highly unlikely (Jones, 2006; Jones, 2007). This can be

disputed, as Shiraz for example is a cultivar grown throughout most of the wine growing regions of South Africa, in cool to hot climates, namely Elgin and Vredendal or Upington respectively, demarcated by growing season temperatures. Shiraz therefore grows and ripens far outside of the demarcated temperature thresholds recommended by Jones (2006). The wine style produced at each of the climates is unique, with cooler areas having a white pepper characteristic and warmer areas being more black/ripe fruit driven and typically richer in colour and tannins (A.E. Strever, personal communication, 2016). Regional scale studies are therefore essential in cultivar adaptations, and cultivars are able to grow and ripen in hot regions outside of the thresholds recommended. Some South African wine growing regions such as the Olifants River and Orange River valley are classified as hot and too hot by some indices (*i.e.* the Winkler index), however these regions are known for high production potential for many cultivars with acceptable wine quality, but with a high dependency on water resources. The latter will therefore possibly be more of a limiting factor for future viticulture than climate, but it is known that climate will affect wine styles. When early ripening grape varieties are planted in warm climates not suited to their growth, aromatic expressions and wine quality is reduced due to ripening being too fast. In contrast, late ripening cultivars planted in cool climates will not reach optimal maturity, resulting in reduced wine quality that will have the tendency to be more vegetative in aromatic character (Mehmel, 2010). Climate change studies worldwide suggest that some regions could lose their climate advantage which allows a particular style of wine production with a particular cultivar to be shifted.

Heat summations over the growing seasons are used extensively in viticulture studies, but may only be applicable for interregional and global comparisons of potential grape growth and maturation. Some studies have highlighted the need for more long term and consistent monitoring of grapevine growth stages at the vineyard level (Jones & Davis, 2000) as well as on a regional level. Rather than only focusing on bioclimatic indices or indexes to classify a season or area, it will be beneficial to incorporate the grapevine's reaction to its environment. Without such knowledge, viticulturists do not have the tools necessary to understand historical and future viticulture trends. The temporal data resolution used for the calculation of the bioclimatic indices has some limitation, as data integrity is lost when using monthly temperatures in the calculation of the indices. The summation of general monthly averages could result in larger errors, classifying regions or areas to be warmer or cooler than what the grapevine is subjected to. Daily data is a more acceptable input for the index calculations, as it accounts for the maximum and minimum values in the day, but it is also limited as the diurnal temperature cycle to which the grapevine is exposed is not accounted for. The maximum and minimum values are of value, but even more so is the frequency and duration of the maximum and minimum temperatures which is not accounted for in the indices used worldwide. A study by McIntyre *et al.* (1987) evaluated the growing degree summation indices used in viticulture, highlighting some limitations such as the initial accumulation is often in error due to the non-symmetrical way that heat accumulates diurnally in many areas, which is not taken into consideration by summating the daily mean temperature above 10°C. Secondly, they found the degree day accumulations between bud-break, bloom, and fruit maturity were just as variable as simply using the number of days between the various phenological stages averaged over a period of several years. The individual cultivars tended to show different responses in different locations, due to the influence of other climatic variables and genotype differences.

The inclusion of more climate variables, such as wind and relative humidity would improve the climatic classifications. Therefore, studies have included more variables such as distance from the ocean, elevation *etc.* to improve climate descriptions in a spatial format (Bonnardot & Cautenet, 2009; Van Niekerk & Joubert, 2011). Other studies have classified growing environments based on

the grapevine's physiological requirements in temperature, wind and relative humidity, showing thresholds for optimal functioning could be incorporated into the climate classifications for better selection of cultivars and rootstocks (Hunter & Bonnardot, 2011).

Different climatic parameters (temperature, wind, rainfall and relative humidity) are seldom combined at global scale (Tonietto & Carbonneau, 2004) or at regional and local scales (Knight, 2006) and little consideration is given to finer temporal scales and specific periods during the growth season (Bonnardot *et al.*, 2002; Hunter & Bonnardot, 2011). There is also a need for including other factors, such as solar radiation, day length, daily temperature ranges, soil moisture *etc.* for more accurately describing climatic regions (McIntyre *et al.*, 1987).

This becomes all the more important in the light of a global climate change which may impact on growth, grape composition, wine style and spatial distribution of grapevines (Tonietto & Carbonneau, 2004; Jones *et al.*, 2010; Hunter & Bonnardot, 2011). Despite the dependence of proper physiological functioning of the grapevine on climate, *i.e.* temperature, humidity, wind, it is therefore necessary to assess at finer scale the climatic suitability (in terms of duration) of regions/environments for grapevine cultivation, and more specifically, the physiological requirements of the grapevine affecting the accumulation of components that are viticulturally and oenologically important. This is critical to optimise the functioning of the grapevine in a specific environment and to improve grape and wine quality in the context of climate change and steer away from large scale suitability studies (Figure 10) (Jones, 2006; Hunter & Bonnardot, 2011).

2.6.4 Global considerations in climate change

"The world is now warmer than at any time during the past 1000 years."

Climate change is a complex biophysical process; hence it is not possible to predict precise future climate conditions. The scientific consensus is that global land and sea temperatures are warming, with an averaged combined warming of 0.85°C (ranging from 0.65 to 1.06°C) over the period 1880 to 2012. Temperatures will continue to warm regardless of human intervention for at least the next two decades (IPCC, 2007), with evidence that the global mean temperature is increasing continuously, with reasonable evidence that this change is accelerating. Surface temperature is projected to rise over the 21st century under all assessed emission scenarios (IPCC, 2014). Each of the last three decades has been successively warmer at the Earth's surface than any preceding decades since 1850. The period from 1983 to 2012 was likely the warmest 30-year period of the last 1400 years in the Northern Hemisphere.

The observed changes are likely due to human influence on the climate system, with recent emissions of greenhouse gases being the highest in history. Warming of the climate system is unequivocal and changes in many extreme weather and climate events have been observed since the mid-20th century (IPCC, 2014). The dominant global trends include more frequent hot and fewer cold temperature extremes over most land areas on daily and seasonal timescales, as global mean surface temperature increases. It is very likely that heat waves will occur with a higher frequency and longer duration. Occasional cold winter extremes will continue to occur. The ocean will continue to warm and acidify, and global mean sea level continues to rise. In many regions, changing precipitation or melting snow and ice are altering hydrological systems, affecting water resources in terms of quantity and quality.

Climate change is also inducing shifts in the timing of growing seasons in parts of the northern hemisphere, and even have begun causing shifts in the geographic distribution of natural species.

It is also projected to reduce renewable surface water and groundwater resources in most dry subtropical regions, intensifying competition for water among various sectors (Midgley *et al.*, 2005; IPCC, 2014).

There are uncertainties about the magnitude of global warming and the location of the expected effects. Some climate models show that global warming will be between 2 and 6 °C from 2050-2100 (IPCC, 2014). It is still very difficult to estimate what the local impacts are and, therefore, how to adapt. Future climate adaption strategies require more accurate projections of climate change, more specific model selection depending on the region that is being considered and the variable(s) being used (Hudson & Jones, 2002).

Although Global Climate Models (GCMs) are an appropriate tool for addressing future climate change in many scientific studies (Hudson & Jones, 2002), reliable climate change information is usually required at finer spatial scales than that of a typical GCM grid-cell. The GCM provide adequate simulations of atmospheric circulation at the continental scale, but at more detailed scales there is an over and under estimation of temperature which is particularly evident for heterogeneous regions (like the Western Cape), where sub GCM grid scale variations in topography, vegetation, soils and coastlines have a significant effect on the climate over short distances (Hudson & Jones, 2002).

Finer spatial and temporal detail can be acquired through the use of RCM, with the limitation of covering a limited area of the globe due to the higher resolution. From the first IPCC assessment to the more recent assessment (2014), reports are that there has been a marked increase and improvement in the number of RCM simulations, including better representation of oceanic influences on global and regional climates, resulting in a more moderate view of future climate change (IPCC, 2014). Hence, the importance to keep updating and improving projections based on new model developments, as well as renewing spatial layers with new interpolation methods developed.

The RCM's are, however, not accurate enough to take into account local climate variability; hence nested scale studies (local and regional) allow for better frame adaptation options. Projected directional climate change demonstrates significant warming and changes in rainfall patterns, yet there are still great uncertainties as a result of natural climate variability at local and regional scales and in socio-economic scenarios. Midgley *et al.* (2005) reported significant warming trends for minimum (around +1°C for December to March) and maximum temperatures for nearly each month of the year in a study including 12 weather stations located in the South Western Cape for the study period 1967 to 2000. It was also reported that very warm days have become even warmer and occurring more frequently during the last decade, particularly during January, April and August (Vink *et al.*, 2010).

Local scale studies show important variability in temperature and growing degree days over very short distances which is related to grapevine phenology and productivity (Bonnardot & Cautenet, 2009; Le Roux *et al.*, 2015). Advances in modelling, such as the development of the Weather Research and Forecasting (WRF) model, which is able to more accurately represent atmospheric processes at high resolution (500m), will enable local areas potentially under high daytime heat stress limiting the grapevines physiological functioning to be identified, (Soltanzadeh *et al.*, 2016). The model is able to reproduce spatial and temporal variation of meteorological parameters at 500 m resolution, with the average model temperature bias of 0.1°C, relative humidity of -0.5% and wind speed of 0.6m/s. The limitation of this model is the inability to accurately represent the effects of nocturnal cooling within the complex terrain of the Western Cape, namely the local study area of

Stellenbosch. Higher resolution model outputs may be of greater value in the identification of potential terrain for viticulture due to the climate variability over short distances due to the complexity of topography in the Western Cape (Bonnardot & Cautenet, 2009; Engelbrecht & Engelbrecht, 2016).

Current understanding of the regional dynamics of the climate system of the sub-continent is limited; hence the need for downscaling and applications of newer models at higher resolutions, developing regional/local scale projections of change from the global models is needed for accurate understanding of what the future holds. For Africa, perhaps more so than other regions of the world, this issue is of noted concern.

2.6.5 Climate change impacts in South Africa

Long term temperature and rainfall changes have been noted in all provinces of South Africa and have broadly been attributed to climate change (Benhin, 2005; Bonnardot & Carey, 2007). These changes may put more pressure on the country's scarce water resources, with implications for agriculture, employment and food security. The overall view from GCMs is that South Africa faces a considerably drier and warmer future overall by mid-century, with some indication of an increased risk of intense rainfall events, especially in the coastal areas (Hulme *et al.*, 2001). With further projected changes in global climates into the future, changes in the South African agriculture sector will be inevitable, especially since the regional climate in South Africa is dependent on global climate, both presently and in the future (Schulze, 2011). South Africa lies in one of the regions of the world that is most vulnerable to climate variability and change (IPCC, 2007), but no one knows exactly how the future global climate will develop and what the resulting consequences will be for South Africa.

The Department of Environmental Affairs (DEA), revisited observed climate trends (1960-2012) as well as current climatology for South Africa and compared these with projected trends (DEA, 2013). The observed trends over the last five decades in South Africa were annual mean temperature increases of at least 1.5 times the observed global average of 0.65°C (IPCC, 2014). Maximum and minimum temperatures showed significant increases annually in almost all seasons. A notable exception was the central interior of the country, where minimum temperatures increased less, and/or decreased. It was also observed that high temperature extremes have increased significantly in frequency, and low temperatures decreased in frequency annually in most seasons across the country, but particularly in the western and northern interior. The rate of temperature change has fluctuated, with the highest rates of increase from the middle 1970s to the early 1980s, and in the late 1990s to middle 2000s (Tyson *et al.*, 2002). Statistical evidence suggests that South Africa has been getting hotter over the past four decades, with average annual temperatures increasing by 0.13°C per decade between 1960 and 2003, with varying increases across seasons and an increase in the number of warmer days as well as a decrease in the number of cooler days (Kruger & Shongwe, 2004). One significant finding is that there are seasonal differences in climatic effects, and these differences must not be overlooked by only considering mean annual effects. The impacts of climate change will, therefore, likely vary in nature and intensity over the wine regions of South Africa, especially in the ripening months of the grapevine.

The average rainfall in the country is very low at *ca.* 450 mm per year, which is well below the world's average of 860 mm per year; the evaporation is also comparatively high in South Africa. Only 10% of the country receives an annual precipitation of more than 750 mm and more than 50%

of its water resources are used for agricultural purposes (Benhin, 2005). Rainfall has shown high inter-annual variability, with statistically smoothed rainfall showing amplitudes of *c.* 300 mm, about the same as the national average. Rainfall trends are similar in all the hydrological zones, with rainfall being above average in the 1970s, the late 1980s, and mid to late 1990s, and below average in the 1960s and in the early 2000s, reverting to the mean towards 2010. Overall annual rainfall trends are weak and non-significant, but there is a tendency towards a significant decrease in the number of rain days in almost all hydrological zones. This implies a tendency towards an increase in the intensity of rainfall events and increased dry spell duration. There has also been a marginal reduction in rainfall for the autumn months in almost all hydrological zones (DEA, 2013).

Both commercial farming and especially subsistence farming may be affected by less availability of water owing to adverse climate change. This is expected to vary across the different agro-climatic zones, provinces and different agricultural systems in the country, affecting irrigated farms and dryland farms differently. In addition, surface and underground water are very limited, with more than 50% of the available water resources being used for only 10% of the country's agricultural activities (Benhin, 2005).

The increasing temperatures, sporadic precipitation and increasing atmospheric CO_2 can have positive or negative impacts on the South African wine industry by modifying grapevine yield and berry composition (Carter, 2006; Vink *et al.*, 2010). Furthermore, irrigation is generally used in South African vineyards; the decreasing precipitation would therefore cause a decrease in the water resources, either directly available for the grapevines or available from the dams as irrigation. The need for irrigation will increase with increase in temperatures expected due to higher evapotranspiration rates. The overall decreased precipitation in specific seasons or over a few seasons (carry over effect of minimal winter rainfall), could cause an increase in the demand and price of water resources, which will decrease the wineries' profitability.

Projected climate trends for South Africa

Climate projections predict temperatures to keep rising 0.2°C to 0.5°C per decade during the 21st century over the African continent (Hulme *et al*., 2001). Climate change projections until 2050 and beyond (under high emission scenarios) complied by the DEA in 2013 show significant warming of between 5 to 8°C over the South African interior by the end of this century, with warming to be reduced over coastal zones. Projections highlight a general pattern of drier conditions to the west and south of the country and wetter conditions over the eastern part of the country. Many of the projected changes are within the range of historical natural variability, but the general uncertainty in the projections is still high (Department of Environmental Affairs, 2013). Projections of a regional climate model over Southern Africa show temperature increases from 1 to 3°C (Engelbrecht & Engelbrecht, 2016).

Potential changes in Köppen-Geiger climate zones over southern Africa, temperate regions of eastern South Africa, the Cape south coast, and winter rainfall region of the South Western Cape are projected to contract. The temperate regions of the winter rainfall region of South Africa are robustly projected to be invaded by the hot steppe zone from the east and the hot desert region from the north. These projections may suggest the Fynbos biome of South Africa, which is located in these temperate regions extending to the Cape south coast, to come under increased pressure under future climate change (Engelbrecht & Engelbrecht, 2016).

2.6.6 Climate change trends observed in the Western Cape

The Western Cape is a diverse region that relies on its characteristic Mediterranean type climate regime to underpin many aspects of its economy and the persistence of its natural ecosystems, and is therefore a region very vulnerable in the context of global climate change (Midgley *et al.,* 2005). The wine areas in this region have experienced a significant increase in temperature over the past decades, with annual temperature increases ranging from 0.5°C to 1.7°C depending on regions and periods (Table 2) (Bonnardot & Carey, 2007; Vink *et al.*, 2010). Similar increased tendencies were observed at a local scale (Stellenbosch) with increasing mean annual temperatures from 1967 to 2003 (Hunter & Bonnardot 2011). According to Bonnardot and Carey (2008), the first signs of warming were higher winter maximum temperatures starting in the late 1960s. A significant breaking point occurred in the 1980's for the annual temperature series going from 1967 through to 2006, with a trend of warming acceleration noted since 2000. Temperature increase was on average 0.02°C per year, with the annual temperature increasing by 1°C per decade and growing season temperature increased by 0.7°C per decade. The calculation of the Winkler index for viticulture using a longer data series (1941-2008) confirmed the increasing rate of warming over the last decade. Most significant changes were noted to be in the growing season, with an increase in minimum February temperatures, and the occurrence of extreme events such as heat waves, droughts, floods and a delay in winter rainfall) (Bonnardot & Carey, 2007).

Table 2 Temperatures of the wine regions of the Western Cape Source over the past decades: Bonnardot and Carey. (2008).

Wine regions, districts or wards	Increase in annual maximum temperature (°C)	Increase in annual minimum temperature (°C)	Increase in Growing Degree Days (over Sept-March)	Period of record	Duration of records
Stellenbosch	+1.7	+0.7	+150	1967-2006	40 years
Paarl	+1.1	+0.5	+200	1970-2006	36 years
Worcester	+1.0	+1.1	+150	1967-2006	40 years
Olifants River	+1.1	+0.8	+240	1973-2006	34 years
Robertson	+0.5	+1.1	+150	1964-1994	30 years
Constantia	+1.0	+1.0	+180	1967-1999	32 years
Overberg	+1.6	+1.1	+180	1964-1994	30 years
Walker Bay	+0.8	+0.5	+100	1977-1990	13 years

Projected climate trends for the Western Cape

Projected climate conditions for South Africa show that temperatures can be expected to rise everywhere in the South Western Cape, with temperature tendencies accentuated in the inland and less pronounced in the adjoining coastal areas (Midgley *et al.*, 2005; Midgley *et al.*, 2015). Typical increases range from *c.*1.5ºC at the coast to 2-3ºC inland of the coastal mountains by 2050. Rainfall projections for mid-century (2046-2065) over the Stellenbosch, Paarl and Franschhoek wine regions show diminished winter rainfall of approximately 20%, particularly in early winter (Carter, 2006). Therefore, warmer and drier conditions are expected for vineyards in the future with temperature increases during the growing period of about 1°C (Carter, 2006; Vink *et al.*, 2010).

The warming trend in Africa is happening at a rate faster than the global average, and increasing aridity. Climate models and observations indicate increases in both mean temperatures and temperature variances, resulting in more hot weather and extreme events, and less change in cold weather. Some of the induced changes are expected to be abrupt, while others involve gradual shifts in temperature, vegetation cover and species distributions (Oosthuizen, 2014). Projections

for the Western Cape are for a drying trend from west to east, shifting to more irregular rainfall of greater intensity, and rising temperatures. This will encompass a range of consequences that will affect the economy, the livelihoods of people and the ecological integrity of the Western Cape region (Midgley *et al.*, 2005; Midgley *et al.*, 2015).

2.7 Climate change consequences and adaptation

It is expected that as climatic patterns change, so will the spatial distribution of agro-ecological zones, habitats, distribution patterns of plant diseases and pests and ocean circulation patterns which can have significant impacts on agriculture and food production (Schulze, 2011; Oosthuizen, 2014). Global climate models suggest that the agricultural sector in the Southern African region is highly sensitive to future climate shifts and increased climate variability.

The availability of water is a major limiting factor for agricultural production in South Africa, with a highly variable and spatially uneven rainfall distribution, as well as climate-related extremes. Any change in rainfall and temperature attributes could have far-reaching implications for agricultural production, and hence the vulnerability of farming systems (Oosthuizen, 2014).

The vulnerability of agriculture to climate change has become an important issue because of reduced crop productivity from adverse changes. At the national scale in South Africa, an economic study on agricultural impacts indicates that crop net revenues could fall by as much as 90% by 2100, with small-scale farmers affected most severely (Benhin, 2005), although the adoption of mitigation strategies could reduce these negative effects.

Adaptation and mitigation are complementary strategies for reducing and managing the risks of climate change. Substantial emissions reductions over the next few decades can reduce climate risks in the 21st century and beyond by largely eliminating the risk of extreme rainfall changes, both increases and decreases, by mid-century. High resolution regional modelling suggests even larger benefits of effective global mitigation by the end of this century, when regional warming of 5-8°C could be more than halved to 2.5-3°C (DEA, 2013). Effective global mitigation action is projected generally to reduce the risk of extreme warming trends, and to reduce the likelihood of extreme wetting and drying outcomes by at least mid-century. Adaptation can reduce the risks of climate change impacts, but there are limits to its effectiveness, especially with greater magnitudes and rates of climate change. The ability to assess the impacts and vulnerabilities, and to implement adaptions successfully will facilitate the achievement of a sustainable future in the Western Cape.

Climate change consequences will vary by region; and in some places the effect will be minimal at first, except perhaps indirectly, while other places will be affected more severely (Oosthuizen, 2014). Impacts from a changing climate can be considerable, depending on the region, therefore local scale analyses are needed to assess potential impacts (Anderson *et al.*, 2012). Changes in optimum growing areas and yields are anticipated, with many consequential effects ranging from the addition of new varieties and increases in pest infestations, influencing the food security and international trade (Oosthuizen, 2014).

Adaptive strategies defined for the Western Cape by the CSIR (Midgley et al. 2005) to alleviate or avoid the worst effects of climate change when looking to a warmer and drier future are: Improve water resource management, possible development of new water sources (aquifers and desalination); and ensure protection of the ecological water reserve for estuaries and the maintain the biodiversity of species through management of alien plants and fire hazards for the current health of indigenous terrestrial ecosystems, and for their future persistence (Midgley *et al.*, 2005).

Climate change and responses to climate change are interrelated aspects of South Africa wine industry influencing the future (Vink *et al*., 2010). Despite observed trends at regional scales and predicted climate change for the South African wine regions, the best strategy for surviving climate change is to deal with diversity: diversity in soil, climate, cultivars (heat tolerant cultivars) and people (Vink *et al.*, 2010).

Climate change has the potential of changing the environmental variables (Vaudour, 2002), which could influence grapevine reaction in growth and ripening, and the final wine style (Figure 11). Vintage, soil and topographic related site characteristics and scion clone affect the phenology, growth, yield, berry composition and wine related parameters of grapevines (Bonnardot & Carey, 2007; Carey *et al.*, 2007). Although many individual climate factors play a role in grapevine yield formation, grape development and grape composition (*i.e.* solar radiation, temperature and temperature extremes, precipitation amount and distribution, wind, humidity *etc.*), temperature and water supply are probably the most important (Coombe, 1987). Temperature and water are also the two factors most frequently addressed in reflections on the possible effects of climate change on viticulture (Schultz, 2000; Schultz & Stoll, 2010).

Several studies have shown that grapevine phenology has significantly advanced in many wine growing regions in the past (Duchêne & Schneider, 2005; Jones *et al.*, 2005) and will continue to shift forward in time with the main ripening period occurring at much higher temperatures (Webb *et al.*, 2007a; Webb *et al.*, 2008). This affected grape composition, as temperature altered the fruit composition (Schultz, 2000; Hunter *et al.*, 2010).

The possible changes in macroclimate has implications for meso- and microclimate and the link with grapevine berry temperature changes under different temperature regimes, will affected the photosynthetic active radiation during ripening period and influence the berry composition. Hence, a changing climate can bring about significant changes in grape composition and wine style, as the berry temperature differences have significant implications for terroir selection and where terrain has a dictating impact. Radiation patterns and berry temperatures would affect grape composition and the time of harvest (Hunter *et al.*, 2010).

Spatial changes in grape growing regions seem unavoidable to combat potential effects of climate change and adaptations are challenging as to be viable over the whole spectrum of viticultural practices, oenological techniques and marketing (Hunter *et al.*, 2010).

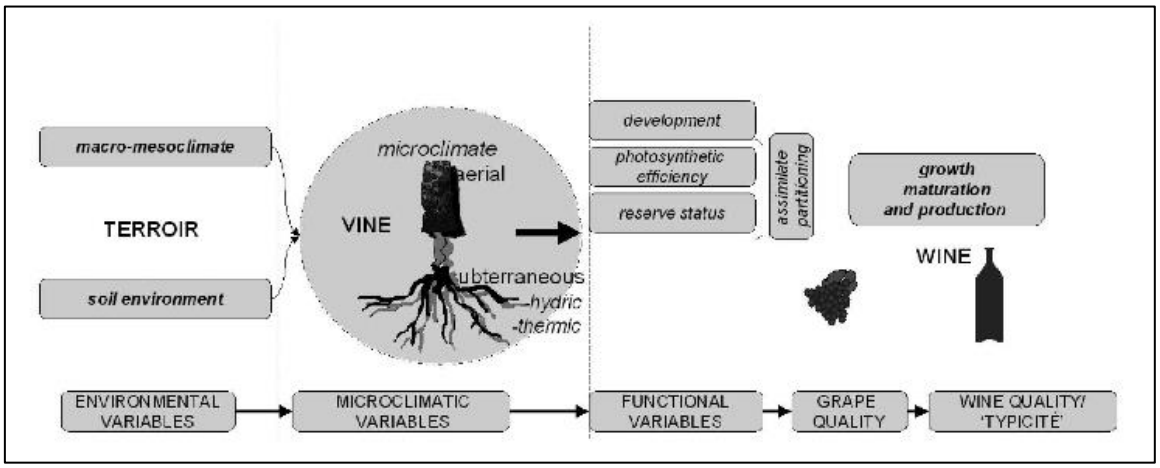

Figure 11 Chain representation of 'terroir/wine/wine' system and interaction (Source: Vaudour, 2002)

Viticulture adaptive strategies

The key to surviving climate change firstly requires an understanding of climate at different scales (especially micro scales) in order to adapt correctly according to the location-specific potential for viticulture. Studies dealing with climate at different scales have shown the effect of inter-annual microclimatic variability on wine aroma and style (Hunter *et al.*, 2010), or the effect of proximity of the Atlantic Ocean and complex topography on local air circulation (sea and slope breezes) resulting in interesting spatial climatic variability for viticulture (Bonnardot *et al.*, 2002; Conradie *et al.*, 2002; Hunter & Bonnardot, 2011).

Modelling of grapevine growth and ripening can become a useful tool to estimate the effect of climate and climate change according to the geographical situation, creating a geographical study of the relationship between the climate and the grapevine ripening in South Africa (Vink *et al.*, 2010).

In the context of climate change in the South African wine industry, adaption strategies should be tailored to the winegrower's perception of change that they are already experiencing and what they expected, as well as to consider their willingness to adapt within short, medium and long term strategies. Suggested adaption frameworks are firstly the short term adaptations, namely, irrigation management of extreme events, secure water resources, modified canopy management, re-evaluation of crop loads and to evolve and adapt wine styles (wine making techniques) and finally improved pest and disease management. For the medium term adaptions, more input costs could be expected such as selecting new varieties and/or rootstocks more suited to the 'new' climate, changing row orientation, canopy managements strategies, pruning techniques and possibly the timing of pruning, shifting marketing approach for new wine styles. Adjustments to the functional variables, such as row orientation (Hunter *et al.*, 2010) or irrigation, could mitigate the impact of climate change, buffering temperature increases by changing row directions or irrigation frequency to allow for a positive or negative final wine styles.

Temperature indices can be used to predict shifts in the varietal spectrum (Schultz, 2000; Jones, 2006). These approaches do not incorporate possible mitigation strategies through cultivation methods, and do not set an upper limit for cultivation thresholds (Schultz & Jones, 2010). Red varieties appear to tolerate warm conditions better than white varieties, and studies have shown a positive correlation of quality ratings and daily mean regional temperature for red but not for white wines, whereas the influence of temperature on vintage variability was strong for white wines but irrelevant for red wines (Schultz & Jones, 2010). Wine quality showed improvement with warming in cool regions, and a decrease in quality in hotter regions, many wine regions are near their optimum growing season temperatures for high quality wine production (Jones *et al.*, 2005). Therefore, further increases in growing season temperatures will likely place some regions outside their theoretical optimum growing season climate.

The final adaption strategies for extreme climate change scenarios on a long term decision making basis would be the shifting to different regions especially if the desire is to maintain wine styles. This implies the selection of new terroirs for certain selected cultivars.

Irrespective of climate change, the current diversity of climatic situations in South Africa allows the elaboration of different types of wine (rosé, red and white wine, port, sparkling and sweet wine) of different styles (tropical or green/herbaceous characteristics), which is mainly related to the climate of a specific region and/or vintage (warm versus cool) (Conradie *et al.*, 2002; Deloire *et al.*, 2009).

"It is not the strongest of species that survives, not the most intelligent that survives. It is the one that is the most adaptable to change."

Charles Darwin.

2.8 Summary

The most recent global assessment of climate change confirms continued warming and changes in rainfall patterns. Each of the last three decades has been successively warmer at the Earth's surface than any preceding decade since 1850. Changes in temperature, together with the already scarce water resources in the country, are expected to have a significant effect on all sectors of the economy, in particular agriculture. Agriculture is highly vulnerable to these changes as it is so dependent on climate variables such as temperature and precipitation. Climate exerts a dominant influence on wine production, driving baseline suitability for cultivation, largely controlling crop production, quality and ultimately driving economic sustainability.

Even minor changes in climate have the potential to bring about the need for significant changes in the management of existing vineyards and changes in the varieties planted. Changes in temperatures, either maximum or minimum, will result in shifts of the suitability zones for viticulture with some regions becoming too warm all together, while others become more viable. The South African wine industry has already shown considerable flexibility in shifting geographically to new production areas that are characterised by cooler climates.

Climate trends and impacts differ from global to local scales, potentially preventing the correct adaptive strategies from being implemented, due to the possible over or under estimation of climate change effects, specifically rainfall and temperature. Incorporating the local atmospheric conditions with the terrain, within localised areas such as provinces, regions, districts and wards, would provide a more realistic understanding of potential impacts.

In the Western Cape, trends show sharp increases in annual maximum and minimum temperatures and declining rainfall. Furthermore, these observed trends are expected to continue into the future. The South African wine grape growing regions are characterised by diversity (in climate, topography, soil type *etc.*), which provides unique adaptive capabilities in managing the effects of climate change.

Accurate quantification of climate and climate change in the Western Cape at higher resolutions, as well as incorporating the complexity of terrain would enable more effective adaptive strategies to be put in place. Every local environment has unique diurnal temperature variations due to the inland penetration of the sea breeze, and other local effects such as synoptic wind, topography, coastline orientation, slope angle and aspect. Climate accuracy strongly relates to surface resolution, as climate variability is often lost at lower spatial resolutions. The local environment can be inferred using higher resolution models, either atmospheric or geostatistical models, to describe the environment over regions and vineyards. Some of the latest atmospheric models and interpolation methods can effectively simulate the local scale meteorology in complex wine growing areas such as Stellenbosch. Remote sensing can be used as an alternative resource to atmospheric and geostatistical modelling to monitor the climate and environment in time and space. The integration of the modelling discussed above and remote sensing allows for detailed studies of the natural environment surrounding the vineyard, also allowing for in time monitoring of climate change, advancing the adaptive strategies to be more in time with seasonal management.

Grapevine and cultivar specific studies in the context of the changing environmental condition would help with decision making for linking specific cultivars to specific regions, for the best fit scenario in terms of yield and quality, as grapevine development and maturity is strongly influenced by temperature. Advantage can be taken of the positive effects, while controlling or reducing the negative effects; hence temperature changes could potentially be beneficial rather than harmful to the country.

2.9 Literature cited

Ainsworth, E.A., Rogers, A., Nelson, R. & Long, S.P., 2004. Testing the "source-sink" hypothesis of down-regulation of photosynthesis in elevated CO_2 in the field with single gene substitutions in Glycine max. Agric. For. Meteorol. 122, 85-94.

Amerine, M.A. & Winkler, A.J., 1944. Composition and quality of musts and wines of California grapes. Hilgard 15, 493-673.

Anderson, J.D., Jones, G.V., Tait, A., Hall, A. & Trought, M., 2012. Analysis of viticulture region climate structure and suitability in New Zealand. J. Int. Sci. Vigne Vin. 46, 149-165.

Benavides, R., Montes, F., Rubio, A. & Osoro, K., 2007. Geostatistical modelling of air temperature in a mountainous region of Northern Spain. Agric. For. Meteorol. 146, 173-188.

Benhin, J.K., 2005. Climate Change and South African Agriculture:Impacts and Adaptation options. Centre for Environmental Economics and Policy in Africa (CEEPA), University of Pretoria, South Africa, 1-60.

Blanco-Ward, D., Queijeiro, J.M.G. & Jones, G.V., 2007. Spatial climate variability and viticulture in the Mino River Valley of Spain. Vitis 46, 63-70.

Bonnardot, V. & Carey, V., 2007. Climate change: observed trends, simulations, impacts and response strategy for the South African vineyards. In: Proc. Global warming, which potential impacts on the vineyards? pp. 1-13.

Bonnardot, V. & Carey, V.A., 2008. Observed climatic trends in South African wine regions and potential implications for viticulture In: Proc. VIIth international viticultural terroir congress 19-23 May 2008, Nyon, Switzerland. pp. 216-221.

Bonnardot, V. & Cautenet, S., 2009. Mesoscale atmospheric modeling using a high horizontal grid resolution over a complex coastal terrain and a wine region of South Africa. J. Appl. Meteorol. Climatol. 48, 330-348.

Bonnardot, V., Planchon, O., Carey, V. & Cautenet, S., 2002. Diurnal wind, relative humidity and temperature variation in the Stellenbosch-Groot Drakenstein wine-growing area. S. Afr. J. Enol. Vitic. 23, 62-71.

Bonnardot, V., Planchon, O. & Cautenet, S., 2005. Sea breeze development under an offshore synoptic wind in the South-Western Cape and implications for the Stellenbosch wine-producing area. Theor. Appl. Climatol. 81, 203-218.

Bonnardot, V., Sturman, A.P., Iman, S., Payman, Z.-R., Jacobus, H. & Quenol, H., 2011. Investigation of grapevine areas under climatic stress using high-resolution atmospheric modelling : case studies in South Africa and New Zealand. In: Proc. 19th International Congress on Biometeorology, 4-8 December 2011, Auckland, paper 338, pp 6.

Buys, M., 1971. The use of electronic resources and statistical techniques in the evaluation of the agro-climate in the South Western Cape (in Afrikaans). Thesis, Stellenbosch University, Private Bag X1, 7602 Matieland (Stellenbosch), South Africa.

Carey, V., A., Archer, E. & Saayman, D., 2002. Natural terroir units: What are they? How can they help the wine farmer? WineLand, February, 86-88.

Carey, V., Archer, E., Barbeau, G. & Saayman, D., 2007. The use of local knowledge relating to vineyard performance to identify viticultural terroirs in Stellenbosch and surrounds. Acta Horticulturae 754, 385-392.

Carey, V.A., 2001. Spatial characteristic of natural terroir units for viticulture in the Bottelaryberg-Simonsberg-Helderberg winegrowing area. Thesis, Stellenbosch University, Private Bag X1, 7602 Matieland (Stellenbosch), South Africa.

Carey, V.A., 2005. The use of viticultural terroir units for demarcation of geographical indications for wine production in Stellenbosch and surrounds. Dissertation, Stellenbosch University, Private Bag X1, 7602 Matieland (Stellenbosch), South Africa.

Carey, V.A., Archer, E., Barbeau, G. & Saayman, D., 2008. Viticultural terroirs in stellenbosch, South Africa. II. The interaction of Cabernet Sauvignon and Sauvignon blanc with Environment. J. Int. Sci. Vigne Vin. 42, 185-201.

Carter, S., 2006. The projected influence of climate change on the South African wine industry. *In* IIASA Interim Report. pp. 33.

Chase, B.M. & Meadows, M.E., 2007. Late Quaternary dynamics of southern Africa's winter rainfall zone. Earth-Science Reviews 84, 103-138.

Conradie, D.C.U., 2012. South Africa's climatic zones: today, tomorrow. International Green Building Conference and Exhibition: Future Trends and Issues Impacting on the Built Environment, 25-26 July 2012, Sandton, South Africa, pp. 1-9.

Conradie, W., J., Carey, V.A., Bonnardot, V., Saayman, D. & Van Schoor, L., H, 2002. Effect of different environmental factors on the performance of Sauvignon blanc grapevines in the Stellenbosch/Durbanville districts of South Africa. I. Geology, soil, climate, phenology and grape composition. S. Afr. J. Enol. Vitic. 23, 78-91.

Coombe, B., 1987. Influence of temperature on composition and quality of grapes. ISHS Acta Horticulturae, 206, 25-35.

De Villiers, F.S., Scmidt, A., Theron, J.C.D. & Taljaard, R., 1996. Onderverdeling van die Wes-Kaapse wynbougebiede volgens bestaande klimaatskriteria. Wynboer Tegnies, January 1996, 10-12.

DEA, 2013. Long-Term Adaptation Scenarios Flagship Research Programme (LTAS) for South Africa. *In* Climate trends and scenarios for South Africa. Phase 1, technical report 1. Department of Environmental Affairs, Pretoria, South Africa.

Deloire, A., Howell, C., Habets, I., Botes, M.P., Van Rensburg, P., Bonnardot, V. & Lambrechts, M., 2009. Preliminary results on the effect of temperature on Sauvignon blanc (Vitis vinifera L.) berry ripening. Comparison between different macro climatic wine regions of the Western Cape Coastal area of South Africa. Presented at the 32st conference of the South African Society for Enology and Viticulture, July 2009, Cape Town, South Africa.

Deloire, A., Vaudour, E., Carey, V.A., Bonnardot, V. & Van Leeuwen, C., 2005. Grapevine responses to terroir: a global approach. J Int Sci Vigne et Vin, Vol 39(4) 149-162.

Downey, M., Harvey, J. & Robinson, S., 2004. The effect of bunch shading on berry deveopement and flavonoid accumulation in Shiraz grapes. Aust. J. Grape Wine Res. 10, 55-73.

Duchêne, E. & Schneider, C., 2005. Grapevine and climatic changes: a glance at the situation in Alsace. Agronomy for Sustainable Development 25, 93-99.

Engelbrecht, C.J. & Engelbrecht, F.A., 2016. Shifts in Köppen-Geiger climate zones over southern Africa in relation to key global temperature goals. Theor. Appl. Climatol. 123, 247-261.

Fraga, H., Costa, R., Moutinho-pereira, J. & Correia, C.M., 2015. Modeling Phenology , Water Status , and Yield Components of Three Portuguese Grapevines Using the STICS Crop Model. Am. J. Enol. Vitic. 66, 482-491.

Freeman, B., M., Kliewer, M.W. & Stern, P.M., 1982. Influence of windbreaks and climatic region on diurnal fluctuation of leaf water potential, stomatal conductance, and leaf temperature of grapevines. Am. J. Enol. Vitic 33, 233.

Gladstones, J., 1992. History of climate selection for Australian viticulture. Viticulture and Environment. Winetitles, Adelaide., 4-7.

Hall, A. & Jones, G.V., 2010. Spatial analysis of climate in winegrape-growing regions in Australia. Aust. J. Grape Wine Res. 16, 389-404.

Hannah, L., Roehrdanz, P.R., Ikegami, M., Shepard, a.V., Shaw, M.R., Tabor, G., Zhi, L., Marquet, P.A. & Hijmans, R.J., 2013. Climate change, wine, and conservation. Proceedings of the National Academy of Sciences 110, 6907-6912.

Hijmans, R.J., Cameron, S.E., Parra, J.L., Jones, P.G. & Jarvis, A., 2005. Very high resolution interpolated climate surfaces for global land areas. Int. J. Climatol. 25, 1965-1978.

Hochberg, U., Degu, A., Fait, A. & Rachmilevitch, S., 2013. Near isohydric grapevine cultivar displays higher photosynthetic efficiency and photorespiration rates under drought stress as compared with near anisohydric grapevine cultivar. Physiol. Plantarum 147, 443-452.

Hudson, D. & Jones, R., 2002. Regional climate model simulations of present-day and future climates of southern Africa. Hadley Centre Technical Note 39, 41.

Huglin, P., 1978. New method for evaluating the potential of solar thermal environments wine. In: Proc. International Symposium on Ecology of Grapevine, I, Constance, Romania, 1978. Ministry of Agriculture and Food Industry, pp. 89-98.

Hulme, M., Doherty, R., Ngara, T., New, M. & Lister, D., 2001. African climate change: 1900–2100. Climate Res. 17, 146-168.

Hunter, J.J. & Bonnardot, V., 2011. Suitability of some climatic parameters for grapevine cultivation in South Africa, with focus on key physiological processes. S. Afr. J. Enol. Vitic 32, 137-154.

Hunter, J.J. & Deloire, A., 2005. Relationship between sugar loading and berry size of ripening Syrah/R99 grapes as affected by grapevine water status. In: Proc. Gesco XIVeme journees du groupe europeen d'etude des systems de conduit de la vigne, 2005, Geisenheim, Germany. pp. 23-27, 127-133.

Hunter, J.J., Volschenk, C.G. & Bonnardot, V., 2010. Linking grapevine row orientation to a changing climate in South Africa. In: Proc. Intervitis Interfructa Conference, 24-28 March, Stuttgart, Germany pp. 60-70.

IPCC, 2007. Summary for Policymakers. In:Parry, M.L., Canziani, O.F., Palutikof, J.P., van der Linden, P.J. and Hanson, C.E. (eds). Climate change 2007. Impacts, adaptation and vulnerability. *In* Fourth Assessment Report of the Intergovernmental Panel on Climate Change. Cambridge University Press, Cambridge, UK.

IPCC, 2014. Climate Change 2014: Synthesis Report. In: Pachauri, R. K. and Meyer, L.A. (eds). Fifth Assessment Report of the Intergovernmental Panel on Climate Change, Geneva, Switzerland.

Jones, G., 2006. Climate and terroir: Impacts of climate variability and change on wine. In: Macqueen, R.W. and Meinert, L.D. (eds). Fine wine and terroir-The geoscience perspective. Geoscience Canada, (Geological Association of Canada, St John's, Newfoundland). pp. 1-14.

Jones, G.V., 2007. Climate Change: observations, projections and general implications for viticulture and wine production. Vasa, 17.

Jones, G.V. & Davis, R.E., 2000. Climate influences on grapevine phenology, grape composition, and wine production and quality for Bordeaux, France. Am. J. Enol. Vitic. 51, 249-261.

Jones, G.V., Duff, A.A., Hall, A. & Myers, J.W., 2010. Spatial analysis of climate in winegrape growing regions in the western United States. Am. J. Enol. Vitic. 61, 313-326.

Jones, G.V., White, M.A., Cooper, O.R. & Storchmann, K., 2005. Climate change and global wine quality. Climatic Change 73, 319-343.

Joubert, S.J., 2007. High-resolution climatic variable generation for the Western Cape. Geology, geography & environmental studies. Thesis, Stellenbosch University, Private Bag X1, 7602 Matieland (Stellenbosch), South Africa.

Kennedy, J.A., 2002. Understanding grape berry development. Practical Winery & Vineyard, July/August 2002.

Knight, F., 2006. A Macro scale analysis of the vineyard production potential of the RSA. Winelands, November, 2006.

Kruger, A.C. & Shongwe, S., 2004. Temperature trends in South Africa: 1960-2003. Int. J. Climatol. 24, 1929-1945.

Le Roux, E.G., 1974. A climate classification for the South Western Cape viticultural areas (in Afrikaanse). Thesis, Stellenbosch University, Private Bag X1, 7602 Matieland (Stellenbosch), South Africa.

Le Roux, R., Neethling, E., Van Leeuwen, C., De Resseguier, L., Madelin, M., Bonnefoy, C., Barbeau, G. & Quenol, H., 2015. Multi-scalar modelling of climate applied to european vineyard sites in the climate change context. Procedia Environmental Sciences 29, 62-63.

Long, S.P., 1991. Modification of the response of photosynthetic productivity to rising temperature by atmospheric CO_2 concentrations. Has its importance been underestimated? . Plant Cell Environ. 14, 729-739.

Mariani, L., Alilla, R., Cola, G., Monte, G.D., Epifani, C., Puppi, G. & Osvaldo, F., 2013. IPHEN—a real-time network for phenological monitoring and modelling in Italy. Int. J. Biometeorol. 57, 881-893.

McGuffie, K. & Henderson-Sellers, A., 2005 (3rd ed). A climate Modelling Primer. John Wiley & Sons, Toronto.

McIntyre, G.N., Kliewer, W.W. & Lider, L.A., 1987. Some limitations of the degree day system as used in viticulture in california USA. Am. J. Enol. Vitic. 38, 128-132.

Mehmel, T.O., 2010. Effect of climate and soil water status on Cabernet Sauvignon (Vitis vinifera L.) grapevines in the Swartland region with special reference to sugar loading and anthocyanin biosynthesis. Thesis, Stellenbosch University, Private Bag X1, 7602 Matieland (Stellenbosch), South Africa.

Midgley, G.F., Chapman, R.A., Hewitson, B., Johnston, P., De Wit, M., Ziervogel, G., Mukheibir, P., Van Niekerk, L., Tadross, M., Van Wilgen, B.W., Kgope, B., Morant, P.D., Theron, A., Scholes, R.J. & Forsyth, G.G., 2005. A Status Quo, Vulnerability and Adaptation Assessment of the Physical and Socio-Economic Effects of Climate Change in the Western Cape. CSIR Environmentek, Stellenbosch CSIR Report No. ENV-S-C 2005-073.

Midgley, G.F., New, M., Johnston, P., Methner, N., Cole, M., Cullis, J., Drimie, S., Dzama, K., Guillot, B., Harper, J., Jack, C., Knowles, T., Louw, D., Mapiye, C., Oosthuizen, H.J. & Smit, J., 2015. A status quo review of climate change and the agriculture sector of the Western Cape Province. CSIR Environmentek, Stellenbosch CSIR. CSIR, P.O. Box 395; Pretoria 0001; South Africa.

Midgley, G.F., New, M., Methner, N., Cole, M., Cullis, J., Drimie, S., Dzama, K., Guillot, B., Harper, J., Jack, C., Johnston, P., Knowles, T., Louw, D., Mapiye, C., Oosthuizen, H.J., Smit, J. & Van dern Broeck, D., 2016. A status quo review of climate change and the agriculture sector of the Western Cape Province. CSIR Environmentek, Stellenbosch CSIR Report No. ENV-S-C 2005-073. CSIR, P.O. Box 395; Pretoria 0001; South Africa.

Moffat, T., 2013. Sensor technology to assess grape bunch temperature variability in Vitis vinifera L. cv. Shiraz. Thesis, Stellenbosch University, Private Bag X1, 7602 Matieland (Stellenbosch), South Africa.

Mountinho-Pereira, J., Gonçalves, B., Bacelar, E., Boaventura Cunha, J., Coutinho, J.F. & Coffeia, C.M., 2009. Effects of elevated CO_2 on grapevine (*Vitis vinifera* L.):Physiological and yield attributes. Vitis 48, 159-165.

Myburgh, P., 2005. Effect of altitude and distance from the Atlantic Ocean on mean February temperatures in the Western Cape Coastal region. Wynboer Technical Yearbook, 49-52.

Neteler, M., 2010. Estimating daily land surface temperatures in mountainous environments by reconstructed MODIS LST data. Remote Sens. 2, 333-351.

Noble, A.C., Elliott Fisk, D.L. & Allen, M.S., 1995. Vegetative flavor and methoxypyrazines in Cabernet Sauvignon. Fruit Flavors 596, 226-234.

Ollat, N., Tandonnet, J.P., Lafontaine, M. & Schultz, H.R., 2003. Short and long term effects of three rootstocks on Cabernet Sauvignon vine behaviour and wine quality. Acta Horticulturae 617, 95-101.

Oosthuizen, H.J., 2014. Modelling the financial vulnerability of farming systems to climate change in selected case study areas in South Africa. Thesis, Stellenbosch University, Private Bag X1, 7602 Matieland (Stellenbosch), South Africa.

Parker, A.K., De Cortázar-Atauri, I.G., Van Leeuwen, C. & Chuine, I., 2011. General phenological model to characterise the timing of flowering and veraison of Vitis vinifera L. Aust. J. Grape Wine Res. 17, 206-216.

Peel, M.C., Finlayson, B.L. & Mcmahon, T.A., 2007. Updated world map of the Köppen-Geiger climate classification. Hydrology and Earth System Sciences Discussions 4, 439-473.

Peterson, R.G. & Stramma, L., 1991. Upper-level circulation in the South Atlantic Ocean. Progress in Oceanography 26, 1-73.

Reason, C., Engelbrecht, F., Landman, W., Lutjeharms, J., Piketh, S., Rautenbach, C. & Hewitson, B., 2006a. A review of South African research in atmospheric science and physical oceanography during 2000–2005. S. Afr. J. Sci. 102.

Reason, C.J.C., Engelbrecht, F., Landman, W.A., Lutjeharms, J.R.E., Piketh, S., Rautenbach, C.J.D. & Hewitson, B.C., 2006b. A review of South African research in atmospheric science and physical oceanography during 2000-2005. S. Afr. J. Enol. Vitic. 102, 35-45.

Reason, C.J.C. & Jury, M.R., 1990. On the generation and propagation of the southern African coastal low. Quarterly Journal of the Royal Meteorological Society 116, 1133-1151.

Robinson, J., 1994. Appellation contrôlée. In: Robinson, J. (ed.). The Oxford companion to wine.Oxford University Press, Oxford. pp. 40-42.

Roux, B., 2009. Ultra high-resolution climate simulations over the Stellenbosch wine producing region using a variable-resolution model by model. Thesis, Pretoria University, South Africa.

Saayman, D., 1977. The effect of soil and climate on wine quality. International symposium on the quality of the vintage, 14-21 February, 1977, Cape Town, South Africa.

Saayman, D., 1999. The development of vineyard zonation and demarcation in South Africa. WineLand, January, T2-T5.

Saayman, D., 2010. Rootstock choice: The South African experience. WineLand, October 2010.

Saayman, D., 2014. South African vineyard soils and climates. Wines of South Africa, (www.wosa.co.za), January 2013.

Saayman, D. & Kleynhans, P.H., 1978. The effect of soil type on wine quality. S.A. Society for Enology and Viticulture, Proceedings, Oct., 105-119.

SAWIS, 2015. South African wine industry statistic. South African Wine Industry Information and Systems. Paarl. http://www.sawis.co.za/.

SAWIS, 2016. South African wine industry statistic. South African Wine Industry Information and Systems. Paarl. http://www.sawis.co.za/.

Schultz, H., 2000. Climate change and viticulture: A European perspective on climatology, carbon dioxide and UV-B effects. Aust. J. Grape Wine Res. 6, 2-12.

Schultz, H.R., 2003a. Differences in hydraulic architecture account for near-isohydric and anisohydric behaviour of two field-grown Vitis vinifera L. cultivars during drought. Plant, Cell Environ. 26, 1393-1405.

Schultz, H.R., 2003b. Extension of a Farquhar model for limitations of leaf photosynthesis induced by light environment, phenology and leaf age in grapevines (*Vitis vinifera* L. *cv*. White Riesling and Zinfandel). Funct. Plant Biol. 30, 673-687.

Schultz, H.R. & Jones, G.V., 2010. Climate Induced Historic and Future Changes in Viticulture. http://dx.doi.org/10.1080/09571264.2010.530098.

Schultz, H.R. & Stoll, M., 2010. Some critical issues in environmental physiology of grapevines: future challenges and current limitations. Aust. J. Grape Wine Res. 16, 4-24.

Schulze, R.E., 1997. South African Atlas of Agrohydrology and Climatology. WRC Report No TT 82/96. Water Research Commission. Private Bag X103, Gezina, Pretoria, 0031, South Africa.

Schulze, R.E., 2011. A 2011 Perspective on Climate Change and the South African Water Sector. In WRC Report 1843/2/11. Water Research Commission, Pretoria

Schulze, R.E. & Maharaj, M., 2006. Temperature database. *In* South African Atlas of Climatology and Agrohydrology. WRC Report No. 1489/1/06. Schulze, R.E. (ed.), Water Research Commission, Pretoria, South Africa.

Smart, R., Robinson, J., Due, G. & Brien, C., 1985. Canopy microclimate modification for the cultivar Shiraz. I. Definition of canopy microclimate. Vitis 24, 17-31.

Smart, R.E., 1985. Principles of grapevine canopy microclimate manipulation with Implications for yield and quality. A review. Am. J. Enol. Vitic. 36, 230-239.

Smart, R.E. & Dry, P.R., 1980. A climatic classification for Australian viticultural regions. Aust. Grapegrow. Winem. 196, 9-16.

Smuts, F., 1979. Die stigting van Stellenbosch. In Smuts, F. (ed). Stellenbosch drie eeue. Stellenbosch City Council, Stellenbosch. pp. 51-66.

Soltanzadeh, I., Bonnardot, V., Sturman, A., Quénol, H. & Zawar-Reza, P., 2016. Assessment of the ARW-WRF model over complex terrain: the case of the Stellenbosch Wine of Origin district of South Africa. Theor. Appl. Climatol., 1-21.

Spayd, S.E., Tarara, J.M., Mee, D.L. & Ferguson, J.C., 2002. Separation of sunlight and temperature effects on the composition of Vitis vinifera cv.Merlot berries. Am. J. Enol. Vitic. 53, 171-182.

Theron, J.N., 1995. The Geology of the Cape Town area. Department of Mineral and Energy Affairs, Pretoria, South Africa.

Tonietto, J. & Carbonneau, A., 2004. A multicriteria climatic classification system for grape-growing regions worldwide. Agricultural Forest Meteorol. 124, 81-97.

Tyson, P.D., Cooper, G.R.J. & McCarthy, T.S., 2002. Millennial to multi-decadal variability in the climate of southern Africa. Int. J. Climatol. 22, 1105-1117.

Vaudour, E., 2002. The quality of grapes and wine in relation to geography: Notions of terroir at various scales. J. Wine Res. 13, 117-141.

Van Huyssteen, T., 1983. Hart van die Boland. Deel een: Die Nedelandse komponent. Tafelberg, Cape Town.

Van Leeuwen, C., Friant, P., Choné, X., Tregoat, O., Koundouras, S. & Dubourdieu, D., 2004. Influence of climate, soil, and cultivar on terroir. Am. J. Enol. Vitic. 3, 207-217.

Van Leeuwen, C., Schultz, H.R., Garcia de Cortazar-Atauri, I., Duchêne, E., Ollat, N., Pieri, P., Bois, B., Goutouly, J.-P., Quénol, H., Touzard, J.-M., Malheiro, A.C., Bavaresco, L. & Delrot, S., 2013. Why climate change will not dramatically decrease viticultural suitability in main wine-producing areas by 2050. Proceedings of the National Academy of Sciences 110, 3051-3052.

Van Niekerk, A. & Joubert, S.J., 2011. Input variable selection for interpolating high-resolution climate surfaces for the Western Cape. Water SA 37, 271-280.

Van Schalkwyk, D., 2013. The impact of climate change on the bud and flowering dates of grapevine cultivars at Nietvoorbij in Stellenbosch. Wynboer, January, 62-66.

Van Zyl, D.J., 1975. Kaapse Wyn en Brandewyn 1795-1860. Hollandsch Afrikaansche Uitgewers Maatschappij.

Van Zyl, D.J., 1979. Ekonomie: Landbou In: Smuts F (ed.), Stellenbosch drie eeue. Stellenbosch City Council, Stellenbosch. pp. 177-206.

Vink, N., Deloire, A., Bonnardot, V. & Ewert, J., 2010. Terroir, climate change, and the future of South Africa's wine industry. J. British Sociolog. Ass., 7-9.

Wang, Z.P., Deloire, A., Carbonneau, A., Federspiel, B. & Lopez, F., 2003a. An in vivo experimental system to study sugar phloem unloading in ripening grape berries during water deficiency stress. Ann. Bot. London 92, 523-528.

Wang, Z.P., Deloire, A., Carbonneau, A., Federspiel, B. & Lopez, F., 2003b. Study of sugar phloem unloading in ripening grape berries under water stress conditions. J. Int. Sci. Vigne Vin.

Webb, L., Whetton, P. & Barlow, E.W.R., 2007a. Modelled impact of future climate change on phenology of wine grapes in Australia. Aust. J. Grape Wine Res. 13, 165-175.

Webb, L.B., Whetton, P.H. & Barlow, E.W.R., 2007b. Modelled impact of future climate change on the phenology of winegrapes in Australia. Aust. J. Grape Wine Res. 13, 165-175.

Webb, L.B., Whetton, P.H. & Barlow, E.W.R., 2008. Modelling the relationship between climate, winegrape price and winegrape quality in Australia. Climate Res. 36, 89-98.

Webb, L.B., Whetton, P.H., Bhend, J., Darbyshire, R., Briggs, P.R. & Barlow, E.W.R., 2012. Earlier wine-grape ripening driven by climatic warming and drying and management practices. Nature Climate Change 2, 259-264.

Zhang, H., Pu, Z. & Zhang, X., 2013. Examination of Errors in Near-Surface Temperature and Wind from WRF Numerical Simulations in Regions of Complex Terrain. Weather and Forecasting 28, 893-914.

Zorer, R., Rocchini, R., Delucchi, L., Zottele, F., Meggio, F. & Neteler, M., 2011. Use of multi-annual MODIS land surface temperature data for the characterization of the heat requirements for grapevine varieties. In: Proc. Analysis of Multi-temporal Remote Sensing Images (Multi-Temp), 2011 6th International Workshop pp. 225-228.

Zorer, R., Rocchini, D., Metz, M., Delucchi, L., Zottele, F., Meggio, F. & Neteler, M., 2013. Daily MODIS land surface temperature data for the analysis of the heat requirements of grapevine varieties. IEEE T. Geosci. Remote 51, 2128-2135.

Chapter 3

Literature review

Satellite remote sensing and its application in agriculture to monitor land surface temperature

CHAPTER 3: SATELLITE REMOTE SENSING AND ITS APPLICATION IN AGRICULTURE TO MONITOR LAND SURFACE TEMPERATURE

3.1 Introduction

Remote sensing is the observation of the Earth's land and water surfaces by means of reflected or emitted energy from an overhead perspective using radiation in one or more regions of the electromagnetic spectrum (Campbell & Wynne, 2011). The land surface temperature (LST) product is a basic determinant of the terrestrial thermal behaviour, measuring the effective radiating temperature of the Earth's surface. Simply put, LST is the radiative skin temperature of the land derived from solar radiation, how hot the "surface" of the Earth would feel to the touch in a particular location (ESA, 2016).

Remote sensing is the science of investigating an object without touching it (Fischer *et al.*, 1976). The origins of remote sensing, as described by Campbell and Wynne (2011), emanates from the 1800's with the practice of photography. Many improvements have been made in photographic technology and methods of acquiring photographs of the Earth from balloons, kites, and use of powered aircraft as a platform for cameras over the years. Tailored cameras for use on aircrafts opened up the science of photogrammetry which is the practice of making accurate measurements from photographs, with instruments specifically designed for image analysis. World War II (1939-1945) saw great advancements in the use of the electromagnetic spectrum for the collection of images extending from the visible to infrared and microwave ranges. In the late 1960's, the CORONA strategic reconnaissance satellite combining aircraft and camera, extended aviation and optical systems far beyond their limits, as the satellite provided the ability to routinely collect imagery from space. Remote sensing was first applied in plant sciences with the use of infrared film for the identification of diseases in small grain cereal crops, marking a milestone in the development of remote sensing and plant sciences. In the mid to late 1900's aerial photography had been institutionalised in both government and civil society as a reliable source of information.

The National Oceanic and Atmospheric Administration (NOAA) satellites have a very long and distinguished history. The first meteorological satellite (TIROS-1, Television and Infrared Observation Satellite) was launched in 1960, designed for climatological and meteorological observations, and used as a basis for later developments. These developments extended the reach of aerial observations outside of the visible spectrum into the infrared and microwave regions (remote sensing), allowing image acquisition during both night and day. The U.S. National Aeronautics and Space Administration (NASA) established a research programme in remote sensing in 1960. During the same period, the U.S. National Academy of Sciences (NAS) looked into opportunities for the application of remote sensing in the field of agriculture and forestry (Campbell & Wynne, 2011).

3.2 Satellite remote sensing

The launch of Landsat 1 in 1970 marked a milestone as the first of many Earth-orbiting satellites designed for land mass observation. Landsat provides systematic repetitive observations of the Earth's land areas, with each image depicting large areas of its surface in several regions of the electromagnetic spectrum. Hence, the world relies on Landsat data to detect and measure land cover/land use change, the health of ecosystems, and water availability (NASA, 2015). Landsat's

main contribution is the routine availability of multispectral data for large regions, which expanded the interest in analysis of multispectral data. The routine availability of digital data in a standard format created the context for the growth in popularity of digital analysis and development of image analysis software that is now readily available.

The evolution of the Landsat mission is described in Figure 1, with the Landsat 1 programme providing a model for future developments and improvements of other land observation satellites. The launch of Landsat 2, Landsat 3, and Landsat 4 followed in 1975, 1978, and 1982, respectively, with higher resolution imaging capabilities, collecting imagery at resolutions of 30 m, 20 m and 10 m, improving to 0.5- 1 m by the 1990's. When Landsat 5 was launched in 1984, it continued to deliver high quality global data for 28 years, officially setting a new Guinness World Record for "longest-operating Earth observation satellite". Landsat 6 failed to achieve orbit in 1993, Landsat 7 was successfully launched in 1999 and along with Landsat 8, launched in 2013, continues to provide daily global data (USGS, 2015).

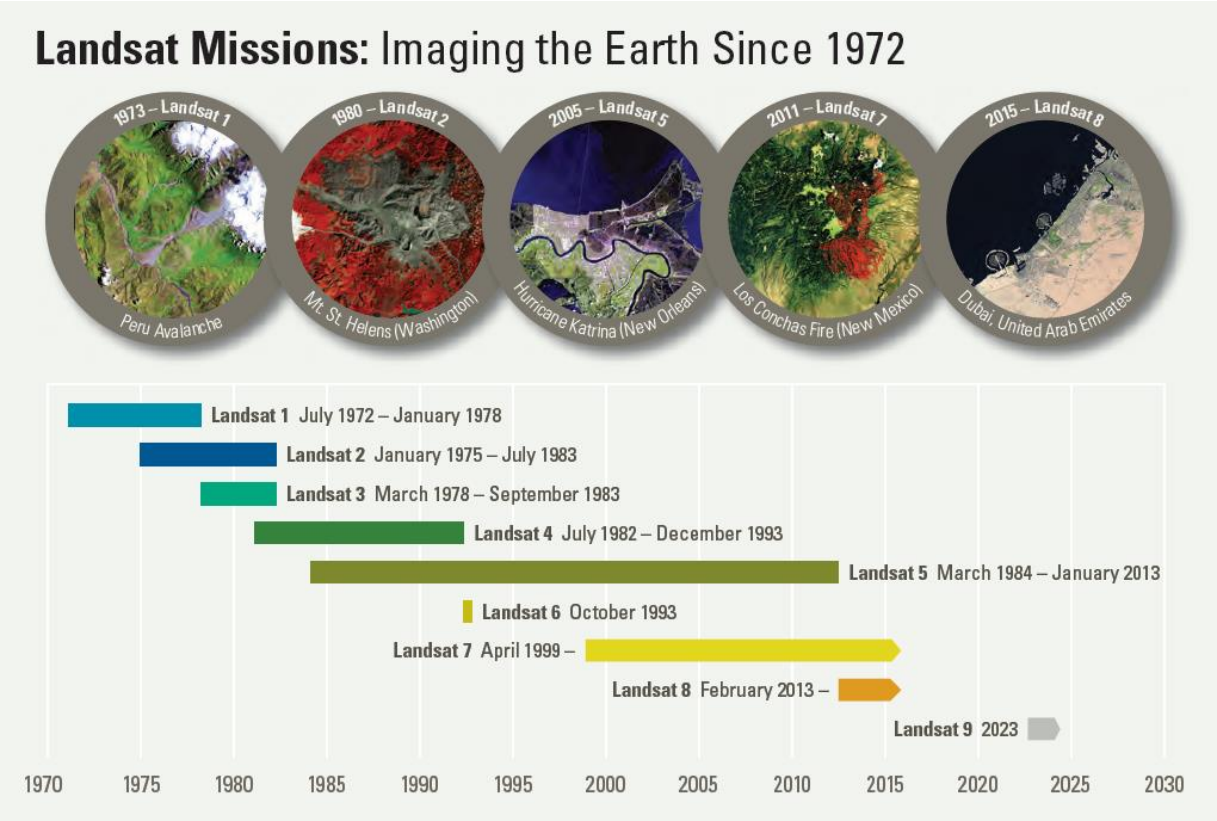

Figure 1 Timeline and history of the Landsat Missions, which started in 1972 (USGS, 2015).

By the late 1900's, satellite systems had been designed specifically to collect remotely sensed data representing the entire surface of the Earth. Landsat offered the capability in principle but, in practice, has a resolution which is too fine (<100 m) for effective global remote sensing. Therefore, Landsat requires sensors and processing techniques specifically designed to acquire broad-scale coverage with course spatial resolution (over kilometres) and high temporal resolution. This ensures the imaging of the entire earth at more frequent intervals to sufficiently monitor the terrestrial activity and change over the entire globe. As of 1978, NOAA satellites were equipped with the Advanced Very High Resolution Radiometer (AVHRR), an instrument sensing in the visible, near infrared, mid-infrared and thermal infrared portions of the electromagnetic spectrum (NOAA, 2016). Since 1981 land surface processes (daily time series of satellite data) have been

successfully monitored by the initiation of the remote sensing techniques using the AVHRR (Justice *et al.*, 1985; Neteler, 2010). Long term remote sensing data records have incorporated AVHRR data into the modern product generation.

The advent of a new era of remote sensing systems started in 1997 and 1998 with the launch of Sea-Viewing Wide Field-of-View Sensor (SeaWiFS) and SPOT VEGETATION, respectively, and has been complemented with Moderate Resolution Imaging Spectroradiometer (MODIS) and Medium Resolution Imaging Spectrometer (MERIS) in the new millennium. MODIS improves on the performance of AVHRR by providing higher spatial resolution and greater spectral resolution, but like AVHRR produces daily LST maps with global coverage (Neteler, 2010). In 1999, NASA launched Terra-1, the first satellite of a system specifically designed with global coverage to monitor change in the nature and extent of the Earth's ecosystem (Zhang *et al.*, 2004; Campbell & Wynne, 2011). This was followed by the launch of Aqua in 2002 to collect information on the Earth's water cycle, originally developed for a six-year design life but has now far exceeded that original goal (NASA, 2016a). This opened up an era of broad scale remote sensing. Data collection starting in 2000, providing spatial patterns of environmental changes during recent years.

Terra collects data about the Earth's bio-geochemical and energy systems using five sensors integrated into a single platform as shown in Figure 2. The sensors observe the atmosphere, land surface, oceans, snow and ice, and energy budget of the earth. Each sensor has unique features that enable scientists to meet a wide range of scientific objectives, especially to monitor the earth's surface in the context of climate change. The different sensors have varying perspectives of the same event, and can therefore yield unique insights into the processes that connect Earth's systems. An overview on Terra and its instruments can be obtained from (NASA, 2016b).

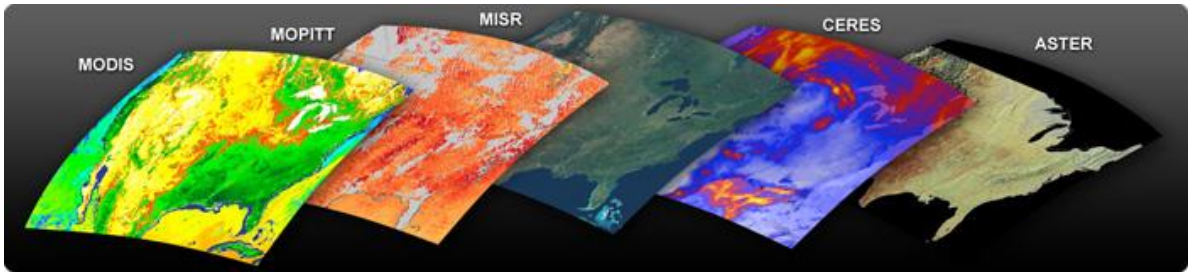

Figure 2 The five sensors imaging the Earth surface on board Terra (NASA, 2016b), namely MODIS (Moderate-resolution Imaging Spectroradiometer); MOPITT (Measurements of Pollution in the Troposphere); MISR (Multi-angle Imaging SpectroRadiometer); CERES (Clouds and the Earth's Radiant Energy System) and ASTER (Advanced Space borne Thermal Emission and Reflection Radiometer).

Aqua has six instruments on board. Of these six instruments, four of them, namely Atmospheric Infrared Sounder (AIRS), Advanced Microwave Sounding Unit (AMSU), Clouds and the Earth's Radiant Energy System (CERES), and Moderate-Resolution Imaging Spectroradiometer (MODIS) continued transmitting high-quality data. There was also reduced quality data from a fifth instrument, AMSR-E. The sixth Aqua instrument, HSB, collected approximately nine months of high quality data but failed in February 2003.

SeaWiFS and MERIS sensor design is oriented towards oceanographic applications, and the bands are limited to the visible and near infrared wavelengths. They have successfully been used for some terrestrial applications and land-cover classification. SPOT VEGETATION has only four spectral bands, limiting the discrimination of land-cover classes. MODIS, however, has 36 bands which cover a wider range of the electromagnetic spectrum, and offers a higher spatial resolution. With the heritage of multiple sensors including AVHRR, TM/ETM+, and CZCS, MODIS faces up to

the challenge to suit atmospheric, oceanographic, and terrestrial needs (Colditz & Dech, 2007). Taking the above-mentioned into consideration, MODIS is an ideal LST product to supplement meteorological temperature data for applications in agriculture and decision making in the context of climate change.

3.2.1 Processing of satellite remote sensing

The sensor data is formed when an instrument (camera or radar) views a physical object by recording electromagnetic radiation emitted or reflected from it. Data can be abstract (distorted) or foreign due to the overhead perspective, unusual resolution, and spectral region outside of the visible spectrum. Therefore, the analysis of satellite images is essential for the true accuracy of the intended image to be interpreted. F for interpretation, the factors interfering between the imaging and sensor needs to be removed. The corrected image can be analysed further for specific applications combining other geospatial data types to address specific practical problems. Some agricultural areas of application are listed in Figure 3 (Campbell & Wynne, 2011).

The remotely sensed images are therefore formed from many interrelated processes, simply described in Figure 3. Hence, an isolated focus of any single component in the processing chain results in a fragmented understanding of the image due to the many terrestrial factors influencing the image and the image containing a large amount of information in the spectra bands. Photogrammetric processing originally implemented the use of manual processes on mechanical instruments to monitor change from satellite images, but today there are highly efficient automated digital analyses. This has resulted in improvement in precision, streamlined acquisition, processing, production and the distribution of satellite remotely sensed data.

The Terra and Aqua satellites both image the entire surface temperature of the earth on a daily basis with the MODIS sensors. A crucial requirement of the land community is a complete and accurate atmospheric correction, including scattering reduction and correction for aerosol and ozone. This can be corrected using a radiation transfer models (based on measured atmospheric variables) for the accurate surface reflectance retrieval. The corrections result in a more accurate thermal layer of the earth surface, however the clouds on the surface of the earth reflects negative values, resulting is some areas of the image depicting the incorrect surface values. Hence, more processing is required for accurate sub-pixel cloud identification, especially for land studies and even more so LST studies in the context of climate change. Continuous LST maps are required for accumulative thermal time calculations relating to the grapevines growth expression over the growing seasons.

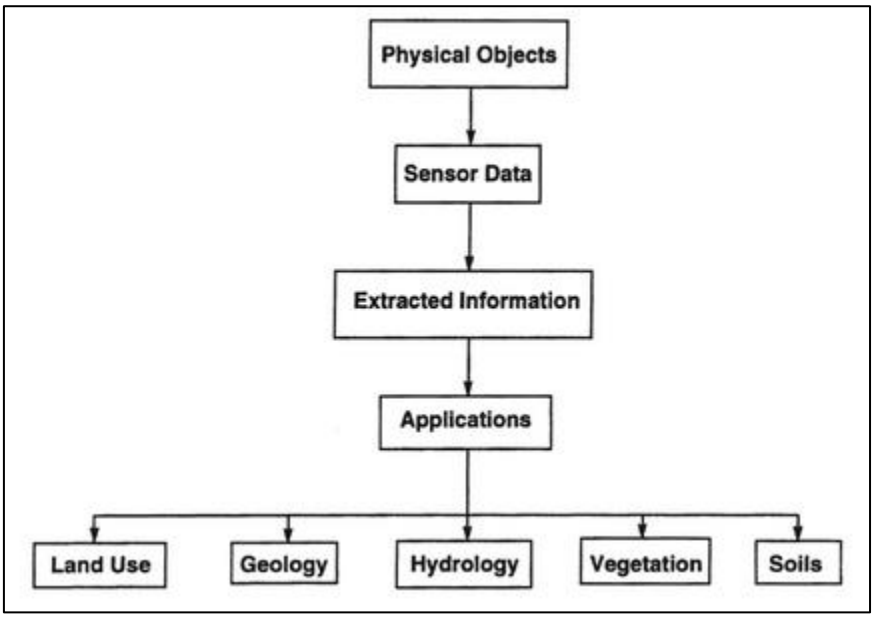

Figure 3 Overview of the remote sensing process and uses in agriculture (Campbell & Wynne, 2011).

3.2.2 Geospatial data

Technologies advanced and converged in the early 2000's to create systems with unique capabilities that each enhanced and reinforced the value of the others to create geospatial data, a term applied collectively to technologies such as primarily remote sensing, geographic information systems (GIS) and global positioning systems (GPS) (Neteler *et al.*, 2012). The progress in the field of remote sensing advanced in parallel with advances in GIS, providing the ability to bring remotely sensed data and other geospatial data into a common analytical framework to support practical applications, mapping of urban infrastructures, precision agriculture and floodplain mapping *etc.* (Campbell & Wynne, 2011). Geospatial data has a geographic component in space and time, meaning that the records in datasets have locational information tied to them such as geographic data in the form of coordinates. Some of the geospatial datasets used in terroir studies are GIS data (soil maps, climate interpolations), GPS data (vineyard sites, specific point measurements) and satellite imagery (LST, NDVI *etc.*).

The needs of the application will determine the spatial and temporal resolution required from the satellite remote sensing images, where spatial resolution refers to the pixel size of the data collected by the sensor. For example, Landsat collects relatively high resolution imagery (clearly focused, with pixels ranging from 15 - 60 m) whereas the AVHRR collects coarse resolution imagery (pixels are >1 km across). Temporal resolution refers to the time frequency with which sensors can collect data from the same place. The AVHRR and Vegetation (VGT) sensors collect data from a particular region every day, whereas Landsat 8, returns data every 16 days (also termed the revisit time of the satellite). The multispectral data collected from such sensors can be combined (*i.e.* in vegetation indices) or used as input for models to develop measurements for specific field applications (Kerr & Ostrovsky, 2003; Neteler *et al.*, 2011; Zorer *et al.*, 2011). Sensor selection is application driven, *e.g.* the leaf area index (LAI) and normalised difference vegetation index (NDVI) show that SPOT and Landsat could predict LAI with acceptable accuracy, but MODIS and AVHRR cannot quantify the spatial variation in LAI measurements, but MODIS is able to provide land surface temperatures at higher temporal resolutions (Kerr & Ostrovsky, 2003). Depending on the spatial and temporal resolution of satellites, they have very significant roles to play in viticulture, especially in the context of climate change.

Over the past few years, a growing number of open source applications are available. Open source refers to software with source code that anyone can inspect, modify and enhance, allowing the development of interrelated technologies to form integrated systems that can acquire imagery and data (Neteler, 2010; Neteler *et al.*, 2012). In the open source platform, GIS, Web mapping and GPS projects are established with different goals, with projects of open source interaction listed on the "FreeGIS portal" (FreeGIS, 2016). These projects link programmers to solve problems and advance geospatial processing at a faster pace. In 2006, the open source geospatial foundation (OSGeo) was created to support and promote worldwide use and collaborative development of open source geospatial technologies and data (Neteler & Mitasova, 2008). Open source resources are becoming more available to aid in the processing of remote sensing data sets, increasing the precision and integrity of the applications, forming fully integrated and synergistic instruments that each reinforce the value of the other (Campbell & Wynne, 2011).

Scientists are finding new ways to approach their research in the utilisation of the open source geospatial tools and data available (to a large extent also freely available). A variety of agricultural (Benali *et al.*, 2012; Zorer *et al.*, 2013) and ecological (Kerr & Ostrovsky, 2003) applications require data from broad spatial extents, which is difficult or impossible to collect through field-based methods. Traditional field data does not translate readily to regional or global extents, and models derived purely from such local data are unlikely to predict the global consequences of human activities (Kerr & Ostrovsky, 2003; Neteler, 2010). However, the use of remote sensing has the advantage of being intrinsically spatialised and representing global to regional areas with spatial and temporal resolutions based on the applications required. Remote sensing compliments the information that can be attained with the traditional field observations, that in the light of remote sensing is seen to be very limited resource. The integration of these layers provides new and innovative ways to approach terroir related research, as there is the capability to integrate remote sensing data, vineyard block information and weather station interpolations into single datasets even with freely available software (Carey, 2005; Zorer *et al.*, 2013).

3.3 General satellite remote sensing applications

Human activities affect most of the terrestrial biosphere and are increasing in intensity therefore changes in our natural environment are becoming more pronounced. Satellite remote sensing is capable of monitoring the activity and development of species distribution, vegetation and environmental shifts over time (Colditz & Dech, 2007). Although with scientists improving their understanding of the factors limiting the distribution of species and environmental changes (Gaston, 2000), extinction rates and environmental shifts continue to accelerate (Kerr & Ostrovsky, 2003), and the use of satellite remote sensing can accelerate adaption to change.

Due to the complexity of the earth's biophysical systems, satellite images are sometimes the only means to comprehensively assess the surface characteristics of large areas. Spatially explicit methods have the potential to contribute greatly towards improved environment and water management from field to regional level. Specialised applications of remote sensing draw most extensively on a few satellite-borne optical remote sensors that vary in their respective spatial and temporal resolutions. Different methods have been developed to provide information at a range of temporal and spatial scales and hence for different applications.

A high temporal frequency of image acquisition, forming a time series of satellite data, can be employed for mapping the development of vegetation in space and time. The repeated measurements of multispectral data collected from remote sensing sensors can detect

photosynthetically active vegetation, phenological development and variability within seasons and sites. High temporal frequency and low spatial resolution is effective in the mapping LST of the entire globe on a daily basis (Neteler, 2010). Time series allows for detecting and assessing changes and multi-year transformation processes of high and low intensity, or even abrupt events such as fire and flooding (Colditz & Dech, 2007; Neteler, 2010).

Water is a finite resource in quality and quantity and its sustainable management requires careful planning, monitoring and management of environmental change. Global changes impose additional constraints such as an increase in extreme rainfall occurrences in amounts and distribution (droughts and floods), increase in temperature as well as changes in evaporation. Therefore, the quantification of the water cycle components is a fundamental requirement in the assessment and management of water resources, especially under the impacts of human induced land use and climate change (Jovanovic *et al.*, 2015).

For agricultural (field scale) applications, there are a number of models that have been developed, *eg.* the Surface Energy Balance Algorithm for Land (SEBAL) model developed by (Bastiaanssen *et al.*, 1998) to estimate aspects of the hydrological cycle, mapping the evapotranspiration (ET), biomass, growth, water deficit and soil moisture. The model has been applied operationally for field scale agricultural water management and evaluated extensively, locally and internationally in assessing the water use efficiency (WUE) of crops and identifying problem areas in terms of suboptimal yield (Jarmain *et al.*, 2013). Remote sensing is a key parameter in the SEBAL model and many other models, measuring the solar radiation reaching the crop, reflecting off the plants, and heating up the soil surface, with stressed plants radiating more heat than unstressed plants, on which irrigation strategies are based on. Therefore the mapping vegetation water status with remote sensing provides useful information to monitor plant drought stress (Penuelas and Et (1993) in text (Cheng *et al.*, 2013)), manage irrigation of agricultural crops (Ben-Gal *et al.*, 2009), and improve our understanding of the vegetation and climate relationship (Cheng *et al.*, 2013).

Spatial vegetative responses can be monitored using the NDVI, which combines reflected red and near infrared (NIR) radiation according to the simple equation: NDVI=(NIR−RED)/(NIR+RED) (Cheng *et al.*, 2013). Through its strong correlation with above ground net primary productivity and absorbed photosynthetically active radiation, the NDVI provides an index of ecosystem and vegetation function. Leaf area index (LAI) is a ground truth measurement and not a vegetative index per se, yet serving more specific purposes or that can reduce some errors associated with NDVI, such as sensitivity to differences in soil reflectance. Another biophysical variable related to optical remote sensing is vegetation canopy water content (CWC), which is the total amount of water accumulated in leaves per unit area (Cheng *et al.*, 2013). The diurnal CWC variation provides valuable information about the partitioning of surface energy and carbon exchange between vegetation and atmosphere, which increases our understanding of whether vegetation activities such as photosynthesis and evapotranspiration peak in the morning or afternoon (Wilson, 2005; Cheng *et al.*, 2013).

Satellite remote sensing data is able to provide information for improved site management in viticulture, especially using the MODIS images for more than just the LST product, but the incorporation of other spectral band for identifying grapevine reaction to the environment within a management block, isolating areas of stronger and weaker growth and adjusting management accordingly is recommended.

The Fruitlook programme, formerly known as Grapelook, is an industry based application of geospatial data integration using multiple satellite remote sensing images with specific application

requirements namely the improvement of water managed over different agricultural crops. It is an operational project where satellite remote sensing based data maps and other information is available at a weekly time-step *via* the Fruitlook website (Klaasse *et al.*, 2011). Information is available for table and wine grape producing areas of the Western Cape, deciduous fruit (Jarmain & Klaasse, 2012; Jarmain *et al.*, 2012), sugar cane and grain (Jarmain *et al.*, 2013) as reported in Gibson (2013). Fruitlook uses SEBAL, and is based on the LANDSAT images covering the Western Cape wine producing areas. It has a spatial resolution of 30 m, and a temporal resolution of 16 days, hence used to create land cover maps, using sequential unsupervised classifications (ISODATA clustering) to isolate specific crops of interest based on the crop NDVI's. When crops are not distinguishable, cloud free ASTER images, with a resolution of 15 m, in combination with the LANDSAT images, could distinguish table and wine grapes from other orchards and further improve the grape map as described by Jarmain *et al.* (2012).

Remote sensing estimates of LST require integration with regional scale study areas using ancillary data and LST can be used to measure the surface temperature with acceptable accuracy and precision (Goetz *et al.*, 2000; Kerr & Ostrovsky, 2003; Neteler, 2010) and as an input for biophysical models. Remote sensing can, and should, be integrated into more applications in the future, relating specially to viticulture, with a high demand for LST at an accurate spatial and temporal resolution that can be applied to grapevine functioning. Agricultural applications that are based on routinely extracted climatic indices, can be used to identify extreme events (late frost periods, heat waves *etc.*) or to quantify the growing season in time by the accumulation of growing degree days. The aggregated LST maps could therefore be used to predict crop maturing or insect development within season and aid in adaptive strategies for better seasonal management (Neteler, 2010; Neteler *et al.*, 2011; Zorer *et al.*, 2013).

Remote sensing data products for analysing and monitoring land surface changes in relation to global warming require continuous datasets of spatial and temporal consistency (Colditz & Dech, 2007) This can be ensured using automated processing. Data from MODIS provides an improved understanding of the global dynamics and processes occurring on the land, in the oceans, and in the lower atmosphere.

3.3.1 Moderate Resolution Imaging Spectroradiometer (MODIS)

The MODIS sensor has a good match between temporal and spatial resolutions and is an excellent data source for both local and global changes, with the advantage that the data is freely available (Neteler, 2010). MODIS LST is a favourable source of LST used to supplement meteorological stations in the complex terrains and monitor the plant responses to a changing environment. MODIS is also playing a vital role in the development of validated, global, interactive Earth system models able to predict global change accurately enough to assist policy makers in making sound decisions concerning the protection of our environment.

The MODIS instruments mounted on the Terra and Aqua platforms were launched on December 18th, 1999 and on May 4th, 2002, respectively (Barnes *et al.*, 1998; Barnes *et al.*, 2003), with Terra operating on a descending orbit with a mean equatorial crossing time at 10:30 am and Aqua in an ascending node crossing the equator at 1:30 pm. It has a viewing swath width of 2,330 km and views the entire surface of the Earth every one to two days. Its detectors measure 36 spectral bands between 0.4 and 14.4 µm, and it acquires data at three spatial resolutions – 250 m, 500 m, and 1,000 m. Depending on the wavelength, the spatial resolution ranges from 250 m to 1 km at nadir, bands 1-2 are imaged at a nominal resolution of 250 m at nadir, with bands 3-7 at 500 m,

and the remaining bands 8-36 at 1 km (Guenther *et al.*, 2002; Justice & Townshend, 2002). Each product is abbreviated with MOD, MYD, and MCD to indicate Terra, Aqua, or combined Terra / Aqua products, respectively.

The product generation of MODIS imagery follows a well-defined procedure with several levels; each product is accompanied by product quality estimators as metadata and at the pixel levels (Wan, 2014). The pixel level quality assurance in particular indicates the usefulness of an observation, and more detail can be viewed on the MODIS websites, (NASA, 2016b, 2016a). The following sections will mostly focus on MODIS land (MODLand) products, specifically LST (Justice & Townshend, 2002; Justice *et al.*, 2002).

3.3.2 MODIS Land Surface Temperature and Emissivity (MOD/MYD11)

Land Surface Temperature (LST) is a good indicator of the energy balance at the Earth's surface and the so-called greenhouse effect because it is one of the key parameters in the physics of land-surface processes on a regional as well as global scale (Wan, 2014). It combines the results of surface-atmosphere interactions and energy fluxes between the atmosphere and the ground (Wan, 1999a), indicating how hot the "surface" of the Earth would feel to the touch in a particular location. Figure 4 shows the LST for January 2016, with temperatures range from -25°C (deep blue) to 45°C (pinkish yellow). Temperatures vary at mid to high latitudes all year, but equatorial regions seem to remain consistently warm (NEO, 2016). In contrast, Antarctica and Greenland remain consistently cold. The LST is very variable due to extreme variability of most natural land surfaces such as in mountainous areas. This makes estimating LST and the validation thereof difficult to due to the deviations such as angle variations, surface spectral emissivity, atmospheric temperature, humidity variations, clouds and aerosol particles such as dust (ESA, 2016).

The MODIS/Terra LST and Emissivity (LST/E) products provide per-pixel temperature and emissivity values in a sequence of swath-based to grid-based global products. The MODIS/Terra/Aqua LST/E Daily L3 Global 1 km Grid product (MOD11A1/MYD11A1, respectively) is tile-based and gridded in the sinusoidal projection (Figure 4), and produced daily at 1 kilometre spatial resolutions (Wan *et al.*, 2002a).

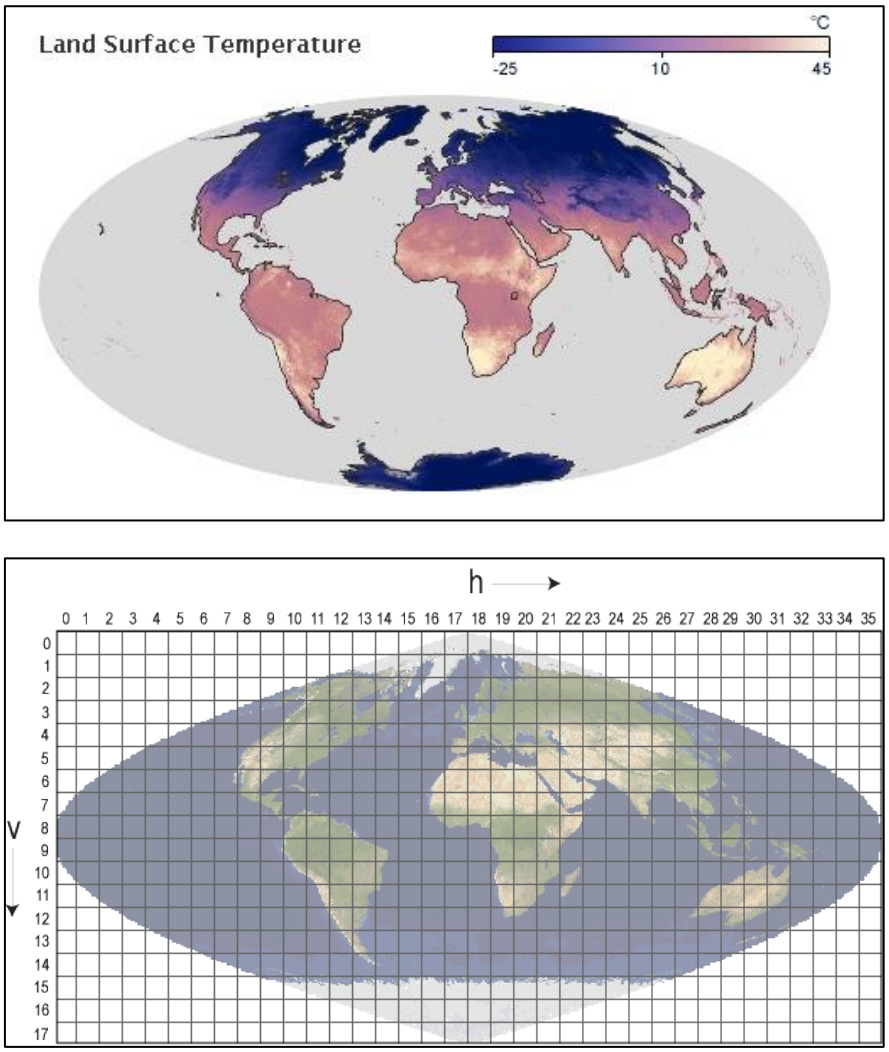

Figure 4 LST for January 2016, from data collected during the daytime by the Moderate Resolution Imaging Spectroradiometer (MODIS) on NASA's Terra satellite and below an image of the sinusoidal grid layout for data acquisition (NEO, 2016).

3.4 MODIS LST image processing

Current advances in satellite remote sensing are focused on the validations and refinement of satellite images collected from satellites observing the Earth's systems, especially improving the accuracy of LST's from the MODIS sensor aboard the Terra and Aqua satellites. Each satellite and sensor requires very specific validations for the most accurate practical application of the product; with possible post processing required from the user for specific applications.

The signal acquired by satellite sensors is composed of energy emitted from the Earth's surface, energy absorbed by the atmosphere, primarily by water vapour, or re-emitted from the atmosphere (Czajkowski *et al.*, 2000). LST combines the results of surface-atmosphere interactions and energy fluxes between the atmosphere and the ground (Wan, 1999b; Wan *et al.*, 2002a). Satellite remote sensing data are subject to large errors, due to sensor characteristics, atmospheric conditions, variations in spectral emissivity, surface type heterogeneity, soil moisture variability, visualisation geometry, and assumptions related to the split-window method (Wan & Dozier, 1996b; Vogt *et al.*, 1997; Czajkowski *et al.*, 2000). If errors are left uncorrected, it can substantially reduce satellite data's usefulness in practical applications. Before reflected radiation reaches a satellite, it interacts with two 'noisy' environments, namely the surface of the Earth and the atmosphere. Surface

temperatures are governed by land-atmosphere interactions and the energy fluxes between both. The surface energy balance is governed by down and upward radiation fluxes, and, latent and sensible heat loss fluxes. Atmospheric contamination of the remote sensing signal can arise through interaction with ozone, water vapour, aerosols, and other atmospheric constituents. On a cloudy day, satellite-borne optical remote sensors see little but the tops of clouds. Shadows, particularly when they vary across the fields of view of a sensors that see across broad areas, haze and scatter from terrestrial surfaces can severely reduce data consistency and such effects are very difficult to remove (Chen *et al.*, 2002; Kerr & Ostrovsky, 2003).

3.4.1 Primary post-processing of LST

The MODIS LST is derived from two thermal infrared (TIR) band channels, 31 (10.78-11.28 µm) and 32 (11.77-12.27 µm). The LST data products (MOD11_L2, MOD11A1, MOD11B1, and MOD11A2) are produced in a sequence, processing for LST for Terra (MOD) and Aqua (MYD) are the same. The sequence begins in a swath (scene) of MODIS data at a nominal pixel spatial resolution of 1 km, the second product is LST daily tile (1 km), the third product is the daily emissivity's (5km) and the fourth products is the 8-day LST products (Wan, 2014).

The second product (MOD11A1) is selected for this study to use as a supplement for meteorological data, daily LST product at 1 km spatial resolution (the exact grid size is 0.927 km, or 0.5 arc-min at the equator). The atmospheric effects are corrected using a spilt window algorithm, considering that the signal difference in the two TIR bands is caused by differential absorption of radiation in the atmosphere and land, so also considering the land cover emissivity's with the MOD11_L2 products, for the extraction of LST for a day at locations on the integerised sinusoidal projection (Wan *et al.*, 2002b; Benali *et al.*, 2012). In estimating LST from space, methods have been validated and used to make corrections for the atmospheric and surface emissivity effects with surface emissivity as an input based on the differential absorption in a split window (Wan & Dozier, 1996a; Wan *et al.*, 2002a; Wan, 2014).

There are two kinds of methods in the validation of the LST products retrieved from satellite thermal infrared data: conventional temperature-based method and advanced radiance-based method (Figure 5) (Wan, 2014). Because of the difficulties in correcting both atmospheric effects and surface emissivity effects, the development of accurate LST algorithms is not easy. The accuracy of atmospheric corrections is limited by radiative transfer methods and uncertainties in atmospheric molecular (especially water vapour) absorption coefficients and aerosol absorption/scattering coefficients and uncertainties in atmospheric profiles as inputs to radiative transfer models (Wan *et al.*, 2002a; Wan, 2014).

The MODIS MOD11 (Terra) and MYD11 (Aqua) Collection 5 (C5) products have been validated *via* a series of field experiments (Figure 5) conducted over different locations and time periods through radiance-based validation studies (Wan, 1999a; Wan, 2014). Refinements and updates were made to improve the quality of the LST products and to use both Terra and Aqua MODIS data in the LST retrieval. The estimated MODIS LST products are validated within an error of 1°K at 1 km resolution under clear-sky conditions, over validation sites in a wide range of surface and atmospheric conditions. The major advantages of the additional Aqua MODIS data for the LST product include the increase in quantity and the improvement in quality of the surface emissivity and temperature over the global land due to the increasing number of MODIS observations in clear-sky conditions since 2002 (Wan, 2014). Comparisons between LSTs and *in-situ* values indicate that the accuracy of the MODIS LST product is better than 1°K in most cases. However,

cases with heavy aerosol loadings and errors may occur at large view angles and in semi-arid regions. Higher errors in some arid regions are apparent due to effects of heavy dust aerosols and greater uncertainties in classification-based surface emissivity's (Wan, 1999a; Wan, 2014).

It is very difficult for the MODIS cloud-mask to discriminate all pixels affected by clouds and heavy aerosols from clear-sky pixels, particularly near cloud edges and/or with sub-pixel clouds such as coastal areas or very mountainous areas. The LSTs that are severely contaminated by clouds and heavy aerosols are removed from LST products using empirical constraints on temporal variations in clear-sky LSTs. Due to the large spatial variation in LSTs, especially during daytime, it is very difficult to make ground-based measurements of LSTs at the 1 km scale reaching a required accuracy (better than 1°K) with single or small number of TIR radiometers in most sites including weather stations (Wan, 2014). However, the Aqua overpass time after midday allows the LSTs retrieved from the MODIS data to more closely represent the maximum temperature of the land surface. Therefore, it is more suitable for regional and global change studies, especially in applications for estimating soil moisture condition and water requirements of crops, and for monitoring daily air temperature (Wan, 2014). Fortunately, many freely available remote sensing datasets have already been processed to reduce contamination and other errors and readily available for a wide variety of climate, hydrologic, ecological and biogeochemical studies (Camillo, 1991; Schmugge & Becker, 1991; Wan, 1999a; Kerr & Ostrovsky, 2003).

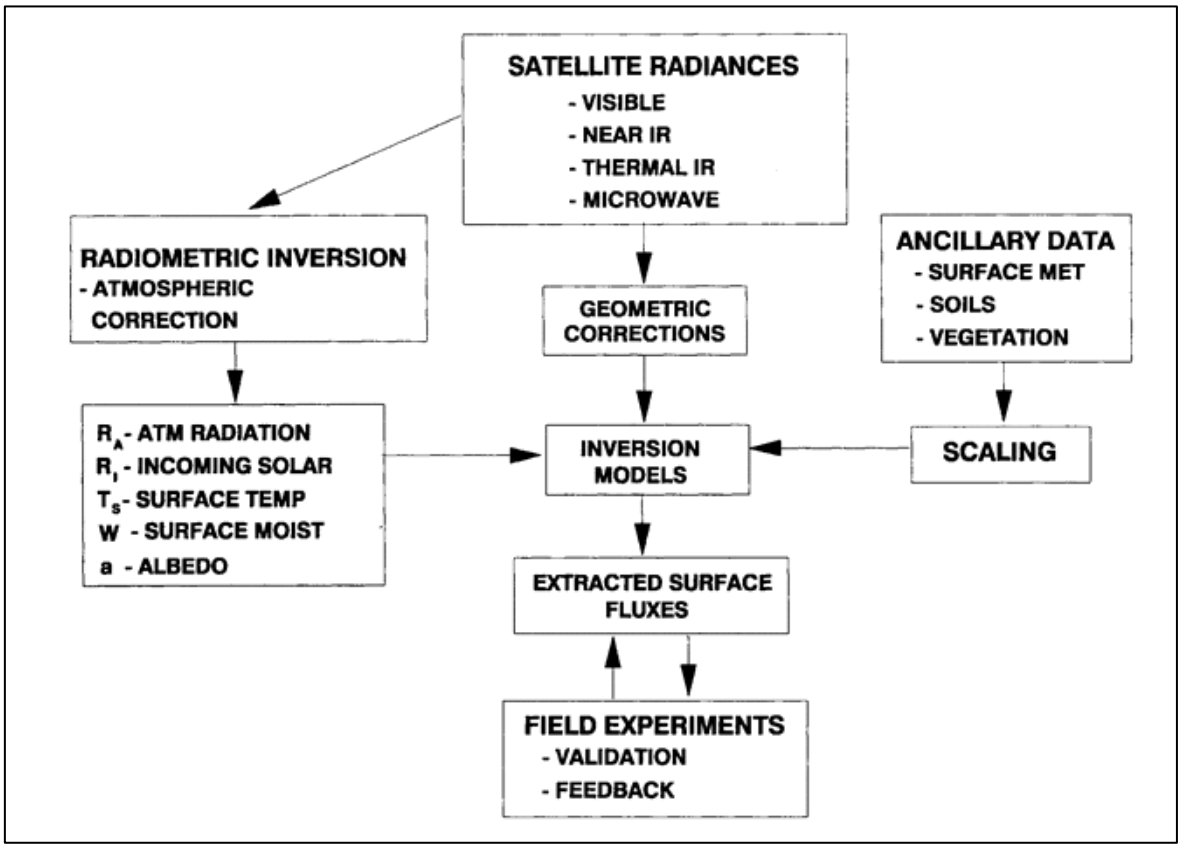

Figure 5 Schematic diagram of the process necessary to obtain surface fluxes from measured radiances (Schmugge & Becker, 1991).

3.4.2 Secondary post-processing

Despite a series of algorithms applied by NASA to filter clouds in the LST product, outliers still remain. These outliers are undetected clouds which introduce very low temperatures in the LST maps and re-projection artefacts. While remote sensing data is more easily available nowadays, the important preparation steps are still very time-consuming, and need to be adjusted for specific applications. Clouds and other atmospheric disturbances, which may obscure parts of or even the entire satellite image, may constitute a significant problem, especially in the seasonal application of LST to monitor seasons and the supplement weather station networks. Therefore, a data validation, secondary post processing is required for specific study areas and applications based on *in situ* measurements to improve the errors in LST layers.

A novel approach to reconstructing MODIS LST data in complex terrains was introduced by Neteler (2010). Processing included the rejection of poor quality pixels by application of MODIS quality maps, and the elimination of low-range temperature outliers based on histogram data. The void map areas were filled using temperature gradient-based map reconstruction with volumetric spline interpolation, resulting in continuous LST maps for complex terrains (Neteler, 2010). The processing of the original MODIS LST data is shown in a few steps in Figure 6. The steps are: 1) projection and import; 2) histogram based outlier removal using MODIS LST quality assurance layers; 3) linear regression on all maps to calculate preliminary map gradients and quality control of those; 4) second filtering of all pre-filtered LST maps; 5) final linear regression to calculate definite map gradients and 6) volumetric splines based on LST map reconstruction (Neteler, 2010). The processing has been implemented as almost automated procedures (scripts) which can run on large grid or cluster infrastructures for parallel computing and to minimise user errors during data processing (Neteler, 2010). Advances in open source geospatial tools have allowed for the processing of MODIS NDVI/EVI and LST time series satellite data in a GIS. The required data preparations for the integration of MODIS data in GIS with focus on the re-projection from MODIS/Sinusoidal projection to national coordinate systems, removal of low quality pixels (using MODIS quality maps) and the final filtering of LST maps with an outlier detector to eliminate originally undetected cloud pixels is automated. The secondary automated processing of MODIS LST using open source geospatial tools allows for easier spatial applications useful in decision making.

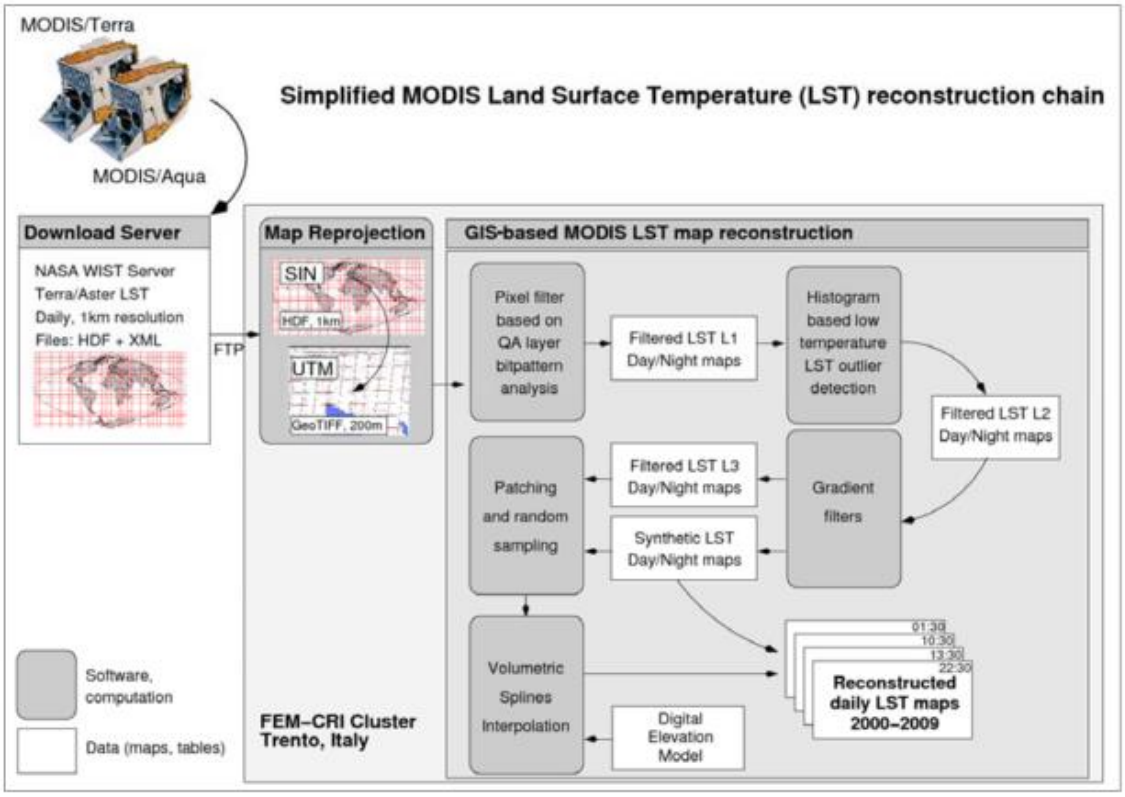

Figure 6 Simplified sketch of MODIS LST reconstruction processing chain (Neteler, 2010).

3.5 Application of MODIS

Spatially continuous thermal satellite data can aid in understanding the consequences and drivers of change in the grapevine response to its direct environment, at local and regional scales where *in situ* observations are scarce. In order to account for processes at the Earth's surface, multiple measurements have to be recorded at various temporal scales. In particular, the length of the record as well as the temporal resolution, is very important for process analysis (Colditz & Dech, 2007). The use of time series provided by modern remote sensing platforms improves the quality of derived maps as indicators of environmental change. The quality of indicators, especially in the complex terrain of the Western Cape, can be determined by thorough pre- and post-processing of the data in order to minimise artefacts in the resulting maps as done in a study by Neteler (2010) in the North of Italy.

Processes of the Earth's surface occur at different scales of time and intensity. Climate, in particular, determines the activity and seasonal development of vegetation. These dynamics are predominantly driven by temperature in the humid mid-latitudes and by the availability of water in semi-arid regions (Colditz & Dech, 2007).

3.5.1 MODIS LST used to supplement meteorological time series

One of the most important potential applications of the LST retrieved from satellite data is to validate and improve the global meteorological model prediction (Wan *et al.*, 2002b; Neteler, 2010; Zorer *et al.*, 2013). Air temperature, typically measured at the shelter height 2 m above ground is a key variable in a wide range of environmental applications including plant reaction, vector-borne disease bionomics, terrestrial hydrology, biosphere processes and climate change research (IPCC,

2007). Depending on the scale, the spatio-temporal air temperature patterns can be highly variable and complex due to the heterogeneity of the environmental factors that control the energy balance of the land-atmosphere system. In complex terrains, meteorological stations and ground surveys are usually sparsely and/or irregularly distributed and often favour agricultural areas. In addition, the application of traditional geospatial interpolation methods in complex terrain remains challenging and difficult to optimise (Neteler, 2010; Benali *et al.*, 2012). Regardless of the method, interpolation accuracy is highly dependent on station network density and the scale of spatial and temporal variability of the parameter, with interpolation errors generally ranging from 1 to 3°K (Vogt *et al.*, 1997; Anderson, 2002; Mostovoy *et al.*, 2006).

Reconstructed daily LST time series are considered to be a valid dataset which can substitute meteorological temperature observations. With the added advantage that the daily LST layers are intrinsically spatialised and therefore a great alternative to supplement and improve the air temperature spatiotemporal pattern, improving the knowledge of climate and terrestrial biological processes at global and regional scales (Neteler, 2010). The performance of reconstructed LST maps was compared with instantaneous observations, and showed good correlations for each station at four daily observations which directly compared to the *in situ* measurement at local solar time (Neteler, 2010; Zorer *et al.*, 2013).

In a study by Williamson *et al.* (2014) in a complex alpine environment, two methods were compared for producing daily temperature fields from the MODIS LST images. The first of these was the Interpolated Curve Mean Daily Surface Temperature (ICM) method, which interpolates single daytime Terra LST values to daily means using the coincident diurnal air temperature curves. The second method calculates daily mean LST from daily maximum and minimum LST (MMM) values from MODIS Aqua and Terra LSTs. Both methods used for producing mean daily surface temperatures have advantages and disadvantages. The ICM signals are strongly correlated to air temperature, but with large variability, while MMM values had a stronger correlation to air temperature with smaller variability. The ICM is a viable gap filling technique for situations where only single observations of day-time LST are available due to cloud cover. However, the MMM produce a better result when compared to air temperature (Williamson *et al.*, 2014).

One of the most important potential applications of the LST retrieved from satellite data is to validate and improve the global meteorological model prediction after appropriate aggregation and parameterisation (Diak & Whipple, 1993; Wan, 2014). Surface emissivity is a necessity in the LST retrieval, and is also used to discriminate senescent vegetation (French *et al.*, 2000a). Many recent studies have found strong linear correlations between MODIS LST (maximum, minimum & average) and air temperatures for many land cover types in Africa (Vancutsem *et al.*, 2010), in Portugal (Benali *et al.*, 2012), on the Tibetan Plateau (Zhu *et al.*, 2013) and over the United States (Crosson *et al.*, 2012). The typical range of errors when correlating LST to air temperature is approximately 2-3°C (Zakšek & Schroedter-Homscheidt, 2009) irrespective of the methodology, spatial or temporal resolutions (Williamson *et al.*, 2014). Land surface temperature is also an important parameter in energy budget models, evapotranspiration (ET) models, soil moisture estimation, forest detection, monitoring the state of crops, studying land and sea breezes and nocturnal cooling (Jovanovic *et al.*, 2015).

3.5.2 Mapping and monitoring vegetation

Mapping and monitoring of agricultural areas and crop yield estimation are challenging fields in which time series are analysed in depth using multiple satellite remote sensing images (*e.g.* MODIS, Landsat *etc.*). Seasonal patterns of plant growth including budburst, growth plateau, senescence, and dormancy are referred to as phenology. The timing, length, and intensity of the growing season and of each phenological phase depends on the region. Multi-year studies on the seasonal variability of phenological phases indicate a clear relation to climatic variables and land cover (Yui *et al.*, 2004). The climatic variability is relevant to many ecosystems, especially in semi-arid regions where precipitation is the principal determining factor for plant growth (Colditz & Dech, 2007). Land surface phenology (LSP) is defined as the seasonal pattern of variation in vegetated land surfaces observed from satellite remote sensing (Friedl *et al.*, 2002). The LSP characterises episodes of greening and browning of the vegetated land surface from remote sensing imagery (MOD13), with the limitation of only working well in regions with well-defined growing seasons, where the Enhanced Vegetation Index (EVI) amplitude is high (Broich *et al.*, 2015). Therefore, retrieving LSP in arid, evergreen or cloudy environments represents an on-going challenge. The absence of clear patterns may be related to climatic variability causing high LSP variability or indicate that a product specifically designed for specific study area conditions is required. However the LSP provides valuable information to scientists and practitioners interested in vegetation and ecosystem response to climate variability such as drought and land use change, as well as possible shifts in seasons such as earlier or later phenology in grapevines (Broich *et al.*, 2015).

Another application of satellite remote sensing is the estimation of leaf area index (LAI) from remotely sensed data (*i.e.* MODIS LAI) which has been applied in various ways, including its potential contribution to calculate the stomatal conductance component (gs) and calculation of gross primary productivity (GPP) (Cleugh *et al.*, 2007; Palmer *et al.*, 2008). Each MODIS LAI pixel provides an estimate of daily water use, which can be integrated for an entire catchment. Evapotranspiration (ET) is a key process within the hydrological cycle and arguably the most difficult component to determine, especially in arid and semi-arid areas where a large proportion of low and sporadic precipitation is returned to the atmosphere *via* ET. This makes the process of ET very dynamic over time and variable in space, due to variations caused by landscape heterogeneity. The MOD16 ET algorithm has been developed and improved (Cleugh *et al.*, 2007), and may be suitable to identify temporal changes and for relative comparisons of data between climatic regions in South Africa (Jovanovic *et al.*, 2015). However, the algorithm underestimated ET by up to 15% for water balance models at national scale. The relatively coarse resolution of ~1 km^2 pixels may have implications for applications in restricted areas, especially where there are heterogeneous vegetation, land use/cover and landscapes. The MODIS LAI-ET model can be used with greater confidence to estimate catchment-scale water use by vegetation and soil than was previously possible using the results of field campaigns of limited duration (Palmer *et al.*, 2008).

Referring to MODIS data specifically, the resolution in the reflective bands ranges from 250-500 m, making it possible to calculate NDVI at 250 m resolution, and can subsequently be used in decision making and selective management within large vineyard blocks. Good correlations between NDVI and crop yield indicate the possibility of yield estimations using the satellite images for better in seasonal planning of cellar space (Mika *et al.*, 2002; Colditz & Dech, 2007). Satellite remotely sensed time series may contribute significantly to yield estimations at an early stage of the cropping season, and is deemed useful as an input to crop models for crops in Europe, India,

and Uzbekistan (Roebeling *et al.*, 2004; Patel *et al.*, 2006; Colditz & Dech, 2007). This may also be applicable in studies in South Africa.

3.6 Limitations and possible future developments

Despite valuable information that is gained from the use of satellite remote sensing, users and practitioners from outside of the remote sensing community often find it time consuming to derive accurate information for their specific regions and applications (Broich *et al.*, 2015). A major advantage of MODIS LST is that it is freely available data that is intrinsically spatialised with sufficient accuracy for further processing for improved accuracy on a regional or field scale. Downloading of images and the post processing can be automated and conducted in open source software, making it even more attractive for large scale and continuous time scale use to monitor climate change.

A major constraint for the MODIS LST as well as other MODIS land products is that they are only available in clear sky conditions due to cloud contamination, as the visible and thermal infrared spectral ranges can't penetrate clouds. The MODIS LST algorithm as well as most of the existing LST algorithms is based on the basic assumption that a land surface pixel could be described by different spectral emissivities and a single effective radiometric temperature in all TIR bands. In the case of LST maps, land/sea surface temperatures in cloud covered areas are simply unavailable since cloud-top temperatures are measured instead. Statistically, greater cloud contamination is found in night-time LST maps because at night only TIR band data can be used in the spectral tests needed for cloud mask production (Wan *et al.*, 2002a; Wan *et al.*, 2004b).

The cloud contaminated LST pixels which remain undetected by the NASA LST map production algorithms (Wan *et al.*, 2004a; Wan, 2014) appear to occur near cloudy areas (coastlines, mountainous areas), identified as outliers in the LST data (negative °C values) due to the cold surfaces of undetected clouds (Neteler, 2010). These outlier areas would have to be identified in the MODIS LST images so that in situ temperature loggers or weather stations can be put in areas of interest to ensure possible gap filling for a continuous LST layer. This process for removal of cloud contamination still in the images can be automated as a secondary post processing for gap filling, which is essential for the use of LST as an alternative source to supplement meteorological stations (Neteler, 2010; Metz *et al.*, 2014) and for the creation of bioclimatic maps relating the grapevine growth and ripening.

Topographic effects in complex terrains is another limitation as only the first order of topographic information, such as elevation of the surface, is considered in radiative transfer simulations in the development of MODIS LST algorithms. However, the second order terrain effects like distance from the ocean, aspects *etc*. are not considered.

When linking pixel value of a vineyard or a farm to a fixed grid on the Earth surface coordinates, the MODIS LST as well as all other land products will experience difficulties with complicated mixed pixels along land cover boundaries in terms of their quantitative definitions, quality assessments, and applications (Wan, 1999a). This is an important factor to consider on the data interpretation level, and a possible solution it the future downscaling of the MODIS LST with the use of digital elevation models (DEM) that is of higher spatial resolutions than LST (1 km).

The use of geospatial techniques to consider specific bioclimatic indices and characteristics of the territory, primarily the soil type, are needed for a better understanding of the viticulture potential of a region. The use of MODIS LST to build bioclimatic indices classification maps, *i.e.* growing

degree days (Amerine & Winkler, 1944), provides a very detailed description of the landscape, despite the complex topography, as the maps are spatialised in nature (Neteler, 2010; Zorer *et al.*, 2010; Benali *et al.*, 2012; Zorer *et al.*, 2013). Research showed that the Huglin Index, Biologically Effective Degree Days, and Growing Season Average Temperature tend to better represent known wine regions, while the Winkler Index leaves out many existing higher latitude locations (Jones *et al.*, 2005). This is due to the fact that WI does not include any adjustment for increasing day lengths at higher latitudes. All of these bioclimatic indices can be calculated from MODIS LST daily data, and future work will evaluate these additional indices and environmental phenomena (sea breeze, distance from the ocean *etc.*) and application to viticulture within the complexity of the Western Cape terrain.

3.7 Summary

Satellite remote sensing data, specifically products with high temporal and thermal resolution such as MODIS LST offers new opportunities to compliment and supplement field based studies in viticulture and monitoring of temperature.

Continuous monitoring of seasonal temperatures within complex terrain or large areas is hampered by the sparse and/or irregular distribution of meteorological stations. The point data from the meteorological stations can be interpolated to create continuous temperature maps, but the accuracy of the interpolation product is limited by the sparsely distributed stations. This is especially difficult in more complex terrains such as the Western Cape. Therefore, the spatialised satellite thermal remote sensing data can be used as an alternative and greatly improving the estimation of air temperature spatiotemporal patterns. Consequently, the knowledge of both climate and terrestrial biological processes at regional and global spatial scales in the context of climate change has improved. The latest refinements in the MODIS LST products have significantly improved the spatial coverage of LSTs, with the accuracy of the MODIS LST product being better than 1°K in most validated cases with in situ measurements.

The strengths of MODIS include freely available data with a global coverage, high radiometric resolution and dynamic ranges suitable for atmosphere, land, or ocean studies, and accurate calibration in multiple TIR bands designed for retrievals of SST, LST and atmospheric properties. Due to the limitations caused by cloud cover and topography, secondary post processing is needed for site and application specific studies. While remote sensing data is currently more easily available, post-processing steps are still time consuming for the creation of continuous LST maps. However, the processing can be implemented as an almost entirely automated procedure which can be run on cluster infrastructures for parallel computing and incorporating other geospatial layers for application specific studies. Therefore, MODIS LST shows to be a good supplement for meteorological station networks, for monitoring seasonal variability in temperature, detecting photosynthetically active vegetation, its phenological development and variability, multi-year transformation processes, and irregular events.

Spatially continuous satellite infrared temperature measurements are essential for understanding the consequences and drivers of change, at local and regional scales, especially in complex terrains such as the Western Cape and where *in situ* observations are scarce.

3.8 Literature cited

Amerine, M.A. & Winkler, A.J., 1944. Composition and quality of musts and wines of California grapes. Hilgard 15, 493-673.

Anderson, S., 2002. An evaluation of spatial interpolation methods on air temperature in Phoenix, AZ. Department of Geography, Arizona State University Tempe, 80104-85287.

Barnes, W.L., Pagano, T.S. & Salomonson, V.V., 1998. Pre-launch characteristics of the Moderate Resolution Imaging Spectroradiometer (MODIS) on EOS AM-1. IEEE Trans. Geosci. Remote Sens. 36, 1088-1100.

Barnes, W.L., Xiong, X. & Salomonson, V.V., 2003. Status of Terra MODIS and Aqua MODIS. Advances in Space Research 32, 2099-2106.

Bastiaanssen, W., Meneti, M., Feddes, R. & Holtslag, A., 1998. The surface energy balance algorithm for land (SEBAL): Part 1 formulation. J. Hydrol. 212, 198-212.

Ben-Gal, A., Agam, N., Alchanatis, V., Cohen, Y., Yermiyahu, U., Zipori, I., Presnov, E., Sprintsin, M. & Dag, A., 2009. Evaluating water stress in irrigated olives: Correlation of soil water status, tree water status, and thermal imagery. Irrigation Sci. 27, 367-376.

Benali, A., Carvalho, A.C., Nunes, J.P., Carvalhais, N. & Santos, A., 2012. Estimating air surface temperature in Portugal using MODIS LST data. Remote Sens. Environ. 124, 108-121.

Broich, M., Huete, A., Paget, M., Ma, X., Tulbure, M., Restrepo, N., Evans, B., Beringer, J., Devadas, R., Davies, K. & Held, A., 2015. Environmental modelling & software. A spatially explicit land surface phenology data product for science, monitoring and natural resources management applications. Environ. Modell. Softw. 64, 191-204.

Camillo, P.J., 1991. Using one- or two-layer models for evaporation estimation with remotely sensed data. In: Camillo, Peter J. (ed). Land surface evaporation. Springer New York. pp. 193-197.

Campbell, J.B. & Wynne, R.H., 2011. Introduction to Remote Sensing. In: Campbell, J.B., and Wynne, R.H. (eds). Guilford Publications.

Carey, V.A., 2005. The use of viticultural terroir units for demarcation of geographical indications for wine production in Stellenbosch and surrounds. Dissertation, Stellenbosch University, Private Bag X1, 7602 Matieland (Stellenbosch), South Africa.

Chen, J.M., Pavlic, G., Brown, L., Cihlar, J., Leblanc, S.G., White, H.P., Hall, R.J., Peddle, D.R., King, D.J., Trofymow, J.A., Swift, E., Van der Sanden, J. & Pellikka, P.K.E., 2002. Derivation and validation of Canada-wide coarse-resolution leaf area index maps using high-resolution satellite imagery and ground measurements. Remote Sens. Environ. 80, 165-184.

Cheng, T., Riaño, D., Koltunov, A., Whiting, M.L., Ustin, S.L. & Rodriguez, J., 2013. Detection of diurnal variation in orchard canopy water content using MODIS/ASTER airborne simulator (MASTER) data. Remote Sens. Environ. 132, 1-12.

Cleugh, H.A., Leuning, R., Mu, Q. & Running, S.W., 2007. Regional evaporation estimates from flux tower and MODIS satellite data. Remote Sens. Environ. 106, 285-304.

Colditz, R.R. & Dech, S., 2007. Time Series Generation and Classification of MODIS Data for Land Cover Mapping. Dissertation, Julius Maximilian University of Würzburg, Germany. pp. 334.

Crosson, W.L., Al-Hamdan, M.Z., Hemmings, S.N.J. & Wade, G.M., 2012. A daily merged MODIS Aqua-Terra land surface temperature data set for the conterminous United States. Remote Sens.Environ. 119, 315-324.

Czajkowski, K.P., Goward, S.N., Stadler, S.J. & Walz, A., 2000. Thermal remote sensing of near surface environmental variables: application over the Oklahoma Mesonet. The Professional Geographer 52, 345-357.

Diak, G.R. & Whipple, M.S., 1993. Improvements to models and methods for evaluating the land-surface energy balance and 'effective' roughness using radiosonde reports and satellite-measured 'skin' temperature data. Agric. For. Meteorol. 63, 189-218.

ESA, 2016. Land Surface Temperature. In: esa sentinel online. https://sentinel.esa.int/web/sentinel/user-guides/sentinel-3-slstr/overview/geophysical-measurements/land-surface-temperature.

Fischer, W.A., Hemphill, W.R. & Kover, A., 1976. Progress in remote sensing (1972–1976). Photogrammetria 32, 33-72.

FreeGIS, 2016. The FreeGIS Project aims to promote the freedom in the scope of Geographic Information Systems (GIS). In: FOSSGIS e.V. http://freegis.org/.

Friedl, M.A., McIver, D.K., Hodges, J.C.F., Zhang, X., Muchoney, D., Strahler, A.H., Woodcock, C.E., Gopal, S., Schneider, A., Cooper, A., Baccini, A., Gao, F. & Schaaf, C., 2002. Global land cover mapping from MODIS: algorithms and early results. remote Sens. Environ. 83, 287-302.

Gaston, K.J., 2000. Global patterns in biodiversity. Nature 405, 220-227.

Gibson, L.A., 2013. The application of the surface energy balance system model to estimate evapotranspiration in South Africa. Dissertation, Department of Environmental and Geographical Science, Faculty of Science, Univeristy of Cape Town, Private Bag X3 Rondebosch 7701.

Goetz, S.J., Prince, S.D. & Small, J., 2000. Advances in satellite remote sensing of environmental variables for epidemiological applications. Advances in Parasitology 47, 289-307.

Guenther, B., Xiong, X., Salomonson, V.V., Barnes, W.L. & Young, J., 2002. On-orbit performance of the Earth Observing System Moderate Resolution Imaging Spectroradiometer; first year of data. Remote Sens. Environ. 83, 16-30.

IPCC, 2007. Summary for Policymakers. In:Parry, M.L., Canziani, O.F., Palutikof, J.P., van der Linden, P.J. and Hanson, C.E. (eds). Climate change 2007. Impacts, adaptation and vulnerability. In Fourth Assessment Report of the Intergovernmental Panel on Climate Change. Cambridge University Press, Cambridge, UK.

Jarmain, C. & Klaasse, A., 2012. Fruitlook: An operational service to improved crop water and nitrogen management in grapes and other deciduous fruit trees using satellite technology for the season of 2011-12. In progress report. Department of Agriculture: Western Cape, Private Bag X1, Elsenburg, South Africa.

Jarmain, C., Klaasse, A., Bastiaanssen, W.G.M. & Roux, A.S., 2012. Remote sensing tools for water use efficiency of grapes in the Winelands Region, Western Cape. http://citeseerx.ist.psu.edu/viewdoc/download?doi=10.1.1.520.5531&rep=rep1&type=pdf.

Jarmain, C., Singels, A., Obando, E., Paraskevopoulos, A., Olivier, F., Münch, Z., Van der Merwe, B., Walker, S., Van der Laan, M., Messehazion, M., Savage, M., Pretorius, C., Annandale, J. & Everson, C., 2013. Water use efficiency of irrigated agricultural crops determined with satellite imagery. Deliverable 6 of WRC project No. K5/2079//4. Water Research Commission, Private Bag X103, Gezina, Pretoria, 0031, South Africa.

Jones, G.V., White, M.A., Cooper, O.R. & Storchmann, K., 2005. Climate change and global wine quality. Climatic Change 73, 319-343.

Jovanovic, N., Mu, Q., Bugan, R.D.H. & Zhao, M., 2015. Dynamics of MODIS evapotranspiration in South Africa. Water SA 41, 79-90.

Justice, C.O. & Townshend, J.R.G., 2002. Special issue on the moderate resolution imaging spectroradiometer (MODIS): a new generation of land surface monitoring. Rem. Sens. Environ., pp. 1-2.

Justice, C.O., Townshend, J.R.G., Holben, B.N. & Tucker, C.J., 1985. Analysis of the phenology of global vegetation using meteorological satellite data. Int. J. Remote Sens. 6, 1271-1318.

Justice, C.O., Townshend, J.R.G., Vermote, E.F., Masuoka, E., Wolfe, R.E., Saleous, N., Roy, D.P. & Morisette, J.T., 2002. An overview of MODIS Land data processing and product status. Remote Sens. Environ. 83, 3-15.

Kerr, J.T. & Ostrovsky, M., 2003. From space to species: ecological applications for remote sensing. Ecol. Evol 18, 299-305.

Klaasse, A., Jarmain, C., Roux, A., Becu, O. & Ginati, A., 2011. GrapeLook: space based services to improve water use efficiency of vineyards in South Africa. Proc. 62nd International Astronautical Congress, 3-7 October, Cape Town, South Africa.

Metz, M., Rocchini, D. & Neteler, M., 2014. Surface temperatures at the continental scale: tracking changes with remote sensing at unprecedented detail. Remote Sens. 6, 3822-3840.

Mika, J., Kerényi, J., Rimóczi-Paál, A., Merza, Á., Szinell, C. & Csiszár, I., 2002. On correlation of maize and wheat yield with NDVI: Example of hungary (1985–1998). Advances in Space Research 30, 2399-2404.

Mostovoy, G.V., King, R.L., Reddy, K.R., Kakani, V.G. & Filippova, M.G., 2006. Statistical estimation of daily maximum and minimum air temperatures from MODIS LST data over the state of Mississippi. IEEE T. Geosci. Remote 43, 78-110.

NASA, 2015. Subcommittee on Space Committee on Science. Presented at the Space and Technology U.S House of Representatives in April 2015.

NASA, 2016a. Aqua project science. *In*, http://aqua.nasa.gov/.

NASA, 2016b. Terra, The EOS flagship. *In*, http://terra.nasa.gov/.

NEO, 2016. Global Maps, Land Surface Temperature. In NASA Earth Observatory, http://earthobservatory.nasa.gov/GlobalMaps/view.php?d1=MOD11C1_M_LSTDA.

Neteler, M., 2010. Estimating daily land surface temperatures in mountainous environments by reconstructed MODIS LST data. Remote Sens. 2, 333-351.

Neteler, M., Bowman, M.H., Landa, M. & Metz, M., 2012. Environmental modelling & software GRASS GIS : A multi-purpose open source GIS. Environ. Modell. Softw. 31, 124-130.

Neteler, M. & Mitasova, H., 2008. Open source GIS A GRASS GIS approach. 3rd Ed.Springer, New York (ISBN-10: 038735767X; ISBN-13: 978-0387357676).

Neteler, M., Roiz, D., Rocchini, D., Castellani, C. & Rizzoli, A., 2011. Terra and Aqua satellites track tiger mosquito invasion: modelling the potential distribution of Aedes albopictus in north-eastern Italy. Int. J. Health Geographics 10, 49.

NOAA, 2016. National Oceanic and Atmosperic Adminstration. In:http://eoedu.belspo.be/en/satellites/noaa.htm.

Palmer, A.R., Fuentes, S., Taylor, D., MacInnis-Ng, C., Zeppel, M., Yunusa, I., February, E. & Eamus, D., 2008. The use of pre-dawn leaf water potential and MODIS LAI to explore seasonal trends in the phenology of Australian and southern African woodlands and savannas. Aust. J.Bot. 56, 557-563.

Patel, N.R., Bhattacharjee, B., Mohammed, A.J., Tanupriya, B. & Saha, S.K., 2006. Remote sensing of regional yield assessment of wheat in Haryana, India. Int. J. Remote Sens. 27, 4071-4090.

Penuelas, J. & Et, A., 1993. The reflectance at the 950-970nm region as an indicator of plant water status. Int. J. Remote Sens. 14, 1887-1905.

Roebeling, R.A., van Putten, E., Genovese, G. & Rosema, A., 2004. Application of Meteosat derived meteorological information for crop yield predictions in Europe. Int. J. Remote Sens. 25, 5389-5401.

Schmugge, T.J. & Becker, F., 1991. Remote sensing observations for the monitoring of land-surface fluxes and water budgets. In: Land Surface Evaporation, Springer New York, USA. pp. 337-347.

USGS, 2015. Timeline and history of the Lansat Missions, which started in 1972. In Fact shoot 2015-3081, November 2015. USGS (US Geology Survey).

Vancutsem, C., Ceccato, P., Dinku, T. & Connor, S.J., 2010. Evaluation of MODIS land surface temperature data to estimate air temperature in different ecosystems over Africa. Remote Sens. Environ. 114, 449-465.

Vogt, J.V., Viau, A.A. & Paquet, F., 1997. Mapping regional air temperature fields using satellite-derived surface skin temperatures. Int. J. Climatol. 17, 1559-1579.

Wan, Z., 1999a. MODIS land-surface temperature algorithm theoretical basis document. MODIS Land-surface Temperature Algorithm Theoretical Basis Document (LST ATBD).

Wan, Z., 1999b. MODIS Land-Surface Temperature Algorithm Theoretical Basis Document Version 3.3.

Wan, Z., 2014. New refinements and validation of the collection-6 MODIS land-surface temperature/emissivity product. Remote Sens. Environ. 140, 36-45.

Wan, Z. & Dozier, J., 1996a. A Generalized Split-Window Algorithm for Retrieving Land-Surface Temperature from Space. IEEE T. Geosci. Remote 34, 892-905.

Wan, Z. & Dozier, J., 1996b. A generalized split-window algorithm for retrieving land surface temperature from space. IEEE T. Geosci. Remote. 34, 892-905.

Wan, Z., Zhang, Q. & Li, L., 2004a. Quality assessment and validation of the MODIS global land surface temperature. Int. J. Remote Sens. 25, 261-274.

Wan, Z., Zhang, Y., Zhang, Q. & Li, Z.-l., 2002a. Validation of the land-surface temperature products retrieved from Terra Moderate Resolution Imaging Spectroradiometer data. Remote Sens. Environ. 83, 163-180.

Wan, Z., Zhang, Y., Zhang, Q. & Li, Z.-L., 2004b. Quality assessment and validation of the MODIS global land surface temperature. Int. J. Remote Sens. 25, 261-274.

Wan, Z., Zhang, Y., Zhang, Q. & Li, Z.L., 2002b. Validation of the land-surface temperature products retrieved from terra moderate resolution imaging spectroradiometer data. Remote Sens. Environ. 83, 163-180.

Williamson, S.N., Hik, D.S., Gamon, J.a., Kavanaugh, J.L. & Flowers, G.E., 2014. Estimating temperature fields from MODIS land surface temperature and air temperature observations in a sub-arctic alpine environment. Remote Sens. 6, 946-963.

Wilson, B.G., 2005. Theory and method as tools: Reflections on research on the pedagogical uses of ICT in education. Computers in Human Behavior 21, 541-546.

Yui, X., Chen, H., Zhuang, D. & Hou, X., 2004. Forest classification based on MODIS time series and vegetation phenology. In: IEEE T. Geosci. Remote Symposium, IGARSS '04.

Zakšek, K. & Schroedter-Homscheidt, M., 2009. Parameterization of air temperature in high temporal and spatial resolution from a combination of the SEVIRI and MODIS instruments. ISPRS J. Photogramm 64, 414-421.

Zhang, X., Friedl, M.A., Schaaf, C.B. & Strahler, A.H., 2004. Climate controls on vegetation phenological patterns in northern mid- and high latitudes inferred from MODIS data. Glob Change Biol 10, 1133-1145.

Zhu, W., Lű, A. & Jia, S., 2013. Estimation of daily maximum and minimum air temperature using MODIS land surface temperature products. Remote Sens. Environ. 130, 62-73.

Zorer, R., Delucchi, L., Neteler, M. & Nicolili, G., 2010. Development of a GRASS-GIS application for the characterization of vineyards in the Province of Trento (Poster). In:VIII International Terroir Congress, June 14th-18th, 2010. Soave, Italy.

Zorer, R., Rocchini, R., Delucchi, L., Zottele, F., Meggio, F. & Neteler, M., 2011. Use of multi-annual MODIS land surface temperature data for the characterization of the heat requirements for grapevine varieties. In: Proc. Analysis of Multi-temporal Remote Sensing Images (Multi-Temp), 2011 6th International Workshop pp. 225-228.

Zorer, R., Rocchini, D., Metz, M., Delucchi, L., Zottele, F., Meggio, F. & Neteler, M., 2013. Daily MODIS land surface temperature data for the analysis of the heat requirements of grapevine varieties. IEEE T. Geosci. Remote 51, 2128-2135.

Chapter 4

Research results

High resolution monitoring of seasonal weather variation over four growing seasons, over a climatic band

CHAPTER 4: HIGH RESOLUTION MONITORING OF SEASONAL WEATHER VARIATION OVER FOUR GROWING SEASONS, OVER A CLIMATIC BAND

4.1 Introduction

The Western Cape Province of South Africa is situated in the south-western part of the country and covers *ca.* 129 370 km^2. The South African wine industry is mostly concentrated in this province. The wine areas are demarcated into regions, districts and wards. The province is bordered seaward by the Indian Ocean in the south and the Atlantic Ocean in the west. The Western Cape has a unique climate. In contrast to much of southern Africa which experiences summer rains and dry winters, t receives the bulk of its' rainfall in winter months, with mild to cool winters and summers that are warm to hot and dry. This unique climate is mainly ascribed to the influence of the Benguela current of the Atlantic Ocean and the westerly winds introduced by the northward displacement of high pressure systems during winter, creating cold polar air in the region. One of the outstanding natural components of the Western Cape vineyards and wine landscapes is the distinctive, diverse topography and geology. The topography is complex, ranging from coastal plains to complex mountain ranges and valleys, dominated by the Cape Fold Belt, forming L-shaped mountain ranges oriented in a north to south and east to west direction (Van Niekerk & Joubert, 2011). Terroir and geology are indirectly linked through the formative effects of geological processes on landscapes, its soil assemblages and associated diversity in mesoclimates due to variation in altitude, sunlight interception and exposure to prevailing winds and its effects on temperature and water availability (Saayman, 2014). In addition to distance from the coast, elevation and latitude have significant effects (Smart & Dry, 1980), and the complex topography of this region therefore results in varied mesoclimatic conditions (Carey, 2005) over short distances. There is also a significant contrast between the cool ocean and warm inland temperatures, resulting in a frequent occurrence of sea breeze, especially during ripening in the summer months when the land temperatures are high and the ocean temperatures cool due to the Benguela current (Bonnardot *et al.*, 2001). The mesoclimate variation in the Western Cape winelands is exacerbated by the renowned sea breeze effect, affecting the relative humidity, maximum temperature and the increase in wind velocity in the mornings and early afternoons. The sea breeze contributes to the variation in the diurnal temperature cycles, with the common midday cooling in warmer regions due to the sea breeze effect, the diurnal temperature variation is affixed by the penetration of the cool and moist air from the sea. Vineyard nearer to the coast experience smaller temperature fluctuations compared to further inland (Bonnardot *et al.*, 2001; Carey, 2005).

Observed and predicted trends in rainfall and air temperature have been published for, *inter alia*, South African wine regions (Midgley *et al.*, 2005; Carter, 2006; Bonnardot & Carey, 2008). Grapevines are highly sensitive to their climatic environment, being driven largely by suitable temperature and precipitation regimes (Becker, 1985;Irimia *et al.*, 2014). Aspects impacting variability include macroclimatic variables such as latitude, proximity to the ocean (Bonnardot *et al.*, 2001) as well as mesoclimatic factors such as elevation, slope, aspect and sun hours. However, while many factors other than temperature drive viticultural suitability and wine production (Jackson & Lombard, 1993; Jones & Davis, 2000), simple to complex indices of temperature are the most common measures used to assess what types of grapes can be grown in which climates (Jones *et al.*, 2010). Bioclimatic indices portray the accumulation of plant function over the growing season (1

September to 31 March in the Southern Hemisphere) and have been used to put upper and lower limits on suitability for grapevine cultivation worldwide (Jones, 2006). Other temperature-based climate measures in viticulture suitability studies typically account for either simple temperature characteristics such as the mean temperature of the warmest month (Smart & Dry, 1980) or growing degree-day formulations that may also include atmospheric moisture or solar radiation parameters (Amerine & Winkler, 1944; Winkler, 1965; Huglin, 1978; Smart & Dry, 1980; Tonietto & Carbonneau, 2004).

There is a need to quantify the extremes and duration of the events affecting the surface of the earth and the plant's reaction. In general, climate is studied on three spatial scales, namely on a macroclimatic scale, which describes the regional climate, a mesoclimatic scale, describing smaller areas, *e.g.* vineyards (topographically linked, and also termed "topoclimate"), and finally the microclimatic scale, describing the plant canopy or the direct surrounding area (Bonnardot *et al.*, 2004). Temporal resolution for analysis and seasonal extremes are sometimes lost in daily and monthly analysis, especially in the context of variability of extremes and duration thereof. High and low temperature extremes are averaged, hence not giving a true account of the environmental conditions at plant level.

Grapevines experience a range of thermal conditions on a daily basis that have an impact on their growth and the development of primary (*e.g.* sugar and organic acids) and secondary (*e.g.* colour and aroma) grape quality metabolites. These conditions are largely controlled by the prevailing regional scale weather conditions and complexity of the local terrain. Finer scale models can be used to identify areas in which the grapevines are likely to be under significant climatic stress in relation to the regional scale weather conditions. In particular, areas in which low/high night temperature stress is likely to affect grape composition, and where low/high day temperature stress is likely to affect grapevine photosynthesis, can be identified in future climate change scenarios. Every local environment has unique diurnal temperature variations due to the inland penetration of the sea breeze, and other local effects such as synoptic wind, topography, coastline orientation and slope angle and aspect (Soltanzadeh *et al.*, 2016). Suitability of climatic parameters for key grapevine physiological processes need to be assessed at finer scales, using hourly weather data, to optimise the functioning of the grapevine in a specific environment for wine quality (Hunter & Bonnardot, 2011).

Grapevine physiological functions, such as photosynthesis, grape colour development, sugar and organic acid formation and flavour development (Coombe, 1987), are dependent on climate, and more particularly temperature (Kliewer, 1971; Coombe, 1987), relative humidity (Champagnol, 1984) and wind speed (Hamilton, 1989). The period between 09h00 and 15h00 is the optimum window for photosynthesis, and for photosynthesis to occur at an optimal rate, the temperature should range between 25-30°C, wind speed <4 m/s and relative humidity should be *c.* 60-70% (Hunter & Bonnardot, 2011). A study by Hunter and Bonnardot (2011) concluded that the day temperatures for optimal wine grape colour and flavour development ranges between 20-25°C from 06h00 to 18h00, and ideally night temperatures between 18h00 and 06h00 should range between 10-15°C.

The aim of this chapter is to present an update on the observed seasonal weather variability over a climatic band (cooler to warmer areas) for four of the Western Cape wine producing areas, namely Elgin, Somerset West, Stellenbosch and Vredendal. In addition to presenting observed seasonal weather variability for selected sites in the Western Cape, a further aim of this chapter is to use selected climatic variables, specifically temperature, relative humidity and wind to highlight the

main site variability and seasonal variability within sites that could influence the grapevine's response to the different environments.

4.2 Materials and Methods

4.2.1 Study area

Study areas were selected over a climatic band within the Western Cape wine regions (Figure 1), namely the winter-rainfall Coastal Region (Somerset West & Stellenbosch), Cape South Coast (Elgin) and the semi-arid Olifants River Region (Vredendal). The topographic diversity of the wine growing regions were also considered in the site selection, as factors such as the occurrence of the sea breeze during the ripening period, will have an impact on the afternoon and evening temperatures as well affecting the relative humidity and wind of the region (Bonnardot *et al.*, 2001). The selected sites and their detailed descriptions (slope, elevation, aspect, distance from the ocean) are given in Table 1. It should be noted that the Stellenbosch area is represented by three sites due to its complex topography inducing significant mesoclimatic variability across the viticultural area (Carey, 2001; Bonnardot *et al.*, 2012). All the study sites had sufficient sunlight hours, with the average daily sun hours ranging from *c.a.* 12.3 to 12.5 hours.

4.2.2 Climate data and classification

Hourly data was collected from six automatic weather stations (AWS) from the Institute for Soil, Climate and Water (ISCW) of the Agricultural Research Council (ARC). Air temperature, relative humidity, wind speed and rainfall were obtained from the AWS within a 1 km radius from the study sites for the period January 2012 to March 2016, *i.e.* for four years, as shown in Figure 1. Additional mesoclimatic ambient temperature and relative humidity sensors (Tinytag® model TGP-4500, Gemini Data Loggers, West Sussex, United Kingdom) housed in a radiation shield (Tinytag® model LS-1, Gemini Data Loggers, West Sussex, United Kingdom) were installed at all the study sites above the grapevine canopy logging at 30 minute intervals. The sensor's temperature measurement range is between -25°C and +85°C, with a relative humidity measurement range of between 0% and 100%, logging for the four-year period of the study.

The logger sensor data were processed to average hourly data to be comparable to the weather station time intervals. The hourly data for the weather station and loggers were processed to average daily and monthly values for further analysis. Missing data within the years of the study were gap filled as a continuous climate dataset is required for climatic indices calculations. The gap filling procedure was done using the nearest weather station or logger to calculate the correlation equations. Refer to Table 4 in Addendum 4.1 for the regression equations used for gap filling.

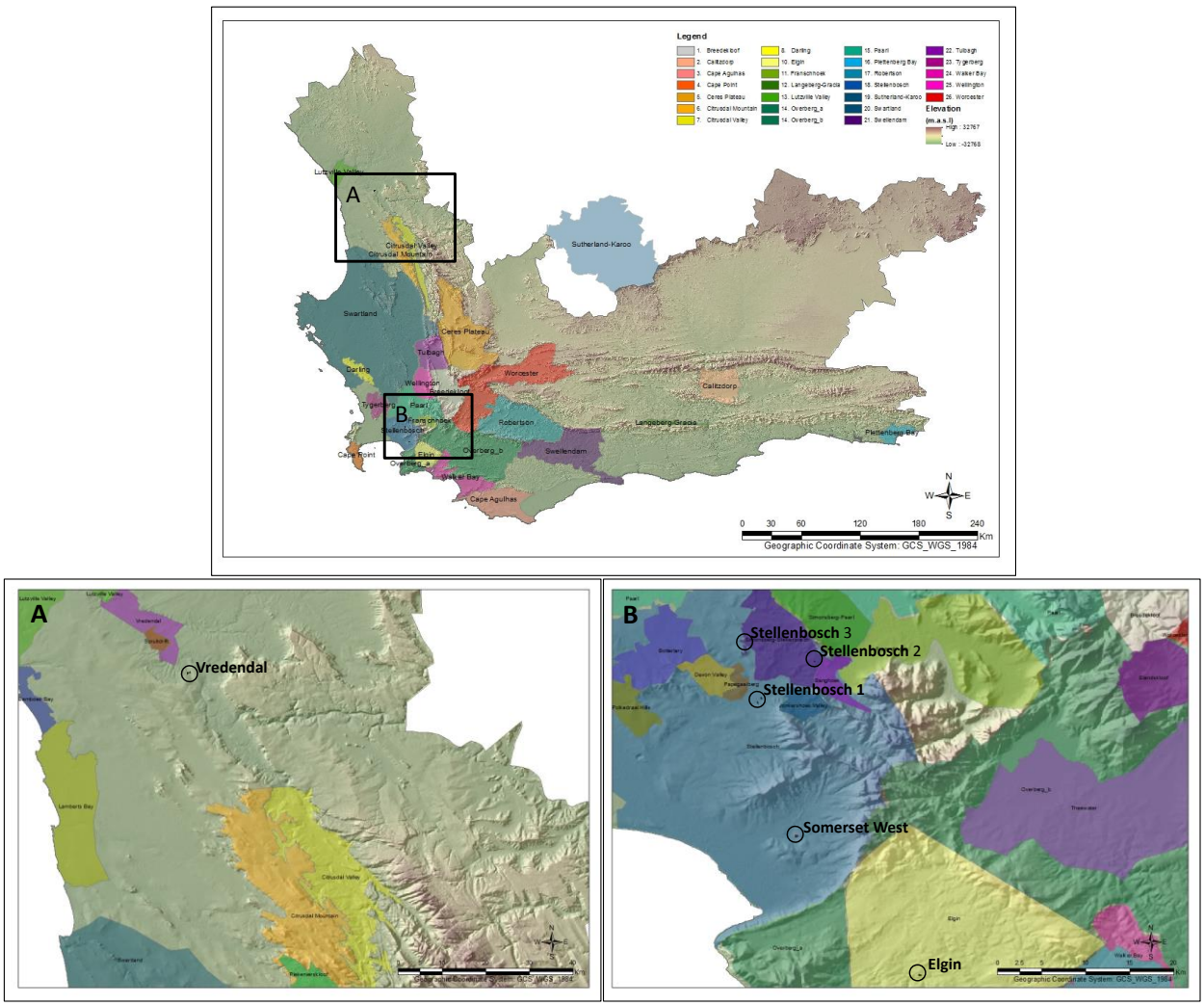

Figure 1 Map showing the Western Cape extent, with districts highlighted and main study areas (A & B) outlined (Top). Zoomed in sections A (bottom left) and B (bottom right) show the main study areas with the selected sites (encircled areas).

Table 1 Descriptions of study sites selected over a climatic band within region and districts of the Western Cape extent.

Region/ District	Locality	Latitude	Longitude	Distance from the ocean	Elevation in (m)	Aspect	Slope (%)	Hill-shade (degrees)	Global Radiation (kWh/ m^2)
Cape South Coast/ Elgin	Elgin	-34.165	19.031	15.4	196	103 (ESE)	6.3	192	1073.5
Coastal/ Stellenbosch	Somerset West	-34.089	18.907	7.7	136	271 (W)	6.5	164	1071.6
Coastal/ Stellenbosch	Stellenbosch_1	-33.923	18.873	21.0	112	184 (S)	5.5	181	1092.0
Coastal/ Simonsberg-Stellenbosch	Stellenbosch_2	-33.902	18.919	25.1	413	158 (SSE)	11.0	170	1071.2
Coastal/ Simonsberg-	Stellenbosch_3	-33.890	18.899	25.5	359	223 (SW)	6.2	155	1090.7
Olifants River	Vredendal	-31.792	18.626	34.9	74	339 (NNW)	2.3	187	1084.1

Mesoclimate classification

The hourly climatic data was used to quantify the diurnal environment at each of the study sites over the climatic band for all four seasons. Hourly data was also used in a frequency data analysis, based on a set of thresholds range (classes) for temperature (T), relative humidity (RH) and wind speed (U2) assimilated from literature (Hunter & Bonnardot, 2011). Temperature classes ranged from 0<x<5 to 50<x<55°C in 5°C intervals, relative humidity ranged from 0<x<20 to 100<x<120% RH in 20% intervals and wind speed (U2) ranged from 0<x<2 to 20<x<22 m/s in 2 m/s intervals. Using frequency tables on datasets, the amount of hours observed in each of the classes was attained for months and sites. The climatic requirements of the physiological processes were studied using hourly temperature, wind speed and relative humidity data of four seasons (2012/2013 to 2015/2016) for all the months of the year (Hunter & Bonnardot, 2011).

The daily datasets from the weather stations and loggers were used as the input for the calculation of climatic indices to quantify the growing season over the climatic band and seasons. The average daily maximum and minimum temperature were used as inputs to derive climatic indices for areas of interest (Table 2). Grapevine growth is usually determined by the climatic potential of a region, calculated with different thermal indices for viticulture as described in Table 2. Popular indices for climatic demarcation worldwide are the Winkler or Huglin indices (Winkler *et al.*, 1974; Huglin, 1978; Tonietto & Carbonneau, 2004). Different climatic parameters (temperature, wind, rainfall and relative humidity) are seldom combined at global scale (Tonietto & Carbonneau, 2004) or at regional and local scales (Knight, 2006). These indices (heat summations over the growing season) result in classification of climatic regions broad enough to take short-term variation in climate into account that affect wine grape production and wine style that can be produced within a given climate and season (Jones *et al.*, 2010; Hunter & Bonnardot, 2011; Anderson *et al.*, 2012).

Table 2 Climate indexes and bioclimatic index equations used to classify the climate.

Equation	Climatic Indices	Calculations	References
Eq 1	Growing season average Temperature (GST)	$GST = \frac{\sum_{31.03}^{01.09}(Tmax + Tmin)/2}{n}$	(Anderson *et al.*, 2012)
Eq 2	Winkler Index (WI) expressed as Growing Degree Days (GDD)	$GDD = \sum_{31.03}^{01.09}(Tmax - Tmin)/2 - 10°C; \geq 0$	Winkler index (Amerine & Winkler, 1944) as adapted by Le Roux (1974)
Eq 3	Huglin Index (HI)	$HI = \sum_{31.03}^{01.10}\frac{(Tmean - 10°C) + (Tmax - 10\,°C)}{2}\,\mathrm{d}; \geq 0$	(Huglin, 1978)
Eq 7	Biologically Effective Degree Days (BEDD)	$BEDD = \sum_{31.03}^{01.09}\frac{\min[\max([Tmax + Tmin]}{2} - 10{,}0)K + DTRadj, 9$	(Anderson *et al.*, 2012)
Eq 4	CI (Cool night Index)	Mean minimum temperature of the ripening month, Southern Hemisphere ranges from January to March depending on the cultivar (early or late ripening)	(Tonietto & Carbonneau, 2004)
Eq 5	MJT	Mean January temperature	(Smart & Dry, 1980)
Eq 6	MFT	Mean February temperature	Smart and Dry (1980) adapted by De Villiers *et al.* (1996)

4.2.3 Software and statistical analysis

Tinytag® Explorer® 4.6 (Gemini Data Loggers, West Sussex, UK) was used for data downloading and configuring the Tinytag® devices. ArcGIS 10 (ESRI, California, USA) was used to create maps and extract layer information. Continuous hourly datasets for each station was processed in Statistica 10 ® (Statsoft, Tulsa, UK). Statistical analysis was conducted using Statistica 10 ® (Statsoft, Tulsa, UK), for the analysis of plots of hourly means per site or per season over the climatic band, as well as the linear regressions analysis for climatic variables.

4.3 Results and discussion

4.3.1 Site mesoclimates and diurnal differences

Climate differences over sites are driven by a number of environmental interactions (Table 1). The occurrence of the sea breeze during the ripening period, and the impact thereof on the afternoon and evening temperatures and relative humidity of the region, cannot be ignored (Bonnardot *et al.*, 2001). The cooler sites are Elgin and Stellenbosch 3, the intermediate sites over the climatic band is Somerset West and Stellenbosch 2, the warmer and warmest sites are Stellenbosch 1 and Vredendal respectively. More detail of the sites is described in Table 5 in Addendum 4.1. The meso-scale climates of each study site is described in Table 5 (in Addendum 4.1) and classified into classes based on the Anderson *et al.* (2012) classifications. The Elgin study site is situated in the Cape South Coast Region. Elgin has a “warm” growing season (GST) and classified as “intermediate to warm” based on WI and HI with a “cool to warm” CI, receiving an average of 814 mm annual rainfall. The Stellenbosch 3 site is situated in the Coastal Region, within the district of Stellenbosch, on the upper slopes of the Simonsberg Mountain. The GST is “warm”, with a “warm to hot” region for WI and HI and the CI of “warm to cool”, receiving an average of 780 mm rain annually.

The intermediate sites in Somerset West site is situated on the west facing lower slopes of the Helderberg Mountain, within the Stellenbosch district of the Coastal region. This particular site is

classified with a “warm to hot” GST and “hot” for WI and HI with “warm” nights and receives, on average, *c.* 654 mm rain per year. The other intermediate site, namely Stellenbosch 2 site is situated on the SSE facing slopes of the Simonsberg in Stellenbosch at an elevation of 413 m within the district of Stellenbosch in the Coastal region and. The Stellenbosch 2 site is comparable to the Somerset West site, but receives substantially more annual rainfall (1003 mm/year). The WI and HI ranges from “warm to hot”, with a “cool to warm” CI.

The Stellenbosch 1 site is the warmest compared to the other Stellenbosch sites and receives the least rainfall at 631 mm/year. This can probably be attributed to the south facing site being positioned on the lower foothills of the Stellenbosch Mountain at an elevation of 112 m. The GST is “hot” with the WI and HI classifying the site as “very hot” with “cool to warm” nights for CI. The warmest site is Vredendal, receiving the lowest rainfall at 188 mm/year over the study period. The Vredendal site is the furthest from the ocean (35 km) compared to all of the other sites and at the lowest elevation of 74 m experiencing “very hot” GST and the WI and HI ranging from “very hot“ to “too hot” with a CI of “hot to warm“ (Table 5 in Addendum 4.1). The Vredendal area is a popular wine producing area, with grape production highly dependent on the supply of water for irrigation. Successful wine grape production in Vredendal confirms the importance of water resources to overcome environmental conditions that could be detrimental to wine grape production. Even in the most extreme cases of climate change, wine grapes could still be produced if there are sufficient water resources available.

Diurnal variations at the different sites

Diurnal temperature differences are affected by relative humidity and wind velocity at the site driven by the surrounding topographic attributes. Before 08h00, there were groupings of three warmer and three cooler sites in winter and summer with respect to diurnal mean hourly temperatures (Figure 2). After 08h00, there were similar trends but there were differences between the two warmer sites having the highest amplitudes in summer and winter. Stellenbosch 1 had the largest variability in minimum and maximum diurnal temperatures for summer and winter. Elgin was cooler than all the other sites throughout the day. As expected, Vredendal was the warmest site in minimum and maximum mean temperatures in the diurnal cycle. In addition to this, temperatures at the Vredendal site took the longest to cool down after the hottest part of the day. This would influence the grapevine recovery from the day’s stress. Hence, the sites are highly dependent on irrigation. The two intermediate sites, *i.e.* Stellenbosch 2 and Somerset West, had the smallest daily temperature variations between the maximum and minimum values.

Before 07h00 and 09h00 in summer winter, respectively, there were groupings of four lower relative humidity and two higher relative humidity sites (Figure 3). As the day progresses in both summer and winter, the highest humidity was observed at the cooler sites and sites nearer to the ocean with the lowest humidly at the warmest site. Shifts in RH could be due to distance from the ocean, but could also be due to less wind at Elgin compared to Vredendal. Even though Vredendal is the furthest site from the sea, there is an ocean breeze effect that brings about diurnal cooling and lower RH (Figure 4). Elgin is close to the ocean, experiencing low wind velocities and high RH. Tis could be due to the Overberg Mountain range, which encourages a build-up of mist in the Elgin basin. Wind velocity at Vredendal and Somerset West were most variable over seasons (summer/winter) and years (Figure 4). Lower wind velocity resulted in higher relative humidity in (2014/15) season. The RH trend was most different for Vredendal compared to other sites, which could be due to the area being more semi-arid and the air drier in general, with less topographical variability as is the case in the other sites.

The occurrence of wind is very variable and complex within the Western Cape and this complexity is reflected in the study sites (Figure 4).The Somerset West site experienced the highest wind velocity and duration throughout the average day over the four seasons for summer and winter. The Stellenbosch 2 site is positioned similarly to that of the Somerset West site in terms of proximity to a mountain range and is located at the foot of the Simonsberg. However, it did not experience the same wind velocities and frequency compared to the Somerset West site. This is due to distance from the ocean, but even more so due to wind direction, with the summer wind blowing towards the Simonsberg, rather than down the Helderberg. The Somerset West site is also exposed to the well-known South Easter that is very dominant in the summer months.

The diurnal variation in climatic factors at a site is important for understanding the shifts in climate and the grapevine's response to more extreme growing conditions. It is of great value to be able to quantify the extremes in more than just temperature, such as looking into wind and relative humidity, as the grapevine has physiological processes that are reliant on the surrounding environmental conditions for optimal functioning (Hunter & Bonnardot, 2011).

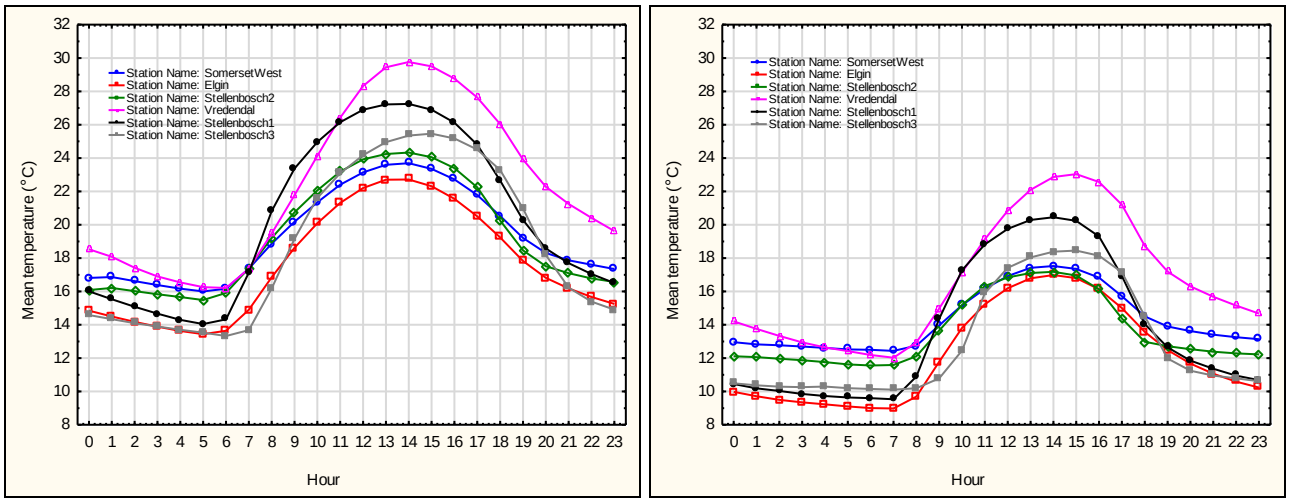

Figure 2 Diurnal mean hourly temperature variations for all study sites summarised over all four study seasons, split into summer (September to March) on the left and winter on the right (April to August).

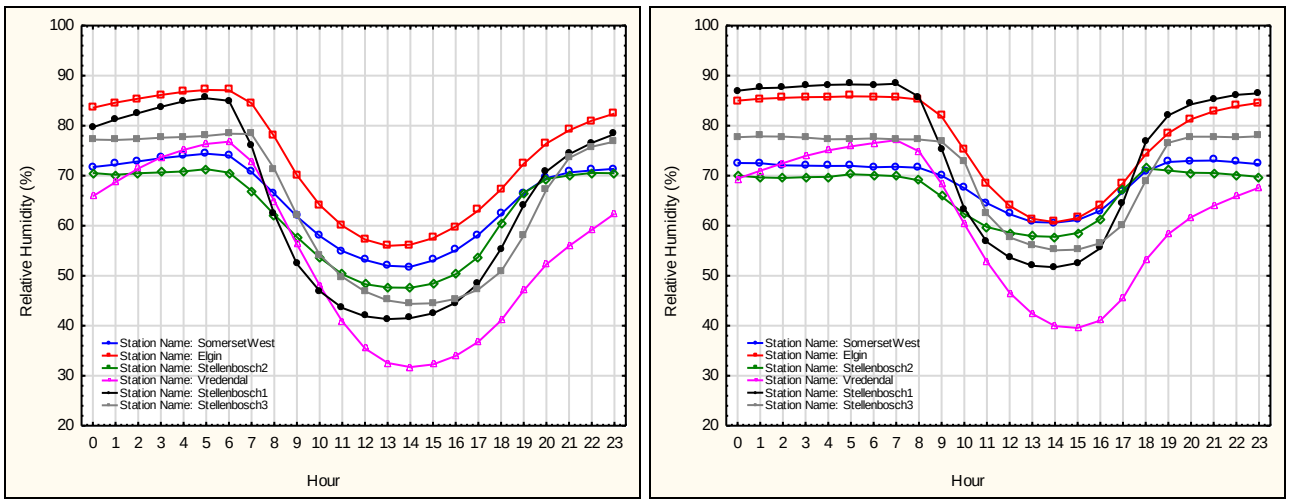

Figure 3 Diurnal mean relative humidity variations for all study sites summarised over all four study seasons, split into summer (September to March) and winter on the right (April to August).

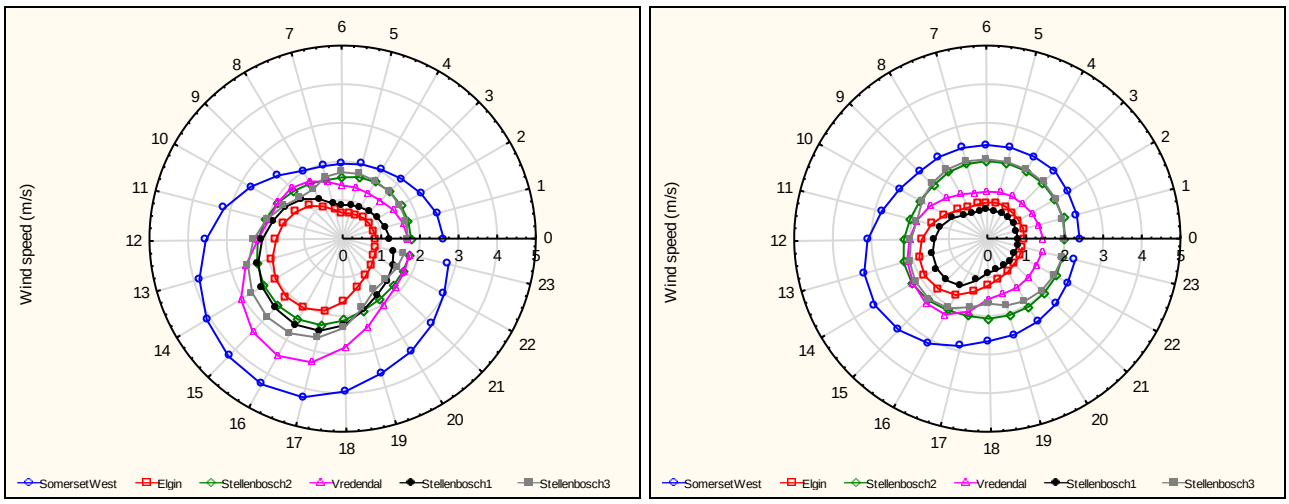

Figure 4 Diurnal mean wind velocity variations for all study sites summarised over all four study seasons, summarised into summer (September to March) on the left, and on the right, summarised for winter (April to August).

4.3.2 Seasonal variability and trends

Grapevine growth is usually determined by the climatic potential of a region, quantified using different thermal indices as described in Table 2. The most frequently used indices for climatic demarcation worldwide are the Winkler and Huglin indices (Winkler *et al.*, 1974; Huglin, 1978), expressed as growing degree days (GDD). For the purpose of this discussion, only the WI will be used to describe the growing season at the different sites selected over a climatic band for presentation purposes. The Elgin and Stellenbosch 3 sites are the coolest and Vredendal is the hottest site, also in terms of accumulated GDD from 1 September to 31 March. Seasonal variability (Figure 5) is similar in extremes, but with seasonal differences noticed in the median data of sites over seasons. It is evident that there is a larger variation over the climate band separating sites from warmer to cooler, yet within the larger trend there is a clear seasonal variability noticed. The thermal heat accumulation over the growing season only accounts for the accumulated temperatures, which are indirectly influenced by other environmental variables, but not explaining possible monthly shifts. It is of importance in the context of climate change and predicted extreme events to also account for other environmental factors, such as rainfall, wind, relative humidity *etc.* causing seasonal shifts at specific sites, and to account for when in the season the events take place.

Mean monthly air temperature, relative humidity and wind indicated that the atmospheric conditions varied during the four growing seasons (data not shown). The most evident changes observed over the four seasons and six sites are described in Table 5 in Addendum 4.1. This includes an evident increase in mean January temperatures by 2°C in the last season and decrease in March mean temperatures, with 2015/16 being the coolest of all the seasons. Mean February temperatures remained comparable over all the seasons. There is a cooling trend over all seasons seen in the months of August and September, cooler than the long term mean, which could influence the timing and homogeneity of budburst. Rainfall in season 2013/14 was more than double compared to other seasons; with most of the rainfall received in the summer months. The analysis over the four seasons highlights a general trend of decreased rainfall over all the sites, but it was still unpredictable in the timing and quantity as described in Table 5 in Addendum 4.1.

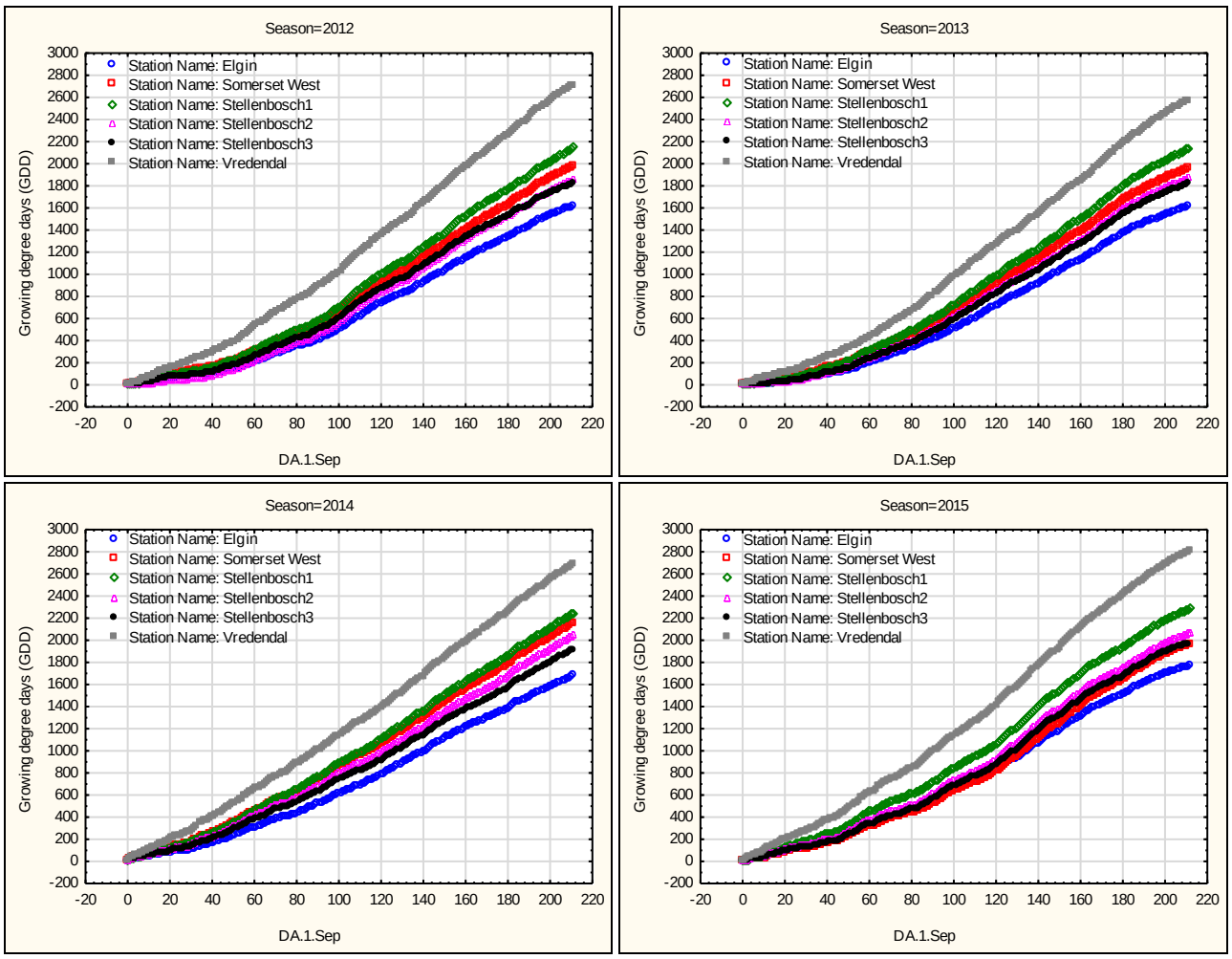

Figure 5 Growing degree days calculated using the Winkler Index, starting from 1 September and indicating days after that date (DA.1.Sep) on the X-axis for the four growing seasons categorised by sites.

Overall there was no significant seasonal variability over the sites, other than the expected seasonal variability within sites, *i.e.* the vintage effect. The seasonal variability is, however, expected to increase in the context of climate change; the largest difference expected and already noted as temperature increases in early summer months and shifts in rainfall quantity and timing. The increase noted in spring and summer temperatures may accelerate the growing and ripening period of the grapevine. However, the cooler February and March temperatures may slow down ripening, with possible enhanced colour formation and flavour retention in later ripening red cultivars.

4.3.2.1 Frequency data analysis for seasons.

Although variability over seasons and sites are reported using climate classifications and averaged diurnal analysis, finer scale analysis using frequency analysis can be applied to ascertain the in-season and between-site variability in the context of climate change. Hourly datasets were separated into temperature, relative humidity and wind speed classes based on previously reported thresholds for grapevine physiological functioning (Hunter & Bonnardot, 2011). Temperature classes were divided into 5°C intervals ranging from 0-5°C to 50-55°C, yielding 11 classes (Figure 6). Relative humidity was divided into classes of 20% RH intervals as shown in Figure 7, with Figure 8 showing wind velocity, classified into 2 m/s intervals ranging from 0 to 22 m/s (also 11 classes). Overall seasonal and site differences based on the grouped frequency

analysis is described in Figure 9 and Figure 10 (in Addendum 4.1) highlighting the finer scale differences that will affect the grapevine's response.

The most prominent seasonal differences over all seasons was in the month of January, with a noted decrease in hours at cooler temperatures and increasing warmer temperatures (25-40°C) over the seasons from 2012 to 2015. December is getting cooler over the seasons from 2012 to 2015 as hours at higher temperatures of 20-35°C are decreasing. The month of March is warming for the last two seasons with decreased hours at lower temperatures and increased hours at higher temperatures. The winter months are slightly different over seasons, with July showing a slight trend of cooling with more hours at 5-10°C, and less at warmer classes, with the last month of winter showing a warming trend with more hours at 10-25°C. The first month of spring, September has shown a warming in the last two seasons with more hours' between15-30°C. The coolest season of the study is the 2012/2013 season, with more hours at cooler temperatures throughout the year.

Temperature differences driven by site variability over the climatic band are shown in the frequency analysis results for temperature classes for all the months of the year averaged over the seasons (refer to Figure 9 and Figure 10 in Addendum 4.1). The analysis overall highlighted the three warmest sites as discussed in sections above, which showed more hours at warmer temperature classes, with the cooler sites showing more hours at lower temperature classes as expected. Overall, the Somerset West site had more than double the hours at 10-15°C compared to the other sites. This could be due to windy conditions, with the other sites yielding more hours at 15-25°C in the summer, while Vredendal had more observations at higher temperatures (20-40°C).

Of all the months, January showed more noticeable seasonal and site differences, and hence is the only month discussed in more detail to emphasise the need and applicability of finer scale climate analysis to describe seasons and sites. This month's hours at cooler temperatures (10-20°C) are decreasing, and observations at warmer temperatures (20-40°C) are increasing over the seasons (Figure 6, left). Relative humidity shows the inverse trend, with observations at lower relative humidly at 20-60% increasing and decreasing for higher relative humidly of 60-100% (Figure 7, left). The summer wind speeds were the highest in the 2012/13 and 2013/14 seasons, with less light breezes at 0-2 m/s but more hours at higher wind speeds of between 4-10 m/s, the lowest wind speeds were noted in the 2014/15 season at 0-2 m/s (Figure 8, left).

Site variability was more prominent in the extreme months such as the middle of summer and winter. For January, Somerset West had most of its observations at 10-20°C, Elgin, Stellenbosch 2 and Vredendal at 15-25°C and Stellenbosch 1 and 3 at 15-30°C (Figure 6, right). Warmer sites had more observations at 25-40°C, and cooler sites at 10-20°C. The higher frequency of cooler temperatures at Somerset West is attributed to the site having the highest wind speeds with more observations at 4-10 m/s, and fewer observations at 0-4 m/s compared to other sites. Elgin experienced light breezes of between 0-2 m/s with a few observation at 2-4 m/s. Vredendal and Stellenbosch sites experienced wind speeds of 0-4 m/s only (Figure 8, right). Cooler sites with less wind showed more observations at higher relative humidity, with the Elgin site having more observations between 60-80% and, Somerset West at 40-80%. Warmer sites such as Vredendal, and Stellenbosch 1 have similar observation at all RH classes (Figure 7, right). More wind is experienced in the summer months compared to winter in most of the Western Cape (data not shown).

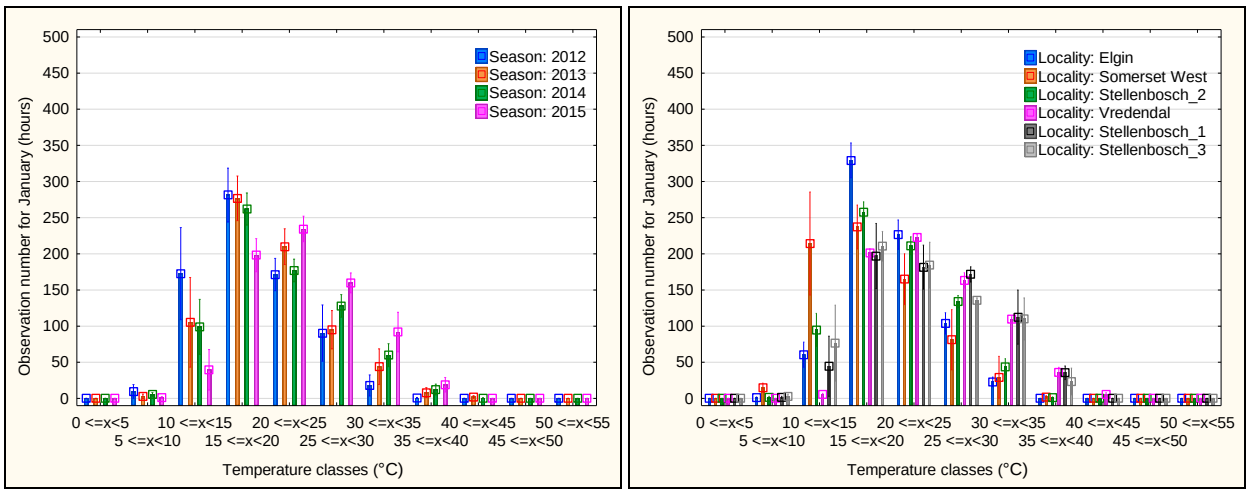

Figure 6 Frequency observations for January, hours observed at different temperature classes (0<=x<5; 5<=x<10; …50<=x<55) degrees Celsius for the four seasons over all sites (left) and sites for all seasons (right).

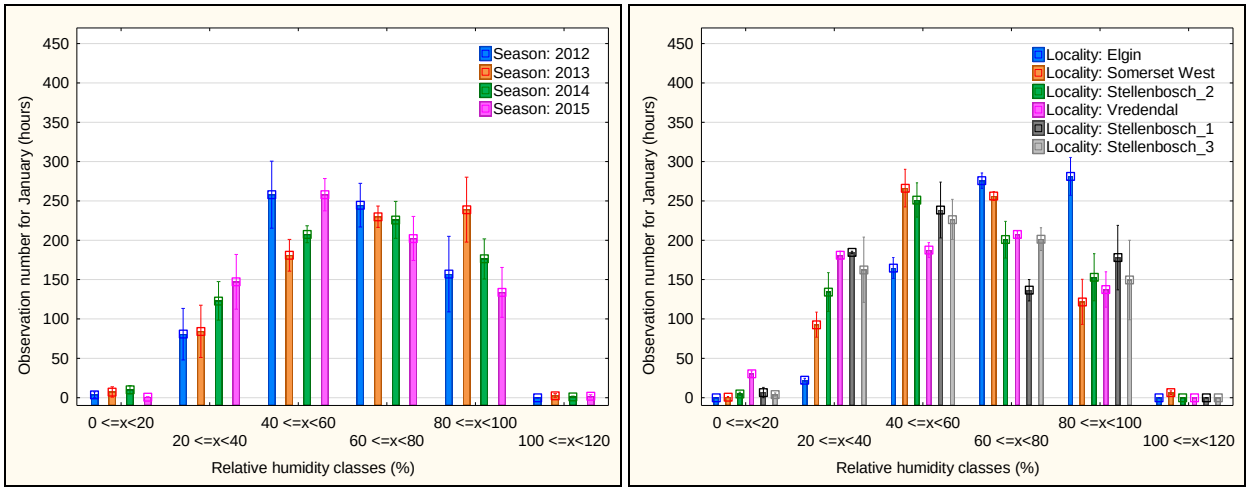

Figure 7 Frequency observations for January, hours observed at relative humidity classes (0<=x<20; 20<=x<40; …100<=x<120) in percentage for the four seasons over all sites (left) and sites for all seasons (right).

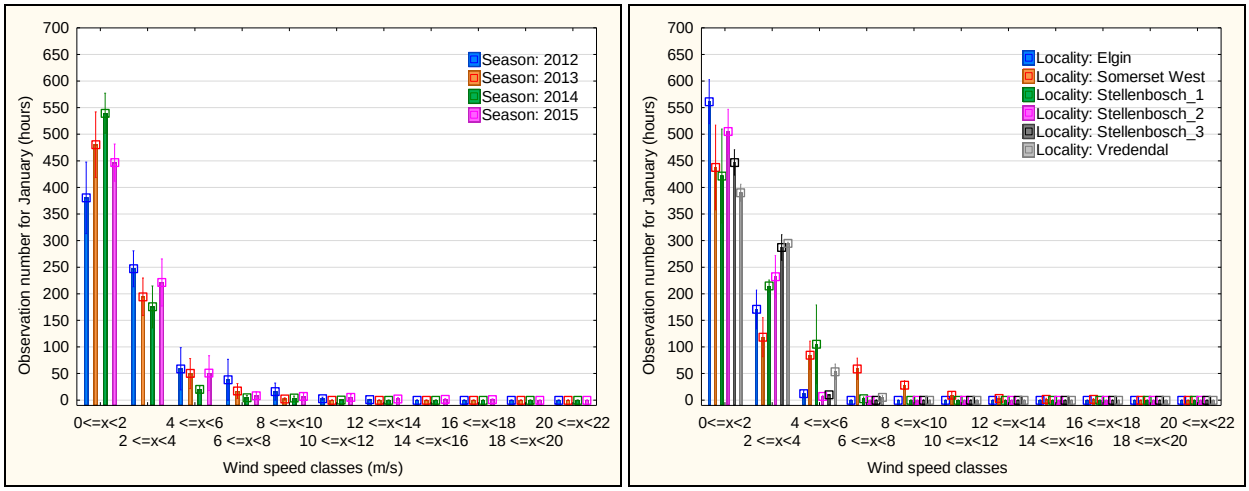

Figure 8 Frequency observations for January, hours observed at wind speed classes (0<=x<2; 2<=x<4; 20<=x<22) in meters per second for the four seasons over all sites (left) and sites for all seasons (right).

Temperature frequency data can possibly be used to explain the vintage effects summarised in the annual harvest reports published for the wine industry. Historical observed grapevine response can

be assessed in the context of the climate of the growing season to better understand the grapevine's response. The frequency analysis is seen as a more robust way to ascertain what climatic factors mostly affect the grapevines response in growth and ripening. The 2008/2009 season was marked as South Africa's best compared to past seasons (Vinpro, 2009), with the 2012/2013 season having the biggest harvest. In the 2013/2014 season, white cultivars ripened late and the season was overall later, with the 2014/15 season being the earliest season in decades (Vinpro, 2013, 2014, 2015). Frequency analysis of hourly climate data could highlight the environmental factors that were more predominant to drive the grapevine's response. More detail regarding this aspect; will be given in Chapter 7. The later or early phenology is driven by cooler or warmer temperatures, as expressed through the number of hours observed at specific classes.

4.3.2.2 Temporal and spatial resolution of temperature data.

Temperature data of higher temporal and spatial resolution could describe a site with better accuracy; and including other climatic elements such a relative humidity and wind speed would improve the current demarcations for wine growing regions in the Western Cape.

Hourly data captures the extremes in timing and duration, information that was masked in the maximum and minimum daily averages used in most climate classification equations and even more so when describing areas based on monthly data. It is expected that hourly data moderates the extremes if it is computed by computing the "real" average daily temperature, *i.e.* the average temperature over the entire day to use as the mean temperature input for indices, rather than using the daily maximum and minimum, which tends to slightly overestimate the climate as the daily data only captures the warmest and coolest hours in the computation.

The selection and application of climatic indices need to be reviewed in the context of climate change, especially the classification classes internationally used to describe the indices. South Africa is warm to intermediate, with many areas classified as too hot. There are however many environmental factors moderating the daily temperatures as well as irrigation buffering the too hot areas, making these areas cooler and viable for high quality table wines. In the context of climate change, where more extreme events of higher frequency and duration are predicted, it could be of value to use climatic indices that include some of the daily extremes such as the Huglin Index, as it includes a stronger weighting for maximum temperatures (Huglin, 1978), compared to other indices such as the Winkler Index. In the context of climate change and seasons shifting earlier, there is a need for new indices that quantify the ripening season with more detail and including more climatic indices understanding the diurnal nature of an area.

Temperature logger resolution and position is important for accurate data acquisition, especially when loggers are placed above the canopy of the grapevine to measure mesoclimatic factors. Slightly warmer temperatures and higher relative humidity are collected by these loggers compared to the weather stations, as seen in Table 6 in Addendum 4.1. Even though there is an excellent correlation ($R^2 \geq 0.96$) for logger and weather station temperatures for all sites (n=5) and seasons (n=4) (Table 3), the small offsets in the slope and intercept of graphs can cause bigger differences in climatic indices, as it is accumulative. The regression equations for each site and season can be used for gap filling of weather station data, to ensure a continuous dataset for index calculations.

Table 3 Correlation of temperature data sourced from a vineyard logger and weather station, averaged over all sites and over all seasons.

Analysis	Regression Equation	*r*	*p*	*R 2*
AllGroups	y = 0.2905 + 1.0015*x	0.98	0.000	0.96
SomersetWest	y = 1.0926 + 0.9719*x	0.95	0.000	0.9
Elgin	y = -0.3693 + 1.0703*x	0.98	0.000	0.96
Stellenbosch_2	y = -0.1704 + 1.0323*x	0.98	0.000	0.96
Vredendal	y = -0.4777 + 1.0109*x	0.99	0.000	0.98
Stellenbosch_1	y = 0.3282 + 0.9892*x	0.99	0.000	0.97

4.4 Conclusions

Seasonal variability within the study period showed a general increase in the heat based indices (WI and HI), and a decrease in the cool night index (CI). The most evident changes observed over the four seasons for the six sites were an increase in mean January temperatures and a decrease in March mean temperatures. The increase in January temperatures will probably accelerate the ripening period of the grapevine. However, the cooler temperatures in February and March will likely slow down ripening, with enhanced colour formation and flavour retention in later red cultivars. Seasonal variability seemed to be the driving factor possibly affecting the grapevine over and above site differences, as the seasonal differences were evident over all the sites. The warmer sites and cooler sites in the context of climate change are shifting to possibly “too hot” and “hot” sites (as classified by Anderson *et al.* (2012)), respectively for grapevines. However, this can be buffered with short term practices such as irrigation and canopy management at the respective sites, negating the “too hot” classification. As South Africa is warm to intermediate over all, with many areas classified as too hot, the selection and application of climatic indices need to be reviewed in the context of our local terrain and climate change, especially the classification classes used internationally to describe the climates of sites.

The study shows that the mean climatic data and indices are not sufficient to properly understand variation in climatic conditions or to quantify the impact on grapevine growth and ripening at a particular location within a specific season in the context of climate change in the Western Cape. Due to the complexity of factors influencing the environment and the sensitivity of the grapevine to change, the site and seasonal variability should be explained using hourly data, where the diurnal trend of warming, speed of warming and recovery rate for temperature, relative humidity and wind are quantified. Finer scale analysis using hourly data for frequency analysis and for diurnal analysis of sites and seasons is important, within the climatic indices describing a site or season. The specific climatic kinetics within seasons and sites would influence the grapevines physiological functioning. Sites classified as “too hot” for viticulture, such as at Vredendal, yet it is an area producing high yields and acceptable quality wines, albeit more focused at bulk wine production. Within the context of climate change and the predicted changes in rainfall distribution over the typical rainfall season, careful water management is important. Frequency data could improve in season management, as more hours at high temperatures in the critical growing periods with lower relative humidity as a site will mean more water constraints. Similarly, analysis only based on temperature shows Somerset West to be a more favourable site, but further insight into the wind speeds experienced throughout the year changes the perspective for varietal selection and management practices to be applied for best grapevine responses.

The overall climatic indices, diurnal site description and frequency detail will give insight into changes in the varieties planted in wine regions as well as shifting planting to more suitable zones for viticulture with some regions becoming warmer or too warm all together while others become

more viable. The extreme sites in the study, Vredendal and Elgin, can be better managed in the future based on finer scale analysis, aiding in better adaptive strategies in the context of a changing climate, shifting short and long term practices, shifting the wine marketing for more realistic wine styles that match the environmental conditions.

Spatial and temporal resolution of climate data is important in the context of climate change, to describe a site with better accuracy; and including more than temperature, other climatic elements such a relative humidity and wind speed would improve the current demarcations for wine growing regions in the Western Cape. The input resolution should be selected based on the output required. Daily data is sufficient for use in climatic indices, to account for the maximum and minimum daily extremes. Results showed that vineyard temperature loggers and weather stations have a good correlation. However, loggers seemed to report slightly warmer temperatures and higher relative humidity. The small differences in observed temperatures between the loggers and weather stations can result in larger errors in heat summation indices. These errors may be so substantial that climate of a particular site could be classified incorrectly the.

Climate exerts a dominant influence on wine production, driving baseline suitability, largely controlling crop production and quality and ultimately driving economic sustainability. Hence, an understanding of the finer scale climate analysis as the diurnal cycle and frequency observations of temperature, wind and relative humidity for a specific site is especially important in the context of climate change in the Western Cape. Considering the relationships between climate and grapevine responses, slight climatic differences have implications for the physiological functioning of grapevines, causing significant changes in the management of existing vineyards. Therefore, optimising the grapevines growth and ripening responses based on hourly frequency observations is important for adaption to climate change.

4.5 References

Amerine, M.A. & Winkler, A.J., 1944. Composition and quality of musts and wines of California grapes. Hilgard 15, 493-673.

Anderson, J.D., Jones, G.V., Tait, A., Hall, A. & Trought, M., 2012. Analysis of viticulture region climate structure and suitability in New Zealand. J. Int. Sci. Vigne Vin. 46, 149-165.

Becker, N., 1985. Site selection for viticulture in cooler climates using local climatic information. In: Heatherbell, D.A., Lombard, P.B., Bodyfelt, F.W. and Price, S.F. (eds). Proc. The IVth International Symposium on Cool Climate Viticulture and Enology, Oregon State Univ., Agricultural Experiment Station Technical Publication no. 7628, 16-20 July, Rochester, New York. pp. 20-34.

Bonnardot, V., Carey, V., Planchon, O. & Cautenet, S., 2001. Sea breeze mechanism and observations of its effects in the Stellenbosch wine producing area. WineLand. pp. 107-113.

Bonnardot, V., Carey, V. & Strydom, J., 2004. Weather stations: applications for viticulture. Wynboer, May. pp. 88-90.

Bonnardot, V. & Carey, V.A., 2008. Observed climatic trends in South African wine regions and potential implications for viticulture. In: Proc. VIIth international viticultural terroir congress 19-23 May, Nyon, Switzerland. pp. 216-221.

Bonnardot, V., Carey, V.A., Madelin, M., Cautenet, S., Coetzee, Z. & Quénol, H., 2012. Spatial variability of night temperatures at a fine scale over the Stellenbosh wine district, South Africa. J. Int. Sci. Vigne Vin 46, 1-13.

Carey, V.A., 2001. Spatial characteristic of natural terroir units for viticulture in the Bottelaryberg-Simonsberg-Helderberg winegrowing area. Thesis, Stellenbosch University, Private Bag X1, 7602 Matieland (Stellenbosch), South Africa.

Carey, V.A., 2005. The use of viticultural terroir units for demarcation of geographical indications for wine production in Stellenbosch and surrounds. Dissertation, Stellenbosch University, Private Bag X1, 7602 Matieland (Stellenbosch), South Africa.

Carter, S., 2006. The projected influence of climate change on the South African wine industry. In IIASA Interim Report. pp. 33.

Champagnol, F., 1984. Eléments de physiologie de la vigne et de viticulture générale. François Champagnol, Saint-Gely-du-Fesc, France, 351.

Coombe, B.G., 1987. Influence of temperature on composition and quality of grapes. Acta Horticulturae., 23-36.

De Villiers, F.S., Scmidt, A., Theron, J.C.D. & Taljaard, R., 1996. Onderverdeling van die Wes-Kaapse wynbougebiede volgens bestaande klimaatskriteria. Wynboer Tegnies, January 1996, 10-12.

Hamilton, R.P., 1989. Wind and its effects on viticulture. Aust. Grapegrow Winem 303, 16-17.

Huglin, P., 1978. New method for evaluating the potential of solar thermal environments wine. In: Proc. International Symposium on Ecology of Grapevine, I, Constance, Romania, 1978. Ministry of Agriculture and Food Industry, pp. 89-98.

Hunter, J.J. & Bonnardot, V., 2011. Suitability of some climatic parameters for grapevine cultivation in South Africa, with focus on key physiological processes. S. Afr. J. Enol. Vitic 32, 137-154.

Irimia, L.M., Patriche, C.V. & Quenol, H., 2014. Analysis of viticultural potential and delineation of homogenous viticultural zones in a temperate climate region of Romania. J. Int. Sci. Vigne Vin 48, 145-167.

Jackson, D.I. & Lombard, P.B., 1993. Environmental and management practices affecting grape composition and wine quality. A review. Am. J. Enol. Vitic 44, 209-230.

Jones, G., 2006. Climate and terroir: Impacts of climate variability and change on wine. In: Macqueen, R.W. and Meinert, L.D. (eds). Fine wine and terroir-The geoscience perspective. Geoscience Canada, (Geological Association of Canada, St John's, Newfoundland). pp. 1-14.

Jones, G.V. & Davis, R.E., 2000. Climate influences on grapevine phenology, grape composition, and wine production and quality for Bordeaux, France. Am. J. Enol. Vitic. 51, 249-261.

Jones, G.V., Duff, A.A., Hall, A. & Myers, J.W., 2010. Spatial analysis of climate in winegrape growing regions in the western United States. Am. J. Enol. Vitic. 61, 313-326.

Kliewer, W.M., 1971. Effect of day temperature and light intensity on concentration of malic and tartaric acids in *Vitis vinifera* L. grapes. J. Amer. Soc. Hort. Sci. 96, 372-377.

Knight, F., 2006. A Macro scale analysis of the vineyard production potential of the RSA. Winelands, November, 2006.

Le Roux, E.G., 1974. A climate classification for the South Western Cape viticultural areas (in Afrikaanse). Thesis, Stellenbosch University, Private Bag X1, 7602 Matieland (Stellenbosch), South Africa.

Midgley, G.F., Chapman, R.A., Hewitson, B., Johnston, P., de Wit, M., Zievogel, G., Mukheibir, P., van Niekerk, L., Tadross, M., van Wilgen, B.W., KGOPE, B., Morant, P.D., Theron, A., Scholes, R.J. & Forsyth, G.G., 2005. A Status Quo , Vulnerability and Adaptation Assessment of the Physical and Socio-Economic Effects of Climate Change in the Western Cape. Analysis, 157.

Saayman, D., 2014. South African vineyard soils and climates. Wineland, January. http://www.wosa.co.za/The-Industry/Terrior/Related-Articles/Terroir-South-African-Vineyard-and-Soils-and-Climate/

Smart, R.E. & Dry, P.R., 1980. A climatic classification for Australian viticultural regions. Austr. Grapegrow. Winem. 196, 9-16.

Soltanzadeh, I., Bonnardot, V., Sturman, A., Quénol, H. & Zawar-Reza, P., 2016. Assessment of the ARW-WRF model over complex terrain: the case of the Stellenbosch Wine of Origin district of South Africa. Theor. Appl. Climatol., 1-21.

Tonietto, J. & Carbonneau, A., 2004. A multicriteria climatic classification system for grape-growing regions worldwide. Agricultural Forest Meteorol. 124, 81-97.

Van Niekerk, A. & Joubert, S.J., 2011. Input variable selection for interpolating high-resolution climate surfaces for the Western Cape. Water SA 37, 271-280.

Vinpro, 2009. 2009 Harvest Report. www.wosa.co.za.

Vinpro, 2013. South African Wine: Harvest Report. pp 1-16. http://www.sawis.co.za/info/download/VINPRO_OESVERSLAG_2013_ENG.pdf.

Vinpro, 2014. South African Wine: Harvest Report. http://www.sawis.co.za/info/download/SA_HarvestReport_VinPro_8May2014_ENG.pdf.

Vinpro, 2015. South African wine:Harvest Report 2015. www.wosa.co.za.

Winkler, A.J., 1965. General Viticulture. Univ of California Press, University of California, Berkeley.

Winkler, A.J., Cook, J.A., Kliewer, W.M. & Lider, L.A., 1974. General Viticulture. Univ. Calif.

Addendum 4.1

Table 4 Correlation analysis between temperature loggers and weather stations used for gap filling ares of missing data.

Site and season	Loggers				Weather station			
	r	*p*	R^2	Mean temperature	*r*	*p*	R^2	Mean temperature
Somerset West	**0.96**	**0.000**	**0.92**	**1.5852+0.9159*x**	**0.96**	**0.000**	**0.92**	**-0.1302+1.0054*x**
Somerset West_2012/13	0.95	0.000	0.90	5.2243+0.8071*x	0.96	0.000	0.90	-3.4783+1.1103*x
Somerset West _2013/14	0.96	0.000	0.91	1.7231+0.9076*x	0.96	0.000	0.91	-0.2181+1.0052*x
Somerset West _2014/15	0.96	0.000	0.93	1.5213+0.9142*x	0.96	0.000	0.93	-0.1816+1.0121*x
Somerset West _2015/16	0.92	0.000	0.86	2.6661+0.8622*x	0.92	0.000	0.86	0.4348+0.9917*x
Elgin	**0.98**	**0.000**	**0.96**	**0.8783+0.9913*x**	**0.98**	**0.000**	**0.96**	**-0.2086+0.9684*x**
Elgin_2012/13	0.99	0.000	0.98	-3.1031+1.2048*x	0.99	0.000	0.98	2.9991+0.8115*x
Elgin_2013/14	0.98	0.000	0.97	1.1568+0.9714*x	0.98	0.000	0.97	-E90.6955+0.995*x
Elgin_2014/15	0.97	0.000	0.94	0.9026+0.9836*x	0.97	0.000	0.94	0.0007+0.9587*x
Elgin_2015/16	0.97	0.000	0.95	1.5133+0.9694	0.97	0.000	0.95	-0.5118+0.9785x
Stellenbosch 2	**0.82**	**0.000**	**0.67**	**2.921+0.8374*x**	**0.82**	**0.000**	**0.67**	**3.5781+0.796*x**
Stellenbosch 2_2013/14	0.81	0.000	0.66	2.7984+0.8357*x	0.81	0.000	0.66	3.5309+0.7901*x
Stellenbosch 2_2014/15	0.82	0.000	0.67	2.7268+0.8462*x	0.82	0.000	0.67	3.5001+0.7917*x
Stellenbosch 2_2015/16	0.60	0.000	0.36	8.0338+0.6165*x	0.60	0.000	0.36	8.6522+0.59*x
Vredendal	**0.80**	**0.000**	**0.64**	**3.463+0.7854*x**	**0.80**	**0.000**	**0.64**	**5.0518+0.8155*x**
Vredendal_2013/14	0.43	0.005	0.18	13.6001+0.4198*x	0.43	0.005	0.18	14.5892+0.4359*x
Vredendal_2014/15	0.80	0.000	0.64	3.0636+0.7926*x	0.80	0.000	0.64	4.8568+0.8137*x
Vredendal_2015/16	0.66	0.000	0.44	7.4375+0.626*x	0.66	0.000	0.44	8.1319+0.7025*x
Stellenbosch 1a	**0.96**	**0.000**	**0.92**	**0.797+0.9372*x**	**0.96**	**0.000**	**0.92**	**0.6511+0.9818*x**
Stellenbosch 1a_2012/13	0.85	0.000	0.72	5.5633+0.6699*x	0.85	0.000	0.72	-1.0241+1.0697*x
Stellenbosch 1a_2013/14	0.91	0.000	0.82	2.7644+0.8201*x	0.91	0.000	0.82	0.3712+1.003*x
Stellenbosch 1a_2014/15	0.97	0.000	0.94	0.3211+0.9587*x	0.97	0.000	0.94	0.7088+0.9809*x
Stellenbosch 1a_2015/16	0.91	0.000	0.83	4.5116+0.8006*x	0.91	0.000	0.83	-0.9075+1.0428*x
Stellenbosch 1b	**0.97**	**0.000**	**0.95**	**0.1089+0.9686*x**	**0.97**	**0.000**	**0.95**	**0.762+0.9799*x**
Stellenbosch 1b_2012/13	0.94	0.000	0.89	1.624+0.8486*x	0.94	0.000	0.89	-0.1792+1.0501*x
Stellenbosch 1b_2013/14	0.97	0.000	0.95	-0.0192+0.9853*x	0.97	0.000	0.95	0.8827+0.9632*x
Stellenbosch 1b_2014/15	0.97	0.000	0.95	0.0744+0.9692*x	0.97	0.000	0.95	0.8545+0.9783*x
Stellenbosch 1b_2015/16	0.94	0.000	0.89	0.375+0.9675*x	0.94	0.000	0.89	2.036+0.9179*x

Table 5 Climatic indices calculated from daily weather station data to quantify the four growing seasons, summer (1 September-31 March) and winter (1 April-31 August).

Season	Site	[1]GST	[1]WI	[1]BEDD	[1]HI	[1]MFT	[1]MJT	[1]MMT	[1]CI	Annual Rainfall (mm)	Summer Rainfall (mm)	Winter Rainfall (mm)
2012/13	Somerset West	18.9	1974	1569	2211	21.05	21.20	20.67	15.3	647.8	272.4	375.4
2013/14	Somerset West	18.8	1961	1568	2226	22.69	21.63	18.80	15.7	1345.6	758.0	587.6
2014/15	Somerset West	19.7	2160	1713	2437	21.10	22.35	21.55	17.1	680.4	0.0	680.4
2015/16	Somerset West	18.9	1969	1544	2301	22.17	24.64	19.48	14.2	632.4	220.0	412.4
2012/13	Elgin	17.2	1615	1413	1972	19.48	19.43	18.48	13.9	868.7	277.5	591.3
2013/14	Elgin	17.1	1613	1426	1981	20.60	20.10	17.26	15.0	1449.2	527.8	921.3
2014/15	Elgin	17.5	1683	1518	2039	18.57	20.30	18.95	14.5	895.8	211.6	684.1
2015/16	Elgin	18.0	1769	1496	2110	19.76	21.94	17.67	13.7	676.9	246.3	430.6
2012/13	Stellenbosch_2	18.3	1862	1468	2280	20.66	21.12	20.24	15.4	1394.5	705.1	689.4
2013/14	Stellenbosch_2	18.3	1871	1491	2279	22.58	21.01	18.15	13.9	1315.6	480.5	835.1
2014/15	Stellenbosch_2	19.2	2054	1645	2411	20.12	21.44	21.25	17.3	934.0	189.8	744.2
2015/16	Stellenbosch_2	19.4	2072	1575	2390	21.50	24.76	19.41	13.3	681.1	241.5	439.6
2012/13	Vredendal	22.3	2715	1791	3147	24.57	24.82	23.96	19.7	228.1	89.8	138.2
2013/14	Vredendal	21.7	2577	1740	3015	25.58	24.40	21.88	17.9	313.3	80.2	233.1
2014/15	Vredendal	22.2	2697	1848	3020	23.02	24.62	23.32	17.7	192.2	70.8	121.4
2015/16	Vredendal	22.8	2809	1852	3170	24.90	26.88	21.52	16.9	142.8	33.5	109.3
2012/13	Stellenbosch_1a	20.2	2210	1677	2732	21.67	23.21	20.14	13.5	850.4	293.6	556.8
2013/14	Stellenbosch_1a	20.6	2309	1730	2823	23.14	22.94	19.90	14.5	955.1	379.0	576.1
2014/15	Stellenbosch_1a	20.8	2351	1822	2838	21.92	22.35	19.39	14.3	593.8	89.8	504.0
2015/16	Stellenbosch_1a	20.4	2286	1703	2788	22.54	25.68	20.21	14.8	449.4	141.1	308.3
2012/13	Stellenbosch_1b	20.2	2210	1677	2732	21.67	23.21	20.14	13.5	850.4	293.6	556.8
2013/14	Stellenbosch_1b	20.6	2309	1730	2823	23.14	22.94	19.90	14.5	955.1	379.0	576.1
2014/15	Stellenbosch_1b	20.8	2351	1822	2838	21.92	22.35	19.39	14.3	593.8	89.8	504.0
2015/16	Stellenbosch_1b	20.4	2286	1703	2788	22.54	25.68	20.21	14.8	449.4	141.1	308.3
2012/13	Stellenbosch_3	18.2	1826	1481	2362	20.17	21.26	19.04	15.7	927.4	308.8	618.6
2013/14	Stellenbosch_3	18.1	1817	1485	2377	22.37	21.07	17.92	14.8	1170.0	424.4	745.6
2014/15	Stellenbosch_3	18.6	1920	1624	2446	19.66	21.16	20.40	16.9	876.6	200.8	675.8
2015/16	Stellenbosch_3	18.9	1971	1543	2465	21.28	24.55	18.72	13.7	578.4	171.2	407.2

[1] GST: growing season temperatures; WI: Winkler index; BEDD: biologically effective degree days; HI: Huglin Index; MFT: mean February temperature; MJT: mean January temperature; MMT: mean March temperature and CI: Cool night index (minimum March temperature).

Table 6 Indices calculated using daily data sourced from temperature and relative humidity loggers (Log) and weather stations (Stat) to quantify the four growing seasons.

Season	Site	[1,2]GST_Log	[1,2]GST_Stat	[1,2]WI_Log	[1,2]WI_Stat	[1,2]MFT_Log	[1,2]MFT_Stat	[1,2]CI_Log	[1,2]CI_Stat
2012/13	Somerset West_1	19.2	18.9	2046	1974	21.2	21.1	16.9	15.3
2013/14	Somerset West_1	19.5	18.8	2114	1961	23.4	22.7	16.6	15.7
2014/15	Somerset West_1	20.2	19.7	2266	2160	21.4	21.1	18.2	17.1
2015/16	Somerset West_1	20.4	18.9	2291	1969	22.4	22.2	15.3	14.1
2012/13	Somerset West_2	19.1	18.9	2027	1974	21.2	21	16.9	15.3
2013/14	Somerset West_2	19.5	18.9	2111	1961	23.2	22.7	16.6	15.7
2014/15	Somerset West_2	20.1	19.7	2251	2160	21.4	21.1	18.2	17.1
2015/16	Somerset West_2	20.3	18.9	2277	1969	22.3	22.2	15.5	14.2
2012/13	Elgin	17.7	17.2	1717	1615	20.3	19.5	13.8	13.9
2013/14	Elgin	18.1	17.1	1808	1613	20.6	20.6	15.2	15
2014/15	Elgin	19	17.5	2007	1683	20.2	18.6	14.9	14.5
2015/16	Elgin	19.2	18	2035	1769	21	19.8	14.5	13.7
2012/13	Stellenbosch_2	18.4	18.3	1888	1862	21.2	20.7	16	15.4
2013/14	Stellenbosch_2	18.9	18.3	1982	1871	23.5	22.6	13.9	13.9
2014/15	Stellenbosch_2	19.9	19.2	2199	2054	21.1	20.1	18	17.3
2015/16	Stellenbosch_2	20.1	19.4	2220	2072	22.3	21.5	13.5	13.3
2012/13	Vredendal	22.3	22.3	2715	2715	24.6	24.6	19.7	19.7
2013/14	Vredendal	21	21.7	2437	2577	24.6	25.7	17.2	17.9
2014/15	Vredendal	21.3	22.2	2494	2697	22.2	23	16.6	17.7
2015/16	Vredendal	22.8	22.8	2809	2809	24.9	24.9	16.9	16.9
2012/13	Stellenbosch_1a	20.2	20.2	2210	2210	21.7	21.7	13.5	13.5
2013/14	Stellenbosch_1a	20.3	20.6	2239	2309	23.1	23.1	14.5	14.5
2014/15	Stellenbosch_1a	20.3	20.8	2239	2351	21.8	21.9	14.3	14.3
2015/16	Stellenbosch_1a	20.6	20.4	2344	2285	22.7	22.5	14.9	14.8
2012/13	Stellenbosch_1b	20.1	20.2	2195	2210	21.7	21.7	13.5	13.5
2013/14	Stellenbosch_1b	20.1	20.6	2224	2309	21.4	23.1	14.5	14.5
2014/15	Stellenbosch_1b	20.9	20.8	2373	2351	21.9	21.9	19.4	14.3
2015/16	Stellenbosch_1b	20.7	20.4	2381	2286	22.9	22.5	14.9	14.8
2012/13	Stellenbosch_1c	20.1	20.2	2198	2210	21.7	21.7	13.5	13.5
2013/14	Stellenbosch_1c	20	20.6	2219	2309	23.7	23.1	14.5	14.5
2014/15	Stellenbosch_1c	20.8	20.8	2335	2351	21.9	21.9	19.4	14.3
2015/16	Stellenbosch_1c	20.6	20.4	2341	2286	22.6	22.5	15.1	14.8

[1] GST: growing season temperatures; WI: Winkler index; MFT: mean February temperature and CI: Cool night index (minimum March temperature). [2] Log_: meso logger; Stat_weather station

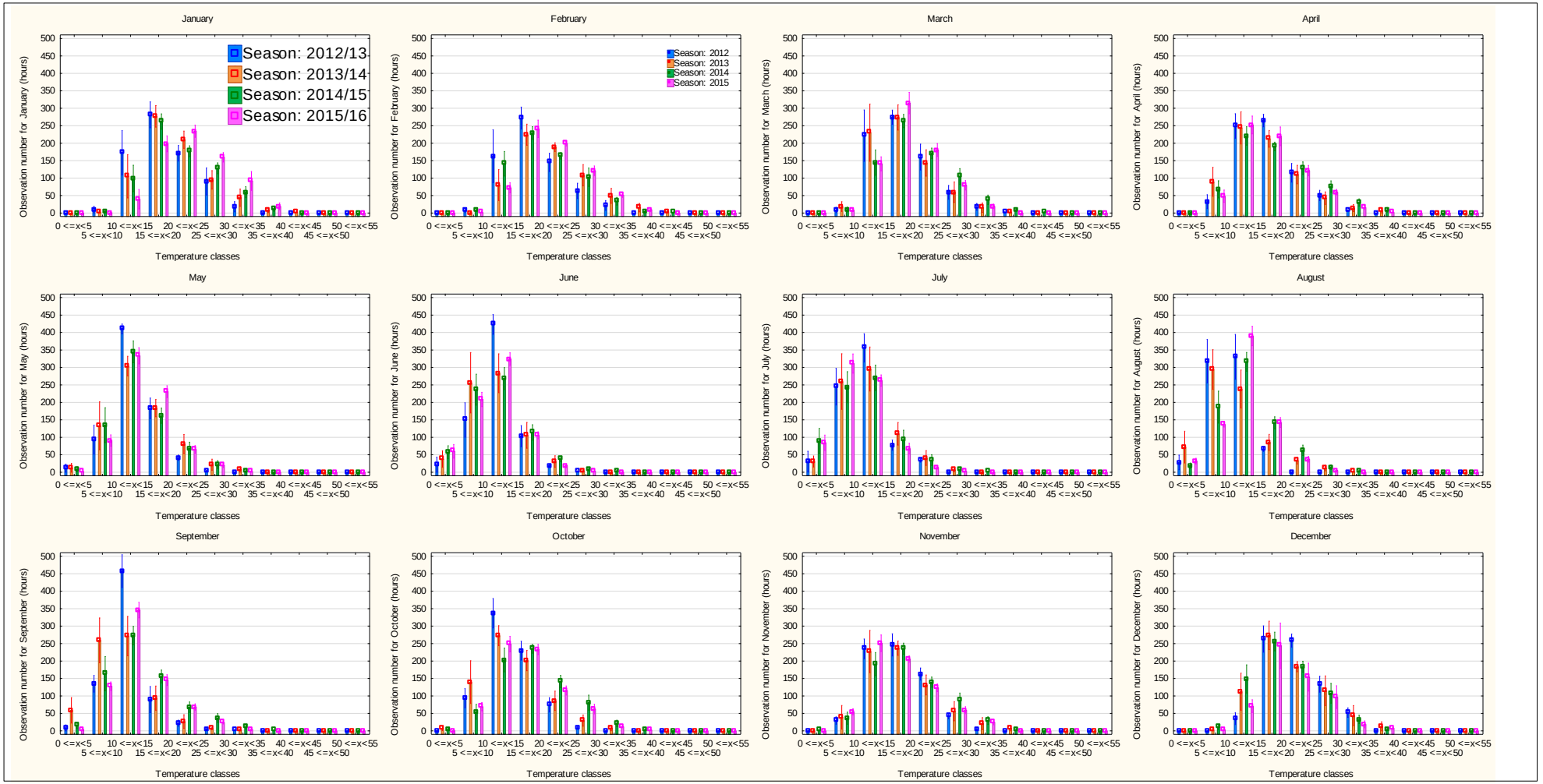

Figure 9 Frequency observations for January to December, hours observed at temperature classes (0<=x<5; 5<=x<10; …50<=x<55 °C) for all the sites over the four seasons.

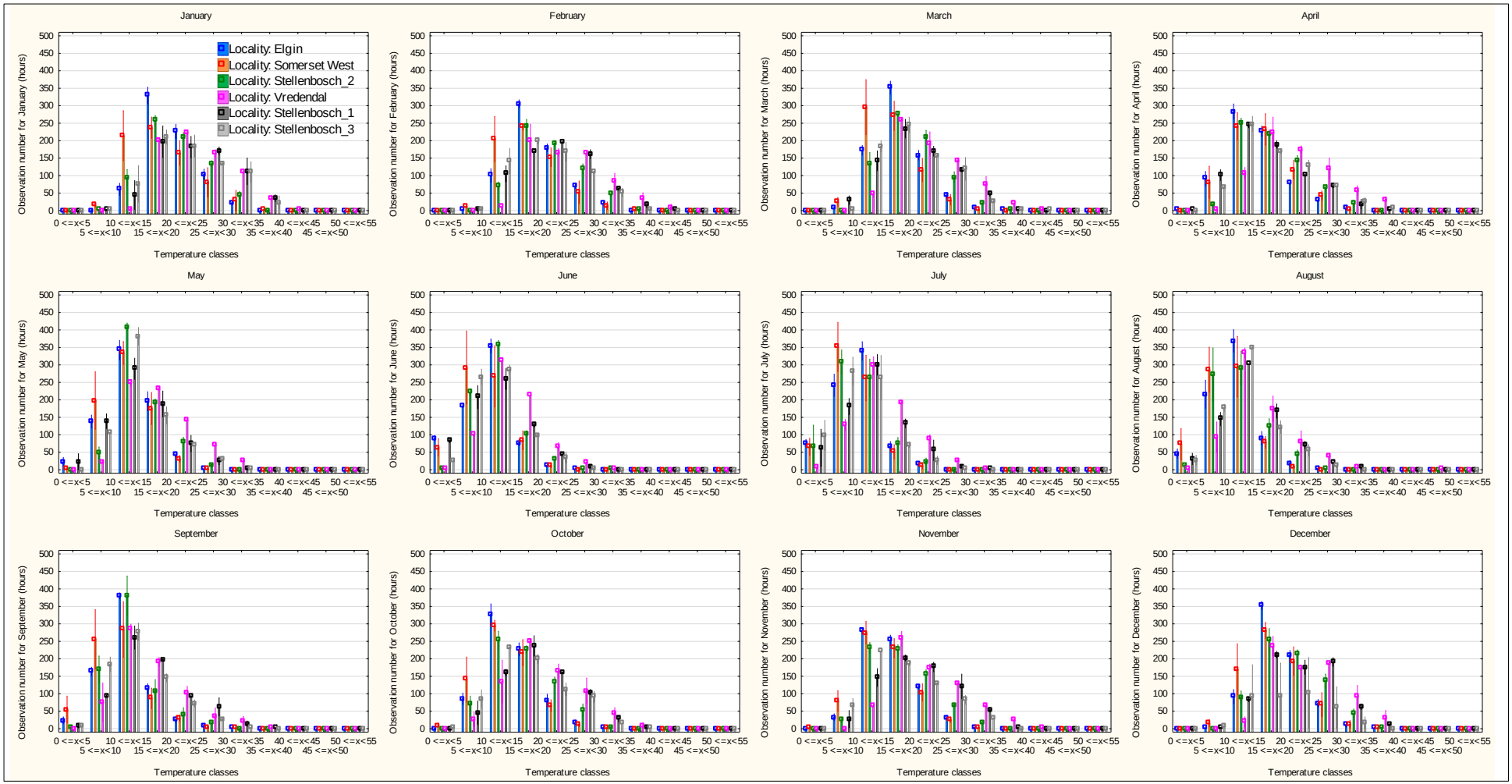

Figure 10 Frequency observations for January to December, hours observed at temperature classes (0<=x<5; 5<=x<10; …50<=x<55 °C) for all the seasons over the sites.

Chapter 5

Research results

Overview of long term climate trends in the Western Cape and possible impacts for the future of viticulture

CHAPTER 5: OVERVIEW OF LONG TERM CLIMATE TRENDS IN THE WESTERN CAPE AND THE POSSIBLE IMPACTS FOR THE FUTURE OF VITICULTURE

5.1 Introduction

Global warming is scientifically and widely accepted, with consistency across observations worldwide. The last three decades have being successively warmer at the Earth's surface than any preceding decade since 1850 (IPCC, 2014). Global trends may have a very different expression at the regional scale (Midgley *et al.*, 2005). South Africa lies in one of the regions of the world that is most vulnerable to climate variability and change, with the impacts being increasingly felt (IPCC, 2007; Vink *et al.*, 2010). Climate change is projected to reduce renewable surface water and groundwater resources in most dry subtropical regions, intensifying competition for water among sectors, especially with the incidence and duration of heat waves increasing (Midgley *et al.*, 2005; IPCC, 2014).

Statistical evidence suggests that South Africa has been getting hotter over the past four decades. Average annual temperatures have increased, with varying increases across the seasons. Increases of 0.21°C, 0.13°C, 0.08°C and 0.12°C in autumn, winter, spring, and summer, respectively, and a general increase in the number of warmer days have been reported (Kruger & Shongwe, 2004). 1983 was highlighted as the breaking point in warming, with the annual temperature increasing by 1°C and growing season temperature by 0.7°C. Warming has accelerated since the year 2000, with the most significant climate changes noted in the growing season (1 September to 31 March, in the Southern Hemisphere). The increase of minimum February temperatures, the occurrence of extreme events (heat waves, droughts, floods *etc*), and a delay in winter rainfall have been noted in literature as possible climate change effects (Bonnardot & Carey, 2007). The wine regions of the Western Cape have experienced a significant increase in temperature over the past decades, with annual temperature increases ranging from 0.5°C to 1.7°C depending on regions and periods (Bonnardot & Carey, 2008; Vink *et al.*, 2010). Temperatures can be expected to rise everywhere in the South Western Cape, with temperature tendencies accentuated in the inland and less pronounced in the adjoining coastal areas. Projected increases range from *ca.* 1.5ºC at the coast to 2-3ºC inland of the coastal mountains by 2050 (Midgley *et al.*, 2005). Rainfall is projected to decrease in the Western Cape, showing a drying trend from west to east, with the likelihood of less rainfall in winter but more summer rainfall, and shifts to more irregular rainfall of possible greater intensity (Midgley *et al.*, 2005; DEA, 2013).

Future climate projections indicate benefits for some regions and challenges for others (Jones, 2006). Economically sustainable production of wine grapes depends on suitable terroir, consequently the increasing temperatures are playing a role in "morphing" terroir shifting wine grape production into new areas (Carey *et al.*, 2007). The increasing temperature dictates the annual growth, reproductive cycle, rate of fruit development and maturation. Increasing temperatures as well as shifts in relative humidity and wind have the potential to alter the grapevine's growing season by moving the dates of phenological events such as bud break, flowering, véraison and harvest either later or earlier (Winkler, 1965; Webb *et al.*, 2007).

This chapter focuses specifically on climate change in the Western Cape, where most of the South African vineyards are situated, by examining observed climatic trends annually, over 5 years and over decades for the past 30 years. Two selected datasets based on different spatial distribution of weather stations were used for data analysis. The aim of this particular study was to identify and understand the possible impacts of climate change over regions, localised areas, seasons and

months for more effective adaptation strategies for winegrowing regions in the context of climate change in the Western Cape.

5.2 Materials and methods

5.2.1 Meteorological stations and data selection

The Institute for Soil, Climate and Water (ISCW) of the Agricultural Research Council has installed a countrywide network of weather stations (mechanical and automatic) since 1940. This network monitors climate over the Western Cape and South Africa.

Figure 1 shows the past and current status of ISCW weather stations servicing agriculture (yellow, green and blue markers) in the Western Cape. The stations still logging (yellow/blue) have decreased substantially since the 1980's, in both their distribution as well as data quality (past stations are green markers). In the past five years, the Hortec weather station network (HORTEC, 2012) (red markers) have extended their commercial services into the wine regions to supplement the ISCW weather stations and service the demand for a better spatial distribution of weather stations and consistent data quality (Figure 1 and Figure 2). The last of the mechanical weather stations (MWS) requiring manual downloads by ISCW were upgraded to automatic weather stations (AWS) towards the end of 2015. Unfortunately, this resulted in a few gaps in datasets of some of the weather stations when the transition was made.

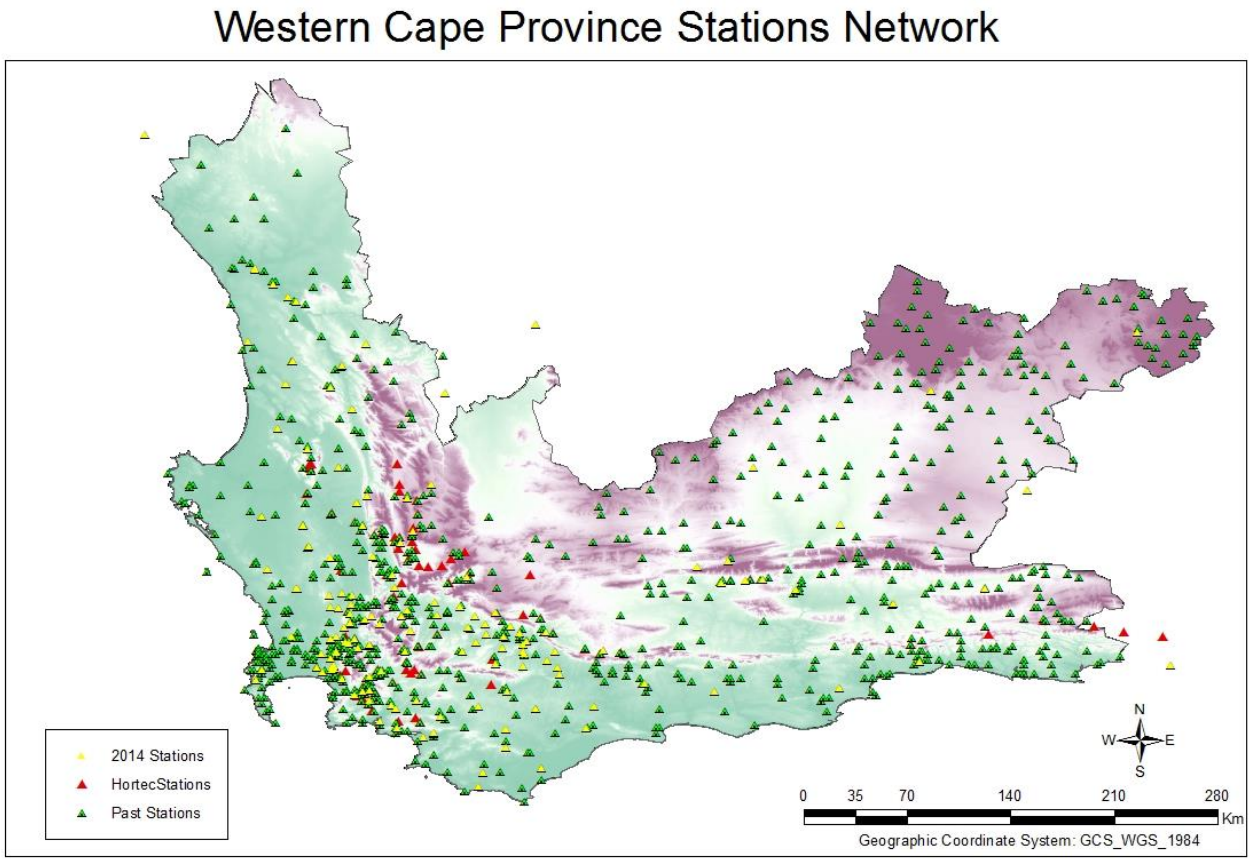

Figure 1 Past weather station distribution in the Western Cape.

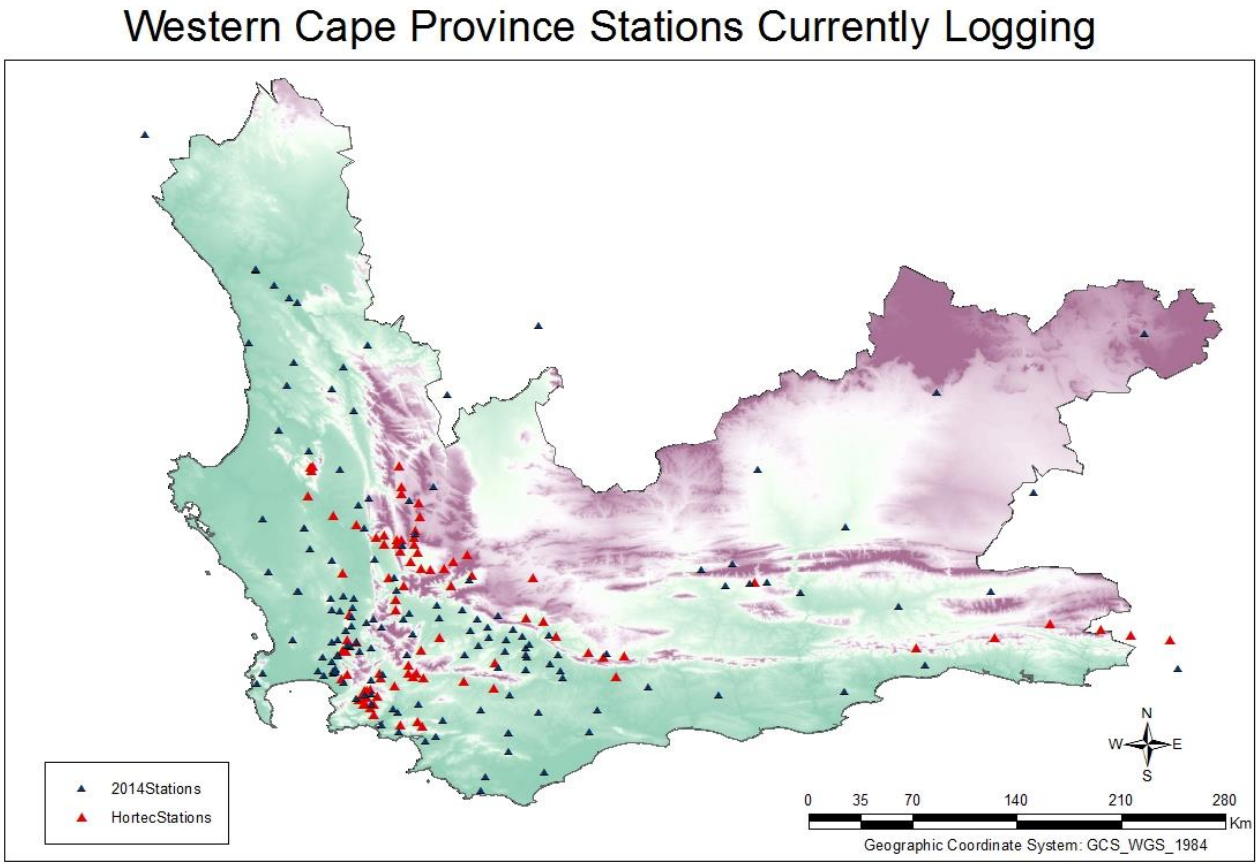

Figure 2 Current weather station distribution in the Western Cape (stations still logging in 2016).

Long term ISCW weather stations (Figure 3), defined here as stations logging for more than 20 years (dataset 1) and more than 10 years (dataset 2) were selected over a large spatial area distributed throughout the wine growing regions of the Western Cape. Monthly and daily data were acquired from the ISCW for use in further climate analysis. Figure 3 highlights the stations selected for analysis, with the black markers and red markers indicating the data series selections, 1984 to 2015 (N=70) and 1984 to 2016 (N=47), respectively (Table 1). The two datasets were selected based on the data series range. Dataset 1 has 70 stations logging for more than 20 years up to 30 years and dataset 2 has 47 stations logging for more than 10 years up to 30 years (Table 7 and Table 8 in Addendum 5.1). Dataset 1 has more MWS in the data set, hence there being more stations that have logged for longer with some of the stations no longer logging, whereas dataset 2 is made up of mostly AWS and MWS that have been upgraded to AWS. Most of the stations in this dataset are still logging to date. Dataset 1 has more stations (N=70) and a wider distribution of stations throughout the Western Cape as seen in Figure 3 represented by the black markers. Dataset 2 is made up of a selection of stations that are still logging to date and have a reliable source of data, leaving only 47 stations that are not as widely spread throughout the Western Cape, but more concentrated in the wine growing areas (red markers in Figure 3). Continuous data sets are required for computation of indices and averaging over decades, months and regions for temperature and rainfall. Gap filling was completed by a process of correlating the station with gaps with one of the nearest weather stations (ISCW or HORTEC stations). For large gaps in the datasets, the regression equation calculated from the two sources of data was then used to fill the gaps (data not shown). If the gaps were small (a few days), the previous year and future year daily/monthly average was used to fill the gaps and create a continuous dataset (data not shown).

Temperature and rainfall were selected as the descriptors to define the climate over decades, half decades, years, regions and months, as these elements were readily available from the MWS and

AWS network datasets and also described in other studies as a reliable resource for processing and describing climate (Deloire *et al.*, 2005; Bonnardot & Cautenet, 2009).

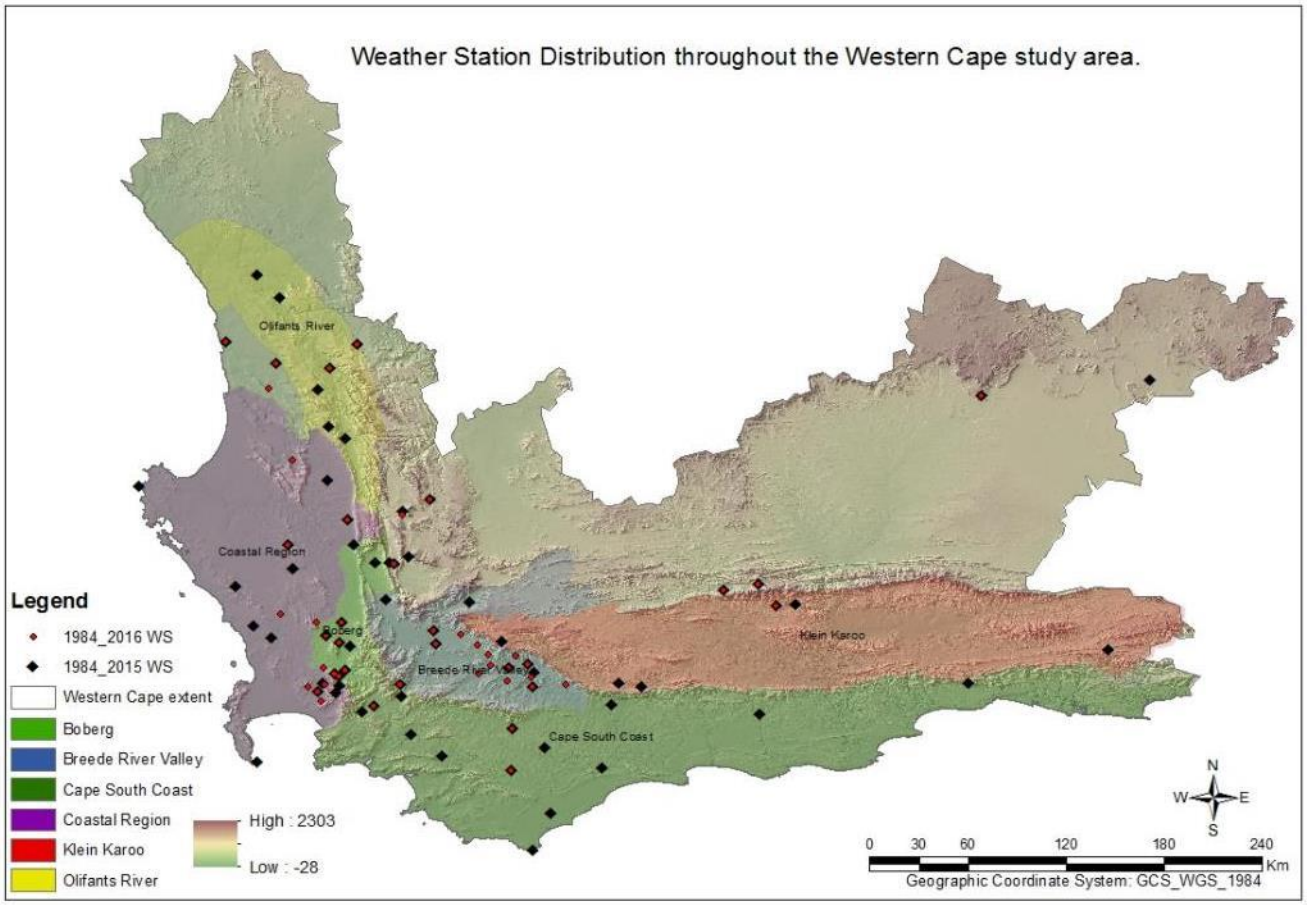

Figure 3 Weather station distribution throughout the Western Cape, black markers and red markers indicating the data series selections, 1984 to 2015 (N=70) and 1984 to 2016 (N=47), respectively.

Table 1 Description of station network selection for analysis as dataset 1 and 2 (for more detail see **Table 7** and **Table 8** in Addendum 5.1).

Dataset	Range	Logging period	Station Number	Station Status
1	1984-2015	at least more than 20 years (>20 yrs)	70	Stopped logging
2	1984-2016	at least more than 10 years (>10 yrs)	47	Still logging

5.2.2 Statistical analysis

Statistical analysis was conducted using Statistica 10 ® software (Statsoft, Tulsa, UK), to process dataset 1 and 2 into decades, half decades, regions and months. This involved computing means for each year, month and region and processing into decades and half decades (N=10 and N=5, respectively). The software was also used to process the annual data for climate trends for temperature and rainfall for a 30-year period and for the analysis of seasonal shifts using indices. One-way ANOVA was used to compare mean climate values between decades. The Kruskal-Wallis non-parametric test was also calculated, but in most cases found to have similar outcomes as the ANOVA f-tests. For post hoc analysis, Fisher least significant difference (LSD) testing was done. Both datasets 1 and 2 were processed for statistical analysis over decades (1980-1990, 1991-2000, 2001-2010 and 2011-2016). For the statistical analysis over five year intervals and over years, only dataset 2 (1984-2015) was used for further descriptive trend analysis and anomaly analysis.

5.3 Results and discussion

5.3.1 Climate trends: decadal analysis

The wine regions of the Western Cape have experienced a significant increase in temperature over the past four decades, with annual temperature increases ranging from 0.5°C to 1.7°C depending on regions and periods (Figure 4). Similar results were reported by Carey *et al.* (2009); Vink *et al.* (2010).

The mean temperature (T_m) increased over the four decades (1980-1990, 1991-2000, 2001-2010 and 2011-2016) with a significant increase noted between the 1980 decade and 2010 decade for dataset 1 and the first two and last two decades for dataset 2 as described in Figure 4. A general trend of warming in both datasets, for all seasons and regions combined, was observed with increases of 1.0 and 0.7°C noted for datasets 1 and 2, respectively (Table 3). The difference in the warming trend between the two datasets is most likely ascribed to the station distribution of each dataset, as both datasets have a large amount of stations in the analysis (N=70 and N=47, respectively), with both datasets including about 18 stations logging for 30 or more years. Dataset 1 has a wider spread of stations, whereas dataset 2 is more concentrated in the wine growing areas of the Western Cape. In addition to this, dataset 1 includes more stations in extreme locations, over more regions, including further inland and nearer to the coast stations, highlighting the possible regional influence on climate change, that some regions are more affected than others (Midgley *et al.*, 2005). The results emphasise the importance of a representative spatial distribution of stations before statements regarding climate change are made and adaptation strategies put in place.

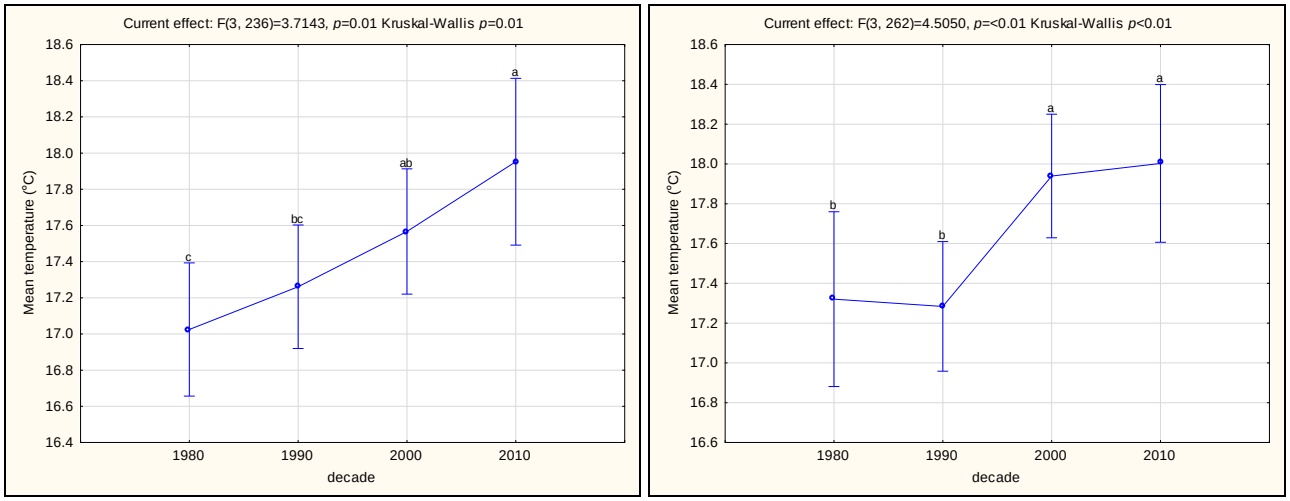

Figure 4 Least square means analysis over decades for mean temperature (T_m) for dataset 1 (left) and dataset 2 (right) as described in Table 1. Vertical bars denote 0.95 confidence intervals. Same letters are not significantly different at the $p \leq 0.05$ level.

The change in T_m can be better understood when considering the maximum temperature (T_x) and minimum temperature (T_n) trends over decades for all stations (Figure 5 and Figure 6, respectively). There was a warming trend for all temperature elements (T_m, T_x and T_n) for the period 1984 to 2015 with 0.9°C, 1.3°C and 0.5°C, respectively, for dataset 1 and 0.7°C, 1.2°C and 0.2°C, respectively, for dataset 2 (Table 3). However, T_n increased comparably over the four decades for dataset 1 and 2 (Figure 6). The shift in mean temperature is therefore driven by T_x (Figure 5) in the datasets, with the exception of T_n playing a role in the T_m for the 1990 decade in dataset 2. The abrupt increase in T_m in dataset 2 is due to the decrease in T_n in the 1990 decade.

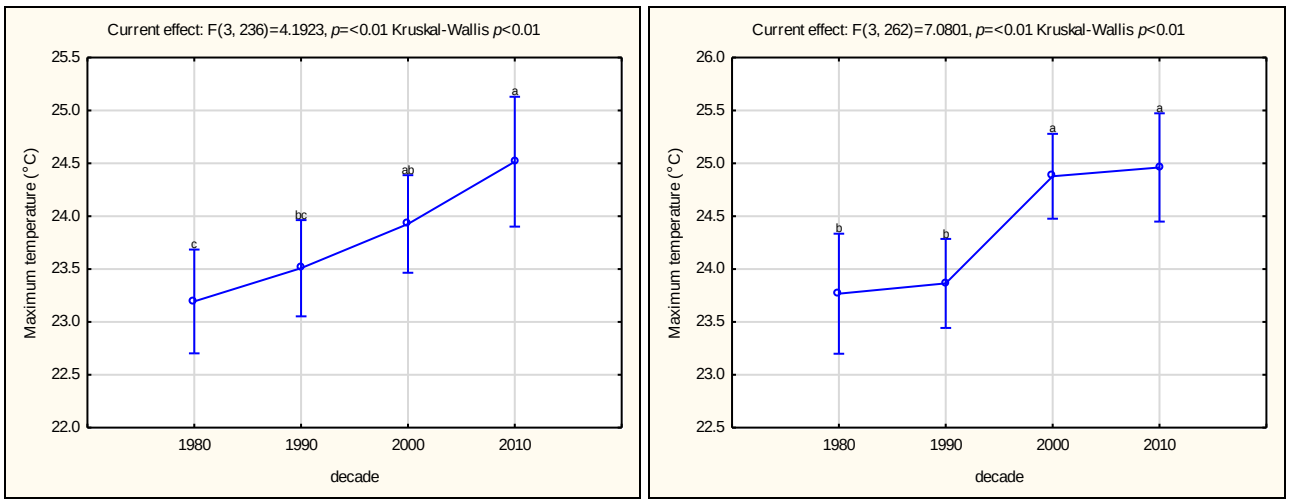

Figure 5 Least square means analysis for maximum temperature (T_x) over decades for dataset 1 (left) and dataset 2 (right) as described in Table 9. Vertical bars denote 0.95 confidence intervals. Same letters are not significantly different at the $p \leq 0.05$ level.

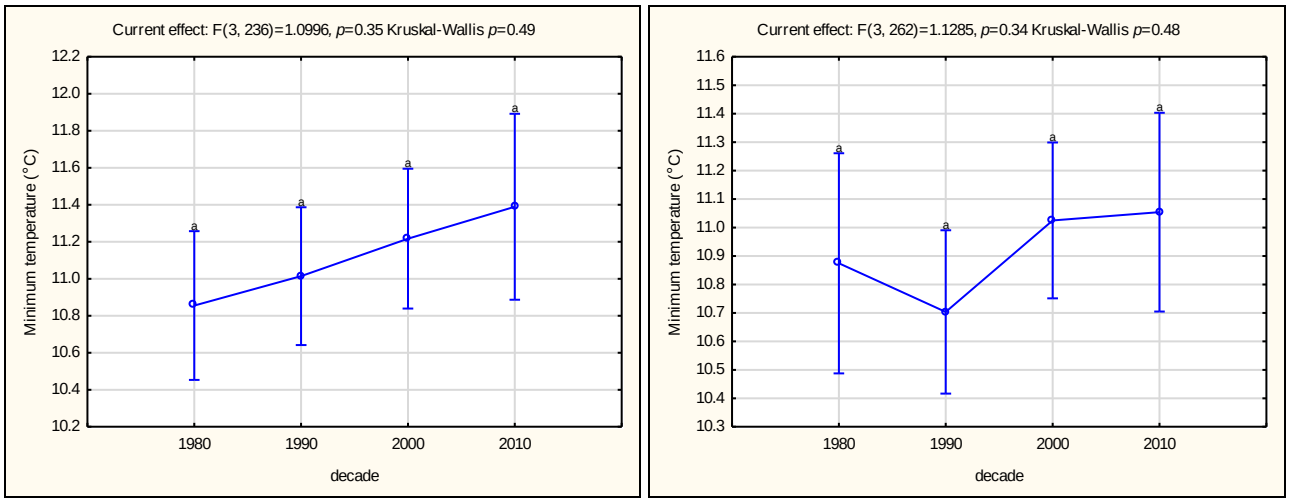

Figure 6 Least square means analysis for minimum temperature (Tn) over decades for dataset 1 (left) and dataset 2 (right) as described in Table 9. Vertical bars denote 0.95 confidence intervals. Same letters are not significantly different at the $p \leq 0.05$ level.

With respect to rainfall, results were not always significant and inconsistent; therefore, interpretation should be made with caution. In both datasets, the rainfall showed a similar trend over the decades, with the rainfall in dataset 1 always being higher than that in dataset 2 (Figure 7). Dataset 1 and 2 showed an average annual rainfall of 515 and 460 mm, respectively, with a difference of approximately 55 mm over all decades (Table 2). In dataset 2, the highest value for rainfall is also the lowest value observed in dataset 1. This could be due to station distribution near the ocean and orographic rainfall in more inland extreme areas at the upper edges of the Western Cape. Rainfall is becoming more sporadic in nature, and hence not much can be concluded from the rainfall volume, timing and distribution (Bonnardot & Carey, 2007; Midgley *et al.*, 2015). From the two datasets, it is clear that there is a possible regional differentiation in terms of temperature and possibly rainfall.

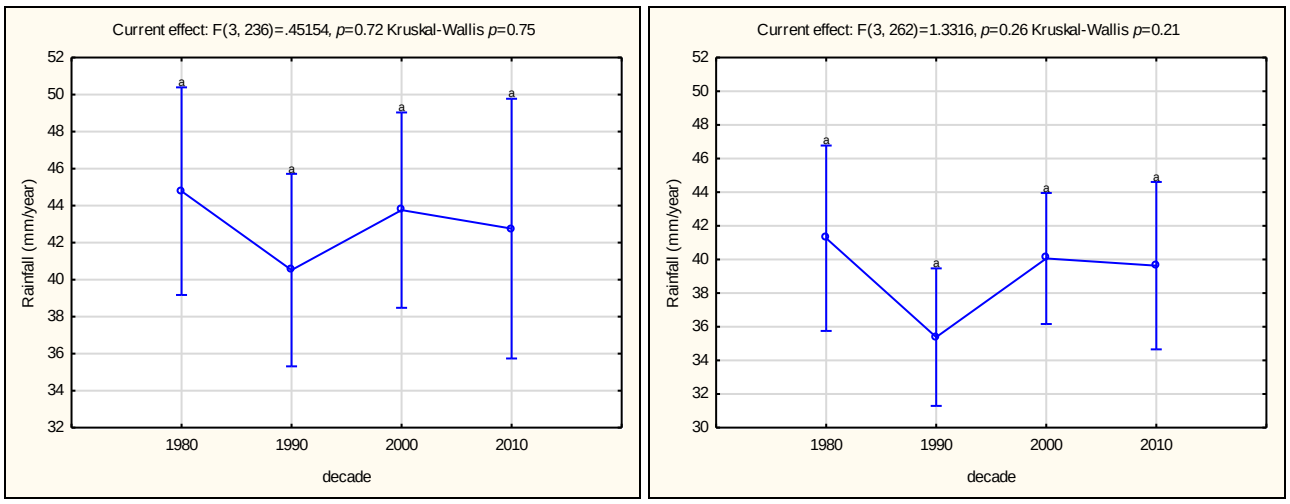

Figure 7 Least square means analysis for average rainfall in mm per year (mm/year) over decades for dataset 1 (left) and dataset 2 (right) as described in Table 9. Vertical bars denote 0.95 confidence intervals. Same letters are not significantly different at the $p \leq 0.05$ level.

Table 2 Analysis of temperature and rainfall over decades, for two data sets 1 and 2 for maximum (T_x), minimum (T_n), mean (T_m) temperatures and mean monthly rainfall (rain).

Element	Decade	>20 years dataset1					>10 years dataset2				
		N	Mean	Std.Dev.	-95%	95%	N	Mean	Std.Dev.	-95%	95%
T_x	1981-1990	61	23.2	2.1	22.6	23.7	44	23.8	1.7	23.2	24.3
T_x	1991-2000	71	23.5	1.9	23.1	24	80	23.9	1.8	23.5	24.3
T_x	2001-2010	69	23.9	1.9	23.5	24.4	88	24.9	2.1	24.4	25.3
T_x	2011-2016	39	24.5	1.7	24	25.1	54	25	2	24.4	25.5
T_n	1981-1990	61	10.9	1.8	10.4	11.3	44	10.9	1.3	10.5	11.3
T_n	1991-2000	71	11	1.6	10.6	11.4	80	10.7	1.5	10.4	11
T_n	2001-2010	69	11.2	1.6	10.8	11.6	88	11	1.2	10.8	11.3
T_n	2011-2016	39	11.4	1.3	11	11.8	54	11.1	1.1	10.7	11.4
T_m	1981-1990	61	17	1.7	16.6	17.4	44	17.3	1.4	16.9	17.7
T_m	1991-2000	71	17.3	1.4	16.9	17.6	80	17.3	1.5	17	17.6
T_m	2001-2010	69	17.6	1.4	17.2	17.9	88	17.9	1.5	17.6	18.3
T_m	2011-2016	39	18	1.3	17.5	18.4	54	18	1.5	17.6	18.4
Rain	1981-1990	61	44.8	22.4	39	50.5	44	41.3	20.1	35.1	47.4
Rain	1991-2000	71	40.5	22.8	35.1	45.9	80	35.4	17.6	31.5	39.3
Rain	2001-2010	69	43.8	22.2	38.4	49.1	88	40.1	19.4	35.9	44.2
Rain	2011-2016	39	42.8	21.1	35.9	49.6	54	39.6	17.2	34.9	44.3

5.3.2 Climate trends: regional trends over decades

It is well known that climate varies over short distances in the Western Cape, and can be attributed to the terrain complexity and distance from the ocean. The seven regions demarcated in Figure 3 differ in temperature and rainfall, with Table 3 describing the climate of the main regions in the Western Cape (Refer to Table 9 in Addendum 5.1for more detial). The Olifants River region is the warmest and driest region, and the Boberg region has the highest Tn. The Cape South Coast is the coolest region with the lowest average Tm, T_x and T_n over the four decades, compared to the other. The temperatures in the Cape South Coast during the 2010 decade were comparable to those of the Coastal region in the 1980 decade (Table 9), highlighting regional climatic shifts which were also predicted by Carey (2005). Temperature increased in all the regions over the four decades of the study. The T_x showed the most pronounced increases in temperature over the four decades, ranging from *ca.* 1°C to 2°C. Minimum temperature increases were observed over all the regions but with less intensity and the increases ranged from <0.6°C to >1°C over the four decades.

The Boberg and Cape South Coast regions had the highest rainfall, possibly attributed to distance from the ocean and orographic rain, respectively. The Boberg region is made up of a network of stations with great variability as the demarcated region covers the mountainous areas and moves into the drier, plateau areas of Paarl (Figure 8). Due to the distribution, the rainfall ranged from 370 mm/year to 1000 mm/year, which are not a true representation of the region and the majority of stations in the demarcated area. Highlighting the need for finer scale climatic demarcations within the context of climate change, this can be achieved with a higher distribution of stations within complex terrains. Rainfall showed a slight but general trend of decrease but was still very sporadic over all regions, with the exception of the more inland stations (Table 9). It was evident that there was an increase in rainfall over the past two decades. It has previously been reported that rainfall is increasing in the north eastern part of the Western Cape (Midgley *et al.,* 2005).

Results highlight the effects of topography and distance from the ocean, driving the regional shifts over the four decades, as there seems to be a more pronounced effect in the coastal region, hence some regions being more prone to change. The Coastal and Boberg regions have the most popular winegrowing areas within their demarcation, namely Stellenbosch, Franschhoek and Constantia. Wine growing areas have been shifting and continue to shift into the Cape South Coast region which is becoming more suitable for a wider spectrum of cultivars. The Cape South Coast region is today (2016) more comparable to what the well renowned wine growing regions were in the 1980's, highlighting the impact of climate changing shifting wine growing regions and varietal selections. The Boberg results are similar to what the Coastal region was in the 1980's, but the results are not a true representation of the region due to the stations in the mountainous area, possibly moderating the temperature to be cooler than what the region actually is (Figure 8).

The accuracy of regional demarcation is important and requires more detail on a finer scale, hence higher resolution demarcation will account for changes in mesoclimate over short distance and allow for more suitable wine growing shifts to take place, into new areas, changing varietal selection *etc*. Some regions are warming and others cooling as described in Table 4, hence the need for more detailed demarcation for the future. Over the four decades all the regions were warming in Tm, mostly driven by the increase in T_x over the decades. However, focusing on only the last decade, temperatures seemed to be cooler for all element of temperature (T_x, T_n and T_m), with a few exceptions such as the Breede River, Boberg and Coastal region showing general warming (Table 4). Rainfall decreased for all regions with the exception of an increase in rainfall in the upper areas of the Western Cape. Due to the complexity of the terrain in the Western Cape, studies at higher resolution (more regions and monthly changes defined) are important in the context of quantifying change and the possibility of adapting grapevine distribution in future.

Table 3 Average mean (T_m), maximum (T_x), minimum (T_n) temperatures and rainfall (mm) over four decades for dataset 2 categorised by regions. Red highlights and blue indicating the highest and lowest values respectively.

Region	T_m	T_x	T_n	Annual Rainfall (mm)
Breede River Valley	17.91	24.77	11.07	293.7
Boberg	17.64	23.42	**11.89**	786.6
Cape South Coast	**16.37**	**22.40**	**10.39**	**702.0**
Coastal Region	17.92	24.27	11.57	478.7
Olifants River	**19.34**	**27.05**	11.64	**255.7**
Klein Karoo	17.85	24.53	11.18	331.8

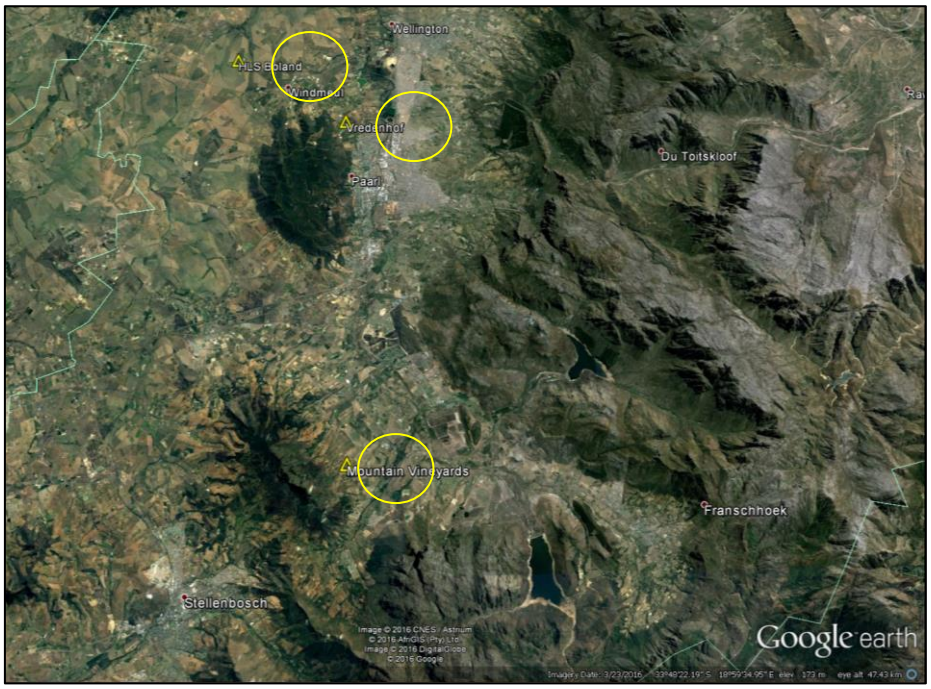

Figure 8 Weather station distribution in the demarcated region Boberg, stations ranging from mountainous areas (Mountain Vineyards) to far inland (HLS Boland).

Table 4 The degree of change in maximum (T_x), minimum (T_n), mean (T_m) temperatures and rainfall (rain) averaged over four decades and the last decade compared to the first decade for dataset 2 categorised by regions. The red/blue indicating warming/increase and the black indicating cooling/decrease or no change.

Region	1980-2010 (over 4 decades)				2000-2010 (last decade compared to 1980 decade)			
	T_x	T_n	T_m	Rain	T_x	T_n	T_m	Rain
Breede River Valley	0.28	-0.75	-0.28	6.03	0.09	0.13	0.07	1.59
Boberg	0.49	0.05	0.27	-5.44	0.26	-0.01	0.16	-6.02
Cape South Coast	0.67	0.49	0.58	-10.88	-0.21	-0.01	-0.04	-4.99
Coastal Region	1.16	-0.22	0.47	3.74	0.42	-0.04	0.19	-5.08
Olifants River	0.92	0.41	0.66	-1.54	-0.06	-0.04	-0.05	-0.20
Klein Karoo	0.90	-0.03	0.44	2.27	-0.07	-0.08	-0.08	1.59
Western Cape Centre	0.52	0.39	0.46	-7.77	-0.05	0.15	0.05	1.21
Western Cape Upper	-0.35	-0.71	-0.53	3.13	0.16	-0.09	0.03	1.07
Western Cape Out	-0.58	-0.04	-0.31	6.76	-0.58	-0.04	-0.31	6.76

5.3.3 Half decade climate trends analysis

The temperature (T_x, T_n, T_x) and rainfall averaged for 5 year intervals for the period 1984-2015 indicates a general trend of warming (Table 5). The T_x and T_n (data not shown) had a similar trend to T_m (Figure 9), with the last three 5 year periods (15 years) being significantly warmer than the previous years (Refer to in Table 10 in Addendum 5.1). There were no significant differences in T_x from 2004 to date, only gentle and continual warming (Table 5). The year to year variation of climate is ascribed to the El Niño/Southern Oscillation (ENSO) cycle, the warm phase of which is referred to as El Niño and the cold phase La Niña. The ENSO originates in the tropical Pacific through coupled interactions of the ocean and the atmosphere, impacting the climate (McPhaden *et al.*, 2011). The most recent year (2015) was significantly warmer with higher T_x, T_n and T_m compared to 30 years ago. Over the 30 year period (1984-2015), T_m, T_x and T_n increased by 0.9°C, 1.4°C and 0.3°C, respectively over all stations for dataset 1 (Table 5). Overall, the warming trend is still evident, with the exception of the Cape South Coast, which is cooling in T_x and warming in T_n in the last few years. Rainfall showed a decreasing trend of about 6.2 mm over the last 30 years, with the greatest reduction in rainfall occurring in the last 15 years (Table 10 and 19 in Addendum

5.1). However, the rainfall was still not as low as what was experienced in the 1994-2004 period (Figure 9).

The trends are confirmed in literature, the prior three record years, 2014, 2010 and 2005, each of which exceeded the preceding record by only a few hundredths of a degree, 2015 increased more than the previous records by more than 0.1°C, comparable to the 1998-1999 spike in temperatures (Hansen *et al.*, 2016). The 1998 temperature was boosted by the strong 1997-98 El Niño, similarly with a comparable magnitude occurred again in 2015 (Hansen *et al.*, 2016).

On a regional scale, the half decade analysis show some regions to be cooling and warming over the 5 year intervals that are not visible in the decade analysis. Higher temporal resolution is therefore important in the context of climate change to account for inter annual variability and apply effective adaptive strategies. Finer scale mesoclimates can shift the vineyard management and planting decisions in accordance to the changing environmental conditions.

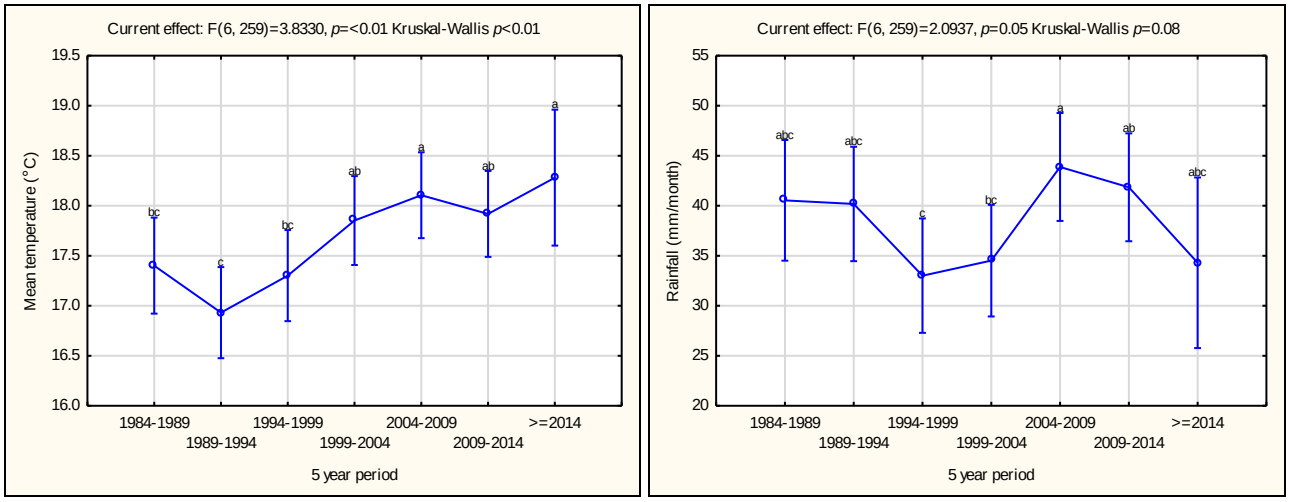

Figure 9 Least square means for 5 year increments over 30 year period for dataset 2 for mean temperature (Tm) and Rainfall, as averaged per month over the half decade. Vertical bars denote 0.95 confidence intervals. Same letters are not significantly different at the p ≤ 0.05 level.

5.3.4 Monthly climate trend analysis over decades

Monthly temperature shifts provide more detail within the regional scale analysis, providing a finer temporal scale which is more closely related to the grapevine's growing seasons. Monthly temperatures better illustrate the fluctuations of temperature across the decades. The monthly changes over decades are given in Table 6 and Table 12 to ascertain the true impact of climate change for the grapevine's growing and ripening season. It is accepted that the grapevine's growing season starts in September (Southern Hemisphere) with budburst (timing is cultivar dependant). The ripening stage starts from December, with the grapevine shifting from vegetative growth to its' ripening phase. Depending on the cultivar, harvesting occurs from January to March. It is generally accepted that the grapevine summer season is from 1st September to 31st March, and the winter season is 1st April to 31st August, and further discussion of months will be based on the above assumptions.

Temperature shifts over the four decades and for the most recent decade is described in Table 6 for the whole year, over all stations combined. Over the four decades, warming in T_x, T_n and T_m occurred in October, December, January, February and March, with the highest increases being in January, December and March, the main ripening months for wine grapes. The most significant shifts to warmer temperatures is in December, January and March, with increasing rainfall in

January and March, which could accelerate ripening and influence the grape composition as well as possibly increase in the incidence of diseases by rainfall in the ripening months.

Table 5 Maximum (T_x), minimum (T_n), mean (T_m) temperatures and rainfall (rain) for 5 year intervals for the 30 year period (1984-2015) in dataset 2 for 47 stations.

Years	Element	Mean	Standard Deviation	Standard Error	Confidence Intervals		Difference per 5 years	Difference over all
					-0.95	0.95		
1984-1989	**T_x**	23.873	1.715	0.286	23.293	24.453		
1989-1994	**T_x**	23.444	1.762	0.279	22.880	24.007	-0.429	
1994-1999	**T_x**	23.869	1.605	0.254	23.356	24.382	0.426	
1999-2004	**T_x**	24.702	1.968	0.304	24.088	25.315	0.832	
2004-2009	**T_x**	25.121	2.110	0.315	24.487	25.755	0.419	
2009-2014	**T_x**	24.793	1.952	0.291	24.206	25.379	-0.328	
>=2014	**T_x**	25.362	2.171	0.512	24.283	26.442	0.570	1.489
1984-1989	**T_n**	10.929	1.330	0.222	10.479	11.379		
1989-1994	**T_n**	10.419	1.748	0.276	9.860	10.978	-0.510	
1994-1999	**T_n**	10.734	1.083	0.171	10.388	11.081	0.315	
1999-2004	**T_n**	11.002	1.288	0.199	10.601	11.404	0.268	
2004-2009	**T_n**	11.137	1.145	0.171	10.793	11.481	0.134	
2009-2014	**T_n**	11.044	1.164	0.174	10.695	11.394	-0.092	
>=2014	**T_n**	11.227	1.150	0.271	10.655	11.799	0.183	0.298
1984-1989	**T_m**	17.401	1.398	0.233	16.928	17.874		
1989-1994	**T_m**	16.931	1.610	0.255	16.416	17.446	-0.469	
1994-1999	**T_m**	17.302	1.216	0.192	16.913	17.691	0.370	
1999-2004	**T_m**	17.852	1.483	0.229	17.390	18.314	0.550	
2004-2009	**T_m**	18.105	1.529	0.228	17.646	18.564	0.253	
2009-2014	**T_m**	17.918	1.446	0.216	17.484	18.353	-0.187	
>=2014	**T_m**	18.281	1.567	0.369	17.502	19.060	0.362	0.880
1984-1989	**Rain**	40.536	20.294	3.382	33.670	47.403		
1989-1994	**Rain**	40.179	20.185	3.192	33.724	46.635	-0.357	
1994-1999	**Rain**	33.009	15.448	2.442	28.068	37.949	-7.171	
1999-2004	**Rain**	34.514	15.475	2.388	29.691	39.336	**1.505**	
2004-2009	**Rain**	43.880	21.516	3.207	37.416	50.344	**9.366**	
2009-2014	**Rain**	41.846	17.124	2.553	36.702	46.991	-2.033	
>=2014	**Rain**	34.295	16.717	3.940	25.982	42.608	-7.551	-6.241

November is the only month that shows cooling for T_x, T_n and T_m and September was warmer in T_x and cooler in Tn. The increase in T_x could have an effect on grapevine phenology as well as on grape ripening due the higher T_x and T_n over all the ripening months. Cooler minimum temperatures in September could affect budburst, whereas the cooler temperatures in November, along with more rainfall, could delay phenology, or promote vegetative growth in the grapevine, increasing vigour. December, January and March seem to be warming, with increases in T_x, T_n, and T_m, while November and February is cooler. In the winter and post-harvest months, *i.e.* April to August, there was a warming in T_x and a cooling in T_n, while T_m was warmer, driven by T_x, with the exception of May and June having a cooler T_m over the four decades. However, over the last decade, warming was not so prevalent over all months, a trend confirmed globally and noted in literature as to the “hiatus effect” (IPCC, 2013).

Overall increases in spring and summer rainfall in October, November, January and February were observed. In contrast, there was a a decrease in December and winter rainfall, with the exception of June. Rainfall seems to be decreasing over all the decades, and shifting to be earlier in both winter and summer. In the last decade, the rainfall has increased in January, March, June and August, and decreased in all the other months. Rainfall also seems to be sporadic, shifting towards summer rainfall (January/March) and early winter rainfall (shifting from July to June), with an increase in early spring rainfall. The shift in rainfall could affect grapevine growth in early stages having potential effects on ripening and grape health (pest and diseases) in the summer months (Table 6).

Winter temperatures are important for achieving even and timeous budburst. Rainfall is shifting from winter into early spring and summer, possibly affecting the soil temperature and therefore an indirect impact on grapevine responses can be expected. In general, winter temperatures are showing a warming trend in averaged Tm, and the increase is driven by the increase in T_x as the T_n is decreasing. These changes could affect grapevine physiology of budburst, as the chill requirement could be achieved earlier in the season, with the warmer ambient and drier soils driving earlier, and possibly uneven budburst. The physiological function of budburst in relation to climate requirements will be discussed further in Chapter 7.

Table 6 Maximum (T_x), minimum (T_n), mean (T_m) temperatures and rainfall (rain) change per month, for the average of the four decades and the last decade compared to the first decade for dataset 2, the red indicating warming/increase and the black indicating cooling/decrease or no change.

Month	1980-2010 (over 4 decades)				2000-2010 (last decade)			
	T_x	T_n	T_m	Rain	T_x	T_n	T_m	Rain
January	2.2	1.49	1.85	10.11	1.54	0.96	1.25	1.74
February	0.85	0.22	0.54	2.67	-0.14	-0.44	-0.29	-0.92
March	1.71	0.6	1.16	-20.98	0.42	0.34	0.43	1.03
April	1.09	-0.38	0.27	-19.24	0.04	-0.74	-0.39	-9.9
May	0.3	-0.6	-0.22	-22.83	0.27	-0.16	0.02	-12.97
June	0	-0.34	-0.17	17.43	-0.71	-0.18	-0.42	32.32
July	0.93	-0.17	0.38	-19.64	-0.5	-0.2	-0.35	-24.7
August	0.49	-0.35	0.06	-6.6	0.5	0.03	0.26	5.08
September	1.31	-0.46	0.43	-29.13	0.19	-0.56	-0.18	-7
October	1.61	0.79	1.19	0.38	-0.12	0.14	0	-1.03
November	-0.32	-0.83	-0.58	18.01	-0.38	-0.52	-0.46	-3.49
December	1.77	1.19	1.49	-8.07	0.59	0.95	0.77	-4.41

5.3.5 Annual temperature trends and anomalies

Despite the multi-decadal warming, there is inter-annual to decadal variability in the rate of warming, with several periods exhibiting weaker trends (IPCC, 2013). The natural climate variability can appear to slow down surface warming over short periods, but does not negate long-term climate change trends (Kosaka & Xie, 2013; England *et al.*, 2014). Multiple weather stations in dataset 2, grouped by year for the 30 year period from 1984 to 2015 as described in Figure 10, highlighted an increasing trend in warming from 1998 and stabilising from 2001 at a higher T_m, T_x and T_n, as documented in other studies (Bonnardot & Carey 2007). The long-term mean for the 30 year period was used in the anomaly analysis, which provides a more detailed description of change in temperature over the 30 year period [Figure 10 (right)]. Trends given in Figure 10 are confirmed by Bonnardot & Carey, (2007), the exceptionally warm year of 1998 is ascribed to the El Nino year, an outlier from the continuing temperature trend, however the outlier for this dataset was 1998-1999. The plateau trend for the period from 1998-2013 is ascribed to the global warming hiatus, a period of relatively little change in the globally averaged temperatures (McPhaden *et al.*, 2011; Meehl *et al.*, 2011). IPCC (2013) reported the hiatus effect as the 15 year period from 1998 to 2012 with much smaller linear trend increases compared to the 60 year dataset from 1951 to

2012. This pause in global warming (hiatus) is confirmed in Figure 10, as the anomaly analysis from 1998 to 2012 seems to be constant. IPCC (2007) reported 1998 and 2005 to be the warmest two years in the global surface air temperature record since 1850. The current study shows a similar cooling trend, seen both before 1998 and 2013, with a warming trend following. It could be expected that temperatures will stabilise at a higher base line such as in 2001 (Figure 10 (left)). Hansen *et al.* (2015) noted that the "stand still" temperature is at a much higher level than existed at any year in the prior decades except for the single year 1998, which was the strongest El Nino of the century.

Possible cooling noted in the inter-annual variability before the documented warming from 1998 to 2001. Another warming spike was observed in 2004 and 2010 for T_x and T_n. Similar inter annual variability is noticed with a general cooling trend from 2011 to 2013, followed by warmer years from 2014 for maximum and minimum temperatures and further warming noted in 2015, with maximum temperature increasing and minimum temperatures possibly cooling compared to 2014 but still warmer than long term mean (Figure 10). From 2013 until 2015, a similar trend can be noticed with increased T_x and T_n, with T_x being more pronounced and hence driving the increase in mean temperatures. In a recent study by Hansen *et al.* (2016), it was noted that 2015 is much warmer than any of the preceding years, already before the El Nino conditions started. The effects of the El Nino in the Western Cape, situated at the edge of tropical regions and yet still in the warm temperature zone, could be further illustrated by correlating the climatic data with the Southern Oscillation Index (SOI) in future work.

The trend of warming could be ascribed to extreme stations in the dataset driving the warming. Figure 11 represents the raw station data highlighting the station distribution in the dataset, which highlights the increase of temperature anomalies since 2013, with some stations showing cooling anomalies but the majority of the data points warming. Figure 11 (right) is a zoomed-in version, highlighting the increase of T_x and T_n in the last few years of the study. This may be an indication of climate change, as these increases could be ascribed to increase extreme events in the context of other climate change observations (Midgley *et al.*, 2005; Midgley *et al.*, 2015). Recent increases in global temperatures is said to be a catch-up of a recent hiatus, "We are returning to normality: rising temperatures. This is an absolute warning of the gangers that lie ahead", as noted by Professor David Vaughan (Mckie, 2016).

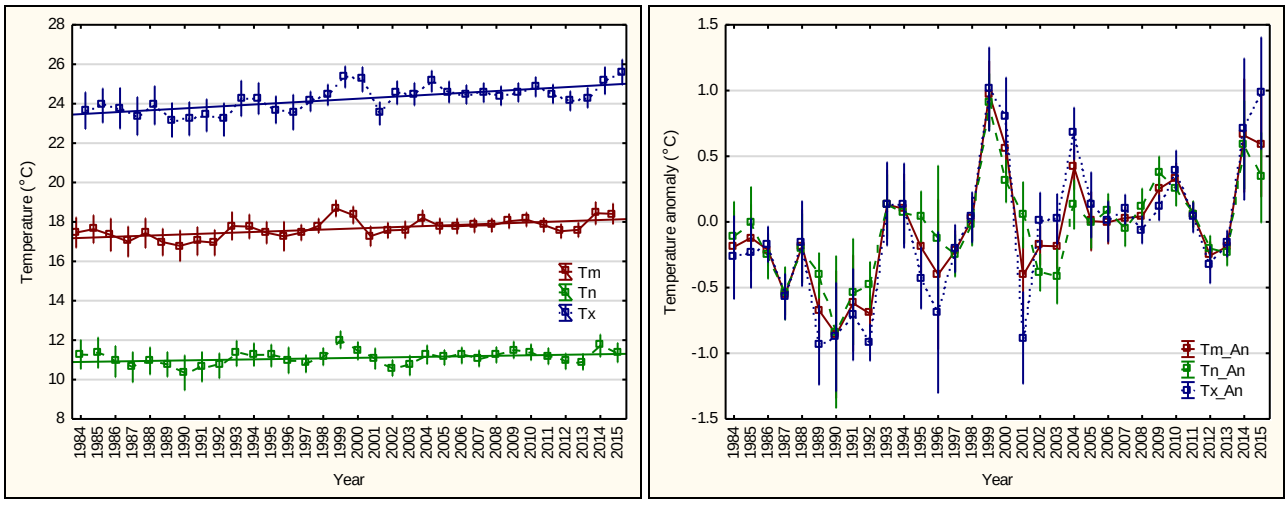

Figure 10 Averaged mean (T_m), maximum (T_x), minimum (T_n) temperature plots (left) for dataset 2 for multiple weather stations grouped by years for a 30 year period (1984-2015). Temperature anomalies (right) for dataset 2, representing the difference from the long term mean. Vertical bars represent 95% confidence intervals.

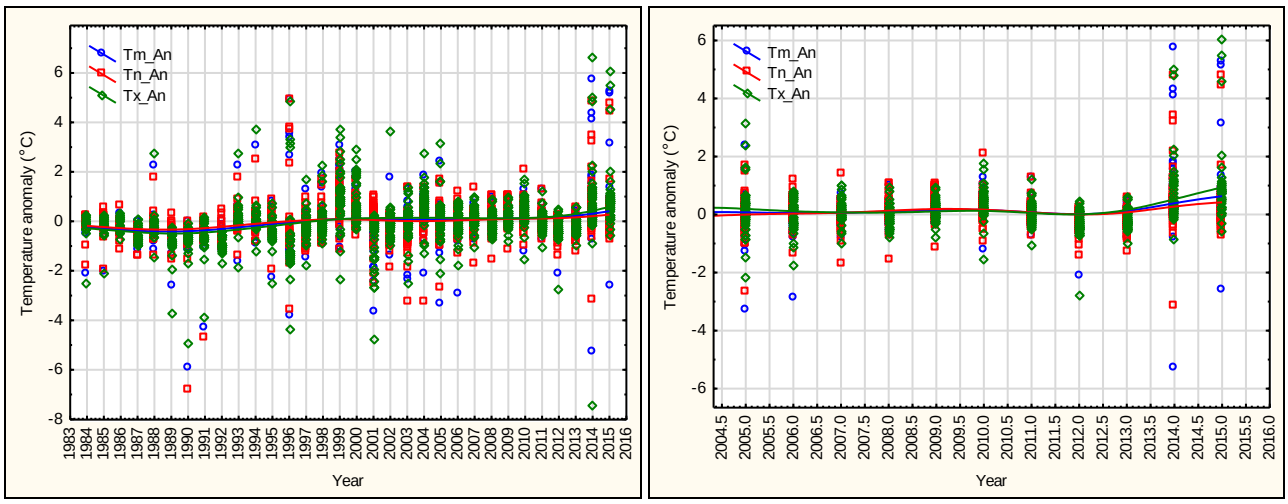

Figure 11 Mean, minimum and maximum temperature anomalies (T_m/T_n/T_x_An), over years from 1984 to 2015 (left), zoomed in section (right) for the last 10 years.

5.3.6 Rainfall trends and anomalies

With respect to rainfall, the results were not always highly significant (Figure 9) but trends were noted, therefore interpretation of these results should be made with great care. The statistical mean plot of multiple weather stations, grouped by years for the 30-year period, shows the variability in annual rainfall over weather stations. There is no consistent trend in the average annual rainfall or rainfall anomalies (Figure 12), other than waving decreases and increases, where a fitted straight line would effectively show no trend. Rainfall has, however, shifted from winter (showing a decreasing trend) to sporadic rainfall in summer months (data not shown), which could affect the grapevine's response to its' environment.

Figure 12 highlights the large variability in annual rainfall patterns over the selection of stations, driven by the complex topography in the Western Cape. Some areas show a decrease in rainfall and others an increase. The general trend as seen in rainfall anomalies (Figure 12, right) seems to be decreasing over time. The annual rainfall anomaly shows a trend of a 200 mm reduction in rainfall over all the stations, with the trend being driven by the majority decreasing, as seen in Figure 12 (left). There are few stations where rainfall has increased in in dataset 2, mainly in the Breede River Region as described in Table 12 (in Addendum 5.1) and two stations in the warmer areas of the Coastal region. The year 2000 and the year 2015 showed to be similar in anomaly of decrease in annual rainfall (Figure 12), the lowest annual anomaly points in the 30 year period.

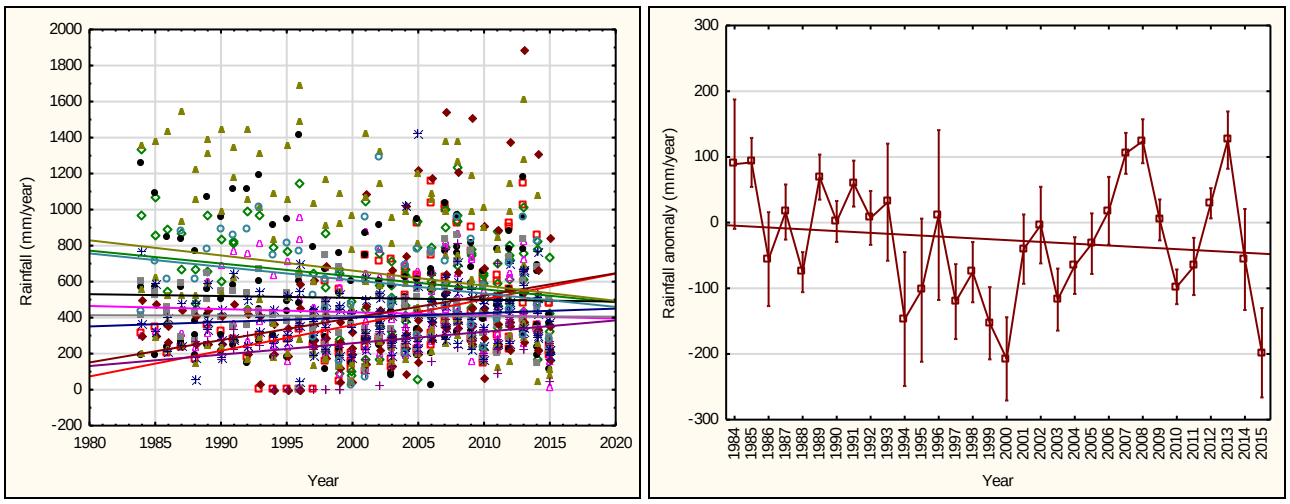

Figure 12 Annual rainfall (mm/year) categorised by stations (left) and anomalies of rainfall (mm/year) (right) grouped by years for a 30 year period in dataset 2. Vertical bars representing 95% confidence intervals.

Rainfall has been documented as being highly variable over seasons and regions, with no distinct pattern in rainfall distribution and amount. Findings are confirmed by literature: there appears to be a shift in rainfall occurrence with a decrease in rainfall in autumn and an increase in rainfall during early winter due to an increase in rainfall amount in June and August (Bonnardot & Carey, 2007). The shifts in annual rainfall are not that large, but the timing and duration thereof is changing. The effects vary over regions, driven by the complex topography in the Western Cape, with some areas showing a decrease in rainfall and others an increase. This highlights the difficulty of drawing conclusions relating to rainfall patterns and quantity, due to the complexity of the Western Cape topography affecting orographic rain, oceanic influences, and shifting low pressure systems seemingly affecting rainfall more in the past few years (Figure 12).

5.3.7 Climate trends: seasonal variability in climate

The increase of T_m in February (Figure 13) from 1984 to 2000 is similar to that shown in previous studies (Bonnardot & Carey, 2007) . The MFT started to cool down from 2010 to 2015, with the exception of 2013. In 2014, the coolest MFT was observed, February is considered to be a general ripening period for most of the cultivars in the Western Cape Province, and these shifts could alter the ripening period and final wine style to some degree. Figure 13 highlights the seasonal variability, with cooler and warmer seasons shown within the general warming trend based on anomaly analysis. January and March have become more important months for ripening wine grapes, especially early and late ripening cultivars, as the seasons are shifting earlier or later due to temperature shifts in other months and rainfall shifts. January is showing a strong increase in temperatures since the year 2000. Figure 13 shows the inverse after 2000 compared to the former years. High temperatures in January are definitely expected to affect grape ripening for early cultivars.

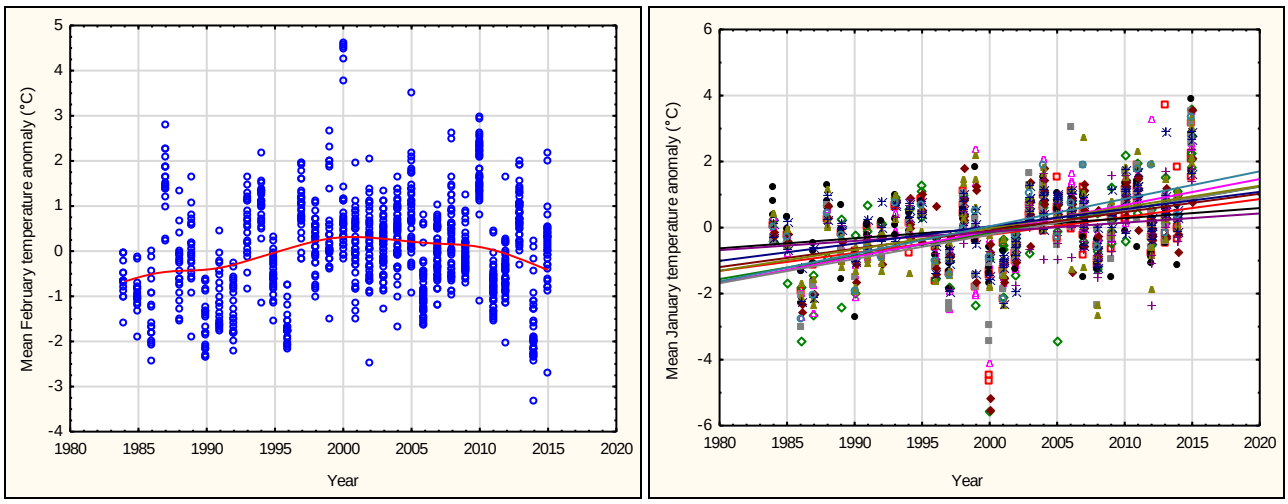

Figure 13 Mean February temperature anomalies averaged over all sites (left) and mean January anomalies categorised by sites (right) for a 30 year period in dataset 2.

The cool night index (minimum March temperature) increased from 1984 to 1990 and then stabilised by 2010, from which temperatures started to decrease by 0.5°C to date as shown in Figure 14. The cool night index is a night coolness variable during the month when ripening usually occurs (Tonietto & Carbonneau, 2004). There is no significant trend in the March temperature anomalies but a definite seasonal effect is evident, having possible impact on colour and aroma development.

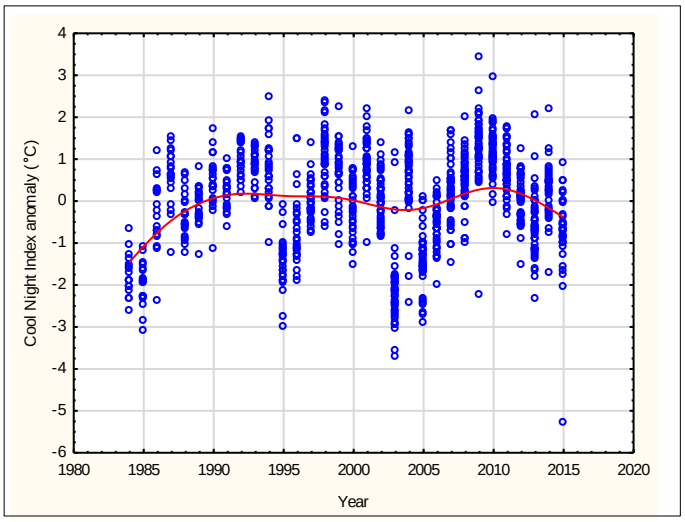

Figure 14 The cool night index (CI) anomalies averaged over all sites for a 30 year period from 1984 to 2015 for dataset 2.

The Winkler (WI) and Huglin (HI) indices calculated for the different wine-producing regions in a study by Bonnardot and Carey (2007) that showed years with lower values occurred at the beginning of the time series (before 1980's), and became less frequent after 1985, with both indices being regularly higher from the mid 1980's (Bonnardot & Carey, 2007). A breaking point in warming from the mid 1980's was observed, which validates the trends observed in regional climate of Southern Africa. Similar patterns of increased values after the mid 1980's were observed over all the stations of the current study, with a plateau from 2003 to 2010, with indices increasing again to the highest point yet in the year 2015 (Figure 15). The trend of increase in WI and HI for the period 2010 to date is about 20 units per season reaching 100 units over five seasons (2010-2015). This represents a general increase of up to 200 units over the 30 year period of the study from 1984-2015, which has the possible implications of shifting the area of classification into a warmer or cooler regions. The classifications of the Winkler and Huglin indices are separated into

classes with unit differences of about 278 and 300 units respectively (Tonietto & Carbonneau, 2004; Anderson *et al.*, 2012). Increases in the indices over time can mostly be explained by increases in the T_n or T_x in the ripening months (Table 12).

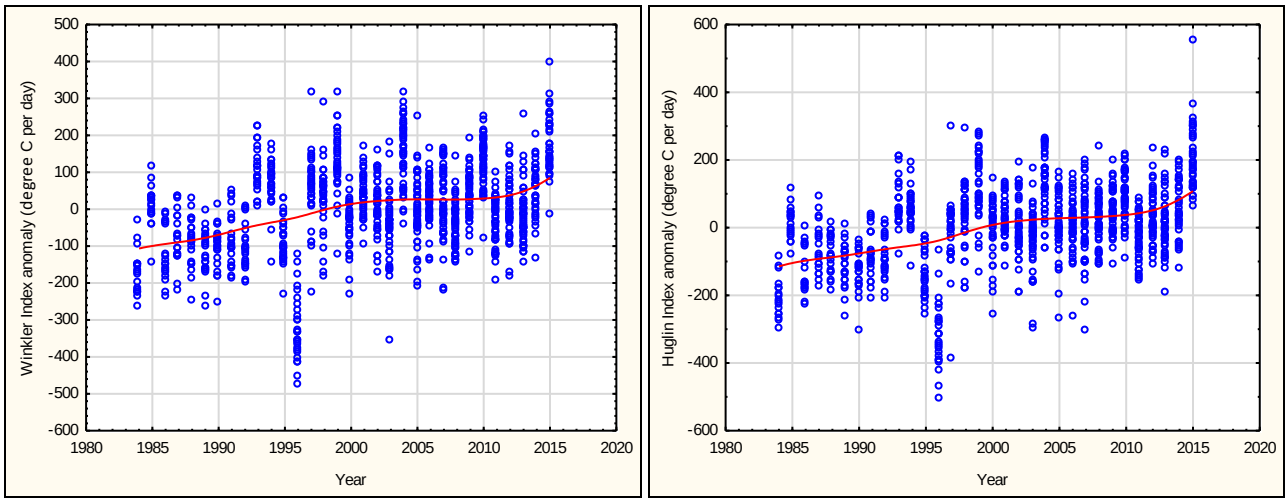

Figure 15 Winkler index anomalies (left) and Huglin index anomalies (right) expressed as growing degree days over a 30 year period from 1984 to 2015 for dataset 2.

The increase in temperature caused shifts in the current climatic regions to warmer classifications, which could be alarming for an already warmer wine producing country, possibly necessitating adaptation of cultivars in other regions and shifting viticulture into non-traditional cooler regions (Bonnardot & Carey, 2007). Bioclimatic indices are important to quantify the seasons and changes over years, including the months of growth and ripening specifically, directly or indirectly affecting the plant and hence the potential of a specific area for the future. A significant increase in the annual temperature values for the Western Cape was noted in previous studies in South Africa. Previous studies by Bonnardot and Carey (2007) showed February to be warmer in terms of minimum (>1.3°C) as well as maximum (>2°C) temperatures for a study period from 1980 to 2001, for a specific station in the district of Stellenbosch in the coastal region.

5.4 Conclusions

Spatial and temporal resolutions are important factors to consider under the umbrella of climate studies. Finer scale analysis provides more detail of where the shifts and changes are taking place in the context of the long term trends, specifically with regards to months and regions. The data range used for analysis can also have an effect on the prediction of climate change in an area of interest. In this study, the decadal analysis showed a general trend of warming in the Western Cape, but when considering the half decade analysis, there were some years cooling and some extreme warmer years. Consequently, when averages are used the meaning of the data could be masked. Over all temperature elements, there was a warming trend from 1984 to 2015 in the Western Cape. Maximum temperatures showed the most increases over the last three decades, ranging from about 1°C to 2°C. Minimum temperature increases were observed over all the regions but with less intensity, increases ranging from <0.6°C over the three decades. Rainfall was not well explained by specific trends, but there were regional and monthly changes of annual increases and decreases over decades, with rainfall shifting more into the summer season of the Western Cape. The shift in annual rainfall may not be significant, but the timing and duration of rainfall are changing and the effects vary over regions, driven by the topography.

Separating the months and the regions is of utmost importance to get a true reflection of climate shifts. Some regions are getting cooler and others warmer; this knowledge will aid in the adaption

strategies for the future of viticulture. A trend of increase in seasonal growing degree day summations was noticed for the period 2010 to date, represented by a general increase of up to 200 units over the 30 year period of the study, confirming that the growing season is warming. Monthly temperature shifts, rather than regional temperatures better illustrate the fluctuations of temperatures across the decades. The most significant shift to warmer temperatures was noted in December, January and March, with increasing rainfall in January and March, which could speed up ripening and affect grape composition as well as the possibly of diseases if rainfall occur during ripening. Cooler minimum temperatures in September could affect budburst, and the cooling temperatures in November, along with more rainfall, could delay phenology, or promote vegetative growth of the grapevine, increasing vigour. Winter months are key for chill unit calculations and efficient budburst for an even and timeous start to the growing season. April, May, June and July showed increasing maximum temperatures and decreasing minimum temperatures. Rainfall is decreasing overall in the winter months with the exception of increases in June for the last decade. August is increasing in mean temperatures driven by the increase in maximum temperatures with an increase in rainfall.

Future work to quantify climate change in the Western Cape and South Africa can be complimented with the use of intrinsically spatialised remote sensing products, such as land surface temperature layers (refer to Chapter 6). Resources such as Fruitlook can be useful to optimise water usage in the future, due the irregular rainfall patterns and possible trends of decreases in annual rainfall. Crops can be cultivated in warmer areas due to the water availability, if water resources become more limited, this will be the factor limiting the future of agriculture in some regions.

The study showed that the spatial input of stations selected for analysis is important. With a wider spatial distribution, there is a significant difference in the warming and cooling over decades, years, regions and months. The correct spatial distribution of reliable stations is key for accurate analysis and to quantify climate change as well as highlighting the possible regional influence on climate change, with some regions possibly more affected than others. Topography and distance from the ocean seemed to drive regional shifts over the three decades, as there seemed to be a more pronounced effect on temperature in the coastal region, with some regions being more prone to change, emphasising the need for finer scale demarcation when climate aspects are considered.

There is a significant climatic trend of warming over the two datasets analysed for the 30 year period, with a similar trend across the different wine regions of South Africa. However, within regions the climate change impacts are more specific in terms of temperature and rainfall, some months being more affected than others, and some months cooling and others warming. South Africa's wine grape growing regions are characterised by diversity in climate, topography, soil type, *etc*. this diversity is a key for effective adaptive strategies, it allows for more complexity in the management of climate change. Changes in the areas of suitability for certain cultivars could be of major importance for the regional economy. Adaptation, change in production practices and development of new wine regions are the keys to surviving climate change. The South African wine industry has already shown considerable flexibility in shifting geographically to new production areas that are characterised by cooler climatic conditions, but this may come at a cost with regards to less favourable conditions such as more summer rainfall or more wind during critical phenological stages such as flowering.

5.5 References

Anderson, J.D., Jones, G.V., Tait, A., Hall, A. & Trought, M., 2012. Analysis of viticulture region climate structure and suitability in New Zealand. J. Int. Sci. Vigne Vin. 46, 149-165.

Bonnardot, V. & Carey, V., 2007. Climate change: observed trends, simulations, impacts and response strategy for the South African vineyards. In: Proc. Global warming, which potential impacts on the vineyards? pp. 1-13.

Bonnardot, V. & Carey, V.A., 2008. Observed climatic trends in South African wine regions and potential implications for viticulture. In: Proc. VIIth international viticultural terroir congress 19-23 May, Nyon, Switzerland. pp. 216-221.

Bonnardot, V. & Cautenet, S., 2009. Mesoscale atmospheric modeling using a high horizontal grid resolution over a complex coastal terrain and a wine region of South Africa. J. Appl. Meteorol. Climatol. 48, 330-348.

Carey, V., Archer, E., Barbeau, G. & Saayman, D., 2007. The use of local knowledge relating to vineyard performance to identify viticultural terroirs in Stellenbosch and surrounds. Acta Horticulturae 754, 385-392.

Carey, V.A., 2005. The use of viticultural terroir units for demarcation of geographical indications for wine production in Stellenbosch and surrounds. Dissertation, Stellenbosch University, Private Bag X1, 7602 Matieland (Stellenbosch), South Africa.

Carey, V.a., Archer, E., Barbeau, G. & Saayman, D., 2009. Viticultural terroirs in stellenbosch, South Africa. III. Spatialisation of viticultural and oenological potential for Cabernet-Sauvignon and Sauvignon blanc by means of a preliminary model. Journal International des Sciences de la Vigne et du Vin 43, 1-12.

DEA, 2013. Long-Term Adaptation Scenarios Flagship Research Programme (LTAS) for South Africa. *In* Climate trends and scenarios for South Africa. Phase 1, technical report 1. Department of Environmental Affairs, Pretoria, South Africa.

Deloire, A., Vaudour, E., Carey, V.A., Bonnardot, V. & Van Leeuwen, C., 2005. Grapevine responses to terroir: a global approach. J Int Sci Vigne et Vin, Vol 39(4) 149-162.

England, M.H., McGregor, S., Spence, P., Meehl, G.A., Timmermann, A., Cai, W., Gupta, A.S., McPhaden, M.J., Purich, A. & Santoso, A., 2014. Recent intensification of wind-driven circulation in the Pacific and the ongoing warming hiatus. Nature Climate Change 4, 222-227.

Hansen, J., Sato, M., Ruedy, R., Schmidt, G.A. & Lo, K., 2015. Global temperature in 2014 and 2015, 16 January 2015 Communication, available at http://www.columbia.edu/~jeh1.

Hansen, J., Sato, M., Ruedy, R., Schmidt, G.A. & Lo, K., 2016. Global temperature in 2015, 19 January 2016 Communication, available at http://www.columbia.edu/~jeh1.

HORTEC, 2012. HORTEC weather services, ileaf. In, http://www.ileaf.co.za/.

IPCC, 2007. Summary for Policymakers. In:Parry, M.L., Canziani, O.F., Palutikof, J.P., van der Linden, P.J. and Hanson, C.E. (eds). Climate change 2007. Impacts, adaptation and vulnerability. In Fourth Assessment Report of the Intergovernmental Panel on Climate Change. Cambridge University Press, Cambridge, UK.

IPCC, 2013. "Despite the robust multi-decadal warming, there exists substantial interannual to decadal variability in the rate of warming, with several periods exhibiting weaker trends (including the warming hiatus since 1998) . Fifteen-year-long hiatus periods are common in both the observed and CMIP5 historical GMST time series", "Box TS.3: Climate Models and the Hiatus in Global Mean Surface Warming of the Past 15 Years". In Climate Change 2013: Technical Summary. pp. 37 and 61-63.

IPCC, 2014. Climate Change 2014: Synthesis Report. In: Pachauri, R. K. and Meyer, L.A. (eds). Fifth Assessment Report of the Intergovernmental Panel on Climate Change, Geneva, Switzerland.

Jones, G., 2006. Climate and terroir: Impacts of climate variability and change on wine. In: Macqueen, R.W. and Meinert, L.D. (eds). Fine wine and terroir-The geoscience perspective. Geoscience Canada, (Geological Association of Canada, St John's, Newfoundland). pp. 1-14.

Kosaka, Y. & Xie, S.-P., 2013. Recent global-warming hiatus tied to equatorial Pacific surface cooling. Nature 501, 403-407.

Kruger, A.C. & Shongwe, S., 2004. Temperature trends in South Africa: 1960-2003. Int. J. Climatol. 24, 1929-1945.

Mckie, R., 2016. February was the warmest month in recorded history, climate experts say. The Guardian, 20 March.

McPhaden, M.J., Lee, T. & McClurg, D., 2011. El Niño and its relationship to changing background conditions in the tropical Pacific Ocean. Geophysical Research Letters 38, n/a-n/a.

Meehl, G.A., Arblaster, J.M., Fasullo, J.T., Hu, A. & Trenberth, K.E., 2011. Model-based evidence of deep-ocean heat uptake during surface-temperature hiatus periods. Nature Climate Change 1, 360-364.

Midgley, G.F., Chapman, R.A., Hewitson, B., Johnston, P., de Wit, M., Zievogel, G., Mukheibir, P., van Niekerk, L., Tadross, M., van Wilgen, B.W., KGOPE, B., Morant, P.D., Theron, A., Scholes, R.J. & Forsyth, G.G., 2005. A Status Quo, Vulnerability and Adaptation Assessment of the Physical and Socio-Economic Effects of Climate Change in the Western Cape. Analysis, 157.

Midgley, G.F., New, M., Johnston, P., Methner, N., Cole, M., Cullis, J., Drimie, S., Dzama, K., Guillot, B., Harper, J., Jack, C., Knowles, T., Louw, D., Mapiye, C., Oosthuizen, H.J. & Smit, J., 2015. A status quo review of climate change and the agriculture sector of the Western Cape Province. CSIR Environmentek, Stellenbosch CSIR. CSIR, P.O. Box 395; Pretoria 0001; South Africa.

Tonietto, J. & Carbonneau, A., 2004. A multicriteria climatic classification system for grape-growing regions worldwide. Agricultural Forest Meteorol. 124, 81-97.

Vink, N., Deloire, A., Bonnardot, V. & Ewert, J., 2010. Terroir, climate change, and the future of South Africa's wine industry. J. British Sociolog. Ass., 7-9.

Webb, L.B., Whetton, P.H. & Barlow, E.W.R., 2007. Modelled impact of future climate change on the phenology of winegrapes in Australia. Aust. J. Grape Wine Res. 13, 165-175.

Winkler, A.J., 1965. General Viticulture. Univ of California Press, University of California, Berkeley.

Addendum 5.1

Table 7 Weather station network descriptions for dataset 1, logging for at least 20 years from 1984 to 2015.

#	Station Name	Latitude	Longitude	Altitude	Logged	Dataset 1	Region
1	AAN-DE-DOORNS WYNKELDER	-33.700	19.483	220	32	>20yr _1984-2015	Breede River Valley
2	AMALIENSTEIN	-33.483	21.460	457	23	>20yr _1984-2015	Klein Karoo
3	ATLANTIS	-33.600	18.483	125	20	>20yr _1984-2015	Coastal Region
4	AVONTUUR	-33.733	23.183	878	22	>20yr _1984-2015	Klein Karoo
5	BIEN DONNE PP	-33.843	18.984	139	23	>20yr _1984-2015	Boberg
6	BO-KLAASVOOGDS	-33.808	19.989	221	20	>20yr _1984-2015	Breede River Valley
7	BOONTJIESKRAAL	-34.200	19.350	128	22	>20yr _1984-2015	Cape South Coast
8	CAPE COLUMBINE - VRT	-32.833	17.850	60	20	>20yr _1984-2015	Coastal Region
9	CHILTERN DAMWAL	-34.041	19.142	308	32	>20yr _1984-2015	Cape South Coast
10	CITRUSDAL (NIVV)	-32.567	18.983	198	22	>20yr _1984-2015	Olifants River
11	DARLING	-33.383	18.383	110	22	>20yr _1984-2015	Coastal Region
12	DE DOORNS (NIWW)	-33.467	19.667	457	22	>20yr _1984-2015	Breede River Valley
13	DE HOEK	-33.150	19.033	115	20	>20yr _1984-2015	Boberg
14	DE KEUR	-32.967	19.300	947	30	>20yr _1984-2015	Western Cape Centr
15	DIE VLAKTE	-33.913	20.492	712	20	>20yr _1984-2015	Klein Karoo
16	DOORNKRAAL	-33.249	19.227	922	21	>20yr _1984-2015	Boberg
17	DRIEFONTEIN	-34.383	20.400	91	22	>20yr _1984-2015	Cape South Coast
18	DROSTDY WYNKELDER	-33.250	19.150	190	22	>20yr _1984-2015	Boberg
19	DROSTERSNES	-34.075	19.077	394	21	>20yr _1984-2015	Cape South Coast
20	DUNGHYE PARK	-34.317	19.517	122	22	>20yr _1984-2015	Cape South Coast
21	DWARSRIVIERSHOEK	-33.928	18.952	307	25	>20yr _1984-2015	Coastal Region
22	FLEURBAIX	-33.959	18.834	125	27	>20yr _1984-2015	Coastal Region
23	GRAAFWATER KO-OP	-32.153	18.605	205	32	>20yr _1984-2015	Olifants River
24	H.L.S. BOLAND	-33.654	18.883	151	32	>20yr _1984-2015	Boberg
25	H.L.S.AUGSBURG	-32.178	18.904	89	31	>20yr _1984-2015	Olifants River
26	HIGH NOON	-33.920	19.287	606	30	>20yr _1984-2015	Cape South Coast
27	HOEKO	-33.490	21.359	614	32	>20yr _1984-2015	Klein Karoo
28	IDEAL HILL	-32.798	18.888	171	23	>20yr _1984-2015	Coastal Region
29	JONASKRAAL	-34.395	19.902	106	30	>20yr _1984-2015	Cape South Coast
30	JONKERSHOEK - BOS	-33.967	18.933	244	20	>20yr _1984-2015	Coastal Region
31	KAAP AGULHAS - VRT	-34.833	20.017	8	20	>20yr _1984-2015	Cape South Coast
32	KAAPPUNT - VRT	-34.350	18.500	11	20	>20yr _1984-2015	Coastal Region
33	KLAWER WYNKELDER	-31.792	18.627	67	23	>20yr _1984-2015	Olifants River
34	LA PLAISANTE	-33.457	19.207	249	27	>20yr _1984-2015	Breede River Valley
35	LANDAU	-33.578	18.968	126	32	>20yr _1984-2015	Boberg
36	LANGGEWENS - AGR	-33.283	18.700	91	20	>20yr _1984-2015	Coastal Region
37	LANGGEWENS (WRS)	-33.283	18.700	177	22	>20yr _1984-2015	Coastal Region
38	LORRAINE	-32.050	19.054	318	32	>20yr _1984-2015	Olifants River
39	MERLE	-33.863	18.929	381	22	>20yr _1984-2015	Boberg
40	MIDDELTUIN	-32.300	18.833	573	21	>20yr _1984-2015	Olifants River
41	MOORREESBURG KO-OP	-33.154	18.673	199	30	>20yr _1984-2015	Coastal Region
42	MORGENSTOND:	-33.937	20.015	121	23	>20yr _1984-2015	Breede River Valley
43	MOUNTAIN VINEYARDS	-33.874	18.951	278	30	>20yr _1984-2015	Boberg
44	NEDERBURG	-33.714	19.013	144	29	>20yr _1984-2015	Boberg
45	NIETVOORBIJ	-33.917	18.860	149	24	>20yr _1984-2015	Coastal Region
46	NOOITGEDACHT - CERES	-33.217	19.333	1040	21	>20yr _1984-2015	Western Cape Centr
47	NORTIER (WRS)	-32.035	18.332	98	32	>20yr _1984-2015	Coastal Region
48	OUTENIQUA (WRS)	-33.917	22.417	361	22	>20yr _1984-2015	Cape South Coast
49	PAARDEKLOOF	-33.261	19.259	878	30	>20yr _1984-2015	Boberg
50	PHILADELPHIA POLISIE	-33.665	18.582	71	23	>20yr _1984-2015	Coastal Region
51	PORTERVILLE KO-OP	-33.013	19.000	149	32	>20yr _1984-2015	Coastal Region
52	PRINSKRAAL	-34.633	20.117	15	22	>20yr _1984-2015	Cape South Coast
53	PROSPECT	-33.854	20.025	149	28	>20yr _1984-2015	Breede River Valley
54	PROTEM	-34.269	20.081	283	25	>20yr _1984-2015	Cape South Coast
55	RIETVLEI	-33.368	21.257	839	28	>20yr _1984-2015	Klein Karoo
56	RIVERSDAL KO-OP	-34.083	21.267	122	22	>20yr _1984-2015	Cape South Coast
57	ROBERTSON PP	-33.828	19.885	156	24	>20yr _1984-2015	Breede River Valley
58	ROUXPOS	-33.405	21.066	641	29	>20yr _1984-2015	Klein Karoo
59	SNEEUWKOP	-32.906	19.452	312	32	>20yr _1984-2015	Western Cape Centr
60	STAGMANSKOP	-32.501	18.891	597	29	>20yr _1984-2015	Olifants River
61	STELLENBOSCHVLEI	-32.246	23.414	958	22	>20yr _1984-2015	Western Cape Upper
62	STOLSHOEK KNP	-32.334	22.489	919	28	>20yr _1984-2015	Western Cape Upper
63	SWELLENDAM - TNK	-34.033	20.450	125	21	>20yr _1984-2015	Cape South Coast
64	TOT-U-DIENS	-33.684	19.843	919	23	>20yr _1984-2015	Klein Karoo
65	TYGERHOEK PP.	-34.162	19.907	183	20	>20yr _1984-2015	Cape South Coast
66	VELDRESERWE	-33.622	19.469	307	32	>20yr _1984-2015	Breede River Valley
67	VILLIERSDORP	-33.986	19.297	355	21	>20yr _1984-2015	Cape South Coast
68	VREDENDAL	-31.667	18.500	37	20	>20yr _1984-2015	Olifants River
69	VREDENHOF	-33.693	18.953	161	32	>20yr _1984-2015	Boberg
70	WELTEVREDE	-33.933	20.617	405	22	>20yr _1984-2015	Klein Karoo

Table 8 Weather station network descriptions for dataset 2, logging for at least 10 years from 1984 to 2016.

#	Station Name	Latitude	Longitude	Altitude	Distance from Ocean	Start_Year	End_Year	Logged_years	DataSet 2	Region
1	AAN-DE-DOORNS	-33.700	19.483	220	78.4	1984	201	32	>10yr_1984-2016	Breede River
2	AGTERVINKRIVIER	-33.702	19.715	361	90.1	1998	201	18	>10yr_1984-2016	Breede River
3	ALTO	-34.014	18.856	251	10.5	1998	201	18	>10yr_1984-2016	Coastal
4	BIEN DONNE PP	-33.843	18.984	139	34.4	1993	201	23	>10yr_1984-2016	Boberg
5	BOESMANSPAD	-33.922	20.203	191	64.9	1998	201	18	>10yr_1984-2016	Breede River
6	BO-KLAASVOOGDS	-33.807	19.989	221	84	1996	201	20	>10yr_1984-2016	Breede River
7	BONFOI	-33.935	18.780	156	17.2	1998	201	17	>10yr_1984-2016	Coastal
8	CHILTERN DAMWAL	-34.041	19.142	308	29.4	1984	201	32	>10yr_1984-2016	Cape South
9	DE HOOP	-33.764	19.928	297	90.6	1998	201	18	>10yr_1984-2016	Breede River
1	DE KEUR	-32.989	19.304	947	96.7	1992	201	24	>10yr_1984-2016	Western
1	ELSENBURG	-33.582	18.830	171	39.3	1995	201	21	>10yr_1984-2016	Coastal
1	FLEURBAIX	-33.959	18.834	125	15.7	1989	201	27	>10yr_1984-2016	Coastal
1	GOREE	-33.815	19.787	171	84.4	1997	201	19	>10yr_1984-2016	Breede River
1	GOUDMYN	-33.879	20.010	143	76.2	1997	201	18	>10yr_1984-2016	Breede River
1	GRAAFWATER KO-OP	-32.153	18.605	205	25.7	1984	201	32	>10yr_1984-2016	Olifants River
1	H.L.S. BOLAND	-33.654	18.883	151	41.1	1984	201	32	>10yr_1984-2016	Boberg
1	H.L.S.AUGSBURG	-32.178	18.904	89	51.9	1985	201	31	>10yr_1984-2016	Olifants River
1	HELDERFONTEIN	-33.923	18.873	133	21	2003	201	13	>10yr_1984-2016	Coastal
1	HIGH NOON	-33.920	19.287	606	46.6	1984	201	30	>10yr_1984-2016	Cape South
2	HOEKO	-33.490	21.359	614	93.5	1984	201	32	>10yr_1984-2016	Klein Karoo
2	JONASKRAAL	-34.395	19.902	106	38.5	1984	201	30	>10yr_1984-2016	Cape South
2	KONINGSRIVIER	-33.903	19.882	196	79.9	1997	201	19	>10yr_1984-2016	Breede River
2	LANDAU	-33.578	18.968	126	51.3	1984	201	32	>10yr_1984-2016	Boberg
2	LE BONHEUR	-33.829	18.868	259	31.4	1998	201	16	>10yr_1984-2016	Boberg
2	LE CHASSEUR	-33.861	19.724	176	75.8	1997	201	19	>10yr_1984-2016	Breede River
2	LORRAINE	-32.050	19.054	318	67.9	1984	201	32	>10yr_1984-2016	Olifants River
2	MARBLE HALL	-25.026	29.366	846	300.6	2002	201	14	>10yr_1984-2016	Western
2	MERLE	-33.863	18.928	381	29.8	1994	201	22	>10yr_1984-2016	Boberg
2	MOORREESBURG KO-	-33.154	18.673	199	49.7	1984	201	30	>10yr_1984-2016	Coastal
3	MORGENSTOND:	-33.937	20.015	121	70.5	1993	201	23	>10yr_1984-2016	Breede River
3	MOUNTAIN VINEYARDS	-33.874	18.951	278	29.6	1984	201	30	>10yr_1984-2016	Boberg
3	NORTIER (WRS)	-32.035	18.332	98	2.9	1984	201	32	>10yr_1984-2016	Coastal
3	NUY	-33.647	19.625	225	90.6	1997	201	19	>10yr_1984-2016	Breede River
3	PAARDEKLOOF	-33.260	19.259	878	91.5	1986	201	30	>10yr_1984-2016	Boberg
3	PORTERVILLE KO-OP	-33.012	18.999	149	74.2	1984	201	32	>10yr_1984-2016	Coastal
3	RIETVLEI	-33.368	21.257	839	109	1988	201	28	>10yr_1984-2016	Klein Karoo
3	RIVIERA	-32.685	18.696	90	35.9	1998	201	18	>10yr_1984-2016	Coastal
3	ROBERTSON PP	-33.828	19.885	156	86.4	1992	201	24	>10yr_1984-2016	Breede River
3	ROUXPOS	-33.405	21.066	641	111.3	1987	201	29	>10yr_1984-2016	Klein Karoo
4	SANDBERG	-32.290	18.566	102	19.5	1998	201	18	>10yr_1984-2016	Coastal
4	SKAAPKRAAL	-33.535	18.631	138	24.7	1997	201	17	>10yr_1984-2016	Coastal
4	SNEEUWKOP	-32.906	19.452	312	106.1	1984	201	32	>10yr_1984-2016	Western
4	STOLSHOEK KNP	-32.334	22.489	919	190.2	1988	201	28	>10yr_1984-2016	Western
4	TYGERHOEK PP.	-34.162	19.907	183	57.9	1996	201	20	>10yr_1984-2016	Cape South
4	VELDRESERWE	-33.622	19.469	307	84.4	1984	201	32	>10yr_1984-2016	Breede River
4	VINKRIVIER	-33.756	19.776	257	88.8	1997	201	18	>10yr_1984-2016	Breede River
4	VREDENHOF	-33.693	18.953	161	46.3	1984	201	32	>10yr_1984-2016	Boberg

Table 9 Maximum (T_x), minimum (T_n), mean (T_m) temperatures and rain averages for the four decades, describing the mean, standard deviation (Std.D) and standard error (Std.E) with N=station number in each region for dataset 2 only.

Region	Decade	N	T_x			T_n			T_m			Rain (mm/month)		
			Mean	Std. Dev	Std. Err	Mean	Std. Dev	Std. Err	Mean	Std. Dev	Std. Err	Mean	Std. Dev	Std .Er
Breede River Valley	1980-1990	6	24.7	0.4	0.2	11.6	0.1	0.1	18.1	0.3	0.1	22.7	6.2	2.5
Breede River Valley	1991-2000	10	24.7	0.5	0.2	11.3	0.5	0.2	18.0	0.4	0.1	20.3	6.6	2.1
Breede River Valley	2001-2010	10	24.8	0.6	0.2	10.7	0.4	0.1	17.8	0.4	0.1	27.2	7.9	2.5
Breede River Valley	2011-2015	6	24.9	0.4	0.2	10.8	0.3	0.1	17.8	0.3	0.1	28.7	6.2	2.5
Boberg	1980-1990	6	23.3	0.6	0.2	11.9	0.6	0.3	17.6	0.6	0.3	68.8	6.7	2.7
Boberg	1991-2000	10	23.2	0.6	0.2	11.7	0.5	0.2	17.4	0.6	0.2	61.2	11.3	3.6
Boberg	2001-2010	10	23.5	0.3	0.1	12.0	0.4	0.1	17.7	0.3	0.1	69.3	12.0	3.8
Boberg	2011-2015	6	23.8	0.7	0.3	12.0	0.2	0.1	17.9	0.4	0.2	63.3	21.4	8.7
Cape South Coast	1980-1990	6	21.9	0.2	0.1	10.0	0.2	0.1	16.0	0.2	0.1	65.1	13.2	5.4
Cape South Coast	1991-2000	10	22.1	0.7	0.2	10.4	0.6	0.2	16.2	0.6	0.2	56.5	14.6	4.6
Cape South Coast	2001-2010	10	22.8	0.4	0.1	10.6	0.2	0.1	16.6	0.3	0.1	59.2	24.4	7.7
Cape South Coast	2011-2015	6	22.6	0.9	0.4	10.5	0.3	0.1	16.6	0.5	0.2	54.2	14.5	5.9
Coastal Region	1980-1990	6	23.8	0.4	0.2	11.7	0.3	0.1	17.7	0.3	0.1	35.0	4.7	1.9
Coastal Region	1991-2000	10	23.9	0.6	0.2	11.6	0.3	0.1	17.7	0.5	0.1	39.6	6.5	2.0
Coastal Region	2001-2010	10	24.5	0.4	0.1	11.5	0.3	0.1	18.0	0.3	0.1	43.8	9.5	3.0
Coastal Region	2011-2015	6	24.9	0.4	0.2	11.5	0.3	0.1	18.2	0.3	0.1	38.7	11.8	4.8
Olifants River	1980-1990	6	26.5	0.3	0.1	11.4	0.5	0.2	18.9	0.3	0.1	22.6	2.5	1.0
Olifants River	1991-2000	10	26.8	0.9	0.3	11.6	0.6	0.2	19.2	0.7	0.2	20.8	6.7	2.1
Olifants River	2001-2010	10	27.4	0.5	0.2	11.8	0.4	0.1	19.6	0.3	0.1	21.2	6.0	1.9
Olifants River	2011-2015	6	27.4	0.5	0.2	11.8	0.2	0.1	19.6	0.3	0.1	21.0	4.6	1.9
Klein Karoo	1980-1990	6	24.0	0.4	0.2	11.1	0.2	0.1	17.5	0.3	0.1	28.3	10.7	4.4
Klein Karoo	1991-2000	10	24.3	0.7	0.2	11.3	0.6	0.2	17.8	0.6	0.2	24.3	5.4	1.7
Klein Karoo	2001-2010	10	24.9	0.3	0.1	11.2	0.4	0.1	18.1	0.2	0.1	29.0	7.7	2.4
Klein Karoo	2011-2015	6	24.9	0.6	0.2	11.1	0.4	0.2	18.0	0.5	0.2	30.5	8.5	3.5
Western Cape	1980-1990	6	21.5	0.3	0.1	8.1	0.2	0.1	14.8	0.2	0.1	52.0	12.6	5.1
Western Cape	1991-2000	10	21.7	0.9	0.3	8.4	0.5	0.1	15.1	0.6	0.2	32.8	12.9	4.1
Western Cape	2001-2010	10	22.0	0.8	0.2	8.4	0.5	0.2	15.2	0.6	0.2	43.0	13.9	4.4
Western Cape	2011-2015	6	22.0	0.6	0.3	8.5	0.2	0.1	15.2	0.4	0.2	44.2	11.8	4.8
Western Cape Upper	1980-1990	2	26.2	2.5	1.8	11.5	1.1	0.7	18.9	1.8	1.3	24.8	9.4	6.6
Western Cape Upper	1991-2000	10	24.2	1.9	0.6	9.6	2.7	0.8	16.9	2.3	0.7	27.7	9.1	2.9
Western Cape Upper	2001-2010	10	25.7	0.4	0.1	10.9	0.5	0.2	18.3	0.4	0.1	26.8	5.6	1.8
Western Cape Upper	2011-2015	6	25.9	0.8	0.3	10.8	0.8	0.3	18.3	0.8	0.3	27.9	9.5	3.9
Western Cape Out	2001-2010	8	28.9	1.1	0.4	12.4	0.9	0.3	20.7	0.9	0.3	41.3	13.5	4.8
Western Cape Out	2011-2015	6	28.3	0.8	0.3	12.4	0.5	0.2	20.4	0.6	0.3	48.0	10.6	4.3

Table 10 Maximum (T_x), minimum (T_n), mean (T_m) temperatures and rain averages for the half decades over a 30 year period, describing the mean, standard deviation (Std.D) and standard error (Std.E) with N=station number in each region for dataset 2 only.

Region	Half decades	N	T_x			T_n			T_m			Rain (mm/month)		
			Mean	Std.D	Std.E	Mean	Std.D	Std.E	Mean	Std.D	Std.E	Mean	Std.D	Std.E
Breede River	1984-1989	5	24.8	0.2	0.1	11.6	0.1	0.1	18.2	0.1	0.1	21.6	6.2	2.8
Breede River	1990-1994	5	24.4	0.4	0.2	11.6	0.3	0.1	18.0	0.3	0.2	24.0	4.0	1.8
Breede River	1995-1999	5	24.6	0.4	0.2	10.8	0.4	0.2	17.7	0.3	0.1	18.8	8.7	3.9
Breede River	2000-2004	5	25.0	1.0	0.4	10.8	0.7	0.3	17.9	0.8	0.3	20.8	7.2	3.2
Breede River	2005-2009	5	24.9	0.4	0.2	10.7	0.2	0.1	17.8	0.2	0.1	31.9	5.6	2.5
Breede River	2010-2014	5	24.8	0.3	0.1	10.8	0.2	0.1	17.8	0.2	0.1	27.2	6.4	2.9
Breede River	>=2015	2	25.3	0.0	0.0	11.1	0.1	0.1	18.1	0.2	0.2	31.0	4.4	3.1
Boberg	1984-1989	5	23.4	0.6	0.3	12.1	0.6	0.3	17.7	0.6	0.3	66.9	5.4	2.4
Boberg	1990-1994	5	22.9	0.4	0.2	11.4	0.2	0.1	17.1	0.3	0.1	73.5	4.2	1.9
Boberg	1995-1999	5	23.1	0.5	0.2	11.7	0.3	0.2	17.4	0.4	0.2	52.8	7.8	3.5
Boberg	2000-2004	5	23.6	0.6	0.3	12.0	0.6	0.3	17.8	0.6	0.2	62.8	12.4	5.6
Boberg	2005-2009	5	23.6	0.3	0.1	12.1	0.3	0.1	17.8	0.4	0.2	72.1	11.0	4.9
Boberg	2010-2014	5	23.4	0.3	0.1	12.0	0.3	0.1	17.7	0.3	0.1	71.1	17.4	7.8
Boberg	>=2015	2	24.6	0.5	0.3	12.2	0.0	0.0	18.4	0.2	0.2	51.0	26.0	18.
Cape South Coast	1984-1989	5	22.0	0.1	0.0	10.1	0.2	0.1	16.1	0.1	0.1	64.0	14.5	6.5
Cape South Coast	1990-1994	5	21.8	0.4	0.2	10.1	0.4	0.2	16.0	0.4	0.2	66.9	4.7	2.1
Cape South Coast	1995-1999	5	22.0	0.7	0.3	10.3	0.4	0.2	16.2	0.5	0.2	52.6	16.2	7.3
Cape South Coast	2000-2004	5	22.8	0.6	0.3	10.6	0.5	0.2	16.7	0.5	0.2	45.9	6.9	3.1
Cape South Coast	2005-2009	5	23.0	0.4	0.2	10.6	0.2	0.1	16.7	0.4	0.2	70.2	31.7	14.
Cape South Coast	2010-2014	5	22.8	0.2	0.1	10.6	0.4	0.2	16.7	0.3	0.1	55.0	11.0	4.9
Cape South Coast	>=2015	2	22.3	1.8	1.3	10.6	0.4	0.3	16.5	1.1	0.8	49.7	23.4	16.
Coastal Region	1984-1989	5	23.9	0.3	0.1	11.8	0.3	0.1	17.9	0.3	0.1	33.6	3.6	1.6
Coastal Region	1990-1994	5	23.4	0.4	0.2	11.5	0.2	0.1	17.4	0.3	0.2	41.0	2.8	1.2
Coastal Region	1995-1999	5	24.0	0.4	0.2	11.5	0.2	0.1	17.8	0.3	0.1	38.4	9.1	4.1
Coastal Region	2000-2004	5	24.6	0.6	0.3	11.6	0.6	0.3	18.1	0.5	0.2	39.2	7.9	3.6
Coastal Region	2005-2009	5	24.5	0.2	0.1	11.6	0.1	0.0	18.1	0.1	0.1	47.2	9.9	4.4
Coastal Region	2010-2014	5	24.7	0.2	0.1	11.6	0.3	0.1	18.2	0.3	0.1	43.8	9.2	4.1
Coastal Region	>=2015	2	25.4	0.2	0.1	11.5	0.6	0.4	18.4	0.4	0.3	30.2	12.7	9.0
Olifants River	1984-1989	5	26.5	0.4	0.2	11.4	0.5	0.2	18.9	0.3	0.2	22.5	2.8	1.2
Olifants River	1990-1994	5	26.6	0.8	0.3	11.2	0.5	0.2	18.9	0.6	0.3	21.3	3.0	1.3
Olifants River	1995-1999	5	26.6	0.7	0.3	11.6	0.2	0.1	19.1	0.4	0.2	21.6	9.3	4.2
Olifants River	2000-2004	5	27.6	0.6	0.3	11.9	0.7	0.3	19.7	0.6	0.3	18.4	5.7	2.5
Olifants River	2005-2009	5	27.6	0.6	0.3	11.8	0.2	0.1	19.7	0.4	0.2	22.7	6.5	2.9
Olifants River	2010-2014	5	27.2	0.4	0.2	11.8	0.3	0.1	19.5	0.3	0.1	23.0	2.0	0.9
Olifants River	>=2015	2	27.7	0.5	0.4	11.8	0.1	0.1	19.8	0.2	0.1	17.2	6.7	4.7
Klein Karoo	1984-1989	5	24.1	0.3	0.1	11.2	0.2	0.1	17.6	0.2	0.1	27.7	11.8	5.3
Klein Karoo	1990-1994	5	23.9	0.5	0.2	11.0	0.4	0.2	17.4	0.4	0.2	26.2	4.9	2.2
Klein Karoo	1995-1999	5	24.2	0.7	0.3	11.2	0.4	0.2	17.7	0.5	0.2	25.0	6.2	2.8
Klein Karoo	2000-2004	5	24.9	0.5	0.2	11.6	0.6	0.3	18.3	0.5	0.2	23.7	4.5	2.0
Klein Karoo	2005-2009	5	25.1	0.3	0.1	11.1	0.4	0.2	18.1	0.3	0.1	32.5	9.5	4.3
Klein Karoo	2010-2014	5	24.8	0.6	0.3	11.0	0.4	0.2	17.9	0.5	0.2	31.4	9.2	4.1
Klein Karoo	>=2015	2	25.1	0.1	0.1	11.2	0.2	0.2	18.2	0.1	0.0	26.2	1.8	1.3
Western Cape	1984-1989	5	21.6	0.1	0.1	8.1	0.3	0.1	14.9	0.2	0.1	52.0	14.1	6.3
Western Cape	1990-1994	5	21.3	0.5	0.2	8.1	0.3	0.1	14.7	0.4	0.2	43.8	14.4	6.4
Western Cape	1995-1999	5	21.7	0.7	0.3	8.3	0.1	0.1	15.0	0.4	0.2	25.8	6.8	3.0
Western Cape	2000-2004	5	22.0	1.2	0.5	8.3	0.8	0.4	15.1	1.0	0.4	36.7	9.0	4.0
Western Cape	2005-2009	5	22.4	0.6	0.3	8.6	0.4	0.2	15.5	0.5	0.2	44.7	17.5	7.8
Western Cape	2010-2014	5	21.7	0.5	0.2	8.5	0.3	0.1	15.1	0.4	0.2	48.1	5.0	2.2
Western Cape	>=2015	2	22.5	0.6	0.4	8.6	0.1	0.1	15.6	0.2	0.2	39.3	23.8	16.
Western Cape	1984-1989	1	28.0			12.3			20.1			18.2		
Western Cape	1990-1994	5	23.3	2.3	1.0	8.5	3.5	1.6	15.9	2.9	1.3	24.7	7.5	3.4
Western Cape	1995-1999	5	24.8	0.6	0.3	10.5	0.3	0.1	17.6	0.4	0.2	29.2	9.4	4.2
Western Cape	2000-2004	5	25.6	0.5	0.2	10.9	0.6	0.3	18.2	0.5	0.2	31.5	7.6	3.4
Western Cape	2005-2009	5	25.9	0.4	0.2	11.2	0.6	0.3	18.6	0.3	0.2	24.8	4.0	1.8
Western Cape	2010-2014	5	25.7	0.8	0.4	10.6	0.7	0.3	18.1	0.7	0.3	30.1	8.4	3.7
Western Cape	>=2015	2	26.5	0.2	0.1	11.3	0.6	0.4	18.9	0.4	0.3	21.4	8.3	5.9
Western Cape Out	2000-2004	2	28.9	1.5	1.1	11.8	1.6	1.2	20.3	1.6	1.1	27.0	4.1	2.9
Western Cape Out	2005-2009	5	29.1	1.2	0.5	12.6	0.6	0.3	20.8	0.8	0.4	48.7	11.2	5.0
Western Cape Out	2010-2014	5	28.0	0.2	0.1	12.5	0.5	0.2	20.2	0.3	0.1	47.0	10.1	4.5
Western Cape Out	>=2015	2	28.8	1.4	1.0	12.6	1.0	0.7	20.7	1.2	0.8	42.7	18.3	12.

Table 11 Maximum (T_x), minimum (T_n), mean (T_m) temperatures and rain differences (anomalies) between half decades and 1984-2015, for dataset 2 only.

Region	Halft decades	T_x	T_n	T_m	Rain (mm/month)
Breede River Valley	1984-1989				
Breede River Valley	1989-1994	-0.43	0.00	-0.22	2.45
Breede River Valley	1994-1999	0.22	-0.77	-0.27	-5.27
Breede River Valley	1999-2004	0.37	0.00	0.18	2.07
Breede River Valley	2004-2009	-0.08	-0.12	-0.10	11.09
Breede River Valley	2009-2014	-0.12	0.05	-0.04	-4.74
Breede River Valley	>=2014	0.57	0.35	0.33	3.80
Breede River Valley	**1984-2015**	**0.52**	**-0.49**	**-0.11**	**9.40**
Boberg	1984-1989				
Boberg	1989-1994	-0.52	-0.71	-0.61	6.58
Boberg	1994-1999	0.21	0.34	0.27	-20.73
Boberg	1999-2004	0.54	0.31	0.43	10.05
Boberg	2004-2009	-0.02	0.08	-0.04	9.32
Boberg	2009-2014	-0.23	-0.05	-0.07	-1.07
Boberg	>=2014	1.23	0.12	0.68	-20.11
Boberg	**1984-2015**	**1.21**	**0.10**	**0.66**	**-15.94**
Cape South Coast	1984-1989				
Cape South Coast	1989-1994	-0.21	0.02	-0.09	2.89
Cape South Coast	1994-1999	0.21	0.16	0.19	-14.28
Cape South Coast	1999-2004	0.73	0.34	0.53	-6.69
Cape South Coast	2004-2009	0.23	0.01	-0.02	24.27
Cape South Coast	2009-2014	-0.20	-0.05	0.01	-15.23
Cape South Coast	>=2014	-0.49	0.06	-0.22	-5.25
Cape South Coast	**1984-2015**	**0.27**	**0.54**	**0.41**	**-14.29**
Coastal Region	1984-1989				
Coastal Region	1989-1994	-0.47	-0.35	-0.41	7.44
Coastal Region	1994-1999	0.56	0.05	0.31	-2.64
Coastal Region	1999-2004	0.57	0.05	0.31	0.83
Coastal Region	2004-2009	-0.03	0.02	0.00	7.92
Coastal Region	2009-2014	0.20	0.03	0.12	-3.37
Coastal Region	>=2014	0.63	-0.13	0.25	-13.54
Coastal Region	**1984-2015**	**1.46**	**-0.32**	**0.57**	**-3.35**
Olifants River	1984-1989				
Olifants River	1989-1994	0.11	-0.13	-0.01	-1.27
Olifants River	1994-1999	0.01	0.33	0.17	0.31
Olifants River	1999-2004	0.95	0.36	0.65	-3.22
Olifants River	2004-2009	0.05	-0.11	-0.03	4.38
Olifants River	2009-2014	-0.38	0.02	-0.18	0.27
Olifants River	>=2014	0.49	0.01	0.25	-5.81
Olifants River	**1984-2015**	**1.22**	**0.48**	**0.85**	**-5.35**
Klein Karoo	1984-1989				
Klein Karoo	1989-1994	-0.22	-0.21	-0.22	-1.44
Klein Karoo	1994-1999	0.28	0.26	0.27	-1.20
Klein Karoo	1999-2004	0.76	0.39	0.57	-1.29
Klein Karoo	2004-2009	0.18	-0.56	-0.19	8.81
Klein Karoo	2009-2014	-0.29	-0.04	-0.16	-1.14
Klein Karoo	>=2014	0.31	0.22	0.26	-5.22
Klein Karoo	**1984-2015**	**1.01**	**0.05**	**0.53**	**-1.48**
Western Cape Centre	1984-1989				
Western Cape Centre	1989-1994	-0.28	-0.02	-0.15	-8.14
Western Cape Centre	1994-1999	0.38	0.20	0.29	-18.06
Western Cape Centre	1999-2004	0.35	-0.04	0.15	10.96
Western Cape Centre	2004-2009	0.39	0.29	0.34	7.98
Western Cape Centre	2009-2014	-0.66	-0.05	-0.35	3.42
Western Cape Centre	>=2014	0.76	0.12	0.44	-8.81
Western Cape Centre	**1984-2015**	**0.95**	**0.50**	**0.73**	**-12.64**
Western Cape Upper	1984-1989				
Western Cape Upper	1989-1994				
Western Cape Upper	1994-1999	1.54	1.95	1.74	4.50
Western Cape Upper	1999-2004	0.75	0.40	0.57	2.32
Western Cape Upper	2004-2009	0.32	0.35	0.34	-6.69
Western Cape Upper	2009-2014	-0.20	-0.63	-0.42	5.26
Western Cape Upper	>=2014	0.79	0.73	0.76	-8.73
Western Cape Upper	**1984-2015**	**-1.50**	**-0.96**	**-1.23**	**3.19**
Western Cape Out	1999-2004				
Western Cape Out	2004-2009	0.22	0.74	0.48	21.72
Western Cape Out	2009-2014	-1.07	-0.11	-0.59	-1.69
Western Cape Out	>=2014	0.84	0.17	0.51	-4.31
Western Cape Out	**1984-2015**	**-0.01**	**0.80**	**0.40**	**15.72**

Table 12 Maximum (T_x), minimum (T_n), mean (T_m) temperatures and rain averages for decades grouped by months, describing the mean, standard deviation (Std.D) and standard error (Std.E) with N=station number in each region for dataset 2 only.

Month	Decade	T_x			T_n			T_m			Rain (mm/month)		
		Mean	Std.D	Std.E	Mean	Std.D	Std.E	Mean	Std.D	Std.E	Mean	Std.D	Std.E
January	1980-1990	29.3	1.1	0.4	15.1	1.1	0.4	22.2	1.0	0.4	12.2	11.5	4.7
January	1991-2000	30.0	0.5	0.2	15.4	0.8	0.2	22.7	0.6	0.2	10.0	7.5	2.4
January	2001-2010	29.9	1.1	0.4	15.6	1.1	0.3	22.8	1.0	0.3	20.6	16.9	5.3
January	2011-2016	31.5	1.1	0.4	16.6	0.8	0.3	24.0	0.9	0.3	22.3	27.7	10.5
February	1980-1990	29.9	1.3	0.5	15.7	1.0	0.4	22.8	1.0	0.4	12.2	10.4	4.2
February	1991-2000	29.9	1.2	0.4	15.8	1.1	0.3	22.8	1.1	0.4	12.6	10.8	3.4
February	2001-2010	30.9	0.9	0.3	16.3	0.5	0.2	23.6	0.7	0.2	15.8	7.0	2.2
February	2011-2016	30.8	1.0	0.4	15.9	1.3	0.5	23.3	1.1	0.4	14.9	7.4	2.8
March	1980-1990	27.3	1.3	0.5	14.1	1.2	0.5	20.7	1.2	0.5	41.4	25.1	10.3
March	1991-2000	28.4	1.1	0.3	14.7	0.9	0.3	21.5	0.9	0.3	14.7	6.9	2.2
March	2001-2010	28.6	1.5	0.5	14.3	1.1	0.3	21.4	1.1	0.4	19.4	19.0	6.0
March	2011-2016	29.0	1.1	0.4	14.7	0.9	0.3	21.9	1.0	0.4	20.4	11.2	4.2
April	1980-1990	24.4	1.2	0.5	11.7	0.6	0.2	18.1	0.8	0.3	49.6	18.4	7.5
April	1991-2000	24.7	1.5	0.5	11.8	1.0	0.3	18.2	1.1	0.4	44.9	37.3	11.8
April	2001-2010	25.5	0.8	0.3	12.1	0.6	0.2	18.7	0.6	0.2	40.3	25.1	7.9
April	2011-2016	25.5	0.8	0.3	11.4	0.6	0.3	18.3	0.6	0.3	30.4	17.1	7.0
May	1980-1990	21.5	1.5	0.6	9.7	0.8	0.3	15.6	1.0	0.4	72.4	53.9	22.0
May	1991-2000	21.2	1.2	0.4	9.0	0.9	0.3	15.1	0.9	0.3	58.8	24.6	7.8
May	2001-2010	21.5	1.3	0.4	9.3	1.2	0.4	15.4	1.1	0.3	62.5	31.6	10.0
May	2011-2016	21.8	0.8	0.3	9.1	0.8	0.3	15.4	0.5	0.2	49.5	26.6	10.9
June	1980-1990	18.2	0.8	0.3	7.2	0.8	0.3	12.7	0.8	0.3	76.7	23.5	9.6
June	1991-2000	17.8	1.3	0.4	6.8	0.7	0.2	12.3	0.9	0.3	89.4	38.2	12.1
June	2001-2010	18.9	1.3	0.4	7.1	1.1	0.3	13.0	0.9	0.3	61.8	30.9	9.8
June	2011-2016	18.2	0.5	0.2	6.9	0.5	0.2	12.6	0.3	0.1	94.1	14.5	5.9
July	1980-1990	17.3	0.5	0.2	6.3	0.5	0.2	11.8	0.5	0.2	74.9	21.5	8.8
July	1991-2000	17.3	1.3	0.4	6.4	0.9	0.3	11.8	1.0	0.3	77.4	40.3	12.7
July	2001-2010	18.7	1.2	0.4	6.3	0.9	0.3	12.5	0.8	0.3	80.0	37.4	11.8
July	2011-2016	18.2	1.0	0.4	6.1	0.5	0.2	12.2	0.6	0.3	55.3	16.2	6.6
August	1980-1990	18.7	0.7	0.3	7.3	0.5	0.2	13.0	0.5	0.2	81.3	29.8	12.2
August	1991-2000	18.4	1.1	0.4	6.6	0.9	0.3	12.5	1.0	0.3	45.4	20.0	6.3
August	2001-2010	18.7	1.0	0.3	6.9	0.9	0.3	12.8	0.8	0.3	69.6	20.8	6.6
August	2011-2016	19.2	1.5	0.6	6.9	1.1	0.4	13.1	1.2	0.5	74.7	48.1	19.6
September	1980-1990	20.2	0.6	0.2	8.4	0.5	0.2	14.3	0.5	0.2	61.5	26.5	10.8
September	1991-2000	21.1	1.7	0.5	8.4	0.7	0.2	14.7	1.2	0.4	37.8	29.3	9.3
September	2001-2010	21.3	1.4	0.4	8.5	0.9	0.3	14.9	1.0	0.3	39.4	20.3	6.4
September	2011-2016	21.5	1.2	0.5	8.0	0.7	0.3	14.7	0.9	0.4	32.4	15.5	6.3
October	1980-1990	22.9	1.3	0.5	10.0	1.3	0.5	16.4	1.2	0.5	30.1	22.4	9.2
October	1991-2000	23.7	1.9	0.6	10.5	1.0	0.3	17.1	1.3	0.4	30.3	27.2	8.6
October	2001-2010	24.6	0.1	0.1	10.6	0.9	0.3	17.6	0.4	0.1	31.5	19.9	6.3
October	2011-2016	24.5	1.7	0.7	10.8	0.5	0.2	17.6	1.1	0.4	30.5	18.7	7.6
November	1980-1990	26.9	1.7	0.7	12.9	1.7	0.7	19.9	1.7	0.7	14.7	14.4	5.9
November	1991-2000	25.6	1.6	0.5	12.1	0.8	0.2	18.8	1.1	0.4	23.6	19.3	6.1
November	2001-2010	26.9	1.1	0.3	12.6	1.2	0.4	19.8	0.9	0.3	36.2	26.0	8.2
November	2011-2016	26.5	1.0	0.4	12.1	0.8	0.3	19.3	0.7	0.3	32.7	21.3	8.7
December	1980-1990	27.6	1.3	0.5	14.0	0.6	0.3	20.8	1.0	0.4	23.3	19.4	7.9
December	1991-2000	28.5	1.4	0.5	14.8	1.4	0.4	21.7	1.4	0.4	24.8	18.5	5.9
December	2001-2010	28.7	0.9	0.3	14.3	1.1	0.3	21.5	0.9	0.3	19.6	13.9	4.4
December	2011-2016	29.3	1.4	0.6	15.2	1.0	0.4	22.3	1.1	0.4	15.2	7.8	3.2

Chapter 6

Research results

Evaluating the suitability of satellite land surface temperature data to supplement weather station temperature data for *Vitis vinifera* L.

CHAPTER 6: EVALUATING THE SUITABILITY OF SATELLITE LAND SURFACE TEMPERATURE DATA TO SUPPLEMENT WEATHER STATION TEMPERATURE DATA FOR *VITIS VINIFERA* L.

6.1 Introduction

Air temperature is commonly measured at 2 m above the ground using meteorological stations to describe the direct environment around the station. However, station distribution has limitations such as incurred by the complexity of topography especially in mountainous areas which limits the climatic accuracy describing the climate of larger areas. Interpolation of meteorological data can be used as one method to successfully estimate temperatures near meteorological stations, however, the station-based interpolation techniques suffer from arbitrary location of weather stations and often lack near real-time data accessibility (Neteler, 2010; Vancutsem *et al.*, 2010; Benali *et al.*, 2012). Climatic index maps are used for the assessment of climatic zones (limits) for species distribution in the world, as well as to serve as a basis for agricultural geography, *i.e.* in the evaluation of agricultural land suitability for viticulture worldwide (Jones *et al.*, 2005; Neteler, 2010; Benali *et al.*, 2012) as well as to characterise phenological stages (Wan *et al.*, 2004; Ganguly *et al.*, 2010; Anderson *et al.*, 2013; Thomas *et al.*, 2013; Zorer *et al.*, 2013; Broich *et al.*, 2015). Most of the indices are derived from air temperature, precipitation and solar radiation data collected from the nearest reliable weather station, calculated over a specific time interval (*i.e.* the growing season) for a specific crop, depending on the latitude (Hall & Jones, 2010; Zorer *et al.*, 2013).

One of the most important potential applications of the land surface temperature (LST) retrieved from satellite data is to validate and improve the global meteorological model prediction after appropriate aggregation and parameterization (Diak & Whipple, 1993; Wan *et al.*, 2004). Satellite remote sensing datasets are subject to large errors, sensor characteristics, atmospheric conditions, variations in spectral emissivity, surface type heterogeneity, soil moisture, visualization geometry, assumptions related to the split-window method and cloud cover areas not detected (Vogt *et al.*, 1997; Czajkowski *et al.*, 2000). If errors are left uncorrected, it reduces its utility in practical applications substantially. Earth surface emissivity is a necessity in LST retrieval, but can also be used to discriminate senescent vegetation (phenological stages) (Singh *et al.*, 2014; Broich *et al.*, 2015).

Validation with *in situ* measurements and data reconstruction allow complete time series for specific areas of interest to be obtained, which could require the automation of the data processing at a high-performance computing facility (Neteler, 2010; Zorer *et al.*, 2013). Although comparisons between Moderate-resolution Imaging Spectroradiometer (MODIS), satellite LST_T and *in situ* values from weather stations (WS_T) indicate an accuracy of 1 K in most cases, some cases with heavy aerosol loadings may result in larger errors. Higher errors may occur in some arid regions due to effects of heavy dust aerosols and greater uncertainties in classification based surface emissivities (Wan, 1999; Wan, 2014). The remote sensing based LST_T estimations are usually based on models that are designed to infer from sparse data, measured by WS_T, to estimate the temperature distribution over larger areas (Benali *et al.*, 2012; Zorer *et al.*, 2013). Many recent studies have found strong linear correlations between the MODIS, a polar-orbiting sensor which produces LST maps at global coverage and *in situ* meteorological station temperatures. MODIS LST_T (maximum, minimum and average land surface temperatures) and air temperatures (WS_T) have good correlations for several land cover types in Africa (Vancutsem *et al.*, 2010), Portugal (Benali *et al.*, 2012), on the Tibetan Plateau (Zhu *et al.*, 2013) and across the United States

(Crosson *et al.*, 2012). The typical range of errors when correlating LST_T to air temperature (WS_T) is approximately 2-3°C (Zakšek & Schroedter-Homscheidt, 2009) irrespective of the methodology, spatial or temporal resolutions (Williamson *et al.*, 2014). The level of precision generally accepted as 'accurate' for remote sensing based land surface temperature (LST_T) estimations is between 1 and 2°C (Vazquez *et al.*, 1997).

Climate in the Western Cape is dynamic due to the variation of topography, proximity to the ocean and the sea breeze effect. The current meteorological network is not a dependable source in terms of distribution and consistency of data accuracy due to factors such as financial constraints, vandalism of some stations, out-dated equipment, and lack of efficient monitoring of stations. Hence, there is a need for an alternative temperature resource to supplement current weather station networks. The application of traditional geospatial interpolation methods in complex terrain such as the Western Cape also remain challenging and difficult to optimise, and accuracy will be highly dependent on station network inputs (Neteler, 2010; Benali *et al.*, 2012). Intrinsically spatialised thermal remote sensing data, such as the MODIS LST product, can be used as an alternative, with reconstructed daily time series being potentially useful in many cases to substitute meteorological temperature observations. To assess the performance of the LST reconstruction, the final LST maps can be compared to instantaneous measurements of meteorological stations. It has been reported that for each station up to four daily observations can directly be compared to local solar time (Neteler, 2010; Zorer *et al.*, 2011).

The aim of this study was to validate LST_T for future use in the Western Cape based on three years of LST_T data collected in parallel to *in situ* weather station data using statistical approaches. The study objectives were to: (1) estimate air temperature (WS_T) using remote sensing LST from the MODIS satellite, (LST_T) over a set/limited temporal and spatial coverage, (2) provide temperature estimations with an accuracy which will support future applications, (3) explore factors and processes influencing the temperature estimation errors and (4) highlight the limitations and possible future developments of using LST in agriculture.

This study aims to establish what the possibilities are for the Western Cape in using the MODIS LST_T product, and what is required for future applications, *i.e.* the degree of inputs required and the amount of downscaling required for applications to be effective. The study trial period ranged over three years from 01/04/2012 to 30/04/2015 to test the LST_T product comparison with WS_T points, serving as a means to assess the need for secondary post processing for the supplementation of meteorological data in the Western Cape.

6.2 Materials and methods

6.2.1 Study region and meteorological data

Climate studies the Western Cape require higher temporal and spatial resolution and the integration of these two factors due to the complexity of the terrain and weather patterns dictated by the surrounding ocean. Weather station distribution is an important input for the creation of high resolution temperature maps. Station distribution is limited due to the complexity of the terrain in the Western Cape and other human resource related factors, emphasising the need for a supplementary climate (temperature) resource at a higher temporal and spatial resolution. The LST could be used as alternative resource supplement weather station (WS) temperatures.

Meteorological data was sourced from the Institute of Soil, Climate and Water (ARC-ISCW) of the Agricultural Research Council. Weather stations (points) and vineyard sites (polygons) were selected in extreme locations over a climatic band from a cooler to a warmer region within the

Western Cape (Table 13 in Addendum 6.1). Vineyards were selected from a larger study focusing on grapevine response to a changing environment; in close proximity to a weather station. Each vineyard had a temperature logger (Tinytag® model TGP-4500, Gemini Data Loggers, West Sussex, United Kingdom) housed in a radiation shield (Tinytag® model LS-1, Gemini Data Loggers, West Sussex, United Kingdom), for which the data will further be described as "LOG_T". Daily mean (T_m), maximum (T_x) and minimum (T_n) temperature measured by 16 meteorological stations (WS_T) and seven vineyard loggers were acquired for the period 01/04/2012 to 30/04/2015. The vineyards' spatial layout in the context of the MODIS LST pixel outline (1 km × 1 km) and proximity to the ocean, and the nearest weather stations are displayed in Figure 1.

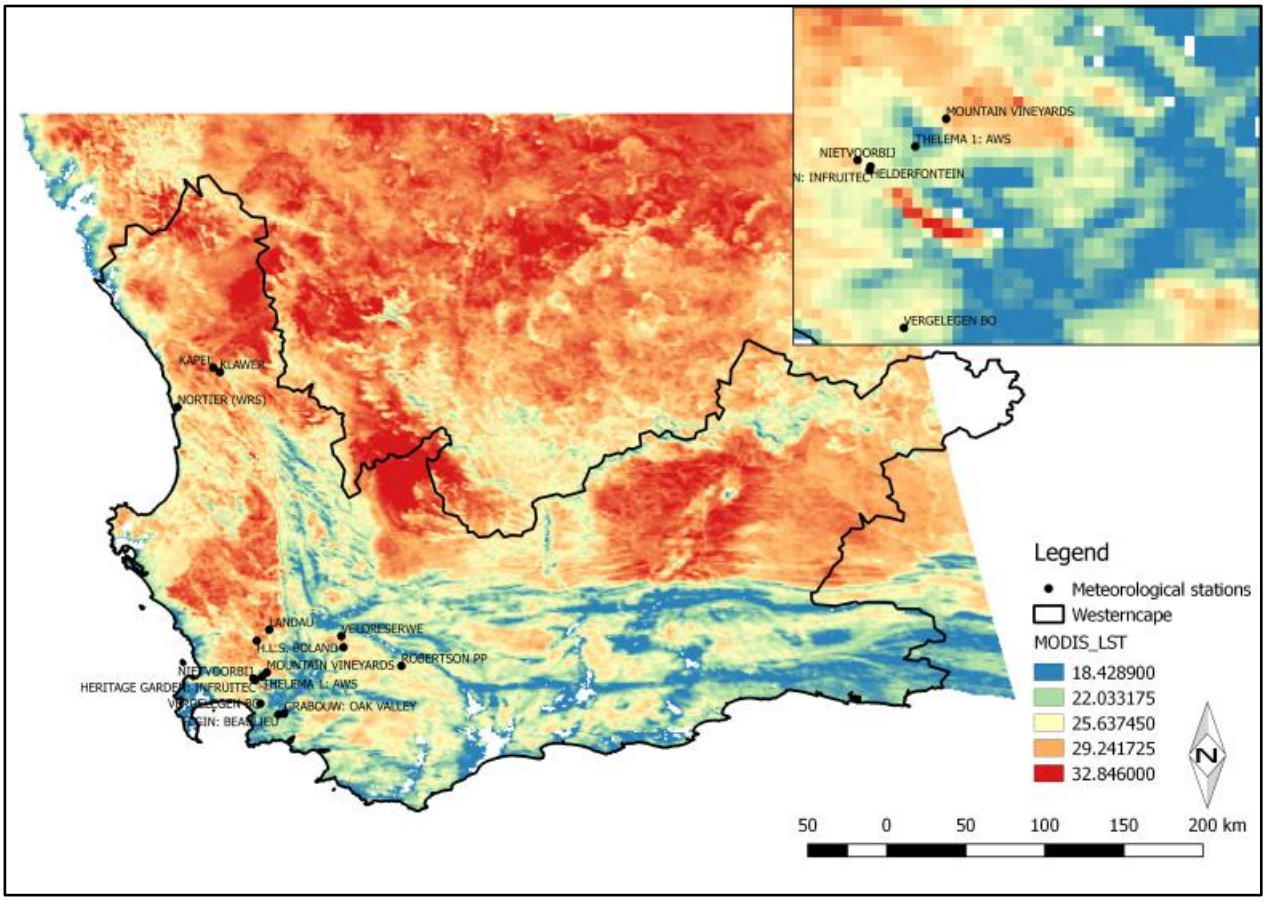

Figure 1 Western Cape extent, with the MODIS tile overlay categorised into growing season temperatures, showing distribution of weather stations selected for the study. In the top right corner is a zoomed in version highlighting the resolution of 1 km × 1 km MODIS pixels.

6.2.2 Land surface temperature

The LST product used in the study has previously been used to derive temperature (Mostovoy *et al.,* 2006; Vancutsem *et al.,* 2010; Benali *et al.*, 2012). The MODIS instrument is operational on both the Terra and Aqua spacecraft. The Terra instrument has been imaging since 03/2000, while Aqua has only been imaging from 08/2002. Both instruments have a viewing swath width of 2,330 km and view the entire surface of the Earth every one to two days. On-board detectors measure 36 spectral bands and acquire data at three spatial resolutions: 250 m, 500 m, and 1000 m. The LST is derived from two thermal infrared (TIR) band channels, 31 (10.78-11.28 µm) and 32 (11.77-12.27 µm). The atmospheric effects are corrected using a spilt window algorithm (Wan & Dozier, 1996) considering that the signal difference in the two TIR bands is caused by differential absorption of radiation in the atmosphere (Wan *et al.*, 2002). Due to the orbit of both satellites around the Earth, the average daily imaging time for the area of the Western Cape (Lat 33.9379, Long 18.856) for Terra (MOD) is around 10:51 am and 18:45 pm local time, and Aqua (MYD)

around 1:55 am and 14:40 pm. The processed data is usually published less than a week after acquisition on a National Aeronautics and Space Administration (NASA) File Transfer Protocol site (ftp://e4ft101.cr.usgs.gov/).

6.2.2.1 Land surface temperature data downloading

The gridded MODIS LST products were used, namely MOD11A1 V005 from the Terra satellite and MYD11A1 V005 from the Aqua satellite which are both provided in equal-area sinusoidal projection, with a 1000 m pixel size. Image data is provided in degrees Kelvin, and delivered in HDF data format from the NASA FTP website (https://lpdaac.usgs.gov/). Thereafter, the files are converted to Geotiff format using the MODIS re-projection tool (MRT) (Wan, 1999; Wan & Li, 2008).

In this study the process was automated in R statistics (further referred to as R) (R-Core-Team, 2014), for downloading and re-projection (sinusoidal to WGS84) of the four daily LST_T images in batches of years from 01/04/2012 to 30/04/2015. Input dates were transformed from day/month/year to day of year for downloads. The MODIS package in R allows tiles to be selected interactively. However, in this study they were selected manually, with the tile of interest being "h19v12" (**Figure 2**). The SDSstring was selected for the MOD (Terra) and MYD (Aqua) products, and automated downloads were stored in a set home directory linked to R.

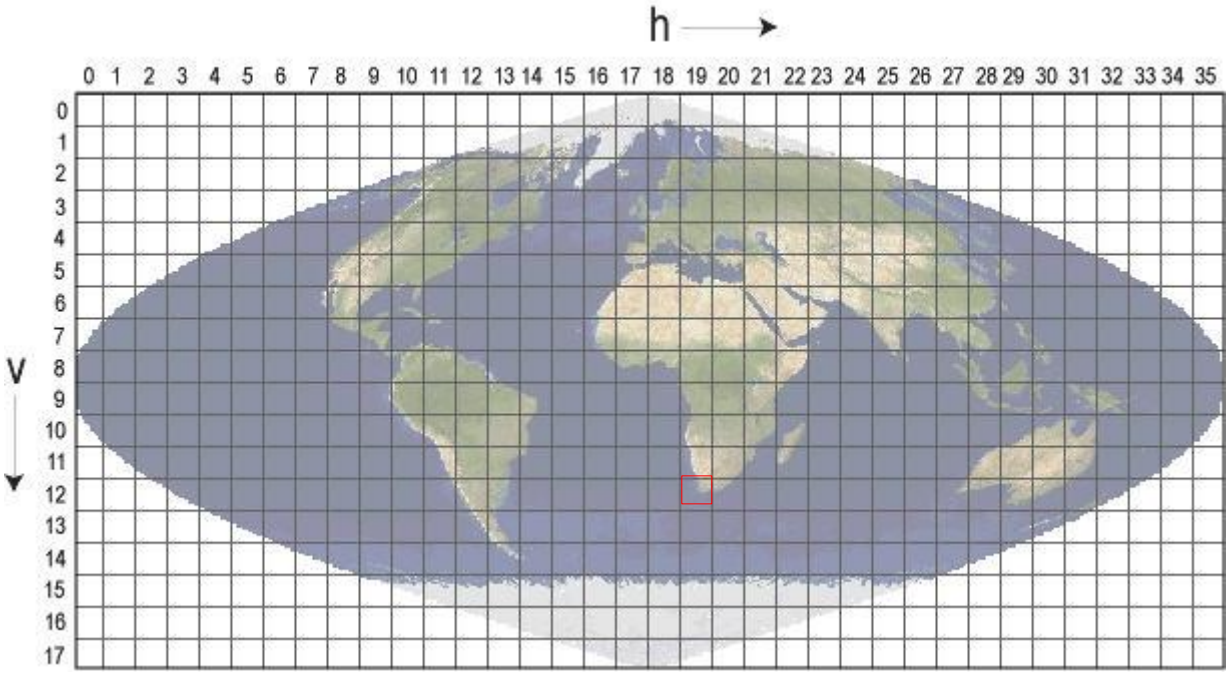

Figure 2 MODIS sinusoidal tile grid, where tile H19V12 is of interest and outlined in red (MODIS-Land-Team, 2015).

The next steps involved scaling of the TIFF files using the scaling factor provided (0.0001), as well as converting images from °K to °C Celsius. Each year of downloads were grouped in one session (3 sessions with four products each) and were processed and stacked separately. Stacking was performed using the RunGdal package (R-Core-Team, 2014), yielding four product types namely (D_MOD (year 1: 01/04/2012-31/03/2013) / D_MODD (year 2: 01/04/2013-31/03/2014) / D_MODDD (year 3: 01/04/2014-31/03/2015). Each year was stacked and processed separately to extract the temperatures from the MODIS LST layers in order to compare to the weather station data. Weather station and polygon locations (latitude, longitude) were loaded into R and it was used to extract values from the MODIS pre-stack created for the date range and for each MODIS product using the RunGdal package.

The extraction of terrain attributes (auxiliary data) was automated in R from an existing 30 m Shuttle Radar Topography Mission (SRTM) Digital elevation model (DEM) (SRTM, 2012), from which elevation, slope and aspect for the weather station points and vineyard polygons could be determined. Global radiation, hill shade and average sunlight hours were extracted from geoTIFFs created in ArcMap (ESRI, 2015) based on a 90 m SRTM DEM (SRTM, 2012). Distance from the ocean was calculated in R using a global self-consistent, hierarchical, high resolution geography database (GSHHS) of the coastline, sourced from https://www.ngdc.noaa.gov/mgg/shorelines/gshhs.html and described in Wessel and Smith (1996).

Extracted information from LST layers for weather station point and polygon area were further processed in Microsoft Excel 2013 (Microsoft Corporation, Redmond, Washington, USA) and statistical analysis was conducted using Statistica 10 ® software (Statsoft, Tulsa, UK). The LST_T extracted for each of the four layers were processed as extracted to test the accuracy of fit, comparing WS_T data to the LST_T layers (Table 1). The extracted T_m, T_x and T_n temperatures for each day for the three-year period from the LST_T images were compared to WS_T point data for the same period combining the extracted LST_T temperature at the weather station points with the WS_T data for the study period. Further analysis was done on a data set of only the temperature means (LST_{Tm}), calculated from the daily maximum (LST_{Tx}) and minimum layer (LST_{Tn}). Land surface temperature values were only included in the LST_{Tm} if both maximum and minimum values were present in the data for a specific day, and these LST_{Tm} values were then further correlated with weather station mean temperature (WS_{Tm}) and logger (LOG_{Tm}) data. The continuous datasets for LST, WS and LOG T_m were used for the calculation of bioclimatic indices and areas climatically described by the (Anderson *et al.*, 2012) classifications (Refer to Chapter 2 and 4 for more information on the indices). The comparison of climatic indices calculated from different data sources (LST_T, WS_T and LOG_T) could establish the more accurate (comparable) indices for future applications if LST_{Tm} was used to supplement WS_T.

For the creation of maps to be overlaid with other elements the file was re-projected to the required projection system in geographic information system (GIS) software and processed to the correct pixel resolution based on the MODIS layer source using the raster calculator function (Digital Number (image)* 0.02) – 273.15 = °C. A colour gradient was set in the GIS programme to show the variation in LST (Figure 1). This process was also automated and used in R statistics, and can be used to create larger time series to monitor seasonal changes and accumulated bioclimatic indices over the growing season.

Table 1 Temperature resources extracted and used in further analysis in the study, land surface temperature (LSTT), weather station temperature (WST) and logger temperature (LOGT) for maximum (T_x), minimum (T_n) and mean (T_m) temperatures.

Temperature sources for analysis	Temperature elements: Maximum (Tx), minimum (Tn) and mean (Tm)
Land surface temperature (LST_T)	**LST_{Tx}** (highest daily value of **10:51am** or **14:40pm**)/ **LST_{Tn}** (lowest daily value of **18:45pm** or **1:55am**)/ **LST_{Tm}** (average of highest and lowest value for the day ((LST_{Tx}+LST_{Tn})/2)/ **LST_{Tm_ALL}** (average of all four images for the day 01:55, 10:51, 14:40 and 18:45 local time)
Weather station temperature (WS_T)	**WS_{Tx}** (daily Tx)/ **WS_{Tn}** (daily Tn)/ **WS_{Tm}** (Daily T_m calculated from ((Tx+Tn)/2))
Logger temperature (LOG_T)	**LOG_{Tx}** (daily Tx)/ **LOG_{Tn}** (daily Tn)/ **LOG_{Tm}** (daily T_m calculated form ((Tx+Tn)/2))

6.2.3 Auxiliary data

Auxiliary variables which have a known direct or indirect impact on environmental temperature and/or on the relation between that temperature and LST were considered, namely elevation (Jarvis *et al.*, 2008) and distance to the coast (based on the GSHHS coastline) (Wessel & Smith, 1996). Temperature increases with an increase in altitude and temperatures also tend to be cooler near the coast due to the sea breeze effect (Myburgh, 2005; Bonnardot & Cautenet, 2009). Other auxiliary data to be used in future analysis, but which were considered in the interpretation of results were factors such as wind velocity, day length, solar radiation and vegetation. These factors influence the energy balance of the land atmosphere system. There is the large variation in the physical properties of soil and water regarding its heat, transparency and density properties (Benali *et al.*, 2012). Proximity to water bodies, which take longer to heat up and retain heat longer than soil, and water bodies also increase the moisture in the air. Water bodies therefore moderate surrounding air temperatures, resulting in smaller measured amplitudes. All the above mentioned factors influence the LST interpretation; hence the need for a high density spatial distribution of weather stations to account for auxiliary variables. The effects of distance from the ocean and altitude were evaluated due to the complexity of the terrain in the Western Cape.

6.2.4 Model selection for supplementing WS_T using LST_T

Model design and assessment were based on a statistical approach, relating the $LST_{Tm/Tx/Tn}$ with $WS_{Tm/Tx/Tn}$ data, and evaluating the correlations and the effect of auxiliary data (altitude and distance from the ocean) on the correlation. The LST_T data used in the models included the daily average of all four layers as LST_{TmAll}, the maximum layer as LST_{Tx}, the minimum layer as LST_{Tn} and the mean as LST_{Tm} computed from the sum of the LST_{Tx} and LST_{Tn} layers divided by 2. The LST_{Tm} was only used if both layers were present for the day as described in Table 1. A preliminary comparison of data was done before further processing to compare the relationship of LTS_T products and WS_T data for one year of data from 01/04/2012-31/03/2013. As the distribution was comparable, two more years of data was downloaded to create a three year dataset for analysis (01/04/2012-31/03/2015). More detailed analysis was done per station and site over the three seasons for all the temperature elements including the bioclimatic indices to study the performance of using LST_T products for supplementing WS_T in viticulture. For further analysis, only the three year (01/04/2012 to 30/04/2015) dataset was used to include more variability in the comparison of LST_T and WS_T. Seasons will not be analysed separately, as seasons by nature are variable and unpredictable, hence adding to the variability and robustness in the model selection, allowing the comparison of LST_T and WST over a larger dataset, which could improve accuracy of the model for future applications.

6.2.4.1 Performance statistics

Descriptive statistics were used to compare continuous daily LST_T to WS_T data, per station and sites and then over all stations and sites. Intra-class correlation coefficients (ICC) are descriptive statistics that can be used when quantitative measurements are made on units that are organised into groups. The relative and absolute biases were calculated when each pair of data was compared individually. The ICC was run on all the stations over the three seasons to describe how strongly units in the same group resembled each other. The ICC agreement includes bias while the ICC consistency excludes bias. If the latter is close to 1, it can affect the ICC (agreement). When the ICC consistency and agreement were both acceptable the Pearson coefficient of correlation (r) was used to describe the relationships between LST_T and WS_T, and the square root of the Pearson coefficient (R^2) explained the variance in the dataset comparisons. The significance of the

correlations was shown as *p,* which was always calculated for a significance level of 5% as a measure of correlation and proportion of observed variability accounted by the model. In addition, the standard error of measure (SEM) was calculated from the ICC, the average error incurred using the LST_T to predict or supplement WS_T. The higher the ICC (agreement and consistency over the dataset) the lower the standard error mean (SEM) values are.

6.2.4.2 Model fitting

In statistical modelling, regression analysis is a statistical process used for estimating relationships among variables. A regression analysis was done for the three year dataset to ascertain what the relationship was between LST_T and WS_T over all three seasons as well as separate seasons. Correlations varied over seasons, hence the longer study period allowed for a more robust calibration between LST_T and WS_T, as seasonal variability was included. The LST_T and WS_T data for T_m, T_x, T_n and GDD were divided into calibration and validation datasets using a 70% and 30% proportions of the datasets, respectively, and each one was defined by randomly resampling the entire observation set several times. The model optimisation was based on the larger dataset of three years, with the calibration (analysis sample) and prediction (validation sample) independently evaluated within the study period of three years, calculating for both a set of performance statistics. This therefore resulted in a calibration set and validation set within the three year period. Each resampling was applied to the LST_T calibration and validation sets independently, which is a method that has already been widely used to test the accuracy of predictive models. The resampling procedures were done regardless of the temporal and spatial components by placing all the observations into global datasets, regardless of measurement data or station location. This procedure was also applied per station and over all stations and sites. For the ICC, the seasons where not separated as the variability of seasons was used for the robustness of the final model. As seasons are variable in nature and cannot be controlled, so a better result would be ascertained across seasons, a larger dataset for better accuracy.

A set of statistical measurements were calculated to evaluate the model adjustments needed to use LST_T to supplement WS_T. The root mean square error (RMSE) is particularly sensitive to outliers and was used as a measure of quadratic error on an individual level, per station and per temperature element as done in other studies evaluating LST (Janssen & Heuberger, 1995; Benali *et al.*, 2012). The RMSE error estimates are given as the unvalidated calibration residuals, called the root mean square error of calibrations (RMSEC) and for the estimated prediction residuals called root mean square error of prediction (RMSEP). The RMSEC represents the calibration error, i.e. the residuals of the calibration data, which measures goodness of fit between the data in the calibration model. The RMSEP results are of interest, as it represents the prediction error to expect in the future, measuring the performance of LST_T to predict/supplement WS_T. The root mean square errors of calibration (RMSEC) and the root mean square errors of prediction (RMSEP) are particularly sensitive to outliers and were used as a measure of quadratic error on an individual level for the temperature elements.

6.2.4.3 Error and uncertainty analysis

Cross validation checks a model by repeatedly sampling out different sub sample sets of calibration sample from the model estimation, using them to test the predictability of the model. Auxiliary data were used in parameter estimations over all stations to test the impact of factors such as distance from the ocean and elevation on the predictability of the model. The comparisons were made at WS_T scale considering all the pairs of observations and predictions for all stations. The assessment of model uncertainty was considered important due to the known and expected

biased distribution of WS according to elevation and distance to the coast, driven by the complexity in topography (Benali *et al.*, 2012).

6.2.5 Statistical software

Open source statistical software R Statistics (R-Core-Team, 2014) was used to download MODIS LST layers as well as extract information from the layers. Statistical analysis was conducted using Statistica 10 ® software (Statsoft, Tulsa, UK) for the calibration/validation analysis. The intra-class correlation analysis was done in R using the "irr" package.

6.3 Results & discussion

6.3.1 Land surface temperature product selection

The LST_T and WS_T (N=16) data showed a good correlation of $R^2 \geq 0.67$ and $R^2 \geq 0.71$ for all the LST_T products for one season's data and three season's data, respectively (Figure 3 and Table 2). The LST_T products acquired from Aqua and Terra show similar correlations with only a very slight slope offset, suggesting the datasets can be used to supplement weather stations in either of the products. However, more detail comparisons showed that the LST_{Tx} temperatures (D_MOD/MYD) overestimated WS_{Tx} temperatures, with a slope of 1.5 despite the good correlations ($R^2 \geq 0.68$). A slope of 1.5 means higher temperatures are overestimated, but there also seems to be an offset in the lower temperatures. The LST_{Tn} night temperature products (N_MOD/N_MYD) seemed to be underestimating the temperature when compared to the $WS_{Tn,}$ with a slope of about 0.8 within the good correlations ($R^2 \geq 0.67$). The LST_T values compared to WS_T data within a pixel showed the LST_{Tm} to have a slightly higher correlation ($R^2 = 0.76$) with the WS_{Tm} compared to the LST_{TmAll} (data not shown), therefore LST_{TmAll} will not be included in further discussion. Taking aforementioned into account, only the LST_{Tm} will be considered for future use in supplementing WS_T.

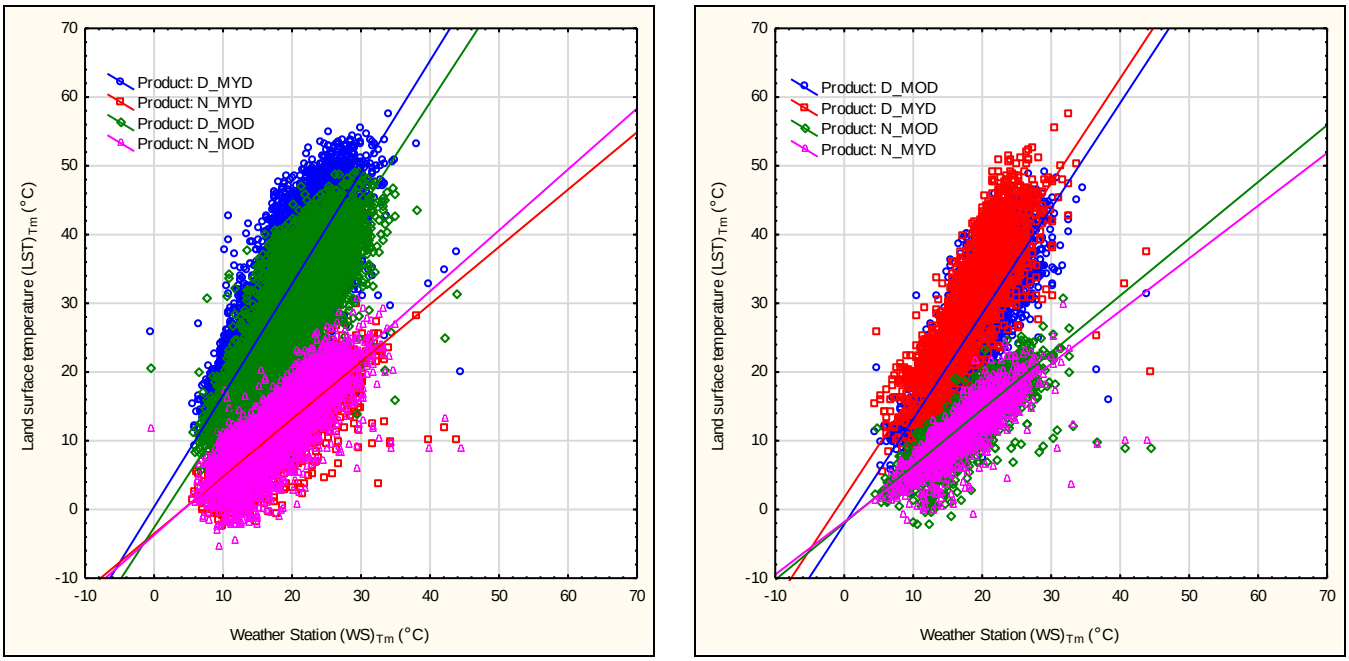

Figure 3 Correlation of land surface temperature (LSTT) against weather station temperature (WST), categorised by the LST products at four times during the day for the period 01/04/2014 to 30/04/2015 (left) and 01/04/2012 to 30/04/2015 (right).

Table 2 Relationship between the four land surface temperature (LST_T) products and the weather station (WS_T) average daily temperatures at comparable acquisition times for one year (01/04/2014 to 30/04/2015) and for three years' data (01/04/2012 to 30/04/2015).

Product (acquisition time)	One year (01/04/2014-30/04/2015)				Three years (01/04/2012-30/04/2015)			
	r	***p***	***R^2***	**Regression equation**	***r***	***p***	***R^2***	**Regression equation**
D_MYD (14:40pm)	0.83	0.00	**0.69**	D_MOD= -2.18+1.53*x	0.84	0.00	**0.71**	D_MYD= 0.35+1.62*x
N_MYD (01:55am)	0.82	0.00	**0.68**	D_MYD= 1.72+1.53*x	0.85	0.00	**0.73**	N_MYD= -3.53+0.83*x
D_MOD (10:51am)	0.84	0.00	**0.71**	N_MOD= -1.97+0.83*x	0.85	0.00	**0.73**	D_MOD= -2.66+1.55*x
N_MOD (18:45pm)	0.82	0.00	**0.67**	N_MYD= -1.80+0.77*x	0.85	0.00	**0.73**	N_MOD= -3.73+0.89*x

6.3.2 Daily land surface temperatures and weather station comparison

The ICC agreement and ICC consistency for T_m, T_n and T_x,was ≥ 0.711 and ≥ 0.770, , ≥ 0.546 and ≥ 0.624 for and ≥ 0.456 and ≥ 0.624, respectively. Overall, there was a better correlation for LST_{Tm} and WS_{Tm} (Table 2). The LST_{Tx} and WS_{Tx} comparison had the lowest ICC of agreement and hence showed a larger SEM. This could be ascribed to how the temperature is acquired from LST and WS. However, over all there was consistency in the temperature datasets for the different elements, but the agreement between the two resources was not always high resulting in higher errors of measure. The weather station points and areas of comparison influenced the ICC, *e.g.* the Kapel/Klawer station had the lowest ICC's, and Elgin the highest ICC's for T_m and T_x, whereas for T_n Kapel again had the lowest and Landau the highest ICC for. The standard error mean (SEM) for all the stations (N=15) for all the temperature elements ranged from 0.8-2.8°C for T_m, 1.7-2.6°C for T_n and 2.5-4.9°C for T_x with the R^2 value for all the elements over all the stations being larger than 0.50 (Table 2). Overall, the Nortier weather station was isolated as an outlier station throughout the analysis. Although this station was left in the analysis as it added to the robustness of the correlations when combining all stations, it will be excluded in this section of the discussion. This analysis highlights the variability in the analysis dataset over the extreme weather station locations included. Addendum 6.3 represents the correlations for each station, and all the temperature elements from the LST_T and WS_T dataset. The inter-class correlations for all temperature elements, namely T_x and T_n are shown in Table 16 and T_m in Table 17 and the Winkler index (GDD) in Table 18 and Table 19 (in Addendum 6.2). The bioclimatic indices calculated for the three growing seasons (1 September to 31 March) from the LST_T and WS_T sources are described in Table 14 (in Addendum 6.1) to isolate the best correlations for the selection of indices for future use to describe growing seasons.

Table 3 Significant ($p < 0.001$) correlations for continuous daily land surface temperature (LST) and weather station (WS) temperature elements. Mean (T_m), maximum (T_x) and minimum (T_n) temperatures and the seasonal summation as growing degree days (GDD) calculated using the Winkler Index are shown.

Element	T_m		T_x		T_n		GDD	
Weather station name	R^2	**SEM**	R^2	**SEM**	R^2	**SEM**	R^2	**SEM**
AAN-DE-DOORNS WYNKELDER	0.85	2.059	0.81	3.206	0.56	2.538	0.59	2.635
ELGIN: BEAULIEU	0.86	1.559	0.77	2.499	0.61	2.020	0.52	2.265
GRABOUW: OAK VALLEY	0.83	1.838	0.77	2.859	0.69	1.679	0.56	2.255
H.L.S. BOLAND	0.85	2.399	0.79	3.980	0.71	1.971	0.62	2.985
HELDERFONTEIN	0.86	1.914	0.76	3.131	0.61	2.302	0.61	2.585
HERITAGE GARDEN: INFRUITEC	0.77	2.274	0.66	3.717	0.56	2.494	0.55	2.914
KAPEL	0.76	2.275	0.66	3.686	0.49	2.597	0.53	2.985
KLAWER	0.66	2.843	0.45	4.914	0.62	2.260	0.48	3.346
LANDAU	0.76	2.202	0.59	3.862	0.71	1.996	0.56	2.775
MOUNTAIN VINEYARDS	0.71	2.499	0.53	4.016	0.71	2.089	0.48	2.975
NIETVOORBIJ	0.74	2.438	0.56	4.169	0.56	2.45	0.52	2.980
NORTIER (WRS)	0.27	3.628	0.15	5.856	0.38	2.335	0.22	3.484
ROBERTSON PP	0.86	2.037	0.79	3.652	0.58	2.404	0.5	2.821
THELEMA 1: AWS	0.67	0.807	0.62	3.264	0.56	2.331	0.37	2.919
VELDRESERWE	0.85	2.425	0.79	3.936	0.66	2.087	0.61	2.983
VERGELEGEN BO	0.79	1.957	0.76	2.861	0.69	1.878	0.61	2.438

Overall, the regression analysis for each station and each element over the three year data range (Table 16 and 37 in Addendum 6.2) showed LST_{Tm} and WS_{Tm} to have the best correlation coefficients for the ICC, with a lower SEM in using LST_T to predict WS_T (Table 3 and Table 4). Mean temperature (T_m) had the better correlation coefficients of $R^2 \geq 0.80$ for LST_{Tm} and WS_{Tm} compared T_x and T_n for all the weather stations in the dataset, except Nortier that showed an $R^2 = 0.50$. The LST_{Tm} can predict the WS_{Tm} with an error ranging from 0.8-2.8°C, depending on the station (Table 4). Calibration and prediction analysis confirmed T_m to be a good fit with $R^2 \geq 0.60$-0.80 range with most of the stations (N=16) having a $R^2 \geq 0.80$ fit for the calibration and the prediction analysis. The RMSE ranged from 1.5 to 2.8°C and 1.8 to 3.4°C for the calibration and prediction analysis, respectively. The prediction error was larger due to fewer samples in the validation sample, as only 30% of the continuous daily data were used. The RMSEC is relatively small and comparable to other studies (Benali *et al.*, 2012; Zorer *et al.*, 2013), making it possible to use LST_{Tm} to successfully supplement WS_{Tm} applying the regression equation to pixels, also where there are no weather stations.

In the larger dataset, which is averaged over all stations and seasons, the T_m also had good correlation ($R^2 = 0.75$) for the analysis and validation dataset, with the lowest RMSEC (2.8°C) compared to other elements and an error of prediction of 4°C (Table 5).

Overall there seemed to be a larger variation in the LST_T dataset compared to the WS_T dataset. It was evident that LST_T consistently underestimated lower temperatures and overestimated higher temperatures. This is probably due to the nature of what LST_T measures, as it does not measure air temperature only but the surface temperature of soil/land which could be cooler when ambient temperatures are lower and hotter when ambient temperatures are higher. The temperature ranges of LST_T are therefore larger than that of the LOG_T and WS_T. These differences are more pronounced in the accumulation of indices over time, where smaller errors can be accumulated over time. For future analyses, a larger calibration data set should be used for the creation of an even more robust regression equation for the use of LST_T to supplement WS_T with the highest accuracy possible.

Table 4 Intra-class correlations (ICC) and regression comparing land surface temperature (LST) and weather station (WS) calibration and validation datasets, for daily mean temperatures (Tm) for all stations. The sample errors of measure (SEM) for all stations and the mean sample errors (MSE) for the calibration and prediction samples are also shown.

Weather station name	All data correlation for T_m			Calibration (70% of the data) sample			Prediction (30%of the data)		
	R^2	*p*	SEM	R^2	MSE	RMSEC	R^2	MSE	RMSEP
AAN-DE-DOORNS WYNKELDER	0.85	0.00	**2.059**	0.84	4.758	**2.181**	0.83	11.757	**3.429**
ELGIN: BEAULIEU	0.86	0.00	**1.559**	0.84	2.545	**1.595**	0.84	3.294	**1.815**
GRABOUW: OAK VALLEY	0.83	0.00	**1.838**	0.86	2.343	**1.531**	0.81	4.312	**2.077**
H.L.S. BOLAND	0.85	0.00	**2.399**	0.84	3.807	**1.951**	0.84	5.527	**2.351**
HELDERFONTEIN	0.86	0.00	**1.914**	0.82	3.375	**1.837**	0.86	4.021	**2.005**
HERITAGE GARDEN: INFRUITEC	0.77	0.00	**2.274**	0.81	3.123	**1.767**	0.75	7.934	**2.817**
KAPEL	0.76	0.00	**2.275**	0.75	4.254	**2.063**	0.81	9.821	**3.134**
KLAWER	0.66	0.00	**2.843**	0.6	8.923	**2.987**	0.66	9.465	**3.076**
LANDAU	0.76	0.00	**2.202**	0.75	5.620	**2.371**	0.61	8.723	**2.953**
MOUNTAIN VINEYARDS	0.71	0.00	**2.499**	0.61	7.801	**2.793**	0.61	7.167	**2.677**
NIETVOORBIJ	0.74	0.00	**2.438**	0.72	5.145	**2.268**	0.74	7.538	**2.745**
NORTIER (WRS)	0.27	0.00	**3.628**	0.32	9.794	**3.129**	0.23	14.952	**3.867**
ROBERTSON PP	0.86	0.00	**2.037**	0.85	3.041	**1.744**	0.86	4.626	**2.151**
THELEMA 1: AWS	0.67	0.00	**0.807**	0.7	6.908	**2.628**	0.66	9.872	**3.142**
VELDRESERWE	0.85	0.00	**2.425**	0.85	2.959	**1.720**	0.84	6.406	**2.531**
VERGELEGEN BO	0.79	0.00	**1.957**	0.85	2.392	**1.547**	0.78	6.050	**2.460**

Table 5 Intra-class correlations (ICC) and regression comparing land surface temperature (LST) and weather station (WS) calibration and validation datasets, for daily mean temperatures for all stations. The sample errors of measure (SEM) for all stations and the mean sample errors (MSE) for the calibration and prediction samples are also shown

Weather Station #	Element	Analysis sample (based on 70% of data)			Validation sample (based on 30% of the data)		
		R^2	MSE	RMSEC	R^2	MSE	RMSEP
All Stations	Tm	0.75	7.718	2.778	0.75	17.321	4.162
All Stations	Tx	0.62	20.011	4.481	0.62	55.273	7.435
All Stations	Tn	0.61	8.687	2.947	0.54	12.105	3.479
All Stations	GDD	0.38	20.106	4.484	0.61	15.861	3.983

6.3.2.1 Station level performance

The outlier stations and some examples of using LST_{Tm} to supplement WS_{Tm} will be discussed here in more detail. The individual station analysis proved to have a good ICC agreement and consistency over all the stations with good correlation coefficients (as discussed above), with the exception of the Nortier station near the coast and some stations in warmer areas such as Kapel and Klawer seemed to have lower ICC and R^2 (Table 16 and Table 17 in Addendum 6.2). With there being larger variability in temperature extremes, and temperature fluctuations within a diurnal cycle at sites selected over the climatic band as described in Chapter 4, this is not captured at the four imaging acquisitions of the LST during the day and night.

Nortier is the outlier station in the continuous daily data comparison of LST_T to WS_T data for the three year period, with a generally low correlation for T_m, T_x, T_n and GDD (Figure 4). With the lowest ICC for the T_x of agreement and consistency as 0.236 and 0.346, respectively (Addendum 6.3), whereas T_n had a much better ICC of 0.606 and 0.617. The higher ICC for T_n could be ascribed to the night temperatures being moderated by the ocean and the lower ICC for T_x due to possible cloud cover being more prominent along the coast or the sea breeze effect cooling the ambient air. The LST_{Tn} underestimated the minimum temperatures, more observations at cooler temperature compared to the WS_{Tn}, measuring more observations above 20°C (Figure 4). This outlier station of Nortier was kept in the dataset and not discarded, contributing to the robustness of the calibration model for LST_T predicting WS_T.

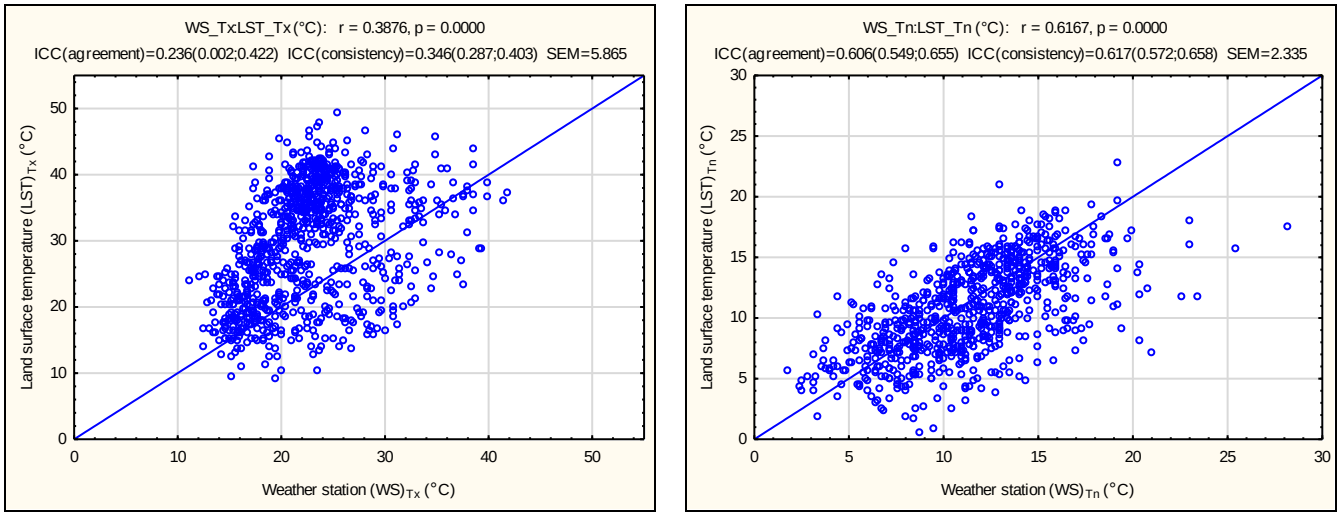

Figure 4 Nortier station correlation of maximum (T_x) (left) and miminim (T_n) (right) temperatures for land surface temperature (LST_T) compared to weather station (WS_T) for three seasons.

It is expected that the LST_T range would be larger than that of the WS_T, as it refers to land surface temperature which will be higher than ambient temperature. The LST_T daytime temperatures could reach >50°C. Hence, the goal of calibration was to compensate for this difference between the LST_T and WS_T data, so as to have an accurate resource to supplement WS_T. The need and future application of LST_T to supplement WS_T is seen in the calculation of the Winkler index (GDD) as described in Table 14 (in Addendum 6.2), and more specifically, the Landau station seasonal accumulation is shown in Figure 5. This highlights the missing WS_T data for season 3, which mean there will be no seasonal description available at the end of that season. The calibrated LST_T could more accurately supplement the missing data and still describe the growing seasons at the Landau station, possibly more accurately than using a nearby weather station.

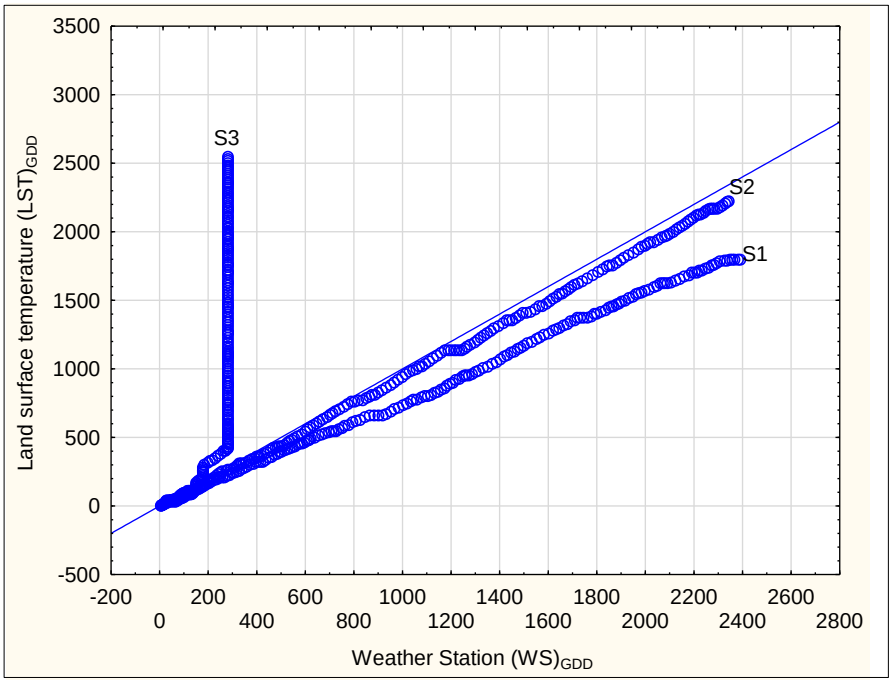

Figure 5 Accumulated growing degree days (GDD) calculated using the Winkler index at Landau weather station comparing three seasons of land surface temperature (LST) and weather station (WS) data. Regression results, r = 0.58, p = 0.00, R^2 = 0.34, ICC(agreement) = 0.56, ICC(consistency) = 0.585, SEM = 459.592. (LST_{GDD}:WS_{GDD} for S1:1796:2390, S2: 2222:2343 and S3: 2547:2800).

Comparing LST_T and a nearby weather station to supplement missing data for the Nietvoorbij station is shown in Figure 6. The Nietvoorbij station stopped logging after the first season; hence the nearby station at Helderfontein was used to supplement the missing data for the last two seasons. From the three seasons described using the Winkler index (Figure 6, left) and Huglin index (Figure 6, right) accumulated over time, the variability in the seasonal analysis can be noticed, with the LST_{GDD} slightly over estimating the second and third seasons and the LST_{GDD} under estimating the first season, which could be ascribed to the weather station source changing. The first season's LST_{GDD} (1722.53) underestimated WS_{GDD} (2179.18). The second and third season showed more comparable LST_{GDD} values (S2=2219 and S3=2507) compared to the WS_{GDD} values (S2=2088 and S3=2315). The seasonal variation in LST_{GDD} is more prominent when GDD is calculated using the Huglin index compared to the Winkler index as seen in Figure 6, and this could be explained by the higher LST_{Tx} values compared to LST_{Tm}.

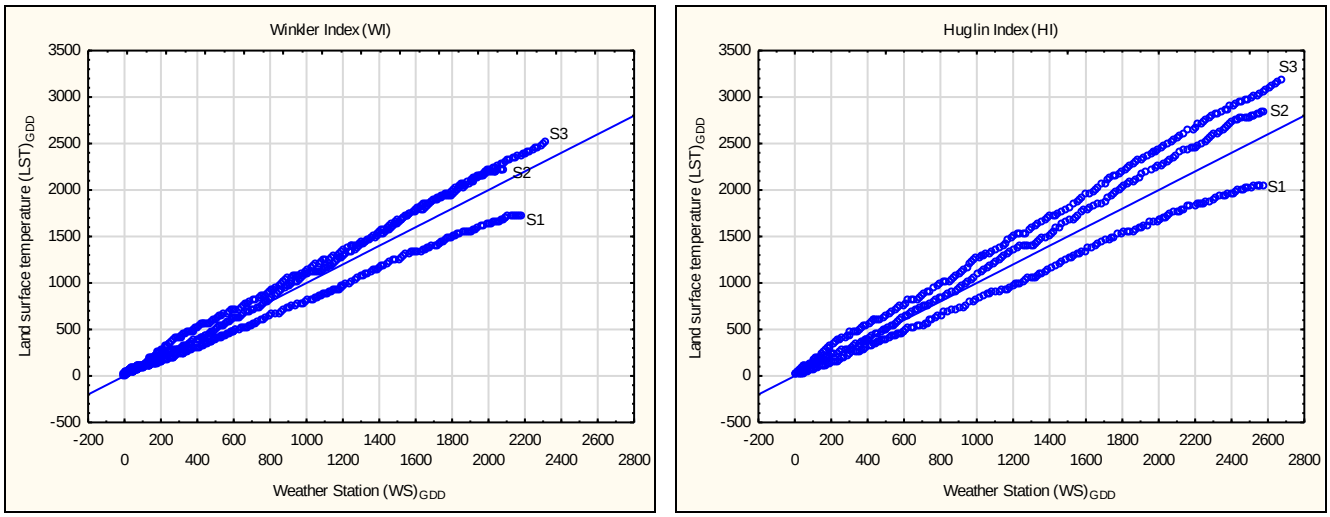

Figure 6 Accumulated growing degree days (GDD) calculated using the Winkler index (left) and Huglin index (right) for Nietvoorbij weather station comparing three seasons of land surface temperature (LST) and weather station (WS) data. Regression results, for Winkler index as r = 0.98, p = 0.00, R^2 = 0.96, ICC (agreement) = 0.975, ICC(consistency) = 0.975, SEM = 110.862 and Huglin index as r = 0.96, p = 0.00, R^2 = 0.92, ICC(agreement) = 0.955, ICC(consistency) = 0.957, SEM = 172.686.

Overall there was seasonal variation similarity over stations: LST_{Tm} underestimated the WS_{Tm} for season one, season two was comparable and in season three, LST_{Tm} overestimated WS_{Tm}. These inconsistencies could be ascribed to many factors such as environmental, image acquisition time *etc.*. The LST_{Tm} could be over estimating the WS_T in season three, as the season was hotter in the summer months compared to the previous seasons (see Chapter 5). This could result in a higher LST_{Tm} and a lower WS_{Tm} due to the ambient temperature being cooled by the sea breeze and afternoon winds. The LST_{Tm} could be used to compliment and supplement WS networks in the future to more accurately describe the growing season in the context of climate change.

6.3.2.2 Vineyard loggers, weather station and land surface temperature correlation

Correlation analysis for LST_T extracted from the vineyard polygons (further referred to as LST_POL_T) showed very weak correlations, with the temperature loggers referred to as LOG_T and WS_T, respectively. LST_POL_{Tx} overestimated the WS_{Tx}, with temperatures ranging up to 40°C and 50°C for LOG_{Tx} and LST_POL_{Tx}, respectively. This was probably due to the representation of the pixel, and land cover having higher temperature due to plant physiological functioning as the

polygon is a vineyard. The LST_POL_{Tx} temperatures were mostly concentrated in the upper temperature ranges of 35-50°C (Figure 7), comparable for all vineyards in the study. The LST_POL_{Tx} had low ICC agreement and consistencies (Table 6), with SEM greater than 5°C for LOG_{Tx} and WS_{Tx}. The WS_{Tx} range was similar to the LOG_{Tx} range but shifted more to the higher temperatures, with a 10°C warmer range and the WS_{Tx} having a 5°C cooler range, yet WS_{Tx} and LOG_{Tx} had a high correlation of a close 1:1 fit (data not shown).

With regard to the correlation analysis for Tn, extracted LST_POL_{Tn} from vineyard polygon area with temperature LOG_{Tn} and WS_{Tn} showed low to good correlations of R^2 = 0.34 and R^2 = 0.64, respectively (Figure 8). The LST_POL_{Tn} underestimated the LOG_{Tn}, with the latter having values ranging from 20-35°C. These high values for T_n could probably be explained by the vineyard canopy influencing the cooling of the air, with open surfaces losing heat faster. Hence, WS_{Tn}, having a better correlation and similar data distribution and ranges, resulted in a better SEM compared to LOG_{Tn} (Table 6). Table 6 describes the correlation coefficients, *p* values, ICC's and SEM over all the sites for the LST_POL_{Tx}, LOG_{Tx} and WS_{Tx} for all the temperature elements. The SEM was larger in the LST_POL to LOG correlation than in the WS. The over estimation of the LST_POL could be ascribed to the pixel (1 km × 1 km) being much larger than the typical vineyard polygon, therefore taking into account other LST_T factors in the polygon areas, which is the situation for the area surrounding the WS. The WS is also generally placed in an open area to measure the environment correctly. In this case with the logger in the vineyard; the temperature was also affected by the plant's direct environment. The T_m from either of the different sources, *i.e.* LST, WS or LOG, is the best temperature element to use in the future to supplement the WS network as described in Table 6 (more detail of temperature elements explained in Addendum 6.2).

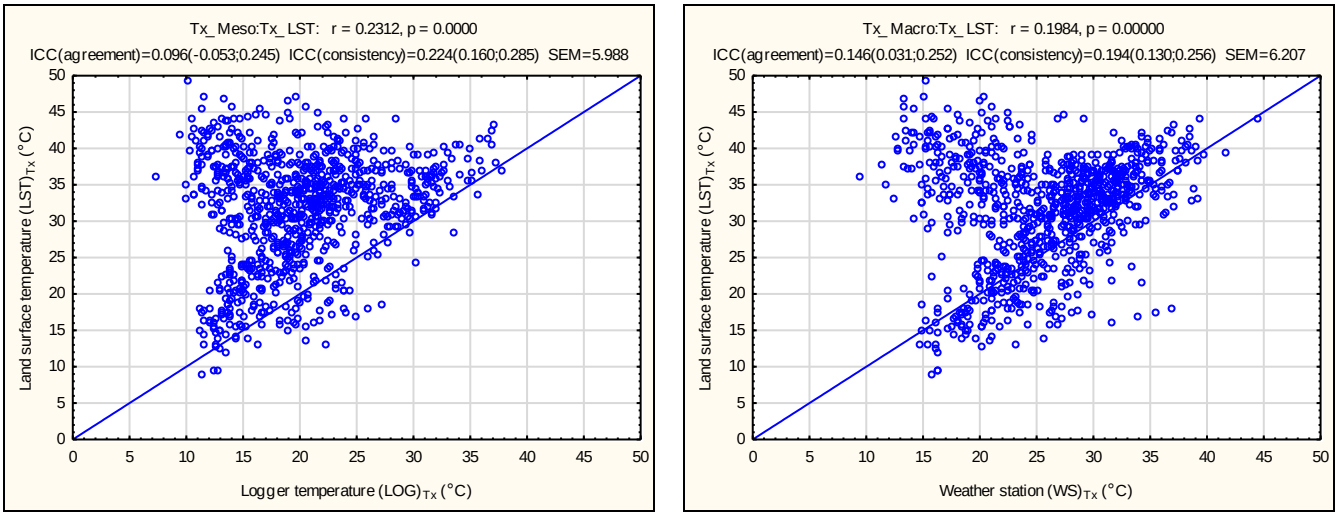

Figure 7 Intra-class correlations of the land surface temperature extracted for the polygon for the site (LST_POL) with the logger temperature (LOG_T) (left) and weather station (WST) (right) maximum temperatures (T_x).

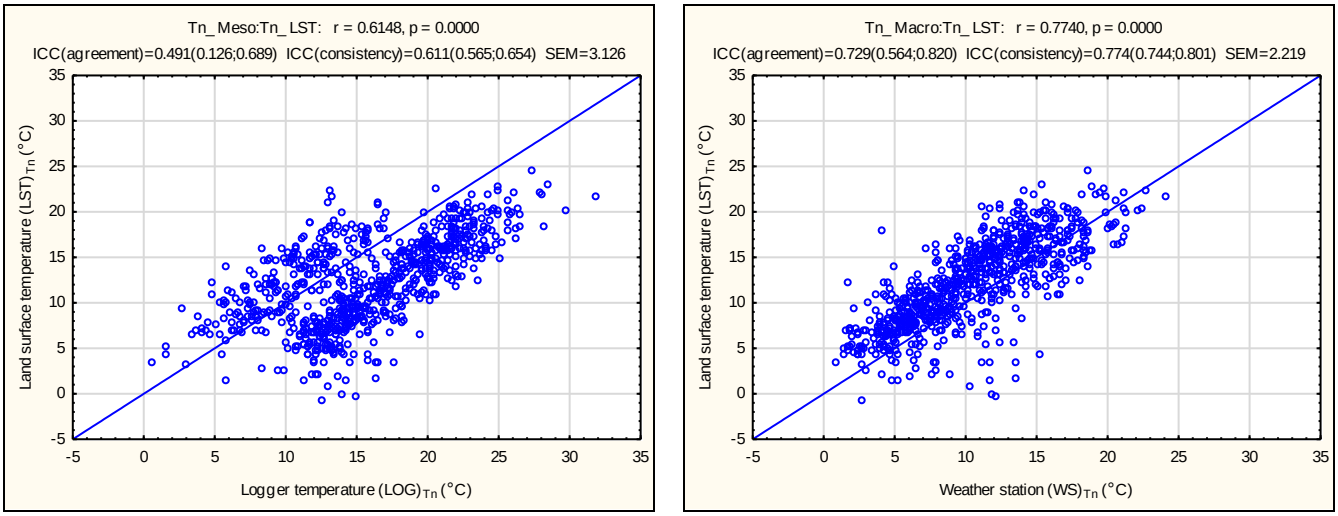

Figure 8 Intra-class correlations of the land surface temperature extracted for the polygon for the site (LST_POL) with the logger temperature (LOG_T) (left) and weather station (WS_T) (right) minimum temperatures (T_n).

Table 6 Intra-class correlations (ICC) of the relationships between the logger (LOG) and extracted land surface temperature for vineyard polygons (LST_POL).

Site	Element	Logger temperature $(LOG)_T$-all data correlation					Weather station temperature $(WS)_T$-all data correlation				
		R^2	*p*	ICC (agree)	ICC (consistency)	SEM	R^2	*p*	ICC (agree)	ICC (consistency)	SEM
SomersetWest_CS	T_m	0.58	0.00	0.502	0.557	2.95	0.63	0.00	0.550	0.622	2.83
SomersetWest_CS	T_x	0.25	0.00	0.209	0.289	5.61	0.23	0.00	0.162	0.254	5.59
SomersetWest_CS	T_n	0.50	0.00	0.428	0.488	3.13	0.84	0.00	0.703	0.774	2.04
Stellenbosch_2_CS	T_m	0.69	0.00	0.646	0.676	2.74	0.61	0.00	0.558	0.613	3.02
Stellenbosch_2_CS	T_x	0.23	0.00	0.231	0.281	5.92	0.20	0.00	0.177	0.217	5.93
Stellenbosch_2_CS	T_n	0.67	0.00	0.608	0.654	2.68	0.77	0.00	0.729	0.733	2.27
Vredendal_CS	T_m	0.53	0.00	0.289	0.528	3.29	0.52	0.00	0.360	0.538	3.48
Vredendal_CS	T_x	0.15	0.00	0.082	0.220	6.91	0.05	0.00	0.057	0.114	7.04
Vredendal_CS	T_n	0.25	0.00	0.297	0.320	4.12	0.80	0.00	0.770	0.770	2.31
Stellenbosch_1_CS	T_m	0.61	0.00	0.463	0.602	2.91	0.64	0.00	0.520	0.643	2.91
Stellenbosch_1_CS	T_x	0.18	0.00	0.096	0.224	5.99	0.17	0.00	0.146	0.194	6.21
Stellenbosch_1_CS	T_n	0.61	0.00	0.491	0.611	3.13	0.80	0.00	0.729	0.774	2.22

The extracted LST from the vineyard polygons (LST_POL) and the LST extracted from the nearest weather station point (LST_{WS}) was compared for T_x, T_n and T_m (Figure 9 & Figure 10). Comparing the LST_POL to the nearest LST_{WS}, there was a low correlation for T_x with a SEM = 5.5°C. In contrast, there was an excellent correlation for T_n with R^2 = 0.94, $p \leq 0.00$ and SEM = 0.73°C. The LST_POL_{Tx} overestimated the LST_{WS_Tx}, which could be due to the surface of the vineyard holding more heat in the growing season. It seems some of the grouped outliers in Figure 9 could be ascribed to the winter (July/August) temperatures at > 30°C for LST_{Tx} and >10°C-20°C for WS_{Tx}. It should be noted that the observed LST_{Tx} were almost double the WS_{Tx} observations. The substantial differences in LST_{Tx} and WS_{Tx} warants more in-depth analysis in future studies. These observations could be better understood and accommodated for by the inclusion of emissivity layers and NDVI layers in the future model calibrations for using LST_{Tm} to supplement, and possibility predict, WS_{Tm} over different surface layers., The T_m was shown to be a better parameter for comparing products (Figure 10), as it incorporates the T_x and the T_n. There was a good correlation of R^2 = 0.56 and SEM = 3.1°C between the LST_{Tm} and WS_{Tm}, mostly driven by the T_x

SEM. Hence, for the calibration of the LST_{Tm} layers the WS_{Tm} temperatures will be used, as it has a lower measurement error compared to the LOG_{Tm}.

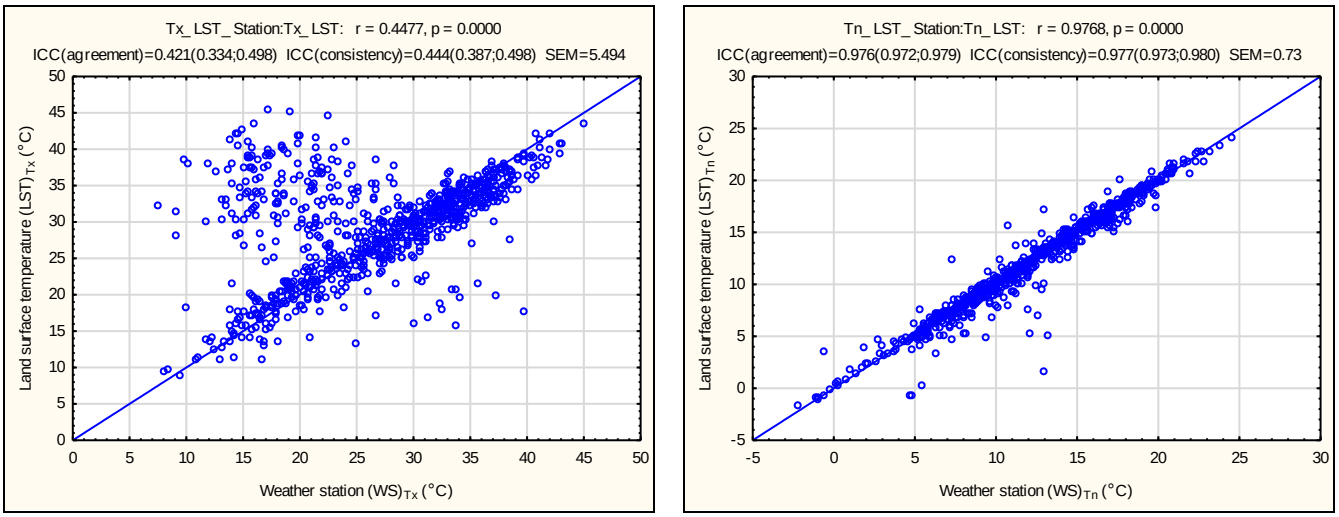

Figure 9 Intra-class correlations of the land surface temperature extracted for the polygon for the Somerset West site (LST_POL) with the nearest weather station (WS_T), maximum temperature (T_x) (left), minimum temperatures (T_n) (right).

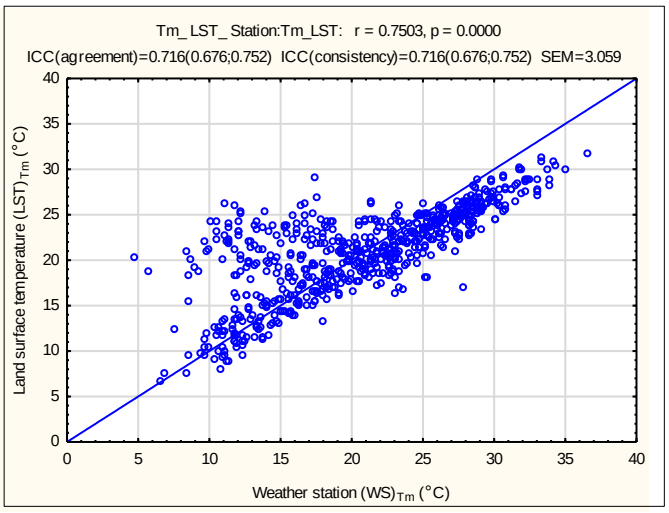

Figure 10 Intra-class correlations of the land surface temperature extracted for the polygon for the Somerset West site (LST_POL) with the nearest weather station (WS_T), for mean temperature (T_m).

6.3.2.3 Climatic index comparison

Indices were calculated from the daily mean temperature data (T_m) over the three seasons, from the sources LST_T, LOG_T and WS_T. The final indices for the growing seasons are compared in Table 7 for one site only (for more detail see Addendum 6.2). Although only the Somerset West site is given as an example of correlations, the discussion is based on all sites, as all sites are used as an input for Table 8. The LOG_T sources showed better correlations for the GST, WI, MMT and MJT compared to the WS_T sources (Table 8), and the WS_T source had better correlation coefficients for the BEDD and HI compared to LST_T. Since the correlations of MFT and CI using LST_T to supplement WS_T were insignificant and very low (Table 8), these climatic indexes should be used with greater caution., The SEM was only slightly lower when LST_T was used to predict WS_T (WI: R^2 = 0.67 and SEM = 2.5°C) indices compared to LOG_T indices (WI: R^2 = 0.63 and *SEM* = 2.6°C).

The correlation coefficients and ICC's over all the sites highlighted GST, WI, HI and BEDD as better indices to use when using LST_T data to supplement WS_T data (Table 7 and Table 8). Accumulative bioclimatic indices for the period 1 September to 31 March were more comparable to WS_T indices than climatic indexes such as mean February temperature (MFT) or minimum March temperatures (Cool night Index). This is probably due to the latter two indices being monthly values, which are sometimes based more on T_n than T_m. From the previous discussion, it was also shown that the use of WS_T seems more reliable to measure ambient temperatures rather than loggers placed above the vineyard canopy.

Table 7 Correlation of selected bioclimatic indices, namely growing season temperature (GST), Winkler index (GDD), biologically effective degree days (BEDD) and Huglin index (HI), calculated from land surface temperature (LST_T) compared to that calculated from logger (LOG_T) and weather station (WS_T) temperatures, over all seasons for the Somerset West site. The bottom three rows are the accumulative bioclimatic indices values averaged over all the season (from 1September to 31 March).

Element	Logger mean temperature (LOG_T)-all data correlation					Weather station temperature (WS_T)-all data correlation				
	R^2	*p*	ICC	ICC	SEM	R^2	*p*	ICC	ICC	SEM
GST	0.45	0.00	0.382	0.386	4.257	0.51	0.00	0.469	0.469	4.089
GDD	0.63	0.00	0.590	0.605	2.587	0.67	0.00	0.623	0.661	2.473
BEDD	0.34	0.00	0.225	0.227	2.153	0.44	0.00	0.371	0.371	2.036
HI	0.55	0.00	0.500	0.556	3.166	0.54	0.00	0.547	0.548	2.995
GDD Acc	*0.91*	*0.00*	*0.790*	*0.857*	*232.695*	*0.94*	*0.00*	*0.875*	*0.901*	*185.779*
BEDD	*0.93*	*0.00*	*0.842*	*0.897*	*150.587*	*0.96*	*0.00*	*0.915*	*0.934*	*117.476*
HI Acc	*0.97*	*0.00*	*0.749*	*0.900*	*207.579*	*0.95*	*0.00*	*0.914*	*0.936*	*141.329*

Table 8 Overall correlations for all stations between growing season temperature (GST), Winkler index (WI), biologically effective degree days (BEDD), Huglin index (HI), mean February temperature (MFT) and cool night index (CI) calculated from land surface temperature (LST), compared to temperature loggers (LOG) and weather station (WS) sources (calculated form daily data).

Source	Climatic Index	*r*	*p*	R^2
Weather station (WS)	GST[(1)]	0.79	0.0000	0.62
Weather station (WS)	WI_GDD[(2)]	0.77	0.0000	0.59
Weather station (WS)	BEDD[(3)]	0.79	0.0000	0.62
Weather station (WS)	HI_GDD[(4)]	0.83	0.0000	0.69
Weather station (WS)	MFT[(5)]	-0.31	0.0037	0.10
Weather station (WS)	CI[(6)]	0.61	0.0000	0.37
Weather station (WS)	MMT[(7)]	0.72	0.0000	0.52
Weather station (WS)	MJT[(8)]	0.64	0.0000	0.41
Logger (LOG)	GST	0.86	0.0000	0.74
Logger (LOG)	WI_GDD	0.85	0.0000	0.72
Logger (LOG)	BEDD	0.69	0.0000	0.48
Logger (LOG)	HI_GDD	0.76	0.0000	0.58
Logger (LOG)	MFT	0.44	0.0046	0.19
Logger (LOG)	CI	-0.03	0.8775	0.00
Logger (LOG)	MMT	0.78	0.0000	0.61
Logger (LOG)	MJT	0.69	0.0000	0.48

[(1)] Growing season temperature; [(2)] Winkler Index; [(3)] Biologically effective degree days; [(4)] Huglin index ; [(5)] Mean February temperature ; [(6)] Cool night index ; [(7)] Mean March temperature and [(8)] Mean January temperature

Indices accumulated over the growing season from continuous daily data (Figure 11) highlighted the performance of the indices with more detail when considering season variability. It seemed that generally over the three seasons, the LST tended to underestimate the climatic indices calculated from WS by a small margin. Climatic indices are commonly used as descriptors in the viticultural sector to make seasonal decisions and to quantify the season in relation to other seasons. Figure 11 and Figure 12 represent the WI, BEDD and HI indices accumulation over time from daily data, accumulated for each of the three growing seasons for the period 1 September to 31 March. Some

seasons were overestimated and other seasons underestimated. Furthermore, it was clear that the seasonal variability seen in WI and HI was not as obvious in the BEDD index. The BEDD had an excellent R^2 = 1 for most stations, the seasonal variability seen in LST_{GGD} and other indices is not as evident in the LST_{BEDD}, but was more comparable to the slight seasonal variability in WS_{BEDD}. This could be due to the BEDD calculation having a lower limit of 10°C and an upper limit of 19°C, and the equation accommodated for an adjustment for diurnal temperature range and has an adjustment for latitude/day length (Figure 11*).* However, the LST_{BEDD} constantly over all seasons and stations underestimated the WS_{BEDD}.Taking the above mentioned into consideration, it seemed that the BEDD is a better index to use for quantifying the season based on the LST_{Tm}. However, the underestimation should be accommodated for in future applications to supplement WS_{BEDD}.

The GDD for stations (Figure 11 & Figure 12) showed the seasonal variability for LST_{GDD} to be larger than that of WS_{GDD}. In the case of the Aan-De Doorns site, the LST_{GDD} both underestimated (season 1) and overestimated (season 3) the WS_{GDD}. Where LST_{GDD} underestimated $WS_{GDD,}$ the difference between the two variables was between 0-200 GDD. However, in the first season (LST_{GDD}: 1820 & WS_{GDD}: 2256), LST tended to underestimate the WI by about 400 units. In both figures, the R^2 = 0.81, the ICC is > 0.99 and the SEM is <100 units. The HI index, expressed the same trends as WI GDD for all the station with the LST_{GDD} underestimating the HI index by about 200-600 units dependent on the season (Figure 12 and Table 14 in Addendum 6.2). The Huglin index should be included when predicting seasonal temperature trends as this index includes T_m and T_x in the equation, and generally showed excellent correlations R^2 = 0.96 and a SEM of <150 for most stations (Figure 12).

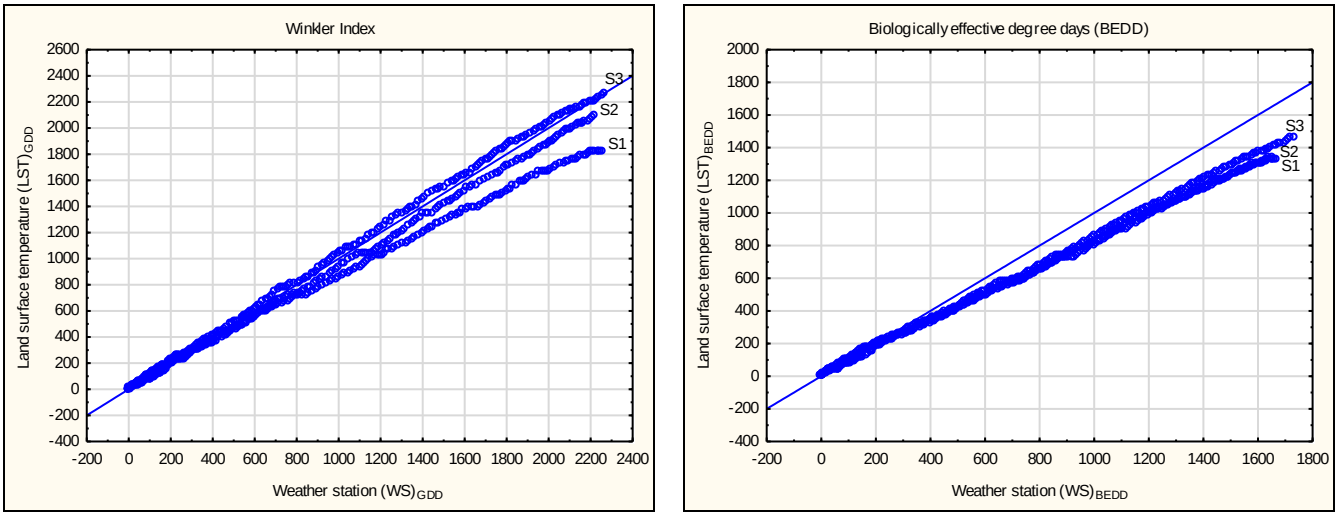

Figure 11 Accumulated growing degree days (GDD) calculated using the Winkler index (left) and Biologically effective degree days (BEDD) (right) for Aan-De-Doorns weather station comparing three seasons of land surface temperature (LST) and weather station (WS) data. Regression results for Winkler index are r = 0.99, p = 0.00, R^2 = 0.98, ICC(agreement) = 0.986, ICC(consistency) = 0.989, SEM = 72.509 and Biologically effective degree days: r = 0.99, p = 0.0000, R^2 = 0.98, ICC(agreement) = 0.948 ICC(consistency) = 0.981, SEM = 65.754.

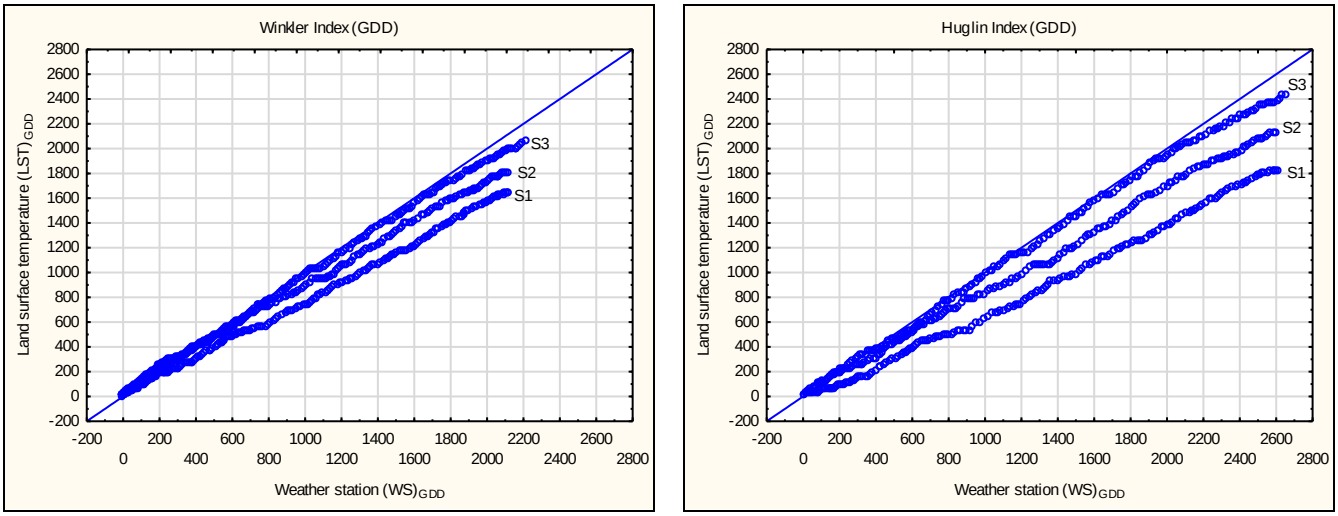

Figure 12 Accumulated growing degree days (GDD) calculated using the Winkler index (left) and Huglin Index (HI) (right) for the Robertson weather station comparing three seasons of land surface temperature (LST) and weather station (WS) data. Regression results for Winkler index are r = 0.99, p = 0.00 R^2 = 0.98, ICC(agreement) = 0.963, ICC(consistency) = 0.978, SEM = 92.905 and Huglin Index (HI) are r = 0.97, p = 0.00, R^2 = 0.94, ICC(agreement) = 0.919, ICC(consistency) = 0.960, SEM = 148.782.

Station data variability as well as faulty or missing WS data can be identified using the correlation between LST_{Tm} and WS_{Tm} and/or the accumulation over time using bioclimatic indices. As seen from Figure 5, showing Landau WS_{GDD} missing data for the one season, the LST_{Tm} could be used to supplement the WS_{Tm} where data was missing from November until end of March. In Figure 12, the variability in the seasonal analysis could be noticed, with the LST_{GDD} slightly overestimating the second and third seasons and underestimating the first season. The seasonal underestimation could be ascribed to site selection, where temperature changes can be influenced by factors such as distance from the ocean etc. Temperature seemed to be more moderate at the coast and more extreme inland; hence the LST_T seemed to be overestimated compared to WS_T. This could be caused by the WST being cooler due to afternoon cooling breezes inland. The under- and overestimation is accentuated or negated on merit of the bioclimatic indices selected to describe the season and environment. The underestimation in season 1 could be ascribed to lower T_m values which could be due to cloud cover, which is a notable risk when using remote sensing as an alternative for temperature variables. This could be incorporated into models in future studies for the Western Cape as done in other research studies (Benali *et al.*, 2012; Zorer *et al.*, 2013). It is also a risk to consider when using remote sensing as an alternative for ambient temperature measurements, and the processing around cloud cover could be incorporated into future studies for the Western Cape. Other studies found that the accumulation over time in climatic indices calculation cannot be supported using LST images that did not have more uncertainties addressed through pre-processing (Benali *et al.*, 2012; Zorer *et al.*, 2013).

6.3.3 Overall performance of land surface temperature calibration and validation

Overall performance is represented in parameter estimates based on all data available for the three year period, with regressions showed over all stations (WS_T, N=16) and polygons/sites (LOG_T, N=13) (Table 9). The correlations for all temperature elements were significant and showed a good relationship with the LST_{Tm} and WS_{Tm}, being slightly higher.

Table 9 Parameter estimates from the calibration (analysis) and validation (prediction) over all stations for Land surface temperature (LST_T) and weather station (WS_T), for mean (T_m), maximum (T_x), minimum (T_n) temperatures and Winkler index (WI) as growing degree days (GDD).

Effect	Para meter	Stdan dard Error	t	*p* value	-0.95 Cnf.limit	0.95 Cnf.limit	Beta (ß)	Std.Err	-0.95 Cnf.limit	0.95 Cnf.limit
LST_{Tm} : WS_{Tm}	0.72	0.01	99.3	0.00	0.71	0.74	0.88	0.01	0.86	0.90
LST_{Tx} : WS_{Tx}	0.62	0.01	82.5	0.00	0.60	0.63	0.78	0.01	0.76	0.80
LST_{Tn} : WS_{Tn}	0.71	0.01	79.9	0.00	0.69	0.72	0.78	0.01	0.77	0.80
LST_{GDD} :	0.45	0.00	53.0	0.00	0.43	0.47	0.60	0.01	0.58	0.62

The final calibration and prediction data analysis showed that the LST_{Tm} had the highest R^2 = 0.74, with a calibration error of 2.4°C and a prediction error of 2.6°C (Table 10). The overall T_m had the lowest RMSEC of 2.3°C (Figure 13), T_x had the highest RMSEC of 3.7°C (Figure 14) and T_n a RMSEC of 2.7°C (Table 10). The element T_m is widely used as a factor in calculating bioclimatic indices relating to agricultural crops. For WS_{Tm} estimation, the results from this study can be considered promising, given the simplicity of the statistical models employed, the robustness of the resampling techniques and the high accuracy achieved under these limitations. To support the findings for T_m, 80% of the stations had an $R^2 \geq 0.85$ and a SEM lower than 2.8°C, for which similar results are noted in other studies (Benali *et al.,* 2012). The LST_{Tm} and WS_{Tm} data exhibited a strong linear relationship (T_m: r = 0.86, $p < 0.001$, and N = 29), and good prediction with an offset of 1.9 and a slope of 0.8. Similar results were reported for a study in Italy (Zorer *et al.*, 2013). The WS_{Tm} can therefore be supplemented/predicted using the LST_{Tm}, based on the regression equations attained from the final analysis.

Table 10 Final calibration and validation over all weather data, after intra class correlations and validation calibration was done per station for Land surface temperature (LST_T) and weather station (WS_T), for mean (T_m), maximum (T_x), minimum (T_n) temperatures and Winkler index (WI) as growing degree days (GDD).

Element	Calibration (70%)				Prediction (30%)			
	R^2	MSE	*r*	RMSEC	R^2	MSE	*r*	RMSEP
T_m	0.74	5.529	0.86	**2.351**	0.74	7.207	0.86	**2.639**
T_x	0.58	13.640	0.76	**3.693**	0.63	16.302	0.79	**4.038**
T_n	0.61	7.189	0.78	**2.681**	0.53	9.182	0.73	**3.030**
GDD	0.36	11.617	0.60	**3.408**	0.62	9.782	0.78	**3.128**

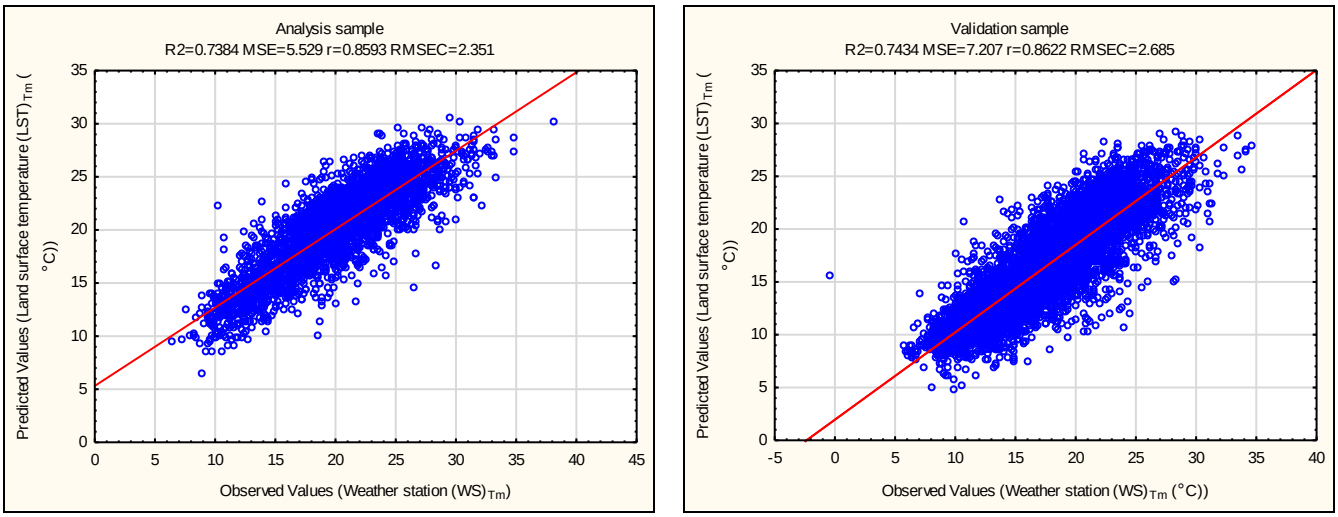

Figure 13 Comparison of predicted mean (T_m) land surface temperature (LST_{Tm}) to observed mean weather station temperatures (WS_{Tm}) for the overall calibration (analysis sample, left) and validation (validations sample, right) data sets.

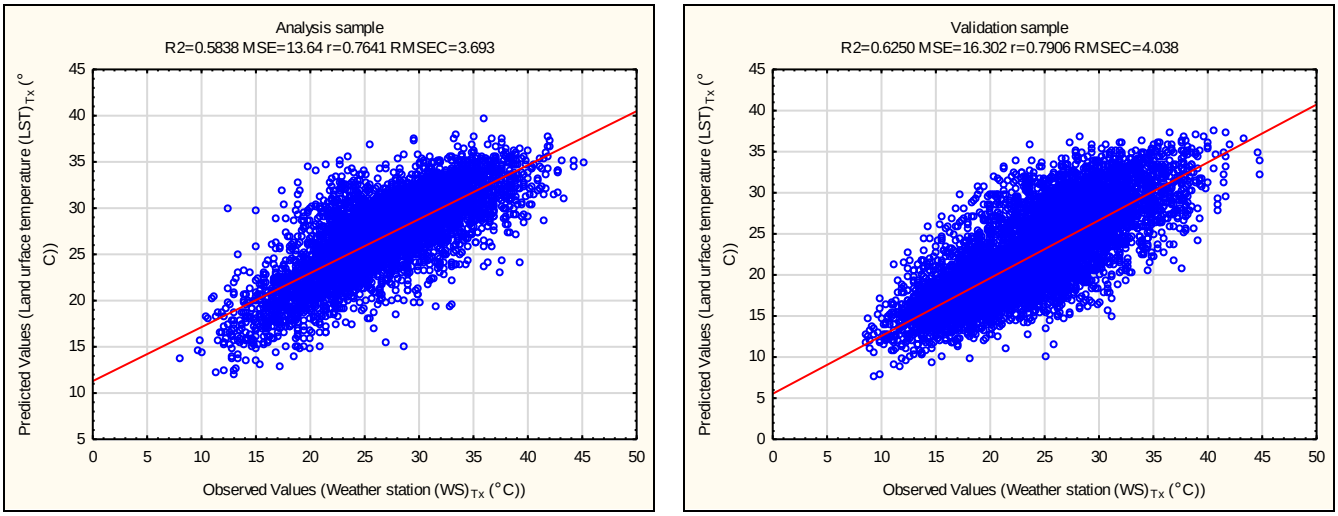

Figure 14 Comparison of predicted maximum (T_x) land surface temperature (LST_{Tx}) to observed mean weather station temperatures (WS_{Tx}) for the overall calibration (analysis sample, left) and validation (validations sample, right) data sets.

6.3.4 Error of uncertainty analysis and auxiliary data

The larger LST_T range could be ascribed to more temperature variables being included within a pixel compared to the *in situ* WS_T measuring a specific area, hence emphasising the importance of including emissivity layers and other auxiliary data inputs into calibration models to more accurately supplement WS_T. Some stations had lower performing subsets and this was possibly due to altitude (Figure 15). However, there was no clear pattern in the global dataset (Figure 16). Altitude has an expected larger, but negative influence on the LST_{Tx} (R^2 = 0.44, $p \leq 0.001$) than the other elements, namely LST_{Tm} (R^2 = 0.21, $p \leq 0.08$) (Figure 15) and LST_n (R^2 = 0.28, $p \leq 0.04$). When all the elements were pooled in a sample analysis, altitude had an overall R^2 = 0.14 and $p \leq$ 0.001 (Figure 16). Altitude did not have a significant effect on the GDD indices calculated from the LST_{Tm} and WS_{Tm}. Distance from the ocean did not show to have significant influence on the relationship between LST_T and WS_T (Table 12). Proximity to the sea did not affect model accuracy, which was expected due to the lower performance noted for stations located nearer to the coast (Table 11 and Table 12)

The lower performance could be ascribed to the moderating effect of the ocean on ambient and possibly land surface temperatures. Other studies found the model to have a general lower performance in stations located near the coast, possibly related to frequent moist sea breezes and fog occurrence (Benali *et al.*, 2012). A slight under- and over estimation of the higher and lower annual temperatures was observed. Areas with more moderate temperatures seemed to have a higher consistency with LST_T and WS_T, the extremes sites far inland and near the coast tend to have had lower consistency (Table 6). The daily LST_T has its limitations in capturing the extremes within a day (very high temperatures or very low temperatures). The temperatures could also be moderated and affected by terrain factors such as topography, distance from the ocean and altitude, as well as the outliers of cloud cover.

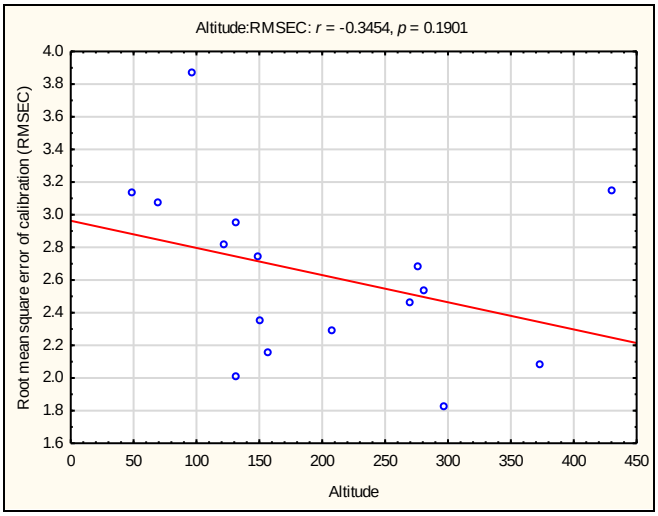

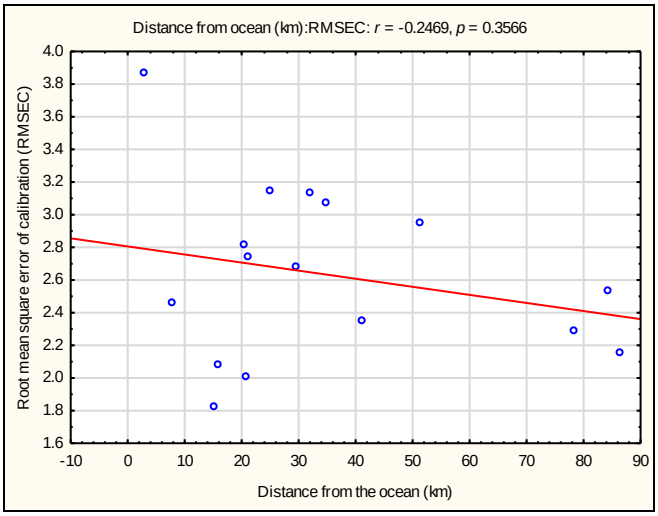

Figure 15 The effect of altitude (left) and distance from the ocean (right) on the correlation between mean temperature from land surface temperature (LST_{Tm}) and weather station (WS_{Tm}) sources analysed by weather station.

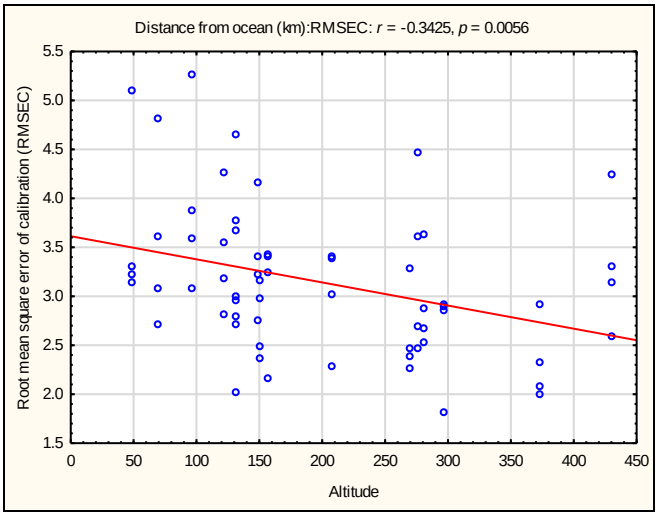

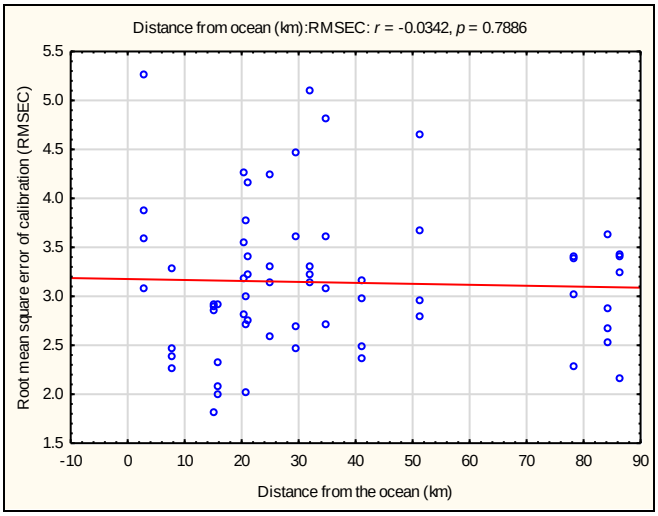

Figure 16 The effect of altitude (left) and distance from the ocean (right) on the correlation between mean temperature from land surface temperature (LST_{Tm}) and weather station (WS_{Tm}) sources analysed for the whole three year dataset, overall weather stations and sites.

Table 11 Effect of altitude and distance from the ocean on the accuracy of correlation between the weather station (WS_T) and land surface temperature (LST_T) for all the temperature elements maximum (T_x), minimum (T_n) and mean (T_m) temperatures and growing degree days (GDD).

StationName	Altitude (m.a.s)	Distance from the Ocean (km)	LST_{Tx} vs WS_{Tx}		LST_{Tn} vs WS_{Tn}		LST_{GDD} vs WS_{GDD}		LST_{Tm} vs WS_{Tm}	
			R^2	RMSEC	R^2	RMSEC	R^2	RMSEC	R^2	RMSEC
AAN-DE-DOORNS WYNKELDER	209	78.4	0.7	3.400	0.4	3.380	0.65	3.008	0.8	2.285
ELGIN: BEAULIEU	297	15.4	0.7	2.898	0.5	2.917	0.65	2.852	0.8	1.815
GRABOUW: OAK VALLEY	373	16.1	0.7	2.909	0.6	1.997	0.63	2.320	0.8	2.077
H.L.S. BOLAND	151	41.1	0.7	3.159	0.6	2.487	0.73	2.961	0.8	2.351
HELDERFONTEIN	132	21.0	0.7	3.768	0.5	2.991	0.72	2.698	0.8	2.005
HERITAGE GARDEN:	123	20.5	0.6	4.250	0.5	3.535	0.63	3.181	0.7	2.817
KAPEL	49	32.0	0.6	5.093	0.4	3.208	0.68	3.295	0.8	3.134
KLAWER	70	34.9	0.4	4.802	0.6	2.710	0.60	3.598	0.6	3.076
LANDAU	132	51.3	0.4	4.652	0.4	2.782	0.51	3.656	0.6	2.953
MOUNTAIN VINEYARDS	277	29.6	0.3	4.470	0.4	2.470	0.53	3.604	0.6	2.677
NIETVOORBIJ	150	21.2	0.5	4.145	0.5	3.211	0.63	3.399	0.7	2.745
NORTIER (WRS)	97	2.9	0.1	5.246	0.3	3.067	0.22	3.582	0.2	3.867
ROBERTSON PP	158	86.4	0.7	3.241	0.5	3.389	0.59	3.429	0.8	2.151
THELEMA 1: AWS	431	25.1	0.6	4.234	0.5	2.588	0.46	3.301	0.6	3.142
VELDRESERWE	281	84.4	0.7	3.625	0.5	2.672	0.66	2.867	0.8	2.531
VERGELEGEN BO	270	7.7	0.7	3.282	0.6	2.247	0.69	2.388	0.7	2.460

Table 12 Summarised outputs from an analysis on how altitude and distance from the ocean affects the root mean square error of calibration (RMSEC) in the different regression analyses, including weather station (WS_T) and land surface temperature (LST_T) for the temperature elements maximum (T_x), minimum (T_n) and mean (T_m) temperatures and growing degree days (GDD).

Regression analysis	Altitude:RMSEC			DistOcean:RMSEC		
	r	*p*	R^2	*r*	*p*	R^2
WholeSample	-0.3425	0.0056	0.12	-0.0342	0.7886	0.00
LST_{Tm} vs WS_{Tm}	-0.3454	0.1901	0.12	-0.2469	0.3566	0.06
LST_{Tx} vs WS_{Tx}	-0.5271	0.0359	0.28	-0.2177	0.4181	0.05
LST_{Tn} vs WS_{Tn}	-0.5835	0.0177	0.34	0.2854	0.2840	0.08
LST_{GDD} vs WS_{GDD}	-0.4619	0.0717	0.21	0.1644	0.5430	0.03

6.3.5 Limitations and possible future developments

The simplicity of the models employed, the robustness and confidence provided by the optimisation and resampling methods, the easy accessibility of the input data at a global scale, along with the good performance attained, suggested that the methodology used in the study has potential to be applied to other regions of the South Africa. The work highlighted future possible improvements when deriving ambient temperature based on remote sensing data, by including more environmental and terrain attributes into the models that may affect temperature. One such improvement can be to increase the quality of LST data by improving cloud detection, decreasing the impact of visualisation geometry and reducing the impact of errors due to incorrect emissivity parameterisation. The integration of NDVI and cloud cover data into the algorithms would increase the robustness of the LST product in supplementing WS data.

6.4 Conclusions

This work showed that daily averages calculated from the maximum and minimum LST_{Tm} layers can be used to accurately estimate WS_{Tm}. Simple statistical methods estimated WS_{Tm} with a calibration error of between 2.3-3.6°C. The study showed that LST can be used as an alternative/supplementary source of temperature data for the Western Cape. However, land surface temperature overestimates the maximum temperatures and measures cooler temperatures at night. Regression equations from the three-year continuous daily data set could be used to calibrate the LST using the actual WS data, providing a temperature layer of better accuracy, a

layer that is already intrinsically spatial in nature taking into account the terrain complexity of the Western Cape. The best correlation was using the T_m of the LST for further analysis and not the average of all four layers. The GDD calculated from the Winkler index and the BEDD were the most promising indices to use for the demarcation of climatic zones. However, minor errors in temperature variability accumulated over time. In further analysis this could be accounted for. The BEDD had an excellent correlation for most stations; the seasonal variability seen in LST_{GGD} and other indices is not as event in the LST_{BEDD}, comparable to the slight seasonal variability in WS_{BEDD}. Overall, LST_{BEDD} underestimated the WS_{BEDD} and will need to be considered in the application of the indices. This could be due to the BEDD calculation having a lower and upper limit, and accommodated for an adjustment for diurnal temperature range and has an adjustment for latitude/day length. From the results obtained in this study, spatial climate maps can be produced using the calibration regression equation, ensuring continuous temperature by supplementing WS_T with LST_T. The use of LST layers as inputs to build bioclimatic indices maps have been done with great success and giving a very detailed description of landscapes, despite the complexity of terrain. With high spatial and thermal resolution allows one to discriminate and select areas best suited areas for specific crop cultivation.

For the daily 1 km products, slightly higher errors may occur than in the other MODIS products, especially at large view angles and in semi-arid regions such as Klawer/Kapel, due to the greater uncertainties in classification based on surface emissivities due to the dust aerosols. Considering results presented in this chapter, it is recommended that the 1 km LST retrieved by generalized split window LST method be used for lakes, snow/ice, and dense vegetated areas, and the 5 km LST product method be used in bare and spare vegetated areas this is a consideration for future work.

We aim in the future to estimate WS_{Tm} for the whole of South Africa for a longer period including more weather station points, estimating temperatures at short temporal scales from hourly to daily and weekly (8-10 day product) resolutions, aiming to describe the intra and inter annual patterns of seasons and crop responses such as phenology at a higher temporal resolution. The scales are relevant for a wide range of environment related applications. Temporal, spatial, and thermal resolutions of T_m acquired from daily LST products, offers a new and powerful tool for classification of viticulture landscapes and seasonal monitoring. A wide scope of applications can benefit from the improved remote sensing based WS_{Tm} estimations presented in this study for the area of Western Cape. Two main practical aspect stands out in terms of the contribution of this work to research applications. Firstly, to provide improved spatial-temporally distributed estimations of temperature and indices maps which are particularly important in regions with low station density or with highly variable spatial patterns between stations. Secondly, a collection of remote sensing layers should be created to compliment and fill weather station gaps and used for integrated grapevine studies for future use in the wine industry as a key tool for decision making.

6.5 References

Anderson, J.D., Jones, G.V., Tait, A., Hall, A. & Trought, M., 2012. Analysis of viticulture region climate structure and suitability in New Zealand. J. Int. Sci. Vigne Vin. 46, 149-165.

Anderson, J.J., Gurarie, E., Bracis, C., Burke, B.J. & Laidre, K.L., 2013. Modeling climate change impacts on phenology and population dynamics of migratory marine species. Ecological Modelling 264, 83-97.

Benali, A., Carvalho, A.C., Nunes, J.P., Carvalhais, N. & Santos, A., 2012. Estimating air surface temperature in Portugal using MODIS LST data. Remote Sens. Environ. 124, 108-121.

Bonnardot, V. & Cautenet, S., 2009. Mesoscale atmospheric modeling using a high horizontal grid resolution over a complex coastal terrain and a wine region of South Africa. J. Appl. Meteorol. Climatol. 48, 330-348.

Broich, M., Huete, A., Paget, M., Ma, X., Tulbure, M., Restrepo, N., Evans, B., Beringer, J., Devadas, R., Davies, K. & Held, A., 2015. Environmental modelling & software. A spatially explicit land surface phenology data product for science, monitoring and natural resources management applications. Environ. Modell. Softw. 64, 191-204.

Crosson, W.L., Al-Hamdan, M.Z., Hemmings, S.N.J. & Wade, G.M., 2012. A daily merged MODIS Aqua-Terra land surface temperature data set for the conterminous United States. Remote Sens.Environ. 119, 315-324.

Czajkowski, K.P., Goward, S.N., Stadler, S.J. & Walz, A., 2000. Thermal remote sensing of near surface environmental variables: application over the Oklahoma Mesonet. The Professional Geographer 52, 345-357.

Diak, G.R. & Whipple, M.S., 1993. Improvements to models and methods for evaluating the land-surface energy balance and 'effective' roughness using radiosonde reports and satellite-measured 'skin' temperature data. Agric. For. Meteorol. 63, 189-218.

ESRI, 2015. ArcGIS Desktop: Release 10.3.1. Redlands, CA: Environmental Systems Research Institute.

Ganguly, S., Friedl, M.A., Tan, B., Zhang, X. & Verma, M., 2010. Land surface phenology from MODIS: Characterization of the Collection 5 global land cover dynamics product. Rem. Sens. Environ. 114, 1805-1816.

Hall, A. & Jones, G.V., 2010. Spatial analysis of climate in winegrape-growing regions in Australia. Aust. J. Grape Wine Res. 16, 389-404.

Janssen, P.H. & Heuberger, P.S., 1995. Calibration of process-orientedmodels. Ecological Modelling 83, 55-66.

Jarvis, A., Reuter, H.I., Nelson, A. & Guevara, E., 2008. Hole-filled seamless SRTM data V4. Cali, Colombia: International Centre for Tropical Agriculture (CIAT) Accessed online in December 2006: http://srtm.csi.cgiar.org.

Jones, G.V., White, M.A., Cooper, O.R. & Storchmann, K., 2005. Climate change and global wine quality. Climatic Change 73, 319-343.

MODIS-Land-Team, 2015. MODIS sinusoildal tile grid. www.modis-land.gsfc.nasa.gov.

Myburgh, P., 2005. Effect of altitude and distance from the Atlantic Ocean on mean February temperatures in the Western Cape Coastal region. WineLands, August.

Neteler, M., 2010. Estimating daily land surface temperatures in mountainous environments by reconstructed MODIS LST data. Remote Sens. 2, 333-351.

R-Core-Team, 2014. R: A language and environment for statistical computing. R Foundation for Statistical Computing, Vienna, Austria.URL http://www.R-project.org/.

Singh, D.K., Agnihotri, R.K., Chauhan, S., Ganie, S.A., Singh, G. & Sharma, R., 2014. Effect of Environmental Changes on Phenology and Reproductive Biology of Sida cordifolia with Special Reference to the Temperature and Relative Humidity. Int. J. Plant Soil Sci. 3, 372-379.

SRTM, 2012. Shuttle Radar Topography Mission (SRTM) 1 Arc-Second Global. Acessed online in 2012: https://lta.cr.usgs.gov/SRTM1Arc.

Thomas, a., Corgne, S., Planchon, O., Bonnefoy, C., Quénol, H. & Lecerf, R., 2013. Phenological monitoring of vine using MODIS imagery in the vineyard of Saumur-Angers (Loire Valley area , France). EGU General Assembly 2012, held 22-27 April, Vienna, Austria., p.9274.

Vancutsem, C., Ceccato, P., Dinku, T. & Connor, S.J., 2010. Evaluation of MODIS land surface temperature data to estimate air temperature in different ecosystems over Africa. Remote Sens. Environ. 114, 449-465.

Vazquez, D.P., Reyes, F.J.O. & Arboledas, L.A., 1997. A comparative study of algo- rithms for estimating land surface temperature from AVHRR data. Rem. Sens. Environ. 62, 215-222.

Vogt, J.V., Viau, A.A. & Paquet, F., 1997. Mapping regional air temperature fields using satellite-derived surface skin temperatures. Int. J. Climatol. 17, 1559-1579.

Wan, Z., 1999. MODIS land-surface temperature algorithm theoretical basis document. MODIS Land-surface Temperature Algorithm Theoretical Basis Document (LST ATBD).

Wan, Z., 2014. New refinements and validation of the collection-6 MODIS land-surface temperature/emissivity product. Remote Sens. Environ. 140, 36-45.

Wan, Z. & Dozier, J., 1996. A generalized split-window algorithm for retrieving land surface temperature from space. IEEE T. Geosci. Remote. 34, 892-905.

Wan, Z. & Li, Z.L., 2008. Radiance-based validation of the V5 MODIS land-surface temperature product. Int. J. Remote Sens. 29, 5373-5395.

Wan, Z., Zhang, Q. & Li, L., 2004. Quality assessment and validation of the MODIS global land surface temperature. Int. J. Remote Sens. 25, 261-274.

Wan, Z., Zhang, Y., Zhang, Q. & Li, Z.L., 2002. Validation of the land-surface temperature products retrieved from terra moderate resolution imaging spectroradiometer data. Remote Sens. Environ. 83, 163-180.

Wessel, P. & Smith, W.H.F., 1996. A Global Self-consistent, Hierarchical, High-resolution Shoreline Database. J. Geophys. Res. 101, 8741-8743.

Williamson, S.N., Hik, D.S., Gamon, J.a., Kavanaugh, J.L. & Flowers, G.E., 2014. Estimating temperature fields from MODIS land surface temperature and air temperature observations in a sub-arctic alpine environment. Remote Sens. 6, 946-963.

Zakšek, K. & Schroedter-Homscheidt, M., 2009. Parameterization of air temperature in high temporal and spatial resolution from a combination of the SEVIRI and MODIS instruments. ISPRS Journal of Photogrammetry and Remote Sensing 64, 414-421.

Zhu, W., Lű, A. & Jia, S., 2013. Estimation of daily maximum and minimum air temperature using MODIS land surface temperature products. Remote Sens. Environ. 130, 62-73.

Zorer, R., Rocchini, R., Delucchi, L., Zottele, F., Meggio, F. & Neteler, M., 2011. Use of multi-annual MODIS land surface temperature data for the characterization of the heat requirements for grapevine varieties. In: Proc. Analysis of Multi-temporal Remote Sensing Images (Multi-Temp), 2011 6th International Workshop pp. 225-228.

Zorer, R., Rocchini, D., Metz, M., Delucchi, L., Zottele, F., Meggio, F. & Neteler, M., 2013. Daily MODIS land surface temperature data for the analysis of the heat requirements of grapevine varieties. IEEE T. Geosci. Remote 51, 2128-2135.

Addendum 6.1

Table 13 List of extraction points (weather stations, N=16) and polygons (sites, N=13) for comparison with land surface temperature (LST).

Source	Weather station name & site name	Latitude	Longitude	Altitude	Distance from the Ocean (km)	Slope (%)	Aspect (°)	HillShade (degree)	Cumulative global radiation (Wh/m^2)	Average daily sun hours
Points	AAN-DE-DOORNS WYNKELDER	-33.7000	19.4833	209	78.35	6.36	293.69	176	1094.29	12.45
Points	ELGIN: BEAULIEU	-34.1652	19.0315	297	15.36	8.39	232.63	156	1066.74	12.36
Points	GRABOUW: OAK VALLEY	-34.1590	19.0728	373	16.14	5.86	267.73	167	1110.74	12.47
Points	H.L.S. BOLAND	-33.6542	18.8828	151	41.14	2.26	338.31	182	1096.51	12.68
Points	HELDERFONTEIN	-33.9233	18.8733	132	20.98	1.56	116.62	179	1079.86	12.42
Points	HERITAGE GARDEN: INFRUITEC	-33.9271	18.8723	123	20.52	3.26	180.00	174	1080.98	12.42
Points	KAPEL	-31.7602	18.5793	49	32.01	5.17	272.58	170	1073.90	12.47
Points	KLAWER	-31.7920	18.6269	70	34.86	3.88	343.71	178	1081.76	12.18
Points	LANDAU	-33.5778	18.9680	132	51.27	2.26	201.67	179	1074.82	12.54
Points	MOUNTAIN VINEYARDS	-33.8742	18.9514	277	29.60	5.24	12.27	192	1111.17	11.70
Points	NIETVOORBIJ	-33.9168	18.8599	150	21.24	2.99	236.98	173	1076.37	12.45
Points	NORTIER (WRS)	-32.0350	18.3324	97	2.86	1.09	90.00	178	1088.80	12.88
Points	ROBERTSON PP	-33.8284	19.8853	158	86.36	5.56	270.00	168	1075.76	12.46
Points	THELEMA 1: AWS	-33.9027	18.9196	431	25.12	10.80	150.99	168	1073.49	12.51
Points	VELDRESERWE	-33.6224	19.4689	281	84.35	2.17	149.19	179	1076.71	12.52
Points	VERGELEGEN BO	-34.0899	18.9077	270	7.74	2.40	166.51	168	1097.68	12.34
Polygon	Elgin_CS	-34.1652	19.0315	205	15.36	5.76	84.25	190	1086.88	12.49
Polygon	Stellenbosch_1_CS	-33.9233	18.8733	109	20.98	2.73	178.42	180	1091.98	12.30
Polygon	Stellenbosch_1_CS_HV	-33.9233	18.8733	112	20.98	5.46	183.87	181	1091.98	12.30
Polygon	Stellenbosch_1_CS_LV	-33.9233	18.8733	110	20.98	1.83	152.84	179	1078.84	12.33
Polygon	Stellenbosch_3_CS_SH	-33.8909	18.8994	358	25.52	7.25	238.06	155	1090.65	12.40
Polygon	Stellenbosch_2_CS	-33.9027	18.9196	423	25.12	8.42	165.77	171	1070.95	12.26
Polygon	Stellenbosch_2_CS_HV	-33.9027	18.9196	416	25.12	6.97	172.44	171	1068.89	12.24
Polygon	Stellenbosch_2_CS_LV	-33.9027	18.9196	429	25.12	9.08	160.43	172	1063.59	12.21
Polygon	SomersetWest_CS	-34.0899	18.9077	147	7.74	6.99	258.73	163	1076.81	12.36
Polygon	Vredendal_CS	-31.7920	18.6269	61	34.86	5.33	64.33	191	1078.90	12.34
Polygon	Vredendal_SH	-31.7920	18.6269	78	34.86	4.42	239.78	168	1066.26	12.40
Polygon	Vredendal_SH_HV	-31.7920	18.6269	80	34.86	4.47	265.84	170	1067.95	12.41
Polygon	Stellenbosch_1_SH	-33.9233	18.8733	119	20.98	2.16	154.20	180	1076.79	12.39

Addendum 6.2

Table 14 Climatic indices calculated from land surface temperature (LST) and weather station (WS) over the three growing seasons.

Season	Weather station	LST_{GST}	WS_{GST}	LST_{GDD}	WS_{GDD}	LST_{BEDD}	WS_{BEDD}	LST_{HI}	WS_{HI}	LST_{MFT}	WS_{MFT}	LST_{CI}	WS_{CI}	LST_{MMT}	WS_{MMT}	LST_{MJT}	WS_{MJT}
*S1	AAN-DE-DOORNS	17.0	20.6	1820.	2255.	1324.4	1671.	2116.	2832.	31.5	23.4	14.2	14.	27.9	21.9	31.5	23.6
S2	AAN-DE-DOORNS	18.9	20.5	2091.	2219.	1343.0	1651.	2619.	2803.	28.8	24.7	15.2	13.	25.3	21.1	29.0	24.0
S3	AAN-DE-DOORNS	19.7	20.7	2270.	2271.	1466.7	1730.	2786.	2810.	26.6	21.9	16.0	14.	26.1	22.4	29.4	24.5
S1	ELGIN: BEAULIEU	12.7	17.6	1101.	1615.	922.0	1412.	1346.	2013.	24.7	20.0	14.0	13.	22.1	19.0	26.0	20.0
S2	ELGIN: BEAULIEU	14.8	17.5	1404.	1613.	1070.1	1426.	1815.	2028.	24.7	21.3	12.8	12.	20.5	17.8	25.0	20.7
S3	ELGIN: BEAULIEU	16.0	17.9	1579.	1682.	1236.6	1517.	2014.	2083.	23.0	19.0	13.9	13.	22.7	19.7	24.6	20.9
S1	GRABOUW: OAK VALLEY	12.9	17.4	1159.	1569.	942.0	1375.	1435.	1933.	26.2	19.9	14.0	14.	23.2	19.1	27.4	19.6
S2	GRABOUW: OAK VALLEY	14.4	17.3	1376.	1559.	1030.2	1389.	1808.	1944.	25.5	21.2	13.0	13.	22.4	17.8	26.5	20.2
S3	GRABOUW: OAK VALLEY	16.3	17.8	1615.	1668.	1223.6	1506.	2080.	2068.	22.9	18.7	13.9	14.	23.3	19.7	25.8	20.8
S1	H.L.S. BOLAND	17.1	21.0	1909.	2332.	1264.3	1656.	2306.	2765.	32.5	23.5	16.4	17.	30.9	23.4	32.3	23.8
S2	H.L.S. BOLAND	19.5	20.8	2326.	2281.	1312.3	1645.	2974.	2761.	31.3	25.2	14.4	15.	26.7	21.1	31.5	23.8
S3	H.L.S. BOLAND	21.5	21.6	2675.	2452.	1427.7	1759.	3446.	2873.	29.1	22.8	16.4	16.	28.2	23.5	32.7	24.3
S1	HELDERFONTEIN	15.9	20.1	1657.	2145.	1209.9	1613.	1971.	2691.	28.7	22.8	16.1	15.	25.6	22.0	30.0	22.8
S2	HELDERFONTEIN	18.3	20.1	2103.	2135.	1326.8	1617.	2657.	2713.	28.8	24.2	15.0	13.	24.3	20.5	28.2	23.2
S3	HELDERFONTEIN	20.0	20.6	2340.	2247.	1420.4	1743.	2925.	2800.	26.3	21.8	17.1	13.	26.7	22.3	29.1	23.1
S1	HERITAGE GARDEN:	16.4	20.3	1785.	2185.	1255.4	1681.	2117.	2580.	29.4	22.4	16.2	15.	26.1	21.8	30.9	22.6
S2	HERITAGE GARDEN:	18.9	19.9	2213.	2095.	1310.7	1611.	2768.	2580.	30.2	24.0	15.8	14.	25.3	20.3	29.5	22.9
S3	HERITAGE GARDEN:	20.7	22.8	2493.	2714.	1430.3	1839.	3101.	2930.	27.6	22.3	17.6	18.	27.1	23.8	30.3	23.8
S1	KAPEL	19.9	21.3	2357.	2389.	1539.5	1746.	2686.	2873.	33.3	23.3	15.8	14.	30.4	22.7	32.5	23.0
S2	KAPEL	21.7	20.8	2717.	2294.	1504.4	1694.	3286.	2809.	32.0	24.3	16.8	13.	28.4	21.1	32.0	22.3
S3	KAPEL	23.5	22.7	3014.	2694.	1656.6	1847.	3582.	3066.	30.4	23.6	16.2	16.	28.7	24.2	33.4	25.2
S1	LANDAU	16.5	21.3	1796.	2390.	1273.7	1687.	2141.	2854.	31.4	23.6	16.1	16.	28.0	23.1	31.4	24.3
S2	LANDAU	19.0	21.0	2222.	2343.	1373.8	1655.	2795.	2836.	29.8	25.6	15.5	14.	24.9	21.1	29.1	24.1
S3	LANDAU	21.0		2547.		1481.0		3205.		27.6		16.5		26.2		30.6	

Growing season temperature (GST), Winkler index (GDD), biologically effective degree days (BEDD), Huglin index (HI), mean February temperature (MFT), Cool night index (CI), mean March temperature (MMT) and mean January temperature (MJT).

*S1=2012/13; S2=2013/14 and S3=2014/15

Table 15 Climatic indexes and indices calculated from land surface temperature (LST) and weather station (WS), over the three growing seasons.

Season	Weather station	LST_{GST}	WS_{GST}	LST_{GDD}	WS_{GDD}	LST_{BEDD}	WS_{BEDD}	LST_{HI}	WS_{HI}	LST_{MFT}	WS_{MFT}	LST_{CI}	WS_{CI}	LST_{MMT}	WS_{MMT}	LST_{MJT}	WS_{MJT}
S1	MOUNTAIN VINEYARDS	15.9	20.2	1656.8	2170.0	1197.4	1622.9	1999.2	2551.2	29.4	22.4	15.8	16.3	26.6	21.7	30.3	23.5
S2	MOUNTAIN VINEYARDS	17.6	20.3	1997.7	2187.3	1259.7	1622.4	2545.0	2617.7	29.3	24.5	14.8	16.3	24.8	21.7	28.4	23.3
S3	MOUNTAIN VINEYARDS	20.0		2349.6		1442.5		2975.2		26.8		16.8		26.6		28.5	
S1	NIETVOORBIJ	16.1	20.3	1722.5	2179.2	1217.0	1678.7	2047.5	2574.7	30.2	22.7	16.2	15.6	27.4	21.7	31.4	22.4
S2	NIETVOORBIJ	18.9	19.8	2218.8	2088.2	1336.6	1604.8	2829.4	2583.6	29.9	24.2	14.7	14.4	25.2	20.5	29.3	22.7
S3	NIETVOORBIJ	20.8	20.9	2506.6	2315.4	1452.4	1670.0	3176.0	2673.9	27.6	23.7	17.0	18.4	27.0	23.8	29.8	24.5
S1	NORTIER (WRS)	17.0	18.2	1812.5	1741.5	1379.6	1522.7	2129.0	2099.5	29.3	19.4	12.1	13.8	26.5	19.3	29.3	19.4
S2	NORTIER (WRS)	19.0	17.9	2195.7	1676.9	1396.3	1490.1	2886.5	2080.6	28.1	20.5	12.9	12.2	24.8	17.4	28.7	20.1
S3	NORTIER (WRS)	19.8	18.2	2297.7	1730.6	1500.5	1574.3	2874.6	2052.9	26.7	19.5	13.8	13.2	25.3	18.7	29.0	20.0
S1	ROBERTSON PP	15.6	20.0	1633.0	2122.2	1245.0	1634.0	1819.3	2609.6	32.7	22.8	14.4	14.0	27.3	21.2	29.6	22.9
S2	ROBERTSON PP	16.7	20.0	1806.8	2122.5	1252.5	1644.2	2120.5	2599.5	30.4	23.9	15.1	14.5	25.9	20.7	30.0	23.0
S3	ROBERTSON PP	18.0	20.5	2051.2	2215.6	1350.5	1731.0	2433.4	2660.5	29.6	21.2	16.7	15.1	26.8	22.0	31.8	24.2
S1	THELEMA 1: AWS	13.6	18.7	1183.6	1854.8	951.8	1462.8	1413.3	2317.7	25.7	21.6	15.1	15.2	22.3	20.6	25.7	21.4
S2	THELEMA 1: AWS	15.6	18.7	1595.0	1864.5	1156.8	1485.0	2015.7	2331.5	25.8	23.6	13.7	14.0	20.6	19.1	24.6	21.4
S3	THELEMA 1: AWS	17.4	19.7	1816.5	2048.3	1355.9	1644.2	2260.5	2453.1	22.8	20.5	16.0	15.8	22.7	22.0	25.1	22.4
S1	VELDRESERWE	18.6	20.8	2144.8	2288.8	1410.2	1673.3	2478.7	2770.7	33.8	23.7	16.4	15.2	29.7	22.1	34.4	23.9
S2	VELDRESERWE	20.3	21.2	2443.4	2365.9	1405.3	1714.3	2949.6	2887.3	31.0	25.1	16.4	14.8	28.0	21.7	32.2	24.2
S3	VELDRESERWE	21.6	21.6	2663.0	2455.3	1522.2	1788.9	3246.3	2952.5	29.8	22.8	17.1	15.8	28.1	23.4	32.4	25.2
S1	VERGELEGEN BO	15.4	19.3	1539.4	1973.7	1147.8	1568.9	1813.2	2246.5	27.8	21.6	16.2	17.0	24.7	21.2	29.9	21.6
S2	VERGELEGEN BO	17.9	19.2	2002.7	1960.7	1323.1	1567.7	2546.1	2263.3	27.5	23.2	14.4	15.4	23.2	19.4	27.7	22.0
S3	VERGELEGEN BO	19.5	20.2	2222.3	2160.3	1450.1	1713.4	2790.6	2464.3	26.1	21.4	15.5	16.8	25.2	22.1	27.7	22.6

Growing season temperature (GST), Winkler index (GDD), biologically effective degree days (BEDD), Huglin index (HI), mean February temperature (MFT), Cool night index (CI), mean March temperature (MMT) and mean January temperature (MJT).

*S1=2012/13; S2=2013/14 and S3=2014/15

Table 16 Continuous daily maximum (T_x) and minimum (T_n) temperature correlations for land surface temperature (LST) and weather station (WS) datasets over three years. Model analysis (calibration) and model validation (predictions) for each station over the three year period.

Weather station name	Element	all data correlation					Calibration (based on 70% of data)				Prediction (based on 30% of the data)			
		r	R^2	ICC	ICC	SEM	R^2	MSE	*r*	RMSEC	R^2	MSE	*r*	RMSEP
AAN-DE-DOORNS	T_x	0.90	0.81	0.80	0.835	3.20	0.75	10.529	0.87	3.245	0.79	35.067	0.89	5.922
ELGIN: BEAULIEU	T_x	0.88	0.77	0.82	0.845	2.49	0.74	8.043	0.86	2.836	0.76	21.029	0.87	4.586
GRABOUW: OAK VALLEY	T_x	0.88	0.77	0.779	0.827	2.85	0.76	10.264	0.72	3.204	0.78	23.67	0.88	4.865
H.L.S. BOLAND	T_x	0.89	0.79	0.698	0.784	3.98	0.76	14.461	0.87	3.803	0.79	38.002	0.89	6.165
HELDERFONTEIN	T_x	0.87	0.76	0.805	0.808	3.13	0.78	7.947	0.89	2.819	0.76	34.737	0.86	5.894
HERITAGE GARDEN:	T_x	0.81	0.66	0.657	0.731	3.71	0.74	10.098	0.86	3.178	0.59	47.47	0.77	6.89
KAPEL	T_x	0.81	0.66	0.607	0.758	3.68	0.65	11.437	0.81	3.382	0.69	61.834	0.83	7.863
KLAWER	T_x	0.67	0.45	0.546	0.624	4.91	0.32	30.204	0.57	5.496	0.44	92.277	0.66	9.606
LANDAU	T_x	0.77	0.59	0.719	0.742	3.86	0.52	18.676	0.72	4.322	0.43	70.144	0.65	8.375
MOUNTAIN VINEYARDS	T_x	0.73	0.53	0.653	0.703	4.01	0.38	25.255	0.62	5.025	0.36	68.28	0.6	8.263
NIETVOORBIJ	T_x	0.75	0.56	0.584	0.691	4.16	0.52	20.341	0.72	4.51	0.54	61.226	0.74	7.825
NORTIER (WRS)	T_x	0.39	0.15	0.236	0.346	5.85	0.12	38.094	0.34	6.172	0.12	113.494	0.35	10.653
ROBERTSON PP	T_x	0.89	0.79	0.724	0.789	3.65	0.73	12.229	0.86	3.497	0.78	41.256	0.88	6.423
THELEMA 1: AWS	T_x	0.79	0.62	0.78	0.780	3.26	0.58	14.517	0.76	3.817	0.66	40.296	0.81	6.348
VELDRESERWE	T_x	0.89	0.79	0.719	0.790	3.93	0.72	13.73	0.85	3.705	0.79	52.87	0.89	7.271
VERGELEGEN BO	T_x	0.87	0.76	0.718	0.815	2.86	2.08	8.232	0.88	2.869	0.77	27.285	0.88	5.224
AAN-DE-DOORNS	T_n	0.75	0.56	0.741	0.745	2.53	0.61	9.279	0.78	3.046	0.46	14.474	0.68	3.805
ELGIN: BEAULIEU	T_n	0.78	0.61	0.782	0.784	2.02	0.66	5.882	0.81	2.425	0.54	8.423	0.73	2.902
GRABOUW: OAK VALLEY	T_n	0.83	0.69	0.784	0.806	1.67	0.74	4.283	0.86	2.069	0.62	6.829	0.79	2.613
H.L.S. BOLAND	T_n	0.84	0.71	0.835	0.838	1.97	0.7	6.93	0.83	2.633	0.68	9.101	0.82	3.017
HELDERFONTEIN	T_n	0.78	0.61	0.724	0.772	2.30	0.63	7.734	0.79	2.781	0.53	12.249	0.72	3.5
HERITAGE GARDEN:	T_n	0.75	0.56	0.749	0.749	2.49	0.58	8.87	0.76	2.978	0.55	14.969	0.74	3.869
KAPEL	T_n	0.70	0.49	0.677	0.695	2.59	0.47	11.652	0.69	3.414	0.49	16.146	0.7	4.018
KLAWER	T_n	0.79	0.62	0.752	0.783	2.26	0.58	10.237	0.76	3.199	0.61	11.027	0.78	3.321
LANDAU	T_n	0.84	0.71	0.838	0.838	1.99	0.72	5.961	0.85	2.442	0.44	10.35	0.66	3.217
MOUNTAIN VINEYARDS	T_n	0.84	0.71	0.803	0.828	2.08	0.65	8.276	0.81	2.877	0.47	11.16	0.7	3.341
NIETVOORBIJ	T_n	0.75	0.56	0.745	0.746	2.45	0.47	10.792	0.69	3.285	0.56	13.553	0.75	3.681
NORTIER (WRS)	T_n	0.62	0.38	0.606	0.617	2.33	0.4	7.273	0.63	2.697	0.35	11.165	0.59	3.341
ROBERTSON PP	T_n	0.76	0.58	0.737	0.761	2.40	0.52	10.194	0.72	3.193	0.55	10.305	0.74	3.21
THELEMA 1: AWS	T_n	0.75	0.56	0.721	0.725	2.33	0.59	9.71	0.77	3.116	0.52	12.326	0.72	3.511
VELDRESERWE	T_n	0.81	0.66	0.792	0.802	2.08	0.73	5.76	0.85	2.4	0.57	11.166	0.76	3.342
VERGELEGEN BO	T_n	0.83	0.69	0.738	0.801	1.87	0.78	4.439	0.88	2.107	0.61	9.179	0.78	3.03

Table 17 Continuous daily mean (T_m) temperature correlations for land surface temperature (LST) and weather station (WS) datasets over three years. Model analysis (calibration) and model validation (predictions) for each station over the three year period.

Weather station name	Element	all data correlation					Calibration (based on 70% of data)				Prediction (based on 30% of the data)			
		r	R^2	ICC (agreement)	ICC (consistency)	SEM	R^2	MSE	*r*	RMSEC	R^2	MSE	*r*	RMSEP
AAN-DE-DOORNS WYNKELDER	T_m	0.92	0.85	0.859	0.883	2.059	0.84	4.758	0.92	2.181	0.83	11.757	0.91	3.429
ELGIN: BEAULIEU	T_m	0.93	0.86	0.879	0.902	1.559	0.84	3.246	0.92	1.802	0.84	6.417	0.91	2.533
GRABOUW: OAK VALLEY	T_m	0.91	0.83	0.858	0.868	1.838	0.86	3.579	0.93	1.92	0.81	9.029	0.9	3.005
H.L.S. BOLAND	T_m	0.92	0.85	0.819	0.863	2.399	0.84	6.058	0.92	2.461	0.84	13.884	0.92	3.726
HELDERFONTEIN	T_m	0.93	0.86	0.852	0.882	1.914	0.82	4.469	0.91	2.114	0.86	9.952	0.93	3.155
HERITAGE GARDEN: INFRUITEC	T_m	0.88	0.77	0.787	0.838	2.274	0.81	4.879	0.9	2.209	0.75	16.328	0.86	4.041
KAPEL	T_m	0.87	0.76	0.711	0.834	2.275	0.75	5.714	0.87	2.39	0.81	21.107	0.9	4.594
KLAWER	T_m	0.81	0.66	0.720	0.770	2.843	0.6	12.065	0.78	3.473	0.66	25.991	0.81	5.098
LANDAU	T_m	0.87	0.76	0.853	0.860	2.202	0.75	6.433	0.87	2.536	0.61	19.573	0.78	4.424
MOUNTAIN VINEYARDS	T_m	0.84	0.71	0.812	0.816	2.499	0.61	10.866	0.78	3.296	0.61	22.375	0.78	4.730
NIETVOORBIJ	T_m	0.86	0.74	0.757	0.823	2.438	0.72	7.651	0.85	2.766	0.74	18.272	0.86	4.275
NORTIER (WRS)	T_m	0.52	0.27	0.422	0.488	3.628	0.32	14.861	0.57	3.855	0.23	40.292	0.48	6.348
ROBERTSON PP	T_m	0.93	0.86	0.836	0.885	2.037	0.85	4.448	0.92	2.109	0.86	11.216	0.93	3.349
THELEMA 1: AWS	T_m	0.82	0.67	0.807	0.807	0.807	0.70	7.598	0.83	2.756	0.66	17.413	0.81	4.173
VELDRESERWE	T_m	0.92	0.85	0.803	0.853	2.425	0.85	4.759	0.92	2.181	0.84	16.711	0.92	4.088
VERGELEGEN BO	T_m	0.89	0.79	0.839	0.851	1.957	0.85	3.598	0.92	1.897	0.78	12.001	0.88	3.464

Table 18 Continuous daily growing degree days (GDD) correlations for land surface temperature (LST) and weather station (WS) datasets over three years. Model analysis (calibration) and model validation (predictions) for each station over the three year period.

Weather station name	Element	all data correlation					Calibration (based on 70% of data)				Prediction (based on 30% of the data)			
		r	R^2	ICC (agreement)	ICC (consistency)	SEM	R^2	MSE	*r*	RMSEC	R^2	MSE	*r*	RMSEP
AAN-DE-DOORNS WYNKELDER	GDD	0.77	0.59	0.745	0.747	2.635	0.42	16.722	0.65	4.089	0.65	12.929	0.81	3.596
ELGIN: BEAULIEU	GDD	0.72	0.52	0.702	0.703	2.265	0.35	13.756	0.59	3.709	0.64	7.389	0.80	2.718
GRABOUW: OAK VALLEY	GDD	0.75	0.56	0.721	0.721	2.255	0.45	12.455	0.67	3.529	0.63	8.695	0.80	2.949
H.L.S. BOLAND	GDD	0.79	0.62	0.734	0.747	2.985	0.43	21.615	0.66	4.649	0.73	16.082	0.85	4.010
HELDERFONTEIN	GDD	0.78	0.61	0.744	0.748	2.585	0.42	16.843	0.65	4.104	0.72	11.979	0.85	3.461
HERITAGE GARDEN: INFRUITEC	GDD	0.74	0.55	0.692	0.702	2.914	0.36	20.303	0.6	4.506	0.63	15.871	0.79	3.984
KAPEL	GDD	0.73	0.53	0.662	0.700	2.985	0.24	22.98	0.49	4.794	0.68	20.012	0.83	4.473
KLAWER	GDD	0.69	0.48	0.641	0.659	3.346	0.25	19.414	0.50	5.423	0.6	21.327	0.78	4.618
LANDAU	GDD	0.75	0.56	0.738	0.739	2.775	0.36	18.015	0.60	4.244	0.51	15.015	0.71	3.875
MOUNTAIN VINEYARDS	GDD	0.69	0.48	0.678	0.679	2.975	0.32	20.682	0.57	4.548	0.53	12.828	0.74	3.582
NIETVOORBIJ	GDD	0.72	0.52	0.666	0.692	2.980	0.3	21.915	0.55	4.681	0.63	16.390	0.79	4.048
NORTIER (WRS)	GDD	0.47	0.22	0.403	0.451	3.484	0.18	18.658	0.42	4.319	0.22	28.822	0.47	5.369
ROBERTSON PP	GDD	0.71	0.50	0.696	0.697	2.821	0.32	18.426	0.56	4.293	0.59	15.131	0.77	3.89
THELEMA 1: AWS	GDD	0.61	0.37	0.598	0.602	2.919	0.26	18.599	0.51	4.313	0.46	12.916	0.68	3.594
VELDRESERWE	GDD	0.78	0.61	0.716	0.729	2.983	0.41	20.405	0.64	4.517	0.66	18.781	0.81	4.334
VERGELEGEN BO	GDD	0.78	0.61	0.746	0.746	2.438	0.48	14.745	0.69	3.84	0.69	10.219	0.83	3.197

Table 19 Accumulative growing degree days (GDD_Acc) correlations for land surface temperature (LST) and weather station (WS) datasets over three years. Model analysis (calibration) and model validation (predictions) for each station over the three year period.

Weather station name	Element	all data correlation				
		r	R^2	ICC	ICC	SEM
AAN-DE-DOORNS	GDD_Acc	1.00	0.99	0.986	0.989	72.509
ELGIN: BEAULIEU	GDD_Acc	0.98	0.99	0.947	0.971	83.474
GRABOUW: OAK VALLEY	GDD_Acc	0.99	0.99	0.963	0.982	65.633
H.L.S. BOLAND	GDD_Acc	0.99	0.99	0.983	0.985	91.122
HELDERFONTEIN	GDD_Acc	0.99	0.99	0.981	0.986	80.299
HERITAGE GARDEN:	GDD_Acc	0.98	0.99	0.967	0.979	106.432
KAPEL	GDD_Acc	0.99	0.99	0.976	0.988	88.730
KLAWER	GDD_Acc	0.98	0.99	0.979	0.981	116.565
LANDAU	GDD_Acc	0.58	0.68	0.566	0.585	459.592
MOUNTAIN VINEYARDS	GDD_Acc	0.99	0.99	0.958	0.984	83.347
NIETVOORBIJ	GDD_Acc	0.98	0.98	0.975	0.975	110.862
NORTIER (WRS)	GDD_Acc	0.99	0.99	0.923	0.961	118.826
ROBERTSON PP	GDD_Acc	0.99	0.99	0.963	0.978	92.905
THELEMA 1: AWS	GDD_Acc	0.98	0.99	0.928	0.967	102.361
VELDRESERWE	GDD_Acc	1.00	1.00	0.993	0.995	54.178
VERGELEGEN BO	GDD_Acc	0.98	0.99	0.981	0.985	78.235

Chapter 7

Research results

Phenology expression of *Vitis vinifera* L. in the context of climate shifts over sites and seasons

CHAPTER 7: PHENOLOGY EXPRESSION OF *VITIS VINIFERA* L. IN THE CONTEXT OF CLIMATE SHIFTS OVER SITES AND SEASONS

7.1 Introduction

The phenomenon of phenological succession is the natural seasonal behaviour of plants, a fundamental marker of the changing seasons. Because many such phenomena are very sensitive to small variations in climate, especially to temperature, phenological records can be a useful proxy for temperature in historical climatology, particularly in the study of climate change and global warming (Jones & Davis, 2000; Parker *et al.*, 2011; Webb *et al.*, 2012; Fraga *et al.*, 2015).

The relationship between the grapevine growth cycle and climate has been studied to assess the impact of climate change on viticulture. The phenological observations provide high temporal resolution information on on-going changes related to global warming. The most recent global assessment of climate change confirms that scientific evidence points undoubtedly towards continued warming and changes in rainfall patterns (IPCC, 2014). Each of the last three decades has been successively warmer at the Earth's surface than any preceding decade since 1850 (Midgley *et al.*, 2005). Air temperature is one of the most important parameters affecting grapevine phenology, growth, and has an effect on almost every aspect of the grapevine's physiological functioning (Carey, 2001). Temperatures are expected to rise by up to 6˚C by the end of the 21st century (Luedeling, 2012), with warmer growing regions possibly experiencing less lower temperatures (required to break dormancy in the grapevine) and cooler regions becoming even cooler. Trends in bloom dates of many trees indicate that dormancy breaking processes are indeed changing, most likely in response to climate change (Legave *et al.*, 2009). It is documented in literature that the timing of phenological events have advanced, and exacerbated by a shortening of the periods between phenological events, and higher temperatures have an impact on the shortening of the season (Webb *et al.*, 2007). The impact that projected shifts in phenological timing will have on the grapevine and wine quality could be either positive or negative depending on the present climate of the region (Dry, 1988; Webb *et al.*, 2007). Phenology is shifting to earlier dates in the season on an annual basis, shifting by as much as a month earlier in certain areas (Webb *et al.*, 2007; Parker *et al.*, 2011; Webb *et al.*, 2011; Ganichot, 2002). The observed phenology of the grapevine in different localities in Europe has steadily advanced over the past 50 years with harvest now almost three to four weeks earlier and suggested warming trends are likely to continue (Jones & Davis, 2000; Jones *et al.*, 2005; Le Roux *et al.*, 2015). Mostly flowering, véraison and grape ripening are affected by climatic factors, positively correlating with temperature and negatively correlating with precipitation (Jones et al., 2000). Future temperature increases may shift grape phenology, ripening and consequently also harvest dates, and may affect grape quality and yield (Spayd *et al.*, 2002; Carey *et al.*, 2007; Webb *et al.*, 2007).

The interaction of the grapevine with its immediate environment has long been a research focus in South Africa (Buys, 1971; Le Roux, 1974; Saayman, 1977; Saayman & Kleynhans, 1978). The average annual temperature in all Western Cape viticultural regions has increased over the past 5 decades (Bonnardot & Carey, 2008; Bonnardot *et al.*, 2011), consequently grapes ripen earlier and chilling units have shifted with warmer growing regions resulting in chilling losses and cooler regions gaining chill units. Some studies showed that the phenology of Cabernet Sauvignon was predominantly affected by seasonal climate with little to no contribution of the site (Carey, 2005). The phenology of wine grape (*Vitis vinifera* L.) development is predominantly temperature-driven

(Jones & Davis, 2000; Pearce & Coombe, 2004). Matching the critical developmental phases of grapevines to a suitable climate (best-fit cultivar for a specific climate) is fundamental in the planning of any vineyard development where optimising quality is a priority (Tesic *et al.*, 2001; Webb *et al.*, 2007).

The phenophases are best correlated with budburst, which depends not only on climate and soil, but also on winter temperatures and time of pruning (Jones & Davis, 2000). Environmental factors, such as climate (rainfall, relative humidity, air temperature, soil temperature as well as the direction and intensity of dominant winds), topography (slope, exposition, sunlight exposure and landscape form) and soil (mineralogy, compaction, soil water reserve, depth, and colour), have an overriding effect on the performance of grapevines with regard to phenology, growth, yield, berry composition and wine attributes (Conradie *et al.*, 2002; Deloire *et al.*, 2005; Bonnardot *et al.*, 2011; Hunter & Bonnardot, 2011; Van Schalkwyk, 2013). Grapevine phenology varies from region to region and cultivar to cultivar (Smart & Dry, 1980). Climate is an important consideration during the choice of grapevine varieties, as each variety requires a minimum temperature summation to reach maturity (Tonietto & Carbonneau, 2004; Deloire *et al.*, 2005). According to Barbeau *et al.* (1998), precocity is a genetic characteristic of varieties and the indices used to define the phenological attributes are driven by terroir, number of days until anthesis (flowering) and véraison determined from the reference date 1st of September. The grapevine has always been very sensitive to its' environment and still fared well in the developed grape growing regions of the Western Cape. In present cooler climates, such as the Cape South coast region, future warming should allow successful ripening of varieties that were previously unsuitable.

The aim of this chapter is to correlate climate elements with phenology events to identity driving factors influencing grapevine phenology at a finer scale for two different cultivars over different sites and growing seasons. This study specifically focuses on (a) the effect of temperature and other climate elements (wind, relative humidity and rainfall) on the grapevine's response expressed as phenology; (b) monitoring of main phenological stages for a network of *Vitis vinifera* (L.) *cv.* Cabernet Sauvignon and Shiraz vineyards within different climatic environments and (c) the integration of high resolution climate and phenological data processed to better understand the interactions between phenology and variables over seasons and site. Lastly, an industry case study studying the effect of short term climate patterns on selected phenology events of different grapevine cultivars at two localities will be analysed. The outputs of the study will provide a basis for future modelling of phenology in the context of climate change.

7.2 Materials and methods

7.2.1 Locality and Vineyard site

Six sites in three well known regions, namely the Cape South Coast, Coastal and Olifants River regions (Figure 1) were chosen to represent a range of climates in which the majority of wine grapes are grown in South Africa (for more details refer to Chapter 4). Two red grapevine cultivars were selected for the study, namely Cabernet Sauvignon and Shiraz, as they are popular and two of the later ripening cultivars planted in the Western Cape. The ripening of Cabernet Sauvignon is normally considered a "late" cultivar, and Shiraz can, in some cases, even ripen with it. The inherent growth nature of the two cultivars was considered in the selection for the study, with Shiraz being near isohydric, and Cabernet Sauvignon more near anisohydric, in their responses to the direct environment, hence it is expected that Cabernet Sauvignon would have a higher water use efficiency compared to Shiraz (Schultz, 2003, Soar *et al.,* 2006). This could aid in future

adaption strategies as a basis of understanding the grapevine's response to different climatic environments and could be fitting to other cultivars with similar growth natures.

The vineyard blocks selected at each site were healthy and produced good quality red wines. Variability within vineyard blocks is an important factor that is sometimes overlooked in commercial farming when blocks are treated as a homogenous unit. Within each Cabernet Sauvignon vineyard block, three grapevine vigour plots (namely, high, medium and low) were selected using infrared aerial photography (12-15 vines selected) and monitored over the four growing seasons. Shiraz was selected as an additional cultivar in the last two seasons only, with only a medium vigour site selected in each block. However, the blocks at Vredendal contained low and high vigour plots for both cultivars. The sites selected and the vigour descriptions are shown in Table 1 (for more detail on the study sites refer to Chapter 8).

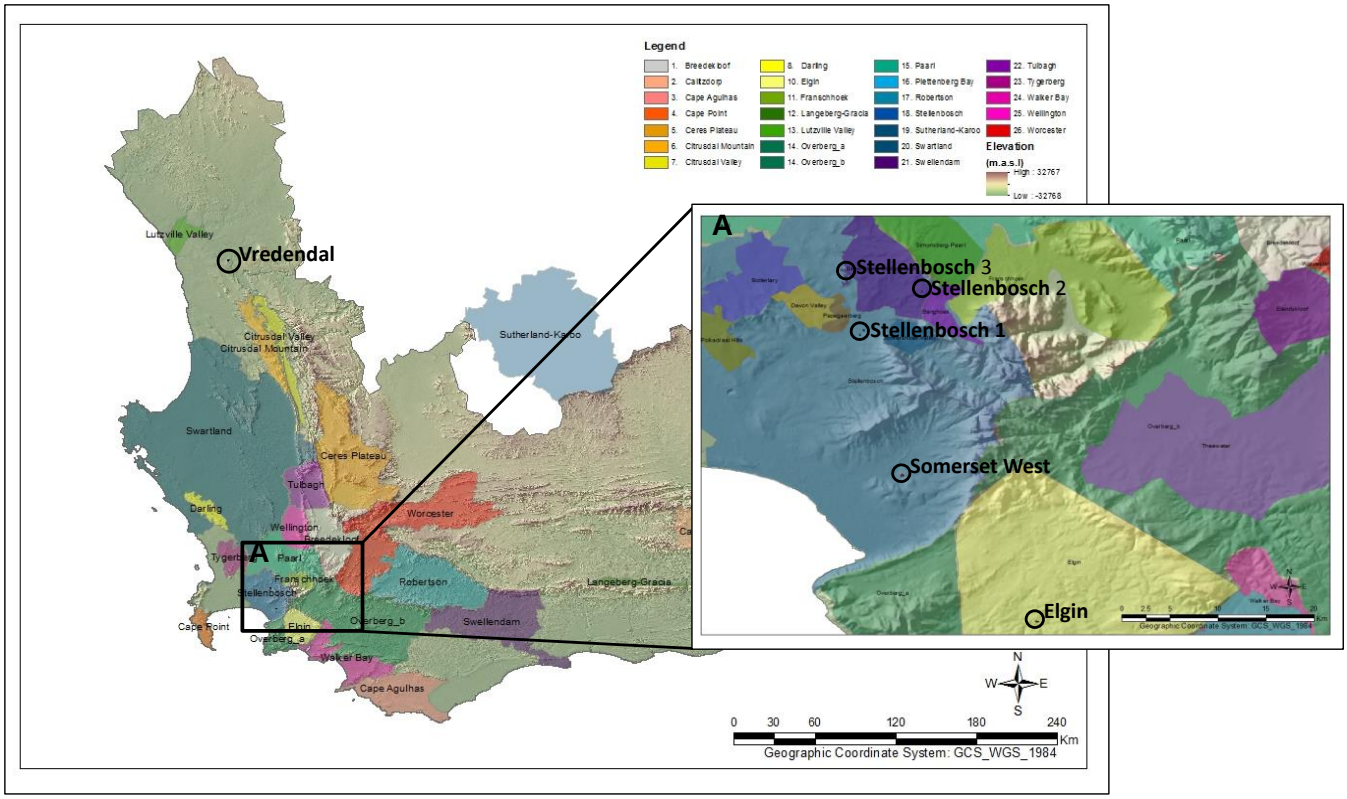

F**igure 1** Maps showing the Western Cape extent, with Districts highlighted and main study areas (A) outlined (bottom). Zoomed in sections A (right) and encircled areas show the selected sites.

Table 1 Cultivation information of the selected commercial vineyards, monitored in season one (S1): 2012/13; season two (S2):2013/14; season three (S3):2014/2015 and season four (S4):2015/2016.

Locality	Cultivar[1]	Treatment[2]	Vigour[3]	Clone	Rootstock	Row width	Vine Spacin	Planting date	Season
Elgin	CS	VSP	HV	CS 46C	101-14	2.5	1.7	2005	S1/S2/S3/S
Elgin	CS	VSP	LV	CS 46C	101-14	2.5	1.7	2005	S1/S2/S3/S
Elgin	CS	VSP	MV	CS 46C	101-14	2.5	1.7	2005	S1/S2/S3/S
Somerset West	CS	VSP	HV	CS 46C	101-14	2.8	1.4	2008	S1/S2/S3/S
Somerset West	CS	VSP	LV	CS 46C	101-14	2.8	1.4	2008	S1/S2/S3/S
Somerset West	CS	VSP	MV	CS1E	R 110	2.8	1.4	2008	S1/S2/S3/S
Stellenbosch_2	CS	VSP	HV	CS 338C	101-14	2.5	2.0	2003	S1/S2/S3/S
Stellenbosch_2	CS	VSP	LV	CS 338C	101-14	2.5	2.0	2003	S1/S2/S3/S
Stellenbosch_2	CS	VSP	MV	CS 338C	101-14	2.5	2.0	2003	S1/S2/S3/S
Vredendal	CS	VSP	HV	CS 46C	R 99	2.5	1.8	2003	S2/S3
Vredendal	CS	VSP	LV	CS 46C	R 99	2.5	1.8	2003	S2/S3
Vredendal	SH	VSP	HV	SH9C	R 99	2.5	1.8	2002	S2/S3
Vredendal	SH	VSP	LV	SH9C	R 99	2.5	1.8	2002	S2/S3
Elgin	CS	VSP	MV	CS 338C	101-14	2.5	1.7	2005	S3/S4
Elgin	SH	VSP	MV	22	101-14	2.5	1.6	2005	S3/S4
Stellenbosch_2	SH	VSP	MV	22	101-14	2.5	1.8	2001	S3/S4
Stellenbosch_1	CS	VSP	HV	CS 338C	101-14	2.5	1.4	2000	S3/S4
Stellenbosch_1	CS	VSP	LV	CS 338C	101-14	2.5	1.4	2000	S3/S4
Stellenbosch_1	SH	VSP_EarlyPrune	MV	SH9C	101-14	2.7	1.5	2000	S3/S4
Stellenbosch_1	SH	VSP_LatePrune	MV	SH9C	101-14	2.7	1.5	2000	S3/S4
Stellenbosch_3	CS	VSP	MV	CS 337C	101-14	2.5	1.5	2001	S3/S4
Stellenbosch_3	SH	VSP	MV	SH9C	101-14	2.5	1.8	2001	S3/S4

[1]CS: Cabernet Sauvignon, SH: Shiraz; [2]VSP: Vertical shoot positioning; [3]HV: high vigour, MV: medium vigour, LV: low vigour.

7.2.2 Environmental conditions

Hourly air temperature, humidity, wind speed and rainfall data was obtained from the nearest automatic weather station stations (AWS) of the Institute for Soil, Climate and Water (ISCW) of the Agricultural Research Council (ARC), Pretoria. In addition, ambient temperature and relative humidity was measured at 30 minute intervals using a temperature/relative humidity sensor (Tinytag® model TGP-4500, Gemini Data Loggers, West Sussex, United Kingdom) housed in a radiation shield (Tinytag® model LS-1, Gemini Data Loggers, West Sussex, United Kingdom), placed above the grapevine canopy.

Climatic indices (Winkler Index, Huglin Index, Biologically effective degree days, average growing season temperature, mean January, February and Cool night index) were calculated both on a macroclimatic (monthly, seasonal) and a mesoclimatic (daily and hourly) temporal scale (Amerine & Winkler, 1944; Tonietto & Carbonneau, 2004; Anderson *et al.*, 2012). Refer to Chapter 2 for more detail about the climatic indices and their calculation and to Chapter 4 for more information about further climate data processing.

7.2.3 Phenology monitoring and the precocity index

The beginning of each phenological stage was determined visually for every site. These phenological stages were defined according to the E-L phenological system developed by Eichhorn & Lorenz as adapted by Coombe (1995). For the purpose of this study, the budburst date was determined at E-L 4 (green tip; first leaf tissue visible), anthesis (flowering) at E-L 23 (17 to 20 leaves separated; 50% caps off), pea size at E-L 31 (berries pea size, 7 mm in diameter), bunch closure just after E-L 32 (bunch closed completely, berries touching), pre-véraison at E-L 34 (berries begin to colour and enlarge), 50% véraison at E-L 36 (berries with intermediate sugar and 50% berries are coloured and enlarged) and véraison at E-L 37 (all berries coloured but not quite

ripe). Grapes were considered ready for harvest (E-L 38; berries harvest-ripe) when berries reached total soluble solids (TSS) concentrations of 23-24°Brix (more information in Chapter 8) so that the time of harvest for all the plots was standardised according to one variable. Phenology was recorded at the different stages at sites over seasons, and data was processed into four phenology groups for the purpose of this study, as described in Table 2. “Phenology 1” represents the calculated precocity index, “phenology 2” denotes calculated as phenological stage dates based on days after 1st of September, “phenology 3” represents the days after budburst for each phenological stage at each site and lastly “phenology 4” represents the amount of days between each phenological stage.

Table 2 Description of the phenology groupings 1 to 4 used in further analysis, showing phenological indices and stages in each grouping.

Phenology 1	Precocity index of flowering (iPf)		Precocity index of véraison (iPv)			Precocity index of the annual cycle (iPcy)		
Phenology 2 (phenology stage as days after 1 September)	BB - 1Sept	Flowering - 1Sept	Pea Size - 1Sept	Bunch Closure - 1Sept	Pre Véraison - 1Sept	Véraison_50%- 1Sept	Véraison_100% - 1Sept	Harvest - 1Sept
Phenology 3 (phenology stage as days after budburst)	Flowering - BB	PeaSize - BB	Bunch Closure - BB	Pre Véraison - BB	V50% - BB	V100% - BB	Harvest - BB	
Phenology 4 (days between phenology stages)	BB to FL	FL to PS	PS to BC	BC to PrV	PrV to V	V to Ver	Ver to H	

Budburst (BB), date measured from (1 Sept), flowering (FL), pea size (PS), bunch closure (BC), pre véraison (PrV), 50% véraison (V), 100% véraison (Ver), harvest (H).

Sites and seasons were compared using indices of precocity developed by (Barbeau *et al.*, 1998) for *cv.* Cabernet franc which were also applied to *cv.* Cabernet Sauvignon by Tesic *et al.* (2001). The indices are used to define the phenological attributes driven by terroir, the number of days until anthesis (flowering) and véraison determined from the reference date 1st of September. The precocity index of flowering (iPf), véraison (iPv) and the phenology cycle (iPcy) describe the phenology per site. The index is based on a baseline of 100, representing a “mean phenological date” of the vintage for all sites per cultivar, which then gives an indication of whether the site is phenologically early (>100) or late (<100). Using this index therefore highlights the extent of the advance or delay over sites and seasons. The iPcy serves as a prediction of the date of harvest according to the dates of flowering and véraison to determine if full ripeness will be reached in a vintage. This is specifically applicable in the Northern Hemisphere, where later vintages are associated with low sugar levels and difficulty to reach optimal ripeness.

The index for precocity of flowering (IPF) for the site j was calculated as:

$$iP_f = 100 \times [1 + \frac{F_m - F_j}{F_m}]$$

Where Fm represents the mean date of flowering for all the studied sites (N=16) and Fj the date of flowering of site j.

The precocity index for the cycle (iPcy) was calculated as:

$$iP_{cy} = iP_f + 100 \times \left[(V_m - F_m) - (V_j - F_j)\right]/(V_m - F_m)$$

Where Vm and Fm represent the mean dates of véraison and flowering, respectively for all the study sites, and Vj and Fj represent the date of véraison and flowering respectively, for the selected site.

7.2.4 Statistical analysis

Mean comparisons of measured variables between sites were compared using one-way ANOVA. Kruskal-Wallis non-parametric statistics were also calculated and reported. Comparisons between seasons were done using mixed model ANOVA where the season effect was treated as fixed, and the sites as random effect. Post hoc testing was done using Fisher least significant difference (LSD). Correlations between variables were tested using Pearson correlations. Multivariate relationships between blocks of variables were described using multiple factor analysis (MFA). RV coefficients were calculated between blocks and used as inputs for cluster analysis with the purpose of clustering similar blocks of variables. All analyses were conducted using Statistica 13 ® software (Statsoft, Tulsa, UK) except for the MFA analyses which were done using the R function “MFA” within the package “FactoMineR”.

The grouping of variables used for the multifactor analysis are described in Table 15 in Addendum 7.1, and compared to the types of phenology described in Table 2.

7.3 Results and discussion

7.3.1 Climatic variability between sites

The average annual temperature in all Western Cape viticultural regions has increased over the past five decades (Refer to Chapter 4), affecting grapevine growth and ripening responses. The most evident climatic changes noticed over the four seasons and six sites (more detail described in Chapter 4) were: a) increases in mean January temperatures, b) mean February temperature remained comparable over all the seasons, c) decrease in March mean temperatures, with 2015/16 being the coolest of all the seasons, and d) lower cool night index (minimum March temperature) with the exception of an increase only in 2014/15 season for the Somerset West and Stellenbosch sites. Early spring temperatures cooled down over the four seasons of the study. Rainfall was variable but showed a shift to more summer rainfall overall. It was observed that the 2013/14 season received more than double the annual rainfall, mostly received in summer months (Refer to Table 6 in Chapter 4 for more detail).

The bioclimatic indices describe the growing season for Elgin and Stellenbosch 3 to be the coolest sites, Stellenbosch 2 and Somerset West warm, and lastly Stellenbosch 1 and Vredendal as the hottest sites over the climatic band (see Table 6 in Chapter 4). Bioclimatic indices such as GDD (Winkler Index) and the growing season temperature (GST) index showed increases with every season in the time frame of this study. The true climatic conditions at the sites affecting grapevine reaction cannot be described only using temperature as a factor, but other environmental factors such as rain, relative humidity and wind, as described in Chapter 4.

7.3.2 Site and seasonal phenology

The four main phenological stages of the phenology 2 cluster (described in Table 2), defined as phenological stages after 1 September, are represented in Figure **2** and Figure 3, namely budburst, flowering, 50% véraison and harvest, grouped over four seasons and cultivars (Cabernet Sauvignon and Shiraz). Somerset West had the earliest budburst at 14 days from 1 September,

significantly different to the Stellenbosch sites. Stellenbosch 3 had the latest budburst date (30 days after 1 September), significantly different to all the other sites with the exception of Stellenbosch 1 which was comparable (Table 16 in Addendum 7.1). The date of flowering was more comparable over sites, showing less site variability. Only the warmest site at Vredendal was highlighted to be significantly different to the all the other sites where the flowering date was 36 days earlier than the other sites.

The phenology stage of 50% véraison was significantly later at the coolest site Elgin, compared to all of the other sites with the exception of Stellenbosch 3 (which was also a relatively cooler site). For harvest, the warmer sites namely Stellenbosch 1 and Vredendal were comparable to one another (Figure 3) and significantly different to the other sites (Table 16 in Addendum 7.1). The warmer site seemed to have had the shortest seasons, with budburst not being much earlier, but resulted in earlier ripening.

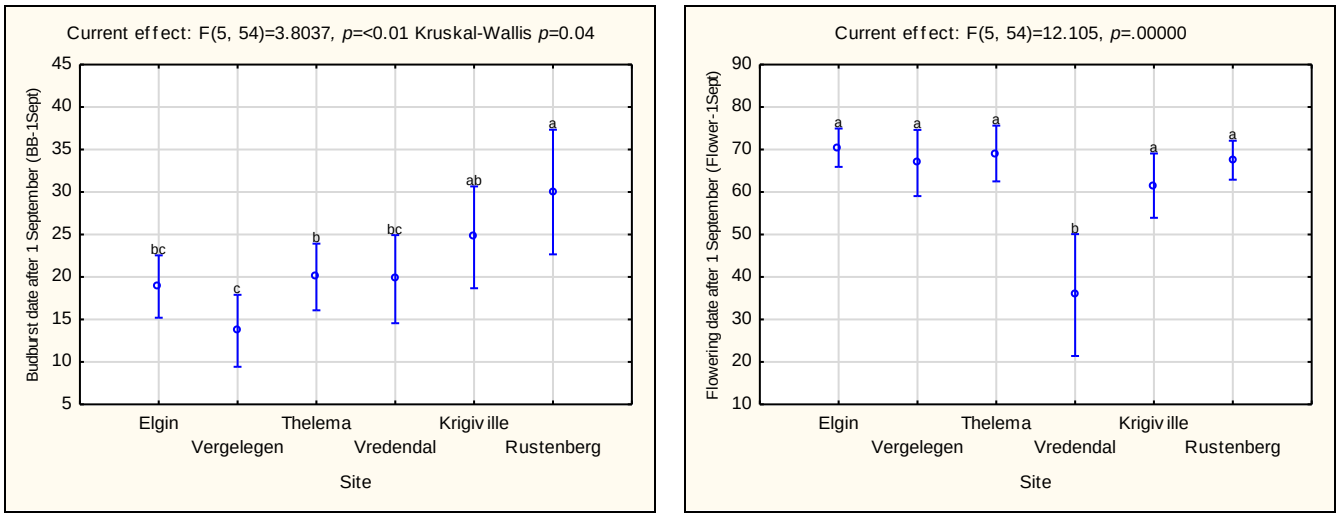

Figure 2 Comparison of study sites over four seasons and two cultivars (Cabernet Sauvignon and Shiraz) for budburst date after 1 September (BB-1Sept) on the left, and flowering date after 1 September (flowering-1Sept) on the right. Vertical bars denote 0.95 confidence intervals. Same letters are not significantly different at the $p \leq 0.05$ level.

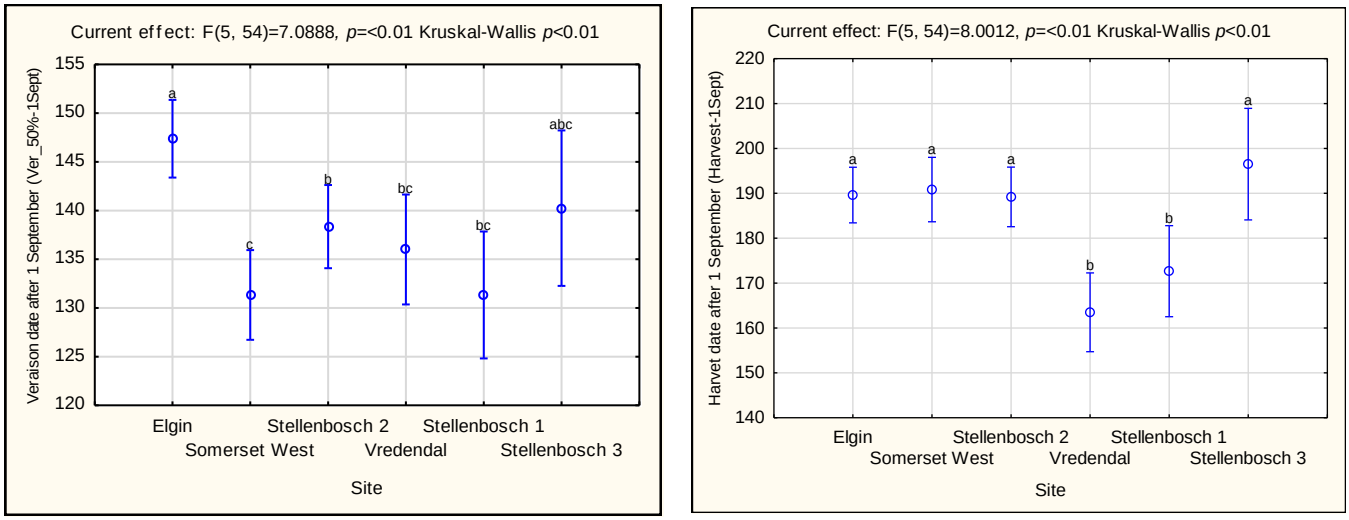

Figure 3 Comparison of study sites over four seasons and two cultivars (Cabernet Sauvignon and Shiraz) for 50% véraison date after 1 September (véraison_50%-1Sept) on the left, and for harvest date after 1 September (harvest-1Sept) on the right. Vertical bars denote 0.95 confidence intervals. Same letters are not significantly different at the $p \leq 0.05$ level.

The number of days between phenological stages seem to be shifting in conjunction with climate warming. The question as to when and why still remains unanswered. The warmest site (Vredendal) had the shortest period between budburst and flowering, significantly different to all the other sites. Stellenbosch 1 and Stellenbosch 3 were comparable in terms of days between budburst and flowering but were significantly less than the other sites. This could be due to budburst of Stellenbosch 3 being the last of the sites, and the warmer temperatures shortening the period between budburst and flowering (Figure **2**). The time frame between flowering and pea size was significantly longer for Vredendal compared to the other sites, with no significant differences for the period pea size to bunch closure (Table 16). The longest period from the start of véraison to the end of véraison (all the berries coloured) was for Stellenbosch 3, at 23 days, significantly different to Vredendal with the shortest period of eight days. The final stage between 100% véraison and harvest was the longest at Somerset West and the shortest at Vredendal. The delay of ripening at Somerset West could be due to wind either limiting grapevine functioning (strong winds) or the cooling sea breeze effect compared to the warmer conditions at Vredendal where sugar loading could be faster. Elgin, the cooler site, was significantly different to the warmer sites but comparable to Stellenbosch 1 and 3 sites at approximately a period of 28-32 days, which could be ascribed to the cooling sea breeze effect on ripening and elevation. The warmer sites were significantly different to the cooler sites; hence temperature and factors affecting temperature were the drivers for grapevine phenology (Table 16 in Addendum 7.1).

Seasons showed significant differences in the phenological stages after 1 September ($p \leq 0.01$) over the four year study period. The seasonal budburst, flowering and pea size shown in Figure 4 and Table 17 in Addendum 7.1 were comparable for the first two seasons (2012/13 & 2013/14) and was significantly different from the last two seasons (2013/14 & 2014/15). Seasons 2012/13 and 2013/14 had later budburst, flowering and pea size compared to 2014/15 season, with season 2015/16 being the earliest.

Seasonal trends started to shift with regards to bunch closure, with significant differences between seasons. In the 2014/15 season, bunch closure was the earliest by *c.* 15 days, whereas the 2012/2013 season had the latest bunch closure (Table 16 in Addendum 7.1). Pre-véraison was significantly different for all the seasons, except the last season. Véraison at 50% (Figure 5) showed that the 2012/13 and 2013/14 seasons were comparable (later). Likewise, the 2014/15 and 2015/16 seasons (earlier) were comparable. There was a significant difference between the first two seasons and the last two seasons. Figure 5 shows véraison to be 14 days later for the 2012/13 and 2013/14 seasons compared to the last two seasons (2014/15 and 2015/16), with the earliest season being 2014/15. Time of harvest seemed to be comparable for all the seasons, with the exception of the 2014/15 season which was the earliest harvest by about 20 days (Figure 5 & Table 16 in Addendum 7.1).

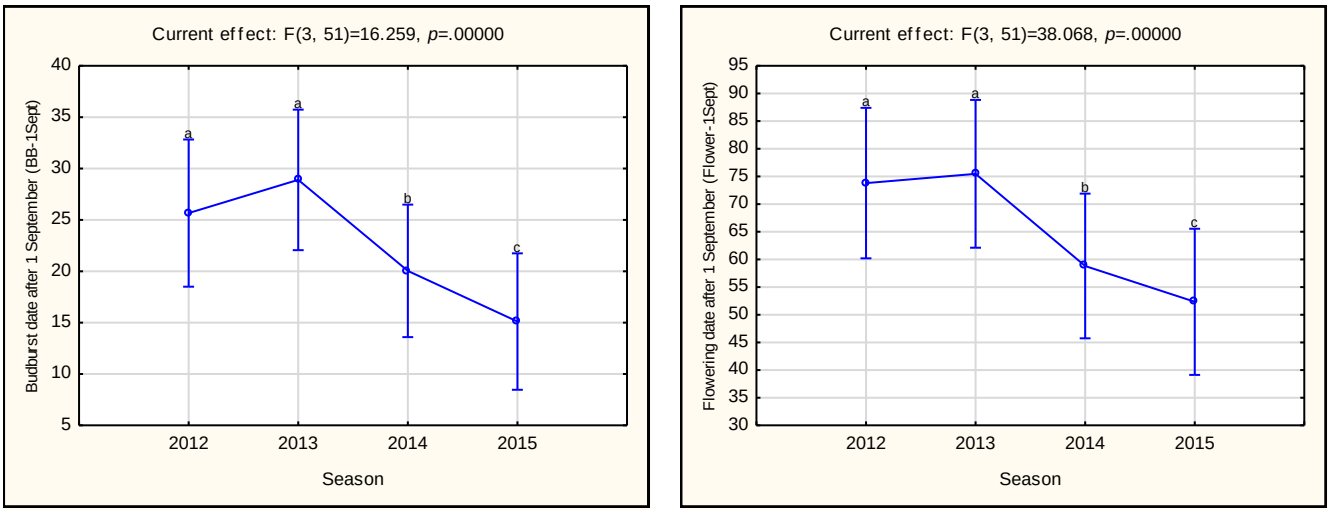

Figure 4 Comparison of study seasons over six sites and two cultivars (Cabernet Sauvignon and Shiraz) for budburst date after 1 September (BB-1Sept) on the left, and for flowering date after 1 September (flowering-1Sept) on the right. Vertical bars denote 0.95 confidence intervals. Same letters are not significantly different at the $p \leq 0.05$ level.

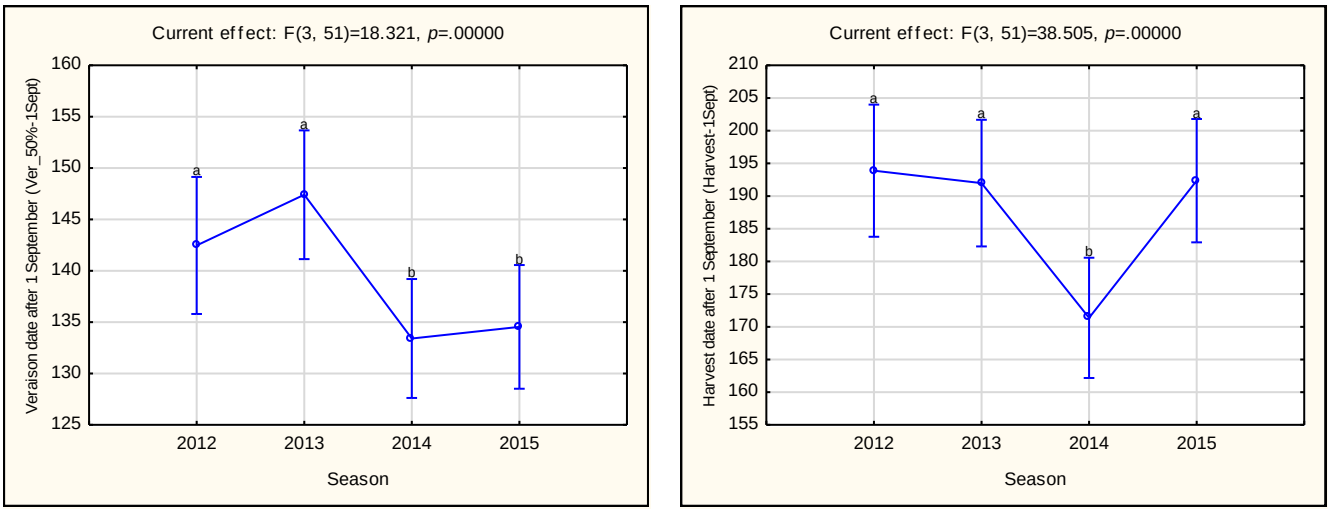

Figure 5 Comparison of study seasons over six sites and two cultivars (Cabernet Sauvignon and Shiraz) for 50% véraison date after 1 September (véraison_50%-1Sept) on the left, and for harvest date after 1 September (harvest-1Sept) on the right. Vertical bars denote 0.95 confidence intervals. Same letters are not significantly different at the $p \leq 0.05$ level.

The number of days between the phenological stages over the seasons gives a more detailed understanding of the possible environmental factors affecting phenology. Figure 6 (left) describes the period between budburst and flowering (BB/FL), which showed a decreasing trend over the seasons, with the first two seasons being significantly longer than the last two seasons (Table 16 in Addendum 7.1). The period between flowering and pea size (FL/PS) showed an increasing trend over the four seasons, with the 2015/16 season being significantly different to the previous seasons (Figure 6). This highlighted possible correlations with increased temperatures over the seasons. The period between pea size and bunch closure (PS/BC) and bunch closure and pre-véraison (BC/PreV) were comparable for the first three seasons (Figure 6), with the 2015/16 season being significantly later and earlier for PS/BC and BC/PreV, respectively, with a standard deviation of about 6 days for both stages (Table 16 in Addendum 7.1).

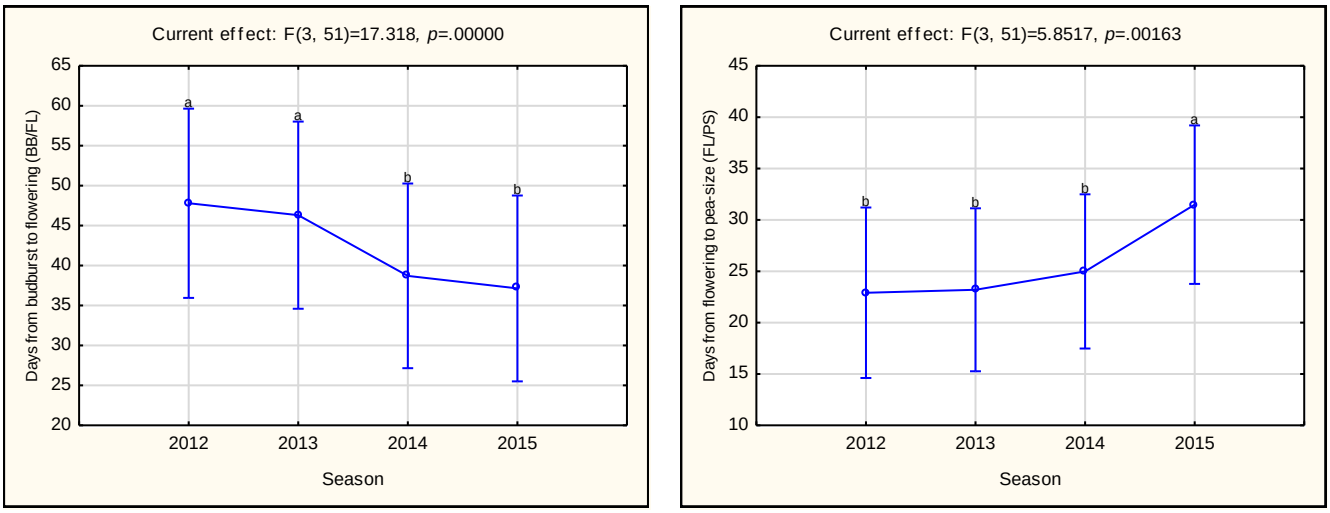

Figure 6 Comparison of study seasons over six sites and two cultivars (Cabernet Sauvignon and Shiraz) for days between budburst and flowering (BB/FL) on the left, and for days between flowering and pea-size (FL/PS). Vertical bars denote 0.95 confidence intervals. Same letters are not significantly different at the $p \leq 0.05$ level.

The start of véraison to full colouring (V/Ver), shown in Figure 7, had a similar trend of increasing over the seasons as shown in Figure 6. The first two seasons were comparable, but significantly earlier than the last two seasons, ranging from 10-22 days difference from the first to the last season. The inverse trend was seen for the ripening period from véraison to harvest [Figure 7 (right)]. The period became significantly longer over the seasons, which could be due to the trend of February and March temperatures decreasing in the last few seasons. This is an important phenological period for colour and flavour development. The longest period was in the 2012/13 season, which was significantly different to the 2014/15 and 201516 seasons, with the shortest period being for the 2014/15 season.

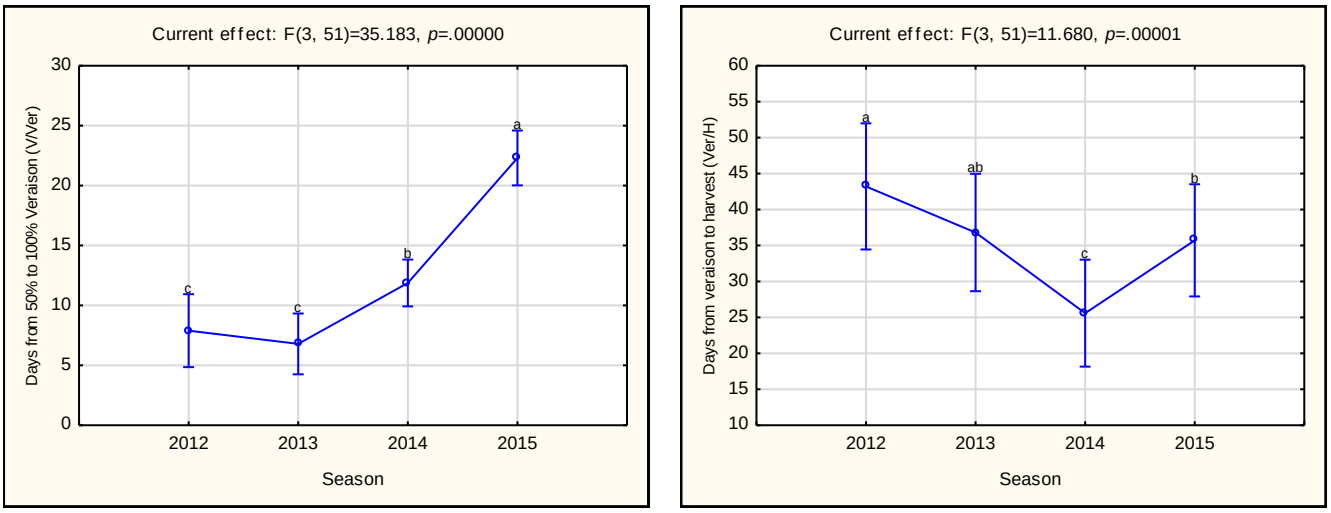

Figure 7 Comparison of study seasons over six sites and two cultivars (Cabernet Sauvignon and Shiraz) for days between 50% véraison and 100% véraison (V/Ver) on the left, and for days between 100% véraison and harvest (Ver/H). Vertical bars denote 0.95 confidence intervals. Same letters are not significantly different at the $p \leq 0.05$ level.

7.3.3 Precocity indices

As can be seen in Table 18 in Addendum 7.1 and Table 19, the phenological dates per phenological stage per site differed significantly, not only between sites per index, but also between seasons, as indicated by the standard deviation (SD) values. It is expected that if a site is delayed or advanced in terms of one of the indices, it will remain delayed or advanced for the other indices and phenological stages; this was not seen over the climatic band selected. The IPF index was significantly different, over seasons (Table 3) and cultivars (Table 4); hence the precocity of flowering was the most variable in the study. The IPF index indicated advanced flowering at Vredendal and Somerset West (possibly more constraints on the plant earlier in the season) and delays for the other sites (Figure 8). The IPV and IPCY were not significantly different for sites and seasons. However, the IPV indicated delays in véraison for all the sites especially Somerset West, and advanced véraison at only the Elgin site. The IPCY indicated an earlier harvest for all the sites, was ascribed to the increased thermal accumulation over the seasons for the period of the study, with the exception of Elgin that had a delayed harvest. The delayed harvest at Elgin was probably due to the cooler conditions at the Elgin site (Figure 8).

The IPF for the Elgin site was significantly different to the Somerset West and Vredendal sites which were the warmer sites, hence there was earlier flowering (above the base line of 100). Overall, the Vredendal site was significantly different from all the other sites, having the earliest flowering at a precocity index of 132 IPV and the latest flowering at 91 for Elgin and Stellenbosch 1 (Figure 8 & Table 3). The weighted means showed the largest variability in flowering to be at Vredendal and Stellenbosch 1, which was due to the inclusion of both cultivars in the analysis. The precocity of véraison was significantly later for Elgin compared to other sites and Somerset West was significantly advanced compared to all sites but comparable to Stellenbosch 1 (Figure 8).

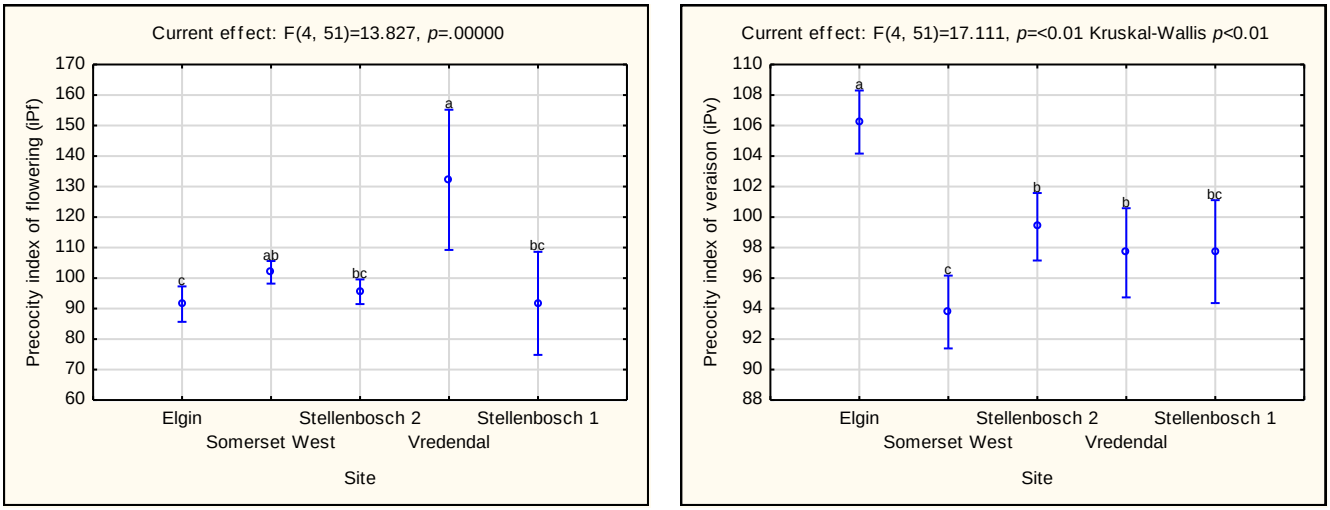

Figure 8 Comparison of study sites over four seasons and two cultivars (Cabernet Sauvignon and Shiraz) for the precocity index of flowering (iPf) on the left, and for precocity index of véraison (iPv) on the right. Vertical bars denote 0.95 confidence intervals. Same letters are not significantly different at the $p \leq 0.05$ level.

Large vintage variability was observed for the IPCY index with the Elgin site being the most delayed and significantly different to the other sites. Somerset West and Vredendal were comparable and were significantly more advanced than the other sites (**Figure 9**). Vredendal is classified as the warmest site according to the bioclimatic indices, and therefore had the earliest flowering and harvest compared to the later Elgin and Stellenbosch 3. The IPF is related to IPCY: earlier flowering resulted in an earlier harvest as seen at Somerset West and Vredendal, late

flowering resulted in a later harvest as seen at Elgin. The IPV, however, contradicted the IPF and the IPCY index, which could possibly be explained on an individual vineyard level by investigating factors such as canopy management, water status of the grapevine *etc.* The IPF and IPCY seemed to be more reactive to climate over sites and seasons than the IPV.

The IPF showed significant variability over seasons (Table 3), having shifted over the seasons, with the 2013/14 flowering being the latest and the 2015/16 season showing the earliest flowering (mean difference of 15.37 days) (Table 20 in Addendum 7.1). The IPCY showed the 2013/14 season to be significantly later than the 2015/16 season with a 7.05 days mean difference. The 2013/14 season had a later harvest and 2015/16 slightly earlier than the other seasons, which could be ascribed to the increase in January temperatures.

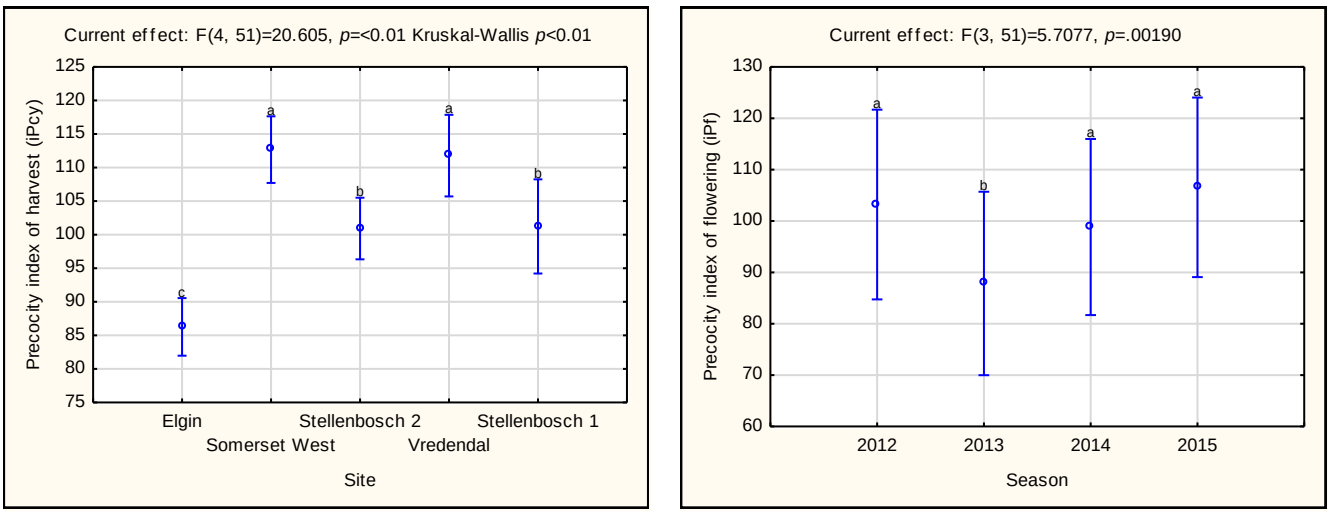

Figure 9 Comparison of study sites over four seasons and two cultivars (Cabernet Sauvignon and Shiraz) for the precocity index of harvest (iPcy) on the left, and for precocity index of flowering (iPf) on the right for seasons over the six sites and two cultivars. Vertical bars denote 0.95 confidence intervals. Same letters are not significantly different at the $p \leq 0.05$ level

Table 3 Least significant distance (LSD), based on probabilities of the Post Hoc test and showing simultaneous confidence intervals for precocity index of seasons, only significant values shown, the fixed effect test was only significant for the IPF index ($p \leq 0.005$) and IPCY ($p \leq 0.05$).

Precocity index	Comparison of seasons		Mean Difference	Standard Error	*p*	Confidence Intervals	
	1st Mean	2nd Mean				-0.95	0.95
IPF	2012	2013	15.37	5.27	0.01	4.78	25.96
IPF	2013	2014	-10.98	4.27	0.01	-19.56	-2.40
IPF	2013	2015	-18.71	4.68	0.00	-28.10	-9.31
IPCY	2013	2015	-7.05	3.32	0.04	-13.72	-0.38

7.3.4 Cultivar differences in phenology

Cabernet Sauvignon is normally a later ripening red cultivar compared to Shiraz, this was confirmed in the phenology over all the sites, with the exception of the 2015/16 season where Cabernet Sauvignon ripened before Shiraz (data not shown). The expected variability in phenology was not seen in the precocity indexes for Cabernet Sauvignon and Shiraz as described in Table 4. Statistically there were no significant differences in the cultivar precocity index to merit the separate analysis over sites and seasons for the purpose of this study. These results highlighted the overall seasonal variability to be the driving factor that affected phenological stages.

Cabernet Sauvignon had a later flowering time and pea size compared to Shiraz (Figure 10 and Table 4). However, the period lengths between the different phenological stages of the two cultivars varied. The period between flowering and pea size was shorter for Cabernet Sauvignon than for Shiraz, whereas the period between véraison and harvest was longer for Cabernet Sauvignon compared to Shiraz. Even with the slight cultivar variability in phenological timing and the period between stages, the climate in seasonal variability seemed to an overriding factor driving phenology for the two cultivars.

Table 4 Precocity index comparison of Cabernet Sauvignon over the four seasons and six sites and Shiraz for two seasons and five sites, $p \geq 0.01$ assuming equal variance.

Precocity	Cultivar	N	Mean	Std.Dev.	Std.Err	-0.95	0.95
IPF	Cabernet Sauvignon	48	99.21	16.14	2.33	94.53	103.90
IPF	Shiraz	12	100.00	28.02	8.09	82.20	117.80
IPV	Cabernet Sauvignon	48	100.00	6.60	0.95	98.08	101.92
IPV	Shiraz	12	100.00	2.84	0.82	98.20	101.80
IPCY	Cabernet Sauvignon	48	100.00	14.05	2.03	95.92	104.08
IPCY	Shiraz	12	100.00	10.61	3.06	93.26	106.74

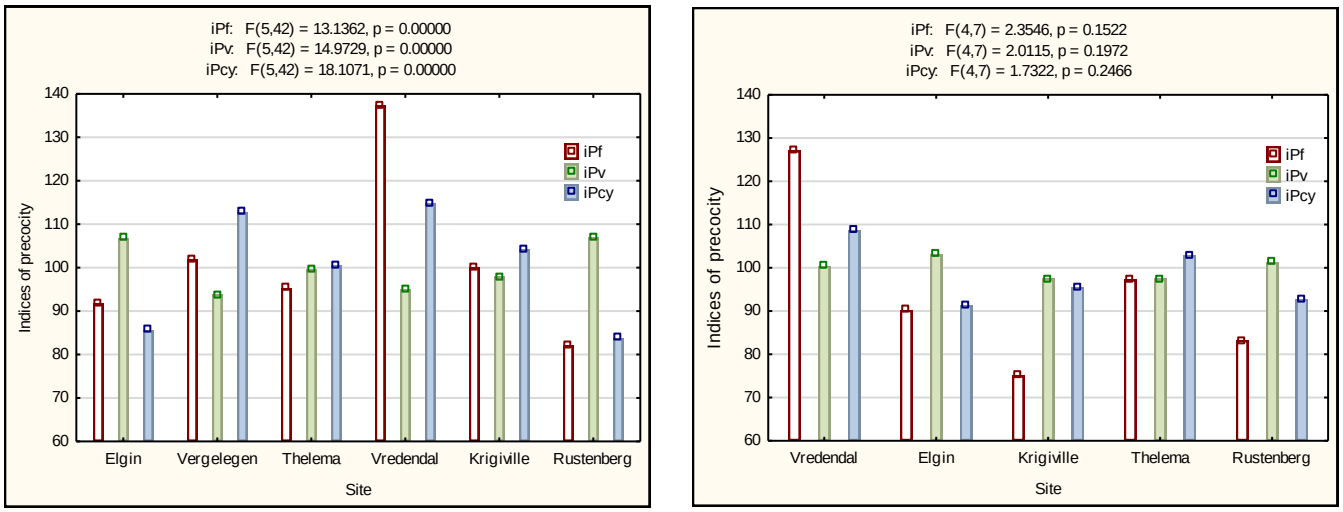

Figure 10 Mean indices of precocity for Cabernet Sauvignon (left) and Shiraz (right) over the different sites, for IPF $p \geq 0.54$, IPV $p \geq 0.76$ and IPCY $p \geq 0.93$.

7.3.5 Multifactor analysis

Multifactor analysis (MFA) isolated the possible driving factors between several climate data blocks affecting grapevine phenology. Due to the size of the dataset and variables compared, only the strong significant interactions will be discussed further. Multidimensional factor analysis on all blocks is presented in Figure 11, along with the final configurations of all the variables and their possible interaction with the phenology grouping (described in Table 2) in the comparison of dimensions (1 and 2). The final cluster analysis based on RV coefficients from the MFA resulted in a tree diagram for 70 variables, assigning cluster identifications for correlation analysis (Figure 12). Results showed two main clusters below the set linkage distance of significance (3.0). Cluster 1 includes the block variables strongly related to phenology 1 and 2 and the second cluster includes the block variables strongly related to phenology 3 and 4 (Figure 12). The phenology clusters 1 and 2 were driven by the climatic factors for the seasons. However, phenology 3 and 4 were driven by temperature changes over sites and seasons. The variables calculated from loggers seemed to

not have a strong influence on the phenology, compared to the climatic indices, relative humidity and temperature from the automatic weather stations.

Cluster 1: Phenology 1 and 2 (black outline) are the precocity indexes and phenological date after 1 September, respectively. It indicates a relationship using a reference date for site and seasonal comparison, linking strongly to the variables explaining site climatic properties. Specifically, relative humidity in the month of September (9_RH), climatic indices calculated from daily and hourly data and lastly rainfall.

Cluster 2: Phenology 3 and 4 (red outline) are the phenological dates after budburst date, and the number of days between phenological stages, respectively. Phenology 3 and 4 seemed to be more temperature sensitive, especially in January, February, May, April, March, December, July, June and November (listed in order of interaction, strongest first).

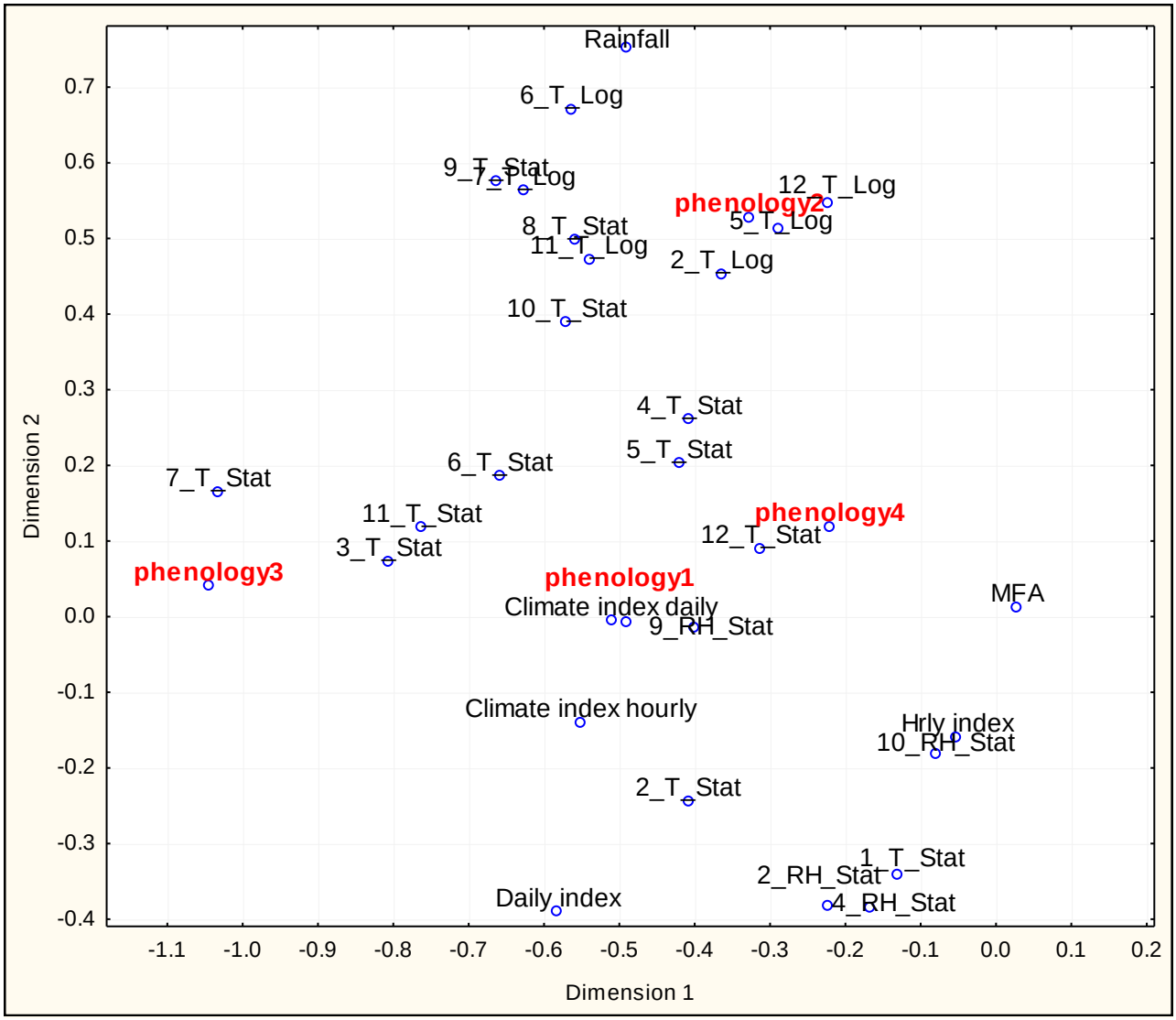

Figure 11 Final configuration of multidimensional factor analysis (MFA) on all block variables for dimension 1 vs dimension 2.

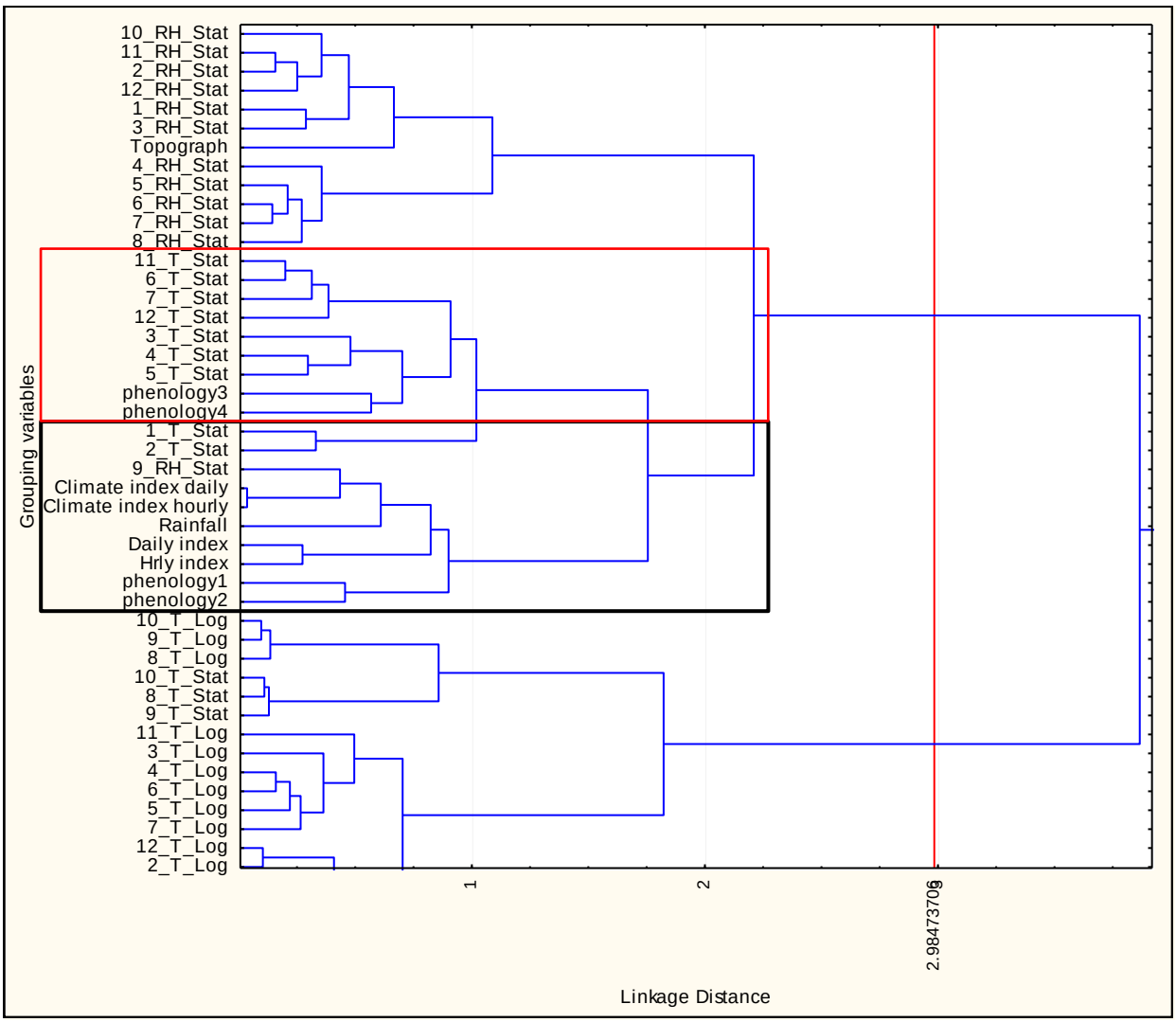

Figure 12 Tree diagram for 70 group variables, from the Wards method cluster analysis based on RV coefficients (1-Pearson *r*). Linkage distance of interaction is 2.9. Clusters in the black and red outline will be discussed as area and interaction of interest.

7.3.6 Correlations between block variables

The variables that were compared in the correlation circle analysis were based on the two cluster groupings of phenology and climate interactions, *i.e.* cluster 1 (black) and secondly cluster 2 (red) as shown in Figure 12 (from the tree diagram). The total amount of data represented in each cluster and variables within the cluster is shown in Table 5, indicating the total percentage of the data population represented on dimension 1 and 2 of the correlation circles discussed further on in the chapter. The RV coefficients measure the closeness of the two sets of points that are each represented in the matrix (Figure 11 & Table 5). Relationships between the block variables from the multifactor analysis are presented as quantitative variables as in principle component analysis (PCA), presented as a correlation circle for each block variable with high RV coefficients of the relationship (Table 6).

Table 5 Correlation circle analysis, percentage data represented on dimension 1 and dimension 2 for the significant interactions of variables listed for cluster 1 and 2 presented in the tree diagram. Strength of interaction between grouped variables is represented as RV coefficients.

Cluster 1	Phenology 1			Phenology 2			Phenology 1	Phenology 2
	Dim 1 (%)	Dim 2 (%)	All (%)	Dim 1 (%)	Dim 2 (%)	All (%)	RV	RV
9_RH_Stat vs Phenology1 & Phenology	50.7	24.3	75.0	53.0	15.0	68.0	0.24	0.40
Climate index daily vs Phenology1 &	64.4	19.9	84.3	65.2	12.3	77.5	0.30	0.61
Climate index hourly vs Phenology1 &	69.7	16.9	86.6	66.0	12.1	78.1	0.38	0.56
Daily index vs Phenology1 & Phenology	56.2	16.8	73.0	48.2	21.0	69.2	0.29	0.27
Hrly index vs Phenology 1 & Phenology	45.4	17.4	62.8	38.8	17.9	56.7	0.42	0.40
Rainfall vs Phenology 1 & Phenology 2	56.8	28.0	84.8	61.3	13.5	74.8	0.19	0.50
Cluster 2	**Phenology 3**			**Phenology 4**			**Phenology 3**	**Phenology 4**
	Dim 1 (%)	**Dim 2 (%)**	**All (%)**	**Dim 1 (%)**	**Dim 2 (%)**	**All (%)**	**RV**	**RV**
1_T_Stat vs Phenology 3 & Phenology 4	47.5	28.5	**76.0**	42.3	17.1	**59.4**	0.33	0.39
2_T_Stat vs Phenology 3 & Phenology 4	48.6	24.6	**73.2**	39.3	17.0	**56.3**	0.35	0.31
3_T_Stat vs Phenology 3 & Phenology 4	51.7	24.9	**76.6**	39.7	19.4	**59.1**	0.51	0.38
4_T_Stat vs Phenology 3 & Phenology 4	49.5	22.6	**72.1**	41.8	18.3	**60.1**	0.36	0.44
5_T_Stat vs Phenology 3 & Phenology 4	46.1	22.6	**68.7**	43.1	18.8	**61.9**	0.36	0.57
6_T_Stat vs Phenology 3 & Phenology 4	51.1	23.5	**74.6**	39.4	17.8	**57.2**	0.47	0.36
7_T_Stat vs Phenology 3 & Phenology 4	55.7	18.3	**74.0**	41.7	21.0	**62.7**	0.46	0.39
11_T_Stat vs Phenology 3 & Phenology	58.3	15.5	**73.8**	41.5	21.0	**62.5**	0.54	0.37
12_T_Stat vs Phenology 3 & Phenology	42.6	22.3	**64.9**	33.5	18.5	**52.0**	0.31	0.25

7.3.7 Correlation circles and regression analysis of selected block variables

For presentation purposes a correlation circle will be shown in text as an example only of each of the clusters discussed. Figure 13 and Figure 16 are examples of the correlation circles for clusters 1 and 2, respectively. All the correlation circles from the cluster analysis will be discussed in the text and summarised in applicable tables (Refer to Figure 22 to 88 in Addendum 7.1). Basic regression analyses are provided to show more detail on the significant or stronger relationship variables within the correlation circles. Variables within the outer circular bands (≥ 0.60) have a strong relationship and a more significant relationship in the direction of dimension 1 (X axis). Results will be discussed in order of interaction on the tree diagram as listed in Table 5. Significant correlations where $p \geq 0.01$, will be discussed further in this section and separated into cluster 1 and cluster 2 variables.

Relative humidity for the month of September had a close link to Phenology 1 and 2 in the tree diagram (RV=0.24 and 0.40, respectively). The correlation circle and regression analysis (Figure 13 and Table 6) highlighted a positive correlation between RH and IPCY of 0-20%. More hours at 0-20% RH, *i.e.* relatively low RH, resulted in an earlier season for both cultivars with the effect on Shiraz being more prominent (R^2 = 0.42) (Table 6). The IPCY had a negative correlation with high RH (80-100%). More observations at high RH resulted in a later season, with a stronger effect on Shiraz (R^2 = 0.65). The higher and lower RH did not have such a strong relationship with Cabernet Sauvignon, which could be ascribed to the higher levels of abscisic acid in the xylem sap (Schultz, 2003, Soar *et al.,* 2006). Soar *et al.* (2006), concluded *Vitis vinifera* cultivars (Grenache and

Shiraz) differ significantly in their response to potentially stressful atmospheric conditions, the abscisic acid physiology drives the contrasting responses. The fact that Shiraz is known to be a more sensitive to the environmental conditions could be a plausible explanation for the better correlation with higher RH has a, as higher RH could influence the water constraints in the grapevine to be less servere (Schultz, 2003). The later seasons could be ascribed to increased vegetative growth due to the more observations at high humidity which could be ascribed to increased spring rainfall in the context of climate change, possibly resulting in less water constraints in the grapevine. It may, therefore, be that water constraints could be an indirect driver of phenology. The lower relative humidity at Vredendal could be a reason aside of the warmer temperatures for an earlier harvest compared to cooler sites. Later flowering and pea size stages were correlated with more hours at higher RH 80-100%. However, more hours at lower RH, *i.e.* 20-40%, had a negative correlation with pea size. Increased hours at RH 40-80% resulted in earlier pea size, which agreed with the IPCY index that had a positive correlation with RH 40-80%. Overall it seemed that more hours at a RH of 40-80% resulted in earlier seasons for both cultivars.

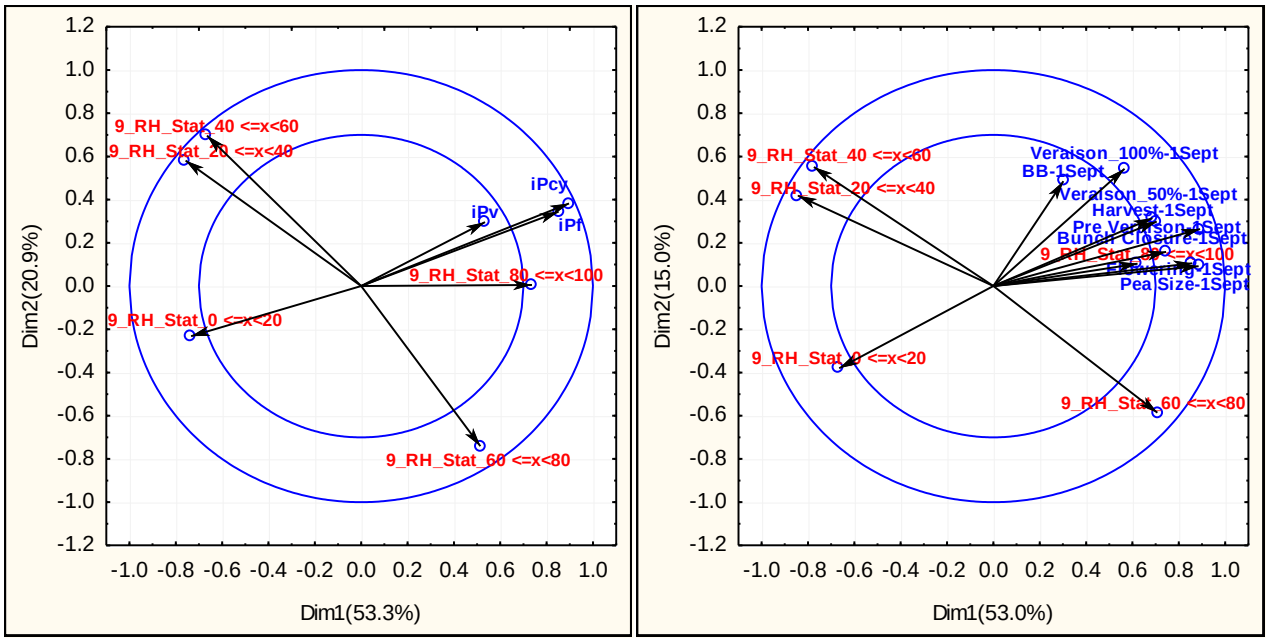

Figure 13 Multifactor analysis (correlation circle), representation of the principal components of separate PCA's of block variables: phenology 1 vs 9 RH_stat (RH from weather station) with an RV=0.24 on the left and phenology 2 vs 9 RH_stat with RV=0.40 on the right.

Table 6 Regression analyses of relative humidity classes from September (9_RH) and precocity index (IPCY) and phenological stages after 1 September (flowering and pea size) for cultivars Cabernet Sauvignon and Shiraz over all sites and seasons.

September relative humidity classes	Phenology	*r*	*p*	R^2	Cultivar
9_RH_Stat_0 ≤ x ≤ 20%	IPCY	0.28	0.05	0.08	CS
9_RH_Stat_0 ≤ x ≤ 20%	**IPCY**	**0.64**	**0.02**	**0.42**	**SH**
9_RH_Stat_20 ≤ x ≤ 40%	IPCY	0.33	0.02	0.11	CS
9_RH_Stat_20 ≤ x ≤ 40%	IPCY	0.59	0.04	0.35	SH
9_RH_Stat_80 ≤ x ≤ 100%	IPCY	-0.56	0.00	0.31	CS
9_RH_Stat_80 ≤ x ≤ 100%	**IPCY**	**-0.81**	**0.00**	**0.65**	**SH**
9_RH_Stat_80 ≤ x ≤ 100%	Flowering-1Sept	0.04	0.01	0.13	CS
9_RH_Stat_80 ≤ x ≤ 100%	Flowering-1Sept	0.63	0.03	0.40	SH
9_RH_Stat_80 ≤ x ≤ 100%	Pea size-1Sept	0.26	0.08	0.07	CS
9_RH_Stat_80 ≤ x ≤ 100%	Pea size-1Sept	0.64	0.02	0.41	SH
9_RH_Stat_20 ≤ x ≤ 40%	Pea size-1Sept	-0.61	0.00	0.38	All

Correlation circle analysis highlighted a strong interaction of the block variable "climatic index daily" (indices calculated from daily data) to phenology 1 (IPCY) (RV = 30), and an even stronger

correlation with phenology 2 (RV = 0.61) (Figure 22 in Addendum 7.1). The phenological stages flowering (R^2 = 0.55) and pre véraison (R^2 = 0.62) both showed negative correlations with GDD, where cooler seasons (lower GDD) resulted in later flowering for all seasons and sites in the study (Figure 14). The precocity index of the ripening cycle (IPCY) confirmed the results, having a positive but low correlation for both cultivars with GDD, indicating an earlier season with higher GDD units comparable to other studies (Jones & Davis, 2000). Phenology of Shiraz was more reactive to the environment compared to the phenology of Cabernet Sauvignon (Table 7), where a warmer season resulted in earlier phenology (R^2 = 0.40) and IPCY (R^2 = 0.32).

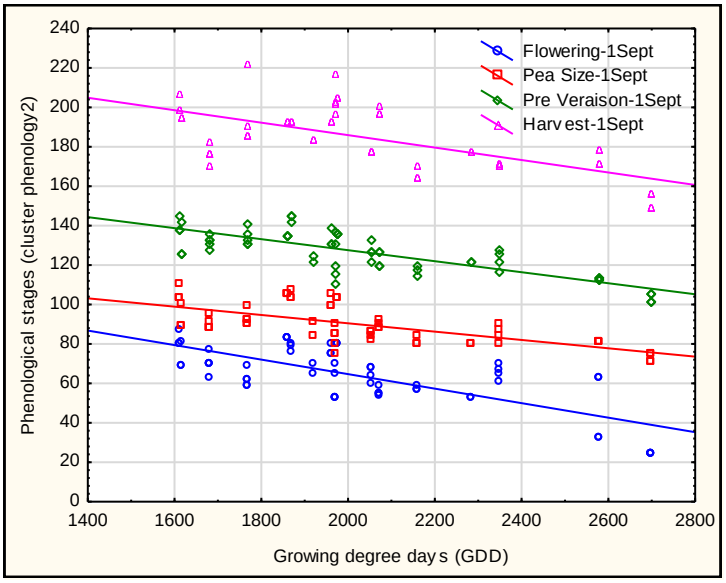

Figure 14 Relationship between phenological stages described as days after 1 September and growing degree days (GDD) for all sites and seasons.

Table 7 Results from regression analyses between growing degree days (GDD) for the clusters phenology 1 (IPCY) and phenology 2. The bottom half of the table represents regression analyses for the different cultivars [Cabernet Sauvignon (CS) and Shiraz (SH)].

Winkler Index	Phenology 1 & 2	*r*	*p*	R^2	
Growing Degree Days	Flowering-1st Sept	-0.74	0	0.55	
Growing Degree Days	Pea size -1st Sept	-0.67	0	0.45	
Growing Degree Days	Pre Véraison-1st Sept	-0.79	0	0.62	
Growing Degree Days	Harvest-1st Sept	-0.63	0	0.40	
Growing Degree Days	IPCY	0.56	0	0.32	
Winkler Index	**Phenology 1 & 2**	***r***	***p***	**R^2**	**Cultivar**
Growing Degree Days	Flowering-1st Sept	-0.74	0	0.55	CS
Growing Degree Days	Flowering-1st Sept	-0.78	0	0.6	SH
Growing Degree Days	Pre Véraison-1st Sept	-0.74	0	0.56	CS
Growing Degree Days	Pre Véraison-1st Sept	-0.88	0	0.77	SH
Growing Degree Days	IPCY	0.60	0	0.35	CS
Growing Degree Days	IPCY	0.65	0.02	0.43	SH

Figure 15 shows the regression analysis comparing flowering dates from 1 September calculated from weather station and logger sources. A warmer season resulted in earlier flowering dates for both sources, but better correlations were found with logger temperatures (R^2 = 0.60) compared to weather station sources (R^2 = 0.55). This could be due to the higher temperatures near the grapevine due to higher carbon dioxide concentrations as a result of grapevine functioning (Schultz, 2000). Flowering had a good correlation with temperature; warmer seasons resulted in earlier flowering over all sites and cultivars.

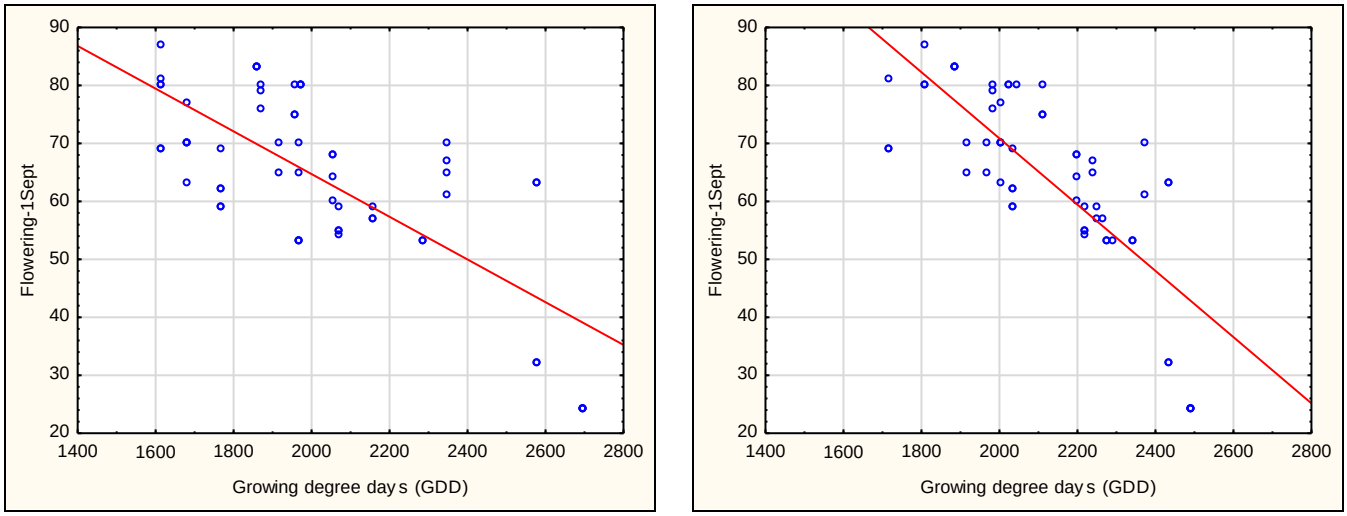

Figure 15 Relationship between flowering date from 1 September and growing degree days calculated from the weather station (left) and logger (right) data. Flowering-1Sept:GDD (weather station) r = -0.74, p = 0.000; $R^2 \geq 0.55$ (left), Flowering-1Sept:GDD(Logger) r = -0.78, p = 0.000; $R^2 \geq 0.60$ (right).

Correlation circle analysis highlighted a strong interaction of the block variable “daily index” (index calculated from daily data) to phenology 1 (IPCY/IPF) (RV = 0.29), and phenology 2 (RV = 0.27) (Figure 14). From the daily index cluster, only the minimum February temperature (MFTn_Stat) had a significant relationship with phenology 1 (IPF and IPCY) and 2 (Flowering and Pre-véraison - 1 Sept) as described in the correlation circles in Figure 23 (in Addendum 7.1). The minimum February temperatures showed a positive correlation with IPF (R^2 = 0.38) and IPCY (R^2 = 0.25): as minimum February temperatures increased, the flowering and vintage precocity indices were earlier. This was confirmed by the negative correlation for flowering (r = -0.46) and pre véraison (r = -0.49), with a warming trend resulting in earlier phenology (Table 8), comparable to other studies (Tesic *et al.*, 2001).

Table 8 Results from regression analyses between minimum February temperature (MFTn) for the clusters phenology1 (IPCY) and phenology2 (phenology at different stages after1 September), for both cultivars over all sites and seasons.

Daily Index	Phenology	r	p	R^2
Minimum February temperatures (MFTn)	IPF	0.62	0.00	0.38
Minimum February temperatures (MFTn)	IPCY	0.50	0.00	0.25
Minimum February temperatures (MFTn)	Flowering-1Sept	-0.46	0.00	0.21
Minimum February temperatures (MFTn)	Pre Véraison-1Sept	-0.49	0.00	0.24

The correlation circles showed significant relationships between the rainfall variable and phenology 1 and 2. The annual rainfall showed a low negative correlation with the IPF and IPCY, with more rainfall resulting in a later season in flowering and vintage (Table 9). Summer rainfall had a low negative correlation with flowering due to the cooler temperatures; which could delay all the phenological stages. Table 7 and Table 9 highlight the cultivar-specific flowering and pea size phenology relationships with annual, summer and winter rainfall: there was a positive relationship for both cultivars for phenology 2 (days after 1 September). More rainfall tended to force the season to be later in terms of flowering and pea size for both cultivars, therefore less water deficits mostly delays phenology. Cabernet Sauvignon had a higher correlation to annual rainfall compared to Shiraz, and Shiraz had a higher correlation to winter rainfall in shifting phenology earlier or later (Table 9). Shiraz had a stronger relationship for flowering compared to Cabernet Sauvignon; this

was the opposite for the phenological stage of pea size. Rainfall variability seemed to have affected the cultivar phenology: more rainfall resulted in later phenology and drier seasons resulted in earlier phenology, therefore confirming the importance of plant water status (Jones & Davis, 2000; Tesic *et al.*, 2001) as well as water availability either through irrigation or seasonal rainfall. The cultivar reaction seemed to depend on the phenological stage, as Shiraz had a stronger correlation at flowering whereas Cabernet Sauvignon showed a stronger correlation at pea size.

Table 9 Results from regression analyses between rainfall (annual, summer and winter rainfall) for the clusters phenology1 (IPF, IPV and IPCY) and phenology2 (phenology at different stages after 1 September) over all seasons and sites. The bottom half of the table represents regression analyses for the separate cultivars [Cabernet Sauvignon (CS) and Shiraz (SH)].

Rainfall (mm)	Phenology1	*r*	*p*	R^2	
Annual Rain	IPF	-0.53	0.00	0.28	
Annual Rain	IPV	0.21	0.10	0.04	
Annual Rain	IPCY	-0.30	0.02	0.09	
Summer Rain	IPF	-0.26	0.04	0.07	
Summer Rain	IPV	0.06	0.67	0.00	
Summer Rain	IPCY	-0.07	0.60	0.00	
Rainfall	Phenology2	*r*	*p*	R^2	Cultivar
Annual Rain	Flowering-1st Sept	0.76	0.00	0.58	CS
Annual Rain	Flowering-1st Sept	0.86	0.00	0.74	SH
Summer Rain	Flowering-1st Sept	0.64	0.00	0.41	CS
Summer Rain	Flowering-1st Sept	0.61	0.04	0.38	SH
Winter Rain	Flowering-1st Sept	0.66	0.00	0.44	CS
Winter Rain	Flowering-1st Sept	0.86	0.00	0.74	SH
Winter Rain	Pea size-1Sept	0.79	0.00	0.62	CS
Winter Rain	Pea size-1Sept	0.72	0.00	0.52	SH

To summarise the results from cluster 1: more rain resulted in later seasons for IPF and IPCY, flowering and pea size (after 1 September). It was evident that the cultivar's reaction was dependent on phenological stage and seasonal rainfall. Drier air, *i.e.* RH at lower values (0-20%) caused earlier phenology, and high RH (80-100%) resulted in later phenology. Furthermore, more hours where RH ranged from 40-80% resulted in earlier seasons for both cultivars. Rainfall could possibly be indirectly related to these factors. As MFT increased, the flowering and vintage precocity index seemed to be earlier, which was confirmed with the negative correlation for flowering (r = 0.46) and pre-véraison (r = 0.49), with a warming trend observed in the month of February, specifically the minimum temperature resulting in earlier phenology.

A warmer season based on GDD was correlated with earlier phenology (R^2 = 0.40). Days after budburst (phenology 3) and time between phenological stages (phenology 4) had a stronger relationship with temperature, hence being more sensitive to temperature frequency and observations at specific temperature classes as described in Chapter 4.

A higher frequency of hours at temperatures between 25°C and 40°C in November decreased the period between budburst and flowering as well as budburst and harvest, therefore cooler temperatures resulted in later bud break (Figure 16 & Table 10). More hours at higher temperatures shortened the season, resulting in fewer days between phenological stages. Results showed that more hours at higher temperatures had a positive correlation (R^2 = 0.62) with the period between pre-véraison and véraison. The warmer temperatures of between 35° and 40°C in November slowed down the ripening period (R^2 = 0.60) and had an overall negative correlation with the period between budburst and flowering. Similar results were obtained in n other studies (Webb *et al.*, 2007). Results showed that an increase in the hours between 30-35°C in the summer

months led to a shorter period between budburst and flowering in November, for both cultivars (R^2 = 0.70 and 0.53 for Cabernet Sauvignon and Shiraz, respectively) over all seasons (Table 10). Both cultivars had a good correlation with the higher temperatures in November, with Shiraz showing a stronger negative correlation with the number of days between budburst and flowering *(r* = -0.94) and a positive correlation with the number of days between pre-véraison and véraison (*r* = 0.96) for temperatures between 35-40°C. From these results, Shiraz grapevines seemed to be more reactive to the warmer and cooler temperatures as compared to Cabernet Sauvignon. This could be ascribed to Shiraz being more sensitive to ambient climatic conditions and water constraints, compared to the over regulating nature of Cabernet Sauvignon confirming finding of Schultz (2003) and Soar *et al*. (2006) (Table 10).

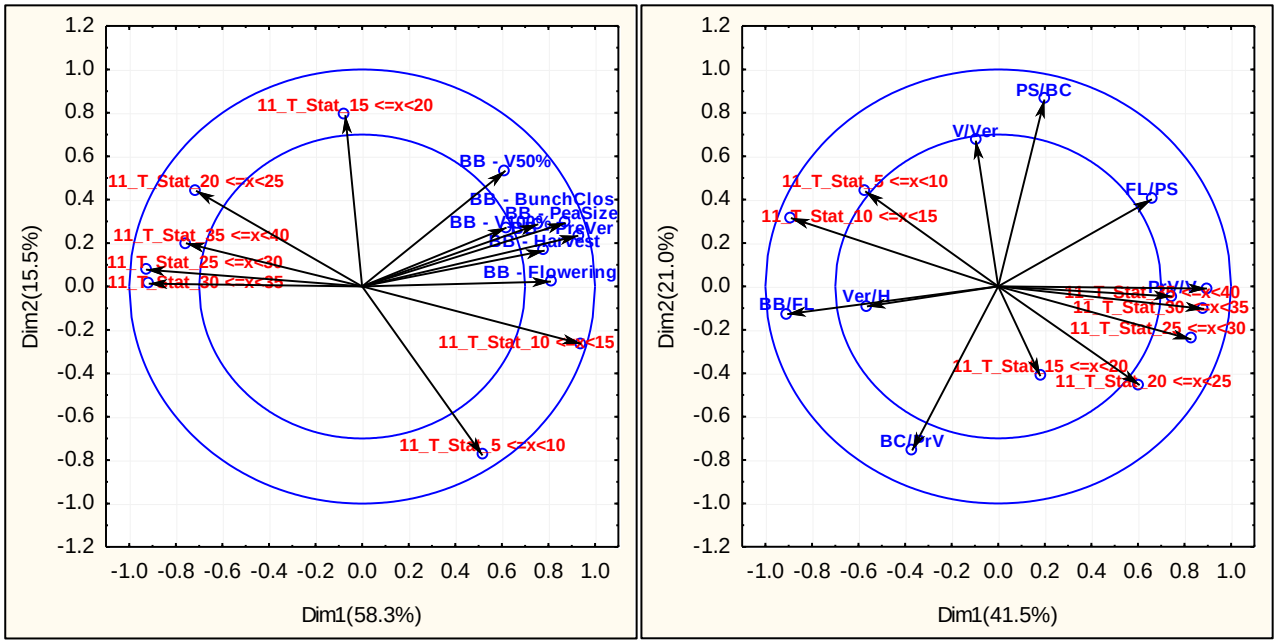

Figure 16 Principal components of separate analyses of each block variable, with phenology 3 with an RV = 0.54 on the left and phenology 4 with RV = 0.37 on the right compared to the temperatures in the month of November (11_T_Stat).

Table 10 Results from regression analyses between November temperature classes (11_T_stat) for the clusters phenology 3 (phenology as days after budburst (BB) and phenology 4 (days between phenology stages) over all seasons and sites. The bottom half of the table represents regression analyses for the separate cultivars [Cabernet Sauvignon (CS) and Shiraz (SH)].

November Temperature classes	Phenology 3	*r*	*p*	R^2	
11_T_Stat_25 ≤ x ≤ 30°C	BB-Flowering	-0.75	0.00	0.57	
11_T_Stat_30 ≤ x ≤ 35°C	BB-Flowering	-0.84	0.00	0.70	
11_T_Stat_35 ≤ x ≤ 40°C	BB-Flowering	-0.80	0.00	0.65	
11_T_Stat_25 ≤ x ≤ 30°C	BB-Harvest	-0.64	0.00	0.40	
11_T_Stat_30 ≤ x ≤ 35°C	BB-Harvest	-0.58	0.00	0.34	
11_T_Stat_35 ≤ x ≤ 40°C	BB-Harvest	-0.51	0.00	0.26	
November Temperature classes	**Phenology 4**	***r***	***p***	R^2	
11_T_Stat_25 ≤ x ≤ 30°C	PrV/V	0.45	0.00	0.20	
11_T_Stat_30 ≤ x ≤ 35°C	PrV/V	0.57	0.00	0.32	
11_T_Stat_35 ≤ x ≤ 40°C	PrV/V	0.79	0.00	0.62	
11_T_Stat_25 ≤ x ≤ 30°C	BB/FL	-0.75	0.00	0.60	
11_T_Stat_30 ≤ x ≤ 35°C	BB/FL	-0.84	0.00	0.70	
11_T_Stat_35 ≤ x ≤ 40°C	BB/FL	-0.80	0.00	0.65	
November Temperature classes	**Phenology 3**	***r***	***p***	R^2	**Cultivar**
11_T_Stat_30 ≤ x ≤ 35°C	BB-Flowering	-0.84	0.00	0.70	CS
11_T_Stat_30 ≤ x ≤ 35°C	BB-Flowering	-0.73	0.01	0.53	SH
11_T_Stat_25 ≤ x ≤ 30°C	BB-Harvest	-0.62	0.00	0.40	CS
11_T_Stat_25 ≤ x ≤ 30°C	BB-Harvest	-0.66	0.02	0.44	SH
November Temperature classes	**Phenology 4**	***r***	***p***	R^2	**Cultivar**
11_T_Stat_35 ≤ x ≤ 40°C	PrV/V	0.67	0.00	0.45	CS
11_T_Stat_35 ≤ x ≤ 40°C	PrV/V	0.96	0.00	0.91	SH
11_T_Stat_35 ≤ x ≤ 40°C	BB/FL	-0.69	0.00	0.47	CS
11_T_Stat_35 ≤ x ≤ 40°C	BB/FL	-0.95	0.00	0.90	SH

The temperatures between 30-40°C recorded in December were negatively correlated with phenological stages between budburst and flowering and positively correlated with the period between pre-véraison and véraison (Refer to Figure 25 in Addendum 7.1). More hours at these temperatures therefore shortened the period of BB/FL and lengthened the period PrV/V. It could be speculated that there was a correlation over seasons, with temperatures in the previous season possibly driving flowering in the succeeding season. The temperatures between 35-40°C had a low positive correlation with the period between pre-véraison and véraison. Prolonging of the period could have been due to higher temperatures affecting grapevine functioning.

Higher temperatures in the month of January had a negative correlation (R^2 = 0.64) with the phenological stage of budbreak to flowering, where more hours at high temperatures between 35-40°C resulted in earlier flowering (Figure 17). Flowering of grapevines (cultivar dependant) is generally expected to occur in November, and ripening is expected to start in January. Therefore, the high correlation with the period between budburst (BB) and flowering may indicate, as for the December temperatures that the previous seasons could possibly affected the following season's flowering time.

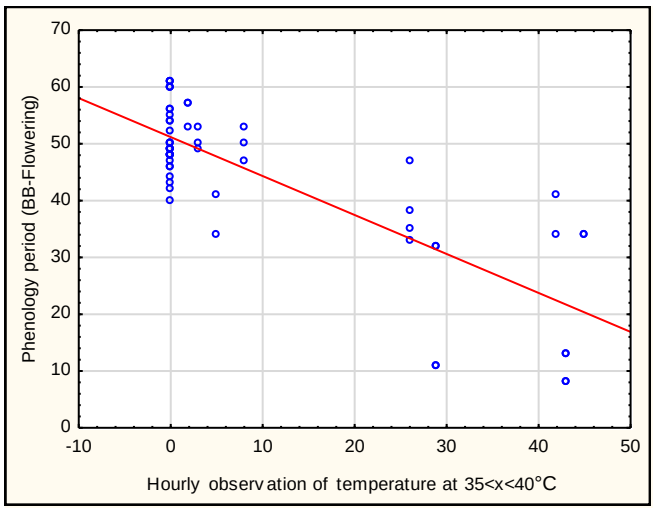

Figure 17 Regression analysis of budburst to flowering (BB-flowering) compared to the hourly observations for the month of January between 35-40°C (1_T_Stat_35<=x<40), *r*=-0.8; *p*= 0.00 and R^2=0.64.

Temperatures in February, in particular the higher temperatures (40-45°C), had a strong relationship with the BB-Flowering stage for phenology 3 and 4 (Refer to Figure 26 in Addendum 7.1). There was a significant correlation for temperature between 25-45°C with BB-Flowering phenology. As February is known to be a ripening month for early ripening cultivars in the Western Cape, hence the high temperatures in the ripening months could have had an influence on the phenological stage BB-Flowering later in the season. The February temperature classes, 25-30, 30-35, 35-40 and 40-45°C was negatively correlated with flowering. Therefore, more observations at higher temperatures in the February resulted in earlier flowering (Table 11).

Table 11 Results from regression analyses between February temperature classes (2_T_stat) for the clusters phenology 3 (flowering phenology as days after budburst (BB)) for both cultivars over all seasons and sites.

February temperatures	Phenology3	*r*	*p*	R^2
2_T_Stat_25<=x<30	BB-Flowering	-0.62	0.00	0.40
2_T_Stat_30<=x<35	BB-Flowering	-0.70	0.00	0.49
2_T_Stat_35<=x<40	BB-Flowering	-0.68	0.00	0.46
2_T_Stat_40<=x<45	BB-Flowering	-0.54	0.00	0.30

Autumn (March, April, May) temperatures affected later occurring phenological stages. Therefore, warmer temperatures, *i.e.* more hours between 20-35°C in April and May, led to longer periods between flowering and pea size. This observation can be explained with further data mining in the future as it is beyond the scope of this study, howver have highlighted the need to review the bioclimatic indices used to monitor the growing season and the expected grapevine responses. More hours at warmer temperatures therefore seemed to have had an effect later in the season or the following season. Yet warmer temperatures had a negative correlation with the time between budburst and flowering, warmer temperatures caused a shorter interval.

Temperatures in March had a negative correlation with BB-flowering, BB-Pea size and BB-Harvest (RV = 0.51), with higher temperatures in March having had a more direct relationship with early phenology (Figure 18). Table 12 represents the regression analysis for the three phenological stages influenced by higher temperatures in March. The temperature classes of 25-40°C in March had a stronger correlation for the BB-Flowering, BB-pea size and BB-harvest periods. More hours between 25-35°C, showed a strong negative correlation with phenology, especially for the flowering stage.

Both cultivars had a high negative correlation of R^2 = 0.70 and R^2 = 0.67 for Cabernet Sauvignon and Shiraz, respectively, for March temperature in the range of 30-35°C. More observations at higher temperatures resulted in earlier flowering, with Cabernet Sauvignon being slightly more responsive compared to Shiraz. This could be due to Cabernet Sauvignon being a later ripening cultivar. Due to a later harvest for Cabernet Sauvignon, the grapevine could still have been functioning at that stage of the season and, hence, be affected by the higher temperatures. This could be the cause of the carry over effect.

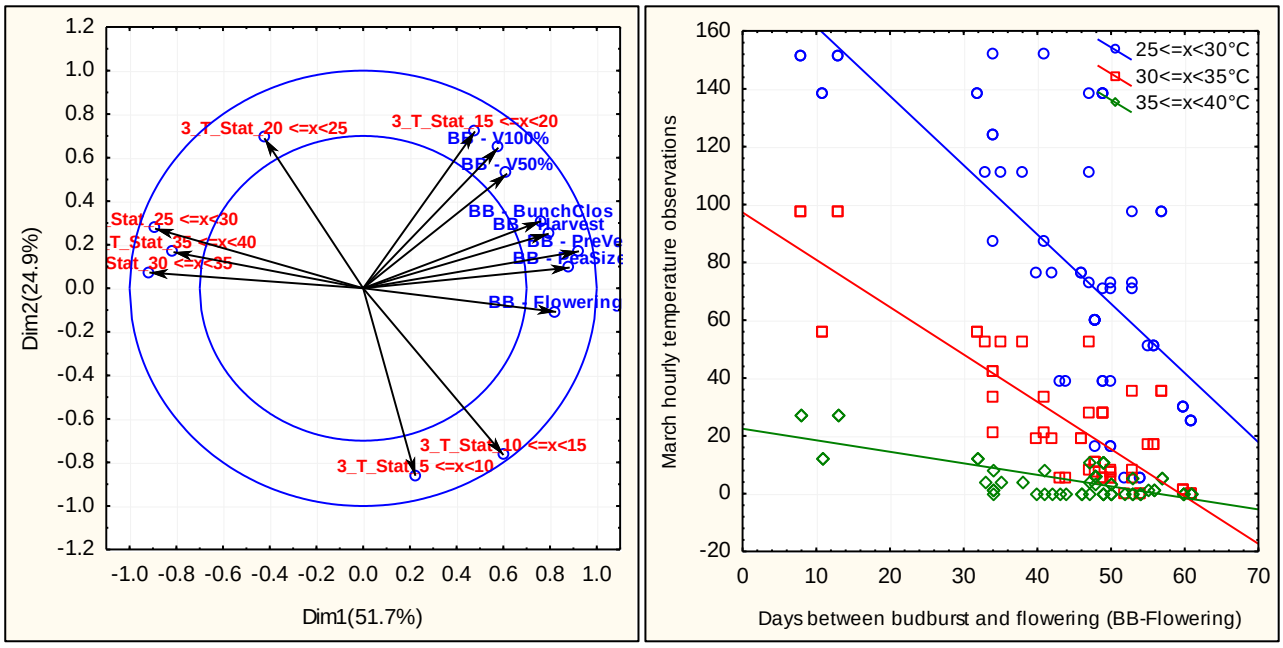

Figure 18 Phenology 3 compared to March temperature classes, with the correlation circle on the left and the regression on the right for budburst to flowering (BB-Flowering).

April temperatures had a significant and strong relationship with flowering. The temperature class of 25-40°C, had a negative correlation with BB-Flowering, overall a higher correlation for hours at warmer temperatures (Table 12). Cooler temperatures between 10-15°C in April had a positive correlation with the period between budburst and flowering, and temperatures between 20-25°C had a low positive correlation with the period between flowering and pea size. More hours at cooler temperatures in April lengthened the interval between BB/FL and FL/PS. It was evident that the relationship for BB/FL was more prominent for Shiraz (R^2 = 0.80) than in Cabernet Sauvignon.

May temperatures had a relationship with phenology 3 (RV = 0.36) and phenology 4 (RV = 0.57). The specific variables of phenology, namely BB-flowering, BB/FL and FL/PS were mostly driven by May temperatures (Figure 28 in Addendum 7.1). The phenological stage BB-Flowering had a high and negative correlation with temperatures between 25-30°C in May. Considering the two cultivars, the correlation for Cabernet Sauvignon *(R^2* = 0.70) was high but was lower than that for Shiraz (R^2 = 0.93).

The period between phenological stages, specifically BB/FL had a negative correlation with more hours at temperatures between 20-35°C, hence the warmer temperatures resulted in earlier flowering, especially between 25°C and 35°C. The period between FL/PS had a positive correlation (R^2 = 0.42) with slightly warmer temperatures between 25-30°C. More hours observed in this temperature class resulted in the advancement of the period between flowering and pea size. The temperatures in this range inMay had the highest correlations with flowering date compared to the other autumn months (Table 12 and Table 13). Literature and other studies showed temperatures between 25-30°C to be the optimal climatic requirements for optimum

photosynthetic activity (Hunter & Bonnardot, 2011), even though the grapevine is known to be dormant in May. The temperature in this range seemed to influence the flowering of the following season and is probably due to some underlying enzymatic processes, which could have had a possible influence on chill requirements and dormancy.

T**able 12** Results from regression analyses between March, April and May temperature classes (3/4/5_T_stat) for the clusters phenology 3 (phenology as days after budburst (BB)) and phenology 4 (days between phenology stages) over all seasons and sites. The bottom half of the table represents regression analyses for the separate cultivars [Cabernet Sauvignon (CS) and Shiraz (SH)].

March temperature classes	**Phenology 3**	***r***	***p***	***R²***	
3_T_Stat_25 ≤ x ≤ 30°C	BB-Flowering	-0.71	0.00	0.50	
3_T_Stat_30 ≤ x ≤ 35°C	BB-Flowering	-0.85	0.00	0.73	
3_T_Stat_35 ≤ x ≤ 40°C	BB-Flowering	-0.76	0.00	0.57	
3_T_Stat_25 ≤ x ≤ 30°C	BB-Pea Size	-0.74	0.00	0.55	
3_T_Stat_30 ≤ x ≤ 35°C	BB-Pea Size	-0.72	0.00	0.52	
3_T_Stat_35 ≤ x ≤ 40°C	BB-Pea Size	-0.57	0.00	0.32	
3_T_Stat_25 ≤ x ≤ 30°C	BB-Harvest	-0.56	0.00	0.31	
3_T_Stat_30 ≤ x ≤ 35°C	BB-Harvest	-0.68	0.00	0.47	
3_T_Stat_35 ≤ x ≤ 40°C	BB-Harvest	-0.68	0.00	0.46	
April temperature classes	**Phenology 3**	***r***	***p***	***R²***	
4_T_Stat_25 ≤ x ≤ 30°C	BB-Flowering	-0.77	0.00	0.60	
4_T_Stat_30 ≤ x ≤ 35°C	BB-Flowering	-0.79	0.00	0.62	
4_T_Stat_35 ≤ x ≤ 40°C	BB-Flowering	-0.86	0.00	0.74	
May temperature classes	**Phenology 4**	***r***	***p***	***R²***	
5_T_Stat_20 ≤ x ≤ 25°C	BB/FL	-0.75	0.00	0.56	
5_T_Stat_25 ≤ x ≤ 30°C	BB/FL	-0.90	0.00	0.80	
5_T_Stat_30 ≤ x ≤ 35°C	BB/FL	-0.81	0.00	0.65	
5_T_Stat_20 ≤ x ≤ 25°C	FL/PS	0.65	0.00	0.42	
March temperature classes	**Phenology 3**	***r***	***p***	***R²***	**Cultivar**
3_T_Stat_30 ≤ x ≤ 35°C	BB-Flowering	-0.85	0.00	0.73	All
3_T_Stat_30 ≤ x ≤ 35°C	BB-Flowering	-0.84	0.00	0.70	CS
3_T_Stat_30 ≤ x ≤ 35°C	BB-Flowering	-0.82	0.00	0.67	SH
April temperature classes	**Phenology 4**	***r***	***p***	***R²***	**Cultivar**
4_T_Stat_10 ≤ x ≤ 15°C	BB/FL	0.47	0.00	0.22	CS
4_T_Stat_10 ≤ x ≤ 15°C	BB/FL	0.92	0.00	0.85	SH
4_T_Stat_20 ≤ x ≤ 25°C	FL/PS	0.32	0.02	0.10	CS
4_T_Stat_20 ≤ x ≤ 25°C	FL/PS	0.67	0.02	0.44	SH
May temperature classes	**Phenology 3**	***r***	***p***	***R²***	**Cultivar**
5_T_Stat_25 ≤ x ≤ 30°C	BB-Flowering	-0.84	0.00	0.70	CS
5_T_Stat_25 ≤ x ≤ 30°C	BB-Flowering	-0.97	0.00	0.93	SH
May temperature classes	**Phenology 4**	***r***	***p***	***R²***	**Cultivar**
5_T_Stat_20 ≤ x ≤ 25°C	BB/FL	-0.64	0.00	0.41	CS
5_T_Stat_20 ≤ x ≤ 25°C	BB/FL	-0.95	0.00	0.90	SH

Moderate to warm temperatures of 15-30°C in the month of June had a negative correlation with BB-Flowering and a positive correlation with the lengthening of the period between Prv/V. The temperatures at 15-30°C had a higher correlation with flowering than Prv/V, yet both were significant. The higher frequency at the temperature classes 25-30°C had a stronger negative correlation with BB-flowering. The correlations for both Cabernet Sauvignon and Shiraz were comparable at R^2 = 0.60 for BB-flowering. The period between Prv/V was lengthened with low correlation for more hours between 25-30°C and 15-25°C (Table 13). Temperatures in July (30-35°C and 25-30°C), had a negative but good correlation of r = 0.74 and 0.70 for BB-Flowering and Prv/V phenology, respectively. More hours at higher temperatures in July resulted in earlier flowering and lengthened the period between the start of véraison and 100% véraison. Comparing the response of the two cultivars indicated that Shiraz tended to be more responsive to higher temperatures than Cabernet Sauvignon for both phenological stages (Table 13).

Table 13 Results from regression analyses between June and July temperature classes (6 and 7_T_stat) for the clusters phenology 3 (phenology as days after budburst (BB)) and phenology 4 (days between phenology stages) over all seasons and sites. The bottom half of the table represents regression analyses for the separate cultivars [Cabernet Sauvignon (CS) and Shiraz (SH)].

June temperature classes	**Phenology 3**	***r***	***p***	***R²***	
6_T_Stat_15 ≤ x ≤ 20°C	BB-Flowering	-0.76	0.00	0.58	
6_T_Stat_20 ≤ x ≤ 25°C	BB-Flowering	-0.73	0.00	0.54	
6_T_Stat_25 ≤ x ≤ 30°C	BB-Flowering	-0.82	0.00	0.67	
June temperature classes	**Phenology 4**	***r***	***p***	***R²***	
6_T_Stat_15 ≤ x ≤ 20°C	PrV/V	0.55	0.00	0.30	
6_T_Stat_20 ≤ x ≤ 25°C	PrV/V	0.55	0.00	0.30	
6_T_Stat_25 ≤ x ≤ 30°C	PrV/V	0.59	0.00	0.35	
July temperature classes	**Phenology 3**	***r***	***p***	***R²***	
7_T_Stat_30 ≤ x ≤ 35°C	BB-Flowering	-0.74	0.00	0.55	
July temperature classes	**Phenology 4**	***r***	***p***	***R²***	
7_T_Stat_25 ≤ x ≤ 30°C	PrV/V	0.70	0.00	0.50	
June temperature classes	**Phenology 3**	***r***	***p***	***R²***	**Cultivar**
6_T_Stat_25 ≤ x ≤ 30°C	BB-Flowering	-0.79	0.00	0.62	CS
6_T_Stat_25 ≤ x ≤ 30°C	BB-Flowering	-0.79	0.00	0.63	SH
July temperature classes	**Phenology 3**	***r***	***p***	***R²***	**Cultivar**
7_T_Stat_30 ≤ x ≤ 35°C	BB-Flowering	-0.71	0.00	0.50	CS
7_T_Stat_30 ≤ x ≤ 35°C	BB-Flowering	-0.73	0.01	0.53	SH
July temperature classes	**Phenology 4**	***r***	***p***	***R²***	**Cultivar**
7_T_Stat_25 ≤ x ≤ 30°C	PrV/V	0.58	0.00	0.33	CS
7_T_Stat_25 ≤ x ≤ 30°C	PrV/V	0.87	0.00	0.76	SH

Temperatures in all the month seemed to affect flowering, with the exception of August and September where there was no significant relationship with flowering. This was interesting as temperatures in August and September would be expected to have had some effect as it is the month prior to flowering. The warmer temperature classes (25-30°C; 30-35°C and 35-40°C) had a negative correlation with flowering phenology. Warmer temperatures resulted in an earlier season in the subsequent year; therefore there is a possible carry over effect. This aspect merits further study,

Over all the sites and vigour levels, flowering had a strong correlation ranging from R^2 = 0.49-0.98 with harvest date and the strength of the correlation was dependent on the season (Figure 19). Flowering tended to dictate the progression of for the phenology in the seasons, with an excellent correlation for the more “normal” seasons, namely 2013/14 and 2014/15. Hence, flowering date as days after budburst could be used to predict harvest date as days after budburst for Cabernet Sauvignon over sites with high accuracy in normal years. The 2012/13 season had a low

correlation of R^2 = 0.56 and this could be ascribed to less sites being monitored in the first year of the study. The 2015/16 season had the lowest correlation, which was probably due to the cooler spring temperatures, or extreme heat was during ripening. It seemed that phenology was affected by temperatures in the previous seasons.

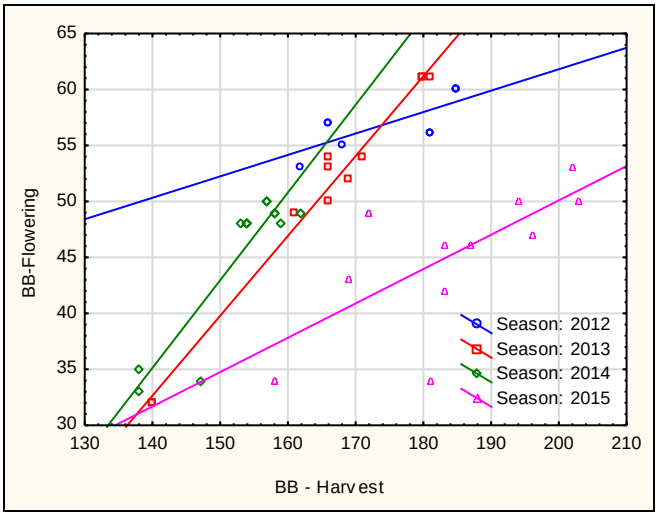

Figure 19 Relationship between BB-Flowering vs BB-Harvest for four seasons, namely 2012: *r* = 0.75, *p* = 0.02; R^2 = 0.56; 2013 *r* = 0.99, *p* = 0.00; R^2 = 0.98; 2014: *r* = 0.91, *p* = 0.00; R^2 = 0.83 and 2015: *r* = 0.70, *p* = 0.01; R^2 = 0.49).

7.3.8 Case study: phenology for cultivars, sites, seasons

To put this five year study into context with more seasons and cultivars, an industry case study was undertaken based on two areas within this study, namely Stellenbosch 2 and Elgin (Refer to Chapter 4). The data collection and analysis was comparable to that of phenology 2, and phenological stages were set as days after 1 September.

Similar seasonal temperature variations were observed in the case study over a diverse climatic band, represented by sites in Elgin and Stellenbosch 2. It was found that variability in budburst of all the cultivars (Chardonnay, Sauvignon Blanc, Wiesser Riesling, Semillon, Grenache, Merlot, Shiraz, Cabernet franc, Petit Verdot and Cabernet Sauvignon) were more dictated by between-season variability rather than variability between the two localities. As the same general cultivar-related trend in budburst was seen at both sites, the seasonal differences were possibly mostly related to the climate.

The general trends over seven seasons at the two localities showed a distinct “V shape” in the data trends (Figure 20) for budburst at 50% (B_50%) and Flowering at 50% (F_50%), with the last four seasons having a similar trend to the Cabernet Sauvignon/Shiraz main study for all cultivars. This indicated that site climate was not the most prominent variable driving the differences at the sites but rather the seasonal variability in weather data.

The trend of budburst and flowering varied greatly between seasons: 2008/09 (white cultivars early and red cultivars late, in a *normal* vintage), 2010/11 (white cultivars early and red cultivars shifted to earlier, *abnormal* vintage) and 2012/13 (white cultivars shifted later and red cultivars late, *abnormal* vintage) (Figure 21). The trend and variability in budburst and flowering were explained through considering hourly temperature data for the two sites over the different growing seasons. Further discussion will focus only on factors affecting the shifts in budburst. These trendss where comparable to the seasonal reports published for the South African wine industry (Table 14), which

also highlighted the seasonal variability to have been the driving factor that affected phenology over and above site variability.

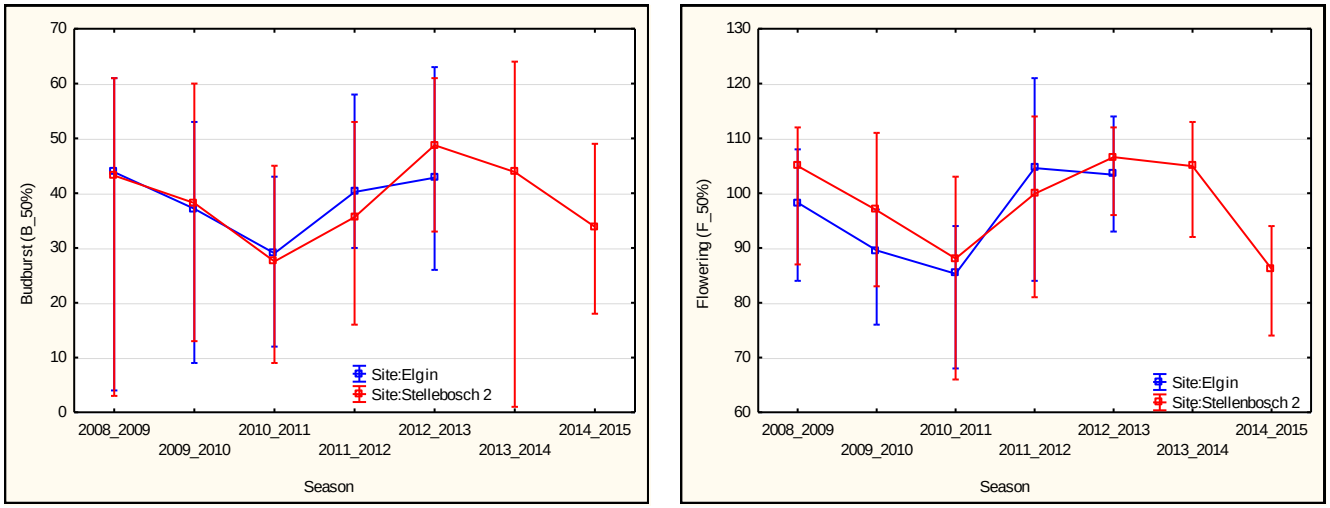

Figure 20 Budburst at 50% (left) and flowering at 50% (right) over seven seasons at the two localities averaged for all the cultivars. Vertical bars denote maximum and minimum values.

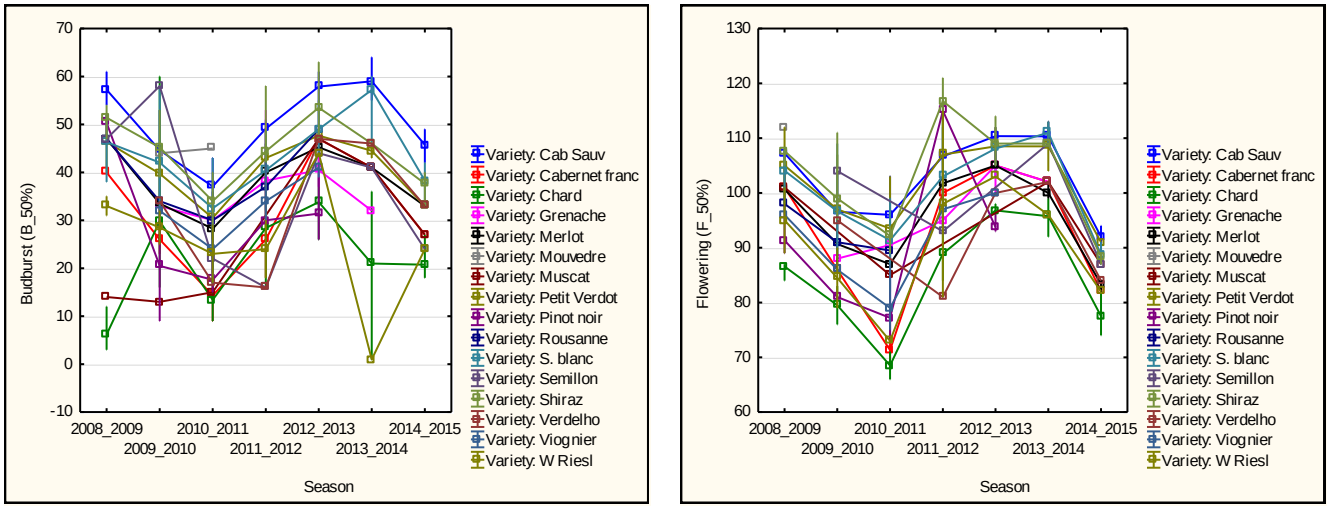

Figure 21 Budburst at 50% (left) and flowering at 50% (right) over seven seasons at the two localities, categorised by cultivars. Vertical bars denote maximum and minimum values.

Statistical processing was based on frequency analysis (described in chapter 4): histograms were used as a means to isolate the differences within temperature classes, set at <5, 5-10, 10-15, 15-20, 20-25 and >25°C. Temperature classes allowed for the identification of the main temperature-related aspects driving variability in budburst over the seasons.

The 2008/2009 season was marked as South Africa's "best" (Vinpro, 2009) compared to other vintages in the past (Table 14), while the 2012/2013 season was the biggest harvest, and the 2013/2014 season had white cultivars ripening later with the season being overall later, and lastly the 2014/15 season was the "earliest season in decades" (Vinpro, 2013, 2014, 2015).

The "best season" (2008/2009) could be ascribed to the cooler conditions in March and April (more hours below 15°C). The winter was also moderate to warm with more hours above 15°C for May and less hours between 5-10°C. The late winter months (July, August and September) was moderate with more hours at 10-15°C, and less at 5-10°C and 15-20°C (data not shown). Hence,

chill units gained in cool early autumn was sufficient for even budburst in spring. Furthermore, even budburst was promoted with warmer late winter and early spring temperatures.

The earlier budburst for the red cultivars was driven by warmer temperatures compared to the long term mean in April (more hours observed between 10-20°C compared to other season between 5-10°C). August and September also had more hours between 15-25°C. Delayed phenology in white cultivars was credited to a cooler season until the end of September, with more hours observed between 5-10°C for August and September compared to the other seasons.

The 2012/2013 and 2013/2014 seasons were not ideal due to late flowering, and the white wine cultivars ripening later than usual. The later flowering was due to the cooler temperatures in August, September and October, with more observations at 5-10°C and less at 20-23°C. The later budburst could have been ascribed to the cooler temperatures in late winter, with more observations at 5-15°C and less at 15-20°C for June and July. The 2013/2014 season received a lot of summer rainfall. The annual rainfall was almost double the norm, which resulted in delayed ripening and an increase in yield. The 2013/14 harvest commenced one to two weeks later than normal, due to late, cold winter conditions and cooler spring temperatures. The red cultivars ripened earlier in the 2014/2015 season, noted as a seasons with the earliest flowering, possibly credited to the warmer months for August, September and October (more observations between 15-30°C and less at 5-15°C).

Table 14 Summary of seasonal reports from the annual South African harvest reports, describing the seasons that were of interest for the case study and including the best season (2008/09).

Season	Industry harvest report description	Source
2008/2009	"The outstanding quality of the 2009 harvest will ensure that it goes down in history as one of South Africa's best"	(Vinpro, 2009)
2012/2013	"The 2013 harvest exceeded the expectations, biggest wine grape crop ever produced, although it had a late and slow start, harvesting later than usual and over a short time"	(Vinpro, 2013)
2013/2014	"Flowering was late and the white wine cultivars ripening later than usual. It was reported as a season with bad, late and uneven bud break", "delayed ripening and the increase in crop size and the harvest commencing one to two weeks later than normal, due to late, cold winter conditions and a cooler spring."	(Vinpro, 2014)
2014/2015	"The 2015 harvest had the earliest start in decades. Warm weather in August resulted in earlier bud break, after which a warm, dry and windy summer kept vineyard growth under control and accelerated ripening by approximately two weeks"	(Vinpro, 2015)

7.4 Conclusions

Seasonal variability was established to be a stronger driving factor than site climatic differences causing shifts in phenology, with the trend over cultivar responses being similar with only the degree of correlation with variables being more prominent for some. Phenology 1 (precocity index) and phenology 2 (days after 1-September) were more driven by seasonal climatic factors, whereas phenology 3 (days after budburst) and phenology 4 (days between stages) categories were driven by finer temperature changes over sites and seasons.

The Winkler and Huglin bioclimatic indices calculated from weather station sources had the strongest relationship with phenology compared to the other indices, and had the best correlation with the absolute dates of flowering and pre-véraison. The higher GDD values (warmer season) resulted in earlier flowering and pre véraison over the different sites. This highlighted the use and strength of using GDD in the future to classify localities for cultivar selection. The use of indices should be complimented with more factors such as relative humidity, rainfall *etc*. The climatic indices calculated from temperature data loggers did not have a strong correlation with phenology,

as the logger could be overestimating temperatures as it is positioned above the canopy; hence it was preferable to use weather station data in this study.

The IPF index indicated advancement in flowering at warmer sites and delays for the moderate to cooler sites. The IPCY indicated an earlier harvest for all the sites with the exception of Elgin that had a delayed harvest over the seasons, possibly ascribed to less water constraints at this site. More rainfall coincided with a delay in the IPF and IPCY, flowering and pea size. The date of flowering was more comparable over sites. However, the warmest site was significantly different to the all the other sites. Rainfall had a positive correlation with flowering, and Shiraz had a stronger correlation due to its climatic sensitivity to temperature and moisture, and hence delayed flowering was more prominent in this cultivar compared to Cabernet Sauvignon.

The drier air (lower RH) tended to drive earlier phenology, with higher RH forcing later phenology. Results showed higher frequency hours at an RH of 40-80%, resulted in earlier seasons for both cultivars, Shiraz had an overall stronger correlation with higher RH. Cabernet Sauvignon is a later ripening red cultivar compared to Shiraz. This was seen in the phenology over all the sites, however the variability of the precocity indexes for Cabernet Sauvignon and Shiraz was very low. Even with the slight cultivar variability for phenological timing and the period between stages, the seasons seemed to be an overriding factor driving phenology for the cultivars discussed.

There was a cooling trend over all seasons seen in August and September. These two months were cooler than the long term mean, which could have influenced the timing and homogeneity of budburst. The delayed budburst could also be ascribed to the cultivar Shiraz which is mostly uneven and slow to start until a certain point of growth. To explain the uneven budburst it could be speculated that Shiraz is possibly more sensitive to chill unit requirements than Cabernet Sauvignon.

Temperatures throughout the season seemed to affect flowering, with the exception of August and September. The summer months (December, January and February) with more observed hours between 30-35°C and 35-40°C, had a negative correlation with flowering date as days after 1 September. As minimum February temperatures increased, the flowering and vintage precocity index was earlier.

In autumn, the temperature classes of 30-35°C, 35-40°C and 25-30°C had the strongest driving impact on flowering. The industry case study highlighted more hours observed at temperatures between 10-20°C rather than at 5-10°C (normal expected), resulted in later budburst. The winter months had the strongest impact on flowering when there were more observations in the temperature class of 20-30°C for June and 30-35°C for July. Shifting in rainfall patterns from July into June would exacerbate the earlier flowering, as the rainfall will bring cooler and warmer temperatures, respectively. Rainfall shift would also influence the water table level, which could have an indirect effect on the plant water status as drier soils will heat up water and increase plant water constraints. The only month in spring that was relevant in the context of flowering and which had a relationship with phenology was November. More hours at warmer temperatures, *i.e.* 30-35°C, seemed to result in earlier flowering in the next season. This could be important considering that November is seemingly becoming more and more variable with regards to temperature, wind and rainfall.

The phenological variables most affected by temperature were the IPF, the flowering date set from 1st September and as days after budburst. Flowering tended to “set the pace” for phenology in the seasons, flowering had a strong correlation with harvest date, the strength of the correlation was dependent on the season ranging from R^2 = 0.49-0.98. Excellent correlation with more “normal”

seasons, 2013/14 and 2014/15 hence flowering date as days after budburst could potentially be used to predict harvest date for Cabernet Sauvignon over sites with high accuracy in normal years. However extreme events like rainfall and extreme heat waves will still affect the season's grapevine ripening responses, but it seems that phenology could also be affected by temperatures in the previous seasons. It seems that months outside the phenological stages are affecting the phenological stages, more in depth studies are required to understand this interaction. This could shed light on the irrelevance of some of the bioclimatic indices used to describe the climate of a season in relationship to the expected grapevine response, as the months possibly influencing the phenological stages are outside of the climatic indices time frames, *i.e.* September/October to March.

The seasonal variability is, however, expected to increase in the context of climate change, with expected increased rainfall in summer months. Over and above the extremity of the sites, the seasonal variability had an overriding impact on phenological stages, and the periods between phenological stages were seen to be shifting (increasing/decreasing) over the seasons. The use of frequency observations at set classes is important for the future in climate change and the adaptation strategies as we move forward, using the extreme cases of Vredendal and Elgin isolating the threshold ranges and frequencies setting the seasons apart within the extreme climates. Results suggested that phenology for the subsequent seasons seemed to be driven by temperatures in the current season. Further studies need to be done on the effect of warmer temperatures in the season influencing the flowering and overall harvest time of the subsequent season.

Historical grapevine responses can be used in the context of climate to better understand the grapevines responses to changing climatic conditions. The frequency temperature analysis seemed to be a more robust way to ascertain what climatic factors mostly influenced the seasonal grapevine responses. Phenology models and climatic indices currently available for predicting phenology in the context of a changing climate need to be reviewed and studied further. Geostatsitical modelling of phenology using the driving factors as inputs, can be used as an in season monitoring and management tool, for better climatic adaptions for the future within farms and regions.

7.5 References

Amerine, M.A. & Winkler, A.J., 1944. Composition and quality of musts and wines of California grapes. Hilgard 15, 493-673.

Anderson, J.D., Jones, G.V., Tait, A., Hall, A. & Trought, M., 2012. Analysis of viticulture region climate structure and suitability in New Zealand. J. Int. Sci. Vigne Vin. 46, 149-165.

Barbeau, G., Morlat, R., Asselin, C., Jacquet, A. & Pinard, C., 1998. Comportement du cépage Cabernet Franc dans différentes terroirs du Val de Loire. Incidence de la précocité sur la composition de la vendange en année climatique normale (exemple de 1988). Journal International des Sciences de la Vigne et du Vin 32(2), 69- 81

Bonnardot, V. & Carey, V.A., 2008. Observed climatic trends in South African wine regions and potential implications for viticulture. In: Proc. VIIth international viticultural terroir congress 19-23 May, Nyon, Switzerland. pp. 216-221.

Bonnardot, V., Sturman, A.P., Iman, S., Payman, Z.-R., Jacobus, H. & Quenol, H., 2011. Investigation of grapevine areas under climatic stress using high-resolution atmospheric modelling : case studies in South Africa and New Zealand. In: Proc. 19th International Congress on Biometeorology, 4-8 December 2011, Auckland, paper 338, pp 6.

Buys, M., 1971. The use of electronic resources and statistical techniques in the evaluation of the agro-climate in the South Western Cape (in Afrikaans). Thesis, Stellenbosch University, Private Bag X1, 7602 Matieland (Stellenbosch), South Africa.

Carey, V., Archer, E., Barbeau, G. & Saayman, D., 2007. The use of local knowledge relating to vineyard performance to identify viticultural terroirs in Stellenbosch and surrounds. Acta Horticulturae 754, 385-392.

Carey, V.A., 2001. Spatial characteristic of natural terroir units for viticulture in the Bottelaryberg-Simonsberg-Helderberg winegrowing area. Thesis, Stellenbosch University, Private Bag X1, 7602 Matieland (Stellenbosch), South Africa.

Carey, V.A., 2005. The use of viticultural terroir units for demarcation of geographical indications for wine production in Stellenbosch and surrounds. Dissertation, Stellenbosch University, Private Bag X1, 7602 Matieland (Stellenbosch), South Africa.

Conradie, W., J., Carey, V.A., Bonnardot, V., Saayman, D. & Van Schoor, L., H, 2002. Effect of different environmental factors on the performance of Sauvignon blanc grapevines in the Stellenbosch/Durbanville districts of South Africa. I. Geology, soil, climate, phenology and grape composition. S. Afr. J. Enol. Vitic. 23, 78-91.

Coombe, B.G., 1995. Growth Stages of the Grapevine: Adoption of a system for identifying grapevine growth stages. Aust. J. Grape Wine Res. 1, 104-110.

Deloire, A., Vaudour, E., Carey, V.A., Bonnardot, V. & Van Leeuwen, C., 2005. Grapevine responses to terroir: a global approach. J Int Sci Vigne et Vin, Vol 39(4) 149-162.

Dry, P.R., 1988. Climate change and the Australian grape and wine industry. The Aust Grapegrow Winem, 300, 14-15.

Fraga, H., Costa, R., Moutinho-Pereira, J., Correia, C.M., Dinis, L.T., Gonçalves, I., Silvestre, J., Eiras-Dias, J., Malheiro, A.C. & Santos, J.a., 2015. Modeling phenology, water status, and yield components of three Portuguese grapevines using the STICS crop model. American Journal of Enology and Viticulture 66, 482-491.

Ganichot, B., 2002. Evolution de la date des vendanges dans les Côtes-du-Rhône méridionales. 6émes Rencontres Rhodaniennes. Ed. Institut Rhodanien. Orange, France. p. 38-41.

Hunter, J.J. & Bonnardot, V., 2011. Suitability of some climatic parameters for grapevine cultivation in South Africa, with focus on key physiological processes. S. Afr. J. Enol. Vitic 32, 137-154.

IPCC, 2014. Climate Change 2014: Synthesis Report. In: Pachauri, R. K. and Meyer, L.A. (eds). Fifth Assessment Report of the Intergovernmental Panel on Climate Change, Geneva, Switzerland. *In*.

Jones, G.V. & Davis, R.E., 2000. Climate influences on grapevine phenology, grape composition, and wine production and quality for Bordeaux, France. Am. J. Enol. Vitic. 51, 249-261.

Jones, G.V., White, M.A., Cooper, O.R. & Storchmann, K., 2005. Climate change and global wine quality. Climatic Change 73, 319-343.

Le Roux, E.G., 1974. A climate classification for the South Western Cape viticultural areas (in Afrikaanse). Thesis, Stellenbosch University, Private Bag X1, 7602 Matieland (Stellenbosch), South Africa.

Le Roux, R., Neethling, E., Van Leeuwen, C., De Resseguier, L., Madelin, M., Bonnefoy, C., Barbeau, G. & Quenol, H., 2015. Multi-scalar modelling of climate applied to european vineyard sites in the climate change context. Procedia Environmental Sciences 29, 62-63.

Legave, J.M., Giovannini, D., Christen, D. & Orger, R., 2009. Global warming in Europe and its impacts on floral bud phenology in fruit species. Acta Horticulturae 838, 21-26.

Luedeling, E., 2012. Climate change impacts on winter chill for temperate fruit and nut production: A review. Scientia Horticulturae 144, 218-229.

Midgley, G.F., Chapman, R.A., Hewitson, B., Johnston, P., de Wit, M., Zievogel, G., Mukheibir, P., van Niekerk, L., Tadross, M., van Wilgen, B.W., KGOPE, B., Morant, P.D., Theron, A., Scholes, R.J. & Forsyth, G.G., 2005. A Status Quo , Vulnerability and Adaptation Assessment of the Physical and Socio-Economic Effects of Climate Change in the Western Cape. Analysis, 157.

Parker, A.K., De Cortázar-Atauri, I.G., Van Leeuwen, C. & Chuine, I., 2011. General phenological model to characterise the timing of flowering and veraison of Vitis vinifera L. Aust. J. Grape Wine Res. 17, 206-216.

Pearce, I. & Coombe, B.G., 2004. Grapevine phenology. In:Viticulture Volume 1 – Resources (eds Dry P, Coombe BG), pp. 150–166. Winetitles, Adelaide, South Australia.

Saayman, D., 1977. The effect of soil and climate on wine quality. International symposium on the quality of the vintage, 14-21 February, 1977, Cape Town, South Africa.

Saayman, D. & Kleynhans, P.H., 1978. The effect of soil type on wine quality. S.A. Society for Enology and Viticulture, Proceedings, Oct., 105-119.

Schultz, H., 2000. Climate change and viticulture: A European perspective on climatology, carbon dioxide and UV-B effects. Aust. J. Grape Wine Res. 6, 2-12.

Schultz, H.R., 2003. Differences in hydraulic architecture account for near-isohydric and anisohydric behaviour of two field grown Vitis vinifera L. cultivars during drought. Plant, Cell and Environment 26 1393-1405

Smart, R.E. & Dry, P.R., 1980. A climatic classification for Australian viticultural regions. Aust. Grapegrow. Winem. 196, 9-16.

Soar, C.J., Speirs, J., Maffei, S.M., Penrose, A.B., McCarthy, M.G. & Loveys, B.R., 2006. Grape vine varieties Shiraz and Grenache differ in their stomatal response to VPD: apparent links with ABA physiology and gene expression in leaf tissue. Aust. J. Grape and Wine Res. 12, 2-12.

Spayd, S.E., Tarara, J.M., Mee, D.L. & Ferguson, J.C., 2002. Separation of sunlight and temperature effects on the composition of Vitis vinifera cv.Merlot berries. Am. J. Enol. Vitic. 53, 171-182.

Tesic, D., Woolley, D.J., Hewett, E.W. & Martin, D.J., 2001. Environmental effects on cv Cabernet Sauvignon (Vitis vinifera L .) grown in Hawke ' s Bay , New Zealand . 1 . Phenology and characterisation of viticultural environments. Aust. J. Grape Wine Res. 8, 15-26.

Tonietto, J. & Carbonneau, A., 2004. A multicriteria climatic classification system for grape-growing regions worldwide. Agricultural Forest Meteorol. 124, 81-97.

Van Schalkwyk, D., 2013. The impact of climate change on the bud and flowering dates of grapevine cultivars at Nietvoorbij in Stellenbosch. Wynboer, January, 62-66.

Vinpro, 2009. 2009 Harvest Report. www.wosa.co.za.

Vinpro, 2013. South African Wine: Harvest Report. pp 1-16. http://www.sawis.co.za/info/download/VINPRO_OESVERSLAG_2013_ENG.pdf.

Vinpro, 2014. South African Wine: Harvest Report. http://www.sawis.co.za/info/download/SA_HarvestReport_VinPro_8May2014_ENG.pdf.

Vinpro, 2015. South African wine:Harvest Report 2015. www.wosa.co.za.

Webb, L.B., Whetton, P.H. & Barlow, E.W.R., 2007. Modelled impact of future climate change on the phenology of winegrapes in Australia. Aust. J. Grape Wine Res. 13, 165-175.

Webb, L.B., Whetton, P.H. & barlow, E.W.R., 2011. Observed trends in winegrape maturity in Australia. Global Change Biology.

Webb, L.B., Whetton, P.H., Bhend, J., Darbyshire, R., Briggs, P.R. & Barlow, E.W.R., 2012. Earlier wine-grape ripening driven by climatic warming and drying and management practices. Nature Climate Change 2, 259-264.

Addendum 7.1

Table 15 Data grouped into blocks (compared to phenology 1-4) and variables within each grouping used in the multifactor analysis. Groupings as blocks are compared to phenology.

Groups for block analysis	**Variables in groups**										
Temperature_(T) °C (month 1-12 for logger and station)	T_0 <=x<5	T_5 <=x<10	T_10 <=x<15	T_15 <=x<20	T_20 <=x<25	T_25 <=x<30	T_30 <=x<35	T_35 <=x<40	T_40 <=x<45	T_45 <=x<50	T_50 <=x<55
RelativeHumidity_(RH) % (month 1-12 for logger and station)	RH_0 <=x<20	RH_20 <=x<40		RH_40 <=x<60		RH_60 <=x<80		RH_80 <=x<100		RH_100 <=x<120	
WindVelocity_(U2) m/s (month 1-12 for station)	U2_0<=x<2	U2_2 <=x<4	U2_4 <=x<6	U2_6 <=x<8	U2_8 <=x<10	U2_10 <=x<12	U2_12 <=x<14	U2_14 <=x<16		U2_16 <=x<18	
[1]**Bioclimatic index daily** (for logger and station)	GST_(DAILY)			GDD_(DAILY)		BEDD_(DAILY)		HI_(DAILY)			
[1]**Bioclimatic index hourly** (for logger and station)	GST_(HRLY)			GDD_(HRLY)		BEDD_(HRLY)		HI_(HRLY)			
[1]**Daily index** (for logger and station)	Dly_MFTx			Dly_MFTn				Dly_CI			
[1]**Hrly index** (for logger and station)	Hrly_MFT		Hrly_MJT		Hrly_MMT		Hrly_MFTx		Hrly_MFTn		Hrly_CI
Rainfall	Rain			Rain_Summer			Rain_Winter				
Topograph	Latitude	Longitude	Altitude (m)	Distance from the Ocean (m)	Slope (%)	Aspect	Hillshade (degrees)	Cumulative Global Radiation		Average Daily Sun Hours	
Culivation	Planting date		Clone		Rootstock		Row Width (m)		Vine Spacing (m)		

Table 16 Regression analysis results of Phenology 2 (phenology after 1 September) for the six sites and over all cultivars (Cabernet Sauvignon and Shiraz) and seasons.

Phenology2 (stage after 1 Sept.)	Site	N	Mean	Standard deviation	Standard error	Confidence Interval		Phenology 3 (stage after budburst)	Mean	Standard deviation	Standard error	Confidence Interval	
						-0.95	0.95					-0.95	0.95
BB-1Sept	**Elgin**	16	18.	5.2	1.3	16.1	21.7	**BB/FL**	51.6	5.9	1.5	48.4	54.7
BB-1Sept	**Somerset West**	12	13.	8.9	2.6	8.0	19.3	**BB/FL**	53.2	4.7	1.3	50.2	56.1
BB-1Sept	**Stellenbosch 2**	14	20.	7.3	2.0	15.8	24.2	**BB/FL**	49.1	4.9	1.3	46.2	51.9
BB-1Sept	**Vredendal**	8	19.	7.9	2.8	13.1	26.4	**BB/FL**	16.0	10.1	3.6	7.6	24.4
BB-1Sept	**Stellenbosch 1**	6	24.	8.2	3.4	16.0	33.3	**BB/FL**	36.8	5.3	2.2	31.3	42.4
BB-1Sept	**Stellenbosch 3**	4	30.	6.9	3.5	19.0	41.0	**BB/FL**	37.5	4.0	2.0	31.1	43.9
Flowering-1Sept	**Elgin**	16	70.	8.5	2.1	65.9	75.0	**FL/PS**	23.8	5.3	1.3	20.9	26.6
Flowering-1Sept	**Somerset West**	12	66.	12.3	3.5	59.0	74.6	**FL/PS**	24.5	2.7	0.8	22.8	26.2
Flowering-1Sept	**Stellenbosch 2**	14	69.	11.4	3.0	62.5	75.6	**FL/PS**	25.5	6.2	1.7	21.9	29.1
Flowering-1Sept	**Vredendal**	8	35.	17.2	6.1	21.4	50.1	**FL/PS**	41.3	14.4	5.1	29.2	53.3
Flowering-1Sept	**Stellenbosch 1**	6	61.	7.2	2.9	53.9	69.1	**FL/PS**	22.0	3.9	1.6	17.9	26.1
Flowering-1Sept	**Stellenbosch 3**	4	67.	2.9	1.4	62.9	72.1	**FL/PS**	20.0	0.8	0.4	18.7	21.3
Pea Size-1Sept	**Elgin**	16	94.	6.8	1.7	90.6	97.8	**PS/BC**	17.9	10.4	2.6	12.3	23.4
Pea Size-1Sept	**Somerset West**	12	91.	11.5	3.3	84.0	98.7	**PS/BC**	18.7	5.0	1.5	15.5	21.9
Pea Size-1Sept	**Stellenbosch 2**	14	94.	9.4	2.5	89.1	100.	**PS/BC**	20.2	5.1	1.4	17.3	23.2
Pea Size-1Sept	**Vredendal**	8	77.	4.5	1.6	73.2	80.8	**PS/BC**	21.3	2.4	0.9	19.2	23.3
Pea Size-1Sept	**Stellenbosch 1**	6	83.	4.3	1.8	79.0	88.0	**PS/BC**	15.8	11.0	4.5	4.3	27.4
Pea Size-1Sept	**Stellenbosch 3**	4	87.	3.5	1.8	81.9	93.1	**PS/BC**	17.0	2.5	1.2	13.1	20.9
BunchClosure-	**Elgin**	16	112	10.8	2.7	106.	117.	**BC/PrV**	22.2	9.3	2.3	17.2	27.2
BunchClosure-	**Somerset West**	12	110	7.5	2.2	105.	114.	**BC/PrV**	15.5	3.9	1.1	13.0	18.0
BunchClosure-	**Stellenbosch 2**	14	114	13.0	3.5	107.	122.	**BC/PrV**	16.6	8.0	2.1	12.0	21.2
BunchClosure-	**Vredendal**	8	98.	4.9	1.7	94.1	102.	**BC/PrV**	9.5	2.2	0.8	7.7	11.3
BunchClosure-	**Stellenbosch 1**	6	99.	9.0	3.7	89.9	108.	**BC/PrV**	23.3	9.0	3.7	13.9	32.8
BunchClosure-	**Stellenbosch 3**	4	104	1.7	0.9	101.	107.	**BC/PrV**	24.3	6.0	3.0	14.7	33.8
Pre Véraison-1Sept	**Elgin**	16	134	5.6	1.4	131.	137.	**PrV/V**	13.1	6.6	1.6	9.6	16.6
Pre Véraison-1Sept	**Somerset West**	12	125	10.3	3.0	118.	132.	**PrV/V**	5.8	3.6	1.0	3.6	8.1
Pre Véraison-1Sept	**Stellenbosch 2**	14	131	8.6	2.3	126.	136.	**PrV/V**	6.9	2.1	0.6	5.7	8.1
Pre Véraison-1Sept	**Vredendal**	8	107	5.3	1.9	103.	112.	**PrV/V**	28.3	3.5	1.2	25.3	31.2
Pre Véraison-1Sept	**Stellenbosch 1**	6	122	4.1	1.7	118.	127.	**PrV/V**	8.7	1.0	0.4	7.6	9.8
Pre Véraison-1Sept	**Stellenbosch 3**	4	128	6.7	3.3	118.	139.	**PrV/V**	11.5	5.2	2.6	3.2	19.8
Véraison_50%-	**Elgin**	16	147	9.9	2.5	142.	152.	**V/Ver**	13.1	9.0	2.2	8.3	17.9
Véraison_50%-	**Somerset West**	12	131	7.0	2.0	126.	135.	**V/Ver**	11.4	7.5	2.2	6.6	16.2
Véraison_50%-	**Stellenbosch 2**	14	138	7.6	2.0	134.	142.	**V/Ver**	13.7	6.8	1.8	9.8	17.6
Véraison_50%-	**Vredendal**	8	136	8.5	3.0	128.	143.	**V/Ver**	8.3	2.1	0.8	6.5	10.0
Véraison_50%-	**Stellenbosch 1**	6	131	4.2	1.7	126.	135.	**V/Ver**	13.5	3.0	1.2	10.4	16.6
Véraison_50%-	**Stellenbosch 3**	4	140	5.3	2.7	131.	148.	**V/Ver**	22.8	8.1	4.0	9.9	35.6
Véraison100%-	**Elgin**	16	160	10.2	2.5	155.	165.	**Ver/H**	29.1	9.9	2.5	23.9	34.4
Véraison100%-	**Somerset West**	12	142	3.0	0.9	140.	144.	**Ver/H**	48.1	15.2	4.4	38.5	57.7
Véraison100%-	**Stellenbosch 2**	14	152	5.4	1.5	148.	155.	**Ver/H**	37.1	7.0	1.9	33.1	41.2
Véraison100%-	**Vredendal**	8	144	7.2	2.5	138.	150.	**Ver/H**	19.3	6.4	2.3	13.9	24.6
Véraison100%-	**Stellenbosch 1**	6	144	5.0	2.0	139.	150.	**Ver/H**	27.8	5.0	2.0	22.6	33.1
Véraison100%-	**Stellenbosch 3**	4	163	8.3	4.1	149.	176.	**Ver/H**	33.5	9.6	4.8	18.3	48.7
Harvest-1Sept	**Elgin**	16	189	13.3	3.3	182.	196.						
Harvest-1Sept	**Somerset West**	12	190	15.9	4.6	180.	200.						
Harvest-1Sept	**Stellenbosch 2**	14	189	8.4	2.3	184.	194.						
Harvest-1Sept	**Vredendal**	8	163	12.3	4.4	153.	173.						
Harvest-1Sept	**Stellenbosch 1**	6	172	3.4	1.4	169.	176.						

Table 17 Descriptive statistics of seasonal variability for phenology 2 averaged over the six sites and cultivars, (-95% and 95% denoting confidence intervals).

Season	Phenology2 (date after 1 Sept.)	N	Mean	Standard Deviation	Standard Error	Confidence Interval		Phenology4 (days between stages)	Mean	Standard deviation	Standard error	Confidence Interval	
						-0.95	0.95					-0.95	0.95
2012/13	BB-1Sept	9	21.56	5.96	1.99	16.97	26.14	BB/FL	57.11	2.47	0.82	55.21	59.01
2013/14	BB-1Sept	13	24.69	4.42	1.23	22.02	27.37	BB/FL	44.69	17.64	4.89	34.03	55.35
2014/15	BB-1Sept	22	19.32	8.55	1.82	15.53	23.11	BB/FL	38.73	14.66	3.12	32.23	45.23
2015/16	BB-1Sept	16	14.50	8.45	2.11	10.00	19.00	BB/FL	43.88	6.05	1.51	40.65	47.10
2012/13	Flowering-1Sept	9	78.67	5.63	1.88	74.34	83.00	FL/PS	21.56	1.51	0.50	20.40	22.72
2013/14	Flowering-1Sept	13	69.38	17.88	4.96	58.58	80.19	FL/PS	27.23	10.03	2.78	21.17	33.29
2014/15	Flowering-1Sept	22	58.05	17.13	3.65	50.45	65.64	FL/PS	25.59	11.64	2.48	20.43	30.75
2015/16	Flowering-1Sept	16	58.38	5.81	1.45	55.28	61.47	FL/PS	28.88	4.76	1.19	26.34	31.41
2012/13	PeaSize-1Sept	9	100.22	6.55	2.18	95.18	105.26	PS/BC	14.78	3.77	1.26	11.88	17.67
2013/14	PeaSize-1Sept	13	96.62	11.21	3.11	89.84	103.39	PS/BC	18.15	6.88	1.91	14.00	22.31
2014/15	PeaSize-1Sept	22	83.64	6.43	1.37	80.78	86.49	PS/BC	15.32	5.07	1.08	13.07	17.57
2015/16	PeaSize-1Sept	16	87.25	6.08	1.52	84.01	90.49	PS/BC	26.25	6.01	1.50	23.05	29.45
2012/13	BunchClos-1Sept	9	115.00	9.99	3.33	107.32	122.68	BC/PrV	19.11	7.64	2.55	13.24	24.98
2013/14	BunchClos-1Sept	13	114.77	11.27	3.13	107.96	121.58	BC/PrV	16.31	6.26	1.74	12.52	20.09
2014/15	BunchClos-1Sept	22	98.95	5.17	1.10	96.66	101.25	BC/PrV	22.55	8.67	1.85	18.70	26.39
2015/16	BunchClos-1Sept	16	113.50	8.83	2.21	108.79	118.21	BC/PrV	12.94	6.81	1.70	9.31	16.56
2012/13	PreVer-1Sept	9	134.11	5.09	1.70	130.20	138.02	PrV/V	8.67	6.84	2.28	3.41	13.92
2013/14	PreVer-1Sept	13	131.08	13.67	3.79	122.82	139.33	PrV/V	15.31	12.05	3.34	8.03	22.59
2014/15	PreVer-1Sept	22	121.50	10.60	2.26	116.80	126.20	PrV/V	12.18	7.20	1.53	8.99	15.37
2015/16	PreVer-1Sept	16	126.44	8.51	2.13	121.90	130.97	PrV/V	9.75	5.78	1.44	6.67	12.83
2012/13	Ver50%-1Sept	9	142.78	5.36	1.79	138.66	146.90	V/Ver	7.89	2.67	0.89	5.84	9.94
2013/14	Ver50%-1Sept	13	146.38	8.28	2.30	141.38	151.39	V/Ver	6.77	2.24	0.62	5.41	8.12
2014/15	Ver50%-1Sept	22	133.68	6.30	1.34	130.89	136.48	V/Ver	11.86	3.38	0.72	10.36	13.36
2015/16	Ver50%-1Sept	16	136.19	12.15	3.04	129.71	142.66	V/Ver	22.31	7.23	1.81	18.46	26.16
2012/13	Ver100%-1sept	9	150.67	6.46	2.15	145.70	155.63	Ver/H	46.33	12.05	4.02	37.07	55.60
2013/14	Ver100%-1sept	13	153.15	9.52	2.64	147.40	158.91	Ver/H	35.69	10.97	3.04	29.06	42.32
2014/15	Ver100%-1sept	22	145.55	6.44	1.37	142.69	148.40	Ver/H	24.64	6.00	1.28	21.97	27.30
2015/16	Ver100%-1sept	16	158.50	12.25	3.06	151.97	165.03	Ver/H	37.19	14.90	3.72	29.25	45.13
2012/13	Harvest-1Sept	9	197.00	6.06	2.02	192.34	201.66						
2013/14	Harvest-1Sept	13	188.85	11.06	3.07	182.16	195.53						
2014/15	Harvest-1Sept	22	170.18	10.08	2.15	165.71	174.65						
2015/16	Harvest-1Sept	16	195.69	12.61	3.15	188.97	202.40						

Table 18 ANOVA analysis shows the Levenes test for homogeneity of variance, IPF p = 0.00, IPV p = 0.84 and IPCY p = 0.42, hence the analysis in table is Games Howell post hoc for IPF and LSD test for IPV and IPCY for all sites.

Phenology	Site	Elgin	Somerset West	Stellenbosch_2	Vredendal	Stellenbosch_1	Statistics
IPF	Elgin		0.03	0.73	0.02	1.00	GAMES HOWELL POST HOC
IPF	Somerset West	0.03		0.12	0.09	0.60	GAMES HOWELL POST HOC
IPF	Stellenbosch 2	0.73	0.12		0.04	0.98	GAMES HOWELL POST HOC
IPF	Vredendal	0.02	0.09	0.04		0.03	GAMES HOWELL POST HOC
IPF	Stellenbosch 1	1.00	0.60	0.98	0.03		GAMES HOWELL POST HOC
IPV	Elgin		0.00	0.00	0.00	0.00	LSD TEST
IPV	Somerset West	0.00		0.00	0.04	0.06	LSD TEST
IPV	Stellenbosch 2	0.00	0.00		0.35	0.42	LSD TEST
IPV	Vredendal	0.00	0.04	0.35		0.97	LSD TEST
IPV	Stellenbosch 1	0.00	0.06	0.42	0.97		LSD TEST
IPCY	Elgin		0.00	0.00	0.00	0.00	LSD TEST
IPCY	Somerset West	0.00		0.00	0.82	0.01	LSD TEST
IPCY	Stellenbosch	0.00	0.00		0.01	0.94	LSD TEST
IPCY	Vredendal	0.00	0.82	0.01		0.03	LSD TEST
IPCY	Stellenbosch 1	0.00	0.01	0.94	0.03		LSD TEST

Table 19 The variability in precocity index between the sites and across the three seasons, as the precocity index for flowering (IPF), véraison (IPV) and the vintage (IPCY).

Precocity Index	Site/Season	N	Mean	Standard Deviation	Standard error	Confidence Interval	
						-0.95	0.95
IPF	Elgin	16	91.46	10.92	2.73	85.64	97.27
IPF	Somerset West	12	101.90	5.82	1.68	98.20	105.60
IPF	Stellenbosch 2	14	95.53	7.00	1.87	91.49	99.57
IPF	Vredendal	8	132.20	27.50	9.72	109.21	155.18
IPF	Stellenbosch 1	6	91.71	16.10	6.57	74.82	108.61
IPV	Elgin	16	106.23	5.75	1.44	103.17	109.30
IPV	Somerset West	12	93.78	2.76	0.80	92.02	95.53
IPV	Stellenbosch 2	14	99.36	3.33	0.89	97.44	101.28
IPV	Vredendal	8	97.66	3.58	1.26	94.67	100.65
IPV	Stellenbosch 1	6	97.74	3.26	1.33	94.32	101.16
IPCY	Elgin	16	86.27	10.49	2.62	80.68	91.85
IPCY	Somerset West	12	112.68	5.07	1.46	109.46	115.90
IPCY	Stellenbosch 2	14	100.92	7.05	1.89	96.85	105.00
IPCY	Vredendal	8	111.79	10.31	3.65	103.16	120.41
IPCY	Stellenbosch 1	6	101.23	9.09	3.71	91.69	110.78
IPF	2012/13	9	100.00	7.16	2.39	94.49	105.51
IPF	2013/14	13	97.09	8.66	2.40	91.85	102.32
IPF	2014/15	22	100.00	29.28	6.24	87.02	112.98
IPF	2015/16	16	100.00	9.93	2.48	94.71	105.29
IPV	2012/13	9	100.00	3.75	1.25	97.12	102.88
IPV	2013/14	13	100.00	5.54	1.54	96.65	103.35
IPV	2014/15	22	100.00	4.69	1.00	97.92	102.08
IPV	2015/16	16	100.00	8.92	2.23	95.25	104.75
IPCY	2012/13	9	100.00	8.80	2.93	93.24	106.76
IPCY	2013/14	13	100.01	11.03	3.06	93.34	106.68
IPCY	2014/15	22	100.00	13.32	2.84	94.10	105.90
IPCY	2015/16	16	100.00	17.72	4.43	90.56	109.44

Table 20 Results from regression analysis between variables in cluster 1 with phenology 1 and phenology 2 (phenology at different stages). Bottom half of the tables, regression analysis for the cultivar Cabernet Sauvignon (CS) and Shiraz (SH) (all regressions significant at the $p \leq 0.01$ level).

Cluster1	**Phenology 1 & 2**	***r***	***p***	***R^2***	
RH_Stat_	**Phenology**				
9_RH_Stat_20<=x<40	Pea size-1Sept	-0.61	0.00	0.38	
Climate Index daily	**Stage**	***r***	***p***	***R^2***	
GDD_Stat_(Daily)	Flowering-1st Sept	-0.74	0.00	0.55	
GDD_Stat_(Daily)	Pea size -1st Sept	-0.67	0.00	0.45	
GDD_Stat_(Daily)	Pre Véraison-1st Sept	-0.79	0.00	0.62	
GDD_Stat_(Daily)	Harvest-1st Sept	-0.63	0.00	0.40	
GDD_Stat_(Daily)	IPCY	0.56	0.00	0.32	
Daily Index	**Phenology**	***r***	***p***	***R^2***	
Dly_MFTn_Stat	IPF	-0.43	<0.01	0.18	
Dly_MFTn_Stat	IPCY	-0.38	<0.01	0.15	
Dly_MFTn_Stat	Flowering-1Sept	-0.46	<0.01	0.21	
Dly_MFTn_Stat	Pre Véraison-1Sept	-0.49	<0.01	0.24	
Rain	**Precocity index**	***r***	***p***	***R^2***	
Rain	IPF	-0.53	0.00	0.28	
Rain	IPV	0.21	0.10	0.04	
Rain	IPCY	-0.30	0.02	0.09	
Summer Rain	IPF	-0.26	0.04	0.07	
Summer Rain	IPV	0.06	0.67	0.00	
Summer Rain	IPCY	-0.07	0.60	0.00	
9_RH_Stat_	**Phenology**	***r***	***p***	***R^2***	**Cultivar**
9_RH_Stat_0<=x<20	IPCY	0.28	0.05	0.08	CS
9_RH_Stat_0<=x<20	IPCY	0.64	0.02	0.42	SH
9_RH_Stat_20<=x<40	IPCY	0.33	0.02	0.11	CS
9_RH_Stat_20<=x<40	IPCY	0.59	0.04	0.35	SH
9_RH_Stat_80<=x<100	IPCY	-0.56	0.00	0.31	CS
9_RH_Stat_80<=x<100	IPCY	-0.81	0.00	0.65	SH
9_RH_Stat_80<=x<100	Flowering-1Sept	0.04	0.01	0.13	CS
9_RH_Stat_80<=x<100	Flowering-1Sept	0.63	0.03	0.40	SH
9_RH_Stat_80<=x<100	Pea size-1Sept	0.26	0.08	0.07	CS
9_RH_Stat_80<=x<100	Pea size-1Sept	0.64	0.02	0.41	SH
Climatic	**Stage**	***r***	***p***	***R^2***	**Cultivar**
GDD_Stat_(Daily)	Flowering	-0.74	0.00	0.55	CS
GDD_Stat_(Daily)	Flowering	-0.78	0.00	0.60	SH
GDD_Stat_(Daily)	Pre Véraison	-0.74	0.00	0.56	CS
GDD_Stat_(Daily)	Pre Véraison	-0.88	0.00	0.77	SH
GDD_Stat_(Daily)	IPCY	0.60	0.00	0.35	CS
GDD_Stat_(Daily)	IPCY	0.65	0.02	0.43	SH
Rainfall	**Phenology**	***r***	***p***	***R^2***	**Cultivar**
Rain	Flowering-1st Sept	0.76	0.00	0.58	CS
Rain	Flowering-1st Sept	0.86	0.00	0.74	SH
Summer Rain	Flowering-1st Sept	0.64	0.00	0.41	CS
Summer Rain	Flowering-1st Sept	0.61	0.04	0.38	SH
Winter Rain	Flowering-1st Sept	0.66	0.00	0.44	CS
Winter Rain	Flowering-1st Sept	0.86	0.00	0.74	SH
Winter Rain	Peas Size-1st Sept	0.79	0.00	0.62	CS
Winter Rain	Peas Size-1st Sept	0.72	0.00	0.52	SH

Table 21 Results from regression analysis between the phenology 3 (BB-Flowering, BB-PeaSize and BB-Harvest):_T_Stat for both cultivar Cabernet Sauvignon (CS) and Shiraz (SH) (all regressions significant at the $p \leq 0.01$ level).

Cluster2	Phenology 3 & 4	*r*	*p*	R^2
1_T_Stat	**Phenology**			
1_T_Stat_35<=x<40	BB-Flowering	-0.80	0.00	0.64
2_T_Stat	**Phenology**	***r***	***p***	R^2
2_T_Stat_25<=x<30	BB-Flowering	-0.62	0.00	0.40
2_T_Stat_30<=x<35	BB-Flowering	-0.70	0.00	0.49
2_T_Stat_35<=x<40	BB-Flowering	-0.68	0.00	0.46
2_T_Stat_40<=x<45	BB-Flowering	-0.54	0.00	0.30
2_T_Stat_35<=x<40	BB/FL	-0.68	0.00	0.46
2_T_Stat_40<=x<45	BB/FL	-0.54	0.00	0.30
5_T_Stat	**Phenology**	***r***	***p***	R^2
5_T_Stat_20<=x<25	BB/FL	-0.75	0.00	0.56
5_T_Stat_25<=x<30	BB/FL	-0.90	0.00	0.80
5_T_Stat_30<=x<35	BB/FL	-0.81	0.00	0.65
5_T_Stat_20<=x<25	FL/PS	0.65	0.00	0.42
4_T_Stat	**Phenology**	***r***	***p***	R^2
4_T_Stat_25<=x<30	BB-Flowering	-0.77	0.00	0.60
4_T_Stat_30<=x<35	BB-Flowering	-0.79	0.00	0.62
4_T_Stat_35<=x<40	BB-Flowering	-0.86	0.00	0.74
3_T_Stat	**Phenology**	***r***	***p***	R^2
3_T_Stat_25<=x<30	BB-Flowering	-0.71	0.00	0.50
3_T_Stat_30<=x<35	BB-Flowering	-0.85	0.00	0.73
3_T_Stat_35<=x<40	BB-Flowering	-0.76	0.00	0.57
3_T_Stat_25<=x<30	BB-Pea Size	-0.74	0.00	0.55
3_T_Stat_30<=x<35	BB-Pea Size	-0.72	0.00	0.52
3_T_Stat_35<=x<40	BB-Pea Size	-0.57	0.00	0.32
3_T_Stat_25<=x<30	BB-Harvest	-0.56	0.00	0.31
3_T_Stat_30<=x<35	BB-Harvest	-0.68	0.00	0.47
3_T_Stat_35<=x<40	BB-Harvest	-0.68	0.00	0.46
12_T_Stat	**Phenology**	***r***	***p***	R^2
12_T_Stat_30<=x<35	BB-Flowering	-0.54	0.00	0.30
12_T_Stat_35<=x<40	BB-Flowering	-0.63	0.00	0.40
12_T_Stat_35<=x<40	PrV/V	0.65	0.00	0.42
7_T_Stat	**Phenology**	***r***	***p***	R^2
7_T_Stat_30<=x<35	BB-Flowering	-0.74	0.00	0.55
7_T_Stat_25<=x<30	PrV/V	0.70	0.00	0.50
6_T_Stat	**Phenology**	***r***	***p***	R^2
6_T_Stat_15<=x<20	BB-Flowering	-0.76	0.00	0.58
6_T_Stat_20<=x<25	BB-Flowering	-0.73	0.00	0.54
6_T_Stat_25<=x<30	BB-Flowering	-0.82	0.00	0.67
6_T_Stat_15<=x<20	PrV/V	0.55	0.00	0.30
6_T_Stat_20<=x<25	PrV/V	0.55	0.00	0.30
6_T_Stat_25<=x<30	PrV/V	0.59	0.00	0.35
11_T_Stat	**Phenology**	***r***	***p***	R^2
11_T_Stat_25<=x<30	BB-Flowering	-0.75	0.00	0.57
11_T_Stat_30<=x<35	BB-Flowering	-0.84	0.00	0.70
11_T_Stat_35<=x<40	BB-Flowering	-0.80	0.00	0.65
11_T_Stat_25<=x<30	BB-Harvest	-0.64	0.00	0.40
11_T_Stat_30<=x<35	BB-Harvest	-0.58	0.00	0.34
11_T_Stat_35<=x<40	BB-Harvest	-0.51	0.00	0.26
11_T_Stat_25<=x<30	PrV/V	0.45	0.00	0.20
11_T_Stat_30<=x<35	PrV/V	0.57	0.00	0.32
11_T_Stat_35<=x<40	PrV/V	0.79	0.00	0.62
11_T_Stat_25<=x<30	BB/FL	-0.75	0.00	0.60
11_T_Stat_30<=x<35	BB/FL	-0.84	0.00	0.70
11_T_Stat_35<=x<40	BB/FL	-0.80	0.00	0.65

Table 22 Results from regression analysis between the phenology 3 (BB-Flowering, BB-PeaSize and BB-Harvest):_T_Stat for both cultivar Cabernet Sauvignon (CS) and Shiraz (SH), bottom of table regression analysis between the phenology 3 (BB-Flowering):T_Stat for cultivar Cabernet Sauvignon (CS) and Shiraz (SH), (all regressions significant at the $p \leq 0.01$ level).

Cluster2	Phenology 3 & 4	*r*	*p*	R^2	Cultivar
5_T_Stat	**Phenology**				**Cultivar**
5_T_Stat_20<=x<25	BB/FL	-0.64	0.00	0.41	CS
5_T_Stat_20<=x<25	BB/FL	-0.95	0.00	0.90	SH
5_T_Stat_25<=x<30	BB-Flowering	-0.84	0.00	0.70	CS
5_T_Stat_25<=x<30	BB-Flowering	-0.97	0.00	0.93	SH
4_T_Stat	**Phenology**	***r***	***p***	R^2	**Cultivar**
4_T_Stat_10<=x<15	BB/FL	0.47	0.00	0.22	CS
4_T_Stat_10<=x<15	BB/FL	0.92	0.00	0.85	SH
4_T_Stat_20<=x<25	FL/PS	0.32	0.02	0.10	CS
4_T_Stat_20<=x<25	FL/PS	0.67	0.02	0.44	SH
3_T_Stat	**Phenology**	***r***	***p***	R^2	**Cultivar**
3_T_Stat_30<=x<35	BB-Flowering	-0.85	0.00	0.73	All
3_T_Stat_30<=x<35	BB-Flowering	-0.84	0.00	0.70	CS
3_T_Stat_30<=x<35	BB-Flowering	-0.82	0.00	0.67	SH
7_T_Stat	**Phenology**	***r***	***p***	R^2	**Cultivar**
7_T_Stat_30<=x<35	BB-Flowering	-0.71	0.00	0.50	CS
7_T_Stat_30<=x<35	BB-Flowering	-0.73	0.01	0.53	SH
7_T_Stat_25<=x<30	PrV/V	0.58	0.00	0.33	CS
7_T_Stat_25<=x<30	PrV/V	0.87	0.00	0.76	SH
6_T_Stat	**Phenology**	***r***	***p***	R^2	**Cultivar**
6_T_Stat_25<=x<30	BB-Flowering	-0.79	0.00	0.62	CS
6_T_Stat_25<=x<30	BB-Flowering	-0.79	0.00	0.63	SH
11_T_Stat	**Phenology**	***r***	***p***	R^2	**Cultivar**
11_T_Stat_30<=x<35	BB-Flowering	-0.84	0.00	0.70	CS
11_T_Stat_30<=x<35	BB-Flowering	-0.73	0.01	0.53	SH
11_T_Stat_25<=x<30	BB-Harvest	-0.62	0.00	0.40	CS
11_T_Stat_25<=x<30	BB-Harvest	-0.66	0.02	0.44	SH
11_T_Stat_35<=x<40	PrV/V	0.67	0.00	0.45	CS
11_T_Stat_35<=x<40	PrV/V	0.96	0.00	0.91	SH
11_T_Stat_35<=x<40	BB/FL	-0.69	0.00	0.47	CS
11_T_Stat_35<=x<40	BB/FL	-0.95	0.00	0.90	SH

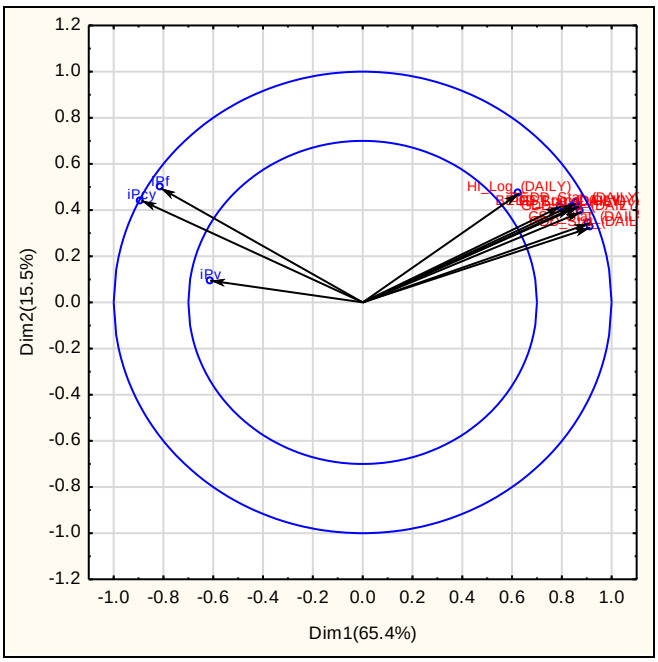

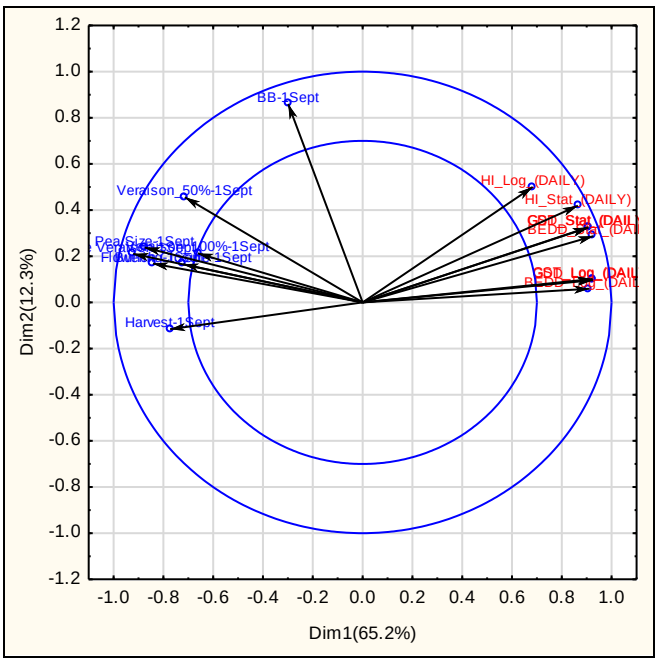

Figure 22 Multifactor analysis, representing the principal components of separate PCA's of each block variable, climatic indices calculated from daily data from weather station and logger sources (HI, GDD, BEDD, GST_Stat/Log) vs the precocity index (phenology 1) with RV = 0.30 (left) and phenology stages as days after 1 September (phenology 2) with RV = 0.61 (right).

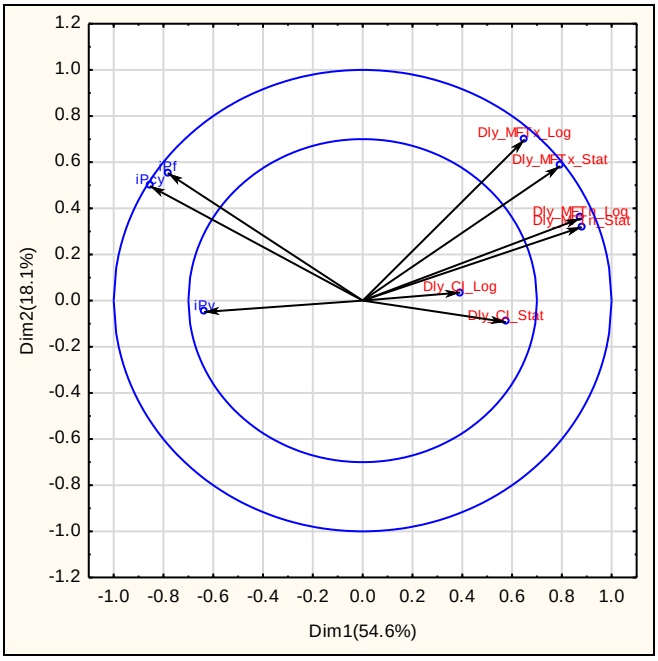

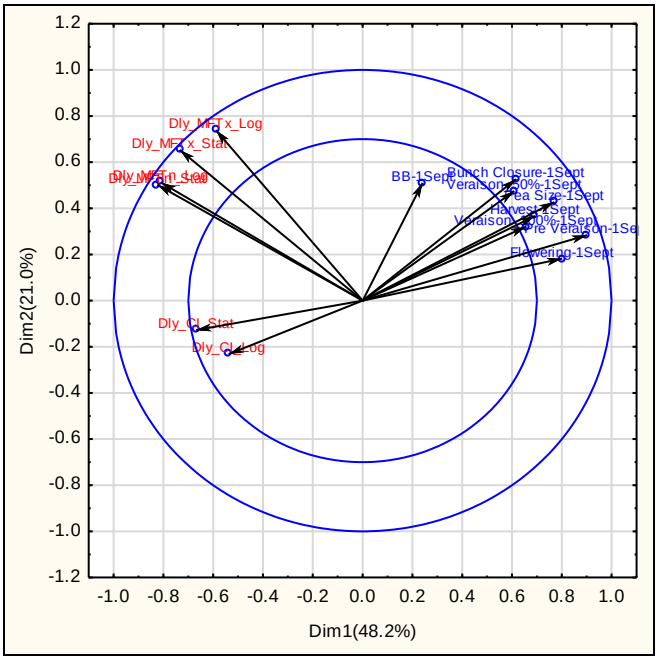

Figure 23 Multifactor analysis, representing the principal components of separate PCA's of each block variable, climatic indices calculated from daily data from weather station and logger sources (MFT, MFT_x, MFT_n, CI_Stat/Log) vs the precocity index (phenology 1) with RV = 0.29 (left) and phenology stages as days after 1 September (phenology 2) with RV = 0.27 (right).

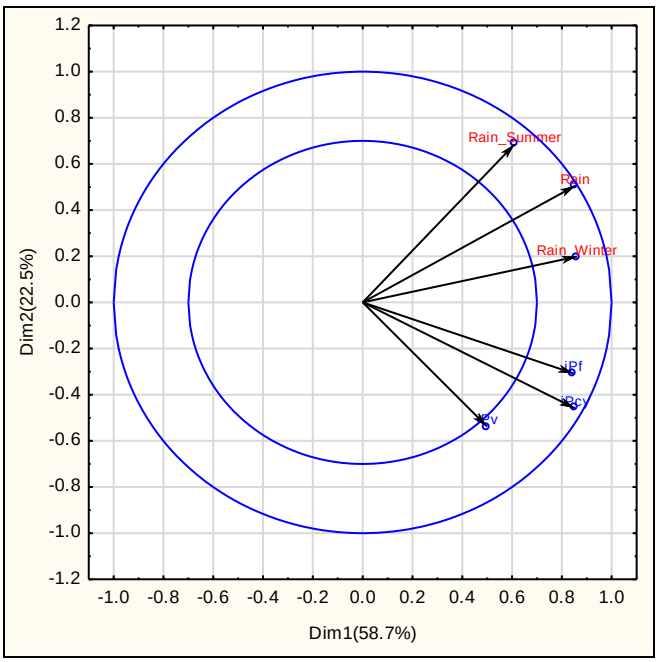

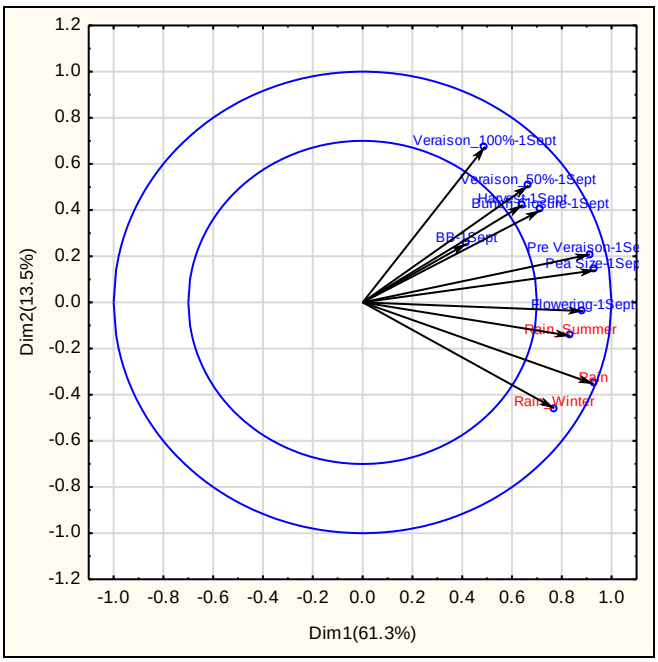

Figure 24 Multifactor analysis, representing the principal components of separate PCA's of each block variable, rainfall (Rain_) vs the precocity index (phenology 1) with RV = 0.19 (left) and phenology stages as days after 1 September (phenology 2) with RV = 0.50 (right). Phenology 1 vs Rainfall is based on 80% of data and phenology 2 vs rainfall is based on 74.8% of data.

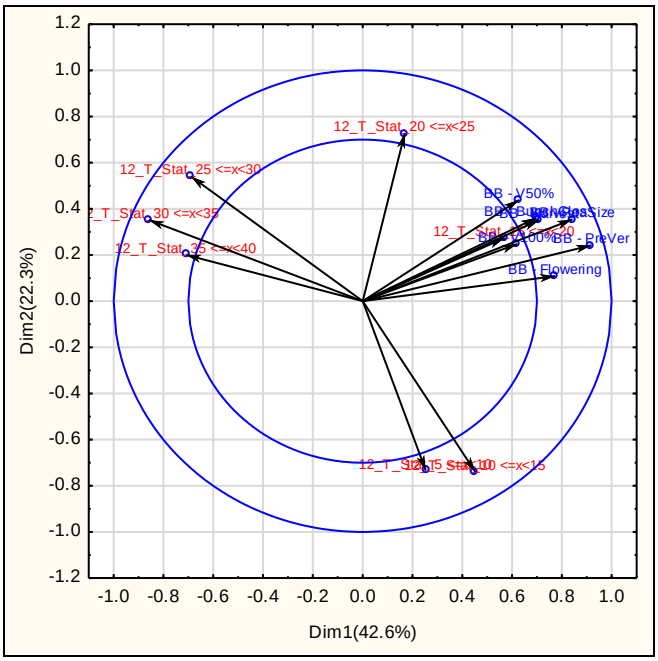

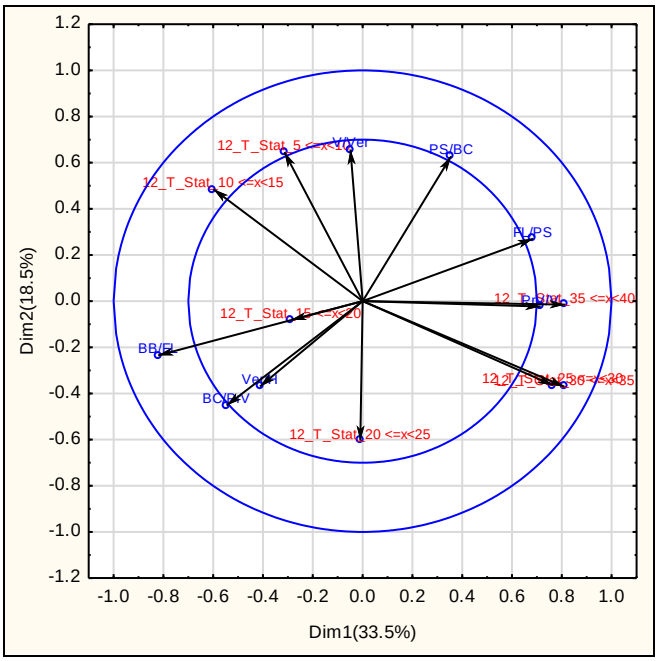

Figure 25 Multifactor analysis, representing the principal components of separate PCA's of each block variable, temperature for the month of December from the weather station (12_T_Stat) vs phenology stages as days after budburst (phenology 3) with RV = 0.31 (left) and days between phenological stages (phenology 4) with RV = 0.25 (right).

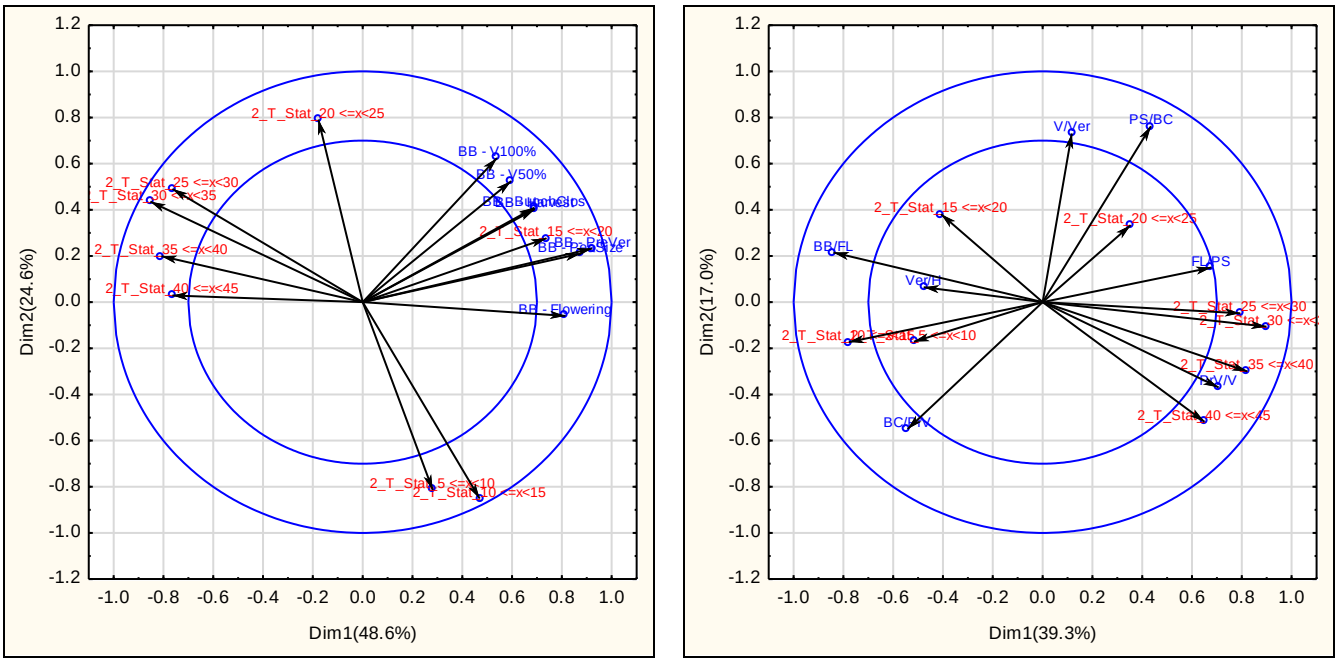

Figure 26 Multifactor analysis, representing the principal components of separate PCA's of each block variable, temperature for the month of February from the weather station (2_T_Stat) vs phenology stages as days after budburst (phenology 3) (left) and days between phenological stages (phenology 4).

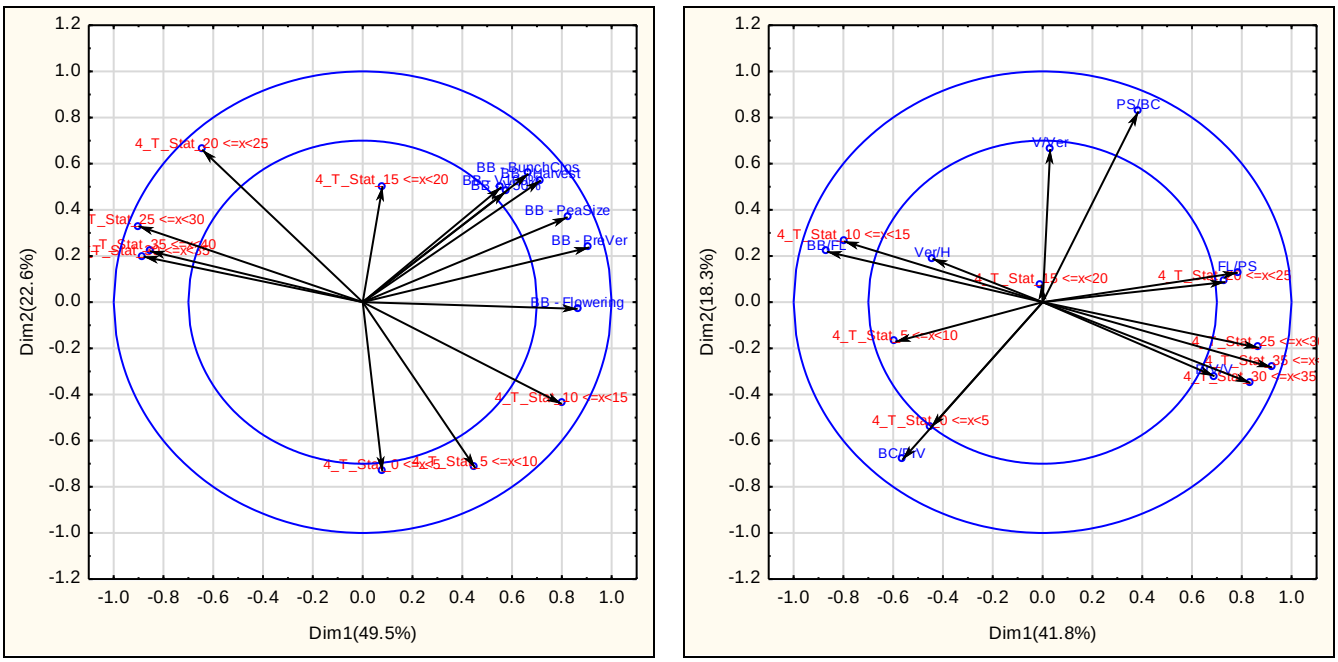

Figure 27 Multifactor analysis, representing the principal components of separate PCA's of each block variable, temperature for the month of April from the weather station (4_T_Stat) vs phenology stages as days after budburst (phenology 3) (left) and days between phenological stages (phenology 4).

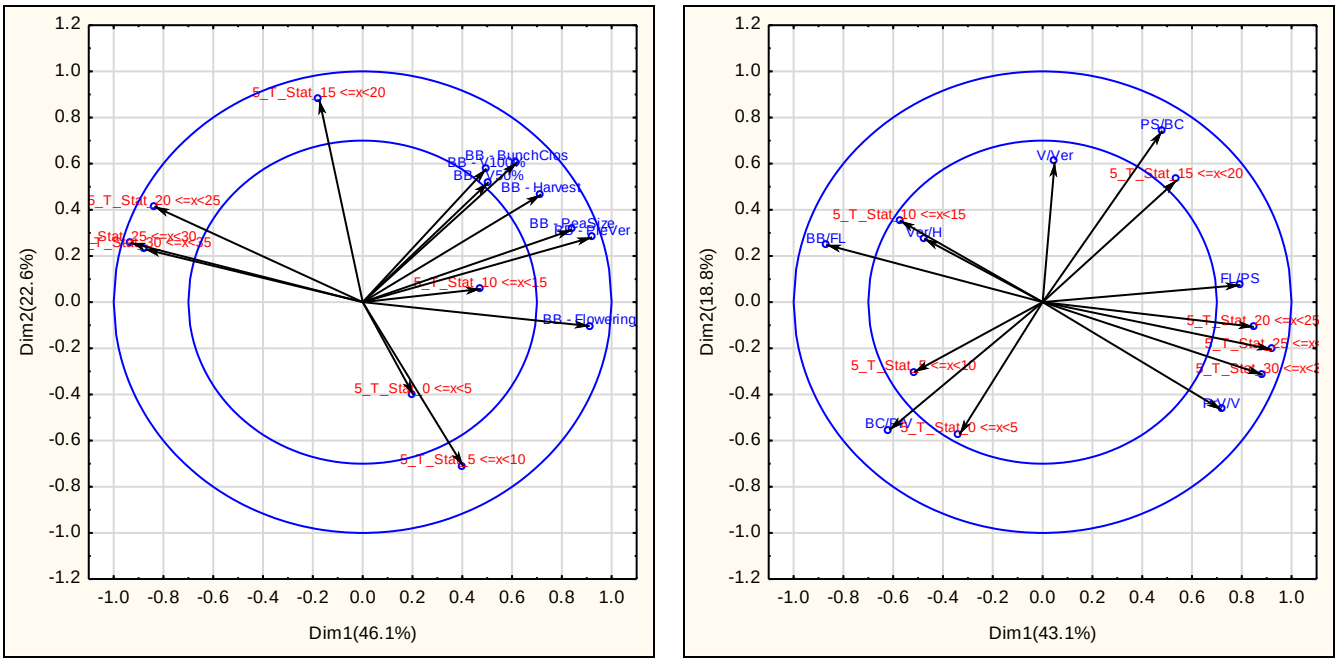

Figure 28 Multifactor analysis, representing the principal components of separate PCA's of each block variable, temperature for the month of May from the weather station (5_T_Stat) vs phenology stages as days after budburst (phenology 3) (left) and days between phenological stages (phenology 4).

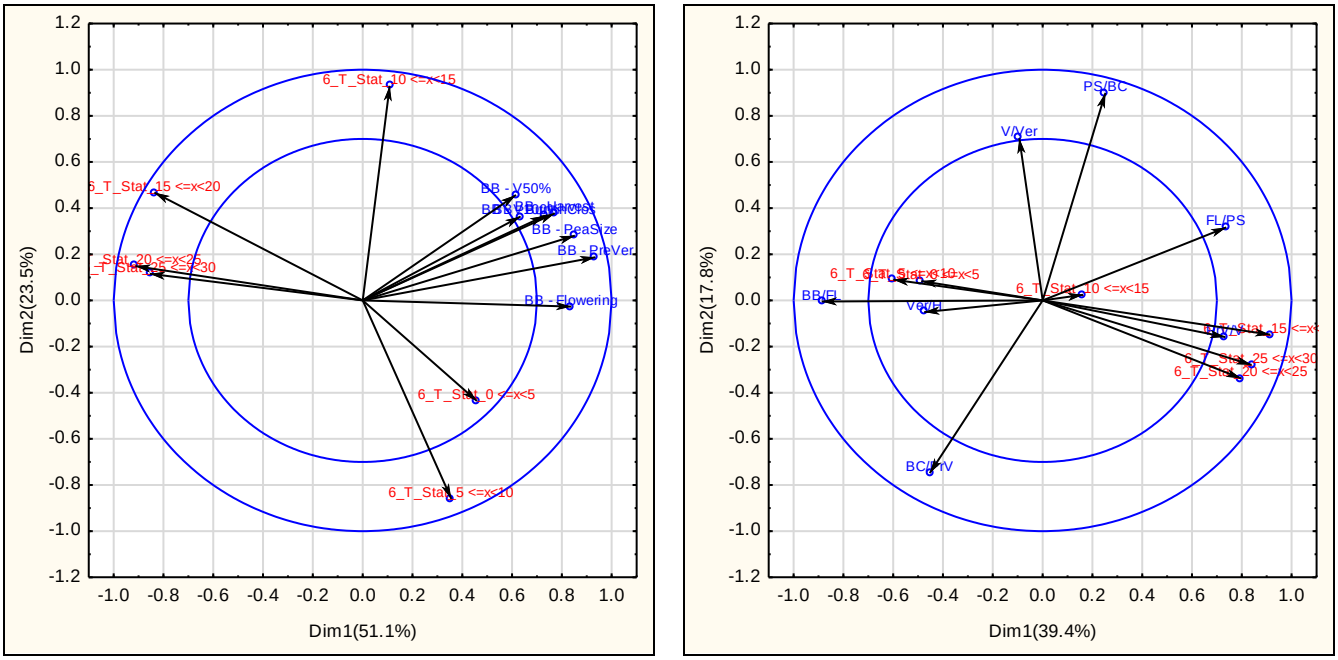

Figure 29 Multifactor analysis, representing the principal components of separate PCA's of each block variable, temperature for the month of June from the weather station (6_T_Stat) vs phenology stages as days after budburst (phenology 3) (left) with (RV = 0.36) and days between phenological stages (phenology 4) with (RV = 0.36).

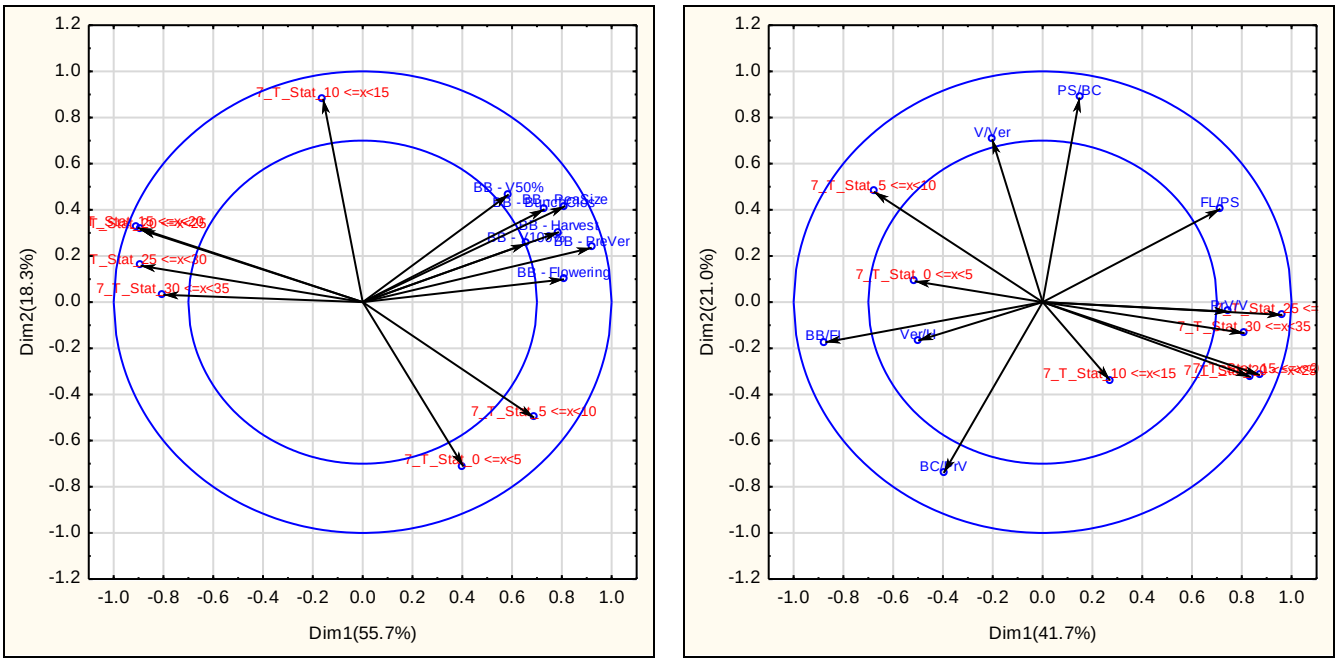

Figure 30 Multifactor analysis, representing the principal components of separate PCA's of each block variable, temperature for the month of July from the weather station (7_T_Stat) vs phenology stages as days after 1 September (phenology 2) (left) and days between phenological stages (phenology 4).

Chapter 8

Research results

Interactive effects of site and season on the performance of (*Vitis vinifera* L.) cv. Cabernet Sauvignon and Shiraz

CHAPTER 8: INTERACTIVE EFFECTS OF SITE AND SEASON ON THE PREFORMANCE OF (*VITIS VINIFERA* L.) *CV.* CABERNET SAUVIGNON AND SHIRAZ

8.1 Introduction

The grapevine growth, yield and ripening response, eventual chemical and colour composition of the berry and final sensory attributes are all results of the interaction between the soil, climate, long term practices (*e.g.* cultivar selection, establishment techniques, row orientation, vine spacing, trellising, training and pruning systems), short term practices (*e.g.* irrigation, fertilisation and canopy management) and harvest criteria applied by the grower (Jackson & Lombard, 1993; Hunter & Archer, 2001a, 2001b; Hunter *et al.*, 2004; Van Leeuwen *et al.*, 2004; Deloire *et al.*, 2005; Carey *et al.*, 2008; Hunter *et al.*, 2010; Hunter & Bonnardot, 2011). These external factors affect physiological processes and the distribution of carbon in the grapevine, altering berry composition and final wine quality (Carbonneau & Deloire, 2001; Hunter *et al.*, 2010). Berry quality may also depend on the temperature during ripening, therefore the best quality is found in a variety grown in a region where the growing season matches the cool portion of the season in that region (Carey *et al.*, 2003; Jones, 2006). Climate, in particular temperature, plays an important role in determining wine style and quality, with a significant variation of wine styles recognised in the complex viticultural terrain of South Africa (Le Roux, 1974; De Villiers *et al.*, 1996).

Research indicates that as climate warms, wine grape phenology progresses more rapidly with an increase in growth tempo and grapes ripening earlier (Chuine *et al.*, 2004; Jones *et al.*, 2005; Webb *et al.*, 2013). Among the most important climate change-related effects are advanced harvest times and higher wine alcohol levels, lower acidities and modification of varietal aroma compounds as higher temperatures increase grape sugar concentrations and influence fruit composition to, as (Conde *et al.*, 2007; Mira de Orduña, 2010; Orduña, 2010; Webb *et al.*, 2013). Grapevine sugar accumulation in the berry is dependent on the photosynthetic activity of the grapevine, which decreases under higher water constraints or water restricted conditions, especially under warmer temperature conditions, resulting in a lower sugar unloading into the berry. It is clear that berry sugar accumulation depends on the source (primarily photosynthesis) and sink activities in the grapevine to be balanced for optimal ripening (Carbonneau & Deloire, 2001). Higher temperatures reduce anthocyanin accumulation (Downey *et al.*, 2006; Joscelyne *et al.,* 2007), for which the optimum temperature ranges between 30°C and 35°C (Spayd *et al.*, 2002). Air temperature is one of the most important atmospheric variables for viticulture (Myburgh, 2005) as it plays an important role in grapevine development, ultimately affecting juice and final wine quality and aroma (Carey, 2001). Anthocyanins are produced during fruit maturation, and their concentration in the berry is affected by growing conditions.

Grape quality tends to be higher on soils that induce moderate water constraints, especially on clayey soils where water deficits in the season are moderate due to the higher water holding capacity - supplementary irrigation is required in more sandy soils and warmer climates (Van Leeuwen *et al.*, 2004; Bruwer, 2010; Mehmel, 2010). Grapevine water status has an effect on vegetative growth, therefore lower vigour areas within vineyards could have lower transpiration per unit leaf area (higher photosynthetic efficiency) and potentially earlier ripening. This could be due to the soil heating up faster, leading to earlier phenology, with vegetative growth eventually being limited by water constraints and warmer temperatures. Managing the grapevine microclimate can therefore possibly contribute to the grapevine's better utilisation of available water resources within

warmer climates. Canopy management strategies where *e.g.* bearing shoots are removed to one shoot per bearer, may severely reduce the source, leading to newly developed leaves benefitting from increased root supply of nutrients, water and hormones, conversely leading to more efficient leaf tissue in the mature stages (Flore & Lakso, 1989; Palliotti *et al.*, 2011; Strever, 2012).

Climate of the season appeared to have a very strong effect on the aroma characteristics of Cabernet Sauvignon wines, where warmer sites and normal seasonal rainfall wines can be expected to have more intense berry aroma characteristics and cooler climates a more vegetative character (Carey *et al.*, 2008; Mehmel, 2010). The typical cultivar aroma of Cabernet Sauvignon can be described as being a fruity flavour of red berry, black currents and green bell peppers (Pineau *et al.*, 2009). A total of 48 active aroma compounds have been identified in Cabernet Sauvignon wines (Carey *et al.*, 2008). The vegetative descriptors for Cabernet Sauvignon are typically bell pepper, herbaceous, tobacco, hay, artichoke, mint, freshly cut green grass and eucalyptus (Carey *et al.,* 2008 and references therein). The vegetative aroma resulted from more dense canopies, with excessive vegetative growth - grapevine water status had a more indirect effect on the flavour and aroma compounds *via* effects on the grapevine canopy (Spayd *et al.*, 2002; Mehmel, 2010).

To avoid the possible negative impacts from climatic shifts, understanding the grapevine reaction in different climatic environments will allow for more effective adaptation strategies. Introducing cultivars that ripen later or earlier in the season, adjusting canopy management strategies and using irrigation strategies to buffer the extremes predicted in the climate change studies, therefore minimizing the plant water stress (Mehmel, 2010) could be applied. Adaption strategies allow for more optimal wine production to be practised into the future within an existing site and within the context of climate change (Webb *et al.*, 2013). Despite the close association between these diverse aspects of temperature, isolation of its effects is important to understand and manipulate the system against warming (Webb *et al.,* 2012). Therefore, it is necessary to assess at fine scale the climatic suitability (in terms of duration) of regions and environments for grapevine cultivation, and more specifically the grapevine requirements that affect the accumulation of components that are viticulturally and oenologically important.

The aim of the study was to isolate possible adaptive strategies within a warming and changing climate within the Western Cape. The objective of the chapter is therefore to correlate climate/weather with the grapevine's growth, ripening and final wine chemistry and sensorial attributes, to identity possible environmental factors affecting grapevine responses, within the context of site and within-site variability.

In light of the above mentioned, *Vitis vinifera* L. *cv.* Cabernet Sauvignon was selected for this study as the cultivar ripens late, has a good tolerance for heat, preferring hotter ripening periods complemented by cooler night temperatures for optimal development of quality and colour (Mehmel, 2010). To add complexity to the data, *Vitis vinifera* L. *cv.* Shiraz grapevines which are less tolerant to heat due their near-anisohydric ("optimistic") growth behaviour, consequently being more reactive to the climate and water availability were also selected. In contrast, Cabernet Sauvignon grapevines regulate more conservatively to their environment due to the inherent near-isohydric nature (Schultz, 2003). In the context of climate change these cultivars were selected to represent cultivars that are more or less sensitive to the climate.

8.2 Materials and Methods

8.2.1 Study area, site selection, experimental layout

Well-renowned commercial wine farms were selected over a climatic band, with vineyards selected based on cultivar/rootstock selections and commercial cultivation practices (Refer to Addendum 8.1). Cabernet Sauvignon grapevine responses to a changing environment was monitored from 01 September to 31 March for three seasons, namely the 2012/13 season (S1), 2013/14 season (S2) and 2014/15 season (S3). Give the detail about the Shiraz for one season. The grapevine was used as a probe to the study the growth and ripening reaction of the grapevine to its environment, hence extreme and representative environmental conditions were selected over a climatic band to study the grapevine in detail. Sites ranged from Elgin (cooler climate) on the coastal side of the Overberg mountain range, to Somerset West (moderate to warm climate) on the west facing slopes of the Helderberg mountain range, to Stellenbosch where three sites (on the foothills of the Simonsberg mountain and closer to town) were selected based on topography (ranging from moderate to cool and moderate to warm climates). Lastly, an extreme site was selected in the Vredendal area (warm to hot climate). The Winkler index classified the Somerset West and Stellenbosch study sites as warm to hot; the Elgin site as intermediate to warm and Vredendal as “too hot” for grapevine cultivation, therefore stressing a high dependency on intensive irrigation. Distances from the ocean, elevation and the influence of the surrounding topography all affected the selected sites and placed them into unique meso-climatic zones. The study area and sites selected over climatic band for three growing seasons is described in Chapters 4 and 6. The study focused specifically on Cabernet Sauvignon as a late ripening cultivar in different climatic environments and over three season, and in the last season of the study Shiraz was added to the study sites.

Experiment layout within sites

Within the sites selected, a visually healthy vineyard was selected that were similar over all the sites, within a radius of 1 km from a representative automatic weather station. The selected vineyards were Cabernet Sauvignon grafted onto 101-14 Mgt rootstock with the exception of a few sites where R110 or R99 were the rootstock (Refer to Addendum 8.1). The commercial vineyard blocks had vertical shoot positioning (VSP) training systems, with moveable canopy wires and conventional viticultural practices were followed at each of these vineyards, including spur pruning and basic canopy management throughout the growing season, with supplementary irrigation (Refer to Addendum 8.1).

The main measurement sites (known as trail sites) in Somerset West (HV, MV, LV), Elgin (HV, MV, LV), Stellenbosch_2 (HV, MV, LV) were monitored for three growing seasons, namely 2012/13 (S1), 2013/14 (S2) and 2014/15 (S3). An additional extreme site at Vredendal was monitored in the 2013/14 (S2) and 2014/15 (S3) seasons. Experimental plots were selected based on once off seasonal Normalised Difference Vegetation Index (NDVI) images taken at the start of the study. The NDVI data was derived from multispectral aerial photographs in January 2012/13 and 2013/14 (at 0.5 m resolution) confirming the variability in growth vigour in each vineyard (Figure 1). The sub-plots were selected to assess the possible interaction of differing soil properties on the expression of the site’s viticultural potential - areas of high, medium and low growth vigour (HV, MV and LV, respectively) were selected within the vineyards (Figure 1), In this figure, the blue demarcation indicates the 2012/13 selection and the red demarcation indicates the new selection in 2013/14 based on visual inspection highlighting sites of lower vigour than originally selected.

Each of the vigour areas selected had 12-15 vines demarcated for detailed measurements over the next three seasons.

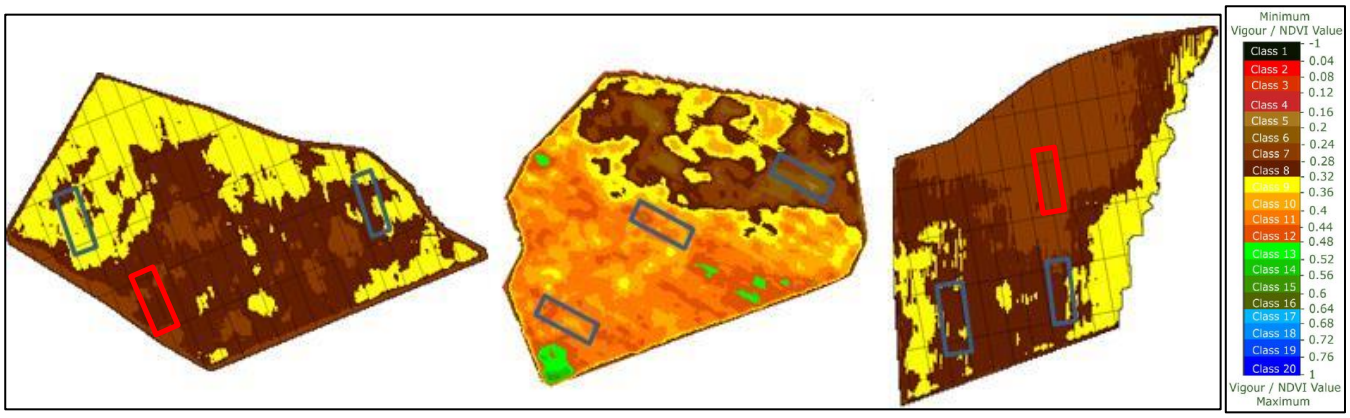

Figure 1 Normalised Difference Vegetation Index (NDVI) images from aerial photography for the Cabernet Sauvignon vineyards in Elgin, Somerset West and Stellenbosch (from left to right), with the demarcated sub-plots in blue rectangles selected in 2012/13 season and the red rectangles selected in the 2013/14 season. Refer to Addendum 8.1 for a more detailed explanation of the other sites.

The site at Somerset West was set out to be the main trial site where more detailed/continuous measurements were made (Figure 2). Additional measurements at the Somerset West site included continuous monitoring of soil temperature and soil water content at weekly intervals during the season and monthly out of season for all the plots (data not included in this study). In the second season, Vredendal was added as an extreme site, and due to the site being further away from Stellenbosch only the main phenological stages were documented.

Figure 2 Detailed experimental layout at the Somerset West site, highlighting the instruments used for continuous logging and probe positioning for monitoring soil water content, and eddy covariance setup (part of another study).

8.2.2 Atmospheric conditions

Air temperature, humidity, wind speed, wind direction and global radiation were obtained at hourly intervals from automatic weather stations (AWS) within a 1 km radius of the study sites. The

stations operate within the network of the Institute of Soil, Climate and Water (ISCW) of the Agricultural Research Council (ARC) in Pretoria. Missing temperature data within the measurement years of the study were filled in using a nearby logger or weather stations, before the data was used for gap filling (Refer to Chapter 4).

Mesoclimate environments where monitored using loggers with a temperature/relative humidity sensor (Tinytag® model TGP-4500, Gemini Data Loggers, West Sussex, UK) housed in a radiation shield (Tinytag® model LS-1, Gemini Data Loggers, West Sussex, UK) was placed above the canopy and logged data at 30 minute intervals, creating a network of eight loggers over the study area. The sensor's temperature measurement range is between -25°C and +85°C, with a relative humidity measurement range of between 0% and 100%.

Calculation of indices

Refer to Chapter 2 for the calculation of bioclimatic indices that are applicable to this chapter, namely the Growing season temperature (GST), Winkler Index (growing degree days (GDD), huglin Index (HI), Biological degree days (BEDD), Mean February temperature (MFT) and Cool night index (CI).

8.2.3 Soil physical and chemical analyses

Soil samples were collected in August 2015 after the completion of the field study to determine what role the soil properties could have had on the above-ground reaction. Samples were collected at three randomised placings in the vine row of each vigour plot and pooled at 0 to 150 mm, 150 to 300 mm, 300 to 600 mm and 600 to 900 mm depth layers to quantify the soil texture and soil chemical properties. Samples were analysed by a commercial laboratory (Elsenburg Soil Laboratory) for five-fraction textural, particle size and soil chemical properties [$pH_{(KCl)}$, Restiance (Ohm), P, K, Ca, Kg, Na and exchangeable acid] according to the Agri-Laboratory Association of Southern Africa (AgriLASA) published methods.

8.2.4 Grapevine water status measurements

Grapevine water status was assessed on mature leaves situated on primary shoots by means of the pressure chamber technique according to Scholander *et al.* (1965). Pre-dawn leaf water potential (PDWP) was measured between 04:00 and 04:30, *i.e.* before day break. Mid-day stem water potential (SWP) was measured in mature leaves fully exposed to the sun, covered in aluminium bags whilst still on the grapevine (Choné *et al.*, 2001) for at least one hour before measurement between 12:00 and 14:00. To quantify grapevine water status, water potentials were Mid-day stem water potentials (ψ_S) was measured in three to five fully expanded leaves per vigour plot over the study sites as regularly as possible on full sunshine days, focusing around main phenological stages. A combination of water constraint classes obtained from Carbonneau *et al.* (1998) and Deloire *et al.* (2004) were used as adapted by (Myburgh, 2015) in another network of Cabernet Sauvignon sites, where a new classification of plant stem water potentials was created to classify readings. This included: class I (≥-0.6 MPa) no constraints, class II (-0.6 > ψ_S ≥ -0.85 MPa), mild constraints; class III (-0.85 > ψ_S ≥ -1.15 MPa), moderate constraints; class IV (-1.15 >ψ≥ -1.4 MPa), high constraints and class V (< -1.4 MPa), severe water constraints. Shiraz stem water potentials were considered, as adapted by Lategan (2011): class I (> -1.3 MPa) no water constraint, class II (-1.3 > ψ_S > -1.7 MPa) weak constraints, class III (-1.7 > ψ_S > -1.9 MPa) medium constraints, class IV (-1.9 > ψ_S > -2.0 MPa) strong constraints and class V (< -2.0 MPa) severe constraints.

8.2.5 Vegetative measurements

8.2.5.1 Cane mass

All grapevines were pruned within one or two weeks during full dormancy (end July) to two-bud spurs. Spurs per grapevine and pruned canes were counted and weighed for each grapevine, using a calibrated hanging scale in the field. Detailed cane measurements were made on a sub-set of the pruned shoots (10 representative shoots), measuring primary cane length, node number and number and length of secondary shoots. The apical sections of each primary cane were inspected, and it was noted if it was topped or not. The spurs per grapevine were counted and weighed for all the grapevines in every treatment at all the sites. The fertile cane percentage was determined by counting the number of canes with bunch stems, along with the total canes per grapevine at pruning. Unfortunately the data of the 2012/13 detialed shoot measurement data was missed placed and hence not included in the data.

8.2.5.2 Early shoot growth measurements

Early shoot growth was monitored on all the fertile shoots of the grapevine, on the three grapevines that were selected based on their Ravaz index. Early shoot growth was monitored in the second and third season at each of the vigour plots at three-day intervals from budswell (E-L 2) (Coombe, 1995), from early September until all the shoots have reached the first canopy wire (approximately 20 cm in length). All the shoots on the grapevine were measured to quantify the variability in shoot growth. Thereafter, two shoots on the right cordon and two shoots on the left cordon were selected for monitoring for the rest of the season, Weekly measurements were performed until vegetative growth ceased. Shoot growth was monitored in the selected 15 vines in each sub-plot.

8.2.5.3 Shoot growth monitoring

Shoot growth monitoring started at the phenological stage of EL5 according to the Eichhorn-Lorenz system, as adapted by Coombe (1995). This stage, hereafter referred to as budburst, corresponded to a stage when 50% of the shoots were 2 cm long, when the first leaves have unfolded and the leaves have reached a length of approximately 2 cm. Due to wind damage at some of the sites, new shoots were selected in the first season at any given time. In the second and third seasons, additional shoots were measured from the start to account for the loss of shoots. Despite this, only a limited number of shoots could be monitored throughout the season.

8.2.5.4 Leaf area

Leaf area was measured destructively as described in Table 1 at post-véraison over all the study sites for each leaf on primary and secondary shoots separately, using an calibrated electronic leaf surface area meter (Delta-T devices Ltd, Cambridge, UK). The leaf L1 length was measured using a measuring tape on a sub-set of shoots to create regressions between the square of the leaf L1 length and individual leaf area (Poni *et al.*, 1994). Each primary shoot length and leaf number was recorded along with the total length of all secondary shoots as well as the number of secondary shoots. Only secondary shoots that exceeded 5 cm in length were recorded. For each of the measurement dates shown in Table 1, three to five representative fertile shoots were collected from different grapevines per vigour plot.

Table 1 Destructive shoot sampling done at the phenological stage post-véraison set at days after budburst (DAB) over all the sites and the three growing seasons

Season	DAB (Phenology)	Measurement details
2012_2013 (S1)	130 (Post-véraison)	Five shoots each for vigour level (HV/MV/LV). All primary and secondary shoots quantified
2013_2014 (S2)	130 (Post-véraison)	Five shoots each for vigour level (HV/MV/LV). All primary and secondary shoots quantified
2014_2015 (S3)	120 (Post-véraison)	Five shoots each for vigour level (HV/MV/LV). All primary and secondary shoots quantified

8.2.6 Reproductive measurements

8.2.6.1 Yield

At harvest, all bunches were counted and harvested on a per-grapevine basis. Grapes were weighed using a top loader mechanical balance to obtain the mass per grapevine Bunches were

8.2.6.2 Yield-related ratios

The yield to cane mass ratio (Y/CM) was determined using cane mass measured at pruning and yield determined at harvest. In addition to this the leaf area using data obtained from destructive measurements was divided by the yield at harvest to determine a per vine ratio of leaf area to yield (LA/Y). An indication of fruit and vegetative growth balance could therefore be provided as well as the incorporation of grapevine balance thresholds as determined in literature (Table 2).

Table 2 Grapevine balance ratios, based on yield and vegetative growth per grapevine

Index	Description	Optimal	References
Ravaz Index (Y/CM)	Yield per vine (kg)/cane mass per vine (kg)	4-10; <10-12	(Zeeman & Archer, 1981; Bravdo *et al.*, 1985; Kliewer & Dokoozlian, 2000)
Leaf area/yield ratio (LA/Y)	Total leaf area per vine (cm^2)/yield per vine (g)	8-20 (single canopy)	(Hunter & Visser, 1990; Smart & Robinson, 1991; Howell, 2001; Kliewer & Dokoozlian, 2005)

8.2.6.3 Berry sampling

The Cabernet Sauvignon and Shiraz berries were sampled on a weekly basis from pre-véraison (pea size) to harvest at each vigour sub-plot to monitor the progression of berry ripening. Six samples of 50 berries each were collected randomly per plot from ten bunches per plot of twelve grapevines. For each sample set, five bunches within and five outside the canopy were selected, with five berries sampled per bunch. For each bunch, one berry was sampled from the bottom of the bunch, two from the middle and two from the top (Mehmel, 2010). Three sets of 50 berries were retained fresh and the remaining three samples frozen at -80°C for later analysis.

8.2.6.4 Berry and juice analysis

On the day of sampling, three of the six 50 berry samples were analysed for berry fresh mass (g) and volume (mL). Berries were weighed on a precision scale (UWE JW-100, UWE, Xindian City, Taiwan). Thereafter, berry volume was determined using volume displacement of water at room temperature. The weighed 50 berries were placed into a glass beaker and the berries were crushed using a household handheld liquidiser (Kambrock essential stick mix KSB7, Braun). There were three consecutive pulses to ensure that the berry skins were broken and the seeds not

damaged. Thereafter, the samples were manually pushed through a sieve so that clear grape juice could be obtained to the volume of at least 25 ml. The clear supernatant was decanted for further analyses of the total soluble solids (TSS), pH and the total titratable acidity (TTA).

Total soluble solids (TSS) concentration was determined using a handheld refractometer (Atago PAL-1 Pocket Refractometer, Atago, Tokyo, Japan). To determine the juice TTA and pH, 50 mL of the supernatant was transferred by means of a pipette into a 150 mL glass beaker. Where 50 mL of juice was not available, the volume was adjusted to 50 mL with distilled water and the volume of the juice noted. The pH and TTA were determined through sodium hydroxide titration with a Metrohm titrator and sample changer (785 DMP Titrino with a LLUnitrode Pt1000 F P, Metrohm AG, Herisau, Switzerland). The conversion of the TTA for the adjusted juice volumes was automatically computed by the device.

8.2.6.5 Sugar accumulation

Sugar loading is defined as the evolution of a quantity of sugar per berry (mg.berry^{-1}) from véraison onwards (Wang *et al.*, 2003). Monitoring the evolution in sugar content of the berry during ripening can indirectly aid in quantifying changes in the physiological functioning of the plant, as affected by factors such as grapevine water status and microclimate (Carbonneau & Deloire, 2001; Wang *et al.*, 2003; Hunter & Deloire, 2005). Sugar loading is calculated on the basis of berry volume (or berry fresh mass, being highly correlated) and TSS (McCarthy & Coombe, 1999; Brenon *et al.*, 2005; Hunter & Deloire, 2005). Sugar loading formulas were used to calculate the sugar loading amount and rate using the Balling (°B) and berry volume, according to the standard calculation method explained in (Deloire *et al.*, 2009).

8.2.6.6 Phenolic measurements in grapes

The three sets of frozen 50-berry samples were used for analysis of phenolic compounds after five to eight months in storage. The berries were weighed and homogenized using an Ultra-Thurrax T25 high-speed homogeniser with an S25N dispersing head (Janke & Kunkel GmbH & Co., Germany) at 24 000 revolutions per minute for two intervals of 120 seconds to prevent heating of the metal shaft. The extraction conditions used for phenolic compounds were essentially according to the method proposed by (Iland *et al.*, 2000). Anthocyanins were extracted from 1 g of homogenate in 10 mL 50% v/v aqueous acidified ethanol (pH 2.0) at 25°C for an hour. After an hour, the solution was centrifuged. The supernatant constituted “the extract” and was used for further colour analysis on the Spectrophotometer (LKB Biochrom Ltd, Cambridge, UK) and high performance liquid chromatography (HPLC). According to literature, the most suitable methods for extraction are 70% methanol at pH 1.5, extracting 95% of the anthocyanins. When using the Iland method, the anthocyanin extracts only provide relative values. This was deemed sufficient for this study as only viticultural sites are being compared. The method proposed by Iland *et al.* (2000) has been used with success with some modifications for optimisation by Jensen *et al.* (2007). Total red pigments and total phenolics in the berries and wine were analysed using a LKB Biochrom Ultraspec II E UV/Visible Spectrophotometer (LKB Biochrom Ltd, Cambridge, UK). These measurements were conducted for all the sites and seasons.

8.2.7 Wine

8.2.7.1 Microvinification

Grapes were harvested when they reached the target sugar content of 24°B in all three seasons, namely the 2012/13, 2013/14 and 2014/15 growing seasons. Wines were made from the grapes (*ca.* 40 kg) of each experimental plot according to the standard procedure for making red wine used by the experimental winery at the Department of Viticulture and Oenology (DVO) at Stellenbosch University.

8.2.7.2 Wine colour and phenolics

Experimental wines were assessed for colour density, modified colour density, colour hue, modified colour hue, total red pigments and total phenolics according to the methods described in (Iland *et al.*, 2000). Wine total acidity, malic acid, lactic acid, pH, volatile acidity, glucose, fructose, ethanol and glycerol were determined using a WineScan FT 120 instrument (FOSS Electric A/S, Hillerod, Denmark).

Wines phenolic profiles were analysed on the HPLC for all the treatments over all the sites and seasons. The wine samples were centrifuged for 10 min at 14 000 rpm before injection. Thereafter, each sample was placed in a 1.5 mL dark coloured vial and protected from oxidation using N gas. The limit of quantification was determined as the smallest area that could be accurately integrated (< 3% standard deviation), measured using reverse phase high performance liquid chromatography (RP-HPLC). Reverse Phase HPLC was performed on an Agilent 1100 series HPLC system equipped with a diode array detector (Angilent Technologies, Palo Alto, CA, USA). Data processing was done with Chemstation® software (Hewlett-Packard, Waldbronn, Germany). A 100 mm x 4.6 mm Chromolith Performance RP-18e column and pre-column was used (Merck, Hohenbrunn, Germany). The mobile phases used were: Solvent A containing de-ionized water adjusted to a pH of 2.04 with ortho-phosporic acid, and Solvent B, consisting of acetonitrile purchased from Chromasolve Reidel-de Haën with 20% of Solvent A. A flow rate of 2 mL/min was used and column temperature was maintained at 35ºC. Quantification was done using external standards: (+)-Catechin Hydrate, gallic acid, vanillic acid, malvidin-3-glucoside, ellagic acid, quercetin-3-glucoside were purchased from Fluka Chemie (Buchs, Switzerland); quercetin purchased from Extrasynthèse (Genay, France) and p-coumaric acid purchased from Sigma-Aldrich (Steinheim, Germany), Flavan-3-ols were quantified at 280 nm as mg/L catechin units, benzoic acids at 280 nm as mg/L vanillic acid units, cinnamic acids at 320 nm as mg/L p-coumaric acid units, anthocyanins at 520 nm as mg/L malvidin-3-glucoside, flavonol-glucoside units at 360 nm as mg/L quercetin-3-glucosides and flavonol aglycones at 360 nm as mg/L quercetin units.

8.2.8 Wine sensory analyses

All the Cabernet Sauvignon wines from all the sites and the three seasons were subjected to sensorial evaluation by two panels of fifteen experienced wine tasters from the South African wine industry. The sensorial evaluation of the wines took place at Stellenbosch University's sensory laboratory according to the standard rate-all-that-apply (RATA) method as described in Ares *et al.* (2014). The RATA method is based on question variants, implemented by asking participants, for terms they selected as ''applies'', to rate intensity using a 3-point scale with anchors 'low', 'medium' or 'high' or rate applicability using a 5-point scale anchored at ''slightly applicable'' and ''very applicable''. The Shiraz wines were analysed but not discussed in the chapter due to there only being one season of data.

8.2.9 Statistical Analyses

Statistical analysis was conducted using Statistica 10 ® software (Statsoft, Tulsa, UK). LoggerNet Datalogger Support Software (Campbell Scientific, Utah, USA) was used to download the data from the data logger (Campbell Scientific, model CR1000, Logan, Utah, USA) Relationships between variables were determined by means of linear regression at the 95% confidence level using Statistica 10 ® software (Statsoft, Tulsa, UK). One-way ANOVA (with Fisher LSD post hoc tests) were used to compare averages between sites and vigour levels. Scatter plots were used to investigate trends of various measurements vs days after budburst. The method of distance weighted least squares were used to calculate trend lines shown on the scatter plots. PCA bi-plots were used to show trends/differences between seasons and sites for various groupings of variables (eg. sensory, wine HPLC, etc). Multiple factor analysis was used to explore relationships between groupings of variables. ANOVA's and scatterplots were done using Statistica 13® software (Statsoft, Tulsa, UK). PCA bi-plots were done in R using the "UBbipl" package. MFA analyses were done using the R function "MFA" in the package "FactoMineR".

8.3 Results and discussion

8.3.1 Climate conditions: sites and seasons

The detailed climatic overview of the sites and seasons of the study is described in Chapter 4s and 6. As an overview for this chapter the average monthly temperatures for the growing season months from the 1st September to 31st March are shown in Figure 3, highlighting the site and seasonal temperature differences of the study. All the sites required some supplementary irrigation, a common practice in South African viticulture, especially in the context of climate change with an increase in seasonal temperatures and less predictable rainfall (Midgley *et al.*, 2015).

There was a marked difference in climate over the three seasons, as expressed in the phenology with the date of budburst having shifted from season to season over all the sites (Refer to Chapter 7). The latest budburst date was observed in season one and the budburst shifted earlier as the study progressed, with the earliest budburst date in the last year of the study (more detail on phenology in Chapter 7).

The 2012/13 season was the windiest of the three growing seasons and the Somerset West site experienced the windiest conditions (Refer to Chapter 4). High wind speeds from October to January, affected the phenology and the size of the canopy, the daily average wind speeds varied from 0.5 to 16 m/s in November 2013/14. The high wind speeds resulted in lower RH, and increased the water constraints in the grapevine and could have limited the photosynthetic activity (Hunter & Bonnardot, 2011). Warmer conditions were experienced in December as seen from the average monthly tempature values (Figure 3).

The 2013/14 growing season had almost double the annual rainfall over all the sites compared to the other seasons (Table 4). Approximately 40% of the rainfall occured in summer, which resulted in higher RH and temperature fluctuations at important stages during the growing season. High rainfall in November resulted in more vegetative growth and higher leaf to fruit ratios. More rainfall in January had a possible negative impact on the berry ripening period due to higher rot incidence, with higher RH levels prevalent in the ripening months. Overall, the 2013/14 growing season was slightly cooler and wetter compared to the other seasons in the study, with higher temperatures for prolonged periods in February followed by cooler March temperatures.

The 2014/15 season can be described as moderate with no extreme events, also with moderate to low wind speeds and the lowest RH compared to the previous seasons in the study. There was also very little rainfall during the growing season. It however, showed the highest accumulated thermal time of the three seasons over all the sites, resulting in the shortest and fastest progressing season; as the season heated up earlier and faster than other years and was cooler during the ripening period as seen in the average monthly temperature graphs for the growing season period (Figure 3).

Overall there was a marked seasonal difference driving the grapevine's reaction to its environment, seemingly more than site variability. Seasonal variability seems to have been driven by more extreme climate events such as extreme wind (2012/13 season), rainfall (2013/14 season) or higher temperatures earlier in growing season and ripening period (2014/15 season), which confirmed the unpredictability of seasons when looking at the weather in the context of climate change research. The seasonal anomalies are highlighted in Chapters 4 and 7.

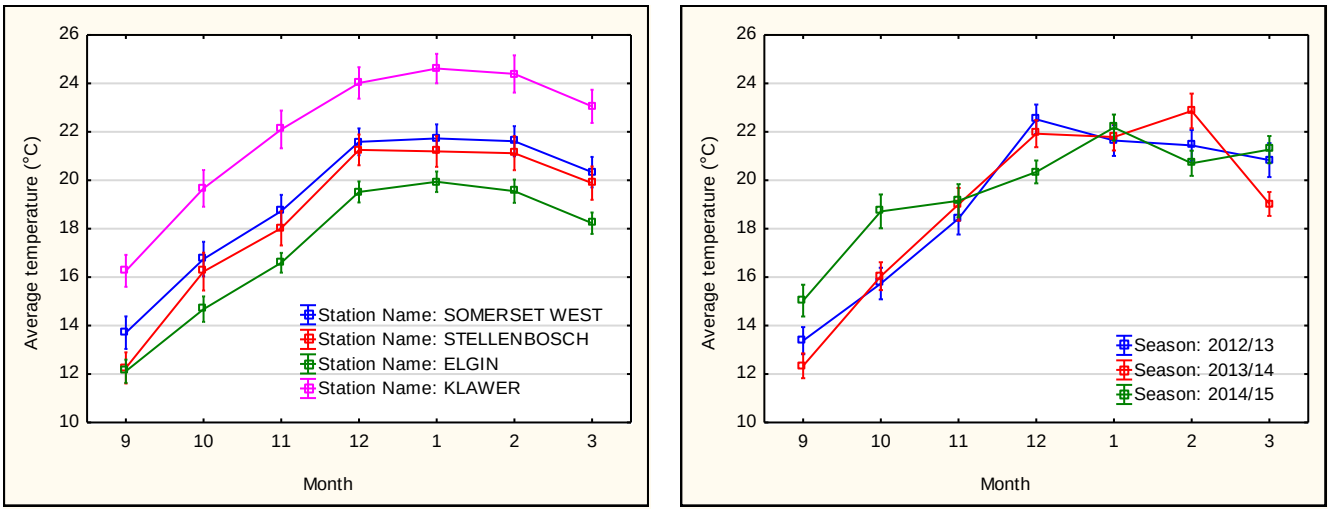

Figure 3 Monthly average temperatures from 1 September to 31 March (all three growing seasons) for the different sites (left) and seasonal monthly mean temperatures over all the sites (right). Vertical bars denote 0.95 confidence intervals.

8.3.2 Soil description

The Western Cape is known to have slightly acidic subsoils, with acidity increasing with depth (<4.0-5.0, measured in 1N KCl), as most basic cations have been lost through leaching and subsequently replaced by hydrogen ions (Saayman, 2013). Soil is classified as acidic when the pH_{KCl} is less than 5.5, as the phosphates become unavailable due to precipitation with free anions (Bates *et al.*, 2002). When the soil pH_{KCl} is greater than 8.0, the soil is classified as alkaline. The soils of the inland areas beyond the coastal mountain ranges, areas further north along the Olifants and Orange rivers, are mainly not acidic, and more often contain free lime (Saayman, 2013). It is therefore not surprising that the sites selected within the climatic band varied accordingly with regards to soil pH, where sites classified as warm to cool seemed to have more acidic soils compared to sites classified as warm to hot (Vredendal and Stellenbosch 1) which had more alkaline soils with pH_{KCl} ranging from 6.0-8.0 (Figure 4). This however is difficult to generalise, as liming practices as well as quite large soil variability within each region and even on farm level can affect such general observations.

The topsoil (0-30cm) pH_{KCl} was more than 5.5 and less than or equal to 8.0, therefore no severe acidity or alkalinity problems occurred in any of the soils at the different sites (Figure 4 and Table 7).

The subsoils seemed to be more acidic <5.0 pH_{KCl}, which could have affected the grapevine vigour within the vineyard block, also considering that the lower vigour sites showed more prominent acidic subsoils, however the pH was not low enough to cause severe negative effects on grapevine growth.

The fine sand was substantially higher than the medium and coarse sandsover all the sites, and was more than 40% (Refer to Table 7 in Addendum 8.2). The highest clay and silt percentages (>15%) were found at Somerset West and Elgin, with the lowest <10% at Stellenbosch 2 & 3 and Vredendal. The soil resistance was lowest at Vredendal, and was on average less than 500 ohms. This could be due to the lower clay and silt contents with higher sand content (Figure 4). The Vredendal soils could also have been affected by the higher frequency irrigation throughout the growing season, the vineyards are irrigated out of a canal irrigation scheme and the site's pH could have possibly been affected by either the irrigation water quality or the geology of the area resulting in more free lime and hence more calcitic and potentially more saline/alkaline soils. There were a few samples from Vredendal where the soil resistance was below the threshold value of 200-250 ohms where symptoms of salinity become apparent on the grapevine (Saayman, 1981). Furthermore, no salinity problems occurred in any of the other sites, and there were no dominating salts in the soil over all the sites, with the exception of Vredendal. The K, Ca and Na and calcium content was much higher at Vredendal compared to the other site as described in Table 7.

The soil nutritional status of all the soils was similar and nutrient levels showed that the grapevines were not subjected to any nutrient deficiencies or toxicities. Therefore, soil chemical properties could be eliminated as a variable that may have caused variation in grapevine growth between the localities, other than for the extreme site, Vredendal, which could have had some salinity effects.

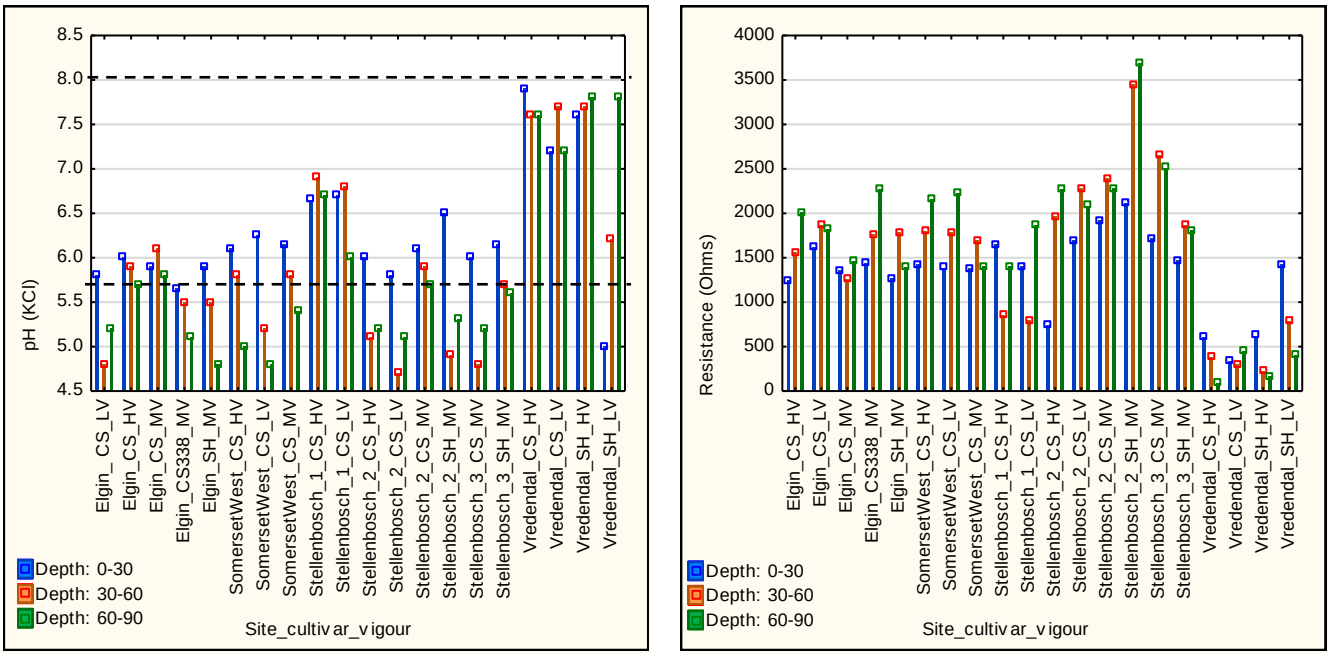

Figure 4 Soil $pH_{(KCl)}$ and resistance for all the sites monitored in the final year of the study. Mean plot of $pH_{(KCl)}$ grouped by site and vigour level and categorised by depth (left) as well as a mean plot of resistance (Ohms) grouped by site and vigour level and categorised by depth (right).

8.3.3 Grapevine water status

Plant water constraints seemed to be site and season dependant (Refer to Table 8 in Addendum 8.2), as sites with higher RH tended to have lower water constraints compared to sites with lower RH, *i.e.* Vredendal. Sites with lower RH had moderate to high water constraints earlier in the

growing seasons, hence confirming their higher dependency on irrigation. The plant water constraints were lowest in the 2013/14 season over all the sites, which were ascribed to summer rainfall. This buffered the water constraints compared to other seasons. Over all the sites and seasons, there seemed to be less water constraints for the high growth vigour areas compared to the low vigour areas within the same vineyard blocks as measured at midday.

The mean midday stem water potential values for Cabernet Sauvignon for the three seasons and sites over time from about flowering to harvest generally transcended the threshold from class I (no stress) to class II and III (mild to moderate water constraints) after about 50 days after budburst (DAB), with values increasing to classes IV (moderate to high water constraints) and in some low vigour sites attained class V (severe water constraints) were recorded after about 110 DAB until harvest (data not shown). The general trend of water constraints was moderate to high for Somerset West, Stellenbosch 2 and Elgin sites, over the three growing seasons, with the exception of the lower water constraints experienced in the 2013/2014 season due to the summer rainfall (Refer to Table in Addendum 8.2). These sites received supplementary irrigation to prevent severe water constraints, as a management strategy at the commercial farms. The Vredendal site is in a hot area and highly dependent on higher frequency irrigation to maintain the water constraints at moderate to low (Figure 34 in Addendum 8.3). The Stellenbosch 3 site had the lowest water constraints (mild to moderate) compared to all the other sites; which could be due to high soil water holding capacity and the higher relative humidity at the site (Figure 35 in Addendum 8.3). The Stellenbosch 1 site experienced the highest water constraints ranging from moderate to severe, with the low vigour plot experiencing the highest amount of water constraints which could have had an effect on the grapevine reactions in growth and ripening (Figure 35 in Addendum 8.3). Shiraz grapevines showed only weak to medium water constraints over all the sites during the final season of the study. The highest water constraints were measured about two weeks following véraison over all the sites, with the differences more accentuated closer to harvest (Addendum 8.3). Overall, the grapevine water constraints were highly dependent on seasonal weather conditions as cooler sites with higher relative humidity and lower wind speeds tended to have lower water constraints. In addition to this, grapevine water constraints were highly dependent on the management of the vineyard within seasons which could modify grapevine water constraints to be more favourable for ripening and attaining the desired yields.

8.3.4 Vegetative response

8.3.4.1 Shoot growth responses

Longer shoots and faster growth was observed in both the medium and high vigour areas compared to the low vigour plots (Figure 5), however this was irrigation dependant. Shoot growth was slow in the initial stages of the season, ascribed to lower temperatures, and increased rapidly as the growing season progressed. Shoot growth slowed again later on in the season due to increased water constraints. Similar results were obtained in other studies where it was observed that ambient temperatures and soil/plant water status were major factors driving shoot growth (Strever, 2012) The reduction in shoot length (means) between 57 and 65 DAB in season 2012/13 was due to many shoots being damaged by the gale force winds, forcing reselection of generally slightly shorter shoots overall as seen in Figure 5 (left). Similar trends in growth were noticed in the 2014/15 season but not ascribed to wind damage, but rather in reaction to increased temperatures with no water constraints, and after about 80-100 DAB the primary shoot growth ceased, which was expected for normal shoot growth but could possibly also have been ascribed to the increased water constraints and warmer temperatures (Figure 5 (right)).

Grapevine growth tempo was driven by site, vigour and season; with faster growth tempos more evident in warmer sites where grapevines had lower vigour, as described in Figure 5 (left), at the Somerset West site that was dryland for 2012/13 season. The LV growth tempo was faster earlier in the season tapering out to a slower tempo, ending with shorter shoots. This could be ascribed to lower soil water holding capacity, due to the LV sites positioning higher up on the slope, and HV/MV lower down on the slope, with the water drainage down the slope increasing the water content at HV. Similar results was seen in the 2014/15 season over all the sites, with the shoot growth tempo and final length as described in Figure 5 (right) driven by management practices, mainly irrigation and time of pruning. All the sites received supplementary irrigation in the 2014/15 season. The growth tempo was comparable for HV and LV, with the MV being slower and shorter in final length. The site temperatures affecting growth tempo were negated with the management of irrigation to maintain moderate water constraints. The time of pruning, namely late and early compared to the commercial time, of the Shiraz grapevines at one of the study sites, showed an effect on the tempo of growth early in the season but reaching the same total length and growth plateaued at about 120 DAB irrespective of the pruning time. Overall the seasons and sites, growth tempo and final shoot length was driven by temperature and water constraints in the soil and grapevine. The management of irrigation can override the effect of temperature on growth, resulting in longer shoots, possibly a fuller canopy which would be an advantage if managed well to be balanced with grapevine yield.

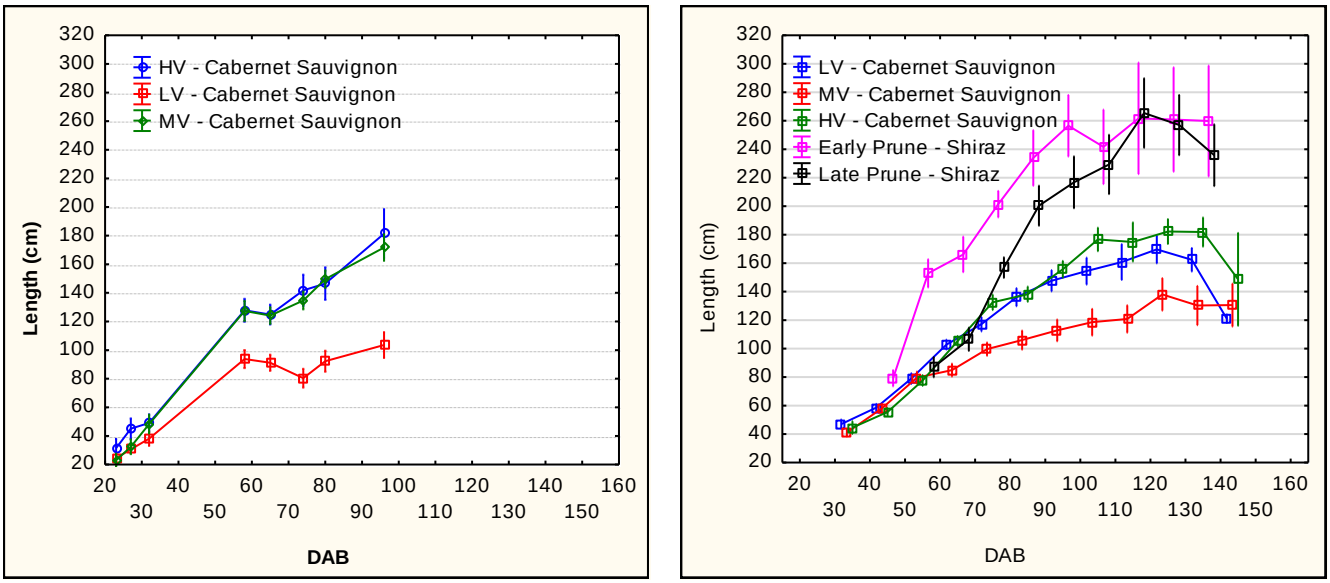

Figure 5 Shoot lengths (cm) describing the growth tempo over the days after budburst (DAB) from 20 DAB to 160 DAB for season 2012/13 (left) and season 2014/15 (right), categorised by cultivar and growth vigour areas demarcated at the measurement sites. Vertical bars denote standard errors.

8.3.4.2 Detailed shoot growth responses during one season

Detailed monitoring of early shoot growth from budburst to shoot growth lag phase for one season of the study showed homogeneity of variances in the Levene's test for the general linear models used to derive parameters of fit for the logistic growth curve over sites and vigour levels (Figure 6). The mid-point of the growth curve, namely the EC50 had an F=0.03 and p=0.97 and for the maximum point of growth namely upper the F=1.86, p=0.16, highlighting significant difference in growth tempo and total shoot length attained within the 2014/15 season at the different sites (Table 3).

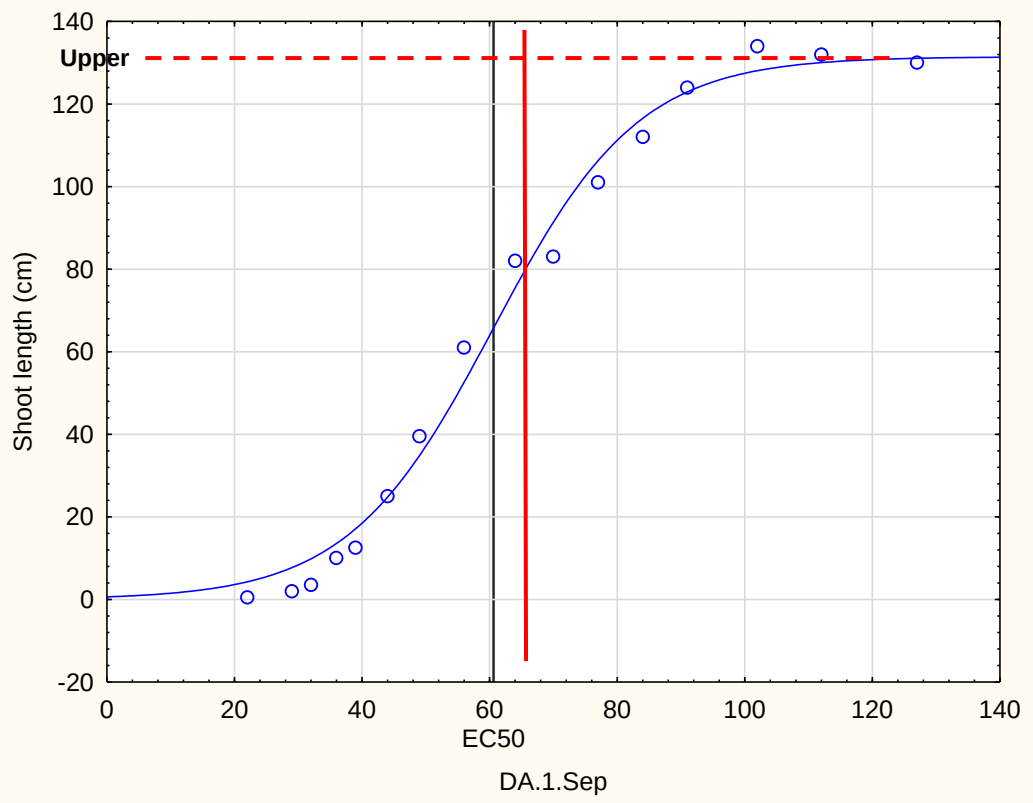

Figure 6 Example of logistic shoot growth curve and parameters measures (EC50).

The climatic band seemed to have affected growth tempo (Figure 7), as the grapevines at the cooler site (Elgin) were significantly later in reaching the midpoint (EC50) of growth compared to the warmer sites (Somerset West). The Somerset West site reached its averaged midpoint of growth significantly earlier than the other sites. The low and medium vigour levels showed a faster tempo of growth compared to the high vigour sites as seen in Figure 7 (right), which may have been ascribed to earlier budburst due to warmer soils as possibly the soil water content could have been lower than the high vigour plots (data not shown).

The cooler sites and high vigour areas within sites reached the midpoint of growth later, which could have been ascribed to more available water resources, resulting in cooler soils and consecutively later phenology and possibly slower growth tempo. The lower water constraints in the high vigour sites later in the season possibly resulted in the longer final shoot lengths (Upper) as seen in Figure 8 (right). The Stellenbosch 2 site was significantly different to the other sites in the 2014/15 season; which was probably due to commercial management of the vineyard as irrigation was applied to ensure the vineyard did not have more than moderate water constraints. Supplementary irrigation was also applied at the other sites, with water constraints not reaching unfavourable levels to limit grapevine growth and functioning. However climatic variable such as the continual cool winds at the Somerset West sites which could have limited final shoot length. Cooler ambient temperatures and higher relative humidity at the Elgin site could have slowed shoot growth tempo and resulted in shorter shoots ascribed to the cooler climate. Temperature seemed to have been the driving factor affecting shoot length, as moderate water constraints with warmer temperatures resulted in longer shoots (Figure 8 and Table 3).

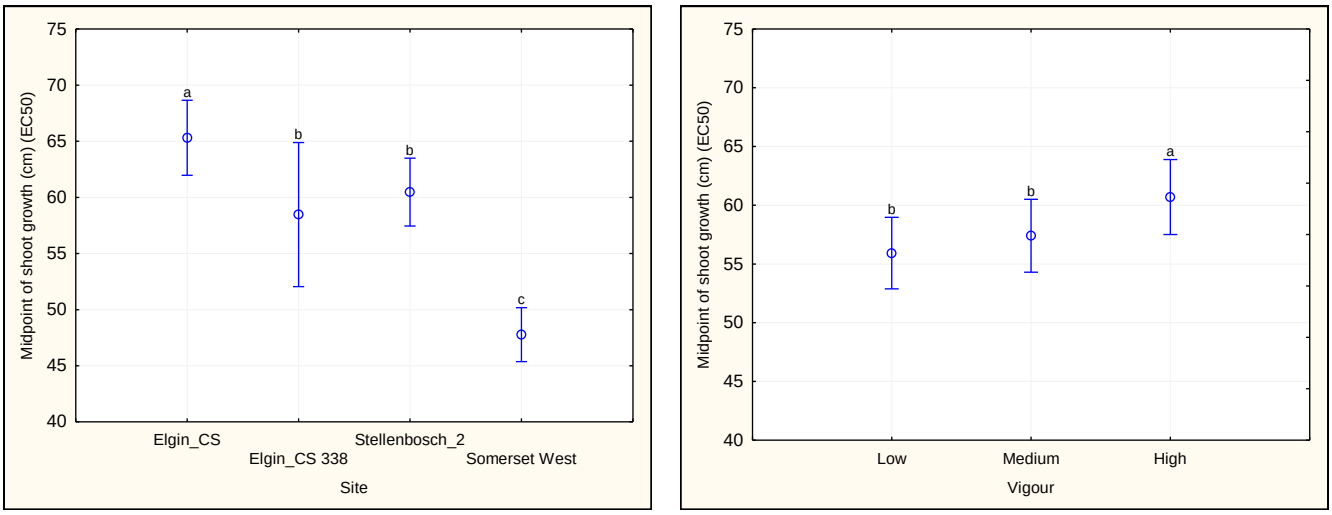

Figure 7 The least square mean of the midpoint of growth (EC50) for the sites (left) current effect F (3,81)=29.35, *p*=0.00 and vigour levels (right) current effect F (2, 81)=3.61, *p*=0.031. Vertical bars denote 0.95 confidence intervals. Same letters are not significantly different at the $p \leq 0.05$ level.

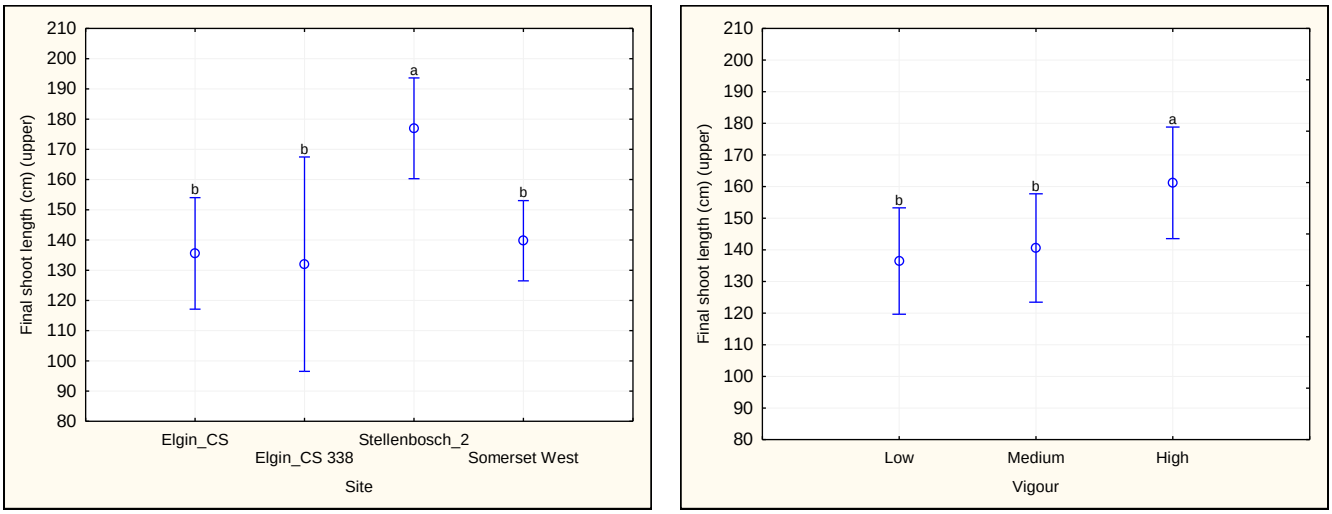

Figure 8 The least square mean of the longest point of growth (upper) for the sites (left) current effect F (3,81)=5.12, *p*=0.03 and vigour levels (right) current effect F (2,81)=3.30, *p*=0.04. Vertical bars denote 0.95 confidence intervals. Same letters are not significantly different at the $p \leq 0.05$ level.

Table 3 Final shoot length (upper) and midpoint of shoot length (EC50), from the general linear models used to derive parameters of fit for the logistic growth curves for sites and vigour levels for the 2014/15 season.

Site/ Vigour	Site	N	Total shoot length (cm) - Upper				Midpoint of shoot length (cm) - EC50			
			Mean	Standard	Confidence -0.95	Confidence 0.95	Mean	Standard	Confidence interval -0.95	Confidence interval 0.95
Site	Elgin_CS	18	135.57	37.72	116.81	154.33	65.31	9.60	60.54	70.09
Site	Elgin_CS 338	6	126.52	33.03	91.85	161.18	57.86	6.32	51.23	64.50
Site	Stellenbosch_2	28	179.70	35.02	166.12	193.28	60.78	5.82	58.52	63.04
Site	SomersetWest	35	138.51	46.29	122.61	154.42	47.52	7.26	45.02	50.01
Vigour	Low	34	144.74	47.37	128.21	161.27	54.02	11.34	50.06	57.97
Vigour	Medium	23	131.15	34.83	116.09	146.21	54.53	9.72	50.33	58.74
Vigour	High	30	171.38	40.85	156.13	186.64	59.90	8.81	56.61	63.19

8.3.4.3 **Leaf area**

The total leaf area of the grapevine canopy seemed to show seasonal variability, but also seemed to directly relate to growth factors discussed above. The seasonal variability over all the sites and vigour levels are highlighted in Figure 9. The 2012/13 season showed higher total leaf area compared to shoot length. In comparision, the 2013/14 season had the longest shoots with the lowest leaf area per shoot. This could have been caused by the unseasonal summer rainfall, which resulted in faster shoot growth, therefore there were less leaves per shoot due to the longer internodes (Figure 9 and Figure 10(left)). The 2014/15 season was reported as being warmer than previous seasons; which could have attributed to increased leaf area per shoot length, due to more and shorter internodes. Overall it seemed that grapevine growth was more sensitive the mesoclimatic effects within the vineyards, such as temperature and plant water status, which could indirectly have been affected by slope and soils at the site, but also managerial practices. The results from the destructive leaf area analysis performed at véraison at all the sites over the three year study period are shown in Table 7 of Addendum 8.2

The total leaf area per vine, combining the primary and secondary growth as shown in Figure 10 (right), was the highest for the 2012/13 season and the lowest for the 2014/15 season. This could be ascribed to the warmer ambient temperatures, as described in Chapter 4, as the seasons become warmer every season over the study period. The warmer temperatures could have resulted in less secondary growth later in the season, as well as having an indirect effect of increased water constraints limiting secondary growth.

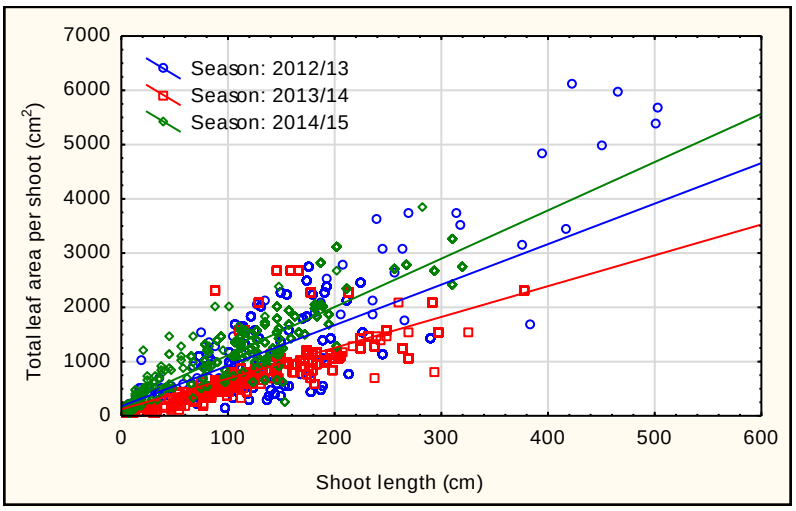

Figure 9 Total leaf area (cm2) per shoot compared to the shoot lengths (cm) for three growing seasons, Season: 2012/13: r = 0.55, p = 0.0000; R^2 = 0.30; Season: 2013/14: r = 0.65, p = 0.0000; R^2 = 0.43 and Season: 2014/15: r = 0.77, p = 0.0000; R^2 = 0.59.

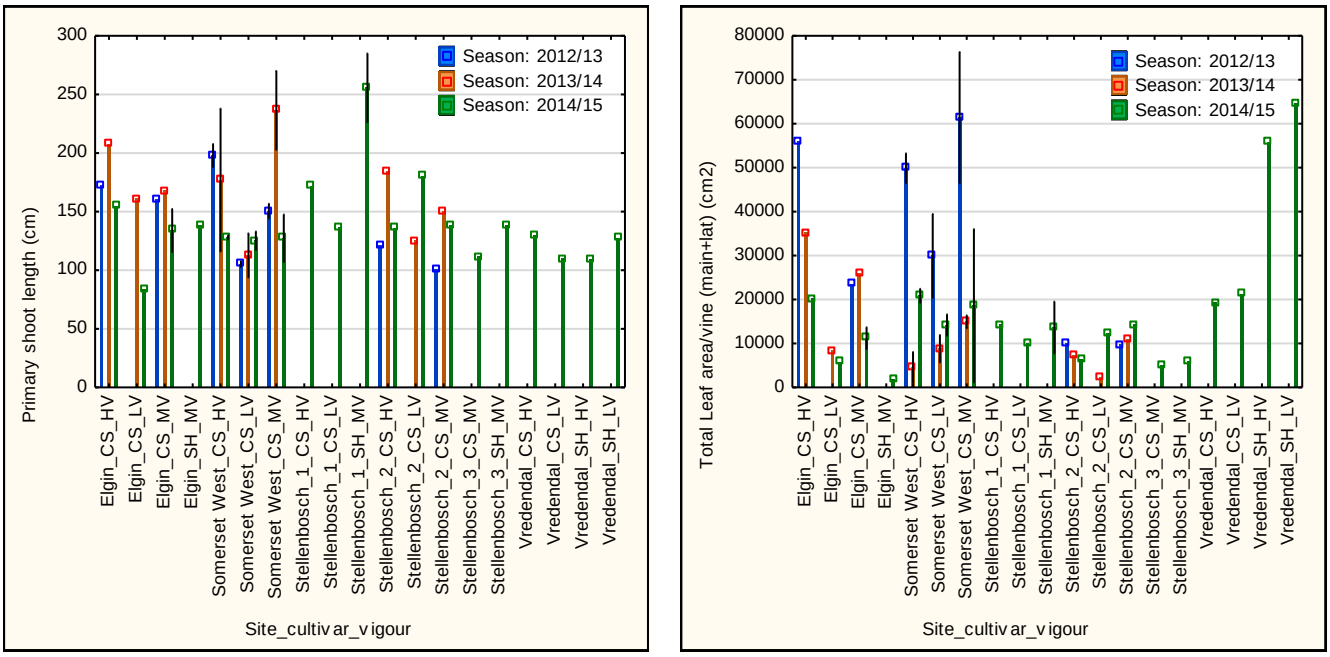

Figure 10 Mean shoot length for the primary (left) and the total leaf area per vine (cm^2) (right) over the different seasons for the different sites and vigour levels. Vertical bars denote stand errors.

8.3.4.4 Pruning measurements

Detailed shoot measurements at pruning showed the total cane length at Stellenbosch 1 and 2 sites to be the highest for the Cabernet Sauvignon sites, with the main canes being slightly longer for the 2014/15 season compared to the 2013/14 season. The total cane lengths at pruning contradicts the shoot length findings at véraison, as the 2014/15 season showed longer primary cane lengths compared to the 2013/14 season at pruning. This could be ascribed to some of the shoots being topped after véraison, which could explain the increase total secondary shoot length. It should be noted that the topping action was a commercial management practice applied at all the sites over all the seasons. The increased secondary cane lengths in the 2013/14 season could be credited to the increased summer rainfall, decreasing summer temperatures and lowering the water constraints so that conditions were favourable for growth (Figure 11). The longer primary cane lengths with less secondary canes in 2014/15 could be ascribed to the warmer growing season and advancement in phenology as described in Chapter 7. The warmer spring temperatures in the 2014/15 season could have initiated faster growth tempo and warmer temperatures later in season possibly resulting in less secondary growth and slightly more primary growth (Figure 11).

From Table 12 it is clear that vigour had a definite effect on shoot length and cane mass, with higher vigour level plots showing higher total cane mass at pruning. The results showed that secondary shoot growth was higher in the higher vigour sites over all seasons and sites. It could be speculated from these results that even though temperature affects the growth of the grapevine, the plant water status possibly had a stronger effect on growth due to lower water constraints at higher vigour sites (Figure 11). The time of pruning of Shiraz at the Stellenbosch site showed no difference in primary shoot length, but a marked difference in the secondary shoot length, with the early pruning (EP) having about 80 percent more secondary growth than the late pruning (LP) treatment.

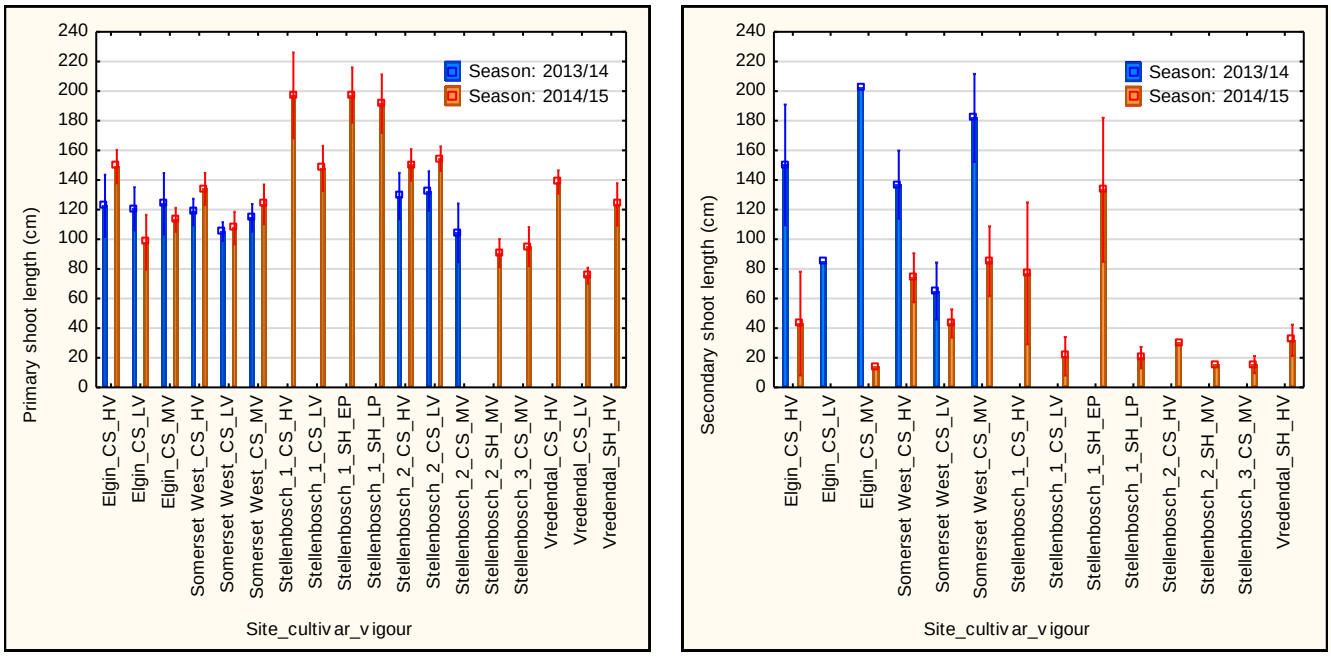

Figure 11 Primary (left) and secondary (right) shoot lengths for all sites, cultivars and vigour levels for season 2013/14 and 2014/15. Vertical bars denote standard errors.

8.3.5 Reproductive response: yield and pruning mass ratios

The yield to pruning mass ratio per vine was affected by the management practices at each of the sites; specifically irrigation and canopy manipulation treatments (Refer to Table 13 in Addendum 8.2). The yield to cane mass ratio known as the Ravaz index, which is used as an index to indicate the balance of the grapevine, was below the optimal range of between 4 to 10 that describes a balanced grapevine with regard to reproductive and vegetative growth (Archer & Strauss, 1989). However, Cabernet Sauvignon is known to be a cultivar, especially in the Stellenbosch region, with a lower Ravaz index. This is likely due to the cultivar's sensitivity to fertility and the pruning methods employed.

Grapevine yield seemed to have been affected by site, vigour and season (Refer to Table 13 in Addendum 8.2), and a respectable yield per vine is between 4 and 7 kg (personal communication, A.E. Strever, 2016). The study showed there was a pronounced seasonal effect, with the highest yield per vine obtained in the 2014/15 season. Considering all the sites, with the Vredendal and Stellenbosch_2 sites produced the highest yields per vine. Stellenbosch_2 was an example of a high yielding Cabernet Sauvignon block however it was rather expected for the Vredendal site to show the highest yield due to the mechanical box pruning. The lower than expected yields at Vredendal could possibly be ascribed to the more saline soils and higher dependency on irrigation, limiting the reproductive growth. However the sites had similar bunches per vine, but the Vredendal site carried much smaller bunches, as expected with mechanical pruning: the canopy management at Vredendal resulted in the highest number of canes and number of bunches per vine, due to mechanical pruning in previous years.

The yield per vine (kg) was highest for the Stellenbosch 2 high vigour site over all three seasons of the study, which could be ascribed to the longer cordon system. Somerset West high and medium vigour sites had the lowest yield per vine, despite their high pruning mass, which resulted in some of the lowest Ravaz index values. This was probably due to overshadowing in the bunch zone which limited the final yield per vine. The Somerset West sites tended to have bad set, with a more

pronounced effect noted in the high vigour site. The high wind speeds at the Somerset West site, especially around the time of flowering could be related to the lower set and therefore lower yield per vine.

Some sites (Somerset West) showed increasing yields per vine over the three growing seasons and some (Elgin) showed decreases (Figure 12). Although Somerset West site had the highest pruning mass per vine for the three seasons, their yields per vine were the lowest. Figure 12 shows the general decrease in average pruning mass per vine over the seasons, which was observed over all the sites as a possible seasonal effect (Table 13). The highest biomass index was recorded at the Stellenbosch 2 high vigour and closely behind was Elgin (Refer to Table 13 in Addendum 8.2). The overall tonnes per hectare was more than double at Stellenbosch 2 sites (highest) compared to the lowest at Somerset West site.

It is well known that Cabernet Sauvignon tends be a cultivar that is sensitive to fertility. Over all the sites, the general fertility was low, as two bunches per bearer shoot is normally expected. Similar results were found in other studies (Carey, 2001). The fertility in the current study showed average values under two bunches per shoot for most sites (Refer to Table 13 in Addendum 8.2), which could be ascribed to the standard practice to prune to 2 bud spurs (or even shorter). However, the cultivar tends to gain fertility with more buds (maximum at positions 4 to 6). A fertility of 1.8 is respectable for Cabernet Sauvignon; this highest estimated fertility for this study was at the Stellenbosch_2 high vigour site, at 1.5 on average.

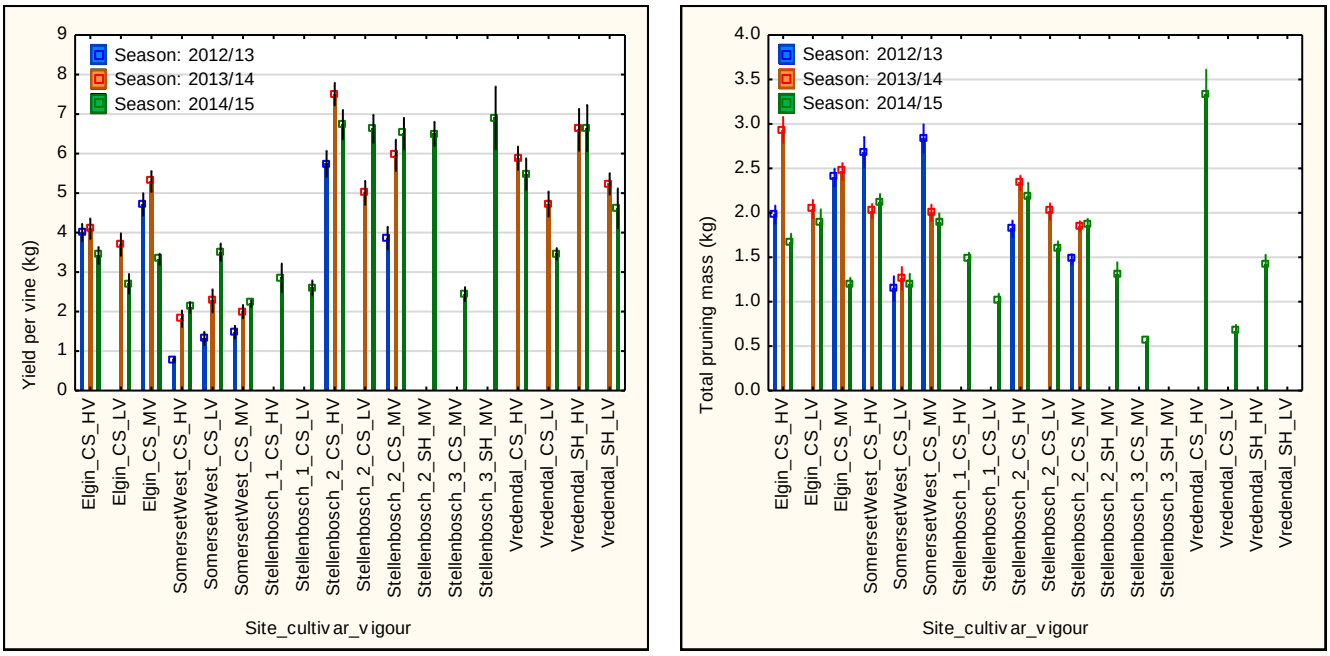

Figure 12 Yield per vine (kg) (left) and total pruning mass per vine (kg) (right) for all three seasons and sites measured over the climatic band including the vigour variability at each site (vertical bars denote standard errors).

Overall the site differences seemed to drive variability in grapevine yield and cane mass over the seasons, which could have been ascribed to the different management strategies at each site and possibly the environmental extremes. Figure 13 shows the clear site separation (Ve: Somerset West, E: Elgin, T: Stellenbosch 2 and Vr: Vredendal), for the factors measured at pruning over all the sites and three measurement seasons (12: season 2012/13, 13: season 2013/14 and 14: season 2014/15). The sites were clearly grouped, and the seasons and plots of differing vigour

grouped within the main site groupings, proving site to be the driving factor affecting the grapevine's balance in growth (considering the yield and cane mass).

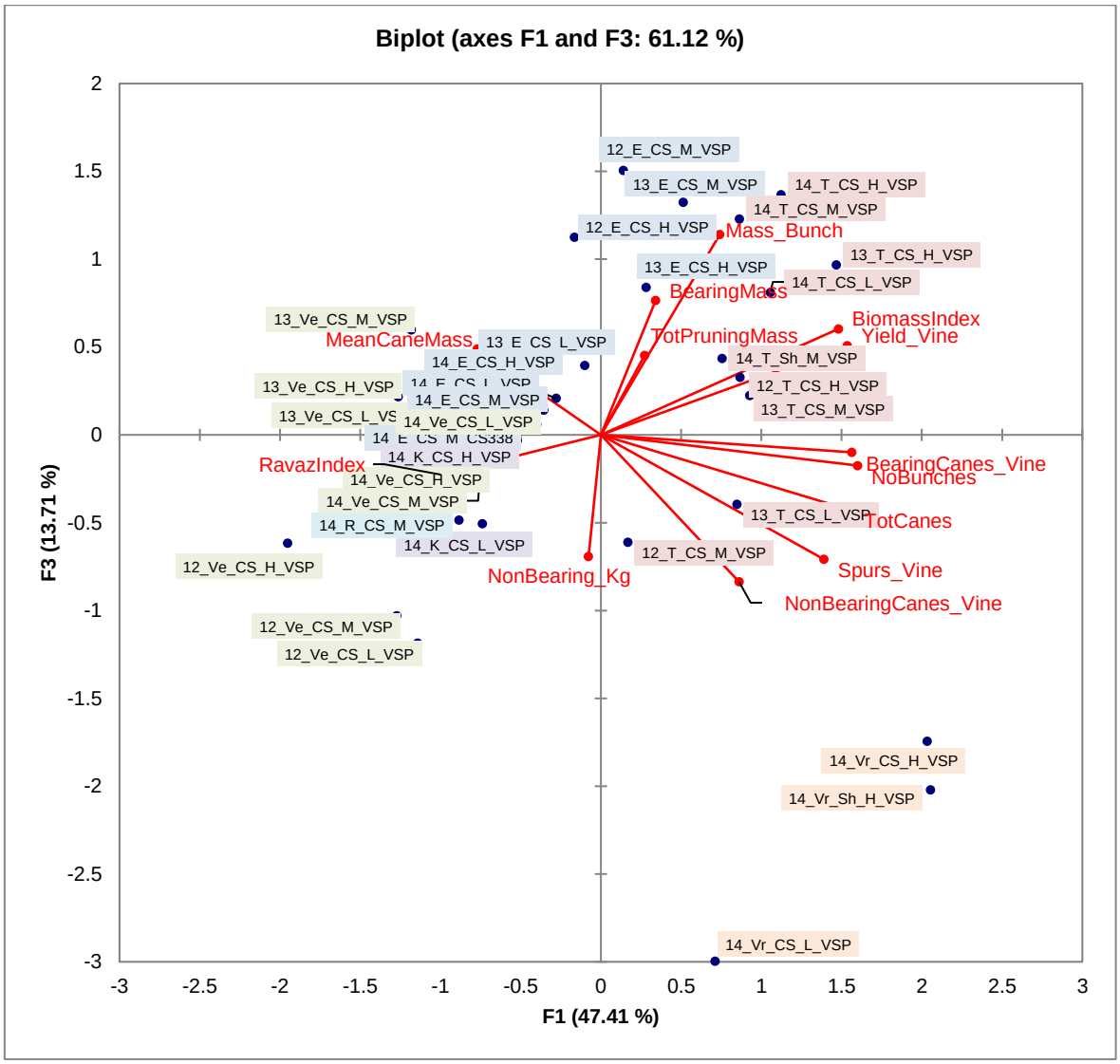

Figure 13 Biplot of the interaction groupings of pruning measurements for all sites, seasons and cultivars, representing 61% of the data population. (Ve: Somerset West, E: Elgin, T: Stellenbosch 2 and Vr: Vredendal), (12: season 2012/13, 13: season 2013/14 and 14: season 2014/15).

8.3.6 Climate interaction with grape berry growth

Detailed monitoring of grape berry mass/volume evolution and ripening over three growing seasons at selected validation sites, proved climate, specifically the mean January temperature (MJT), growing season temperature (GST) and growing degree days (GDD) to be negatively correlated with berry size, berry volume and sugar loading, over all sites and seasons (Figure 14). Warmer temperatures, especially the extreme events and increased plant water constraints resulted in smaller berries, and reduced sugar concentration per berry, which could be ascribed to the reduced photosynthetic activity of the grapevine to assimilate carbon compounds (Wang *et al.*, 2003; Van Leeuwen *et al.*, 2009; Mehmel, 2010).

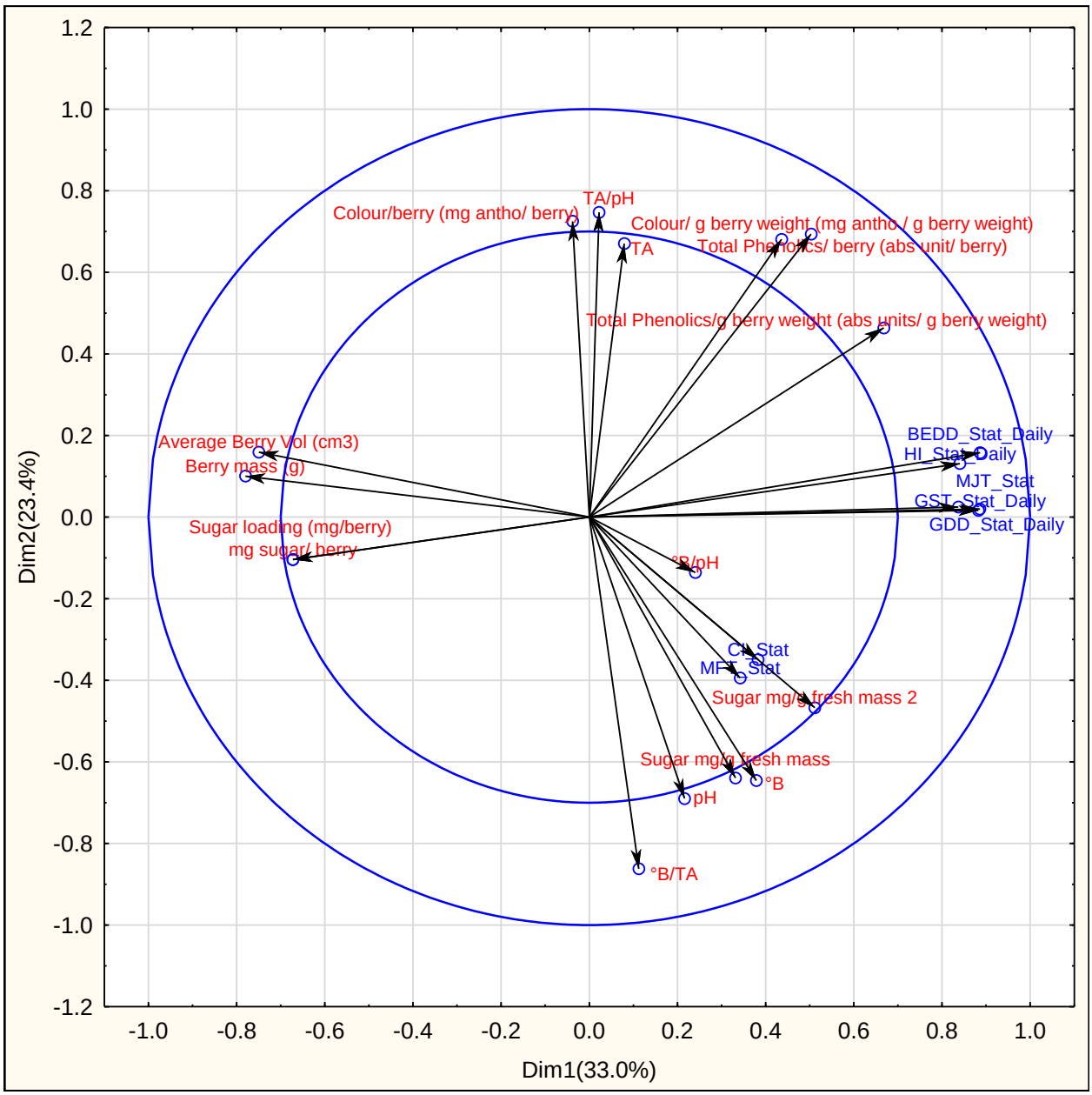

Figure 14 Multifactor analysis (correlation circle), representation of the principal components of separate principal component analysis of block variables: climate indices and grape berry attributes with an RV = 0.21 over all sites and seasons for Cabernet Sauvignon.

8.3.6.1 Berry mass and volume

Berry development over all sites seemed to follow a typical sigmoid curve of development, with season and site affecting the tempo of berry growth and expansion to the point of growth plateauing. Over all sites there was a vigour differentiation (Refer to Table 14 in Addendum 8.2), with cooler sites and higher vigour sites having larger berries. Only the data pertaining to the average of the sites over seasons will be discussed for brevity. Season 2013/14 berry size did not seem to decrease as abruptly as other season but, rather, plateaued for a period that was longer than other seasons. This extended plateau could be credited to the summer rainfall (Figure 15). The berry size varied within limits over sites and seasons for Cabernet sauvignon <1.5g and for Shiraz >1.5g, and was affected mostly by vigour. The cooler sites, namely Stellenbosch 3 and Elgin had the largest berries *ca*. 1.2-1.5 g and the smallest berries were related to the warmest sites, namely Stellenbosch_1 and Vredendal at about 1.1g for Cabernet Sauvignon (Refer to Table

14 in Addendum 8.2). Overall the maximum berry size was reached at different stages dependent on the site. The cooler sites such as Stellenbosch 3 and Elgin tended to have larger Shiraz berries; possibly ascribed to being more sensitive to climate and water, as the sites experienced little to no water constraints in the berry growth period as described in Table and Addendum 8.3. Vigour affected the tempo of growth, which could be indirectly related to the water constraints driving vigour - low water constraints were more associated with higher vigour sites (Table in Addendum 8.2 and 8.3). The berry volume typically decreased with increasing grapevine water constraints, with the berry mass and volume being highest at the lowest water constraints (high to medium vigour level plots) (Figure 16). Similar findings were reported by Mehmel (2010) where large differences in berry volume were directly related to water deficits, placing constraints on the grapevine functioning, in a study over a climatic band for Cabernet Sauvignon. Van Leeuwen *et al*. (2004) showed berry weight to be mainly affected by soil type, followed by cultivar which was confirmed in the current study.

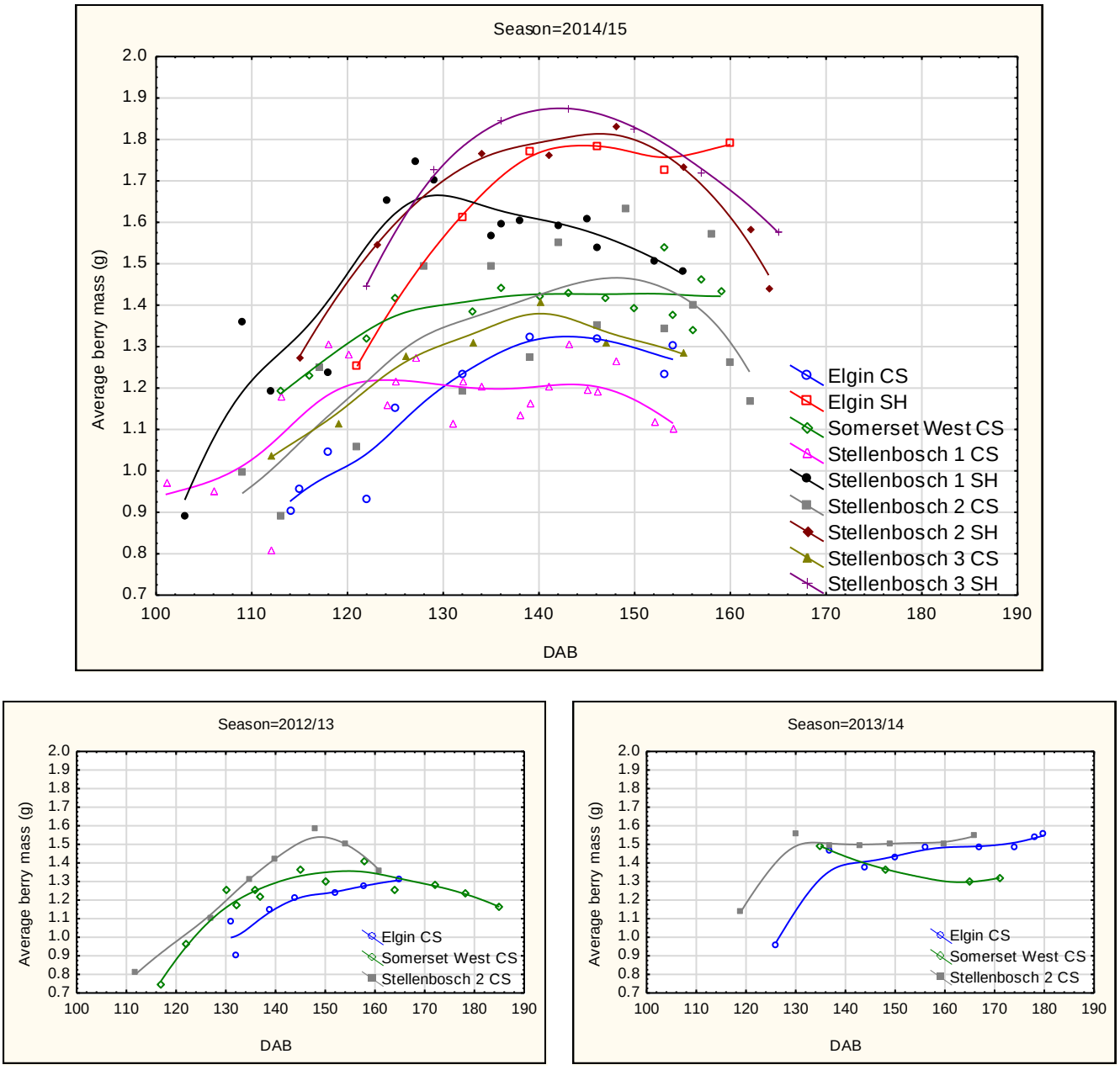

Figure 15 The average berry mass (g) over time from first sampling to harvest, recorded as days after budburst (DAB), for the study sites over the three season.

8.3.6.2 Total soluble solids accumulation

Total soluble solids accumulation (termed sugar accumulation forward for simplicity) showed a trend similar to that obtained for berry volume and mass, with the warmest season (2014/15) showing the earliest maximum rate and the cooler season with more rainfall (2013/14) showing delayed sugar accumulation. Consequintly, there were differences in the maximum potential sugar loaded into the berry (Figure 16). With ripening measurements commencing at pre-véraison, the lower boundaries of the growth curves were not set to zero also for clarity on the graphs. Despite the concentration effect of smaller berries in the low vigour areas within sites, the higher water constraints resulted in lower sugar per berry compared high vigour areas. These results were in agreement with other studies (Mehmel, 2010). Increased water constraints could limit stomatal conductance and hence reduce photosynthetic capacity, limiting carbon assimilation in terms of sugar loading (Van Leeuwen *et al*., 2009). Sugar loading was an indication of how balanced the grapevine was. In Figure 16, the Stellenbosch_1 SH represents a typical graph resembling a balanced vine, whereas unbalanced grapevines showed continued sugar loading as for the Elgin SH or lagging/no accumulation as was the case at the Stellenbosch_1 CS. The accumulation of sugar in the berry depends on the photosynthetic activity of the grapevine, which in turn depends on the plant water status - grapevines experiencing no water constraints normally show higher sugar unloading during ripening (Wang *et al*., 2003). The dynamics of photosynthesis and ripening were highly sensitive to plant water status which is directly linked to the climatic conditions, as moderate to cooler climatic conditions can mask the effects of water constraints (Wang *et al.*, 2003; Mehmel, 2010).

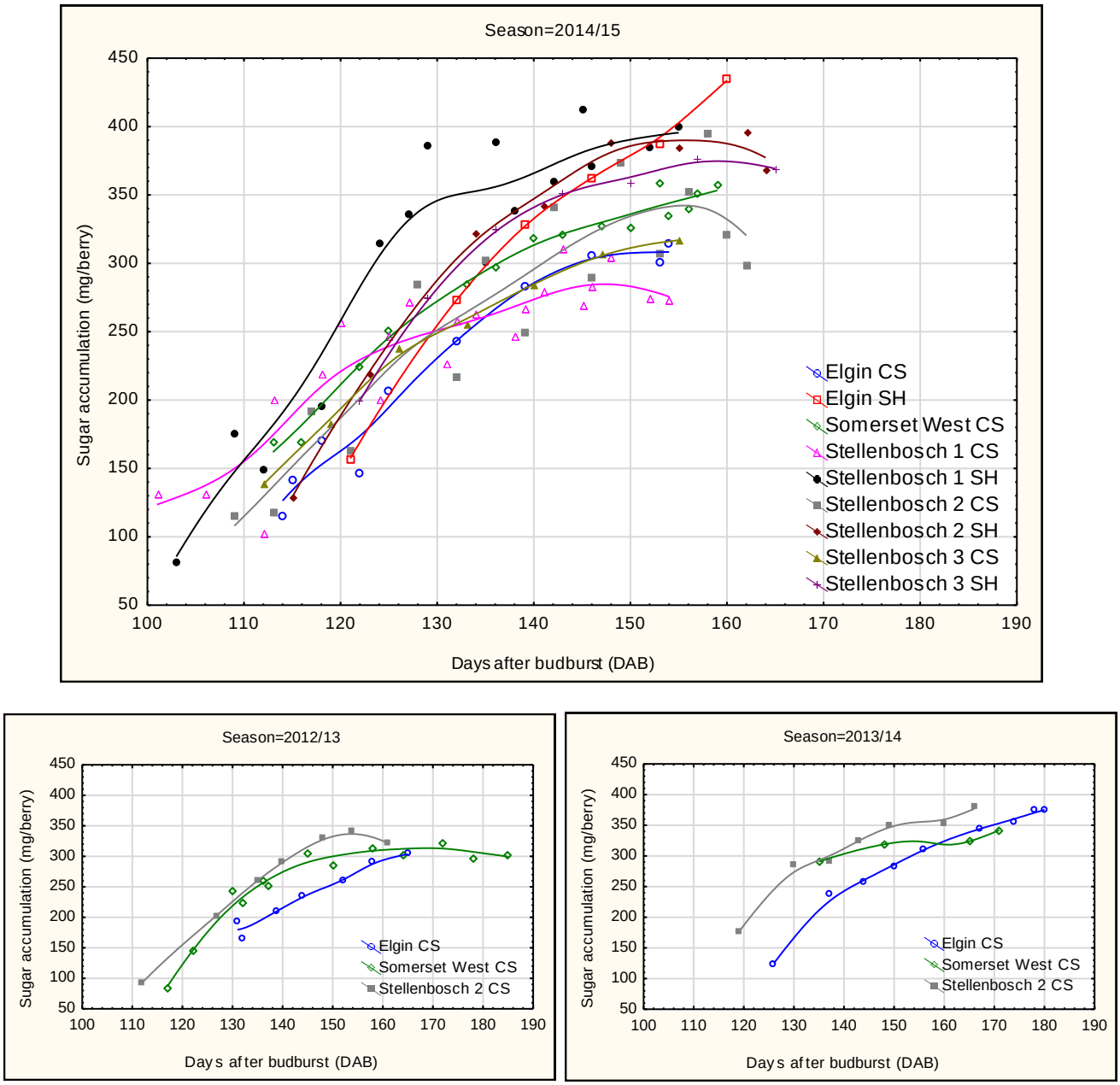

Figure 16 Sugar accumulation as mg sugar per berry mass (g) over time from first sampling to harvest, recorded as days after budburst (DAB), for the study sites over the three seasons.

The 2012/13 season seemed to be the slowest season in terms of sugar accumulation when compared to the other seasons of the study. It was a warm season but still cooler in comparison to the 2013/14 and 2014/15 seasons (Table 4). The 2012/13 season had a cooler summer compared to the other years, with later phenology over all sites. The berry sugar loading in the 2013/14 season was possibly affected by the summer rainfall which could have contributed to the slow start in sugar accumulation and a possible later increase due to the warmer February temperatures. Due to higher temperatures in the 2014/15 season, and associated higher bioclimatic indices, the growing and ripening season was shorter compared to previous seasons, increasing faster and reaching higher total soluble solids content per berry earlier compared to the other seasons (Figure 17). This trend was possibility driven by the increase in January temperatures (increase of about 2°C), which accelerated ripening, with cooler February and March temperatures possibility slowing it down in some areas. Cabernet Sauvignon is normally one of the latest ripening cultivars.

However, in the 2014/15 season Shiraz ripened after Cabernet Sauvignon for all sites, which was an interesting seasonal phenomenon along with the season being about 10-20 days earlier from budburst to harvest.

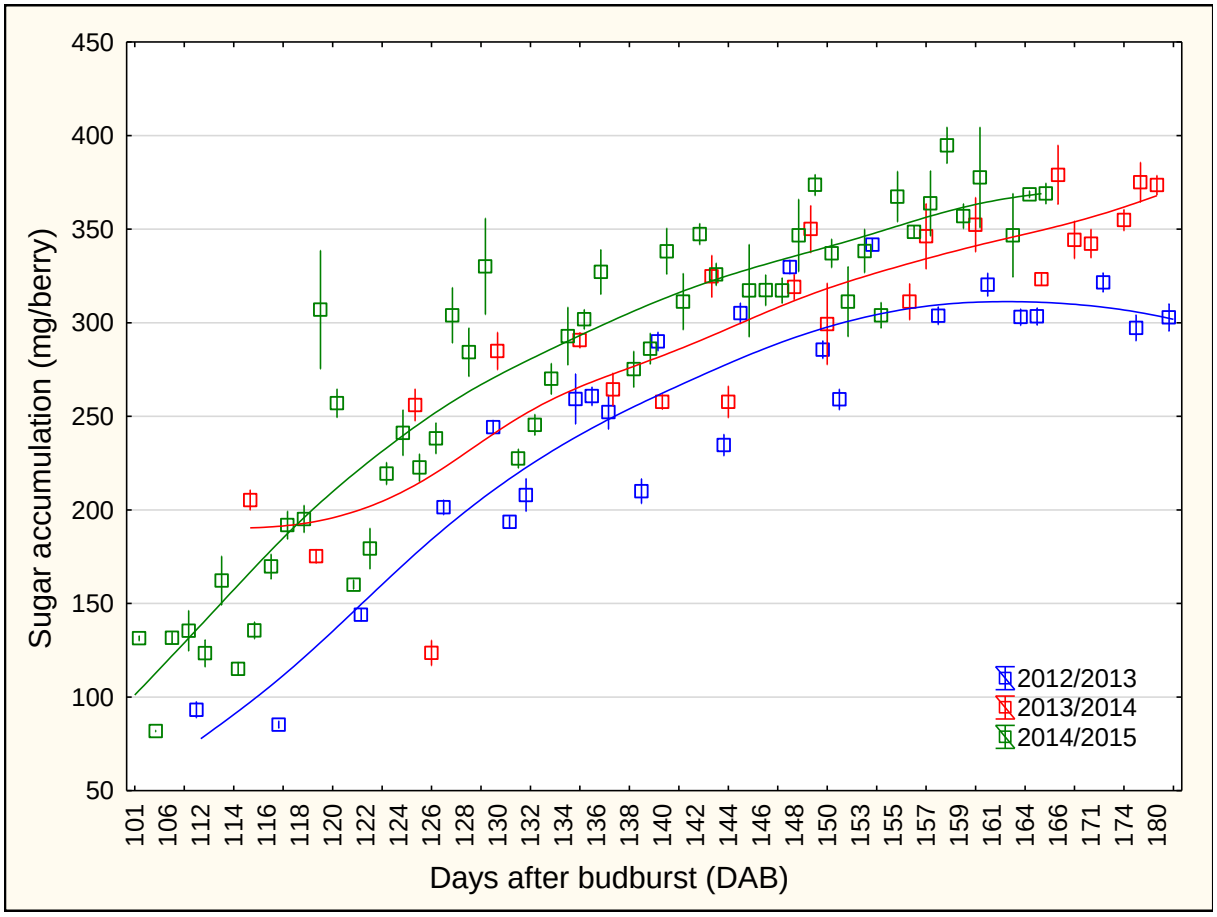

Figure 17 Mean plot of distance weighted least squares for sugar accumulation in the berry as mg/berry for the three seasons' ripening phases over all sites.

8.3.6.3 Total sugar and acid ratio at harvest

The total soluble solids:titratable acidity (TSS:TA) ratios progressed much slower at the cooler sites from Elgin to Somerset West compared to Stellenbosch 2 for all seasons, and highlighted a seasonal affect over all sites. The rate of the biosynthesis and degradation of organic acids are mainly influenced by environmental factors as pathways are mainly enzymatically activated (Coetzee, 2013). The index showed an almost linear increase with days after budburst in Figure 18, and is considered a more sensitive index for harvest ripeness or wine style determination, as it incorporates both total soluble solids and acidity, with malic acid being particularly sensitive to climatic conditions (temperature and light) (Dokoozlian & Kliewer, 1996; Bergqvist *et al*., 2001). Van Leeuwen *et al*. (2004) noted that the season had the strongest influence on total acidity as well as pH of the grape juice, with the cultivar and the soil type influence noticed to a lesser extent.

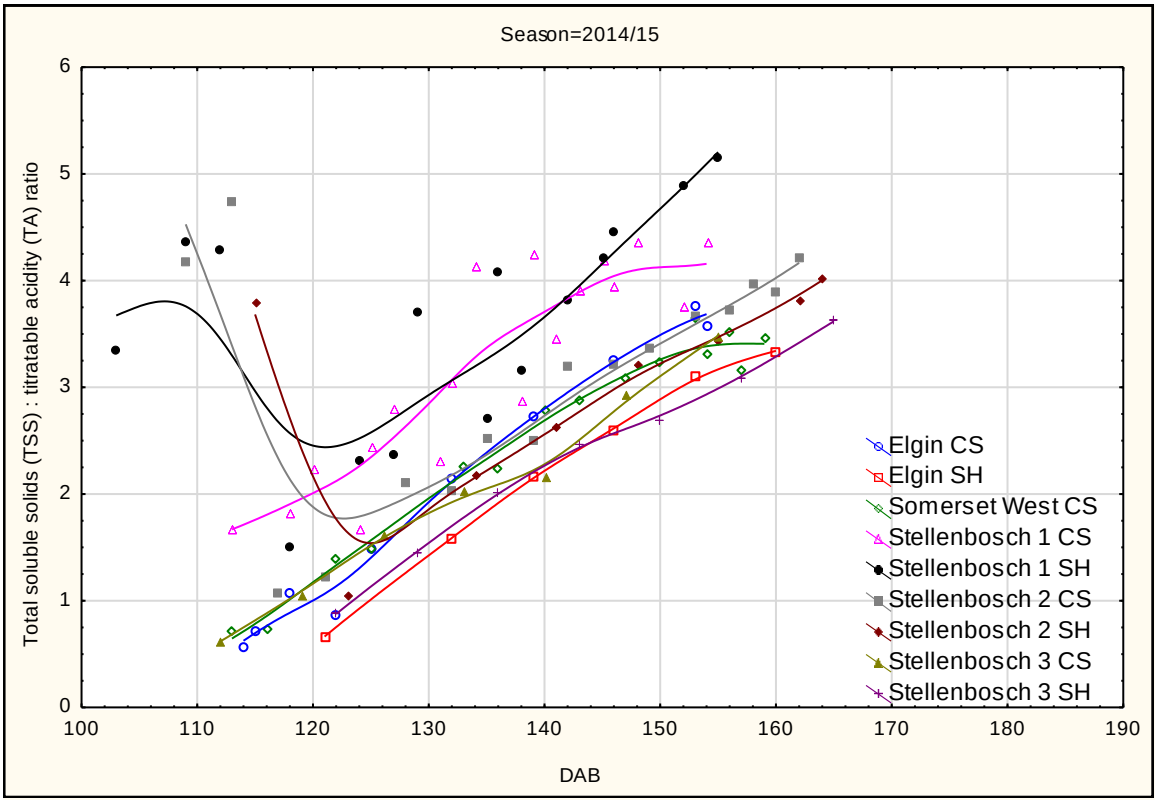

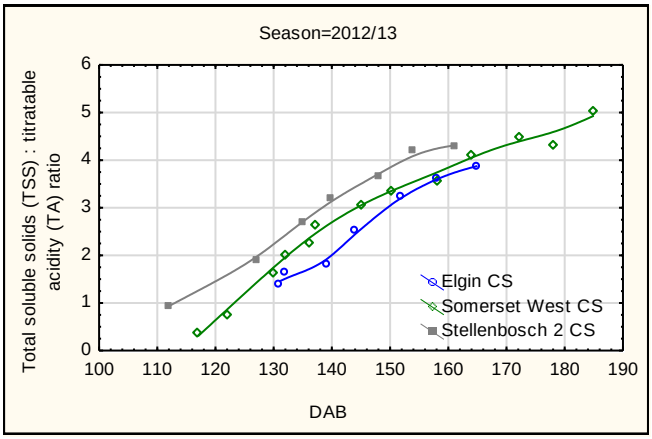

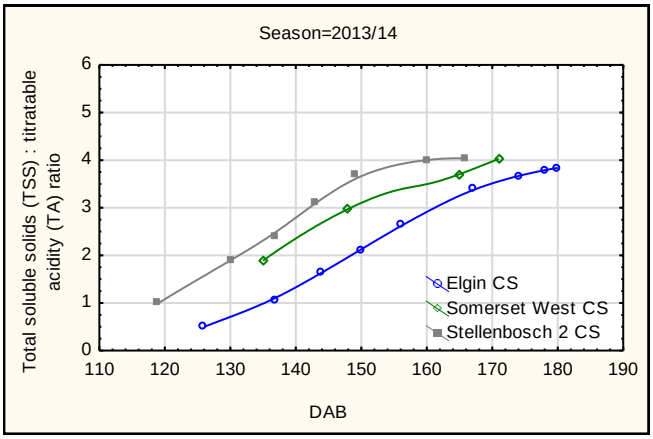

Figure 18 Total soluble solids (TSS) and titratable acidity (TA) ratio for all study sites and over the three seasons, from the time of first sampling to harvest, recorded as days after budburst (DAB), for the study sites over the three seasons.

8.3.6.4 Grape colour at harvest

Moderate to low water constraints allow for optimal physiological functioning, which can affect sugar accumulation and anthocyanin biosynthesis. Both Cabernet Sauvignon and Shiraz showed differences in sugar accumulation and anthocyanin accumulation over all sites and seasons. For the purpose of discussion only the 2014/15 season is shown. The Cabernet Sauvignon

measurements commenced at 100 DAB compared to the Shiraz at 110 DAB, with the Cabernet Sauvignon season also ending earlier at 160 DAB compared to 165 DAB for Shiraz over all sites. The composition of the grape berry changes dramatically during ripening, and anthocyanin biosynthesis starts at véraison and is correlated with increased sugar content (Kennedy, 2002; Fournand *et al.*, 2006). For Cabernet Sauvignon and Shiraz, the anthocyanin and sugar accumulation seemed to be well-related, with a small offset for Cabernet Sauvignon (Figure 19). It was expected from these graphs that there may be more colour in Cabernet Sauvignon wines than in Shiraz, as the Shiraz also showed degradation of anthocyanin at the end of ripening when Cabernet Sauvignon was still accumulating sugar.

The moderate water constraint sites reached the highest sugar and anthocyanin concentrations compared to the hotter sites and lower vigour levels. The increase in anthocyanin content in grape berries subjected to water deficit is a common phenomenon, as the biosynthesis of pigments in the berry is a response to environmental and climatic factors such as temperature, light, partial defoliation, training system, soil characteristics and nitrogen availability (Ojeda *et a*l., 2002).

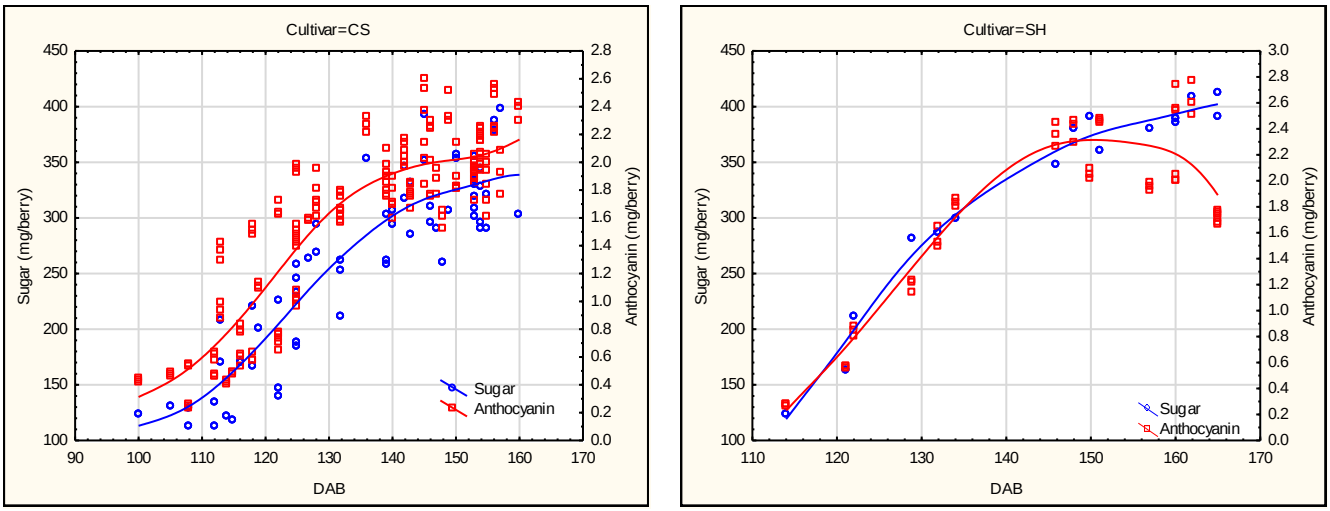

Figure 19 Sugar accumulation (mg per berry) and anthocyanin content (mg/berry) for Cabernet Sauvignon on the left and Shiraz on the right. A distance-weighted least-square mean fit is shown through the data.

Multifactor analysis highlighted a clear seasonal difference in berry colour (Figure 20). All sites seemed to be separated firstly into distinct seasons and then into site differences and vigour levels (Figure 20). The 2012/13 season (S1) showed a stronger correlation with pH and TSS/TA, which could be ascribed to a more “stable season” other than the high wind speeds in the growth phases. The 2013/14 season (S2) that received more than double the annual rainfall was better correlated with berry mass and sugar loading, which could possibly be ascribed to the rainfall causing lower water constraints resulting in more sugar per berry. The 2014/15 season was the warmest and shortest season in terms of GDD, with the warmest January and cooler February and March temperatures. Thus particular season was associated with higher total colour and total phenolics per berry, which could be ascribed to the warmer ripening season with cooler ripening temperatures closer to harvest. Results highlighted a strong negative relationship between climate and berry mass, volume and sugar loading, where the increase of extreme events and warming could result in smaller berries with lower sugar concentrations, as sites with higher water constraints resulted in smaller berries with lower sugar per berry. Over all the sites, it seemed that the seasonality was the driving factor affecting grapevine growth and ripening (Figure 20).

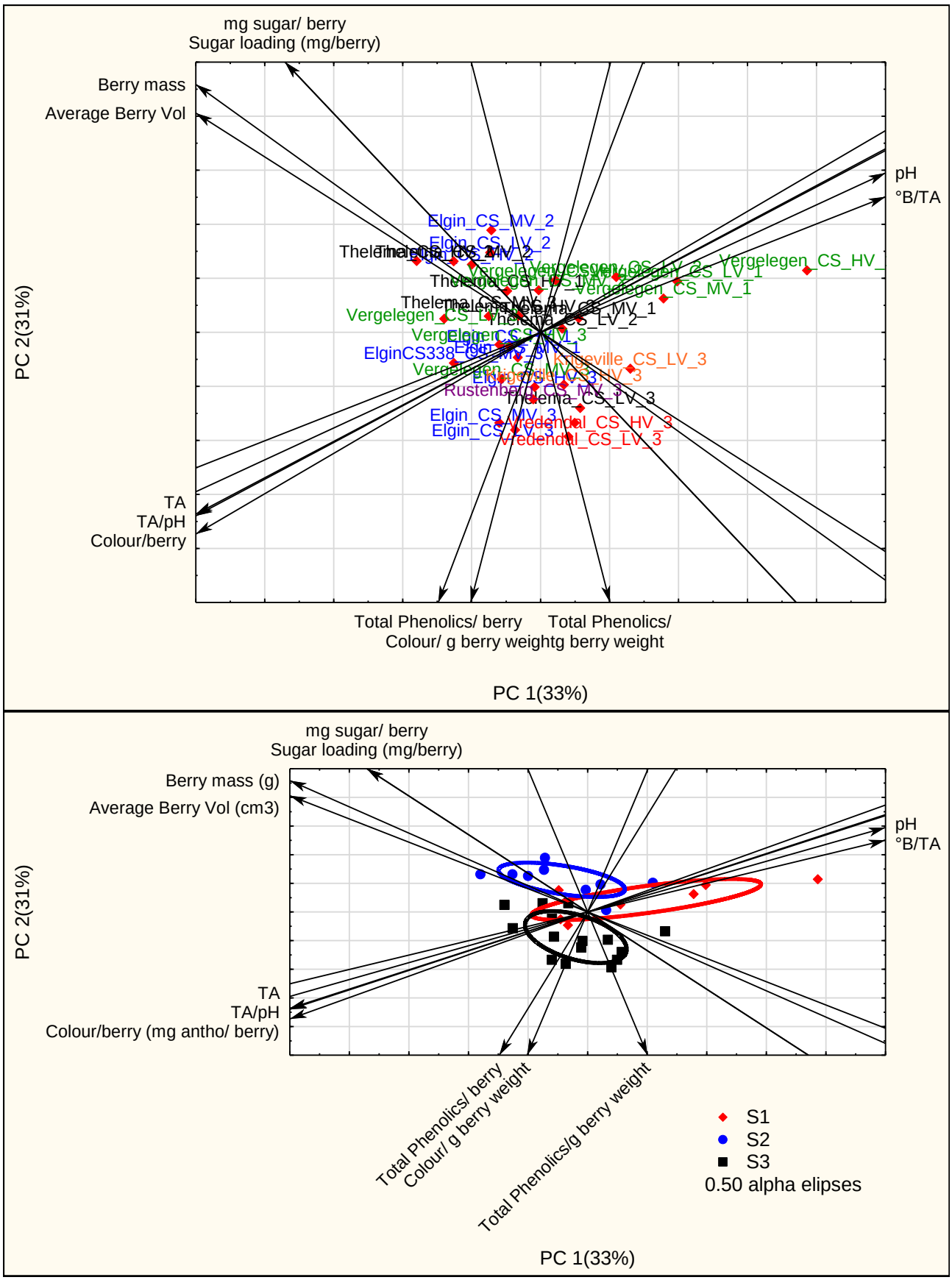

Figure 20 Multifactor analysis, showing the principle components of interaction for grapevine berry growth, sugar accumulation and colour development for the different sites and vigour levels (top) and for seasons (bottom) for Cabernet Sauvignon [2012/13 (S1), 2013/14 (S2) and 2014/15 (S3)].

8.3.7 Wine composition: chemical analysis

Over all sites and seasons the wine chemical analyses were closely related as seen in the grouping in Figure 21. Wine alcohol, pH, TA, volatile acidity (VA) and residual sugar did not show any significant trends with respect to sites and seasons. Wine pH ranged between 3.4 and 4.0 over all seasons and sites and was the highest at Vredendal in the 2013/14 and 2014/15 seasons where values ranged from 3.8 to 4.0. Wine pH at all the other sites was less than 3.8, with the exception of the medium and high vigour level plots at Somerset West site where a wine pH of *ca*. 4.0 in season 2012/13. The higher wine pH observed for Vredendal could be due to warmer climatic conditions and higher water constraints, whereas in the case of the Somerset West site, the higher wine pH was probably due to the occurrence of wind during ripening, which could have limited the photosynthetic activity at the Somerset West site.

The outliers in the 2012/13 (S1) could be ascribed to possible technical issues in the wine making process, the outlier sites are closely related to high malic acid, ethanol, volatile acid and low lactic acid values, there could have been a problem with secondary fermentation for some of the wines.

The wine colour and phenolic components, namely the total red pigments, phenolics, degree of red pigment colouration, colour hue and colour density showed a distinct seasonal separation in the multifactor analysis bi-plots in Figure 22. The warmest and shortest seasons (2014/15) had the highest total red pigments and total phenolics compared to the lowest concentration in the 2012/13 season. The 2012/13 season (S1) showed the highest wine colour hue and degree of red pigment colour (Figure 22). The colour hue of the wine is an indication of the browning of the wine due to oxidation and aging, which may explain why season 2012/13 (S1) had a high colour hue as analysis was done later than the other seasons. The total red pigments and phenolics seemed to increase to almost double from the first season to the last season and this could be due to increase temperatures in January and cooler February and March temperatures in the ripening months enhancing colour development (Figure 23). The seasonal differences seemed to be the driving factor in the groupings seen in the biplots, with the sites separating within the seasonal groupings. The higher vigour areas at the different sites seemed to show slightly higher red pigments and phenolics per berry. These results suggest that anthocyanin biosynthesis may be more sensitive to atmospheric conditions than to water constraints under the given conditions, which is in agreement with earlier findings (Ojeda *et al*., 2001).

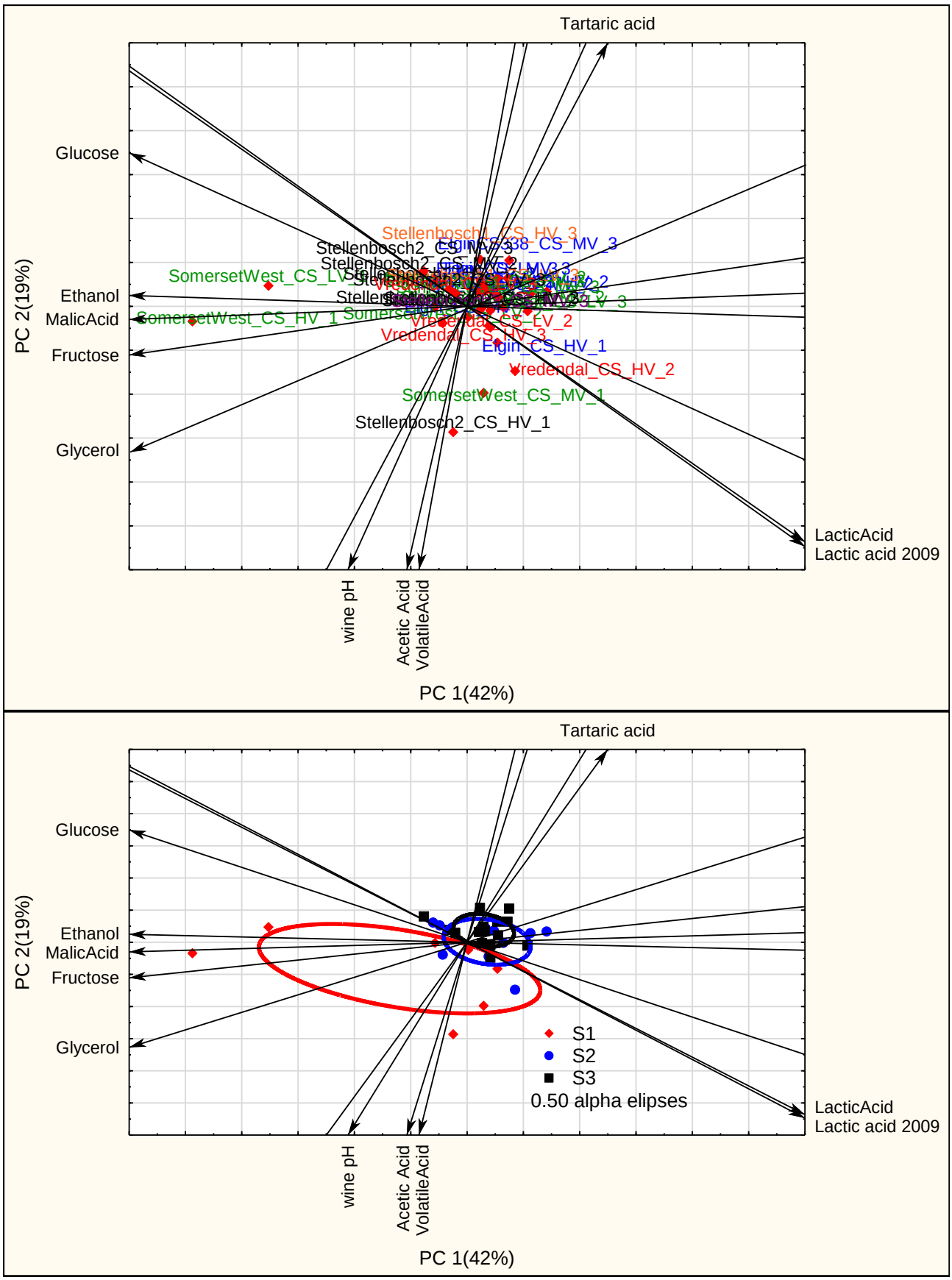

Figure 21 Multifactor analysis, showing the principle components of interaction for wine chemical analysis for sites and seasons (top) and over three seasons for all sites (bottom).

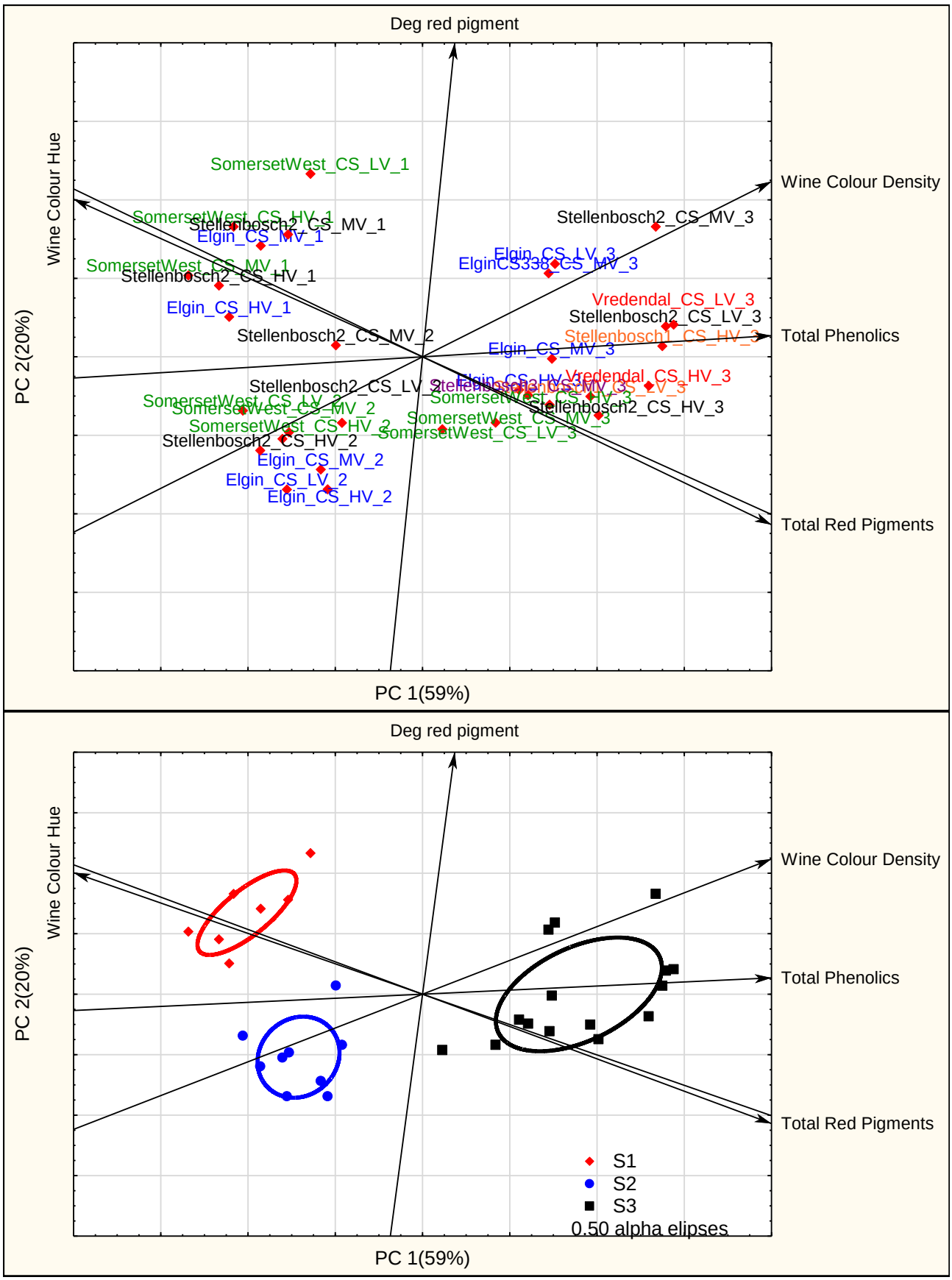

Figure 22 Multifactor analysis, showing the principle components of interaction for wine colour for different sites and vigour levels (top) and for the different seasons (bottom) for Cabernet Sauvignon [2012/13 (S1), 2013/14 (S2) and 2014/15 (S3)].

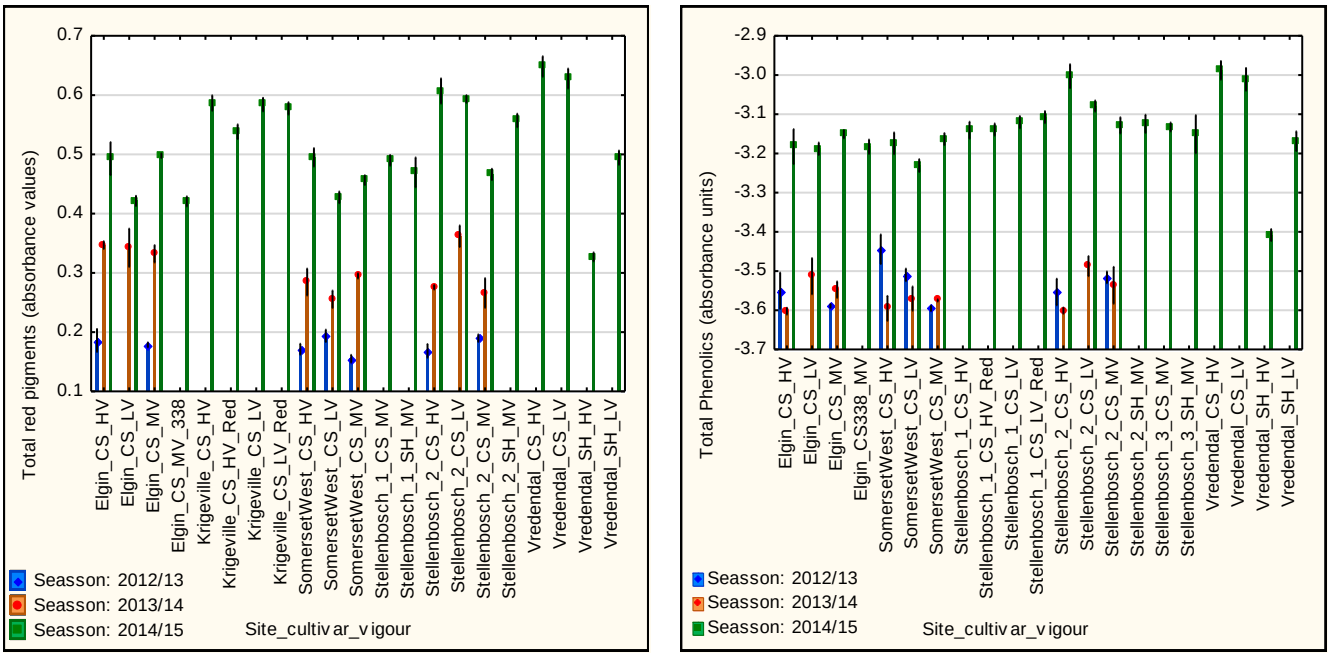

Figure 23 Total red pigments (left) and total phenolic concentration (right) in Cabernet Sauvignon and Shiraz wines over the three seasons and sites. Vertical bars denote standard error.

Correlation analysis based on a RV coefficient of 0.61 showing a strong interaction between climate and wine groups, was done to isolate the possible factors that could be used for modelling ripening and wine style in the context of climate change for *Vitis vinifera* L. *cv* Cabernet Sauvignon. The wine colour components, namely total red pigments, phenolics and colour density were positively correlated with the bioclimatic indices (Figure 24). The total colour pigments and phenolics increased over the three growing seasons with an increase in GDD.

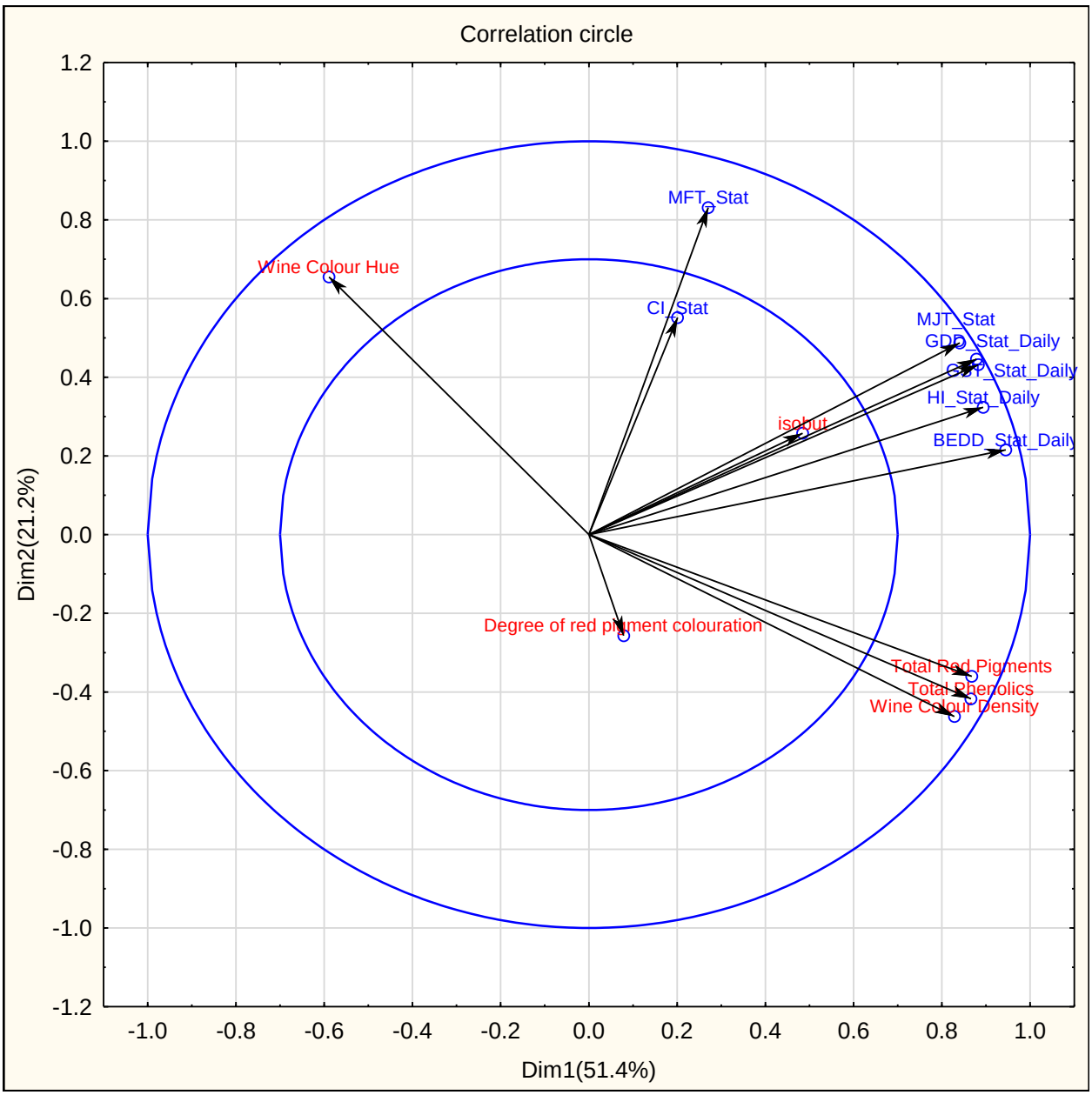

Figure 24 Multifactor analysis (correlation circle), representation of the principal components of separate PCA's of block variables: climate indices vs wine colour attributes with an RV=0.61 over all sites and seasons for Cabernet Sauvignon.

Wine phenolic profiles for Cabernet Sauvignon showed that the season was an overriding factor over vigour levels and sites, with seasons being more strongly grouped together and sites and vigour levels grouped within the seasonal groupings (Figure 25). Cooler and warmer sites also seemed to be grouped within the seasonal groups. There was a distinct seasonal grouping, season 2012/13 (S1) had a closer grouping with acids in the phenolic profile, season 2013/14 (S2) with malvidin and petunidin nonacylated glucosides and acetylglucosides and lastly season 2014/15 (S3) with peonidin, malvidin, petunidin and delphinidin coumaroyl derivatives as well as the delphinidin nonacylated glucosides and acetylglucoside derivatives for the cooler sites. Spayd *et al.* (2002) also reported that cooling the fruit decreased coumaroyl derivatives and heating caused an increase in coumaroyl derivatives. This shift in the anthocyanin composition suggested that warm climate fruit tended to have a higher proportion of malvidin, petunidin and delphinidin coumaroyl derivatives; while the "cool climate" grapes had more peonidin and cyanidin nonacylated glucosides and acetylglucosides. The anthocyanin composition from cooler areas and

shaded fruit was more readily extracted from the grape berries in the wine making process than the anthocyanin composition in grape berries from warmer areas, due to coumaroyl derivatives decreasing in cooler conditions. Overall, the seasons and hence the temperature affected the anthocyanin biosynthesis and final composition of anthocyanins. It is important that the total phenolic composition in the grape berry is balanced, to produce a quality wine that will age well (Spayd *et al.*, 2002; Downey *et al.*, 2004).

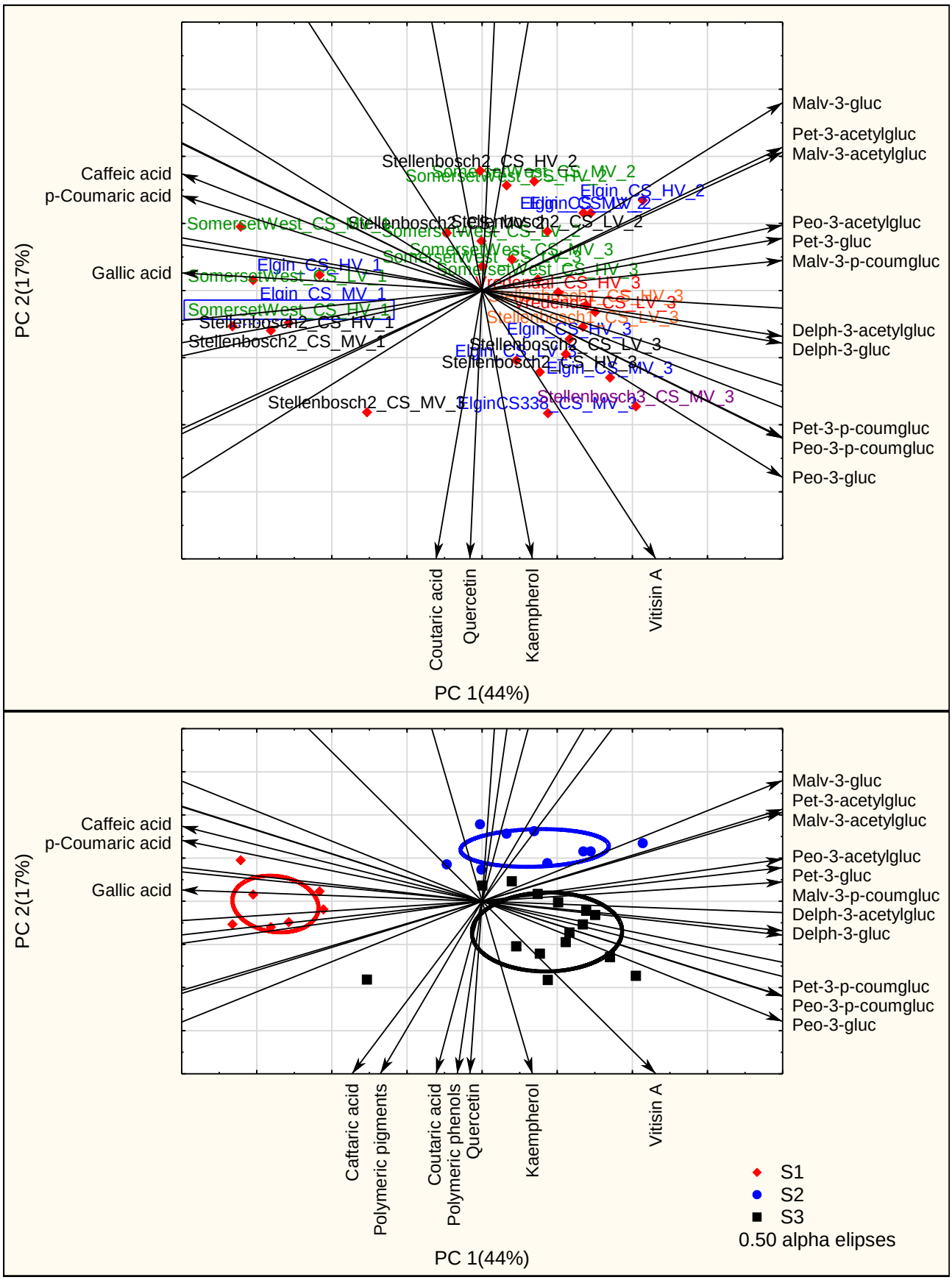

Figure 25 Multifactor analysis, showing the principle components of interaction for wine phenolic profiles for all sites and seasons (top) and for the three seasons over all sites (below).

As previously shown multifactor analysis was used to isolate the possible factors in climate that affects the wine attributes for Cabernet Sauvignon. The analysis was based on an RV coefficient of 0.21. It seems that most of the colour compounds of the anthocyanin profile were positively correlated with climatic indices whereas the compounds caffeic acid, p-coumaric acid and gallic acid were negatively correlated with climatic indices (Figure 26). Therefore, the increase in accumulated seasonal temperatures will affect the wine anthocyanin profile, increasing all the anthocyanin derivatives, which could aid in more complexity and possibly stability of wine colour.

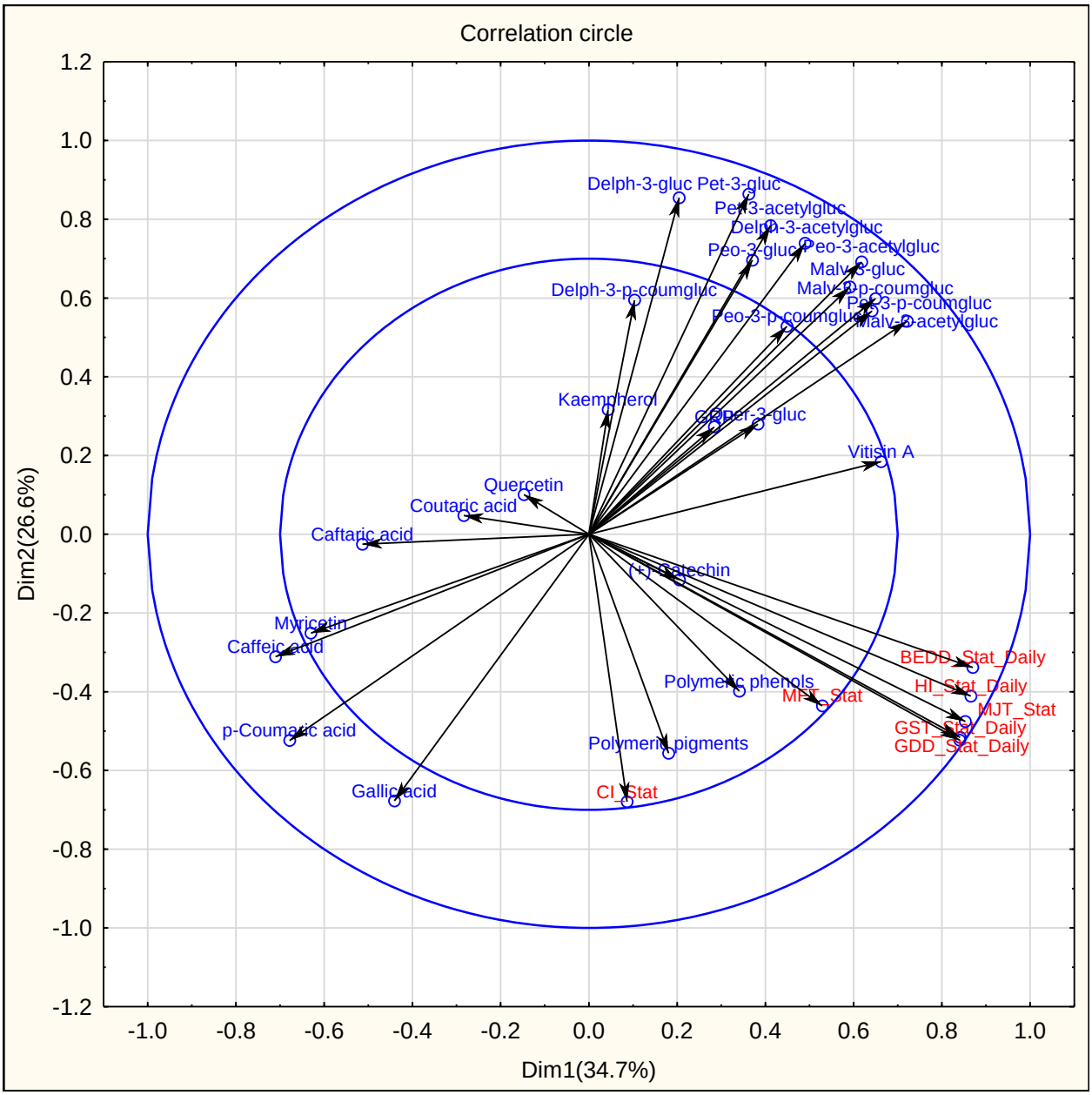

Figure 26 Multifactor analysis (correlation circle), representation of the principal components of separate PCA's of block variables: climate indices vs wine phenolic profile attributes with an RV=0.21 over all sites and seasons for Cabernet Sauvignon.

Temperature and water constraints over sites and seasons affected the methoxypyrazine expression in the Cabernet Sauvignon wines, expressed as 2-isobutyl-3-methoxypyrazine (ibMP) and 2-isopropyl-3-methoxypyrazine (ipMP) (Figure 27). The ipMP over all the sites and samples was <1 ng/L or not detectable. The intensity of the green bell pepper character (ibMP) as perceived on tasting, the threshold value was estimated to be 15 ng/L (Roujou de Boubée *et al*., 2000).

Growing degree days increased over the three seasons due to increased temperatures during the ripening period from September to March, possibly driving the increase in ibMP due to the warmer pre-véraison temperatures. In the cooler climate of Elgin, the ibMP concentration was not seemingly affected by vigour, but rather by season, with the 2013/14 season having the highest concentration in the wines. This could be due to the summer rainfall resulting in more vegetative responses of the grapevine in terms of growth. The lowest ibMP concentrations were in the 2014/15 season at Elgin (Figure 27). This could most likely be due to the cooler pre-véraison conditions limiting the formation of ibMP. Results confirmed findings of other studies, where there were no significant differences in ibMP levels between the shaded and exposed clusters at harvest as pre-véraison light exposure was shown to effect the accumulation of ibMP in the berries (Ryona et al., 2008; Lapalus, 2016).

The Somerset West and Stellenbosch sites harboured moderate to warm climates, hence the warmer pre-véraison conditions are ideal for ibMP formation and higher vigour sites resulting in the higher concentrations as degradation is limited due to shaded conditions. The highest ibMP concentrations were in the 2014/15 season and lowest concentrations in the 2012/13 season. This could be ascribed to the warmer temperatures earlier in the 2014/15 season, possibility resulting in a longer period of formation and accumulation, and with the season being compressed for red cultivars limiting the degradation period. The concentration of ibMP increased over the three seasons at the warmer sites for all the vigour levels with the exception of Somerset West low vigour (Figure 28). This trend was, however, not as obvious at the cooler sites, but ibMP was generally lower which is ascribed to the cooler pre-véraison temperatures. Scheiner *et al*. (2012) reported that vines with less water constraints tended to be more vigorous and bear fruit with higher ibMP levels. Furthermore, it appeared that soils with a greater water-holding capacity (clay-rich soil) will favour vine growth and yield higher levels of ibMP in the grapes. Cabernet Sauvignon grapes grown on sandy-silt soil were reported to have higher ibMP levels than grapes from gravel soils (Roujou de Boubée *et al*., 2000). Thereforem favourable soil conditions and the warmer climate pre-véraison could explain the higher wine ibMP concentrations at Vredendal.

The Stellenbosch_2 medium vigour site had ibMP value higher 40 ng/L. Similar ibMP levels were obtained in previous studies attributed to plots with sandy-silt soil (Roujou de Boubée *et al*., (2000). In the current study, the high ibMP for MV and LV could be ascribed the warmer pre-véraison condition and high light interception in the canopy due to good canopy management. The Stellenbosch_2 vigour sites had some of the highest Ravaz index values in the study at *ca.* 4, indicating balanced grapevines. However, with the 2014/15 season temperatures warming so early and the season being shorter the degradation of IBMP could have been limited. Roujou de Boubée *et al*. (2000), showed the breakdown kinetics to be more gradual on plots with sandy-silt soil, the soil 5 fraction analysis in Table 7 showed the course sand percentage to be highest for Stellenbosch_2.

Overall, the variations in the climate from one season to another affected the ibMP content of the wine, over and above the site differences. It has been established in several studies and regions that the ibMP concentration in grapes decreases during ripening and that this phenomenon depends on climate, the vine's vegetative growth, and vineyard management techniques affecting the sun exposure of the grapes (Allen et al., 1994; Roujou de Boubée *et al.*, 2000). As the green character in Cabernet Sauvignon is sometime frowned upon, this study could shed light on the future planting distribution of Cabernet Sauvignon in the context of the pre-véraison temperatures increasing in warmer areas.

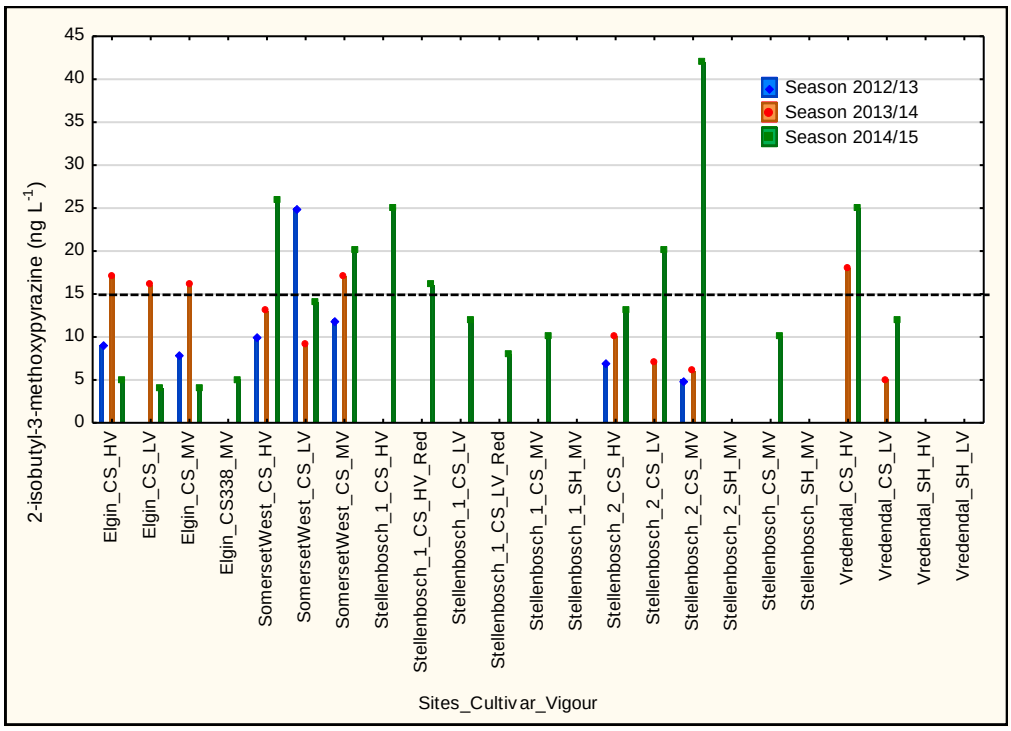

Figure 27 Wine 2-isobutyl-3 methoxypyrazine (ibMP) concentration in Cabernet Sauvignon wines over the three seasons and sites. Only Cabernet Sauvignon results are shown. The line at 15 ng/L^{-1}, represents the threshold value of preception.

8.3.8 Wine sensory analysis

The sensory profile for Cabernet Sauvignon is described as vegetative and fruity, with the vegetative descriptors being bell pepper, herbaceous, tobacco, hay, artichoke, mint, freshly cut green grass and eucalyptus (Roujou de Boubée *et al.*, 2000; Carey *et al.*, 2008b). The vegetative aroma seems to be linked to higher canopy density with excessive vegetative growth. The fruity/berry aroma descriptors in Cabernet Sauvignon seem to be more prominent when there was higher rainfall during the months before harvest, therefore moderate to high water constraints resulted in more fruity aroma wines (Chapman, 2005). Berry aroma was associated with soils with a lower water holding capacity, due to the reduced canopy growth resulting in a more open canopy causing photo degradation of methoxypyrazines (Carey *et al.*, 2008b). The ibMP is a strong aroma active compound, and low levels contribute to the aromatic complexity of red wines, but higher levels are perceived as a lack of ripeness and are detrimental to wine quality (Roujou de Boubée *et al.*, 2000; Lapalus, 2016). The increased fruity aroma significantly decreases the vegetative bell pepper aroma in the wine.

The multifactor analysis showed strong seasonal separations for the sensory attributes; with the seasons 2012/13 (S1) and 2013/14 (S2) more closely related with smokey, soy and red fruit sensory attributes, and the 2014/15 season (S3) being distinctly different to the previous two seasons. It showed sensory attributes of dark fruits, herbaceous and more vegetable attributes (Figure 28 and Figure 29). Climate had a positive correlation with herbaceous, dark fruit, sweetness, sourness and astringency sensory attributes for Cabernet Sauvignon and a negative correlation with smokey and soy sensory attributes (Figure 30). The increase in temperatures, shifts in season and increase in extreme events such as rainfall in season 2013/14 and warmer and shorter season like 2014/15 could affect the sensory profile of the wine.

The 2013/14 season seemed to have more red fruit attributes, compared to the 2012/13 season that was more associated with smokey attributes (Figure 28 and Figure 29) for the Somerset West and Stellenbosch_2 sites. Over both seasons, the sites seemed to separate into vigour levels, with more water constraints increasing the smokey/soy and horsey sensory attributes and lower water constraints being more associated with smokey/red fruit attributes. The very unpleasant aroma of horse sweat could be as a result of the higher water constraints experienced at the low vigour sites, and the higher wind exposure resulting in less photosynthetic activity or just over exposure of bunches. The cooler site, Elgin was more associated with smokey attributes for seasons 2012/13 and 2013/14. The 2014/15 season (S3) was very different in sensory profile compared to the other seasons, which could be due to the phenology being the earliest out of the three seasons and climate being the warmest in terms of accumulated heat units - hence the season was earlier and ripening was faster.

Cooler ripening seasons and sites could result in wines with less intense but more complex aromas, but also potentially wines with poor colour and green vegetative characteristics. Warmer regions can produce good wines with intense aromas, or wines that are thin and have coarse tannin structure. Moderate climates with moderate water constraints seem to produce more complex wine than extreme climates – but it can be emphasised that canopy management and irrigation strategies are important in the context of climate change to ensure complexity and quality in the wines. Cabernet Sauvignon is a cultivar that needs some vigour, but as it is a cultivar that is more sensitive to fertility, vigour needs to be induced but must protect the fertility harbouring more light in the canopy. Sites with too low vigour, result in slowed ripening, with over exposure of bunches, resulting in unfavourable wine aromas, such as at Somerset West low vigour level.

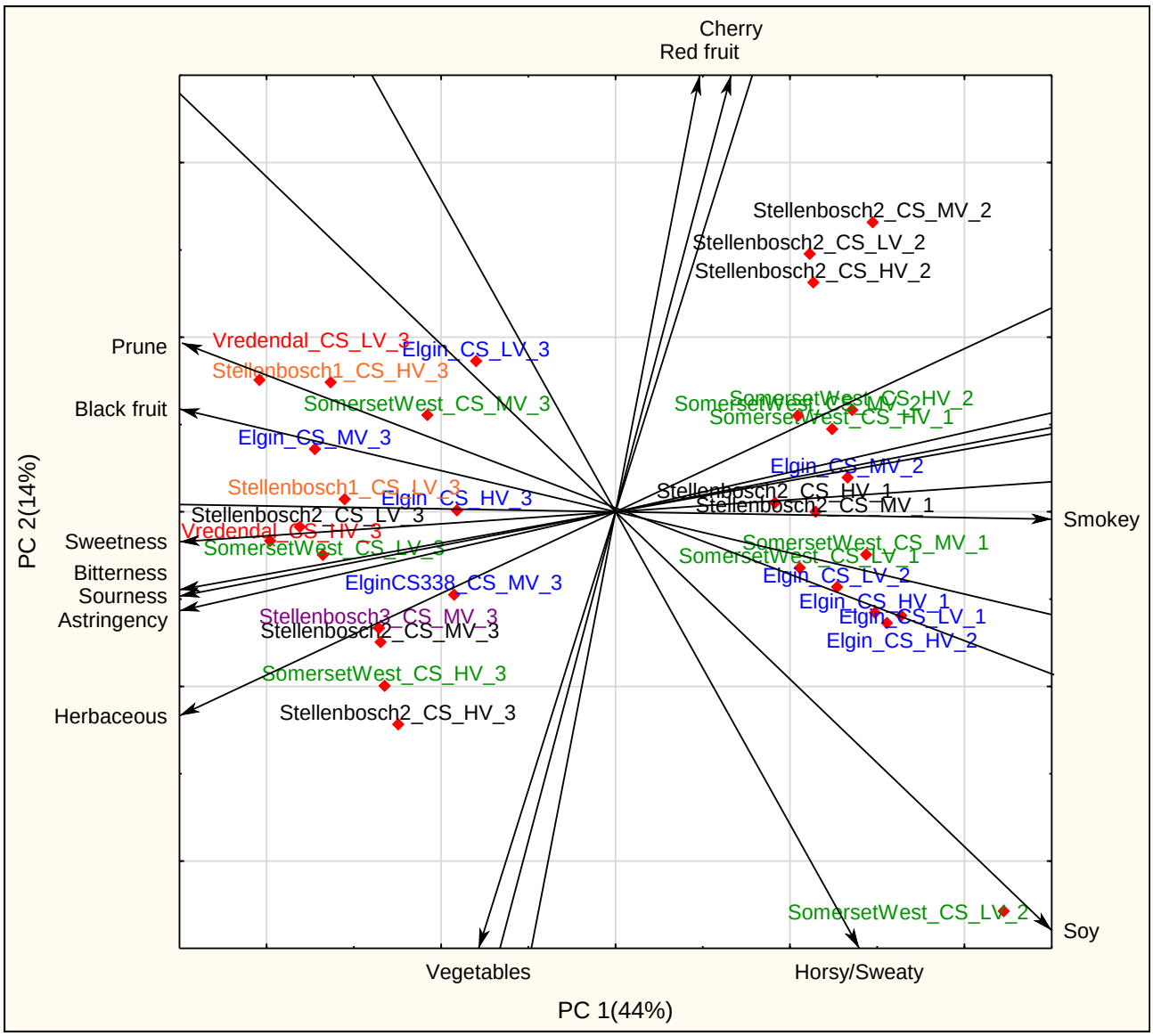

Figure 28 Multifactor analysis, showing the principal components of interaction for wine sensory analysis for Cabernet Sauvignon for the three seasons [2012/13 (S1), 2013/14 (S2) and 2014/15 (S3)] to emphasise the expression of sensory attributes at different sites and vigour levels.

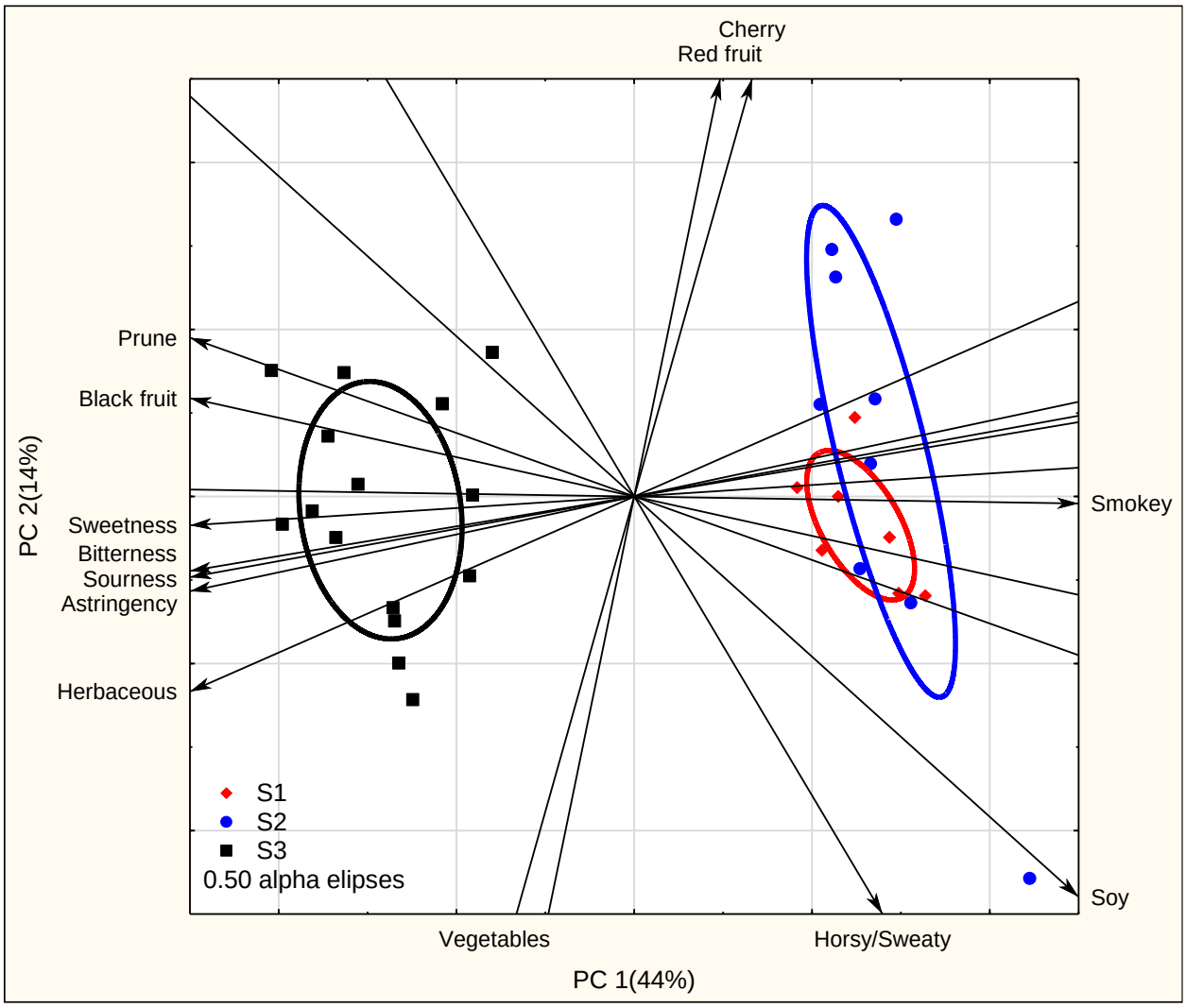

Figure 29 Multifactor analysis showing the principal components of interaction for wine sensory analysis for Cabernet Sauvignon for the three seasons [2012/13 (S1), 2013/14 (S2) and 2014/15 (S3)].

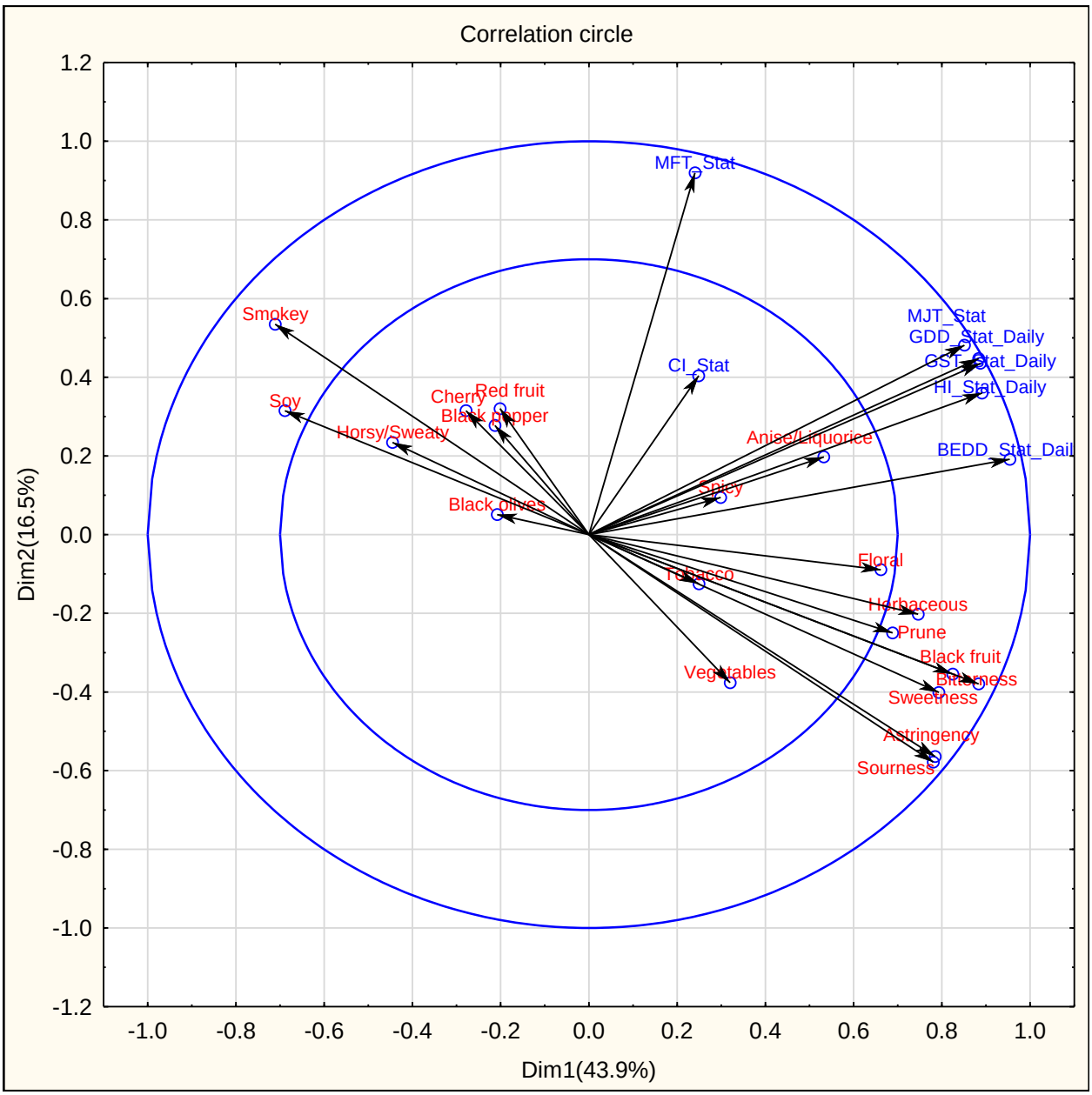

Figure 30 Multifactor analysis (correlation circle), representation of the principal components of separate PCA's of block variables: climate indices describing the season and wine sensory attributes with an RV=0.36 over all sites and seasons for Cabernet Sauvignon.

8.4 Conclusions

Results showed that there was a marked seasonal difference driving the grapevine's response to its environment more so than site variability. Season variability seemed to be driven by extreme out of the ordinary climate events such as extreme wind, rainfall or higher temperatures earlier in growing season and ripening period, confirming the unpredictability of seasons predicted in the context of climate change. The climatic seasonal variability was one of the major driving factors that were isolated as a factor affecting grapevine growth, ripening, final wine colour and composition and wine sensory profile.

Shoot growth tempo was significantly slower for grapevines at the cooler site compared to the warmer sites. Grapevine vigour also had an effect on the tempo of growth and final shoot length, with the low and medium vigour having a faster tempo of growth, but shorter shoots compared to the high vigour. The final shoot length attained seemed to be driven by temperature and water

constraints, hence the longest shoots were attained with moderate water constraints and moderate to warm climatic conditions. Overall temperatures had a positive correlation with growth early in the season and a negative correlation later in the season; however this could be buffered with low to moderate water constraints. Moderate to high water constraints ensure the canopy fills out to have sufficient source to sink ratio to allow for a good tempo of sugar and anthocyanin accumulation. The balance in the grapevine therefore could drive sugar accumulation or lack thereof and indirectly anthocyanin accumulation due to the co-regulation nature of the compounds. Unbalanced grapevines will either not complete sugar loading before harvest is attained, or the opposite, where the sugar accumulation could stop ("gets stuck"), hampering the phenolic development of the berry.

Climate was positively correlated with wine colour, as the total colour pigments and phenolics increased over the three growing seasons in relation to the increase in seasonal growing degree days. The warmer season in terms of accumulated thermal time had the strongest correlation with colour and phenolics. The total red pigments and phenolics seemed to increase to almost double from the first season to the last season. This could be due to increased temperatures in the ripening months enhancing colour development. The results suggested that anthocyanin biosynthesis was more sensitive to atmospheric conditions than to water constraints under the given conditions of the study. Season was the overriding factor influencing the wine anthocyanin profile, with warmer season and sites more closely related to the coumaroyl derivatives; while cooler sites, seasons and vigour levels (shaded fruits) had more glucosides and acetylglucosides derivatives.

Temperature and water constraints over sites and seasons affected the methoxypyrazine expression in the Cabernet Sauvignon wines. Results also showed that unseasonal s summer rainfall could hamper the degradation of ibMP due to the possible increased vegetative growth. In contrast, the warmer per-veraison temperatures were favourable for ibMP synthesis and the shorter season did not allow for effective degradation. The effect seemed to be more prominent in the warmer climates, as the cooler climates had cooler pre-veraison temperatures resulting in less synthesis of ibMP. The kinetics of ibMP degradation seemed to be slower at the sites where the soils had higher silt and course sand contents. This study gives some insights into the management and planting distribution of Cabernet Sauvignon in the context of ibMP expressions, especially as the pre-veraison temperatures seem to increasing in warmer areas where Cabernet sauvignon plantings are prolific.

The study highlights season and secondly water constraints as primary driving factors influencing the sensory attributes of Cabernet Sauvignon wines. Cooler temperatures and lower water constraints sites were strongly associated with herbaceous and vegetable attributes. Whereas warmer sites and areas of medium to low water constraints were more related with back fruit and prune attributes, as well as being sweeter. The final season of the study, also the warmest and shortest had a different sensory profile compared to previous seasons, ascribed to the early phenology and warmer seasonal growing conditions from early spring already, shifting the season earlier and changing the sensory expression.

From this study it seemed that Cabernet Sauvignon needs vigour for a good expression of growth and ripening, but the fertility must be protected by harbouring more light in the canopy. Within this study, low vigour areas that had a good balance of yield to pruning mass, resulted in unfavourable wine attributes, possibly due to over exposure of the bunches. Medium vigour sites that allowed for some vigour but ensured sufficient light in the canopy had well balanced vines in terms of the Ravaz index and had overall respectable tons per hectare. Results showed that wine sensory

attributes depended on climate, soil water content, vegetative growth, and vineyard management techniques affecting the sun exposure of the grapes in the canopy.

Growing degree days increased over the three seasons due to increased temperatures during the ripening period from September to March. Under such conditions the plant water constraints will increase earlier in the season, especially in the light of decreasing winter rainfall or shifting. With the increase of temperatures, there is an every pressing need for supplementary irrigation that is managed judiciously to ensure moderate water constraints for complexity in ripening. This study has provided some insights into the understanding of cultivating Cabernet Sauvignon in the context of warmer and cooler climatic conditions. Every response of the grapevine is influenced by climate, the grapevine growth tempo and final shoot length is sensitive to seasons and water constraints and indirectly influence's the leaf area per vine that influences the ripening tempo and final wine quality. The seasonal climatic conditions could be masked with more detailed viticultural management practices, to ensure a balanced grapevine in the selection of trellis system, pruning and canopy management. In the context of climate change the aim is to match the cultivar growth and ripening response to the climatic conditions of a site.

8.5 References

Allen, M.S., Lacey, M.J. & Boyd, S., 1994. Determination of methoxypyrazines in red wines by stable isotope dilution gas-chromatography-mass spectrometry. J. Agric. Food Chem 42, 1734-1738.

Archer, E. & Strauss, H.C., 1989. Effect of shading on the performance of Vitis vinifera L. cv. Cabernet Sauvignon. S. Afr. J. Enol. Vitic. pp. 74-77.

Ares, G., Bruzzone, F., Vidal, L., Cadena, R.S., Giménez, A., Pineau, B., Hunter, D.C., Paisley, A.G. & Jaeger, S.R., 2014. Evaluation of a rating-based variant of check-all-that-apply questions: Rate-all-that-apply (RATA). Food Qual. Prefer. 36, 87-95.

Bravdo, B., Hepner, Y., Loinger, C., Cohen, S. & Tabacman, H., 1985. Effect of irrigation and crop level on growth, yield and wine quality of Cabernet Sauvignon. Am. J. Enol. Vitic. 36, 132-139.

Brenon, E., Bernard, N., Zebic, O. & Deloire, A., 2005. Grape maturity: Proposal for a method using the berry volume as indicator. Revue des oenologues. 117, 1-3.

Bruwer, R.J., 2010. The edaphic and climatic effects on production and wine quality of Cabernet Sauvignon in the Lower Olifants River region. Thesis, Stellenbosch University, Private Bag X1, 7602 Matieland (Stellenbosch), South Africa.

Carbonneau, A., Champagnol, F., Deloire, A. & Sevila, F., 1998. Harvest and grape quality. In: C. Flanzy. Oenologie. Fondements scientifiques et technologiques. pp. 647-668.

Carbonneau, A. & Deloire, A., 2001. Plant organization based on source-sink relationship: new finding on development, biochemical and molecular responses to environment. Mol. Biol. Biotechnol. 263-280.

Carey, V.A., 2001. Spatial characteristic of natural terroir units for viticulture in the Bottelaryberg-Simonsberg-Helderberg winegrowing area. Thesis, Stellenbosch University, Private Bag X1, 7602 Matieland (Stellenbosch), South Africa.

Carey, V.A., Archer, E., Barbeau, G. & Saayman, D., 2008. Viticultural terroirs in stellenbosch, South Africa. II. The interaction of Cabernet Sauvignon and Sauvignon blanc with Environment. J. Int. Sci. Vigne Vin. 42, 185-201.

Carey, V.A., Bonnardot, V., Schmidt, A. & Theron, J.C.D., 2003. The interaction between vintage, vineyard site (mesoclimate) and wine aroma of Vitis vinifera L. cvs. Sauvignon blanc, Chardonnay and Cabernet Sauvignon in the Stellenbosch-Klein Drakenstein wine producing area. OIV Bull 76 (863-864), 4-29.

Choné, X., Van Leeuwen, C., Dubourdieu, D. & Gaudillère, J.-P., 2001. Stem water potential is a sensitive indicator of grapevine water status. Ann. Botany 87, 477-483.

Chuine, I., Yiou, P., Viovy, N., Seguin, B., Daux, V. & Ladurie, E.L.R., 2004. Historical phenology: Grape ripening as a past climate indicator. Nature 432, 289-290.

Conde, C., Silva, P., Fontes, N., Dias, A.C.P., Tavares, R.M., Sousa, M.J., Agasse, A., Delrot, S. & Gerós, H., 2007. Biochemical changes throughout grape berry development and fruit and wine quality. Food Global Science Books 1, 1-22.

Coombe, B.G., 1995. Growth Stages of the Grapevine: Adoption of a system for identifying grapevine growth stages. Aust. J. Grape Wine Res.1, 104-110.

Deloire, A., Carbonneau, A., Wang, Z. & Ojeda, H., 2004. Grapevine and water. J. Int. Sci. Vigne Vin 38 (1), 1-13.

Deloire, A., Howell, C., Habets, I., Botes, M.P., Van Rensburg, P., Bonnardot, V. & Lambrechts, M., 2009. Preliminary results on the effect of temperature on Sauvignon blanc (Vitis vinifera L.) berry ripening. Comparison between different macro climatic wine regions of the Western Cape Coastal area of South Africa. Presented at the 32st conference of the South African Society for Enology and Viticulture, July 2009, Cape Town, South Africa.

Deloire, A., Vaudour, E., Carey, V.A., Bonnardot, V. & Van Leeuwen, C., 2005. Grapevine responses to terroir: a global approach. J Int Sci Vigne et Vin, Vol 39(4) 149-162.

De Villiers, F.S., Scmidt, A., Theron, J.C.D. & Taljaard, R., 1996. Onderverdeling van die Wes-Kaapse wynbougebiede volgens bestaande klimaatskriteria. Wynboer Tegnies, January 1996, 10-12.

Downey, M.O., Dokoozlian, N.K. & Krstic, M.P., 2006. Cultural practices and environmental impacts on the flavonoid composition of grapes and wine: A review Am. J. Enol. Vitic, 257-267.

Downey, M., Harvey, J. & Robinson, S., 2004. The effect of bunch shading on berry deveopement and flavonoid accumulation in Shiraz grapes. Aust. J. Grape Wine Res. 10, 55-73.

Flore, J.A. & Lakso, A.N., 1989. Environmental and physiological regulation of photosynthesis in fruit crops. Horticultural reviews, 111-157.

Fournand, D., Vicens, A., Sidhoum, L., Souquet, J.M., Moutounet, M. & Cheynier, V., 2006. Accumulation and extractability of grape skin tannins and anthocyanins at different advanced physiological stages. Journal of Agricultural and Food Chemistry 54, 7331-7338.

Howell, G.S., 2001. Sustainable grape productivity and the growth - yield relationship: A review. Am. J. Enol. Vitic. 52, 165-174.

Hunter, J.J. & Archer, E., 2001a. Long-term cultivation strategies to improve grape quality. In: Proc. VIIIth Viticulture and Enology Latin-American Congress, November 2001, Montevideo, Uruguay.

Hunter, J.J. & Archer, E., 2001b. Short-term cultivation strategies to improve grape quality. In: Proc. VIIIth Viticulture and Enology Latin-American Congress, November 2001, Montevideo, Uruguay.

Hunter, J.J. & Bonnardot, V., 2011. Suitability of some climatic parameters for grapevine cultivation in South Africa, with focus on key physiological processes. S. Afr. J. Enol. Vitic 32, 137-154.

Hunter, J.J. & Deloire, A., 2005. Relationship between sugar loading and berry size of ripening Syrah/R99 grapes as affected by grapevine water status. In: Proc. Gesco XIVeme journees du groupe europeen d'etude des systems de conduit de la vigne, 2005, Geisenheim, Germany. pp. 23-27, 127-133.

Hunter, J.J. & Visser, J.H., 1990. The effect of partial defoliation on Cabernet vegetative growth. *In* S.Afr.J.Enol.Vitic., pp. 18-25.

Hunter, J.J., Volschenk, C.G. & Bonnardot, V., 2010. Linking grapevine row orientation to a changing climate in South Africa. In: Proc. Intervitis Interfructa Conference, 24-28 March, Stuttgart, Germany pp. 60-70.

Hunter, J.J., Volschenk, C.G., Marais, J. & Fouché, G.W., 2004. Composition of Sauvignon blanc Grapes as Affected by Pre-véraison Canopy Manipulation and Ripeness Level. South African Journal of Enology and Viticulture 25, 13-18.

Iland, P.G., Ewart, A., Sitters, J., Markides, A. & Bruer, N., 2000. Techniques for chemical analysis and quality monitoring during winemaking. Patrick Iland Wine Promotions.

Jackson, D.I. & Lombard, P.B., 1993. Environmental and management practices affecting grape composition and wine quality. A review. Am. J. Enol. Vitic 44, 209-230.

Jensen, J.S., Blachez, B. & Egebo, M., 2007. Rapid extraction of polyphenols from red grapes. Am. J. Enol. Vitic. 58, 451-461.

Jones, G., 2006. Climate and terroir: Impacts of climate variability and change on wine. In: Macqueen, R.W. and Meinert, L.D. (eds). Fine wine and terroir-The geoscience perspective. Geoscience Canada, (Geological Association of Canada, St John's, Newfoundland). pp. 1-14.

Jones, G.V., White, M.A., Cooper, O.R. & Storchmann, K., 2005. Climate change and global wine quality. Climatic Change 73, 319-343.

Joscelyne, V.L., Downey, M.O., Mazza, M. & Bastian, S.E., 2007. Partial shading of Cabernet Sauvigon and Shiraz vines altered wine color and mouthfeel attributes, but increased exposure had little impact. J. Agric. Food Chem, 10888-10896.

Kennedy, J.A., 2002. Understanding grape berry development. Practical Winery & Vineyard, July/August 2002.

Kliewer, W.M. & Dokoozlian, N.K., 2000. Leaf area/crop weight ratios of grapevines: Influence on fruit composition and wine quality. In: Proc. Amer. Soc. Enol. Viticult. 50th Anniv. Annu. Mtg., pp. 285-295.

Kliewer, M.W. & Dokoozlian, N.K., 2005. Leaf Area/Crop Weight Ratios of Grapevines: Influence on Fruit Composition and Wine Quality. Am. J. Enol. Vitic. 56, 170-181.

Lambrechts, J.J.N., Van Zyl, J., Ellis, F. & Schloms, B.H.A., 1978. Grondkode en kaartsimbool vir detail kartering in die Winterreënstreek. Technical Communication No. 165, Dept. Agric. Tech. Services, Pretoria.

Lategan, E.L., 2011. Determining of optimum irrigation schedules for drip irrigated Shiraz vineyards in the Breede River Valley. Department of Soil Science, 162.

Le Roux, E.G., 1974. A climate classification for the South Western Cape viticultural areas (in Afrikaanse). Thesis, Stellenbosch University, Private Bag X1, 7602 Matieland (Stellenbosch), South Africa.

McCarthy, M.G. & Coombe, B.G., 1999. Is weight loss in ripening grape berries cv. Shiraz caused by impeded phloem transport. Austr. J. Grape & Wine Research. 5, 17-21.

Mehmel, T.O., 2010. Effect of climate and soil water status on Cabernet Sauvignon (Vitis vinifera L.) grapevines in the Swartland region with special reference to sugar loading and anthocyanin biosynthesis. Thesis, Stellenbosch University, Private Bag X1, 7602 Matieland (Stellenbosch), South Africa.

Midgley, G.F., New, M., Johnston, P., Methner, N., Cole, M., Cullis, J., Drimie, S., Dzama, K., Guillot, B., Harper, J., Jack, C., Knowles, T., Louw, D., Mapiye, C., Oosthuizen, H.J. & Smit, J., 2015. A status quo review of climate change and the agriculture sector of the Western Cape Province. CSIR Environmentek, Stellenbosch CSIR. CSIR, P.O. Box 395; Pretoria 0001; South Africa.

Mira de Orduña, R., 2010. Climate change associated effects on grape and wine quality and production. Food Research International 43, 1844-1855.

Myburgh, P., 2005. Effect of altitude and distance from the Atlantic Ocean on mean February temperatures in the Western Cape Coastal region. WineLands, August.

Myburgh, P., 2015. Correct interpretation of soil water monitoring/measurements. Vinpro Road show, September 2015.

Orduña, R.M.D., 2010. Climate change associated effects on grape and wine quality and production. 43, 1844-1855.

Palliotti, A., Gatti, M. & Poni, S., 2011. Early Leaf Removal to Improve Vineyard Efficiency: Gas Exchange, Source-to-Sink Balance, and Reserve Storage Responses. Am. J. Enol. Vitic.

Pineau, B., Barbe, J.-C., Van Leeuwen, C. & Dubourdieu, D., 2009. Examples of perceptive interactions involved in specific "red-" and "black-berry" aromas in red wines. J. Agric. Food Chem 57, 3702-3708.

Poni, S., Intrieri, C. & Silvestroni, O., 1994. Interactions of LeafAge, Fruiting, and Exogenous Cytokinins in Sangiovese Grapevines Under Non-Irrigated Conditions. II. Chlorophyll and Nitrogen Content. Am. J. Enol. Vitic. 45, 278-284.

Saayman, D., 1981. Klimaat, grond en wingerdbougebiede In: BURGER. pp. 48-67, Wingerdbou in Suid-Afrika. Viticultural and Oenological Research Institute, Private Bag X5026, 7600 Stellenbosch, Republic of South Africa

Saayman, D., 2013. South African vineyard soils and climates. In: Wine of South Africa (WOSA) www.wosa.co.za.

Scholander, P.F., Hammel, H.T., Bradstreet, E.D. & Hemmingsen, E.A., 1965. Sap pressure in vascular plants Science 148, 339-346.

Schultz, H.R., 2003. Differences in hydraulic architecture account for near-isohydric and anisohydric behaviour of two field-grown Vitis vinifera L. cultivars during drought. Plant, Cell Environ. 26, 1393-1405.

Smart, R.E. & Robinson, M., 1991. Sunlight into Wine. A Handbook for Wine grape Canopy Management. Winetitles, Adelaide, Australia.

Spayd, S.E., Tarara, J.M., Mee, D.L. & Ferguson, J.C., 2002. Separation of sunlight and temperature effects on the composition of Vitis vinifera cv.Merlot berries. Am. J. Enol. Vitic. 53, 171-182.

Strever, A.E., 2012. Non-destructive assessment of leaf composition as related to growth of the grapevine (*Vitis vinifera* L. cv. Shiraz). Dissertation, Stellenbosch University, Private Bag X1, 7602 Matieland (Stellenbosch), South Africa.

Van Leeuwen, C., Friant, P., Choné, X., Tregoat, O., Koundouras, S. & Dubourdieu, D., 2004. Influence of climate, soil, and cultivar on terroir. Am. J. Enol. Vitic. 3, 207-217.

Van Leeuwen, C., Tregoat, O., Choné, X., Bois, B., Pernet, D. & Gaudillere, J.-P., 2009. Vine water status is a key factor in grape ripening and vintage quality for red Bordeaux wine. How can it be assessed for vineyard management purposes? J. Int. Sci. Vigne Vin 43, 121-134.

Wang, Z.P., Deloire, A., Carbonneau, A., Federspiel, B. & Lopez, F., 2003. Study of sugar phloem unloading in ripening grape berries under water stress conditions. J. Int. Sci. Vigne Vin.

Webb, L.B., Watterson, I., Bhend, J., Whetton, P.H. & Barlow, E.W.R., 2013. Global climate analogues for winegrowing regions in future periods: projections of temperature and precipitation. Aust. J. Grape Wine Res. 19, 331-341.

Webb, L.B., Whetton, P.H., Bhend, J., Darbyshire, R., Briggs, P.R. & Barlow, E.W.R., 2012. Earlier wine-grape ripening driven by climatic warming and drying and management practices. Nature Climate Change 2, 259-264.

Zeeman, A.S. & Archer, E., 1981. Stokontwikkeling, wintersnoei en somerbehandeling. In: Burger, J. & Deist, J. (eds). Wingerdbou in Suid- Afrika. ARC Infruitec- Nietvoorbij, Private Bag X5026, 7599 Stellenbosch, South Africa. pp. 202-233.

Addendum 8.1

8.5.1 **Somerset West –** Measurement seasons: 2012/2013 (S1), 2013/2014 (S2), 2014/2015 (S3), 2015/2016 (S4)

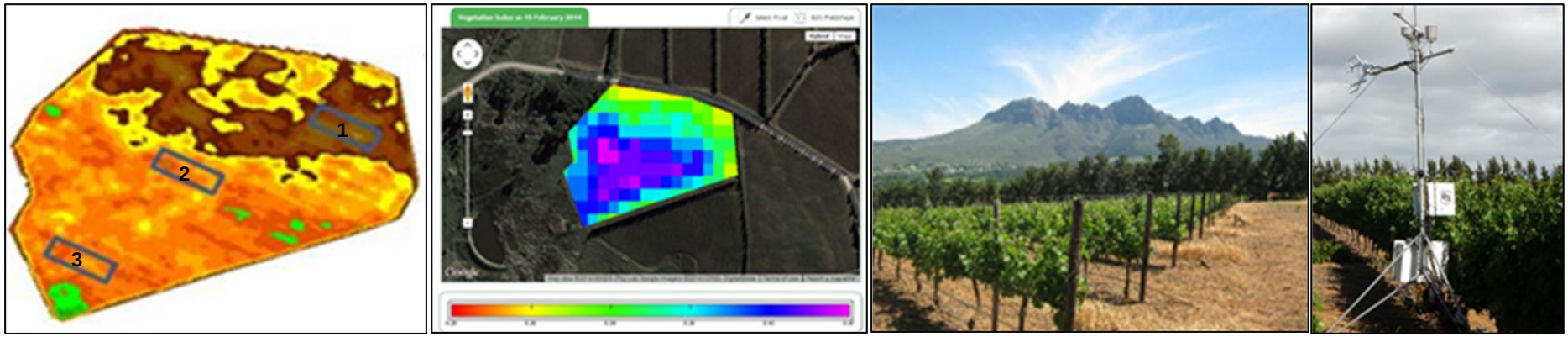

Plot Description: Somerset West site about 7 km from the ocean was selected and the study sites established in the first growing season of 2012/13 as the main FruitLook data validation site. In addition to monitoring the growth at different vigour areas, the ET and surface energy balance are continually measured using an OPEC eddy covariance systems (above, far right). The growth vigour differences is clear in the NDVI image from February 2014 (above, middle), ranging from around 0.34 at the low vigour (1) area and 0.48 at the high vigour (3) areas.

Planting date:	**Spacing:**	**Row Direction:**	**Irrigation:**	**Trellis:**	**Cover Crop**:
2008	2.75 X 1.4 m	NW-SE	Rain fed (V1) and supplementary drip (V2-4)	7-wire hedge trellis (VSP)	Winter only all rows

Vigour plots	**Cultivar**	**Scion/Clone**	**Rootstock**	**Aspect**	**Slope (%)**	**Altitude (m)**	**Terrain Description within vigour**
Plot 1 (LV) (n=12 VSP)	Cabernet Sauvignon(CS)	CS 46C	101-14 Mgt	280	6.5	162	Higher up on slope, more exposure to wind
Plot 2 (MV) (n=12 VSP)	Cabernet Sauvignon(CS)	CS 1E	R110	274	6.7	145	Higher water content
Plot 3 (HV) (n=12 VSP)	Cabernet Sauvignon(CS)	CS 46C	101-14 Mgt	271	6.6	136	Base of slope, more water

8.5.2 **Stellenbosch_2 -** Measurement seasons: 2012/2013 (S1), 2013/2014 (S2), 2014/2015 (S3), 2015/2016 (S4)

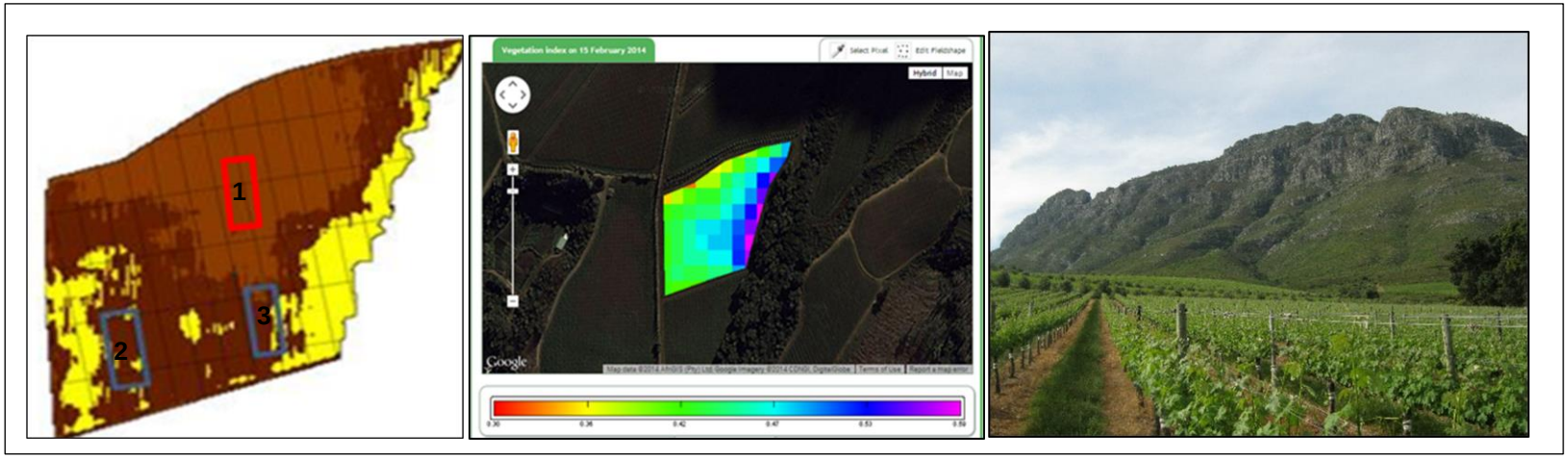

Plot Description: The Stellenbosch 2 site situated 25 km from the ocean was selected, low and high vigour areas was established in 2012/13 (blue outline). In the 2013/14 season a new lower vigour site (marked in red) was selected (abover, left). This site is slightly cooler than the Somerset West site due to altitude and proximity to the Simonsberg mountain. NDVI ranged between 0.4 and 0.58 in February 2014, higher than the Somerset West site (abover, middle). An additional cultivar (shiraz) was monitored for S3 and S4.

Planting date:	**Spacing:**	**Row Direction:**	**Irrigation:**	**Trellis:**	**Cover Crop**:
2003	2.5 X 2 m	N-S	**D**rip	7-wire hedge trellis (VSP)	Permanent/seasonal alternating rows (Korog/Fiscu)

Vigour plots	**Cultivar**	**Scion/Clone**	**Rootstock**	**Aspect**	**Slope (%)**	**Altitude (m)**	**Terrain Description within vigour**
Plot 1 (LV) (n=12 VSP)	Cabernet Sauvignon(CS)	CS 338 C	101-14 Mgt	160	9.1	429	Upper part of block on slope, soil very stony
Plot 2 (MV) (n=12 VSP)	Cabernet Sauvignon(CS)	CS 338 C	101-14 Mgt	158	11.0	413	Bottom of block, tended to have more water
Plot 3 (HV) (n=12 VSP)	Cabernet Sauvignon(CS)	CS 338 C	101-14 Mgt	172	7.0	416	Bottom of block, tended to have more water
Plot 4 (MV) (n=5 VSP)	Shiraz (SH)	SH	101-14 Mgt	169	5.3	425	Bottom of block, tended to have more water

8.5.3 **Elgin** – Measurement seasons: 2012/2013 (V1), 2013/2014 (V2), 2014/2015 (V3), 2015/2016 (V4)

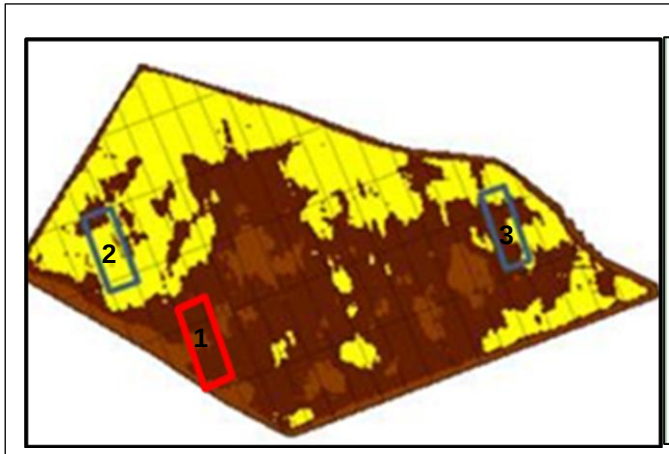

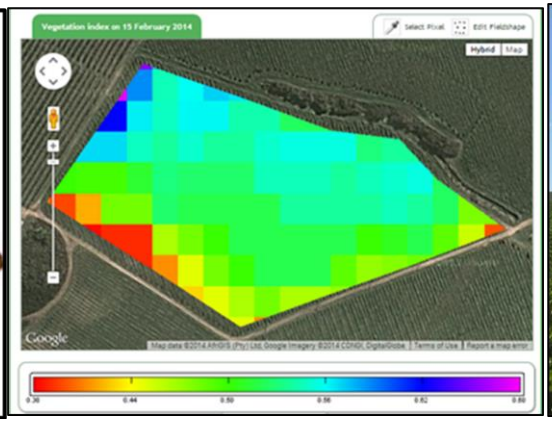


Plot Description: The Elgin experimental site situated about 15km from the ocean, was established in 2012/13 and has a higher relative humidity, cooler temperatures throughout the growing season and represents the cooler end of the climatic spectrum for the sites included for Fruitlook validation (above middle). In 2013/14 a new lower vigour site (marked in red) was selected (above left). This site includes a vigorously growing permanent cover crop.

Planting date:	**Spacing:**	**Row Direction:**	**Irrigation:**	**Trellis:**	**Cover Crop**:
2005	2.5 X 1.7	N-S	Drip	7-wire hedge trellis (VSP)	Permanent cover crop alternative rows

Vigour plots	**Cultivar**	**Scion/Clone**	**Rootstock**	**Aspect**	**Slope (%)**	**Altitude (m)**	**Terrain Description within vigour**
Plot 1 (LV) (n=12 VSP)	Cabernet Sauvignon(CS)	CS 46C	101-14 Mgt	84	5.8	205	Higher up on slope, more exposure to wind
Plot 2 (MV) (n=16 VSP)	Cabernet Sauvignon(CS)	CS 46C	101-14 Mgt	84	5.8	205	Higher up on slope, more exposure to wind
Plot 3 (HV) (n=12 VSP)	Cabernet Sauvignon(CS)	CS 46C	101-14 Mgt	84	5.8	205	Base of slope, more wate r
Plot 4 (MV) (n=3 VSP)	Cabernet Sauvignon(CS)	CS 338 C	101-14 Mgt	84	5.8	205	Mid slope
Plot 5 (MV) (n=5 VSP)	Shiraz (SH)	SH22C	101-14 Mgt	84	5.8	2015	Higher up on slope, more exposure to wind

8.5.4 **Vredendal -** Measurement seasons: 2013/2014 (S2), 2014/2015 (S3)

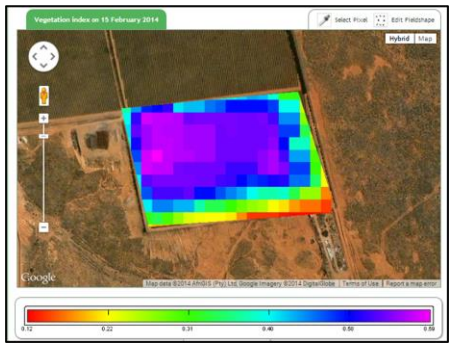
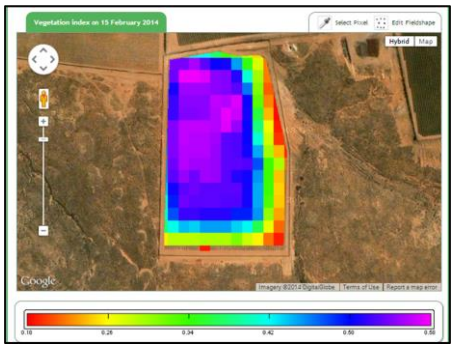


Plot Description: Warmest site of the study, about 34 km form Ocean was selected as the extreme site in the second year of the study. To monitor the grapvines reaction to a warmer and drier climate and (b) to extend the study to include other cultivars, e.g. Shiraz that physiologically behaves very different to Cabernet Sauvignon. The two additional vineyards (one Cabernet Sauvignon and one Shiraz) situated close to Vredendal, are located in close proximity to each other. In addition to monitoring growth over the growing season, ET measurements were made at both the sites, using one-sensor eddy covariance systems. The variation in growth vigour (here visible in the NDVI) is clear from the figures above on the left, depicting the Normalised difference vegetative index (NDVI) on 18 February 2014.

Planting date:	**Spacing:**	**Row Direction:**	**Irrigation:**	**Trellis:**	**Cover Crop**:
2003 (CS) 2002 (SH)	1.8 x 2.5	N-S	High intensity irritgation	5-wire hedge trellis (VSP)	Winter only all rows

Vigour plots	**Cultivar**	**Scion/Clone**	**Rootstock**	**Aspect**	**Slope (%)**	**Altitude (m)**	**Terrain Description within vigour**
Plot 1 (LV) (n=12 VSP)	Cabernet Sauvignon(CS)	CS 46C	R99	64	5.3	61	Higher up on slope, more exposure to wind
Plot 2 (HV) (n=12 VSP)	Cabernet Sauvignon(CS)	CS 46C	R99	64	5.3	61	Lower down on the slope
Plot 3 (LV) (n=12 VSP)	Shiraz (SH)	SH9C	R99	240	4.4	78	Higher up on slope, more exposure to wind
Plot 4 (HV) (n=12 VSP)	Shiraz (SH)	SH9C	R99	240	4.4	78	Lower down on the slope

8.5.5 **Stellenbosch_1 –** Measurement seasons: 2014/2015 (S3), 2015/2016 (S4)

Plot Description: in the final year of the study two sites where added to the study, about 21km from the ocean, these Stellenbsoch 1 sites receive the typical mid day cooling ocean breezes. These site where selected as validation sites within the extreme study sites.

Planting date:	**Spacing:**	**Row Direction:**	**Irrigation:**	**Trellis:**	**Cover Crop**:
2000	CS: 1.4 x 2.5 SH: 1.5 x 2.7	NW-SE	**S**upplementary drip	7-wire hedge trellis (VSP)	Winter only all rows

Vigour plots	**Cultivar**	**Scion/Clone**	**Rootstock**	**Aspect**	**Slope (%)**	**Altitude (m)**	**Terrain Description within vigour**
Plot 1 (LV) (n=5 VSP)	Cabernet Sauvignon(CS)	CS 338C	101-14 Mgt	153	1.8	110	Flat
Plot 2 (HV) (n=5 VSP)	Cabernet Sauvignon(CS)	CS 338C	101-14 Mgt	183	5.5	112	Flat
Plot 3 (Early Pruning) (n=3 VSP)	Shiraz (SH)	SH9C	101-14 Mgt	154	2.1	119	Flat
Plot 4 (Late Pruning) (n=3 VSP)	Shiraz (SH)	SH9C	101-14 Mgt	154	2.1	119	Flat

8.5.6 Stellenbosch_3 – Measurement seasons: 2014/2015 (S3), 2015/2016 (S4)

Plot Description: This site was selected due to is unique topography, situated high up on the Simonsberg mountain in Stellenbosch about 25km from Ocean. The site has a very intresting weather profile, taking longer too warm up in the morning, yet reaching warmer temperature than expected but cools faster in the afternoon. Over all this site is cooler due to low lying mist off the mountain as seen in the image abvove on the right..

Planting date:	**Spacing:**	**Row Direction:**	**Irrigation:**	**Trellis:**	**Cover Crop**:
2001	1.8 x 2.5	N-S	Supplementary drip	7-wire hedge trellis (VSP)	Winter only all rows

Vigour plots	**Cultivar**	**Scion/Clone**	**Rootstock**	**Aspect**	**Slope (%)**	**Altitude (m)**	**Terrain Description within vigour**
Plot 1 (MV) (n=3 VSP)	Cabernet Sauvignon(CS)	CS 337C	101-14 Mgt	238	7.2	358	Higher up on slope, more exposure to wind
Plot 2 (MV) (n=3 VSP)	Shiraz (SH)	SH9C	101-14 Mgt	238	7.2	358	Higher up on slope, more exposure to wind

Addendum 8.2

Table 4 Multifactor analysis results showing the groups in the analysis and the RV coefficients on interaction on which the correlation circles of interaction is based.

	HPLC wine	climate	grape	sensory	wine chemical	wine color	MFA
HPLC wine	1	0.21	0.39	0.39	0.52	0.61	0.74
climate	0.21	1	0.21	0.34	0.10	0.33	0.49
grape	0.39	0.21	1	0.49	0.51	0.49	0.77
sensory	0.39	0.34	0.49	1	0.17	0.76	0.74
wine chemical	0.52	0.10	0.51	0.17	1	0.30	0.63
wine color	0.61	0.33	0.49	0.76	0.30	1	0.82
MFA	0.74	0.49	0.77	0.74	0.63	0.82	1

Table 5 Summary of climatic indices of the study sites for the three growing season of the study, highlighting the site and seasonal variation driven by the climate gradient

Season	Locality	GST	GDD	BEDD	HI	MFT	CI	Rainfall	SummerRain	WinterRain
2012/13	Elgin	17.19	1614.98	1412.73	1972.44	19.45	13.85	868.71	277.46	591.25
2013/13	Somerset West	18.86	1973.74	1568.94	2210.67	21.49	15.28	647.80	272.40	375.40
2012/13	Stellenbosch_1	20.19	2210.31	1676.76	2732.28	22.63	13.52	850.42	293.64	556.78
2013/13	Stellenbosch_2	18.32	1861.75	1468.26	2279.87	21.02	15.43	1394.50	705.10	689.40
2012/13	Stellenbosch_3	18.17	1825.90	1480.60	2361.88	20.25	15.27	927.40	308.80	618.60
2013/13	Vredendal	22.28	2714.89	1791.06	3146.55	26.40	19.66	228.05	89.83	138.22
2013/14	Elgin	17.14	1613.23	1426.25	1980.87	20.95	14.96	1449.18	527.84	921.34
2013/14	Somerset West	18.78	1960.71	1567.72	2226.28	23.79	15.73	1345.60	758.00	587.60
2013/14	Stellenbosch_1	20.64	2309.02	1730.34	2823.46	25.15	14.48	955.12	379.03	576.09
2013/14	Stellenbosch_2	18.34	1870.75	1491.24	2279.18	23.68	13.87	1315.60	480.50	835.10
2013/14	Stellenbosch_3	18.10	1817.20	1484.96	2376.98	23.41	14.81	1170.00	424.40	745.60
2013/14	Vredendal	21.65	2577.01	1739.82	3015.05	29.01	17.89	313.30	80.16	233.14
2014/15	Elgin	17.51	1682.62	1517.92	2039.42	17.59	14.51	895.76	211.63	684.13
2014/15	Somerset West	19.72	2160.29	1713.40	2437.04	21.16	17.14	680.40	0.00	680.40
2014/15	Stellenbosch_1	20.83	2350.50	1821.69	2837.71	23.93	14.30	593.84	89.79	504.05
2014/15	Stellenbosch_2	19.23	2054.15	1645.49	2410.61	20.25	17.29	934.00	189.80	744.20
2014/15	Stellenbosch_3	18.61	1920.20	1624.05	2445.57	19.82	16.85	876.60	200.80	675.80
2014/15	Vredendal	22.20	2696.77	1847.91	3019.88	25.59	17.68	192.19	70.80	121.39

[1] Climatic indices used to classify climate Growing Season Temperature (GST), Growing Degree Days (GDD), Cool Night Index (CI) and Mean February Temperature (MFT) as described by Anderson et al., (2012). *Problems with the accuracy of rainfall information collect from the station

Table 6 Summary of long term (LTM) climatic indices of the study sites, highlighting the site and seasonal variation driven by the climate gradient

Season	Locality	*LTM_GST*	*LTM_GDD*	*LTM_Huglin*	*LTM_BEDD*	*LTM_CI*	*LTM_MFT*	*LTM_Rainfall*	*LTM_Summer*	*LTM_WinterR*
2012/13	Elgin	17.84	1659.20	2116.95	1532.54	13.14	20.59	907.95	303.75	604.20
2013/13	Somerset West	18.38	1775.45	2228.02	1624.12	13.37	20.67	599.29	254.22	345.07
2012/13	Stellenbosch_1	20.22	2164.06	2730.55	1739.64	13.43	23.18	658.45	209.65	448.80
2013/13	Stellenbosch_2	19.18	1944.21	2335.31	1620.36	15.94	22.13	1046.54	350.35	696.19
2012/13	Stellenbosch_3	20.16	2151.48	2534.16	1729.89	16.01	23.34	1272.38	362.87	909.51
2013/13	Vredendal	23.16	2788.73	3292.22	1875.34	16.16	25.87	331.36	144.96	186.40
2013/14	Elgin	17.84	1659.20	2116.95	1532.54	13.14	20.59	907.95	303.75	604.20
2013/14	Somerset West	18.38	1775.45	2228.02	1624.12	13.37	20.67	599.29	254.22	345.07
2013/14	Stellenbosch_1	20.22	2164.06	2730.55	1739.64	13.43	23.18	658.45	209.65	448.80
2013/14	Stellenbosch_2	19.18	1944.21	2335.31	1620.36	15.94	22.13	1046.54	350.35	696.19
2013/14	Stellenbosch_3	20.16	2151.48	2534.16	1729.89	16.01	23.34	1272.38	362.87	909.51
2013/14	Vredendal	23.16	2788.73	3292.22	1875.34	16.16	25.87	331.36	144.96	186.40
2014/15	Elgin	17.84	1659.20	2116.95	1532.54	13.14	20.59	907.95	303.75	604.20
2014/15	Somerset West	18.38	1775.45	2228.02	1624.12	13.37	20.67	599.29	254.22	345.07
2014/15	Stellenbosch_1	20.22	2164.06	2730.55	1739.64	13.43	23.18	658.45	209.65	448.80
2014/15	Stellenbosch_2	19.18	1944.21	2335.31	1620.36	15.94	22.13	1046.54	350.35	696.19
2014/15	Stellenbosch_3	20.16	2151.48	2534.16	1729.89	16.01	23.34	1272.38	362.87	909.51
2014/15	Vredendal	23.16	2788.73	3292.22	1875.34	16.16	25.87	331.36	144.96	186.40

[1] Climatic indices used to classify climate Growing Season Temperature (GST), Growing Degree Days (GDD), Cool Night Index (CI) and Mean February Temperature (MFT) as described by Anderson et al., (2012). *Problems with the accuracy of rainfall information collect from the station

Table 7 Soil analysis of all the study sites at the vigour levels over the climatic band for the Cabernet Sauvignon and Sgiraz vineyards at three depth intervals (0-30, 30-60 and 60-90 cm).

Locality	Cultivar	Vigour	Depth	Clay %	Silt %	Fine Sand %	Medium Sand %	Coarse Sand %	pH (KCl)	Resistance (Ohms)	P (citric acid) mg/kg	Potassium mg/kg	Calcium cmol(+)/kg	Magnessium cmol(+)/kg	Sodium mg/kg
Elgin	CS	HV	0-30	11	15	57	6	11	6	1240	62	317.5	11.08	2.815	32
Elgin	CS	HV	30-60	14	18	51	6	11	5.9	1560	29	214	7.52	1.59	25
Elgin	CS	HV	60-90	18	26	42	5	9	5.7	2010	10	89	4.44	0.86	24
Elgin	CS	MV	0-30	11	16	54.5	6.5	12	5.9	1355	34.5	178	6.32	1.765	29
Elgin	CS	MV	30-60	18	18	48	7	9	6.1	1260	12	82	5.42	0.89	22
Elgin	CS	MV	60-90	16	18	50	6	10	5.8	1460	4	54	3.32	0.58	21
Elgin	CS	LV	0-30	15	8.5	59.5	6.5	10.5	5.8	1620	29	128.5	6.52	1.575	30.5
Elgin	CS	LV	30-60	20	24	35	8	13	4.8	1860	15	62	3.96	0.88	31
Elgin	CS	LV	60-90	14	18	41	6	21	5.2	1820	12	55	4.15	0.65	32
Elgin	338	MV	0-30	12	19	58	4.5	6.5	5.65	1440	29	150	6.485	2.345	37.5
Elgin	338	MV	30-60	16	20	50	4	10	5.5	1760	86	123	6.82	1.15	35
Elgin	338	MV	60-90	16	22	46	4	12	5.1	2270	80	43	5.52	0.71	43
Elgin	SH	MV	0-30	13	22	51	5.5	8.5	5.9	1270	25.5	227.5	7.815	2.24	40.5
Elgin	SH	MV	30-60	12	22	46	7	13	5.5	1780	12	131	5.48	1.35	37
Elgin	SH	MV	60-90	26	34	26	3	11	4.8	1390	2	42	2.68	0.72	35
Somerset West	CS	HV	0-30	17	24	42	9.5	7.5	6.1	1420	18.5	105.5	5.29	1.63	33
Somerset West	CS	HV	30-60	24	36	24	8	8	5.8	1800	8	33	3.84	1.45	32
Somerset West	CS	HV	60-90	20	14	52	6	8	5	2160	2	20	2.19	1.65	23
Somerset West	CS	MV	0-30	13	18	52	9.5	7.5	6.15	1375	51	180	7.82	1.57	32
Somerset West	CS	MV	30-60	16	18	46	9	11	5.8	1690	17	53	4.81	1.27	31
Somerset West	CS	MV	60-90	14	18	52	6	10	5.4	1400	8	34	3.21	1.17	29
Somerset West	CS	LV	0-30	16	21	41	9	13	6.25	1385	30	116.5	8.025	0.97	47
Somerset West	CS	LV	30-60	18	24	27	6	25	5.2	1780	4	41	1.81	0.58	37
Somerset West	CS	LV	60-90	22	26	24	9	19	4.8	2220	3	32	1.16	0.74	32

Table 7 (Continued) Soil analysis of all the study sites at the vigour levels over the climatic band for the Cabernet Sauvignon and Sgiraz vineyards at three depth intervals (0-30, 30-60 and 60-90 cm).

Locality	Cultivar	Vigour	Depth	Clay %	Silt %	Fine Sand %	Medium Sand %	Coarse Sand %	pH (KCl)	Resistance (Ohms)	P (citric acid) mg/kg	Potassium mg/kg	Calcium cmol(+)/kg	Magnessium cmol(+)/kg	Sodium mg/kg
Stellenbosch_1	CS	HV	0-30	11	13	34.5	25.5	16	6.65	1650	94	67	6.63	0.865	35.5
Stellenbosch_1	CS	HV	30-60	10	10	41	17	22	6.9	850	47	31	6.24	0.54	25
Stellenbosch_1	CS	HV	60-90	10	12	42	23	13	6.7	1400	24	23	3.11	0.56	21
Stellenbosch_1	CS	LV	0-30	9	13	42	19.5	16.5	6.7	1400	81	70.5	6.78	0.955	35
Stellenbosch_1	CS	LV	30-60	12	18	39	19	12	6.8	790	95	46	9.26	1.05	52
Stellenbosch_1	CS	LV	60-90	12	18	36	19	15	6	1860	47	37	3.67	0.73	35
Stellenbosch_2	CS	HV	0-30	3	6	45	14.5	31.5	6	735	70	249.5	8.38	2.46	41
Stellenbosch_2	CS	HV	30-60	4	10	38	14	34	5.1	1960	26	138	3.71	0.95	41
Stellenbosch_2	CS	HV	60-90	4	10	37	12	37	5.2	2270	6	56	3.2	0.54	52
Stellenbosch_2	CS	MV	0-30	4	8	55	14.5	18.5	6.1	1915	21	139.5	6.595	1.54	23.5
Stellenbosch_2	CS	MV	30-60	4	8	45	17	26	5.9	2390	8	39	4.73	1.45	39
Stellenbosch_2	CS	MV	60-90	4	10	46	15	25	5.7	2280	7	33	4.04	1.26	37
Stellenbosch_2	CS	LV	0-30	4	6	44.5	16	29.5	5.8	1695	62.5	178	6.575	3.22	32.5
Stellenbosch_2	CS	LV	30-60	4	6	39	13	38	4.7	2280	8	45	1.91	0.77	38
Stellenbosch_2	CS	LV	60-90	6	8	34	14	38	5.1	2080	14	76	3.55	1.23	36
Stellenbosch_2	SH	MV	0-30	2	6	40.5	25.5	26	6.5	2115	41.5	134.5	11.335	3.125	35.5
Stellenbosch_2	SH	MV	30-60	2	6	35	27	30	4.9	3450	16	39	2.18	0.46	29
Stellenbosch_2	SH	MV	60-90	2	6	35	28	29	5.3	3690	13	28	3.41	0.87	34
Stellenbosch_3	CS	MV	0-30	4	9	46.5	17.5	23	6	1720	37	138	8.425	1.865	42
Stellenbosch_3	CS	MV	30-60	4	8	34	19	35	4.8	2650	21	43	2.93	0.91	38
Stellenbosch_3	CS	MV	60-90	8	8	36	16	32	5.2	2510	13	35	3.13	1.26	39
Stellenbosch_3	SH	MV	0-30	11	15	45.5	12	16.5	6.15	1465	24.5	283.5	6.7	1.9	30.5
Stellenbosch_3	SH	MV	30-60	10	8	51	13	18	5.7	1860	11	96	4.3	1.5	35
Stellenbosch_3	SH	MV	60-90	8	12	47	14	19	5.6	1810	55	77	5.47	1.94	39

Table 7 (Continued) Soil analysis of all the study sites at the vigour levels over the climatic band for the Cabernet Sauvignon and Sgiraz vineyards at three depth intervals (0-30, 30-60 and 60-90 cm).

Locality	Cultivar	Vigour	Depth	Clay %	Silt %	Fine Sand %	Medium Sand %	Coarse Sand %	pH (KCl)	Resistance (Ohms)	P (citric acid) mg/kg	Potassium mg/kg	Calcium cmol(+)/kg	Magnessium cmol(+)/kg	Sodium mg/kg
Vredendal	CS	LV	0-30	4	4	60	13	19	7.2	330	102	184	12.75	8.73	165
Vredendal	CS	LV	30-60	4	4	50	10	32	7.7	300	45	191	27.75	11.75	445
Vredendal	CS	LV	60-90	2	2	18	13	65	7.2	450	35	165	9.8	9.67	359
Vredendal	CS	HV	0-30	4	8	64	11	13	7.9	600	119	210	22.95	9.45	177
Vredendal	CS	HV	30-60	4	8	69	17	2	7.6	380	74	236	6.37	6.05	345
Vredendal	CS	HV	60-90	8	6	46	17	23	7.6	90	119	332	5.71	7.66	954
Vredendal	SH	LV	0-30	4	4	58	12	22	5	1420	24	108	0.83	0.98	45
Vredendal	SH	LV	30-60	2	4	64	15	15	6.2	780	7	106	1.99	2.85	92
Vredendal	SH	LV	60-90	2	4	52	15	27	7.8	400	31	211	30.63	10.92	389
Vredendal	SH	HV	0-30	4	4	74	10	8	7.6	620	69	177	9.13	4.74	71
Vredendal	SH	HV	30-60	2	4	63	6	25	7.7	220	100	225	19.2	10.1	97
Vredendal	SH	HV	60-90	4	4	61	8	23	7.8	160	338	267	30.71	8.72	230

Table 8 Midday stem water potentials for all sites and vigour levels at one phenological stage over the three seasons of the study.

Season	DAB	Phenology	Locality	Vigour	Culitvar	SWP (MPa)	N	Std.Dev.	Coef.Var.
2012/13	162	PostVéraison	Elgin	HV	CS	-1.30	5	79.06	6.08
2012/13	162	PostVéraison	Elgin	MV	CS	-1.33	5	44.72	3.36
2012/13	153	PostVéraison	Somerset West	HV	CS	-0.92	5	57.01	6.20
2012/13	153	PostVéraison	Somerset West	LV	CS	-0.85	5	35.36	4.16
2012/13	153	PostVéraison	Somerset West	MV	CS	-0.71	5	54.77	7.71
2012/13	154	PostVéraison	Stellenbosch_2	HV	CS	-0.85	5	50.00	5.88
2012/13	154	PostVéraison	Stellenbosch_2	MV	CS	-0.96	5	41.83	4.36
2013/14	144	PostVéraison	Elgin	HV	CS	-1.15	5	79.06	6.87
2013/14	144	PostVéraison	Elgin	LV	CS	-1.28	5	130.38	10.19
2013/14	144	PostVéraison	Elgin	MV	CS	-1.40	5	136.93	9.78
2013/14	148	PostVéraison	Somerset West	HV	CS	-1.04	5	54.77	5.27
2013/14	148	PostVéraison	Somerset West	LV	CS	-1.29	5	108.40	8.40
2013/14	136	PostVéraison	Stellenbosch_2	HV	CS	-1.19	5	151.66	12.74
2013/14	136	PostVéraison	Stellenbosch_2	LV	CS	-1.74	5	89.44	5.14
2013/14	136	PostVéraison	Stellenbosch_2	MV	CS	-1.50	5	231.84	15.46
2013/14	122	Véraison	Vredendal	HV	SH	-1.34	5	114.02	8.51
2013/14	122	Véraison	Vredendal	LV	SH	-1.32	5	57.01	4.32
2013/14	112	Véraison	Vredendal	HV	CS	-1.48	5	83.67	5.65
2013/14	112	Véraison	Vredendal	LV	CS	-1.22	5	109.54	8.98
2014/15	153	PostVéraison	Elgin	MV	SH	-1.46	3	57.74	3.94
2014/15	146	PostVéraison	Elgin	LV	CS	-1.21	3	28.87	2.37
2014/15	146	PostVéraison	Elgin	MV	CS	-1.10	3	0.00	0.00
2014/15	153	PostVéraison	Somerset West	HV	CS	-1.21	3	28.87	2.37
2014/15	154	PostVéraison	Somerset West	LV	CS	-1.00	3	0.00	0.00
2014/15	154	PostVéraison	Somerset West	MV	CS	-1.03	3	152.75	14.78
2014/15	142	PostVéraison	Stellenbosch_2	HV	CS	-1.26	3	57.74	4.56
2014/15	146	PostVéraison	Stellenbosch_2	LV	CS	-1.80	3	0.00	0.00
2014/15	148	PostVéraison	Stellenbosch_2	MV	SH	-1.53	3	115.47	7.53
2014/15	129	PostVéraison	Stellenbosch_1	HV	CS	-1.78	3	175.59	9.85
2014/15	129	PostVéraison	Stellenbosch_1	LV	CS	-1.75	3	278.39	15.91
2014/15	118	Véraison	Vredendal	HV	SH	-1.10	3	0.00	0.00
2014/15	118	Véraison	Vredendal	LV	SH	-0.90	5	114.02	11.52
2014/15	123	Véraison	Vredendal	HV	CS	-0.95	4	100.00	10.53
2014/15	123	Véraison	Vredendal	LV	CS	-1.25	5	176.78	14.14

Table 9 Destructive shoot measurements for Cabernet Sauvignon and Shiraz for all vigour levels over the study site and the three seasons of the study.

Season	SiteCultVig	Main_Length (cm)	Main_Node#	Total Leaf area/Shoot (main+lat) (cm^2)	Total Leaf area/vine (main+lat) (cm^2)	Ratio Lat:Main leaf area	LeafArea/YieldRatio (g)
2012/13	Elgin_CS_HV	172.5	21.0	4361.9	55947.7	1.1	14.0
2012/13	Elgin_CS_MV	160.3	22.0	3071.3	23470.8	0.4	5.0
2012/13	Somerset West_CS_HV	188.2	32.0	3914.5	46492.5	1.6	60.1
2012/13	Somerset West_CS_LV	107.7	21.7	1590.3	20396.8	1.6	15.5
2012/13	Somerset West_CS_MV	156.6	26.8	2900.7	46467.0	2.4	31.4
2012/13	Stellenbosch_2_CS_HV	121.2	22.9	2006.5	10063.1	0.2	1.8
2012/13	Stellenbosch_2_CS_MV	100.4	19.7	1508.6	9743.2	0.3	2.5
2013/14	Elgin_CS_HV	207.5	32.1	2576.2	35176.2	0.7	8.6
2013/14	Elgin_CS_LV	161.1	26.1	1476.2	8351.3	0.2	2.3
2013/14	Elgin_CS_MV	167.9	29.1	3302.6	25987.6	0.3	4.9
2013/14	Somerset West_CS_HV	237.8	38.5	1898.0	8011.4	0.2	4.4
2013/14	Somerset West_CS_LV	131.4	31.3	1525.1	11891.9	0.7	5.2
2013/14	Somerset West_CS_MV	203.0	35.7	2159.0	13449.1	0.4	6.7
2013/14	Stellenbosch_2_CS_HV	184.4	28.4	1211.0	7168.0	0.2	1.0
2013/14	Stellenbosch_2_CS_LV	125.3	21.5	1150.8	2349.3	0.0	0.5
2013/14	Stellenbosch_2_CS_MV	150.2	25.4	1190.0	10837.0	0.4	1.8
2014/15	Elgin_CS_HV	154.8	22.8	2302.0	20232.1	0.5	5.9
2014/15	Elgin_CS_LV	83.1	16.8	850.8	5756.9	0.3	2.1
2014/15	Elgin_CS_MV	115.6	20.8	1289.7	8754.1	0.4	2.6
2014/15	Elgin_CS_MV	152.2	22.8	2013.6	13667.8	0.4	4.2
2014/15	Elgin_SH_MV	137.9	17.1	2752.9	1721.9	0.6	0.0
2014/15	Somerset West_CS_HV	129.6	17.1	1776.4	22431.7	0.9	10.7
2014/15	Somerset West_CS_LV	117.4	20.4	1675.1	11781.0	0.4	3.4
2014/15	Somerset West_CS_MV	107.0	27.0	1148.8	1148.8	0.0	0.5
2014/15	Stellenbosch_1_CS_HV	171.8	28.4	2753.8	14271.4	0.2	5.0
2014/15	Stellenbosch_1_CS_LV	136.3	22.2	1773.9	9985.8	0.3	3.8
2014/15	Stellenbosch_1_SH_MV	253.5	27.8	3561.5	18268.7	0.3	2.5
2014/15	Stellenbosch_2_CS_HV	135.8	23.2	1208.7	6339.7	0.2	0.9
2014/15	Stellenbosch_2_CS_LV	180.1	24.8	2458.1	12355.8	0.2	1.9
2014/15	Stellenbosch_2_CS_MV	138.0	16.4	1788.3	14249.6	0.3	2.2
2014/15	Stellenbosch_3_CS_MV	111.5	25.0	1112.6	4886.9	0.2	2.0
2014/15	Stellenbosch_3_SH_MV	138.0	22.2	1300.3	5916.4	0.2	0.9
2014/15	Vredendal_CS_HV	129.8	23.2	2047.7	19218.9	0.2	3.5
2014/15	Vredendal_CS_LV	109.9	26.0	1981.3	21225.3	0.4	6.1
2014/15	Vredendal_SH_HV	108.9	17.2	2632.5	55714.9	0.8	8.4
2014/15	Vredendal_SH_LV	127.1	17.2	2797.8	64518.5	1.1	14.0

Table 10 Detailed pruning measurements for Cabernet Sauvignon and Shiraz for all vigour levels over the study site, only the last two seasons recorded as the first season 2012/13 is missing.

Season	Locality_Cultivar_Vigour	Length (cm)				nodes		
		Means	N	Std.Dev.	Std.Err.	Means	Std.Dev.	Std.Err.
2013/14	Somerset West_CS_LV	94.66	38	45.40	7.37	18	8	1
2013/14	Somerset West_CS_HV	125.48	42	66.66	10.29	23	14	2
2013/14	Somerset West_CS_MV	132.98	40	72.46	11.46	25	15	2
2013/14	Elgin_CS_LV	117.36	11	45.18	13.62	18	8	2
2013/14	Elgin_CS_HV	131.80	15	73.38	18.95	22	14	4
2013/14	Elgin_CS_MV	135.21	7	55.02	20.79	18	10	4
2013/14	Stellenbosch_2_CS_LV	132.60	10	42.22	13.35	19	6	2
2013/14	Stellenbosch_2_CS_HV	129.17	9	46.94	15.65	19	6	2
2013/14	Stellenbosch_2_CS_MV	104.33	6	48.61	19.85	16	7	3
2014/15	Somerset West_CS_LV	86.13	15	43.54	11.24	17	7	2
2014/15	Somerset West_CS_HV	113.00	20	49.17	11.00	21	8	2
2014/15	Somerset West_CS_MV	107.76	17	53.33	12.93	21	12	3
2014/15	Elgin_CS_LV	98.00	5	41.48	18.55	16	6	3
2014/15	Elgin_CS_HV	115.97	16	71.71	17.93	19	11	3
2014/15	Elgin_CS_MV	105.46	13	38.62	10.71	19	7	2
2014/15	Stellenbosch_2_CS_LV	154.43	14	31.15	8.33	23	3	1
2014/15	Stellenbosch_2_CS_HV	142.20	15	49.51	12.78	23	7	2
2014/15	Stellenbosch_2_CS_MV							
2014/15	Stellenbosch_3_CS_MV	77.36	18	55.11	12.99	19	13	3
2014/15	Vredendal_CS_LV	75.38	12	18.69	5.40	17	4	1
2014/15	Vredendal_CS_HV	138.67	12	27.35	7.90	23	4	1
2014/15	Vredendal_SH_LV							
2014/15	Vredendal_SH_HV	81.48	24	64.09	13.08	13	8	2
2014/15	Stellenbosch_1_CS_HV	161.10	10	93.91	29.70	27	14	4
2014/15	Stellenbosch_1_CS_LV	126.67	12	66.05	19.07	20	9	3
2014/15	Stellenbosch_2_SH_MV	83.82	11	36.59	11.03	11	4	1
2014/15	Stellenbosch_1_SH_EP	171.75	20	102.09	22.83	24	12	3
2014/15	Stellenbosch_1_SH_LP	148.72	16	96.72	24.18	17	9	2

Table 11 Yield and pruning results for all sites, vigour levels and seasons of the study.

Season	Locality_Cultivar_Vigour	Bunches/ vine	yield (kg/vine)	TotalCanes / vine	Pruning (kg/vine)	Ravaz Index	Biomass Index	Tons/Ha	Estimated fertility
2012/13	Elgin_CS_HV	31.25	4.00	24.06	1.98	2.02	5.98	9.41	1.30
2012/13	Elgin_CS_MV	37.75	4.71	25.88	2.40	1.97	7.11	11.09	1.46
2012/13	Somerset West_CS_HV	13.50	0.77	18.75	2.68	0.29	3.46	2.01	0.72
2012/13	Somerset West_CS_LV	21.08	1.32	20.42	1.25	1.05	2.57	3.42	1.03
2012/13	Somerset West_CS_MV	18.58	1.48	22.42	2.84	0.52	4.31	3.84	0.83
2012/13	Stellenbosch_2_CS_HV	51.50	5.74	32.25	1.82	3.15	7.56	11.48	1.60
2012/13	Stellenbosch_2_CS_MV	40.92	3.86	28.17	1.48	2.61	5.34	7.72	1.45
2013/14	Elgin_CS_HV	31.38	4.10	31.00	2.93	1.40	7.03	9.64	1.01
2013/14	Elgin_CS_LV	30.38	3.70	27.07	2.04	1.81	5.74	8.70	1.12
2013/14	Elgin_CS_MV	37.06	5.29	30.31	2.47	2.15	7.76	12.46	1.22
2013/14	Somerset West_CS_HV	19.08	1.82	19.58	2.02	0.90	3.84	4.72	0.97
2013/14	Somerset West_CS_LV	21.08	2.27	17.42	1.26	1.80	3.53	5.90	1.21
2013/14	Somerset West_CS_MV	19.75	2.00	18.67	2.15	0.93	4.15	5.19	1.06
2013/14	Stellenbosch_2_CS_HV	56.50	7.51	35.25	2.34	3.21	9.84	15.01	1.60
2013/14	Stellenbosch_2_CS_LV	53.25	5.00	33.83	2.01	2.48	7.02	10.01	1.57
2013/14	Stellenbosch_2_CS_MV	49.67	5.96	32.33	1.85	3.22	7.81	11.91	1.54
2013/14	Vredendal_CS_HV	60.33	5.88				5.88	14.32	
2013/14	Vredendal_CS_LV	55.58	4.72				4.72	11.49	
2013/14	Vredendal_SH_HV	53.25	6.60				6.60	12.05	
2013/14	Vredendal_SH_LV	50.25	5.23				5.23	9.55	
2014/15	Elgin_CS_HV	29.31	3.42	24.75	1.67	2.05	5.09	8.05	1.18
2014/15	Elgin_CS_LV	27.60	2.70	25.80	1.89	1.43	4.59	6.36	1.07
2014/15	Elgin_CS_MV	26.25	3.36	23.13	1.33	2.53	4.69	7.91	1.14
2014/15	Elgin_CS338_MV	25.50	3.26	21.57	0.92	3.55	4.18	7.67	1.18
2014/15	Somerset West_CS_HV	26.00	2.10	26.08	2.12	0.99	4.22	5.46	1.00
2014/15	Somerset West_CS_LV	31.08	3.50	24.08	1.20	2.93	4.70	9.10	1.29
2014/15	Somerset West_CS_MV	27.83	2.21	24.17	1.89	1.17	4.10	5.73	1.15
2014/15	Stellenbosch_1_CS_HV	23.10	2.85	26.10	1.48	1.93	4.33	8.15	0.89
2014/15	Stellenbosch_1_CS_LV	23.30	2.60	23.40	1.00	2.59	3.60	7.43	1.00
2014/15	Stellenbosch_1_SH_EarlyPrune_MV			19.00	1.51	0.00	1.51	0.00	0.00
2014/15	Stellenbosch_1_SH_LatePrune_MV	29.00	7.22	17.67	2.16	3.34	9.38	17.83	1.64
2014/15	Stellenbosch_2_CS_HV	44.33	6.73	33.08	2.19	3.08	8.92	13.46	1.34
2014/15	Stellenbosch_2_CS_LV	48.25	6.63	32.08	1.60	4.13	8.23	13.25	1.50
2014/15	Stellenbosch_2_CS_MV	45.83	6.51	30.08	1.86	3.51	8.36	13.01	1.52
2014/15	Stellenbosch_2_SH_MV	38.80	6.50	29.60	1.31	4.96	7.81	14.85	1.31
2014/15	Stellenbosch_3_CS_MV	23.78	2.44	19.11	0.55	4.40	3.00	6.51	1.24
2014/15	Stellenbosch_3_SH_MV	32.00	6.90	24.56			6.90	15.78	1.30
2014/15	Vredendal_ CS_HV	68.00	5.48	47.08	3.33	1.65	8.81	13.33	1.44
2014/15	Vredendal_CS_LV	48.92	3.46	36.17	0.67	5.19	4.13	8.42	1.35
2014/15	Vredendal_SH_HV	57.92	6.65	45.42	1.41	4.70	8.06	12.13	1.28
2014/15	Vredendal_SH_LV	44.89	4.61	43.75			4.61	8.42	1.03

Table 12 Grape berry analysis at harvest, berry mass, total soluable solids (TSS) measured as Balling (°B), sugar accumulation and the final colour and phenolic per berry for all sites, vigour levels and seasons.

Season	Locality_Cultivar_Vigour	N	Average Berry mass (g)	Average Berry Vol (cm3)	Total soluble solids (°B)	Sugar accumulation (mg/berry)	Colour/ berry (mg antho/ berry)	Total Phenolics/ berry (abs unit/ berry)
2012/13	Elgin_CS_HV	9	1.30	1.20	23.70	312.10	1.70	0.30
2012/13	Elgin_CS_MV	9	1.30	1.20	22.90	299.10	1.90	0.30
2012/13	Somerset West_CS_HV	9	1.10	1.00	27.40	295.30	1.00	0.10
2012/13	Somerset West_CS_LV	9	1.20	1.10	26.20	326.60	1.40	0.20
2012/13	Somerset West_CS_MV	9	1.20	1.10	24.30	286.50	1.30	0.20
2012/13	Stellenbosch_2_CS_HV	9	1.40	1.30	23.00	330.00	1.50	0.20
2012/13	Stellenbosch_2_CS_MV	9	1.30	1.10	24.20	310.80	1.60	0.20
2013/14	Elgin_CS_HV	9	1.50	1.40	23.70	359.20	1.50	0.20
2013/14	Elgin_CS_LV	9	1.60	1.40	24.30	379.70	1.70	0.30
2013/14	Elgin_CS_MV	9	1.60	1.40	24.00	380.40	1.50	0.20
2013/14	Somerset West_CS_HV	6	1.40	1.20	25.70	353.20	1.50	0.20
2013/14	Somerset West_CS_LV	6	1.30	1.20	27.00	359.10	1.40	0.20
2013/14	Somerset West_CS_MV	6	1.40	1.30	25.10	347.70	1.50	0.20
2013/14	Stellenbosch_2_CS_HV	9	1.70	1.50	24.10	406.90	2.10	0.30
2013/14	Stellenbosch_2_CS_LV	9	1.30	1.20	24.60	325.70	2.20	0.30
2013/14	Stellenbosch_2_CS_MV	9	1.60	1.50	24.60	404.50	2.10	0.40
2013/14	Vredendal_CS_HV	3	1.00	0.90	25.00	261.80		
2013/14	Vredendal_SH_HV	3	1.50	1.40	24.70	377.60		
2013/14	Vredendal_CS_LV	3	1.00	0.90	25.00	253.60		
2013/14	Vredendal_SH_LV	3	1.50	1.30	21.50	314.70		
2014/15	Elgin_CS338_MV	3	1.50	1.40	23.60	344.90	2.20	2.20
2014/15	Elgin_CS_HV	3	1.30	1.20	24.50	308.80	1.90	2.00
2014/15	Elgin_CS_LV	3	1.20	1.10	24.30	295.00	2.20	2.10
2014/15	Elgin_CS_MV	3	1.20	1.10	23.60	289.60	2.00	2.00
2014/15	Elgin_SH_MV	3	1.60	1.40	24.50	389.60	2.60	2.10
2014/15	Somerset West_CS_HV	3	1.40	1.20	25.50	352.50	1.80	1.80
2014/15	Somerset West_CS_LV	3	1.50	1.40	23.10	354.70	1.90	2.10
2014/15	Somerset West_CS_MV	3	1.30	1.20	25.20	334.00	1.90	2.00

Table 12 (continued) Grape berry analysis at harvest, berry mass, total soluable solids (TSS) measured as Balling (°B), sugar accumulation and the final colour and phenolic per berry for all sites, vigour levels and seasons.

Season	Locality_Cultivar_Vigour	N	Average Berry mass (g)	Average Berry Vol (cm3)	Total soluble solids (°B)	Sugar accumulation (mg/berry)	Colour/ berry (mg antho/ berry)	Total Phenolics/ berry (abs unit/ berry)
2014/15	Stellenbosch_1_SH_EarlyP	3	1.60	1.60	25.80	413.90	2.70	2.50
2014/15	Stellenbosch_1_CS_HV	3	1.20	1.10	24.10	284.50	1.80	1.70
2014/15	Stellenbosch_1_CS_HVRed	3	1.20	1.10	25.00	295.80	1.70	1.80
2014/15	Stellenbosch_1_SH_LateP	3	1.60	1.50	23.90	376.90	2.30	1.90
2014/15	Stellenbosch_1_CS_LV	3	1.10	1.10	23.50	260.60	1.60	1.60
2014/15	Stellenbosch_1_CS_LVRed	3	1.10	1.00	24.60	270.00	1.60	1.70
2014/15	Stellenbosch_1_SH_Red	3	1.60	1.40	26.80	427.90	2.40	2.30
2014/15	Stellenbosch_2_CS_HV	3	1.40	1.30	24.80	351.40	2.00	1.70
2014/15	Stellenbosch_2_CS_LV	3	1.20	1.10	25.30	307.00	2.40	2.10
2014/15	Stellenbosch_2_CS_MV	3	1.50	1.40	25.50	393.10	2.50	2.10
2014/15	Stellenbosch_2_SH_MV	3	1.40	1.20	25.80	360.30	2.50	2.20
2014/15	Stellenbosch_3_CS_MV	3	1.30	1.20	23.00	291.20	1.90	1.80
2014/15	Stellenbosch_3_CS_MV	3	1.20	1.10	24.40	289.60	1.70	1.70
2014/15	Stellenbosch_3_SH_MV	3	1.70	1.60	21.80	379.90	2.00	2.00
2014/15	Stellenbosch_3_SH_MV	3	1.80	1.60	23.30	412.30	1.70	2.20
2014/15	Vredendal_CS_HV	3	1.10	1.00	23.90	270.60	2.00	2.00
2014/15	Vredendal_SH_HV	3	1.70	1.50	21.80	364.10	1.50	1.90
2014/15	Vredendal_CS_LV	3	1.10	1.00	25.00	270.70	1.60	1.80
2014/15	Vredendal_SH_LV	3	1.60	1.50	23.90	390.70	1.80	2.20

Table 13 Wine chemical analyses for Cabernet Sauvignon wines, for all sites and vigour levels over the three growing seasons of the study.

Season	Locality_Cultivar_Vigour	wine pH	Volatile Acid	TotalAcid	MalicAcid	LacticAcid	Glucose	Fructose	Ethanol	Glycerol	Succinic Acid	Tartaric acid	Acetic Acid
2012/13	Elgin_CS_HV	3.72	0.6	6.2	0.7	1.5	-0.1	1.1	14.4	10.9	1747.5	821.5	812.9
2012/13	Elgin_CS_MV	3.62	0.6	6.4	0.7	1.3	0.2	1.1	14.7	11.2	1882.9	956.0	753.7
2012/13	Somerset West_CS_HV	4.02	0.6	6.5	3.4	-0.1	1.4	6.0	17.8	12.2	2138.7	216.9	701.0
2012/13	Somerset West_CS_LV	3.88	0.5	6.8	3.0	-0.2	1.2	2.1	17.3	12.5	1846.0	465.7	578.1
2012/13	Somerset West_CS_MV	4.09	0.6	5.9	1.0	1.3	-0.7	1.5	14.9	11.5	1622.7	232.1	759.8
2012/13	Stellenbosch_2_CS_HV	3.76	1.1	6.7	0.6	1.6	-0.1	1.0	13.6	12.1	2022.3	469.8	1336.4
2012/13	Stellenbosch_2_CS_MV	3.61	0.6	6.7	1.0	1.1	0.3	1.3	15.0	11.5	1986.8	900.1	684.2
2013/14	Elgin_CS_HV	3.73	0.4	5.4	0.5	1.5	0.6	1.0	13.8	10.0	1531.8	812.1	355.8
2013/14	Elgin_CS_LV	3.57	0.5	5.8	0.5	1.0	0.2	1.1	14.7	10.2	1831.9	806.7	539.2
2013/14	Elgin_CS_MV	3.66	0.5	5.5	0.6	1.3	-0.1	1.0	14.5	9.7	1782.8	773.8	458.4
2013/14	Somerset West_CS_HV	3.66	0.5	5.7	0.8	0.8	0.2	1.2	14.7	10.2	1725.2	852.4	552.9
2013/14	Somerset West_CS_LV	3.81	0.6	5.5	1.1	0.8	0.4	1.6	16.1	10.5	1770.8	534.1	649.9
2013/14	Somerset West_CS_MV	3.78	0.5	5.5	0.7	1.0	-0.1	1.1	14.9	10.3	1669.1	660.7	485.9
2013/14	Stellenbosch_2_CS_HV	3.56	0.6	5.8	0.6	1.0	0.2	1.1	14.2	10.7	1982.5	698.2	689.9
2013/14	Stellenbosch_2_CS_LV	3.55	0.6	5.9	0.7	0.5	0.2	1.1	14.9	11.3	2006.5	798.1	620.1
2013/14	Stellenbosch_2_CS_MV	3.45	0.6	6.2	0.8	0.6	0.5	1.1	15.0	11.0	1999.1	987.0	707.6
2013/14	Vredendal_CS_HV	3.99	0.6	5.3	0.6	1.5	-0.2	1.4	15.1	10.3	1672.8	301.2	648.1
2013/14	Vredendal_CS_LV	3.73	0.6	5.7	0.8	1.2	0.0	1.3	14.9	10.4	1795.2	539.8	591.2
2014/15	Elgin_CS_HV	3.51	0.5	5.8	0.6	1.0	0.0	1.0	14.2	11.1	2021.3	692.8	571.8
2014/15	Elgin_CS_LV	3.40	0.6	5.8	0.6	0.8	0.0	1.2	14.1	10.2	1857.6	945.7	614.8
2014/15	Elgin_CS_MV	3.48	0.6	5.9	0.6	0.9	0.1	1.0	14.0	10.0	1809.4	1151	622.9
2014/15	Elgin_CS338_MV	3.42	0.5	6.1	0.6	0.9	-0.1	1.1	14.1	10.2	1874.9	1186	495.8
2014/15	Somerset West_CS_HV	3.66	0.5	5.9	0.7	1.0	0.3	1.2	14.8	10.6	1701.9	819.2	544.2
2014/15	Somerset West_CS_LV	3.61	0.6	5.7	0.6	1.2	0.0	1.0	13.7	10.4	1772.8	783.1	646.8
2014/15	Somerset West_CS_MV	3.68	0.4	5.7	0.6	1.0	0.2	0.9	14.4	10.6	1761.6	718.5	532.1
2014/15	Stellenbosch_1_CS_HV	3.54	0.3	6.2	0.7	0.9	-0.1	1.1	14.3	11.2	1924.9	908.2	352.2
2014/15	Stellenbosch_1_CS_LV	3.63	0.4	5.8	0.7	1.0	-0.2	1.3	14.5	10.9	1946.1	652.0	410.1
2014/15	Stellenbosch_2_CS_HV	3.72	0.5	5.6	0.7	1.2	0.4	1.1	15.0	10.8	1825.2	714.7	550.8
2014/15	Stellenbosch_2_CS_LV	3.53	0.5	5.7	0.7	0.7	0.3	1.1	14.6	11.4	1964.4	643.7	628.4
2014/15	Stellenbosch_2_CS_MV	3.54	0.5	6.1	1.0	0.5	0.6	1.2	15.5	11.2	1931.9	865.7	549.9
2014/15	Stellenbosch_3_CS_MV	3.59	0.5	5.8	0.6	1.2	-0.1	1.1	14.2	11.1	1990.6	579.2	577.3
2014/15	Vredendal_CS_HV	3.80	0.5	5.6	0.7	1.4	0.2	1.3	15.1	10.9	1719.7	550.5	518.2
2014/15	Vredendal_CS_LV	3.65	0.5	5.9	0.8	1.1	0.7	1.4	15.5	11.1	1822.8	678.7	451.4

Addendum 8.3

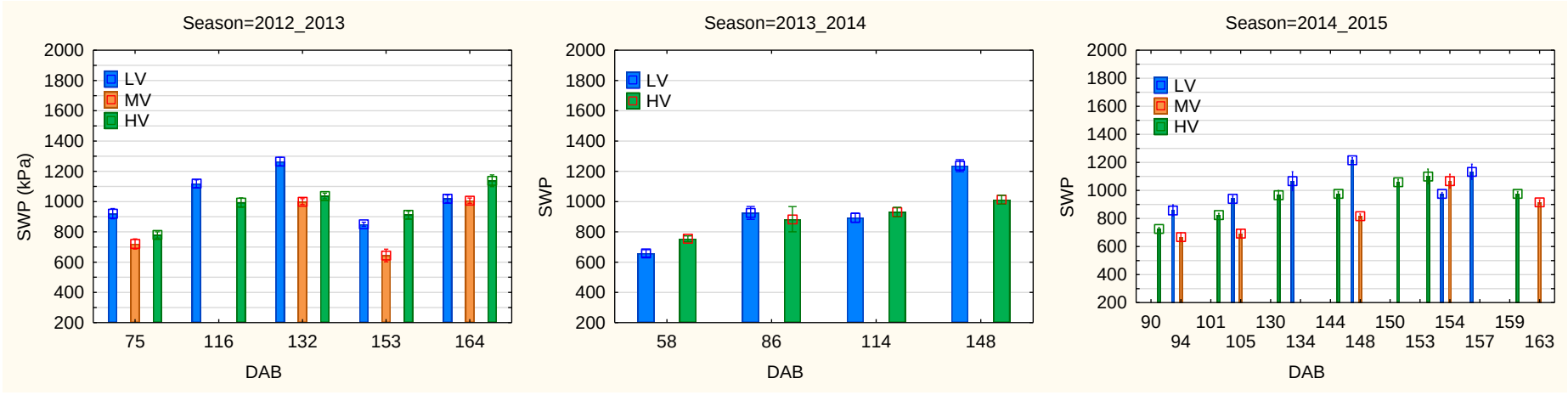

Figure 31 Somerset West SWP over the three growing seasons from left to right, 2012/13, 2013/14 and 2014/15, respectively. Water constraints measured at main phenological stages indicated as days after budburst (DAB) for the three vigours low, medium and high vigour (LV, MV and HV). Vertical bars denote standard errors.

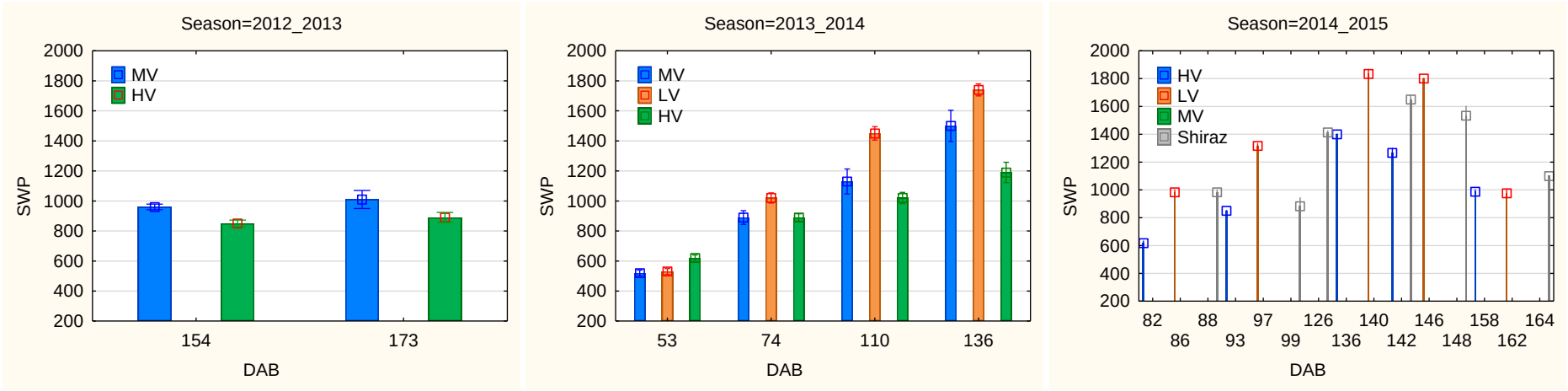

Figure 32 Stellenbosch 2 SWP over the three growing seasons from left to right, 2012/13, 2013/14 and 2014/15, respectively. Water constraints measured at main phenological stages indicated as days after budburst (DAB) for the three vigours low, medium and high vigour (LV, MV and HV).

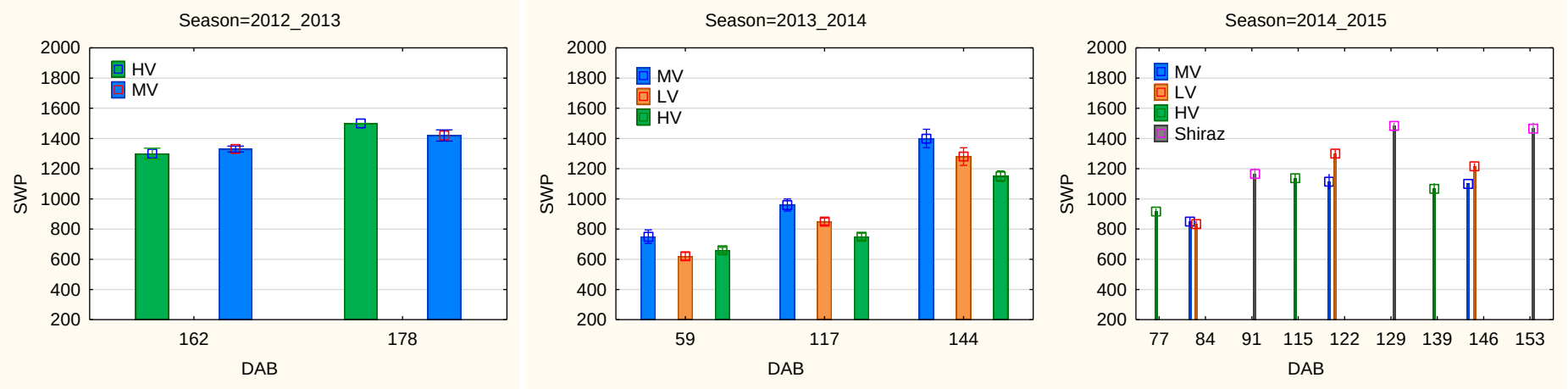

Figure 33 Elgin SWP over the three growing seasons from left to right, 2012/13, 2013/14 and 2014/15, respectively. Water constraints measured at main phenological stages indicated as days after budburst (DAB) for the three vigours low, medium and high vigour (LV, MV and HV).

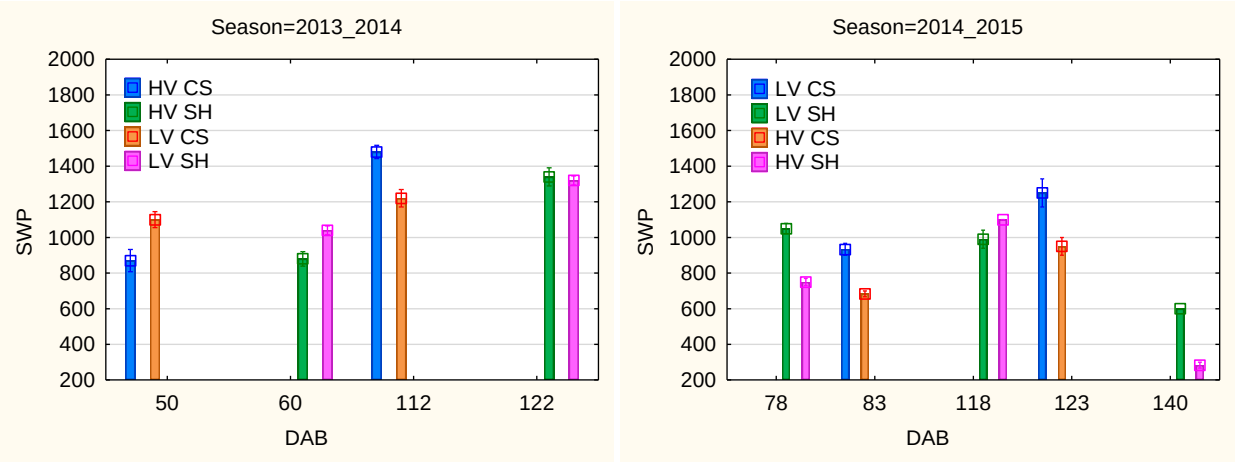

Figure 34 Vredendal SWP over the three growing seasons from left to right, 2012/13, 2013/14 and 2014/15, respectively. Water constraints measured at main phenological stages indicated as days after budburst (DAB) for the three vigours low, medium and high vigour (LV, MV and HV).

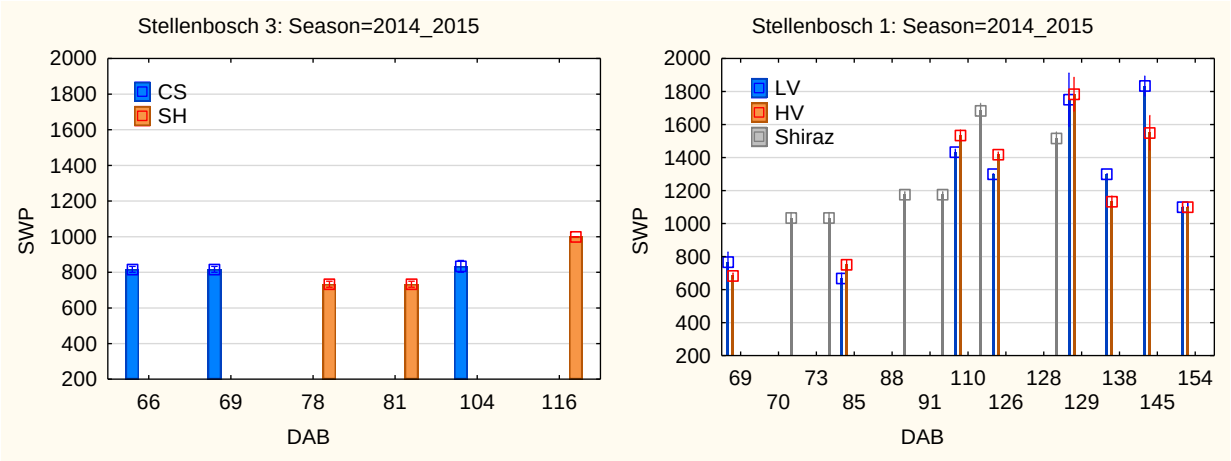

Figure 35 Stellenbosch 1 and 3 on the left and right, respectively for the last season of the study 2014/15 only. Water constraints measured at main phenological stages indicated as days after budburst (DAB) for two vigours low, and high vigour (LV and HV) for two cultivars, Cabernet Sauvignon (CS) and Shiraz (SH).

Chapter 9

General discussion and conclusions

CHAPTER 9: GENERAL DISCUSSION AND CONCLUSIONS

9.1 Introduction/brief overview

The study aimed to provide new insights into the subject of climate change in the Western Cape and to the grapevine's response to climate, namely for *Vitis vinifera* cvs. Cabernet Sauvignon and Shiraz. In the study, climatic parameters were processed on different temporal and spatial resolutions in the study area within the Western Cape and for specific sites selected over a climatic band. The availability of climate and weather data at an applicable spatial and temporal level is crucial to support studies on grapevine phenology, growth, and ripening models, which can be achieved by integrating existing weather station networks and remote sensing resources (Bonnardot & Carey, 2007; Carey *et al.*, 2007; Zorer *et al.*, 2011; Zorer *et al.*, 2013). Hence, the study aimed to evaluate the use of remote sensing sourced land surface temperature as an alternative and supplementary source for weather station temperature which can be used in future climate change adaption strategies.

The plant's reaction to seasonality of environments can be seen in phenology, a sensitive indicator of climate change (Zhao *et al.*, 2013). The application of multiple factor analysis to evaluate the interaction of climate on grapevine phenology, growth, ripening and wine attributes, highlighted possible driving factors that can be used in future modelling. Matching cultivar and terroir requires cultivar-specific studies, such as those described in Van Schalkwyk and Schmidt (2009), together with knowledge of grapevine reaction in terms of growth and ripening when confronted with different climatic/extreme weather conditions.

The overall objective of the study was therefore to study the grapevine's response to climate attributes from a phenology, growth and ripening perspective also evaluating the use of technology to supplement sparse weather station data.

9.2 General discussion of findings according to original aims and objectives

The study had four main aims with its respective objectives:

1. **To perform climate analysis on a site and regional scale**
    a. To analyse hourly data for different sites selected over a climatic band, focusing on temperature and other selected variables (relative humidity, rainfall and wind).

Seasonal variability seemed to be the driving factor possibly affecting the grapevine responses over and above site differences, as pronounced seasonal differences were evident over all the sites. Due to the complexity of factors affecting the environment, and the sensitivity of the grapevine to change, the site and seasonal variability should be explained using hourly data, where the diurnal trend of warming, speed of warming and recovery rate for temperature, relative humidity and wind are quantified. Finer scale analysis of hourly data explained the frequency of hours within specific temperatures, wind and relative humidity classes, which helped to explain the specific climatic kinetics for days, months, seasons and sites affecting the grapevines vegetative and reproductive response. This study did not consider pre-set cut-offs in the climatic variable classes as seen in other climatic studies, but rather analysed the entire temperature, wind and relative humidity profiles, allowing the data to "express itself" and guide the study further.

Seasonal variability within the four year study period showed a general increase in the heat based climatic indices, namely the Winkler and Huglin indices and a decrease in the cool night index. The frequency analysis of hourly data highlighted the specific months within seasonal summations that

are shifting the most and how they are shifting. The most evident changes observed over the four seasons for the six study sites were increases in mean January temperatures and decreases in mean March temperatures. These elements could be further studied on a larger long-term dataset to further elucidate its importance in defining relevant change over different seasons.

The study showed that the mean climatic data and climatic indices could mask seasonal variability, and hence was shown to be insufficient to quantify the finer seasonal variability driving specific grapevine growth and ripening at specific sites. This approach of using the climate profile based on hours at specific classes provides better insights to guide adaptive strategies for the future, especially in the context of climate change and the complex terrain of the Western Cape affecting the diurnal shifts of weather/climate over seasons and short distances.

b. Climate analysis to identifying trends and shifts for the study area of the Western Cape.

The study showed that climate and climate change descriptions are highly dependent on the temporal and spatial resolutions as inputs for the analysis. In this study, the different analysed stations showed significant differences in the warming and cooling over decades, years, regions and months. There was a significant climatic trend of warming over the two datasets analysed for the 30 year period, with a similar trend across the different wine regions of South Africa. Over all temperature elements, there was a warming trend from 1984 to 2015 in the Western Cape. Maximum temperatures showed the most increase over the last three decades, ranging from about 1-2°C. Minimum temperature increases were observed over all the regions but with less intensity, increases ranging up to 0.6°C over the three decades. Rainfall was not well explained by specific trends, but there were regional and monthly changes of annual increases and decreases over decades, with rainfall shifting more into the summer season of the Western Cape. The topography and distance from the ocean seemed to drive regional shifts over the three decades (1984-2015), with a more pronounced effect on temperature in the coastal region, some regions being more prone to change, emphasising the need for finer scale demarcation when climate aspects are considered.

In this study, the higher temporal analysis as half decades, years and months provided more insights into the decadal analysis that showed a general trend of warming in the Western Cape. The half decade analysis showed some years to be cooling and some extreme warmer years. Separating the months and the regions is of utmost importance to get a true reflection of climate shifts in the complex terrain of the Western Cape. Monthly temperature shifts, rather than regional temperatures better illustrated the fluctuations of temperatures across the decades. The most significant shift to warmer temperatures was noted in December, January and March, with increasing rainfall in January and March, insights that could affect the grapevine's growth and especially ripening.

The study highlighted that the climate in the Western Cape wine growing area is changing, with a general trend of warming that was more pronounced in some regions and for some months. The dynamics of how and where the changes are more pronounced can be explained using more integrated climate/weather analysis based on climatic indices, the hourly diurnal nature of the study sites and hourly frequency observations over the climatic band. The study emphasised the need for more climate monitoring sites, especially in the complex terrain of the Western Cape.

2. **To evaluate the use of land surface temperatures for supplementing weather station temperature networks**
    a. Establish an automated workflow to acquire freely available land surface temperature data for any site within South Africa.

In this study the process of downloading freely available daily LST images for the three year period of the study and extracting the final LST values from the images was semi-automated in the applicable software. This process can be adapted slightly to downloading data for other time periods over most areas in the country.

    b. Testing the reliability of land surface temperature (LST) data to supplement daily weather station (WS) temperatures in the complex terrain of the Western Cape.

The best correlation of LST to WS sources was obtained from the T_m of the LST layers calculated form the maximum and minimum layers, rather than using the mean temperature from the average of all four LST layers. This study showed that daily averages calculated from the maximum and minimum LST daily layers to create mean daily LST_{Tm}, sufficiently estimated the WS_{Tm}. Simple statistical methods estimated WS_{Tm} from LST_{Tm} with a calibration error of between 2.3 and 3.6°C. The study showed that LST_{Tm} can be used as an alternative or supplementary source of temperature data for the Western Cape.

From the results obtained in this study, spatial climate maps can be produced using the calibration regression equation to account for the error, ensuring continuous temperature maps by supplementing WS_T with LST_T. As the LST_{Tm} layers are intrinsically spatialised, this would overcome the previous limitations of station distribution limiting climate change analysis. The LST_{Tm} layers can also be used as inputs to build bioclimatic index maps as done in other studies, for detailed description of landscapes, despite the complexity of terrain. This validation was new for the area of the Western Cape and these LST_{Tm} layers can add great value to the climate classification of the Western Cape and the grapevine's expected reaction based on temperature inputs. From the analysis over three seasons, the GDD calculated from the Winkler index and the BEDD were the most promising indices to use for the demarcation of climatic zones. The availability of daily spatial layers could also push modelling of the grapevine's reaction to temperature in a spatial direction. The higher spatial and thermal resolution allows for the discrimination and selection of areas best suited areas for specific crop cultivation.

3. **To study grapevine phenological variability in relation to climate**
    a. Monitoring main phenological stages for a network of *Vitis vinifera* L. cvs Cabernet Sauvignon and Shiraz vineyards selected over a climatic band for four growing seasons.

The study showed that, over and above the extremity of the sites selected over the climatic band, the seasonal variability also had an overriding impact on phenological stages, and the periods between phenological stages were seen to be shifting (increasing/decreasing) between the seasons. The seasonal variability is, however, expected to increase in the context of climate change, with expected increased rainfall in summer months. The Winkler and Huglin bioclimatic indices had the strongest relationship with phenology compared to the other indices, and had the best correlation with the absolute dates of flowering and pre-véraison. The higher indices values (warmer season) resulted in earlier flowering and pre véraison over the different sites.

The precocity index of flowering indicated advancement in flowering at warmer sites and delays for the moderate to cooler sites. The precocity index of vintage indicated an earlier harvest for all the sites over the study period with the exception of the coolest sites which had delayed harvest over the seasons possibly ascribed to less water constraints. More rainfall coincided with a delay in the precocity index of flowering and vintage and the phenological stages of flowering and pea size berries. Rainfall had a positive correlation with flowering. Shiraz had a stronger correlation with flowering probably due to its climatic sensitivity to temperature and moisture, and hence delayed flowering was more prominent in this cultivar compared to Cabernet Sauvignon. Overall, the drier air (lower RH) tended to drive earlier phenology, with higher RH forcing later phenology.

Temperatures throughout the season, with the exception of August and September, seemed to affect flowering. The summer months (December, January and February) with more observed hours between 30-35°C and 35-40°C, had a negative correlation with flowering date calculated as days after 1 September. As minimum February temperatures increased, the flowering and vintage precocity index was earlier. From this study, it is speculated that the months outside the expression of the phenological stages are affecting these stages, and more in depth studies are required to understand this interaction. This could shed light on the irrelevance of some of the bioclimatic indices used to describe the climate of a season in relationship to the expected grapevine response, as the months possibly affecting the phenological stages may be outside of the generally used climatic indices' time frames, *i.e.* September/October to March.

Flowering tended to "set the pace" for phenology in the seasons. Furthermore, flowering had a strong correlation with harvest date, with an excellent correlation in more "normal" seasons. Flowering date as days after budburst could potentially be used to predict harvest date for Cabernet Sauvignon over sites within an accuracy of a few days.

b. Including some other commercial sites and cultivars to assess possible climatic impacts on phenology.

Similar seasonal temperature variations were observed in the case study over a diverse climatic band, confirming the results from the four year study period in the context of the seven seasons assessed in the case study. The phenological variability was dictated by between-season variability rather than variability between the two localities, which again confirms the main study's results.

4. **To study grapevine growth, ripening and wine attributes in relation to climate.**
    a. Monitoring grapevine vegetative responses for the mentioned sites, as well as areas within the vineyards with differing vigour, for four growing seasons.

The study showed overall warmer temperatures to have a positive correlation with growth early in the season and negative correlations later in the season. However, this could be buffered with low to moderate water constraints. Shoot growth tempo was significantly slower for grapevines at the cooler site compared to the warmer sites. Vigour also had an effect on the tempo of growth and final shoot length, with the low and medium vigour having had a faster tempo of growth, but shorter shoots compared to the high vigour plots. The final shoot length attained seemed to be driven by temperature and water constraints, hence the longest shoots were attained with moderate water constraints and moderate to warm climatic conditions. Moderate to high water constraints ensure the canopy fills out to have sufficient balance of vegetative and reproductive growth to allow for a

good tempo of sugar and anthocyanin accumulation. The balance in the grapevine therefore could drive sugar accumulation or lack thereof and indirectly affect anthocyanin accumulation due to the co-regulation nature of the compounds. Unbalanced grapevines will either not complete sugar loading before harvest is attained, or the opposite, where the sugar accumulation could stop ("gets stuck"), hampering the phenolic development of the berry.

As seasonal climatic conditions were shown to be a key driver in grapevine response, it should be considered that this may be counteracted by viticultural practices, such a supplementary irrigation to induce or allow moderate water constraints, ensuring a more balanced grapevine in the selection of trellis system, pruning and canopy management. In the context of climate change, the aim is to match the cultivar growth and ripening response to the climate, for ripening to match the cooler part of the season.

b. Correlating final wine chemical and sensory attributes to climate for the Cabernet Sauvignon sites.

Climate was positively correlated with wine colour, as the total colour pigments and phenolics increased over the three growing seasons in relation to the increase in seasonal GDD. The results suggested that anthocyanin biosynthesis was more sensitive to atmospheric conditions than to water constraints under the given study conditions over sites. Season was the overriding factor affecting the anthocyanin profile, with the warmer seasons and sites being more closely related to the coumaroyl derivatives; while cooler sites, seasons and higher vigour levels (shaded fruits) showed more glucosides and acetylglucoside derivatives.

Season and water constraints were apparently the primary driving factors affecting the sensory attributes of Cabernet Sauvignon. The cooler and lower water constraint sites, such as the high vigour areas, were strongly associated with herbaceous and vegetable attributes. The warmer sites and areas of medium to low vigour were more related with black fruit and prune attributes, as well as tasting sweeter. This was ascribed to the warmer temperatures, and a shorter season in 2014/15.

Temperature and water constraints over sites and seasons affected the methoxypyrazine (ibMP) expression in the Cabernet Sauvignon wines, in particular the summer rainfall in 2013/14 which hampered the degradation of ibMP due to the possible increased vegetative growth. Secondly, the warmer pre-véraison temperatures in the 2014/15 season were probably more favourable for ibMP synthesis and the shorter season did not allow for more effective degradation. The effect seemed to be more prominent in the warmer climates, as the cooler climates had cooler pre-véraison temperatures probably resulting in less synthesis of ibMP. The kinetics of ibMP degradation seemed to be slower at the sites in the study with higher percentage of course sand and silt content. This study gave some insights into the management and planting distribution of Cabernet Sauvignon in the context of ibMP expressions, especially as the pre-véraison temperatures seem to be increasing in warmer areas where Cabernet Sauvignon plantings are prolific.

Moderate climates with moderate water constraints seemed to produce more complex wines than extreme climates – but it can be emphasised that canopy management and irrigation strategies are important in the context of climate change to ensure complexity and quality in the wines. The sensory attributes depend on climate, soil water content, the vine's vegetative growth, and vineyard management techniques affecting the sun exposure of the grapes in the canopy. Within this study, the low vigour areas that had a good balance of yield to pruning mass resulted in

unfavourable wine attributes, possibly due to over exposure of the bunches. The medium vigour sites, which allowed for some vigour but ensured sufficient light in the canopy however had well balanced vines in terms of the Ravaz index and had overall respectable tons per hectare and more favourable sensory attributes.

c. Isolating possible factors affecting grapevine growth, ripening and wine attributes in relation to climate.

The study showed there to be a marked seasonal difference driving the grapevine's response to its environment more so than site variability. Seasonal variability seemed to be driven by extreme climate events such as extreme wind, rainfall or higher temperatures earlier in the growing season and ripening period, confirming the unpredictability of seasons predicted in the context of climate change. The seasons seemed to override even site or vigour differences in many instances; however the seasonal responses also seemed more pronounced at warmer sites.

Results provided some insights into the understanding of cultivating Cabernet Sauvignon in the context of warmer and cooler climatic conditions. Many responses of the grapevine were affected by climate, the grapevine growth tempo and final shoot length was sensitive to seasonal differences and water constraints and indirectly affected leaf area per vine that in turn affected ripening tempo and final wine quality. Major findings: limitations and novelty value-implications

9.3 Major findings: limitations and novelty value implications

The novelty in the study were anchored in the integration of multiple viewpoints to assess the grapevine's response to climate: from climate data analysis to remote sensing combined with a detailed view on the response of the grapevine in growth, ripening and wine style, all in the context of climate change. The study also showed seasonal variability to be driving the grapevines responses, and especially in the context of climate change with seasonal extreme events predicted to increase. Spatial and temporal data sources need to be integrated to create new spatial and temporal layers of higher resolution, which could aid in more insightful within-season decision making and adaptive strategies for a warmer (or cooler) future. The plant-based analysis and aspects of the grapevine most affected by climate as isolated from this study can be used to build models in the context of climate change, learning from the past with historic data, but also projecting into the future. As the LST_{Tm} layers are intrinsically spatialised, this would overcome the previous limitations of station distribution limiting climate change analysis, and can provide continuous layers updated to semi-real time by automated actions, for in season decision making.

9.3.1 Limitations

The main limitation of the study was the frustrations faced in accessing reliable weather station network data in the Western Cape. The network has degraded significantly over the past 10 years, with almost half the stations lost around the year 1998. The spatial station distribution is therefore limited and for the stations that are still functioning, the quality of data could not always be guaranteed. The weather station data had to go through a lengthy process of validating the data, and in many cases, gap filling of missing data.

The study was limited to the study sites and the commercial case study in terms of phenology, growth, ripening and wine attributes, as there is no database for grapevine responses that can be

linked to climate. Due to the lack of information in some form of a geospatial database, the aims for the study in the context of the Western Cape were limited to the results obtained in the study.

9.3.2 Novelty value

Season variability was prominent in driving grapevine response, the variability compelled by extreme out of the ordinary climate events such as extreme wind, rainfall or higher temperatures earlier in growing season and ripening period, confirming the unpredictability of seasons predicted in the context of climate change. This study proves that the climate is warming/cooling, dependant of area and months, which emphasise the need for more semi-real time climate data that can be used within season for decision making.

The finer scale analysis of the climate profile, considering and accounting for the amount of hours at specific classes of temperature, wind and relative humidity with no cut off thresholds, is a novel approach as it gives the climate data the space to express itself and possibly explain the grapevine's responses outside of our scientific frame of reference. This approach provided more detailed insights into the grapevine's requirements and responses to the climate, which will aid in improved adaptive strategies for the future, especially in the context of climate change and the complex terrain of the Western Cape affecting the diurnal shifts of weather/climate over seasons and short distances.

Temporal, spatial, and thermal resolutions of T_m acquired from daily LST products, offer a new and powerful tool for classification of viticultural landscapes and seasonal monitoring. A wide scope of applications can benefit from the improved remote sensing based WS_{Tm} estimations presented in this study for the area of Western Cape. The simplicity of the LST models employed, the robustness and confidence provided by the optimisation and resampling methods, the easy accessibility of the input data at a global scale, along with the good performance attained, suggested that the methodology used in the study has potential to be applied to other regions of the South Africa.

The grapevine phenological stages seem to be more affected by temperatures outside of the September to March growing season, highlighting the need for reviewing the climatic indices used to describe the growing season. In this study, the date of flowering was most effected by climate and tended to "set the pace" for phenology in the seasons. Flowering had a strong correlation with harvest date, hence flowering date as days after budburst could potentially be used to predict harvest date for Cabernet Sauvignon over sites within an accuracy of only a few days.

9.4 Perspectives for future research

In view of climate change, economic pressures and future limitation of water availability to the agricultural sector, informative decisions regarding the suitability of environments for viticulture are paramount. Understanding the interaction between the atmosphere and biosphere is important for the improvement of models relating to the physical system of the earth, and to monitor the impact of global climate change (Cleland *et al.*, 2007). Considering the relationships between climate and grapevine responses, slight climatic differences have implications for the physiological functioning of grapevines, causing significant changes in the management of existing vineyards. Therefore, optimising the grapevine's growth and ripening responses based on hourly frequency observations is important for adaption to climate change. Phenology models and climatic indices currently available for predicting phenology in the context of a changing climate need to be reviewed and studied further. Understanding the finer scale climate analysis as the diurnal cycle and frequency

observations of temperature, wind and relative humidity for a specific site is especially important in the context of climate change in the Western Cape.

Historical grapevine responses can be used in the context of climate to better understand the grapevine's responses to changing climatic conditions. The frequency temperature analysis seemed to be a more robust way to ascertain what climatic factors mostly influenced the seasonal grapevine responses. In the future, there should be more detailed studies on the growth and ripening modelling – integration of climate, remote sensing land surface temperature and plant responses, using open source geospatial tools for adaption to climate. Climatic indices also need to be reviewed in the context of the Western Cape and be used in the context of the cultivar.

9.5 Final Remarks

Future work to quantify climate change in the Western Cape and South Africa can be complimented with the use of intrinsically spatialised remote sensing products, such as land surface temperature layers. Resources such as Fruitlook can be useful to optimise water usage in the future, due the irregular rainfall patterns and possible trends of decreases in annual rainfall. Crops can be cultivated in warmer areas due to the water availability, if water resources become more limited, this will be the factor limiting the future of agriculture in some regions.

This study provides some foundations for a larger database of climate, LST and phenology to build on, for the identification of cultivar distributions compared to more ideal cultivar distribution in the context of a warmer future with possibly more limited water resources. Geostatistical modelling of phenology using isolated driving factors as inputs, can aid as an in-season monitoring and management tool, for better climatic adaptions for the future within farms and regions.

The study confirmed the hypothesis that grapevine will respond to climate change and continue to do so in the expression of phenology, growth and ripening, as the grapevine performances are affected by the constant environmental parameters despite the differences on vineyard and site level.

9.6 Literature cited

Bonnardot, V. & Carey, V., 2007. Climate change: observed trends, simulations, impacts and response strategy for the South African vineyards. In: Proc. Global warming, which potential impacts on the vineyards? pp. 1-13.

Carey, V., Archer, E., Barbeau, G. & Saayman, D., 2007. The use of local knowledge relating to vineyard performance to identify viticultural terroirs in Stellenbosch and surrounds. Acta Horticulturae 754, 385-392.

Cleland, E.E., Chuine, I., Menzel, A., Mooney, H.A. & Schwartz, M.D., 2007. Shifting plant phenology in response to global change. Ecol. Evol 22, 357-365.

Van Schalkwyk, D. & Schmidt, A., 2009. Cultivation of Pinotage in various climatic regions (Part 1): Climatic differences. Wynboer, February.

Zhao, M., Peng, C., Xiang, W., Deng, X., Tian, D., Zhou, Z., Yu, G., He, H. & Zhao, Z., 2013. Plant phenological modeling and its application in global climate change research: Overview and future challenges. Environ. Rev. 21, 1-14.

Zorer, R., Rocchini, R., Delucchi, L., Zottele, F., Meggio, F. & Neteler, M., 2011. Use of multi-annual MODIS land surface temperature data for the characterization of the heat requirements for grapevine varieties. In: Proc. Analysis of Multi-temporal Remote Sensing Images (Multi-Temp), 2011 6th International Workshop pp. 225-228.

Zorer, R., Rocchini, D., Metz, M., Delucchi, L., Zottele, F., Meggio, F. & Neteler, M., 2013. Daily MODIS land surface temperature data for the analysis of the heat requirements of grapevine varieties. IEEE T. Geosci. Remote. 51, 2128-2135.